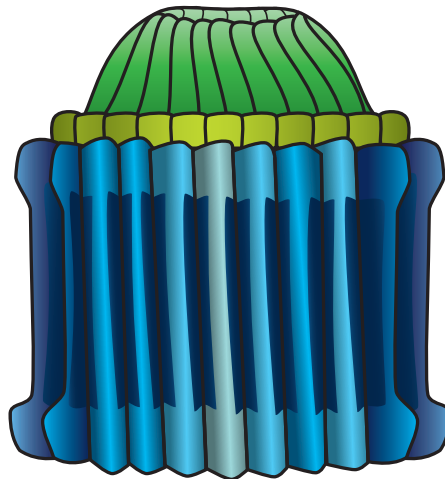


Cenozoic Coccolithophores: Discoasterales



Marie–Pierre Aubry

Rutgers University and Woods Hole Oceanographic Institution

2014

The Micropaleontology Press Foundation, Inc., New York

Online update: November 2018

[Click to Interactive Table of Contents](#)

ISBN 978-0-9766734-1-5

This volume is part of a peer-reviewed taxonomic revision of all fossil and living coccolithophores. Suggested citation: Aubry, M.-P., 2014. *Cenozoic Coccolithophores: Discoasterales (CC-C)*. New York: Micropaleontology Press. Atlas of Micropaleontology series, 328 pp.

Copyright © 12 December 2014 by Micropaleontology Press. All rights reserved. No part of this volume may be reproduced in any form, by print, photographic media, or digitized electronic storage without written permission from the publisher.

“Micropaleontology Press” is the business name of The Micropaleontology Press Foundation, Inc., a 501(c)3 nonprofit corporation housed at CUNY Queens College, 6530 Kissena Blvd., Flushing NY 11367

CONTENTS

Foreword	p. v
Explanatory Note	p. vii
Order Discoasterales Hay 1977 emend. Aubry herein (continued)	
Family Fasciculithaceae	
Genus <i>Gomphiolithus</i>	p. 1
Genus <i>Lithoptychius</i>	p. 17
Genus <i>Fasciculithus</i>	p. 87
Family Heliolithaceae	
Genus <i>Bomolithus</i>	p. 163
Genus <i>Heliotrochus</i>	p. 181
Genus <i>Heliolithus</i>	p. 225
Family Hayellaceae	
Genus <i>Hayella</i>	p. 245
Genera <i>incertae sedis</i>	
Heliolith Genus indeterminate A	p. 269
<i>Nomina dubia</i>	p. 277
References	p. 289
Appendix 1: Alphabetic list of taxa	p. 294
Appendix 2: Supplementary information on illustrations listed in “Figure References”	p. 296
Index	p. 327

FOREWORD

The objective of the *Atlas of Micropaleontology*, in its various forms of publication, is to provide the scientific community with state of the art taxonomy that integrates current knowledge with the observations from more than 150 years of study into the various disciplines of micropaleontology.

Cenozoic Coccolithophores, the first such synthesis in this series, presents a comprehensive re-examination of the taxonomy of the coccolithophores of the present geological era, in consideration of our rapidly growing understanding of the biology, ecology, and biogeography of this enormously important and abundant constituent of the global biosphere. This work continues the study that began with the *Handbook of Cenozoic Calcareous Nannoplankton*, integrating major recent advances in molecular biology with traditional morphologic description as the basis for a comprehensive review of nomenclature up through families and orders. While the more than twenty volumes of *Cenozoic Coccolithophores* are independent from one another, they are complementary within the overall concept of the group. To avoid repetition in each volume of the fundamental principles behind this organization, an introductory volume explains the objectives of the project, the methodological and philosophical approach, and the format that has been followed throughout. The introductory volume also acknowledges the circumstances, and the contributions of my colleagues, that have made this work possible.

I am deeply grateful to my colleagues John Van Couvering (Micropaleontology Press) for his editing of the manuscript, John Steinmetz (Indiana Geological Survey), Maria Triantaphyllou (University of Athens, Greece) and Osmon Varol (Varol Research), for their thoughtful reviews of this work, and also to Sarah Klingler (Rutgers University), for her diligence and accomplishment in creating the artwork in this volume.

Marie–Pierre Aubry

EXPLANATORY NOTE

Organization of the work, and symbols used in text and illustration

Cenozoic Coccolithophores is a series of more than 20 volumes dedicated to the full description of all known and valid species of Coccolithophores from the beginning of the Paleocene to the present day, with an overview volume that synthesizes our knowledge of the group accumulated over 140 years and reviews the objectives of the series, as well as giving full explanation of the organization, style and layout of text and plates found in the descriptive volumes.

Unlike the related *Handbook of Cenozoic Calcareous Nannoplankton*, which was organized around a key of determination for identifying morphostructural groups and associated genera, *Cenozoic Coccolithophores* is organized according to taxonomic hierarchy, from orders to families down to genera, with each order occupying one or more volumes (and in two instances, two low-diversity orders in a single volume). The orders are then subdivided into families of related genera. In each volume, the taxonomic subdivision is first explained, with clear definitions of the order and its families, according to fundamental morphostructural characteristics of the group. The subsequent chapters then treat the genera in succession, as follows:

(1) Description of the genus, beginning with the coccoliths, and (when known) the coccosphere, that characterize the genus, followed by a review of the biology, physiology and ecology of its species, their evolutionary history, and their stratigraphic application. This is followed by the original type description of the genus, and (where appropriate) "Remarks" on the genus from other sources. Wherever possible, a key of determination to the species within a genus is given.

(2) Description of the species, grouped by units for easy comparison of similar morphologies. A unit includes two facing lead-pages with a columnar organization such that facing columns concern the same discrete taxon. The first page illustrates the types of the species in the unit, as seen in light microscopy; the second provides the original descriptions of these species, together with supplementary data on stratigraphic occurrence, preservation, paleoecologic preferences, and phylogenetic relationships. Occasionally the holotype of a species is in the form of an electron micrograph (SEM). In such cases, a light microscope photograph (taken from the original publication whenever possible) is added to make full comparison possible. Descriptions have been shortened (but not truncated) to allow immediate access to the salient taxonomic characters, and all descriptions in foreign languages have been translated to English. Information from the original description is denoted by the short dash "-" at the left margin of the text, while information from subsequent research

is indicated by the long dash "—", also at the left margin. Regarding size, the notation n_1-n_2 indicates the amplitude of size variation along the main dimension, while $n_1 \times n_3$ (or $n_1-n_2 \times n_3-n_4$) denotes size (or size variation) along two dimensions, indicated by [L] for length, [W] for width, [Ø] for diameter, or [H] for height. At the bottom of each column is the code number of the reference from which the type description is taken, with its pagination and, where relevant, the code (with pagination) of the reference from which a recombination or emendation is adopted. The coded references are listed as "Figure References" at the end of each chapter. The units include validly named species (in **bold face italics**) and their synonyms (in *regular face italics*) but also taxa in open nomenclature (regular face). Taxa validly named but which represent artifacts of preservation are best treated as *nomen oblitum* (also in *regular face italics*).

(3) The lead pages are followed by a variable number of pages that further illustrate the species, first in light microscopy then in electron microscopy. Electron micrographs are grouped according to material (coccospheres vs coccoliths, and living vs fossil material) and then sequentially by orientation (for coccoliths: side view > proximal face > distal face; for coccospheres: side view > apical view > antapical view where such terminology is applicable). When no illustrations are available for a desired orientation, the next best illustration(s) to convey the characters of the coccolith in the desired orientation is used. Also, some photographs may illustrate several coccoliths with different orientations. A narrow spacing between illustrations indicates that they correspond to the same specimen. The illustrations are keyed to the source reference by the code number in **bold face** adjacent to the first illustration from each source. Numbers in regular face identify the plate and figure of the illustrations for the individual figures in the source reference(s), which are listed at the end of the unit.

The full citations of references in the text and in "Figure References" are given in the reference list at the end of the volume.

To keep the text concise, as well as to save space in the somewhat constricted format imposed by the multi-column layout, the following abbreviations and symbols have been used:

In the text:

[]	translation
**	modified from original
≠	differs
E.	Early
M.	Middle
L.	Late
e.E.	early Early
m.E.	middle Early
l.E.	late Early
e.L.	early Late
FAD	First Appearance Datum
LAD	Last Appearance Datum
LO	Lowest Occurrence
HO	Highest Occurrence
C.N.	Crossed Nicols
X.P.	Crossed Polarized Light
B.F.	Bright Field
SEM	Scanning electron microscope

In the illustrations:

H	Holotype
L	Lectotype
P	Paratype
S	Syntype
[cf.]	Confer
[aff.]	Affinity
1	Style of reference code
1	Style of illustration code

The coded list of references at the end of each chapter is organized as follows:

1. Albus, X., 1983. Publ. Pal., 99(9): 9-99.
(1, 2, 10): 10/15, 16, 20.

The bold face number that begins the first line is the code for the indicated reference. On the second line, the numbers in parentheses are the codes used herein for the illustrations taken from this reference; following this, "10/" is the plate number, and "15, 16, 20" are the figure numbers, respectively, which identify the referenced illustrations.

Illustrations without any code numbers originate from my personal collection, but in view of the fact that this publication has the goal of synthesizing the published literature (see above) I have used as few of these as possible.

GOMPHIOLITHUS

HIGHLIGHTS

- Fasciculiths consisting of two cycles (the distal one being extremely thin) and a central body.
- Two species.
- Size range: 8–17 μm .
- Slightly concave proximally.
- Deeply concave distally; central opening closed by central body.
- Cocosphere unknown.
- Very short range in upper Danian (Zone NP4).
- Evolved possibly from *Biantholithus sparsus* (insufficiently documented).

SELECTED READING

Aubry, Bord and Rodriguez, 2011; Monechi et al., 2013; Perch-Nielsen, 1977; Perch-Nielsen, 1981a; Romein, 1979.

INTRODUCTION

The first illustrations and substantial descriptions of the *Gomphiolithus* fasciculiths are by Perch-Nielsen (1977) and Romein (1979). Additional photomicrographs have since been published, but little useful documentation of their structure has since become available. Their comprehensive interpretation will necessitate recovery of better preserved material than that which is currently available.

MORPHOLOGY AND STRUCTURE

Coccoliths

Morphology – The fasciculiths of *Gomphiolithus* are large and broadly conical, with a narrow, slightly concave face at one end and a broader, deeply concave face at the other in keeping with the etymology of their name (from Gr. *gomphios*, molar; Gr. *lithos*, stone; text-fig. 1). They exhibit a radial symmetry, highlighted by the occurrence of a marked axial canal.

Originally, the fasciculith *G. magnus* was oriented so that the broad, deeply concave end was proximal, and the narrower and shallower end was distal. This is the general orientation of such morphologies in the bulk of fasciculiths, and is the one preferred by Monechi et al. (2012, 2013). However, Perch-Nielsen (1977) reversed the orientation of the fasciculith based on the difference in shape of the sutures at both ends, and was followed in this by Romein (1979) and Steurbaut and Sztrákos (2008). The same logic is used here.

Structure – The only *Gomphiolithus* fasciculiths currently illustrated in electron microscopy are those of *G. magnus* from DSDP Site 356 in the South Atlantic (Perch-Nielsen, 1977). The smooth surface and angular sides of their elements indicate extensive recrystallization, which hampers thorough description. Nevertheless, they show their basic structural components sufficiently well.

Gomphiolithus fasciculiths mainly consist of a large, sturdy column composed of wedge-shaped elements that are visible at both the proximal and distal ends of the coccoliths (text-fig. 2). At the

proximal end, their sutures radiate from the center of the slightly concave face. At the distal end, they form the periphery of the craterous face, where they also exhibit radial sutures (e.g., Perch-Nielsen, 1977, pl. 11, fig. 6). Deeper in the depression they are covered by elements apparently concentrically arranged and with sutures oriented anticlockwise, interpreted here as corresponding to the calyptra. This is the “thin, upper slice” with sutures “oblique and oriented counter-clockwise” which Romein (1979, p. 76, 79) interpreted as resulting from distal torsion of the elements of the column; it is the cause of the “vague incisions in the inner, upper part of the column” noted by him (op. cit., p. 148, 149). Earlier, Perch-Nielsen (1977, p. 728) had determined that “the central part of the distal side is built up of concentric rings”.

The bottom of the distal depression is occupied by elements arranged in a coarsely radial pattern, as described by Perch-Nielsen (1977, p. 728, pl. 11, fig. 5). This corresponds to the distal surface of the central body (text-figs. 1, 2a). Considering the irregularity of this pattern, it may be best interpreted as reflecting crystal overgrowth on the distal surface of an otherwise porous central body.

Extinction patterns

Gomphiolithus fasciculiths belong to the optical group Heliolithae. In light microscopy and under crossed nicols, they produce an extinction cross with radial arms that fan out from the center of the fasciculith towards the periphery. In lateral view they behave as if they consist of a single cycle, show an equilateral triangular or diamond-shaped central body and a poorly defined distal structure (Romein, 1979, p. 148, 149).

BIOLOGY AND ECOLOGY

Biology

The cocosphere of *Gomphiolithus* is unknown, but probably consisted of juxtaposed fasciculiths radiating around the cell (text-fig. 3). The fasciculiths are bulky and the heterococcolith-stage was likely non-motile. The canal running along the vertical axis of the fasciculith would have permitted water and gas exchanges between the cell and seawater in which the central body may have served as a filter.



TEXT-FIGURE 1

Morphology and structure of *Gomphiolithus fasciculiths* as seen in cross section.

a: *G. magnus*.

b: *G. magnicordis*.

As in all genera of the order Discoasterales the structural units are coded as follows; blue: column; green: calyptra; aqua: central body.

Physiology

The coccolith morphology (shape, size) and the occurrence of a porous central body are suggestive of mixotrophic physiology. The original structure of these fasciculiths is strongly altered by recrystallization in all SEM-illustrated specimens. It is most likely that their sturdy appearance is a diagenetic artifact, and that these fasciculiths were as delicate as those of *Fasciculithus* (although probably not with fenestrae). In side view of *G. magnus*, the elements of the column are seen to split in two where the column expands (i.e., above the constriction), resulting in a regular pattern of alternating broad and narrow notches between the elements (text-fig. 2b). The doubling of the number of elements would have resulted in more than a doubling of the surface of the column, which in turn can be interpreted as a substantial increase of the surface of the coccolith exposed to seawater. This achieves the same as the addition of the collaret in the *Biantholithus-Lithoptychius* transition, seen as an adaptation to late Danian oceanic oligotrophication (Aubry et al., 2012).

Ecology

Specimens of *Gomphiolithus* are always rare, and their ecology is poorly known. They have not been recovered from high latitudes (text-fig. 4).

EVOLUTIONARY HISTORY

Origin

Gomphiolithus magnus is the oldest fasciculith. It is characterized by a sharp constriction in the lower third of the column. Perch-Nielsen (1977, p. 747) saw in this constriction evidence of

“*Markalius inversus* developing its small, simple proximal shield into the small, proximal part of *F. magnus* and its high, distal shield into the high distal part of *F. magnus*, thereby keeping the central depression with the concentric rings of elements” (1977, p. 747; see also 1981a, p. 14, fig. 3).

A placolith, *Markalius inversus* belongs to the Order Coccolithales and is an unlikely ancestor of *Gomphiolithus*.

A more plausible hypothesis is the evolution of *Gomphiolithus* (and all fasciculiths) from *Biantholithus* (Aubry, 1998) in which the tall cycle of the former evolved from a considerable thickening of the column of the latter associated with an even more considerable thinning of the calyptra, and the addition of a central body (text-fig. 5). This possibility was endorsed by Monechi et al. (2013, p. 34; although the so-called “intermediate forms” (ibid, pl. 1, figs. 3, 4) are unconvincing.

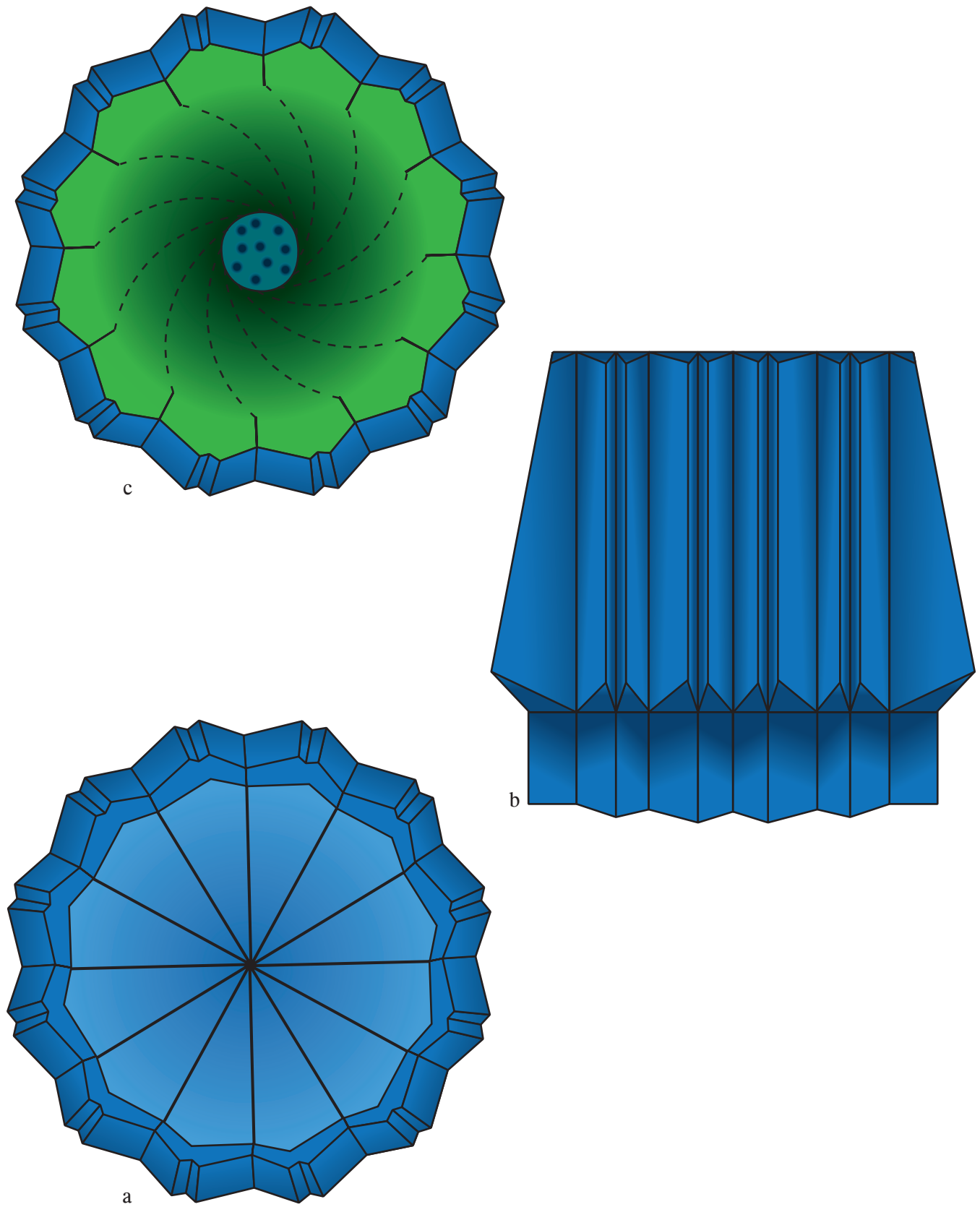
Although logical in all regards, a derivation of *Gomphiolithus* from *Biantholithus* is not fully supported, at least not by the available data, because it would have evolved a radically profound structural transformation with almost complete loss of the calyptra. A possible alternative is that *Gomphiolithus* evolved from a Maestrichtian-earliest Paleocene ancestral lineage of the Order Discoasterales that did not calcify or was not preserved. In this view, *Gomphiolithus* may well have evolved from a species of *Ceratolithoides* (see CC-B, Introduction: Order Discoasterales, text-fig. 1). In brief, as stated by Perch-Nielsen (1977, p. 747) “*Fasciculithus magnus* appears suddenly, without any obvious ancestor”.

Phylogeny

Until proper significance was given to their structure, all fasciculiths were assigned to the genus *Fasciculithus*, and the oldest species *magnus* was regarded as the stem species of a *Fasciculithus* lineage (Romein, 1979, fig. 40; Perch-Nielsen, 1981a, fig. 3). This view is maintained by Monechi et al. (2013).

A different view emerges here, in which the fasciculiths of *Lithoptychius* are directly derived from the biantholiths of *Biantholithus*, giving rise in turn to the fasciculiths of *Fasciculithus* (see Genus *Lithoptychius*, Genus *Fasciculithus*, this volume). In this interpretation, *Gomphiolithus* had no Paleocene descendants. The lack of temporal overlap between its fasciculiths and those of *Lithoptychius*, its extremely low diversity (two species) and short life span are further evidence that *Gomphiolithus* is an isolated genus.

We follow Romein (1979, p. 77) in considering that *G. magnicordis* evolved from *G. magnus*.



TEXT-FIGURE 2
 Structure of *Gomphiolithus fasciculiths* (based on *G. magnus*).
 a: proximal face.
 b: side view.
 c: distal view.

Diversity

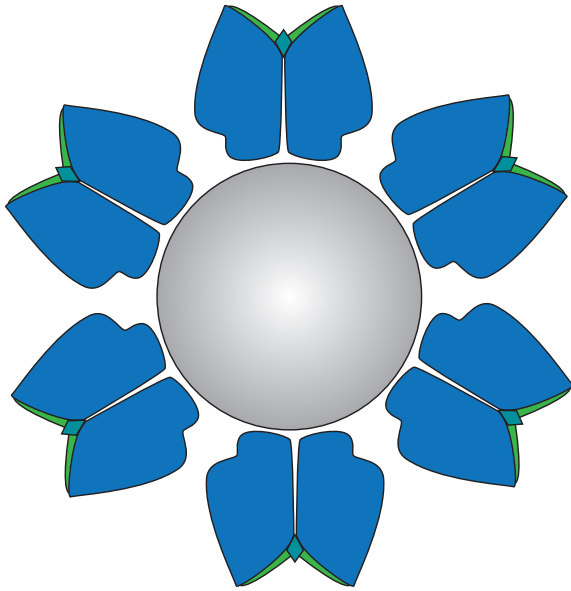
With only two described species, *Gomphiolithus* is one of the genera of the Order Discoasterales exhibiting little diversity. However, scarcity of its fasciculiths is not conducive to firm documentation of true diversity.

STRATIGRAPHY

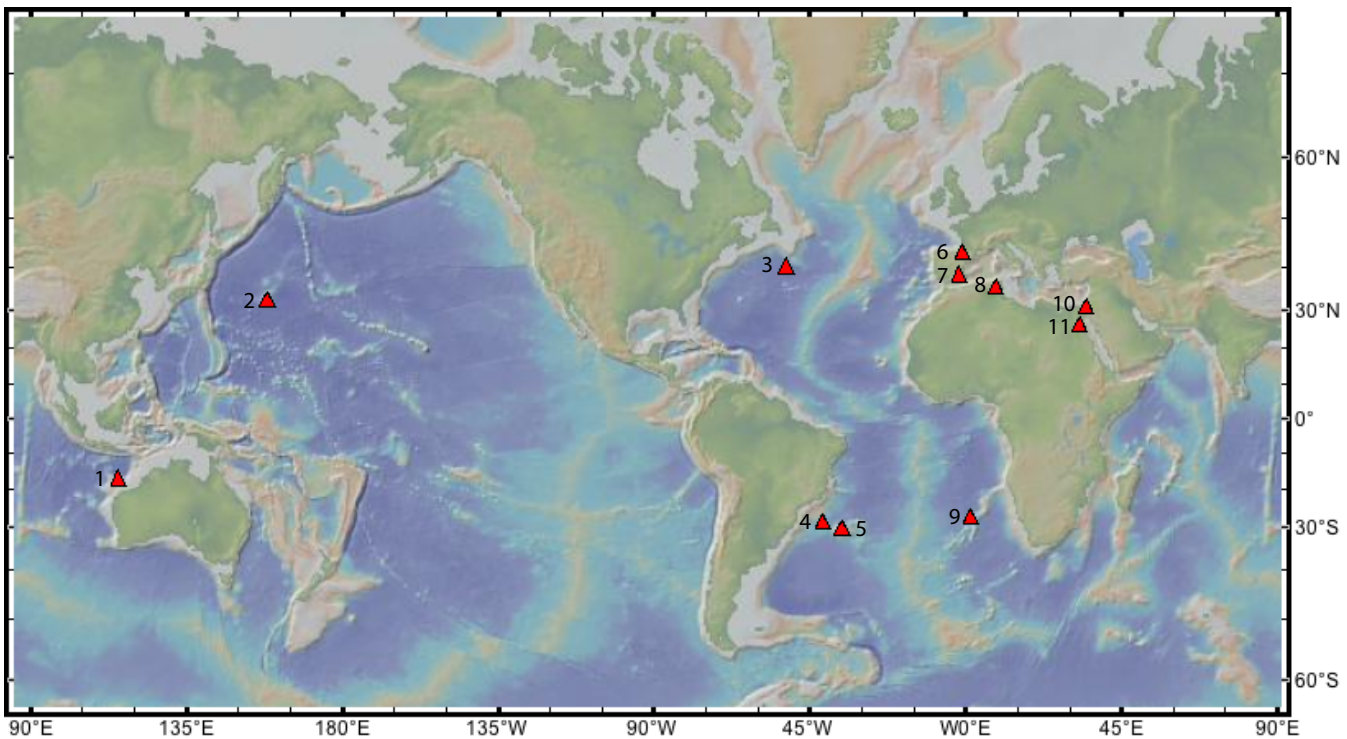
The occurrences of *Gomphiolithus* species are restricted to a thin stratigraphic interval in Subzone NP4a of Zone NP4 (Romein, 1979; Aubry and Salem, 2012), which essentially corresponds to Subzone NTP5c to NTP7 of Varol (1989). At ODP Site 1262, they occur over a 2 m-thick interval assigned to Subzone NTP5-Zone NTP6 (Monechi et al., 2013, table 1). In the Sidi Nasseur section (Tunisia) they are reported from a 40 cm thick interval assigned to Zone NTP6 (Van Iterbeek et al., 2007).

Varol (1989, p. 278) commented that the HO of either species (*magnus* or *magnicordis*) may serve to approximate the upper boundary of his Zone NTP7 (originally named the *Fasciculithus chowii* Zone) in the absence of *F. chowii* or *Sphenolithus primus*, whose respective HO and LO define the top of the zone. (*F. chowii* is a superficial taxon that encompasses the oldest representatives of the genus *Lithoptychius*; *L. collaris* may best be substituted to *F. chowii*; see Chapter *Lithoptychius*, this volume).

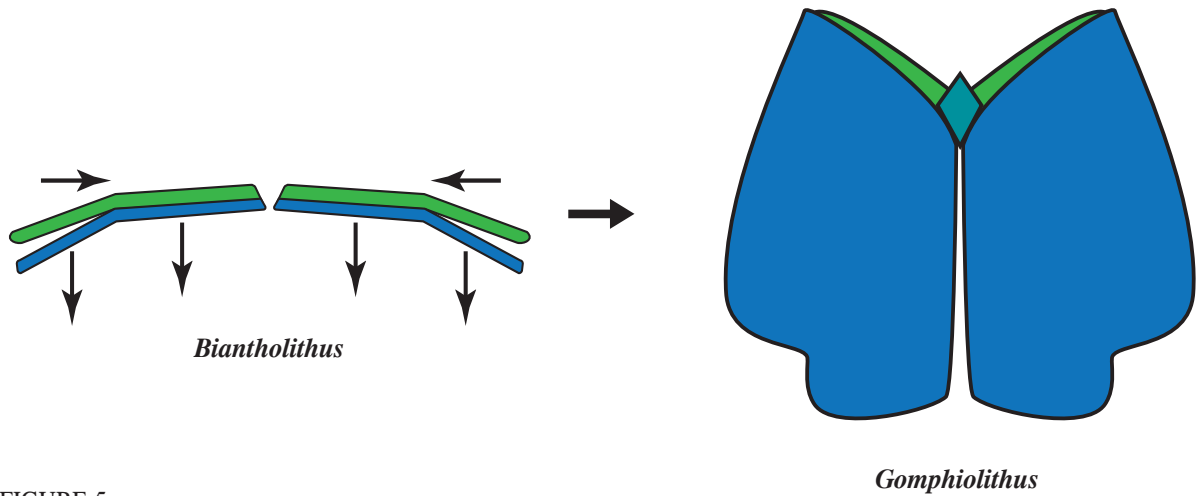
There are unexplained inconsistencies in the range of the two species in different sections. Varol (1989) indicated that the upper ranges of the two species overlap with the upper range of *Lithoptychius collaris* (see above). In contrast, Steurbaut and Sztrákos (2008) and



TEXT-FIGURE 3
Tentative reconstruction of the coccosphere of *Gomphiolithus magnus* (as seen in cross section).



TEXT-FIGURE 4
Geographic distribution of *Gomphiolithus* species.
(1, 2, 3, 9): DSDP Sites 384, 761, Indian Ocean, ODP Site 1209, Pacific Ocean, DSDP Site 384, N. Atlantic Ocean, ODP Site 1262, S. Atlantic Ocean (Monechi et al., 2013); (4, 5): DSDP Sites 356, 357, S. Atlantic Ocean (Perch-Nielsen, 1977); (6): Loubieng, Aquitaine basin (Steurbaut and Sztrákos, 2008); (7, 10): Caravaca, Spain, Nahal Avdat, Israel (Romein, 1979); (8): Sidi Nasseur, Tunisia (Van Iterbeek et al., 2007); (11): Qreyia, Egypt (Sprong et al., 2009).
(Map from GMRT, Ryan 2009; <http://www.geomapapp.org>.)



TEXT-FIGURE 5

Derivation of *Gomphiolithus* fasciculiths from biantholiths of *Biantholithus*. Coccoliths in cross section.

Monechi et al. (2013) showed that the HO of *G. magnus* is older than the LO of *Diantholitha* spp. (itself older than the LO *F. chowii* [probably *L. collaris*]) in sections such as Loubieng, DSDP Sites 384, 761B, and ODP Sites 1209, 1262 (see text-fig. 4). However, whereas the HO of *G. magnicordis* is also older than the LO of *Diantholitha* spp. in the latter four sections, it is much younger in the Loubieng section, and Agnini et al. (2007, fig. 5) determined a small, albeit isolated abundance peak of the “*F. magnicordis* gr.” at ODP Site 1262 (text-fig. 6), which, by correlation with Monechi et al. (2013), is younger than the LO of *Lithoptychius* spp., (and consequently *Diantholitha* spp.).

Chronostratigraphy

Because of their general scarcity, the range of *Gomphiolithus* species are not useful for formal zonal purposes. However, they characterize a short interval of the upper Danian.

Chronology

The stratigraphic range of *Gomphiolithus* is currently best documented at Sites 1262, 384 and 761B where Monechi et al. (2013) shows it to be contained to Magnetozone C27r. These records allow to confidently tie the FAD and LAD of *G. magnus* to early Chron C27r, with dates of 62.4 Ma and 61.5 Ma, respectively (text-fig. 7). The FAD of *G. magnicordis* is also placed at 62.4 Ma. Because of the inconsistent location of its HO with respect to other biohorizons, it seems premature to date the LAD of this taxon.

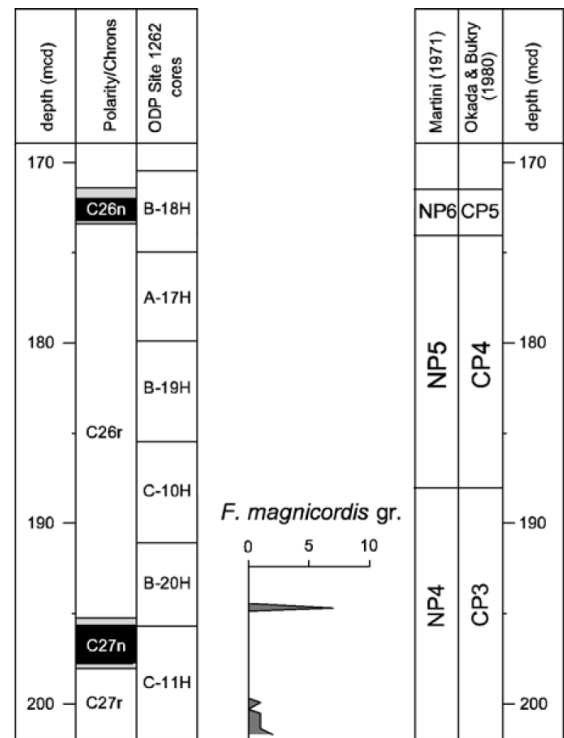
TAXONOMY

Generic taxonomy

Genus: *Gomphiolithus* Aubry in Aubry, Bord and Rodriguez 2011

Type Species: *Gomphiolithus magnus* (Bukry & Percival) Aubry in Aubry, Bord and Rodriguez 2011, p. 273 (= *Fasciculithus magnus* Bukry & Percival 1971, p. 131, pl. 4, figs 9-12 (holotype pl. 4, figs. 9, 10).

“Fasciculiths consisting of a main, tall structural unit (column) of radially arranged, wedge-shaped elements; distal face deeply concave; proximal face flat or slightly

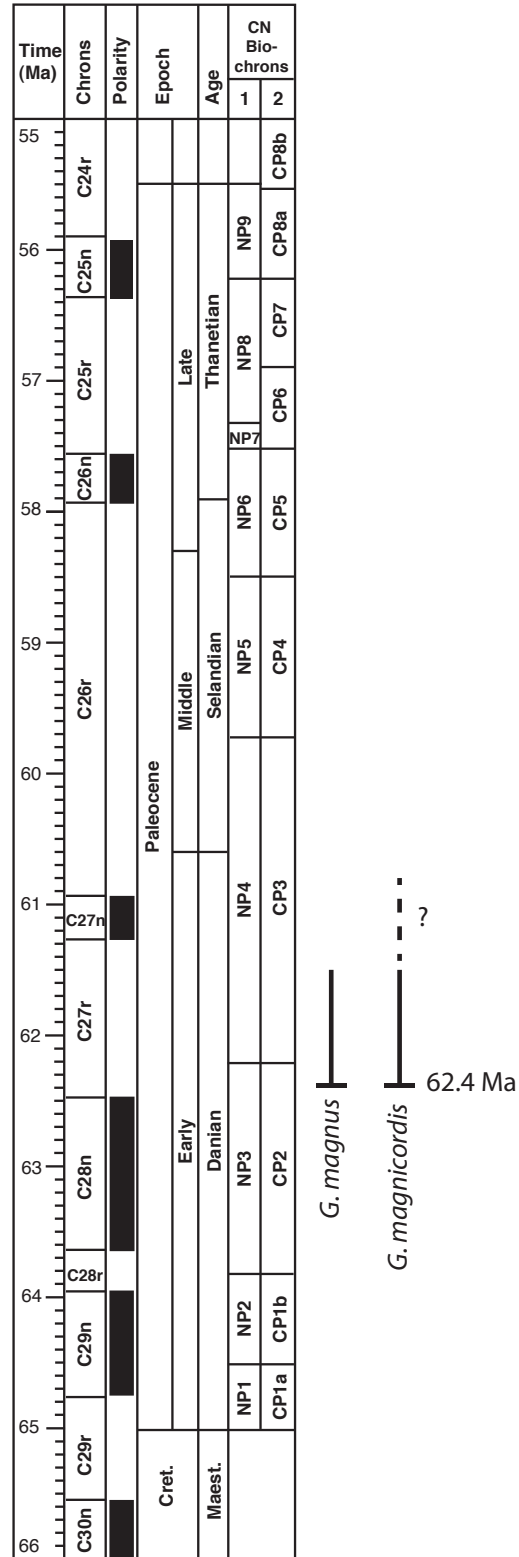


TEXT-FIGURE 6

Abundance pattern of *Gomphiolithus magnicordis* group at DSDP Site 1262. (Modified from Agnini et al., 2007, fig. 5.)

concave. The distal side is marked by the presence of a central body (visible only in side view).

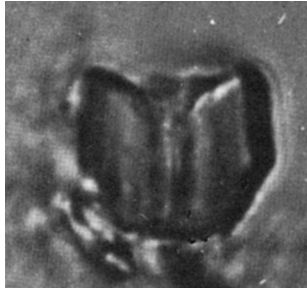
“Species assigned to *Gomphiolithus* were previously placed in the genus *Fasciculithus* Bramlette & Sullivan 1961. Until now this genus has accommodated all fasciculiths (a Paleocene morphostructural group; see Aubry, 1989). The introduction of *Gomphiolithus* is based on 1) the marked morphologic and structural differences between the older two fasciculiths (species *magnus* and *magnicordis*) and all younger fasciculiths, and 2) the disjunct stratigraphic ranges of these older fasciculiths and the younger ones. Unlike *Fasciculithus*, *Gomphiolithus* possesses a central body but it does not possess a calyptra (some specimens may have a tiny distal structural unit). Also, the elements of the column in *Gomphiolithus* delineate a broad central canal whereas in *Fasciculithus* the elements of the column are contiguous along the vertical axis. The fasciculiths of *Lithoptychius* also comprise a column and a central body. They additionally possess a collaret and a calyptra, both of which are absent in *Gomphiolithus*” (Aubry in Aubry et al., 2011, p. 273).



TEXT-FIGURE 7
Biochronology of *Gomphiolithus*.

Gomphiolithus magnus (Bukry & Percival) Aubry & Rodriguez in Aubry et al. 2011
[= *Fasciculithus magnus* Bukry & Percival 1971]

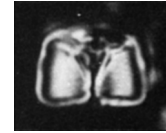
H



BD71/1

Gomphiolithus magnicordis (Romein) Aubry & Rodriguez in Aubry et al. 2011
[= *Fasciculithus magnicordis* Romein 1979]

H



RAJT79/40

Gomphiolithus magnus

- 10–17 μm

- E. Paleocene. Shatsky Rise, Northwestern Pacific.

- Large, characterized by a very deep concave depression at one end and by a distinctive narrowing of the cylindrical body about halfway towards the other end. Body of the cylinder solid, composed of ~20 high wedge-shaped elements. In side view, the outline slopes in toward the central axis from the larger portion of the column (where the conical depression is) to its narrow part.

≠ from *F. schaubi* by lacking six concave sides and pit-and-ridge ornamentation;

≠ from *F. involutus* and *F. tympaniformis* by having a distinctive change in cylinder diameter half way along its length and by having a very deep conical depression at one end.

— The fasciculith was re-oriented by Perch-Nielsen (1977, pl. 11) with the deep concave depression being distal. The occurrence of the central body confirms this orientation (Romein, 1979).

— Romein (1979, p. 148) commented that this sp. consists of a column and a central body, noting that a “well defined [calyptra herein] is absent.”

— Gave rise to *G. magnicordis* (Romein, 1979, p. 77).

- BD71 (p. 131), PNK77 (p. 273).

Gomphiolithus magnicordis

- 6–8 μm x 8–10 μm

- E. Paleocene. Spain.

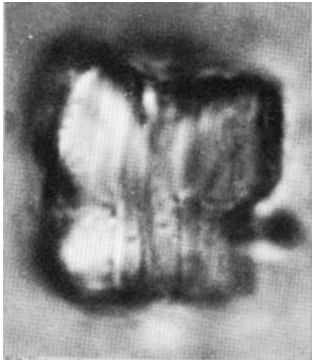
- Composed of a distally tapering column and a central body. Column consisting of 20 to 30 wedges with smooth outer surface. Proximal side flat to slightly concave; distal side concave. Sutures slightly oblique, counterclockwise in distal view, radial in proximal view. Central body relatively large, extending from the distal depression to, or almost to, the proximal side. In the L.M., the body shows a cut-diamond-like cross-section in side view. In the same view, a vague incision can be observed in the upper inner part of the column.

≠ from the closely related *F. magnus* by its smaller size, and by its relatively larger central body.

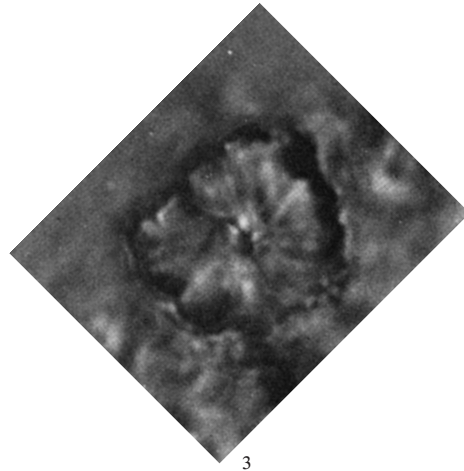
- Short range in the *Ellipsolithus macellus* Zone (NP4) (Romein, 1979, p. 149).

- RAJT79 (p. 149), AMP11 (p. 273).

Gompholithus magnus (continued)



BD71/2



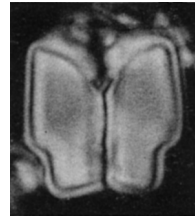
3



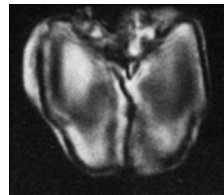
PNK77/6



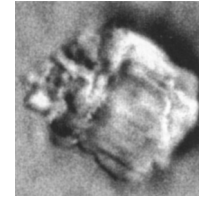
7



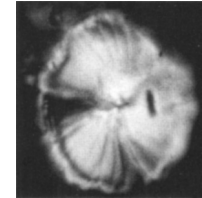
8



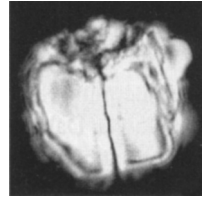
RAJT79/9



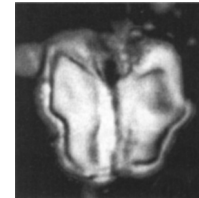
SE08/10



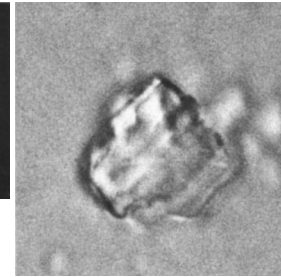
11



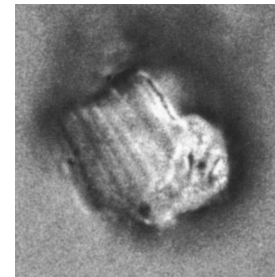
12



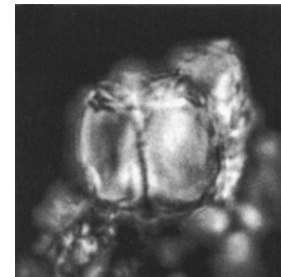
13



14



15



16

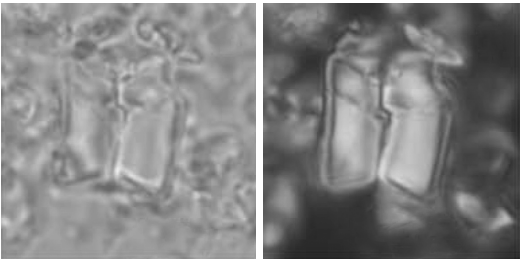


4



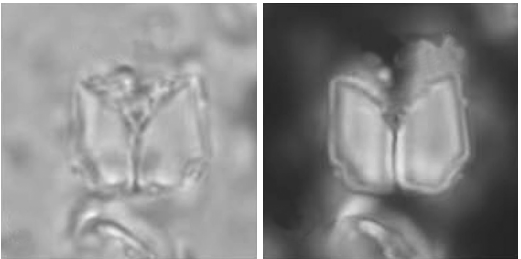
AC07/5

Gomphiolithus magnus (continued)



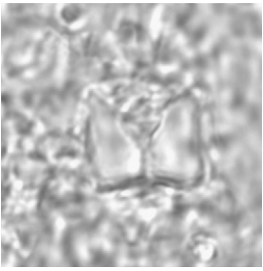
MS12/17

18

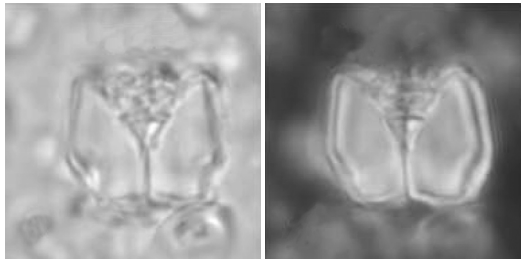


23

24

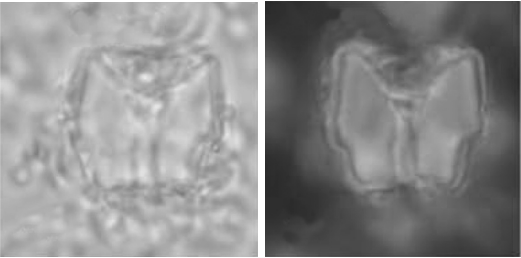


MS13/29



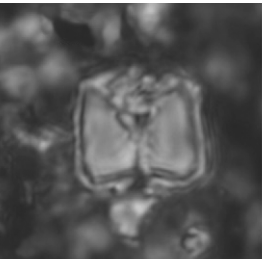
19

20

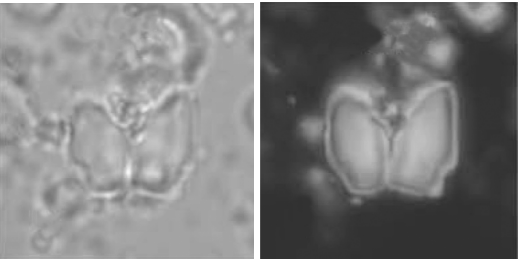


25

26

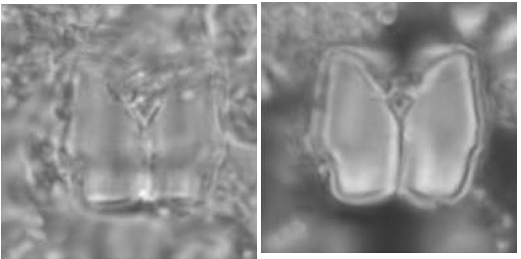


30



21

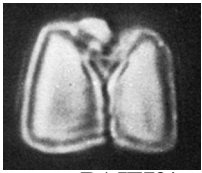
22



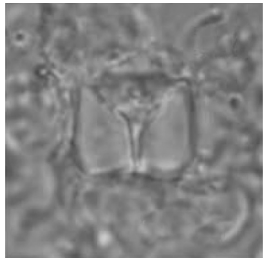
27

28

Gomphiolithus magnicordis (continued)



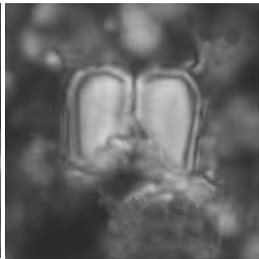
RAJT79/41



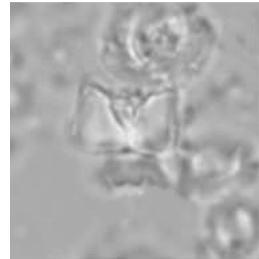
MS12/42



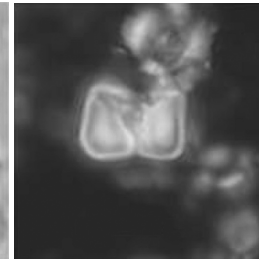
43



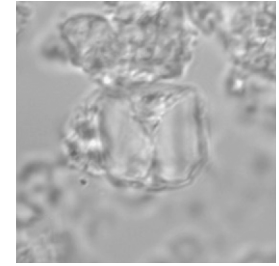
44



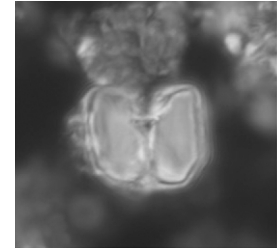
45



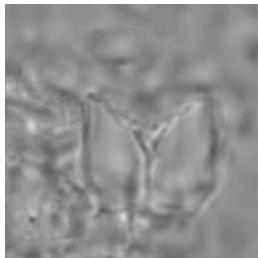
46



MS13/55



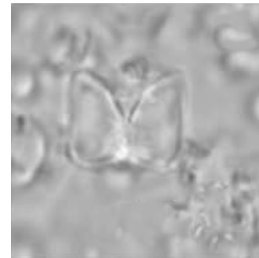
56



47



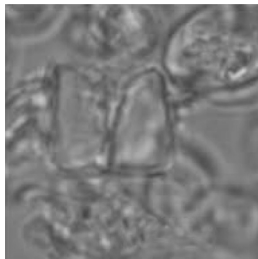
48



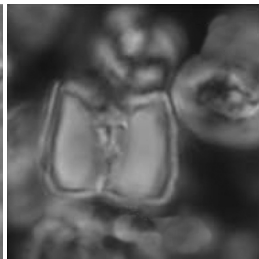
51



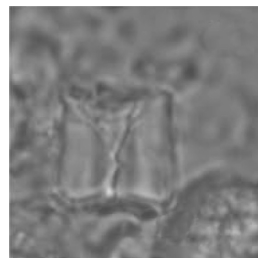
52



49



50



53



54

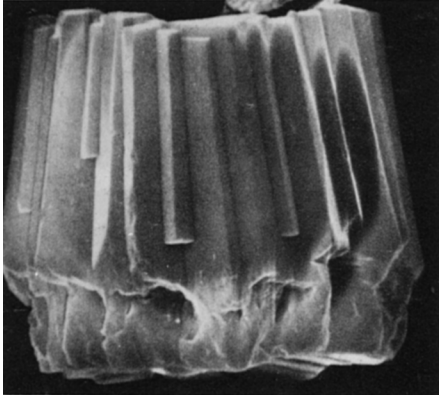


SE08/57

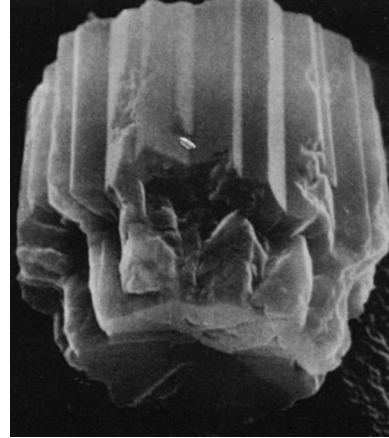
Gompholithus magnus (continued)

SIDE VIEW

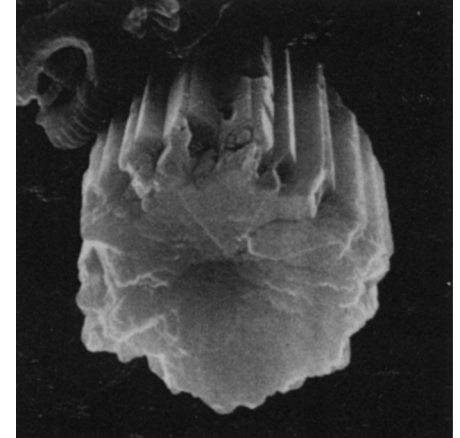
PROXIMAL FACE



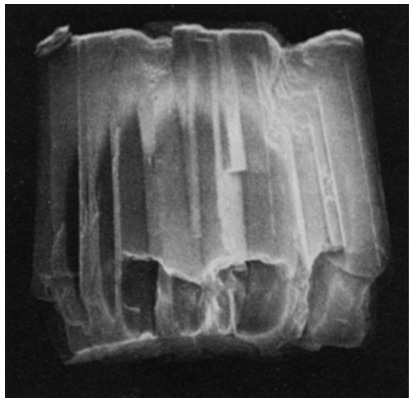
PNK77/31



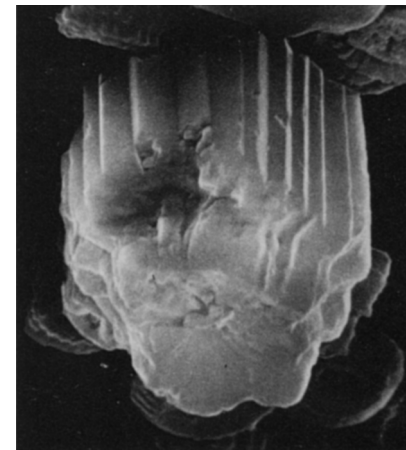
PNK77/33



34



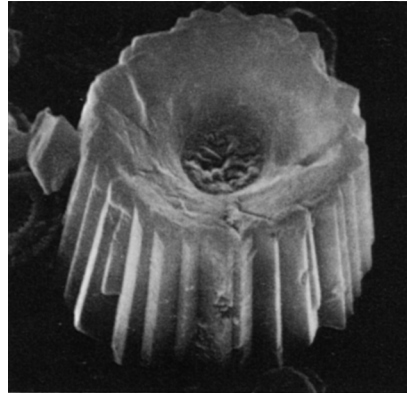
32



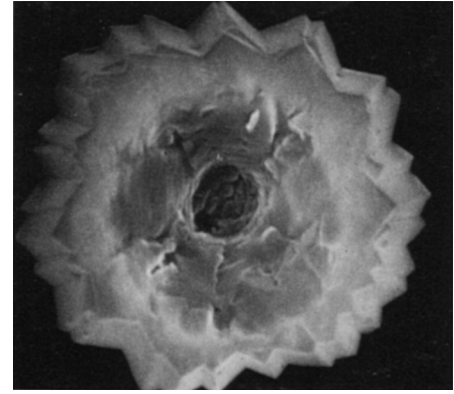
35

Gomphiolithus magnus (continued)

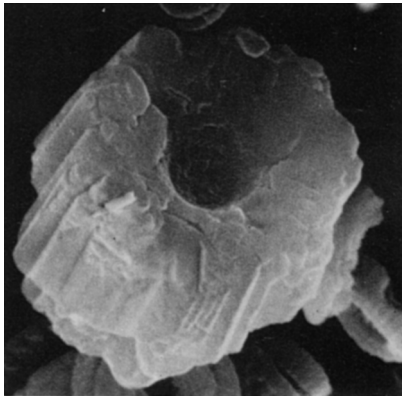
DISTAL FACE



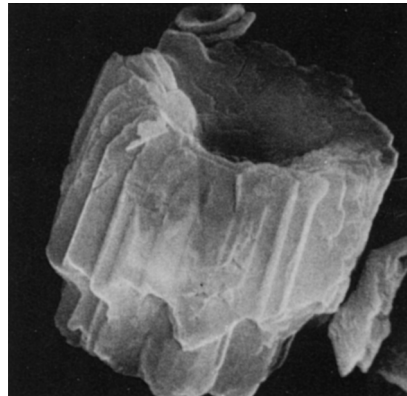
PNK77/36



37



38



39

Figure References

- AC07.** AGNINI, C., FORNACIARI, E., RAFFI, I., RIO, D., RÖHL, U. and WESTERHOLD, T., 2007. *Marine Micropaleontology*, 64: 215–248.
(5): 2/1 (as *Fasciculithus magnus*)
- AMP11.** AUBRY, M.–P., BORD, D. and RODRIGUEZ, O., 2011. *Micropaleontology*, 57: 269–287.
- AMP.** AUBRY, M.–P., this volume.
- BD71.** BUKRY, D. and PERCIVAL, S. F., 1971. *Tulane Studies in Geology and Paleontology*, 8: 123–146.
(1-4): 4/9, 12, 11, 10 (as *F. magnus*)
- MS12.** MONECHI, S., REALE, V., BERNAOLA, G. and BALESTRA, B., 2012. *Micropaleontology*, 58: 351–365.
(17-28): 1/2, 1, 4, 3, 6, 5, 8, 7, 10, 9, 12, 11 (*G. magnus*)
(42-54): 1/15, 14, 13, 21, 20, 17, 16, 19, 18, 23, 22, 25, 24 (*G. magnicordis*)
- MS13.** MONECHI, S., REALE, V., BERNAOLA, G. AND BALESTRA, B., 2013. *Marine Micropaleontology*, 98: 28–40.
(29, 30): 1/7, 6 (*G. magnus*)
(55, 56): 1/10, 5 (*G. magnicordis*)
- PNK77.** PERCH–NIELSEN, K., 1977. In: Supko, P. R., Perch–Nielsen, K., et al., *Initial Reports of the Deep Sea Drilling Project*, 39, 699–823. Washington, D. C.: U.S. Government Printing Office.
(6-8): 49/10, 16, 22 (as *F. magnus*)
(31-35): 11/9, 8, 11, 12, 10 (as *F. magnus*)
(36-39): 11/5, 6, 4, 7 (as *F. magnus*)
- RAJT79.** ROMEIN, A. J. T., 1979. *Utrecht Micropaleontological Bulletins*, 22: 1–231.
(9): 9/14 (as *F. magnus*)
(40, 41): 9/12, 13 (as *F. magnicordis*)
- SE08.** STEURBAUT, E. and SZTRÁKOS, K., 2008. *Marine Micropaleontology*, 67: 1–29.
(10-16): 2/7-9, 10a, b, 11, 12 (as *F. magnus*)
(57): 2/13 (as *F. magnicordis*)

LITHOPTYCHIUS

HIGHLIGHTS

- Fasciculiths consisting, characteristically, of four structural units: column, calyptra, collaret and central body.
- 12 described species, four species in open nomenclature.
- Size range: 3.5–12 μm in width; 3.5–10 μm in height.
- Most fasciculiths are convex distally, with a large central perforation.
- Coccusphere unknown.
- Stratigraphic Range: uppermost Danian (upper Zone NP4) – lower Thanetian (? lower Zone NP7).
- FAD of genus tied to the Chron C27n, at ~ 61.1 Ma.
- LAD probably in Chron C25r, at ~ 56.92 Ma.
- ~ 4 Myr life span.
- Burst of diversification in latest Chron C27n and early Chron C26r.
- Evolved from *Biantholithus sparsus*.

SELECTED READING

Aubry et al., 2011; Aubry et al., 2012; Monechi et al., 2013; Varol 1989.

INTRODUCTION

Lithoptychius was introduced for fasciculiths that have traditionally been assigned to *Fasciculithus*, but differ in possessing a collaret between the column and calyptra. The etymology of their name (from Gr. *lithos*, stone; Gr. *ptychos*, f., fold, leaf, layer) accounts for the presence of this additional structural unit.

This short-lived genus radiated in the latest Early Paleocene (latest Danian) and is mostly restricted to the Middle Paleocene (Selandian).

MORPHOLOGY AND STRUCTURE

The fasciculiths of *Lithoptychius* have a robust appearance, being about as broad as high (text-fig. 1). Their morphology is determined by the component structural units: 1) a cylindrical proximal column, more or less concave proximally, 2) a distal dome-shaped calyptra; 3) a thin cycle or collaret located between the column and calyptra; and 4) a triangular or diamond-shaped central body close to the distal end of the fasciculith and aligned with its central axis. Although easily distinguished in SEM photographs, the collaret is inconspicuous in several species examined under the light microscope, even in crossed-nicols. For those forms, it is practical to refer to the ‘cone’ formed by the collaret and calyptra.

Morphology

Column: In lateral view, the column may be parallel-sided, or it may widen, and eventually flare distally. It may also be constricted at mid height (text-fig. 2). With a few exceptions, it is higher than broad. The proximal surface may be flat, or slightly or deeply concave. The distal surface may be concave, flat or convex. In light microscopy, a canal is seen to run along the vertical axis. The width of the column is species dependent. It is distinctly larger in the

earlier species in which the canal broadens in proximal direction, so that the column then appears to be strongly concave proximally.

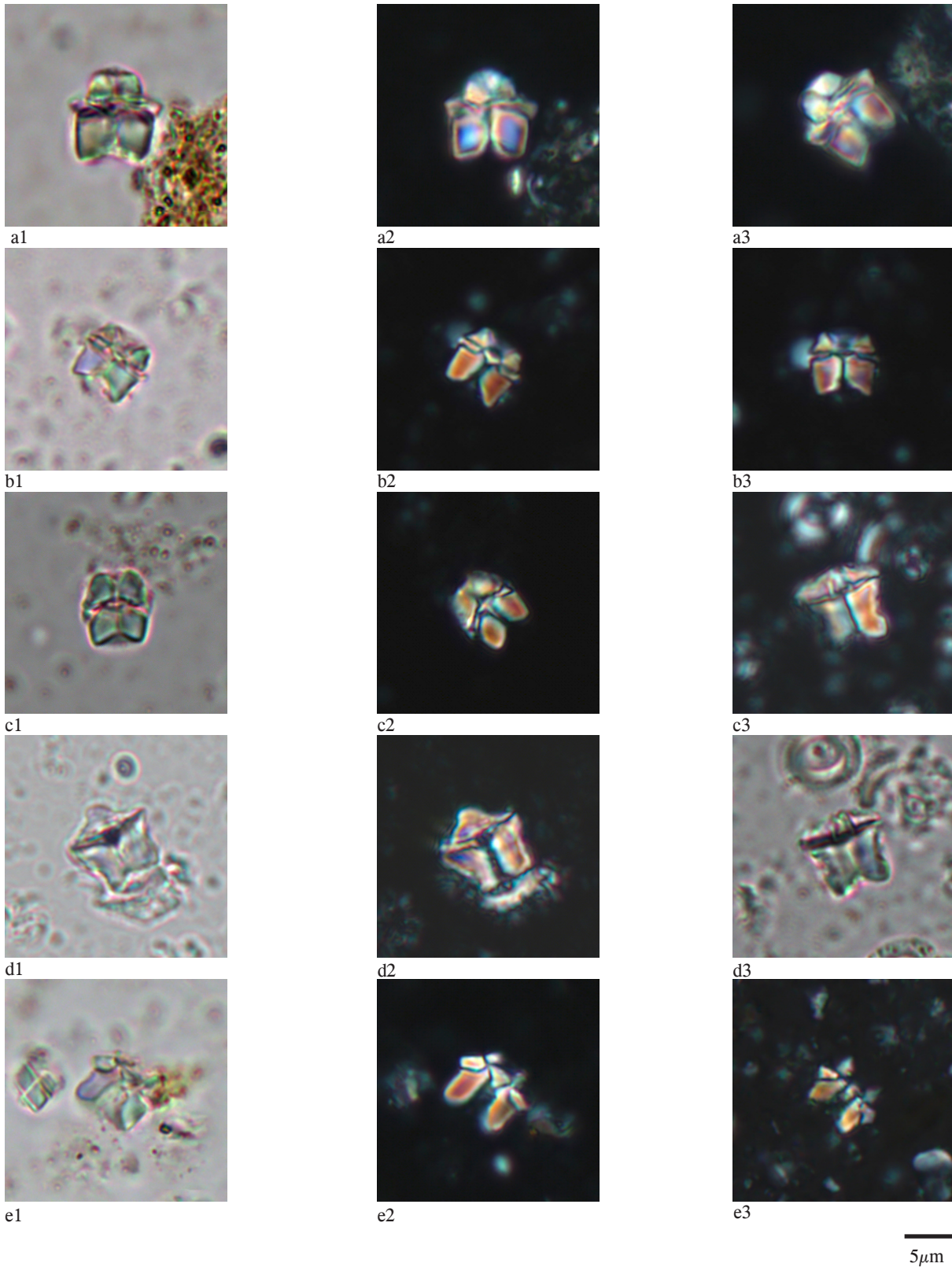
Collaret: This is a low cycle. Its shape differs considerably among species, partly as a function of the shape of the distal end of the column (text-fig. 2):

1) When the distal end of the column is flat or slightly convex, the collaret is a ring of even thickness (e.g., *L. varolii*).

2) When the distal end of the column is more strongly convex, the width of the collaret increases outwardly. In light microscopy, this produces the effect of two narrow isocetes triangles resting upon the column on each side of the central canal, their main axes lying perpendicular to it. The collaret may then be restricted to the width of the column (e.g., *L. merloti*), or it extends beyond it (e.g., *L. collaris*, *L. felis*).

3) When the distal end of the column is concave, the collaret may be entirely within the diameter of the column and barely extend above it (e.g., *L. ulii*, Perch-Nielsen, 1971a, pl. 2, fig.; Romein, 1979, pl. 4, fig. 7; Monechi, 1985, pl. 7, fig. 3). In other species, the collaret extends beyond the column laterally flaring into a cup shape (e.g., *L. jani*; Perch-Nielsen, 1971a, pl. 5, fig. 3; Romein, 1979, pl. 5, fig. 1). In the first case, the low collaret is almost indistinguishable from the column in light microscopy (e.g., *L. billii*, *L. pileatus*, *L. ulii*, *L. vertebratooides*). In the second case, the collaret appears as a marginal thickening of the column without clear sutural extinction lines in light microscopy (e.g., *L. jani*).

Calyptra: The calyptra may be massive (e.g., *L. collaris*, *L. varolii*; *L. bitectus*), delicate (*L. jani*) or tiny (*L. billii*) (text-fig. 2). It may be entirely contained within the circumference of the column (e.g., *L. pileatus*) or it may extend beyond it (e.g., *L. bitectus*). In all species a canal runs through the calyptra, with the distal end being a circular hole.



TEXT-FIGURE 1

Selected species of *Lithoptychius fasciculith*, showing general morphology and its relationship with structure. (Images and taxonomy from Aubry et al., 2011; Specimens are shown as oriented on stage for photography. Scale = 5µm; all specimens at same scale).

a1–a3: *Lithoptychius collaris* Aubry & Rodriguez.

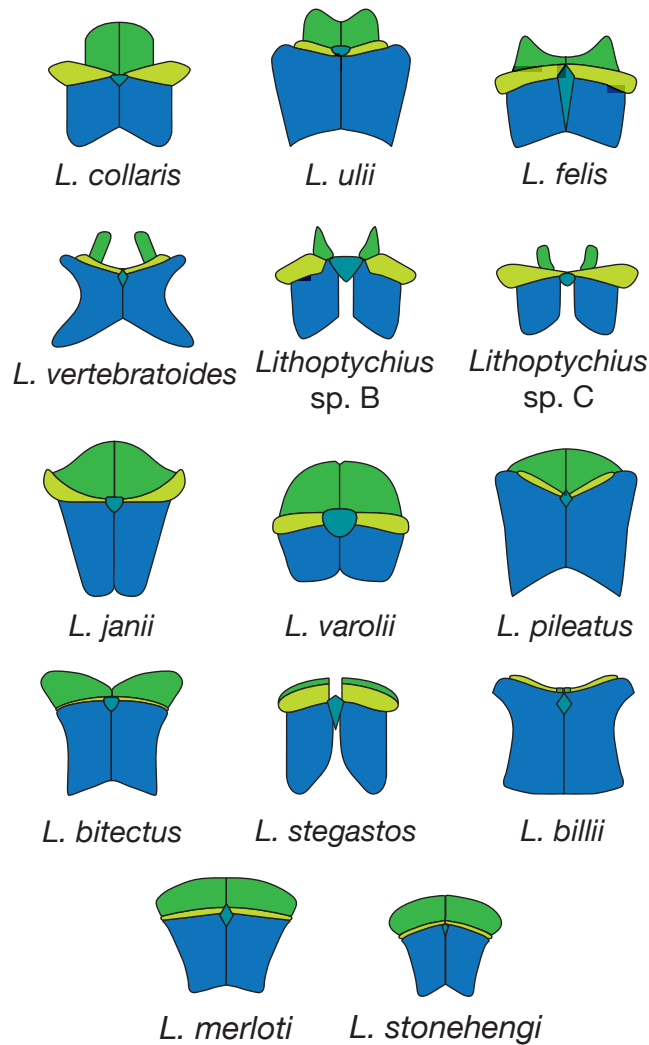
b1–b3: *Lithoptychius felis* Aubry & Bord.

c1, c2: *Lithoptychius varolii* (Steurbaut & Sztrákos) Aubry.

c3, d3: *Lithoptychius merloti* (Pavsic) Aubry.

d1, d2: *Lithoptychius janii* (Perch–Nielsen) Aubry.

e1–e3: *Lithoptychius* sp. A.



TEXT-FIGURE 2

Morphology and structural components of the fasciculiths of *Lithoptychius* species as seen in cross section.

Central body: The triangular or diamond-shaped central body lies at the distal end of the central canal, at the intersection between the calyptra, column and collaret (text-fig. 2). It always points distally when triangular; its two shorter sides are in distal position when diamond-shaped.

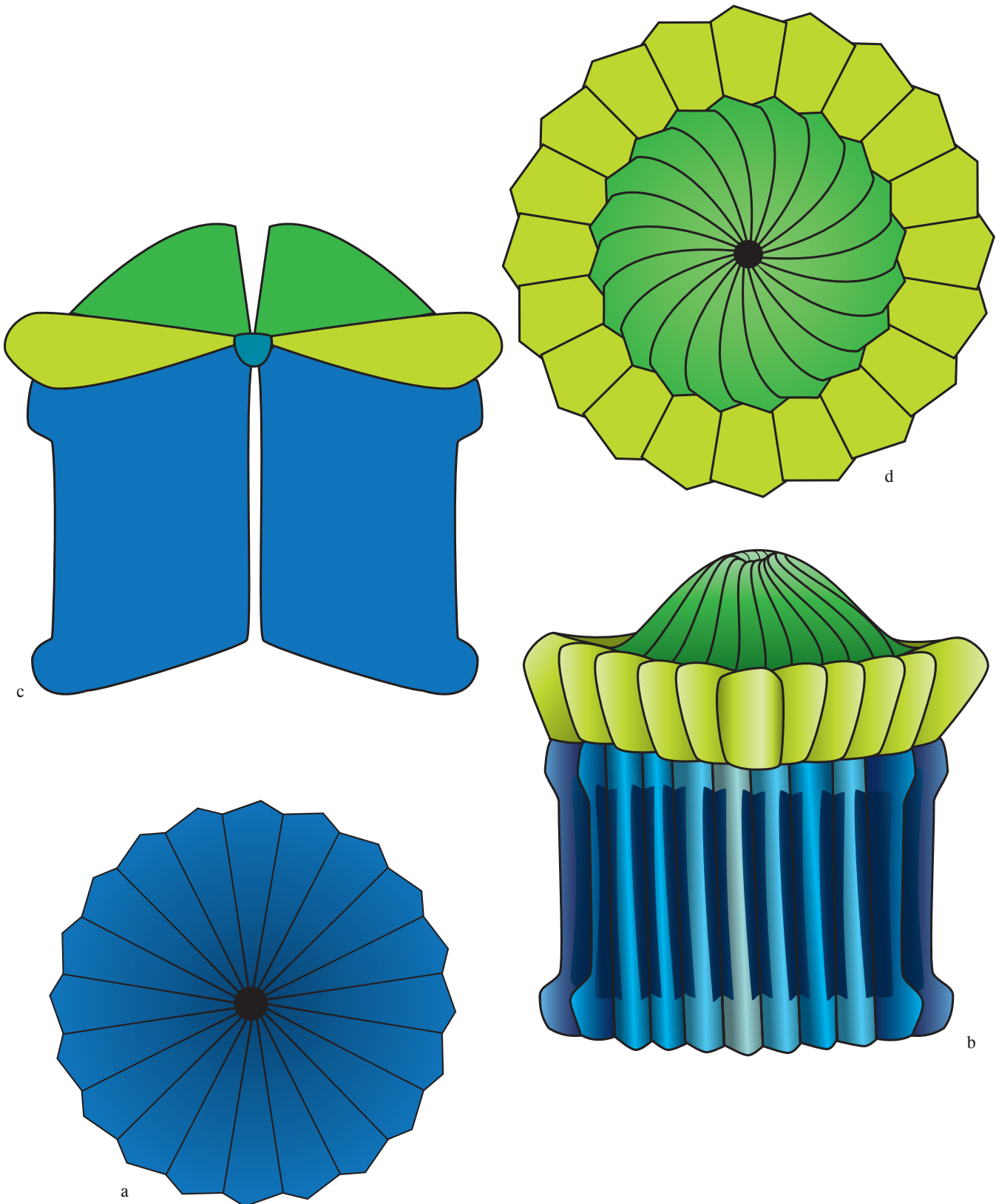
Structure – As stated above, the *Lithoptychius* fasciculiths are characteristically comprised of four structural units (text-figs. 3, 4).

Column: The column consists of 20 to 30 wedge-shaped elements arranged in radial fashion around the axial canal. On the proximal face, they are joined through most of their length and their sutures are radial (text-figs. 3a, 4a). In side view, their surface is often smooth with angular sides, indicative of strong recrystallization and alteration of the original aspect of the column. Less altered specimens (*L. ulii*: Perch-Nielsen, 1971a, pl. 2, figs. 1, 4; *L. billii*: Perch-Nielsen, 1971a, pl. 4, fig. 11, pl. 5, fig. 8) allow a glance into the original structure, in which the elements are delineated by long vertical depressions (or fenestrae) between them (text-figs. 3b, 4b). In some fasciculiths, the recrystallized column shows elements separated by tall vertical ridges that alternate with deep, narrow, vertical depressions (e.g., *F. ulii*, Monechi, 1985, pl. 7, fig. 3), in a pattern that suggests a complicated pattern of narrow vertical fenestrae.

Collaret: The collaret is a cycle of subquadrangular elements with sinistral imbrication and sutures oriented clockwise (as seen from the distal side of the cycle, text-figs. 3b, d, 4b, d; e.g., *L. janii*: Perch-Nielsen, 1971a, pl. 5, fig. 3; Perch-Nielsen, 1977, pl. 12, fig. 2; Romein, 1979, pl. 5, fig. 1). Sutures with the column and with the calyptra delineate it clearly and consistently, its elements being oriented opposite to those in the other two cycles.

Romein (1979, p. 77) first identified the collaret in *L. bitectus* (Romein), naming it “median cycle”. He considered it homologous with the “upper slice” observed by him in *L. ulii* and *L. janii* (and also *Gomphiolithus magnus*).

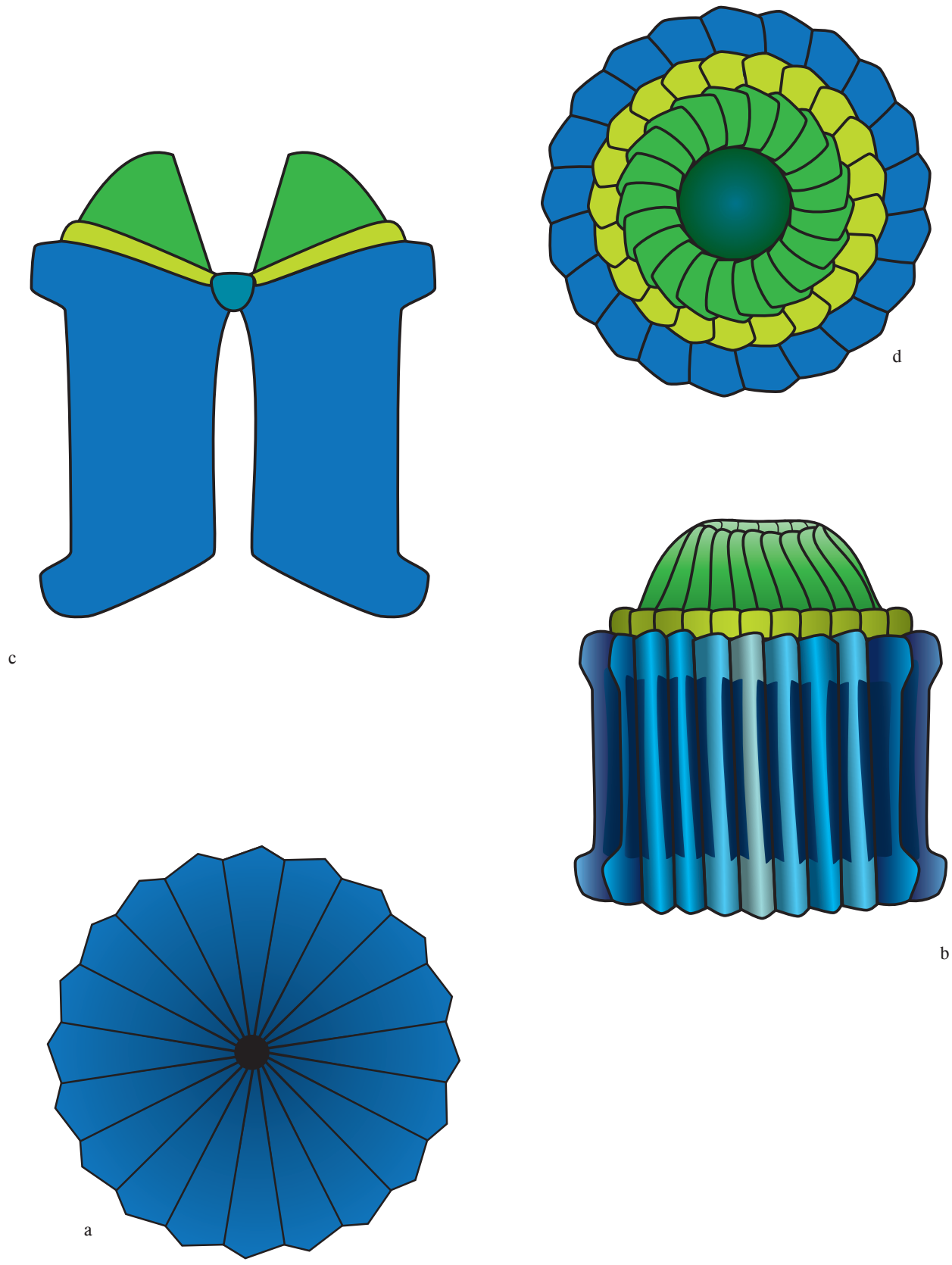
Calyptra: The calyptra consists of elongate elements with dextral imbrication (text-figs. 3d, 4d). In many species the elements are oblique to the vertical axis of the fasciculith (e.g., *L. janii*: Perch-Nielsen, 1977, pl. 12, fig. 16; Romein, 1979, pl. 5, fig. 1). In this disposition the calyptra caps the column and collaret, and may be as broad as them (e.g., *L. pileatus*), narrower (e.g., *L. janii*) or larger (e.g., *L. bitectus*). In other species, the elements are subparallel to the long axis of the fasciculith, i.e., almost perpendicular to the distal face of the column/collaret (e.g., *L. ulii*: Perch-Nielsen, 1971a, pl. 2, figs. 2, 3). In axial views of such species in light microscopy the calyptra appears in the form of two tooth-like projections, one



TEXT-FIGURE 3
 Structure of a *Lithoptychus fasciculith* with a flaring collaret.

- a: proximal face.
- b: side view.
- c: cross-section.
- d: distal view.

It is not clear whether each depression occurs along the central axis of each element or whether it is formed by the depressed sides of two adjacent elements. In the former case the sutures between the elements occur along the ridges. In the latter case a ridge runs vertically in the middle of each elements in a case of convergence with the keeled triades of the sphenoliths (see Order Discoasterales, CC-B).



TEXT-FIGURE 4
Structure of a *Lithoptychus* fasciculith with a small collaret.
 a: proximal face.
 b: side view.
 c: cross-section.
 d: distal view.



TEXT-FIGURE 5
Color patterns in standard orientation for side view in *Lithoptychius bitectus*. (After Romein, 1979, text-fig. 41).

on either side of the axial canal (e.g. *L. ulii*, *L. vertebratoides*) (compare text-figs. 3b, c and 4b, c).

Romein (1979) referred to the calyptra as the “dome” or the “cone” (note that *cone* is used here when the calyptra and collaret are difficult to distinguish from one another in the LM, see above).

Central body: Lying deep in the concavity of the calyptra (text-figs. 3c, 4c), the central body is rarely visible in SEM photographs. The distal surface of the central body is visible in a specimen of *L. ulii* illustrated by Perch-Nielsen (1977, pl. 11, fig. 3). Its granular texture likely results from the overgrowth of an originally porous texture.

Extinction patterns

The four structural components of the *Lithoptychius* fasciculiths are conspicuous in light microscopy, particularly in cross-polarized light where they are strongly birefringent and clearly delineated by extinction lines in which the collaret can be seen between the calyptra and the column as a discrete, low cycle.

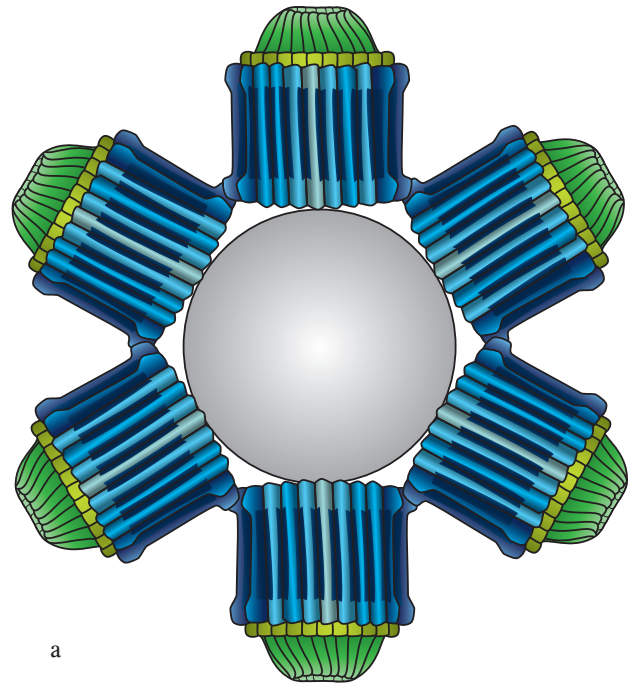
The standard orientations established by Romein (1979, p. 148) for fasciculiths are followed here. In the standard orientation for distal view, the calyptra points upwards and the concave side of the column faces downwards. In this view, the extinction cross is formed by two orthogonal straight lines intersecting at the center of the fasciculith, as in *Sphenolithus* (see CC-B, Genus *Sphenolithus*). In the standard orientation for side view, the calyptra points in the positive direction of the Y-cross-hair, the proximal edge of the column being parallel to the X-cross-hair. In this orientation, the fasciculiths are bisected by a straight median longitudinal line. In addition, the column/collaret and collaret/calyptra contacts are highlighted black. The central body is generally extinct when the axis of the fasciculith is oriented parallel to either polarizer or analyzer, but is highly birefringent and delineated by a black line when oriented at 45°. It is also highly refringent.

The extinction and color patterns in standard orientations with the addition of a gypsum plate was illustrated by Romein (1979, p. 148) for *Lithoptychius bitectus* (text-fig. 5).

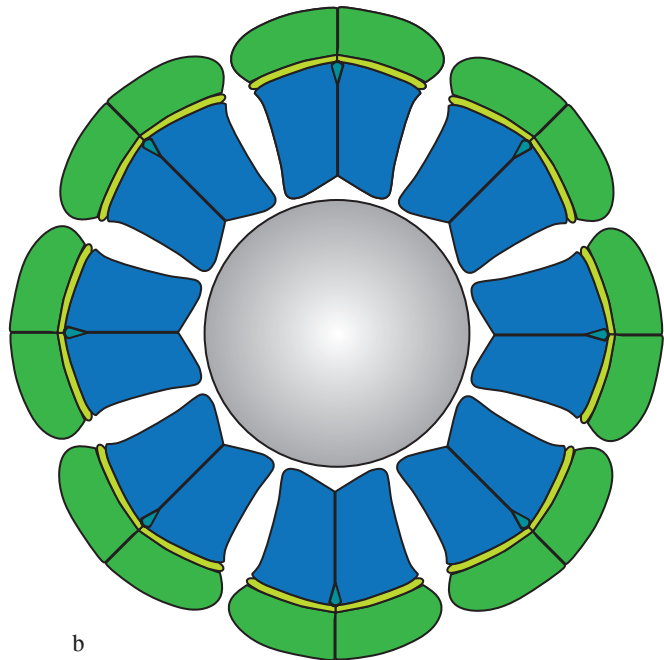
BIOLOGY, PHYSIOLOGY AND ECOLOGY

Biology

The coccosphere of *Lithoptychius* is unknown. It is tentatively reconstructed here as consisting of juxtaposed fasciculiths radiat-



a

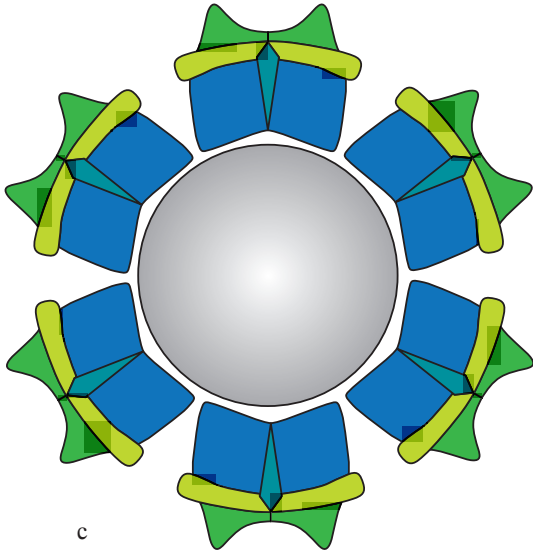


b

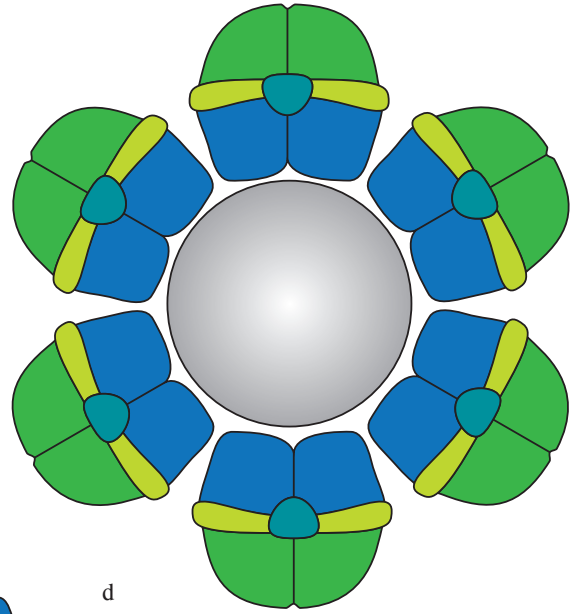
TEXT-FIGURE 6
Tentative reconstruction of a coccosphere as seen in cross section. Cell seen in cross section. Fasciculiths in side view (a) and in cross section (b-g).

- a: *Lithoptychius* (*L. ulii*).
- b: *L. stonehengii*.
- c: *L. felis*.
- d: *L. varolii*.
- e: *L. billii*.
- f: *L. janii*.
- g: *L. collaris*.

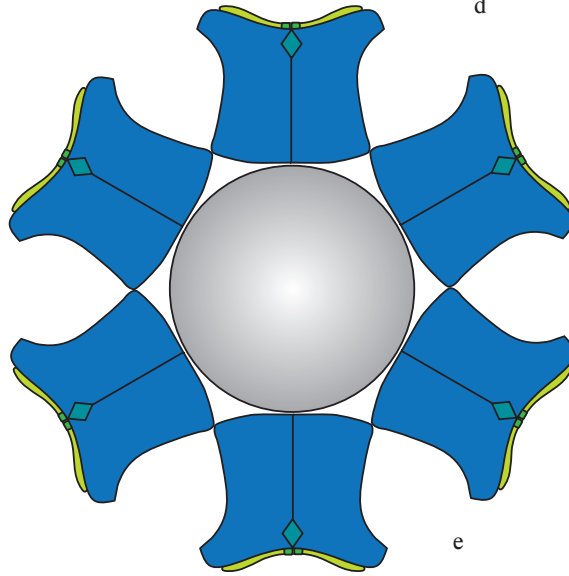
The cells are arbitrarily shown as of the same size. However, cell size was likely different in different species at different times. The coccoliths would appear to have been massive from these drawings, in fact, they were most likely very delicate and light.



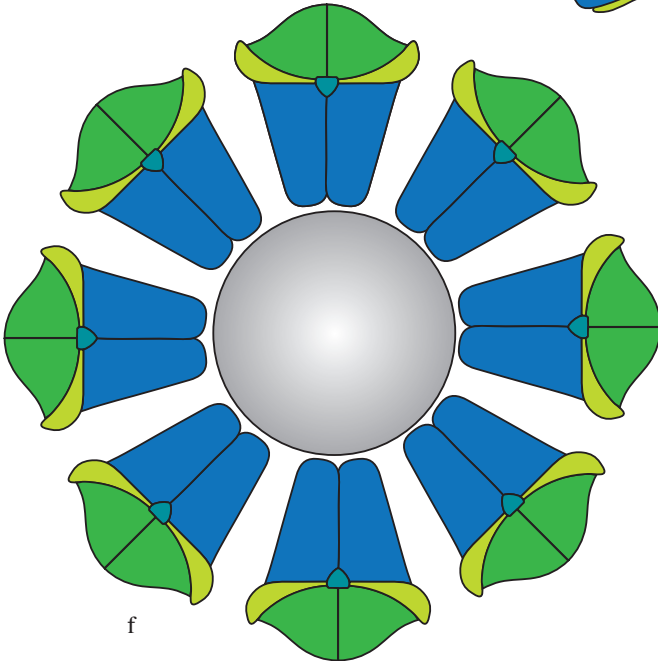
c



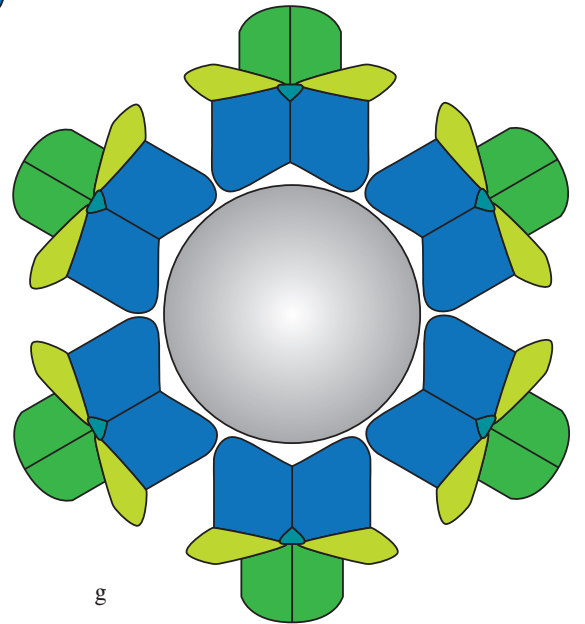
d



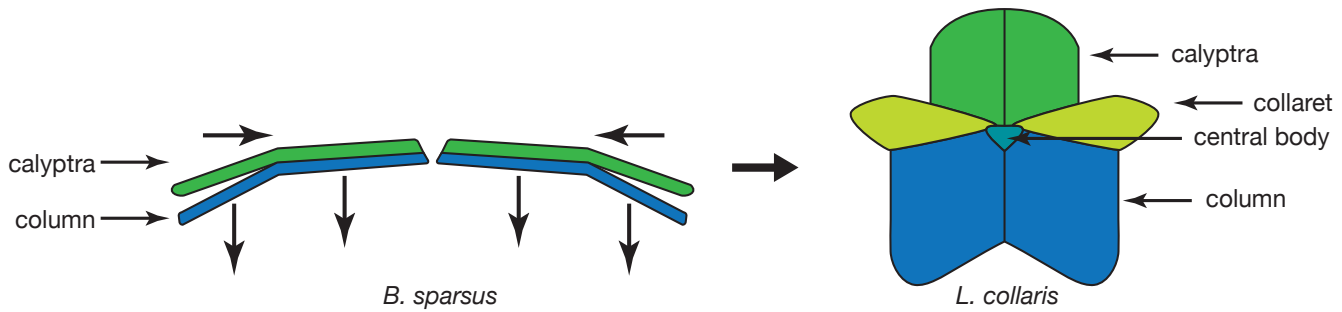
e



f



g



TEXT-FIGURE 7

Derivation of a fasciculith of *Lithoptychius* from a biantholith of *Biantholithus*. The column and calyptra of *Lithoptychius* would have easily resulted from the proximal and distal expansion of the column and calyptra of *Biantholithus*. The collaret and the central body are *de novo* structural units. If *Lithoptychius* evolved from *Biantholithus* and not from *Gomphiolithus*, the central body represents convergent evolution. It is also possible that *Lithoptychius* and *Gomphiolithus* evolved independently from an unidentified ancestor intermediate between them and *Biantholithus*, which possessed a central body.

ing around the cell (text-fig. 6). Even if the fasciculiths during life were delicate and not as massive as their fossils would indicate, their shape was not hydrodynamic. It may be inferred from this, and from the coccosphere of the ancestral *Biantholithus sparsus*, that the heterococcolith-stage was non-motile.

Physiology

The canal running along the vertical axis of the fasciculith would have permitted water, nutrient and gas exchanges between the cell and the environment. As in *Gomphiolithus*, the central body may have acted as a means to control these exchanges.

Aubry et al. (2012) observed that the derivation of *Lithoptychius* fasciculiths from *B. sparsus* involved a considerable increase in surface area, which would have facilitated mixotrophic physiology in a nascent oligotrophic ocean. The description of the column, herein, as being comprised of tall but fluted elements with a U-shaped transversal section, resulting in a pattern of vertical fenestrae around the fasciculiths (text-figs. 3b, 4b) concurs with this interpretation. Food particles and bacteria could have been easily trapped in the fenestrae.

Ecology

Lithoptychius fasciculiths are common at low latitudes.

Fasciculithus chowii (probably *L. collaris*) was reported from the North Sea area where it was exceedingly rare in the late Subchron NNTp7B together with *Ellipsolithus macellus* and *Sphenolithus primus* (Varol, 1989, figs. 12-14).

Fuqua et al. (2008, p. 192) have determined that *Lithoptychius* species were adapted to oligotrophic environments.

EVOLUTIONARY HISTORY

Origin

Interpreted as a fasciculith, *Diantholitha* has been proposed as the ancestor of *Lithoptychius* as part of a *Gomphiolithus-Diantholitha-Lithoptychius* lineage (Monechi et al., 2013, p. 33, fig. 6; see CC-B, Order Discoasterales). This lineage is actually highly improbable, and a derivation of the *Lithoptychius* fasciculith directly from a biantholith is most likely—although not from *Diantholitha*, whose

Biostratigraphic horizons	Varol 1989	Marti 1971
⊥ <i>H. riedelii</i> ⊥ <i>H. dreverli</i>	NTp13	NP8
	NTp12	
⊥ <i>F. billii</i> ⊥ <i>F. ulii</i>		NP7
	NTp11B	
⊥ <i>H. mohleri</i> ⊥ <i>S. anarthropus</i>		
	NTp11A	NTp11
⊥ <i>L. pileatus</i> ⊥ <i>L. jani</i>		NP6
	NTp10c	NTp10
⊥ <i>H. kleinpellii</i>		
	NTp9	NTp9
⊥ <i>N. neocrassus</i> ⊥ <i>F. tympaniformis</i>		NP5
	NTp8C	
⊥ <i>L. pileatus</i> ⊥ <i>L. jani</i>		
	NTp8B	NTp8
⊥ <i>L. billii</i> ⊥ <i>L. ulii</i>		NP4
	NTp8A	
⊥ <i>S. primus</i> ⊥ <i>T. chowii</i>		
	NTp7B	NTp7 NTp5c
⊥ <i>E. macellus</i>		
	NTp5B	NTp5b
		NP3

TEXT-FIGURE 8

***Lithoptychius* species as biozonal markers.** Varol (1989) introduced a Paleocene zonation for low latitudes in which the LOs and HOs of several *Lithoptychius* species are used to define zonal and subzonal boundaries (red lines). Correlation with Martini's zonal scheme (1971) is shown for reference.

Kokaksu Section	Loubieng Section	ODP site 1262 ¹	ODP site 1262 ²	Zumaia	Oreiya
\top { <i>L. billii</i> <i>L. ulii</i> }					
\top { <i>L. pileatus</i> <i>L. janii</i> }			\top <i>L. vertebratooides</i>		
	\perp <i>L. pileatus</i>		\perp <i>L. pileatus</i> ²		
	\perp <i>L. ulii</i>		\perp <i>L. janii</i> ²	\perp <i>L. janii</i>	
\perp { <i>L. janii</i> <i>L. pileatus</i> }	\perp { <i>L. janii</i> <i>L. billii</i> }	\perp <i>L. billii</i>	\perp { <i>L. billii</i> <i>L. vertebratooides</i> }	\perp <i>L. billii</i>	\perp { <i>L. billii</i> <i>L. pileatus</i> }
			\perp <i>L. pileatus</i> ¹		\perp <i>L. janii</i>
		\perp { <i>L. ulii</i> <i>L. pileatus</i> }	\perp <i>L. janii</i> ^a	\perp { <i>L. ulii</i> <i>L. pileatus</i> }	\perp <i>L. ulii</i>
\perp { <i>L. billii</i> <i>L. ulii</i> }			\perp <i>L. ulii</i>		\perp <i>L. ulii</i>
\top <i>T. chowii</i>	\perp <i>L. vertebratooides</i>			\top { <i>L. chowii</i> <i>L. varolii</i> }	\perp <i>L. schmitzii</i>
			\perp <i>L. schmitzii</i>	\perp <i>L. schmitzii</i>	
	\top { <i>L. varolii</i> <i>L. chowii</i> }		\perp { <i>L. chowii</i> <i>L. varolii</i> }	\perp { <i>L. chowii</i> <i>L. varolii</i> }	\perp { <i>L. chowii</i> <i>L. varolii</i> }

TABLE 1

Compared locations of the LOs of selected *Lithoptychius* species in three sections.

Kokaksu Section, Turkey: Varol (1989).

Loubieng Quarry at Pont Labau: Steurbaut and Sztrákos (2008).

South Atlantic ODP Site 1262: (1) Agnini et al. (2007); (2) Monechi et al. (2013).

Zumaia, Spain: Monechi et al. (2013).

Qreiya, Egypt: Monechi et al. (2013).

(a): LRO [lower rare occurrence] as indicated by authors.

calyptra is too specialized (having differentiated, partly trihedral elements) to have given rise to the morphologically simpler calyptra of *Lithoptychius*.

A more attractive ancestor is *Biantholithus* (Aubry et al., 2012; text-fig. 7). The structure of the calyptra of *B. sparsus* is strikingly comparable to that of *Lithoptychius* species (compare Romein, 1979, pl. 1, fig. 9, with Monechi, 1985, pl. 7, fig. 4). The two differ only by the greater number of elements in the latter. The column of the biantholith could have evolved into the column of *Lithoptychius* simply through thickening. The collaret is an innovation characteristic of *Lithoptychius*, that may have developed from distal migration of the tiny proximal cycle sometimes seen in *Biantholithus*.

Phylogeny

The appearance of *L. collaris*, the oldest species of the genus as illustrated in the Qreiya section of Egypt (Aubry et al., 2012, fig. 3), was closely followed by the simultaneous appearances of a minimum of four additional species (*L. felis*, *L. stegastos*, *L. varolii*, and *Lithoptychius* sp. A). This radiation has been illustrated in localities around the Tethys area (Kokaksu section, Turkey [Varol, 1989]; Tunisia [Van Itterbeek et al., 2007]; Loubieng, Aquitaine Basin, France [Steurbaud and Sztrákos, 2008]; Zumaia, Spain [Bernaola et al., 2009; Monechi et al., 2013]; Blaja, Bulgaria [Dinarès-Turell et al., 2010]; Gebel Duwi and Gebel Hamada, Egypt [Farouk and Faris, 2013]) as well as at South Atlantic Site 1262 (Monechi et al., 2013). Monechi et al. have attributed *Lithoptychius* species to two lineages, with *L. varolii* and *L. chowii* as stem species. It is impor-

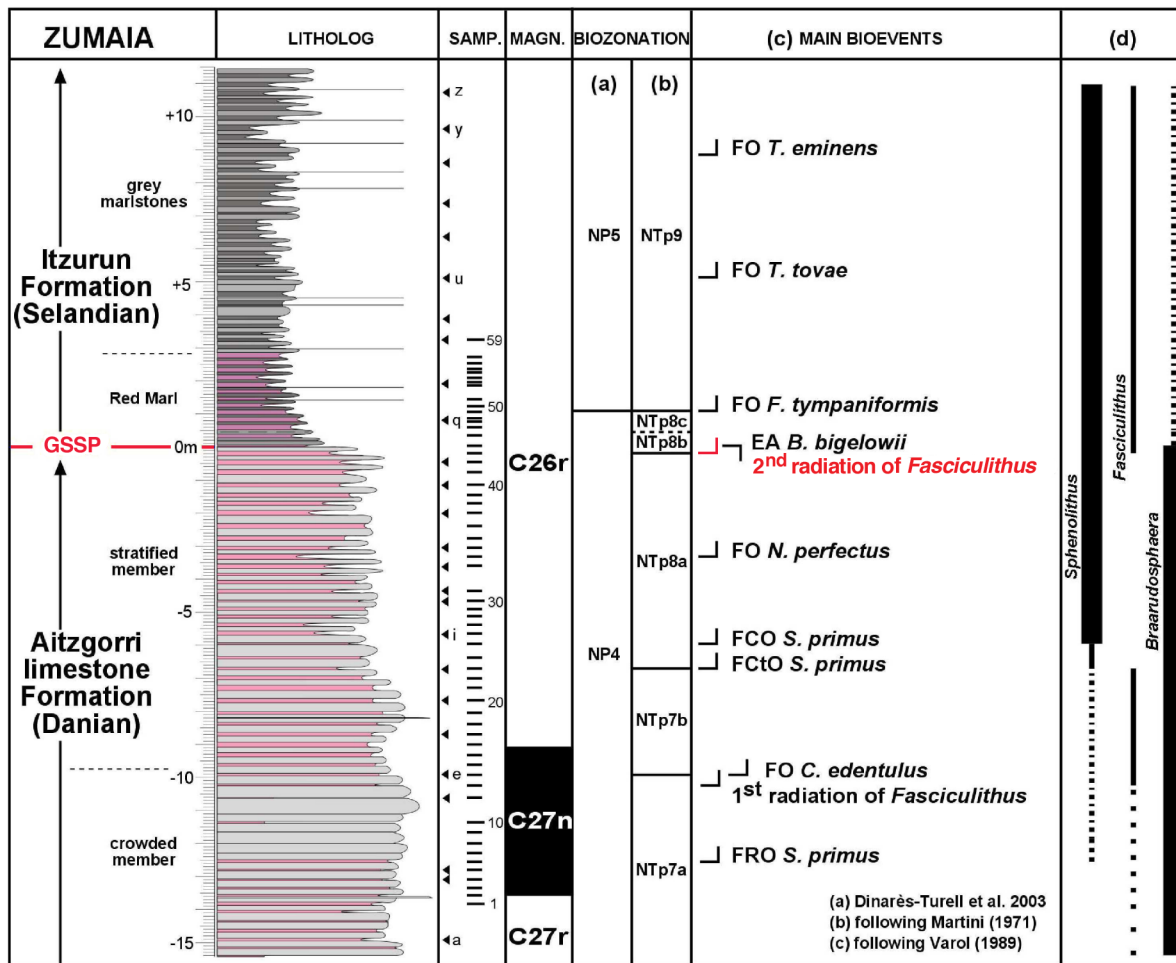
tant to recognize that *L. chowii* is a superficial taxon that encompasses several species of *Lithoptychius* (see below). Considering the enormous potential for diversification conferred to *Lithoptychius* by the presence of four structural units, it would be preferable to refrain from attempting its phylogenetic history until the taxonomy and stratigraphy of its species have been comprehensively documented.

Although the life span of *Lithoptychius* was short (~4 Myr), a marked morphologic trend occurs, in which the oldest species (e.g., *L. collaris*, *L. varolii*, *L. felis*, *L. schmitzii*) have a prominent collaret (as well as a thick, hemispherical calyptra) in contrast to the younger species (e.g., *L. ulii*, *L. billii*) in which the collaret is considerably subdued.

Diversity

The early range of *Lithoptychius* is marked by great morphologic diversity that is difficult to unravel at the species level (Aubry et al., 2012). Species were better individualized in late Chron C26r, and were fewer.

Monechi et al. (2013) have reported on a “*fasciculithus* paracme” of global extent beginning shortly after the evolutionary appearance of *L. schmitzii* and ending with the FAD of *L. ulii*, and during which coccolith assemblages are deprived of *Lithoptychius* fasciculiths. In the Zumaia and Qreiya sections, the “*fasciculithus* paracme” corresponds to a loss of diversity over a short stratigraphic interval due to dissolution (Criscione et al., unpublished).



TEXT-FIGURE 9

GSSP for the base of the Selandian Stage and Middle Paleocene Subseries at Zumaya and the so-called “second radiation of the fasciculiths” (including the LO of *Lithoptychius ulii*). (Modified from Schmitz et al., 2011, fig. 13.) FCTO: first continuous occurrence; FCO: first common occurrence EA: end acme; FRO: first rare occurrence.

STRATIGRAPHY

Biostratigraphy

Romein (1979) restricted the stratigraphic range of fasciculiths now assigned to *Lithoptychius* to (upper) Zone NP4 and Zone NP5. According to the zonal framework of Varol (1989), this range encompasses from the upper part of Zone NP4 to Zone NP7 (where the LADs of *L. billii* and *L. ulii* lie).

Varol (1989) made ample use of *Lithoptychius* species (then assigned to *Fasciculithus*) in his “nannofossil, Tertiary-Palaeocene” (NTp) zonation (text-fig. 8). The HO of *L. chowii* (possibly *L. collaris*) near the LO of *Sphenolithus primus* marks the top of Zone NTp7 (“*Fasciculithus chowii*” Zone) and Subzone NTp7B (*Chiasmolithus edentulus* Subzone). The LOs of *L. ulii* and *L. billii*, and those of *L. pileatus* and *L. jani* mark the base of, respectively, Zone NTp8B and Zone NTp8C (equivalent to the top of Martini’s Zone NP4). The HOs of *L. pileatus* and *L. jani* mark the top of Zone NTp10 and Subzone NTp10C (within Zone NP6). The HOs of *L. billii* and *L. ulii* mark the top of Zone NTp11 and Subzone NTp11B in Zone NP7.

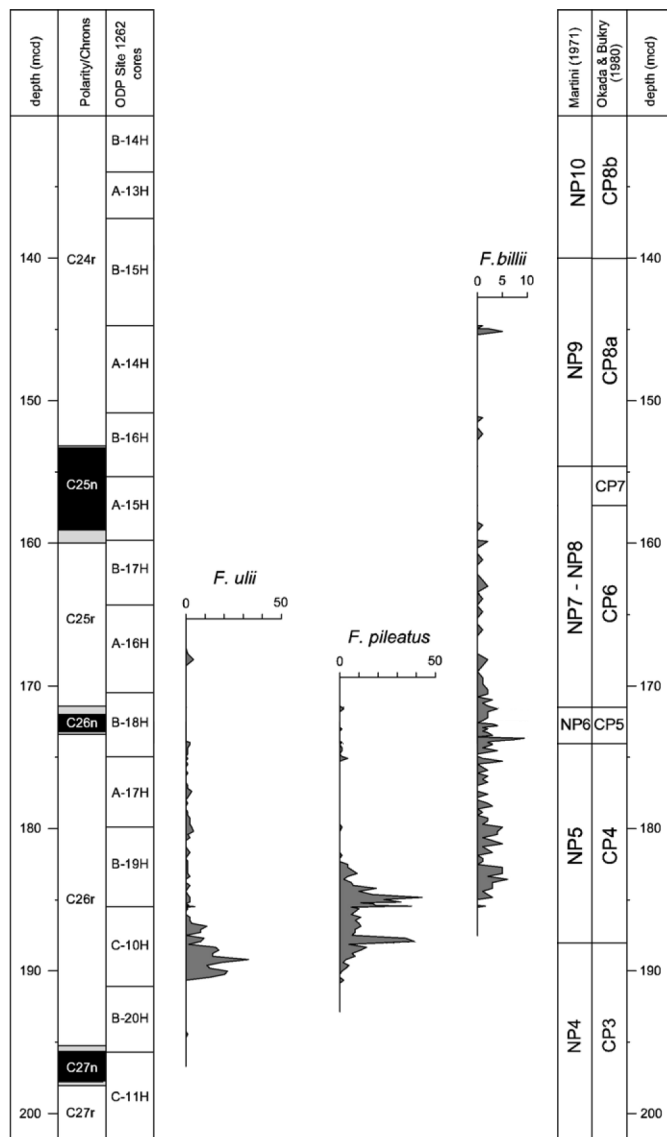
The reliability of Varol’s zonation for long distance correlation is questionable. This is because the stratigraphic ranges of most *Lithoptychius* species are still imprecisely known, owing in large

part to differences in taxonomic concepts among authors. For instance, a species as critical as *L. jani* is rarely identified following the concept intended by its author; likewise *L. ulii* is very difficult to determine consistently. Discrepancies in stratigraphic assignment by different authors are common with regard to several species (table 1). For instance, Steurbaut and Sztrákos (2008, p. 9; table 1) recorded the sequential LOs of *L. vertebratoides*, *L. billii* together with *L. jani*, *L. ulii*, and *L. pileatus* above the simultaneous LOs of *L. varolii* and *L. chowii* in the Loubieng section. In contrast, Varol (1989, fig. 12.4) indicated that the LOs of *L. ulii* and *L. billii* are simultaneous and older than the LOs of *L. pileatus* and *L. jani* (table 1). In turn, Agnini et al (2007, fig. 6; table 1) established that the LO of *F. billii* is >5.6 m above that of *L. ulii* at ODP Site 1262, which is > 880 kyr younger.

Lithoptychius jani was described from Zone NP5. Steurbaut and Sztrákos (2002) confirmed Varol’s determination of its HO in Zone NP6, but their determination of the species is questionable. The report of *L. stonehengii* from Zone NP9 (Haq and Aubry, 1980) may indicate reworking.

Chronostratigraphy

The LO of *L. ulii* s.s. is the primary criterion for correlation of the base of the Selandian Stage, as defined in the base of the Itzurun Formation at the stratotype section of Zumaia (Schmitz et al.,



TEXT-FIGURE 10
Abundance patterns of *Lithoptychius* species at ODP Site 1262.
 (Modified from Agnini et al., 2007, fig. 5.) Core description from Zachos et al. (2004); Magnetostratigraphy from Bowles, 2006.

2011, p. 237; text-fig. 9). This biohorizon is recorded in the uppermost Danian, slightly below the lithological boundary between the Aitzgorri Limestone Formation and the Itzurun Formation. It is used to characterize an event which, for stratigraphic purpose, has been dubbed the second radiation of *Fasciculithus* (a misnomer) and the second radiation of the fasciculiths (Bernaola et al., 2009; see Order Discoasterales, this volume).

Biochronology

The stratigraphic appearance of the genus *Lithoptychius* is consistently tied to the Chron C27n/C26r reversal at Bjala (Bulgaria; Dinarès-Turell et al., 2010, fig. 10), Zumaia and at ODP Site 1262 (Monechi et al., 2013, figs. 2, 4). However, in the Zumaia section, rare to abundant *Lithoptychius* specimens occur in the upper part of the interval representing Chron C27n (Criscione, unpublished data). The extinction level of *Lithoptychius* is difficult to determine. Both

L. ulii and *L. billii*, which are the two youngest species of the genus (Varol, 1989), occur inconsistently and in low frequency in their upper range at ODP Site 1262 (Agnini et al., 2007, fig 5; text-fig. 10). There, the final, isolated abundance peak of *L. ulii* and the highest consistent occurrence (HCO) of *L. billii* at the same level may represent the NTp11B/NTp12 zonal boundary (in Zone NP7, in agreement with Varol, 1989); if so, the LAD of the genus would be tied to the early part of Chron C25r (~56.92 Ma). On the other hand, the scanty record of *L. billii* above its HCO and up to mid Chron C25n in the same hole, if not due to reworking or taxonomic inconsistencies would indicate that *Lithoptychius* became extinct in early Chron C24r, slightly before the PETM (text-fig. 10).

The FAD of *L. collaris* is dated at ~ 61.15 Ma (in reference to the magnetostratigraphy of Cande and Kent (1992, 1995), those of *L. felis*, *L. stegastos*, *L. varolii*, and *Lithoptychius* sp. A being only slightly younger than this date (text-fig. 11).

Based on Agnini et al. (2007) the FADs of *L. ulii* and *L. pileatus* are at 60.306 Ma and the FAD of *L. billii* at 59.426 Ma.

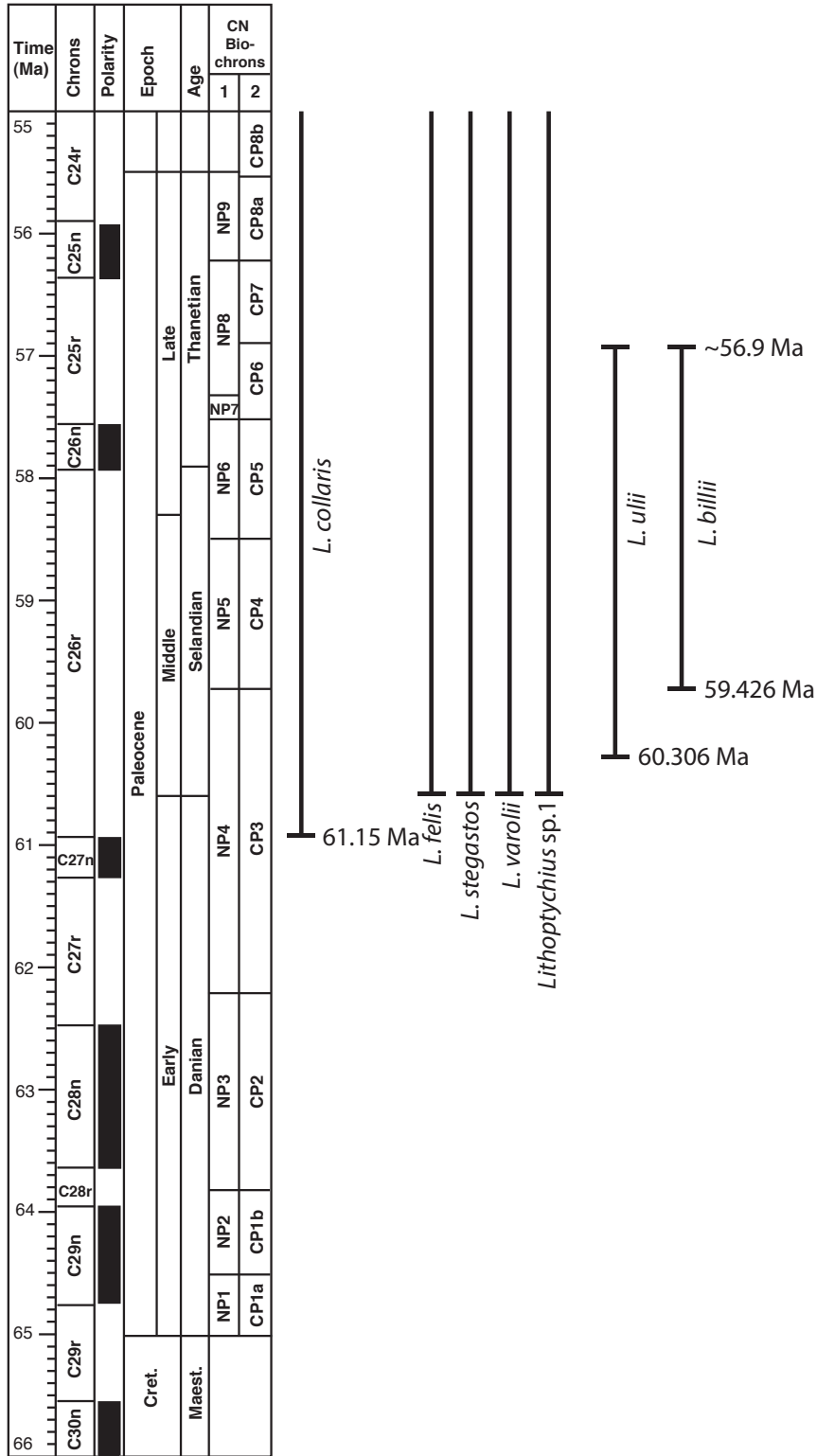
TAXONOMY

Generic taxonomy

Genus *Lithoptychius* Aubry in Aubry, Bord and Rodriguez 2011

Type species: *Lithoptychius ulii* (Perch-Nielsen) Aubry in Aubry et al., 2011, p. 273 (= *Fasciculithus ulii* Perch-Nielsen 1971a).

“Fasciculiths consisting of three superposed structural units and a central body located along the vertical axis at the distal end of the column. The (proximal) column is broadly cylindrical and composed of wedge-shaped elements. Its proximal surface is concave, its distal surface flat, concave or convex. A narrow or broad canal runs along the vertical axis. The intermediate unit (collaret) is a thin, disc-shaped cycle. In some species it is so thin as to be difficult to distinguish from the calyptra (together the calyptra and collaret form the ‘cone’). The collaret is generally thicker laterally than centrally, its thickness progressively increasing outwardly (as seen in longitudinal section). It may be as broad as the column or extend beyond it. It may also be restricted in extent to the periphery of the column. It consists of elements with sinistral imbrication as seen in distal view. In cross-polarized light the collaret is delineated from both the column and calyptra by extinction lines that highlight its contour. The calyptra, dome-shaped or cylindrical, overlaps the collaret, being as broad, broader or narrower. It may be prominent or tiny, with a narrow central canal or with a large central depression. It consists of (sub)radially arranged, wedge-shaped elements with dextral imbrication as seen in distal view. The size of the elements varies considerably between species, producing typical patterns in longitudinal sections seen in light microscopy. When the central canal is narrow, the calyptra is thick and massive. When the central canal is broad, the calyptra is thin and appears either as two narrow, parallel-sided ‘slabs’ on each side of the canal, or two, distally pointed, triangular ‘ears’. The central body occurs in distal position along the vertical axis, as a meeting point between the column, calyptra and collaret. Of variable size, it may be rhomboidal, triangular, or elongate and occupy the whole axis of the column.



TEXT-FIGURE 11

Biochronology of *Lithoptychius* species. Magnetobiochronologic framework from Berggren et al., 1995 updated (Wade et al., 2011, and herein).

“Species are differentiated upon 1) the shape of the column, including that of the distal face and the width of the central canal; 2) the size, shape and extent of the collaret; 3) the size, shape and thickness of the calyptra. Together the collaret and calyptra confer a characteristic appearance to the fasciculiths of *Lithoptychius*. In older species the two units are well developed. In younger species the collaret occupies a more inner position at the distal end of the column, and is less distinct. The taxonomic significance of the collaret remained unrecognized when such younger taxa were first described (Perch-Nielsen, 1971a). *Lithoptychius ulii* is chosen as type species because its structure is well known from SEM studies; its holotype clearly exhibits the collaret” (Aubry in Aubry et al., 2011, p. 271).

Specific taxonomy

Species differ by the shapes of the column, collaret and calyptra, their relative proportions, and the lateral extent of the collaret over the column and the calyptra over the collaret (see above).

The shape and size of the collaret are significant characters for species recognition, but the general lack of consideration given to this structural unit has resulted in taxonomic ambiguity.

Unresolved issues concern the *Fasciculithus* (now *Lithoptychius*) species *jani* Perch-Nielsen 1971a, *bitectus* Romein 1979, *merloti* Pavsic 1977 and *stonehengii* Haq and Aubry 1980. The latter three names are rarely, if ever, used, whereas numerous specimens are assigned to *L. jani* on the base of the shape of the column.

Perch-Nielsen (1971a, 1977) copiously illustrated *F. jani*. In these specimens, the column is of highly variable shape, from massive, almost square (1977, pl. 12, fig. 13), to slightly egg timer-shaped (1971a, p. 5, fig. 1), to markedly fluted (1977, pl. 12, fig. 10). In all these specimens, the collaret flares laterally as if it were a distal extension of the column, forming a large calyx (in morphologic continuity with the column) that surrounds the calyptra nested at its center, an annular depression running at the contact between calyptra and collaret. Romein (1979, pl. 5, fig. 1) assigned to *F. jani* a specimen in which the collaret is not depressed distally, but convex, and with no clear demarcation between the collaret and calyptra. This may represent a late morphotype of the species, or a different taxon (Sample SP624 [Caravaca section] from which the specimen is illustrated, is assigned to Zone NP9; however *F. jani* was only recorded from Zone NP5; op. cit., fig. 8, p. 24, 25).

Romein (1979) introduced *F. bitectus* based on a single light microscope illustration. The column is massive, with a slight constriction 2/3 above the concave base. The collaret (“cone” in Romein) flares distally extending “to, or almost to the margin of the column” (op. cit., p. 150). It is surmounted by a convex, centrally depressed distal cycle with a diameter “larger than that of the column and the cone” (op. cit.). A remarkable SEM illustration of this species is found in Monechi (1985, pl. 7, fig. 4). The specimen was assigned to *F. pileatus*, in which the calyptra is entirely contained within the distal width of the column.

Lithoptychius bitectus and *L. jani* are of very similar shape, both fasciculiths broadening considerably at the distal end. However, the flaring morphology is due to the extent of the calyptra in *L. bitectus*, to that of the collaret in *L. jani*. The difference has probably not been appreciated until now. It is difficult to revise taxonomic assignments from published illustrations of *L. jani*. For this rea-

son, but with one exception, I have refrained from re-interpreting light microscopy illustrations of *L. jani* that may as well be of *L. bitectus*.

Haq and Aubry (1980, p. 301) and Steurbaut and Sztrákos (2008, p. 34) remarked that the light microscope photographs of *F. jani* by Perch-Nielsen (1971a, pl. 14, figs. 37-38; now *Lithoptychius jani*) do not match the electronmicrograph of the holotype (op. cit., pl. 5, fig. 1). The former authors provided a more appropriate light microscope photograph of the species, and the latter authors introduced a new taxon (*Fasciculithus vertebratoides*, op. cit., p. 25, 26; now *Lithoptychius vertebratoides*) in which the elements of the cone stand almost erect in contrast to their gentle oblique inclination in *L. jani*.

Judging from its holotype, *Fasciculithus merloti* Pavsic 1977 is probably a synonym of *L. jani*. However, the specimen attributed to this taxon by this author and illustrated in pl. 7, fig. 2 corresponds in fact to *L. pileatus*. With its calyptra slightly larger than the distal end of the column, *Fasciculithus stonehengii* Haq & Aubry (1981, p. 301) is probably a junior synonym of *Lithoptychius bitectus*. The impression of a calyptra ‘sitting loosely on the’ column probably reflects the intermediate presence of the collaret.

Morphological and structural differences among species are given in figure 2.

Revised species taxonomy

Lithoptychius barakati (El Dawoody) n. comb.

Basionym: *Fasciculithus barakati* El-Dawoody 1988, p. 555, 556, pl. 1, figs. 5a,b, 6a, b, 7a, b.

Lithoptychius sp. A

Basionym: *Fasciculithus* sp. 1 Okada & Thierstein, 1972, p. 523, pl. 6, figs. 6a, b.

Lithoptychius sp. B

Basionym: *Lithoptychius* sp. 1 Aubry et al., 2011, p. 272, pl. 7, figs. 1a-d.

Lithoptychius sp. C

Basionym: *Fasciculithus* sp. 3 Bernaola et al., 2009, figs. 4v, 5a-d.

Lithoptychius sp. D

Basionym: *Fasciculithus* sp. 1 Prins 1971, pl. 6, figs. 5a-c.

Lithoptychius sp. E

Basionym: *Fasciculithus* sp. 5 Bernaola, Martín-Rubio & Baceta 2009, figs. 4i, j.

Key of determination

- I. Fasciculiths with prominent collaret occupying the whole distal diameter of the column. Unit 1
- *L. varolii*
 - *L. collaris*
 - *L. felis*
 - (*L. chowii*)
- II. Fasciculiths with a thin collaret occupying the whole distal diameter of the column. Units 2, 3
- *L. jani*
 - *L. merloti*
 - *L. stonehengii*
 - *L. pileatus*
 - *L. stegastos*
 - *Lithoptychius* sp. A
 - *L. bitectus*
 - *L. barakati*
- III. Fasciculiths with prominent collaret restricted to the distal periphery of the column. Unit 4
- *Lithoptychius* sp. B
 - *Lithoptychius* sp. C
 - *L. schmitzii*
 - *Lithoptychius* sp. D
- IV. Fasciculiths with very thin collaret. Unit 5
- *L. vertebratoides*
 - *L. ulii*
 - *Lithoptychius* sp. E
 - *L. billii*

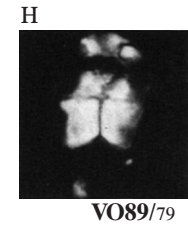
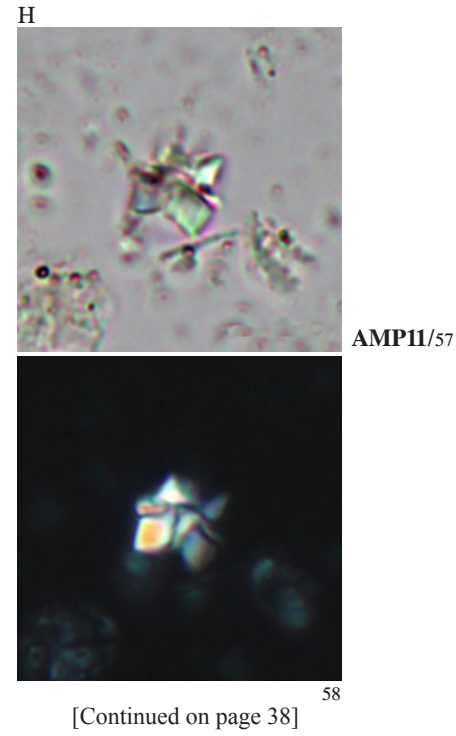
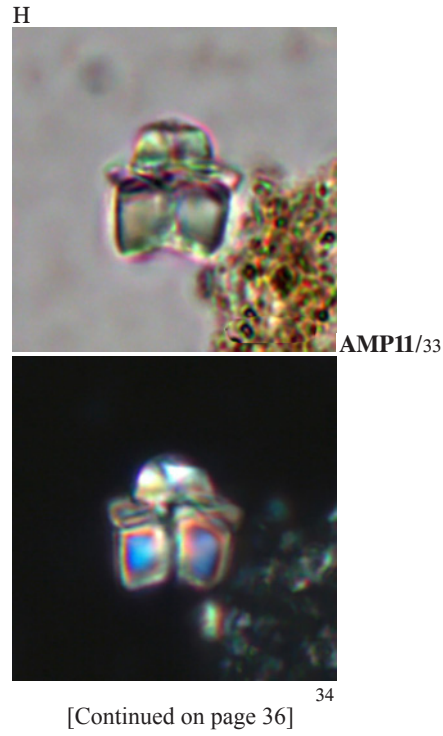
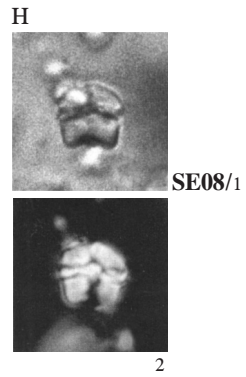
Note: Except when species have been introduced based on specimens figured as part of the description of a former species, all illustrations given by an author to accompany his description of a new taxon have been retained together, even if some of the illustrated specimens clearly represent another taxon. For these, remarks on taxonomic assignment are given in the figure references section.

Lithoptychius varoli (Sturbaut & Sztrákos) Aubry & Rodriguez in Aubry et al. 2011 [= *Fasciculithus varoli* Sturbaut & Sztrákos 2008]

Lithoptychius collaris Aubry & Rodriguez in Aubry et al. 2011

Lithoptychius felis Aubry & Bord in Aubry et al. 2011

Lithoptychius chowii (Varol) Aubry in Aubry et al. 2011 [= *Fasciculithus chowii* Varol 1989]



Lithoptychius varolii

- 5.2–6.4 μm x 5.3–6.2 μm

- L. Danian (l. NP4). Aquitaine Basin, France.

- Small form, as high as broad, with three structural units. Proximal column half the height of the fasciculith, proximally concave, consisting of numerous elements with clear edges; covered by distal dome-shape of unit with a rather small cycle of lateral elements slightly overlapping the column, topped by a much higher, slightly narrower mushroom-shaped cone. The lateral cycle and dome are well distinguishable as two superimposed, optically different structures in CN in side view.

≠ from *L. collaris* in having a collaret as wide as the column or only slightly wider (Aubry in Aubry et al., 2011, p. 273).

— The tall, dome-shaped calyptra is well differentiated from the collaret; distal face of the column markedly convex (Aubry in Aubry et al., 2011, p. 173).

- SE02 (p. 25), AMP11 (p. 273).

Lithoptychius collaris

- H: 5.7–7 μm ; collaret: 5–8 x 0.8–1.5 μm ; calyptra: 3–4.5 x 2–2.5 μm

- E. Paleocene (l. NP4). Egypt.

- Robust, compact, with prominent collaret and dome-shaped calyptra. Column slightly taller than the cone, with vertical sides, gently concave proximally and convex distally, and with a narrow axial canal, conferring each half of the column on either side of the canal a rhomboidal shape. Cone with distinct collaret and calyptra. The collaret is prominent, thick, extending well beyond the periphery of the column; the free part of its proximal face curves upwards whereas the distal surface is (sub)horizontal. Tall, massive, dome-shaped calyptra, narrower than both collaret and column.

≠ from *L. varolii* in having a prominent collaret and a massive calyptra. In *L. varolii*, the collaret is “a rather small cycle of lateral elements slightly overlapping the column”. In *L. collaris* the collaret is thick and extends laterally well beyond the column. The calyptra of *L. varolii* has slanted sides; that of *L. collaris* is almost parallel-sided; ≠ from *L. chowii* that has “a laterally reduced cone extending distally”, and in which “the contact between the column and cone is always straight”. Varol’s illustrations clearly show the presence of a collaret in *L. chowii*, but they are insufficient to show its extent and shape. Also, the calyptra is conical in *L. chowii*, whereas it is massive and dome-shaped in *L. collaris*.

- AMP11 (p. 271).

Lithoptychius felis

- H: ~5 μm ; column W: ~4.5 μm ; collaret: 8–8.5 x 0.5–1 μm ; calyptra: (dw) 3.5–4 μm , (pw) 3.5–5.5 μm x (h) 1.5–2.5 μm

- E. Paleocene (l. NP4). Egypt.

- Broader than high; prominent collaret, wide, crateriform calyptra, elongate central body in axial canal. Column widening distally, axial canal also increasing in \emptyset distally. Collaret slightly extending laterally beyond the column, not reaching central canal, the column being indented distally on both sides of it: collaret rests on the outer two thirds of the \emptyset of distal face of column. Calyptra as an empty truncated cone, broad at base with \emptyset = distal \emptyset of column; resting on collaret and central body, rising gently, narrowing while decreasing in thickness. In section and LM, it forms two symmetrical isosceles triangles slightly bent outwards on either side of a central, crater-like depression with broadly concave bottom. Inner sides of the triangles concave, outer sides slightly convex. Central body tetragonal, elongate, with two short distal sides, and two long proximal sides.

≠ from all other spp. by the shape of calyptra and of central body;

≠ from *L. collaris* in having a calyptra delineating a wide central depression. The calyptra is massive in the latter species;

≠ from *L. chowii* in having a much wider calyptra;

≠ from *Lithoptychius* sp.1 that has a thinner, cylindrical calyptra and in which the collaret is restricted to the periphery of the column.

- AMP11 (p. 271, 272).

Lithoptychius chowii

- ~6.7 μm x 6.5 μm

- L. Paleocene (NTp7). Northern Turkey.

- Fasciculith having a parallel-sided or constricted column and a laterally reduced cone extending distally. Contact between column and cone always straight. Column usually constricted and strongly concave proximally; cone extending distally to a height almost equal to half of the column but reduced laterally, with a diameter always < than that of column.

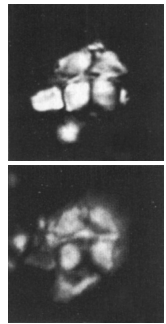
≠ from *L. billii* and *L. ulii* by having a column with a flat distal side and a comparatively high cone. The distal sides of *L. billii* and *L. ulii* are strongly concave and the cone is weakly developed or absent; ≠ from *L. pileatus* and *L. jani* by its laterally reduced cone.

— “*F. chowii* is one of the oldest species of the genus recovered and is widely distributed in both low and high latitudes. It is so far found restricted to Zone NTp7, Lower Palaeocene” (Varol, 1989, p. 298).

— “*L. chowii* included all *Lithoptychius* species with the exception of Middle Paleocene forms *F. mertoti*, *F. ulii* and *F. billii*” (O. Varol, e-mail comm. to author, 16 April 2013).

- VO89 (p. 297, 288), AMP11 (p. 273).

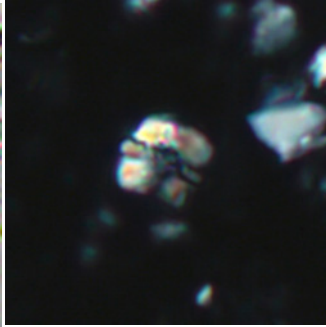
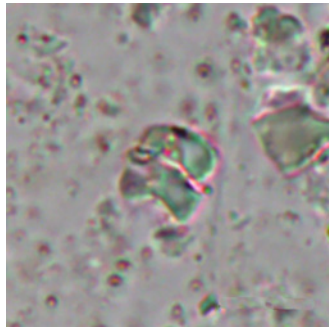
Lithoptychius varolii (continued)



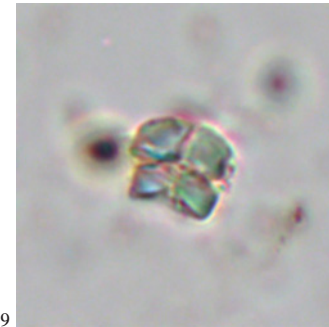
PDF78/3

4

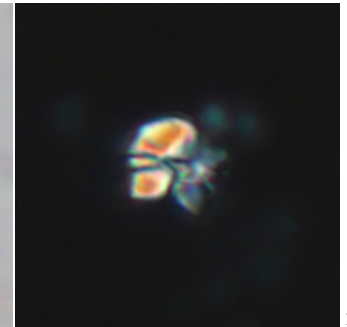
AMP11/5



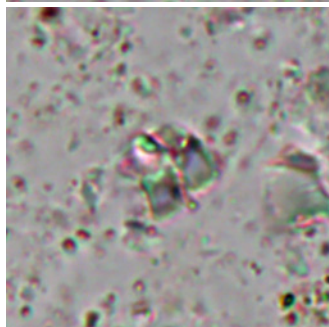
6



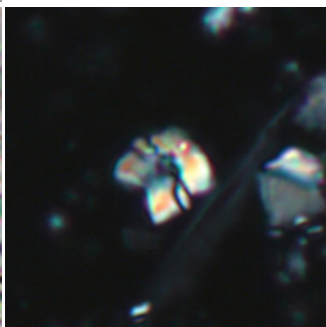
9



10



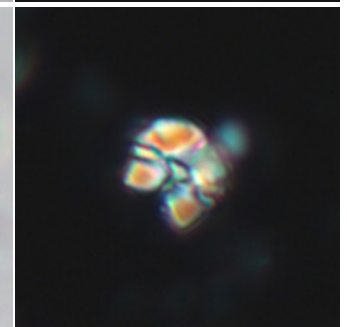
7



8



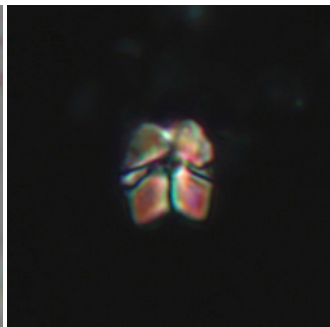
11



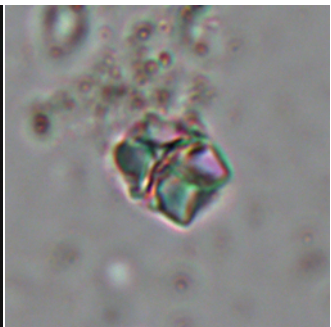
12



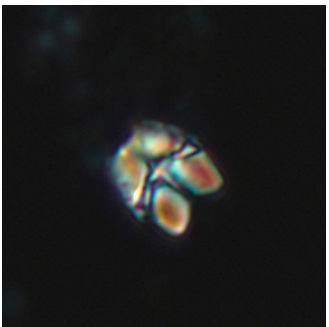
13



14

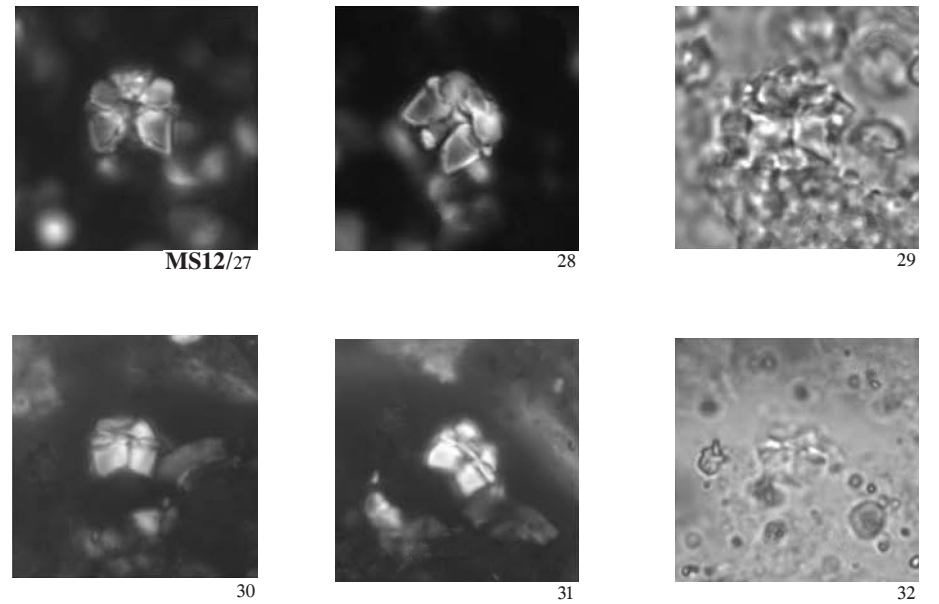
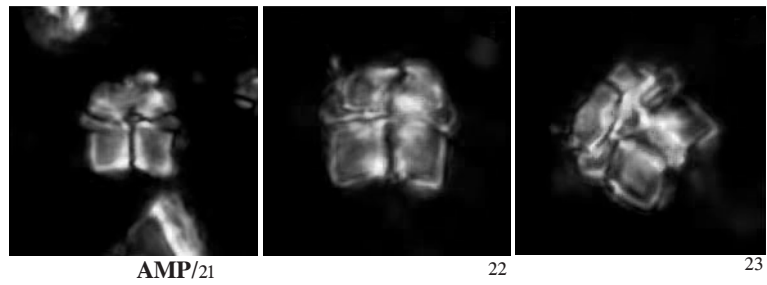
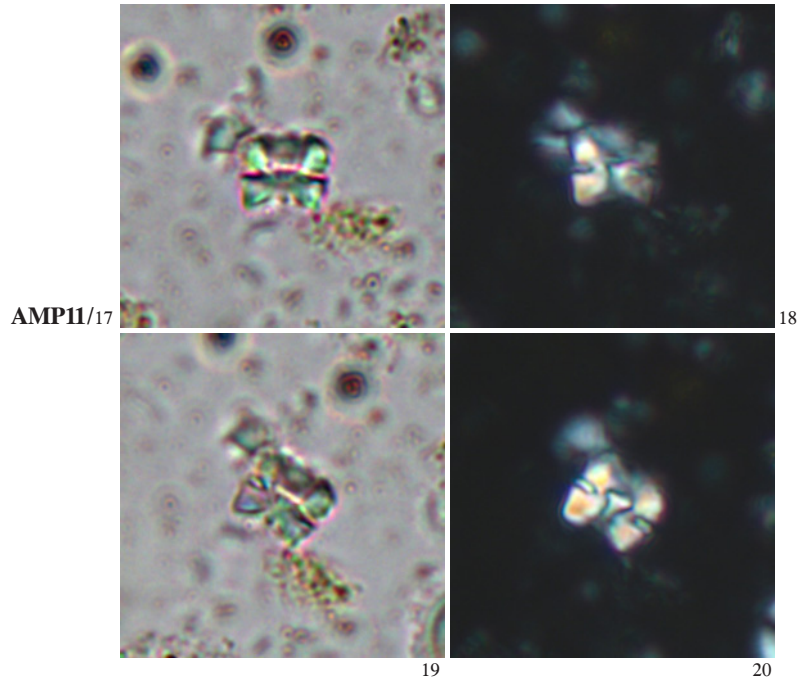


15

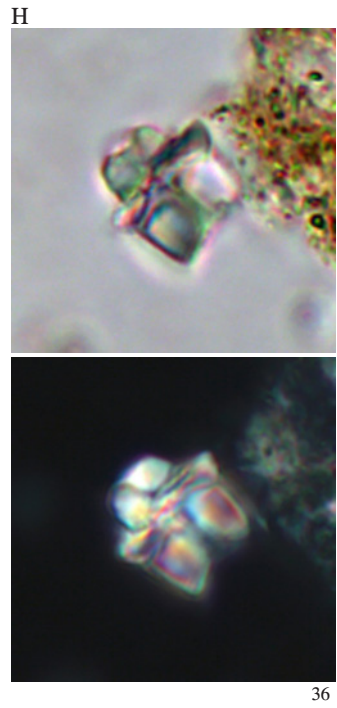


16

Lithoptychius varolii (continued)

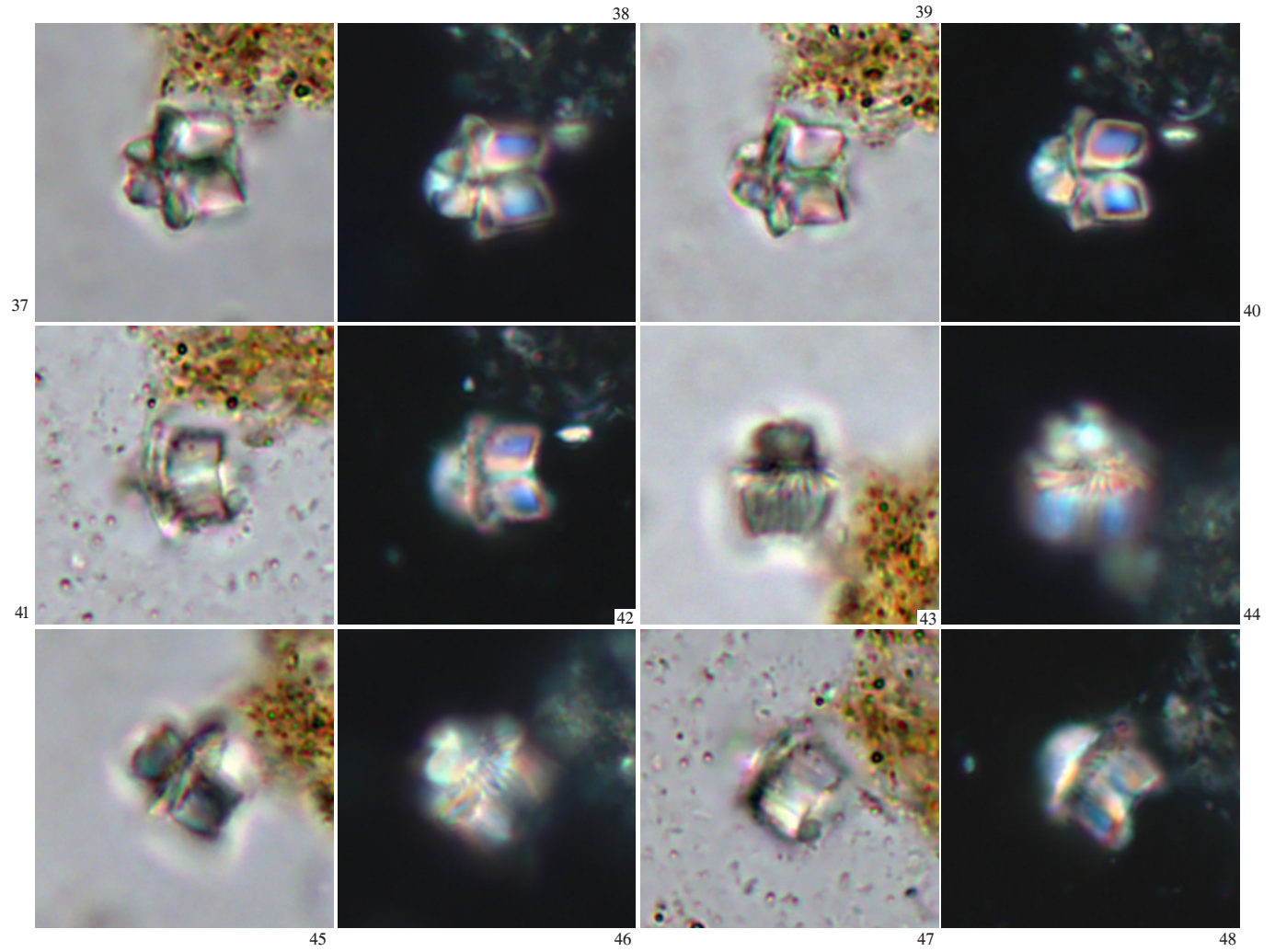


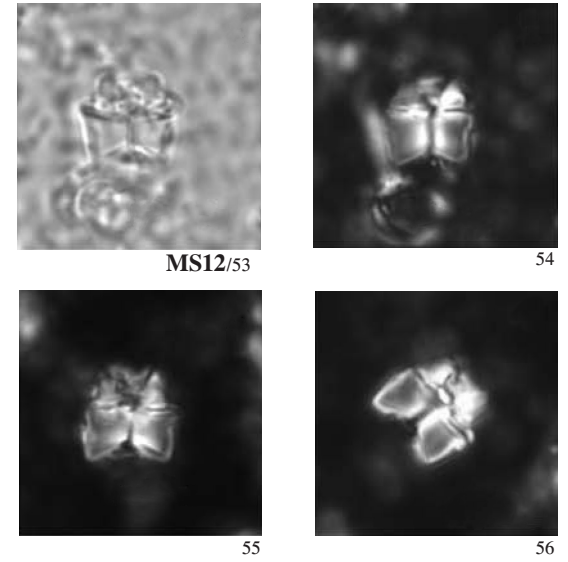
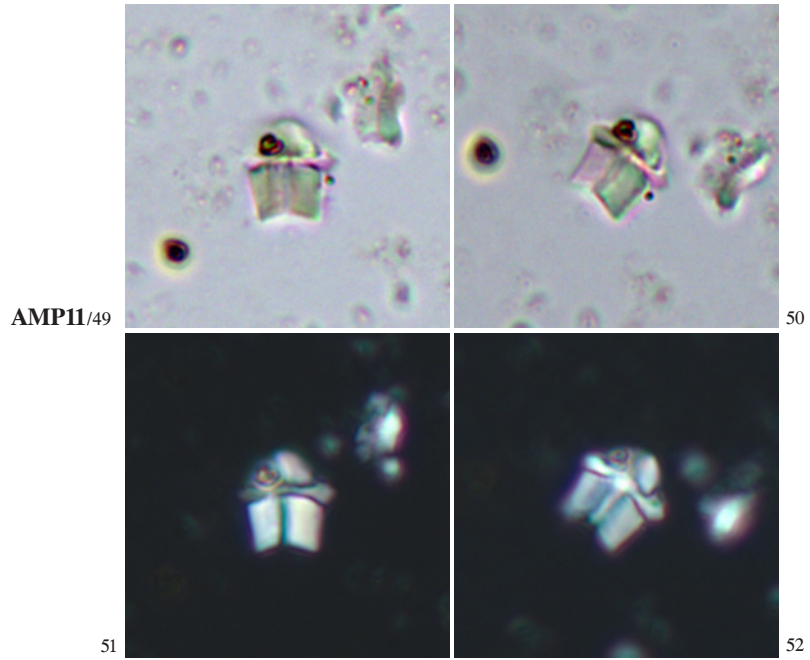
Lithoptychius collaris (continued)



AMP11/35

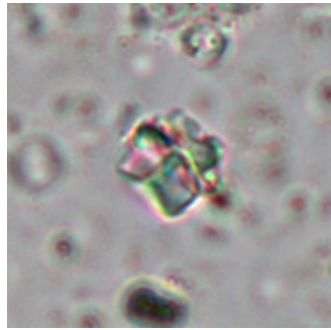
36



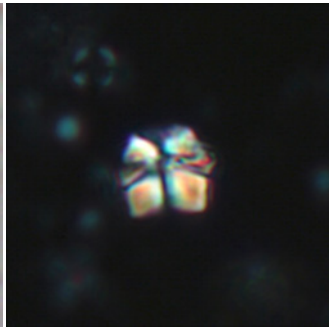
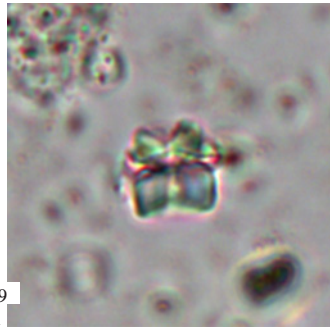


Lithoptychius felis (continued)

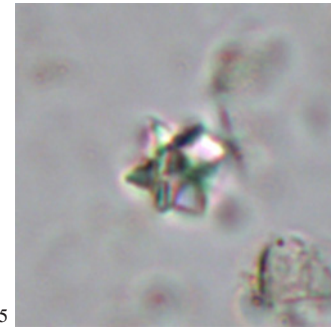
H



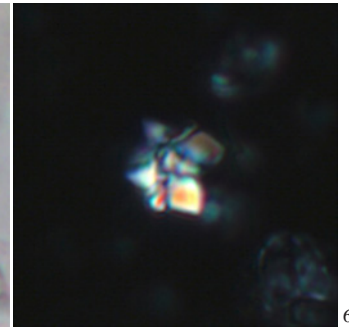
AMP11/59
61



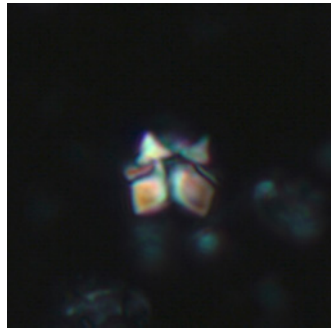
62



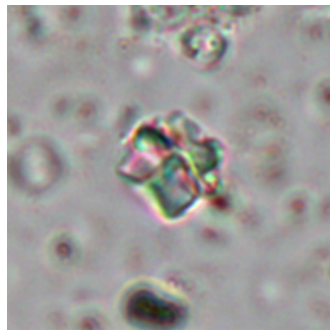
65



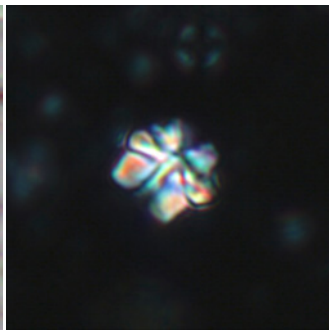
66



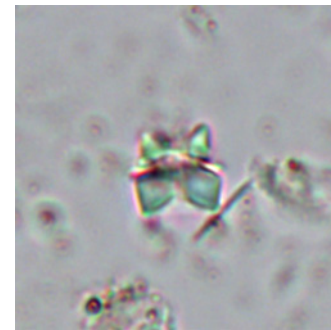
60



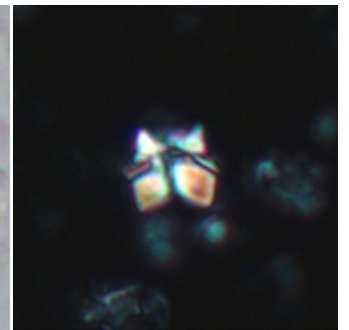
63



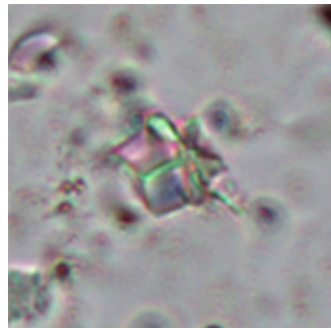
64



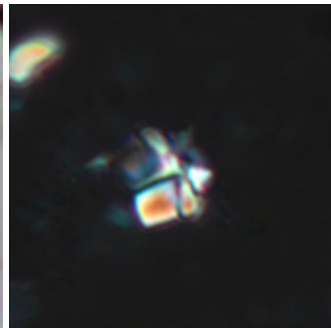
67



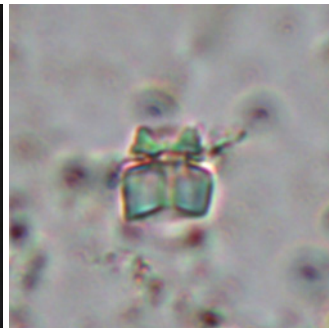
68



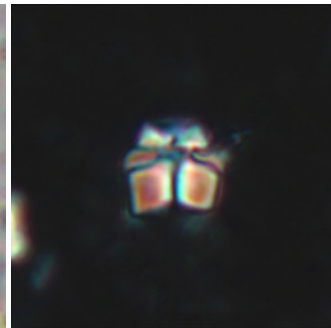
69



70

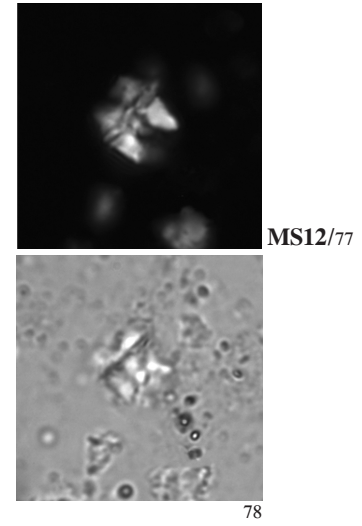
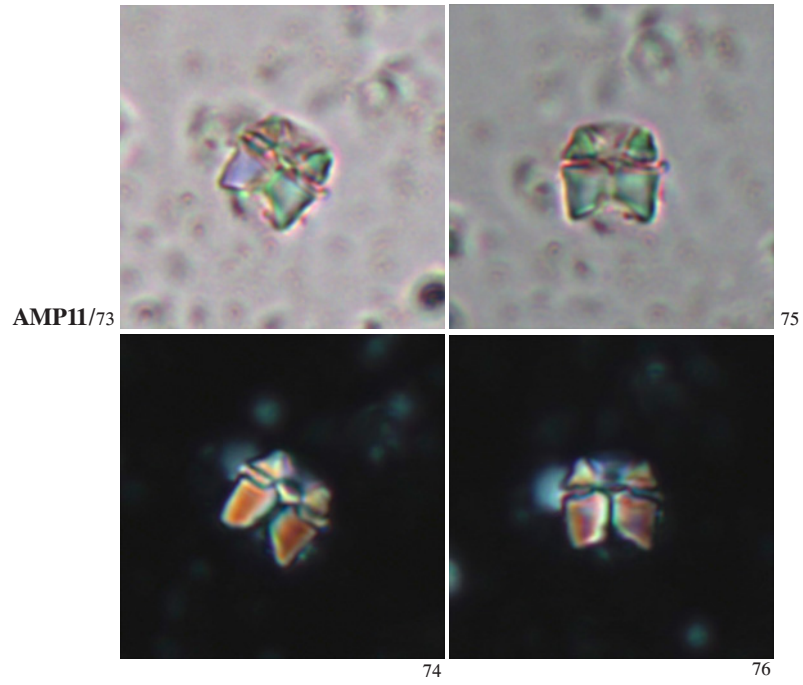


71

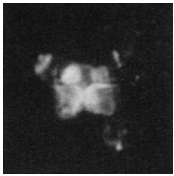


72

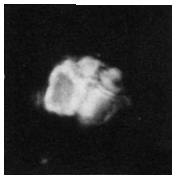
Lithoptychius felis (continued)



Lithoptychius chowii (continued)

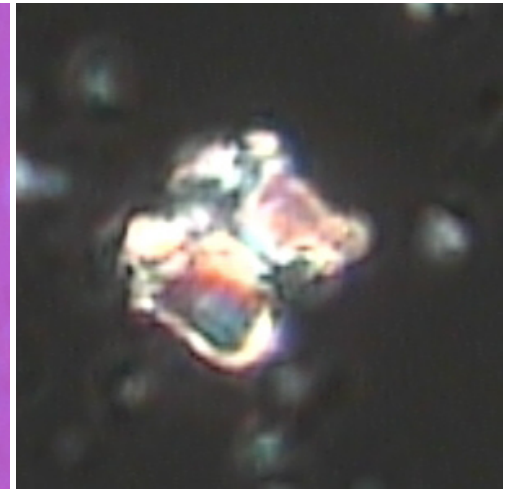
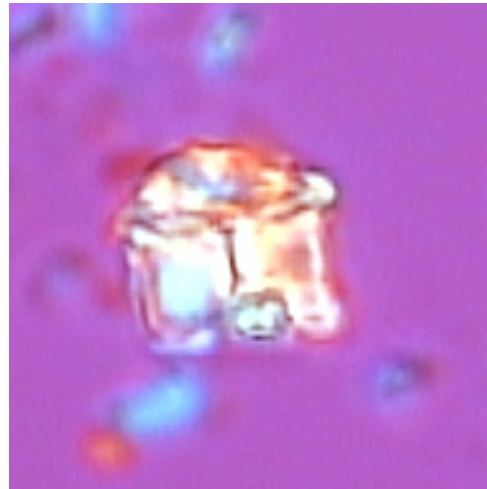


VO89/80

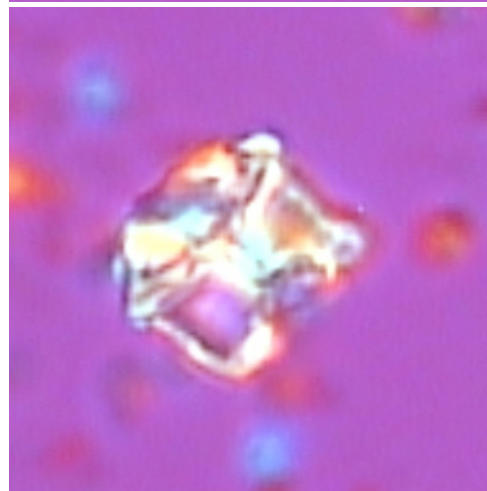


81

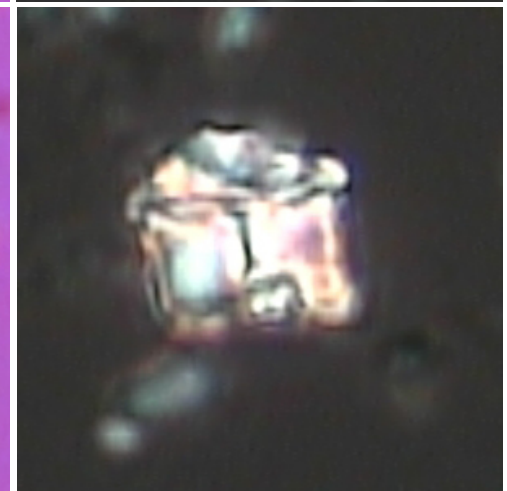
VO13/82



83



84



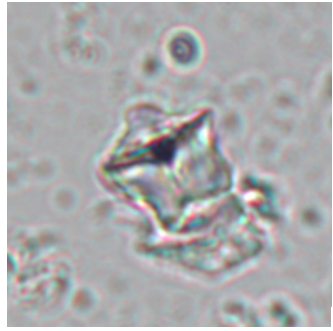
85

Lithoptychius janii (Perch-Nielsen) Aubry in Aubry et al. 2011 [= *Fasciculithus janii* Perch-Nielsen 1971]

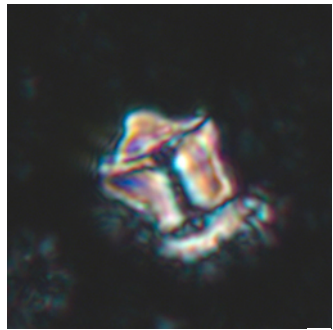
Lithoptychius merloti (Pavšič) Aubry in Aubry et al. 2011 [= *Fasciculithus merloti* Pavšič 1977]

Lithoptychius stonehengii (Haq & Aubry) Aubry in Aubry et al. 2011 [= *Fasciculithus stonehengii* Haq & Aubry 1980]

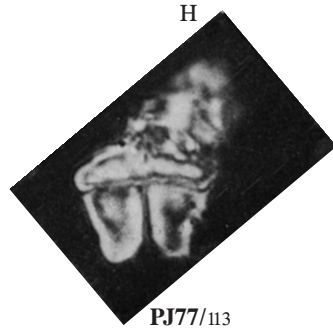
Lithoptychius pileatus (Bukry) Aubry in Aubry et al. 2011 [= *Fasciculithus pileatus* Bukry 1973;= *Fasciculithus* sp. cf. *F. ulii*, Roth 1973]



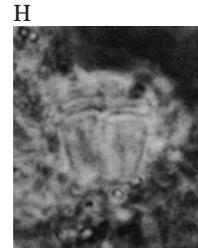
AMP11/86



87



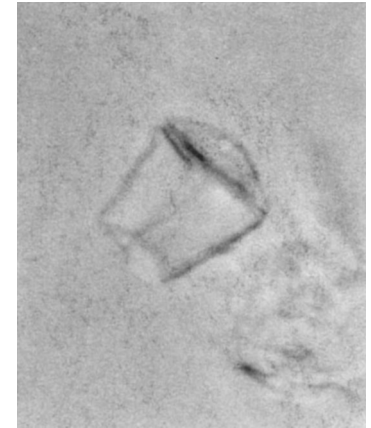
PJ77/113



HBU80/132



133



BD73a/135



136

[Continued on page 44]

Lithoptychius janii

- 5–7 μm x 6–9 μm

- M. Paleocene (NP5). Bay of Biscay (DSDP Site 119), Atlantic.

- [Column made of wedge-shaped elements, showing a wide flange made of enlarged lateral elements. Distal side topped with a flat cone-shaped apical needle. The height of the column as well as that of the needle is variable.]

≠ from other spp. by its characteristic flange, which is reminiscent of the star-shape of *Discoaster*, into which it might have evolved by reduction of the column into a knob.

— The thin collaret is responsible for the flaring shape of the fasciculith just above the column, a shape enhanced by the progressive widening of the column. Calyptra narrower than collaret, occupying depressed distal face of column (Aubry in Aubry et al., 2011, p. 273).

— This sp. has often been confused with *L. pileatus* and *L. bitectus* (Aubry in Aubry et al., 2011, p. 273).

— FAD in NP4 slightly before FAD of *F. tympaniformis*. LAD in NP5 (Romein, 1979, p. 77).

- PNK71b (p. 352), AMP11 (p. 273).

Lithoptychius merloti

- 8–12 μm

- M. Paleocene (NP5). Podsabotin Beds, Gorilka Hills, Hungary.

- [Column in the shape of a truncated cone, overlain by a disc that projects into an apical spine. Inclination of the sides of the cone is 73–75°. Outer wall of column, central opening and central tube smooth. Central tube wide and distinct. Proximal face of column markedly concave. The disc is normally as large as the distal end of the column, although it sometimes extends a little over the edge.]

≠ from the similar *L. ulii* in having clearly inclined column sides. The disc extends into a conical apical spine and not in a step-like fashion as in *L. ulii*.

— The holotype of *L. merloti* suggests that the low dome-shaped cone in this species is comprised of a thick calyptra extending slightly beyond the periphery of the column, being in continuity with it, and a thin collaret lying on the central part of the slightly concave distal face of the column. The central body is tiny. This species has not or has rarely been reported in the literature, and was considered synonymous with *L. janii* by Aubry (1989). A better understanding of the morphologic diversity among fasciculiths of *Lithoptychius* leads to conclude that *L. merloti* is a distinct taxon (Aubry in Aubry et al., 2011, p. 273).

- PJ77 (p. 43), AMP11 (p. 273).

Lithoptychius stonehengii

- 7–8 μm

- M. – L. Paleocene (NP5–NP9). Jordan.

-** Tapering proximal column. Gently curved apical disc, which has the general outline of a curved rectangle, somewhat thickened in the center and only slightly larger than the distal part of the proximal column.

≠ *L. janii*, which has a slightly flared apical disc that is appreciably larger than the proximal column. Both these forms seem to be related morphologically, and specimens with intermediate characters are often encountered.

— Possibly a junior synonym of *L. bitectus*.

- HBU80 (p. 301), AMP11 (p. 273).

Lithoptychius pileatus

- 5–12 μm

- Paleocene. Pacific, Indian and Atlantic Oceans; Caribbean Sea.

-** Truncated, cone-shaped column with smooth straight walls that expand from the base to the apex. A large, convex-topped, lens-shaped cap covers the entire top of the column and can extend beyond it. A central stud may connect the cap and column in some specimens. In C.N., side views have a straight dark line bisecting the column and a straight dark line separating the column and cap, forming three bright areas.

≠ *L. ulii*, which has concave column walls and small flat-topped apex that fails to cap the entire column and gives only weak optical relief in side view.

- Remarks: Its long stratigraphic range through the Paleocene is matched only by *F. tympaniformis*, a conservative, parallel-sided, cylindrical form with no distinctive ornamentation.

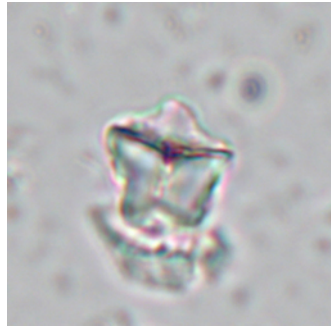
— Bukry (1973a) erroneously referred to his new species, the specimen illustrated by Roth, 1973, pl. 16, figs. 1a-c under the name *Fasciculithus* sp. cf. *F. ulii*. As the stratigraphic range given by Bukry shows, Roth's specimen is that illustrated in pl. 16, figs. 2a, b.

— Typical low latitude guide sp. (Bukry, 1978, p. 691).

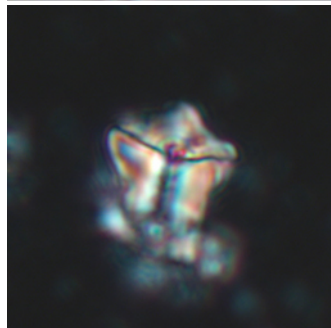
- BD73a (p. 307), AMP11 (p. 273).

Lithoptychius janii (continued)

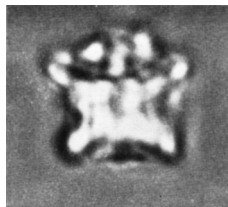
Lithoptychius merloti (continued)



AMP11/88



89



91

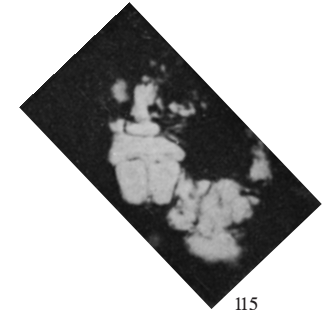
PB71/90



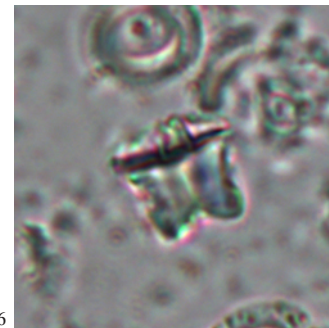
92



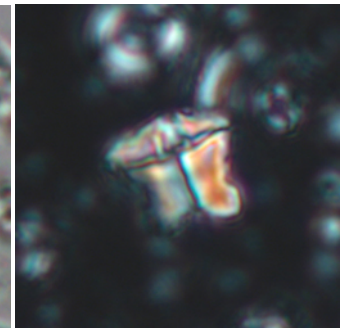
PJ77/114



115



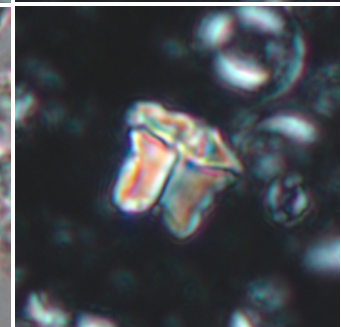
AMP11/116



117



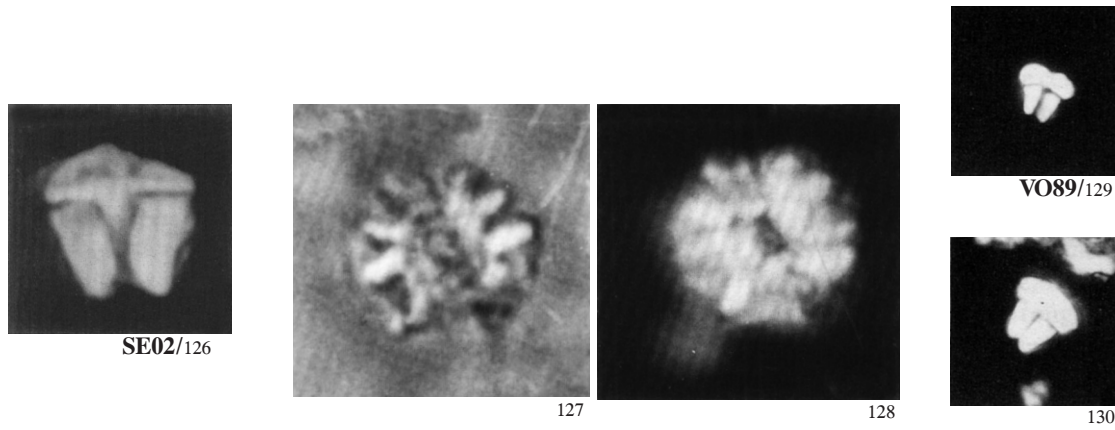
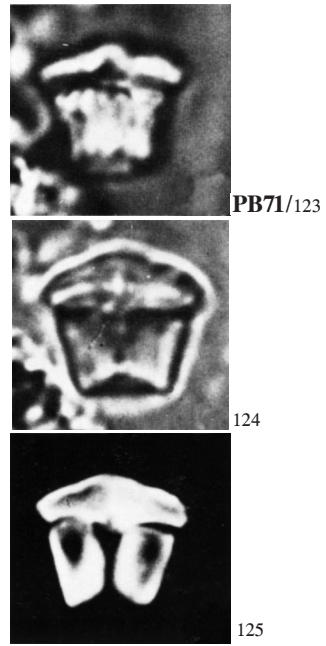
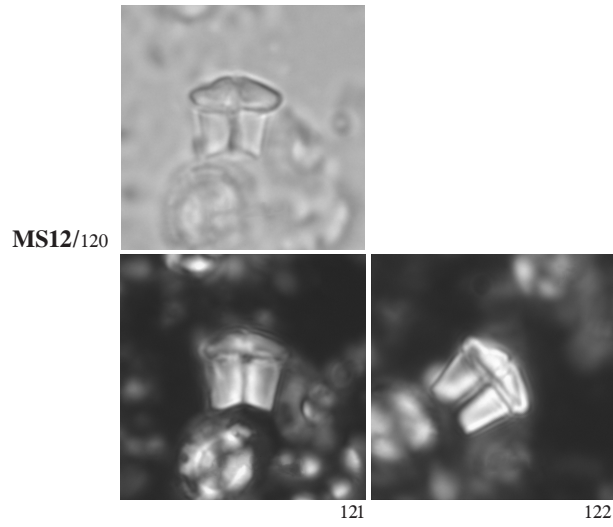
118



119

Lithoptychius merloti (continued)

Lithoptychius stonehengii (continued)



Lithoptychius pileatus (continued)

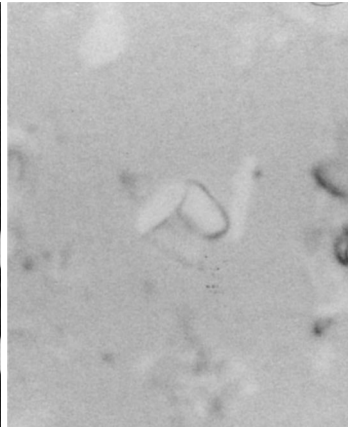
BD73a/137



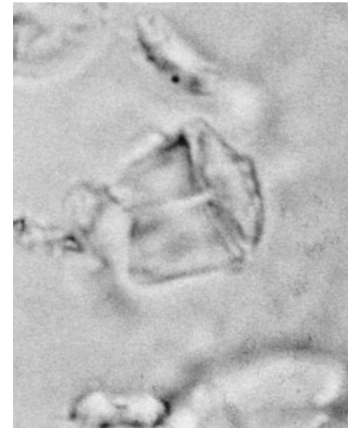
138



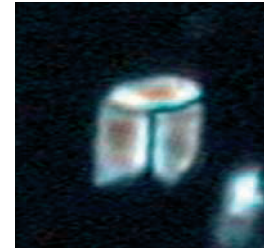
139



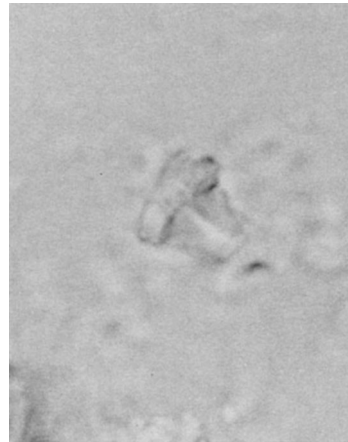
140



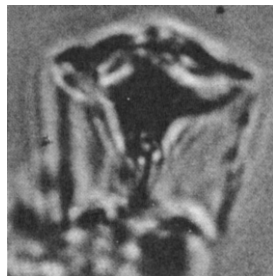
141



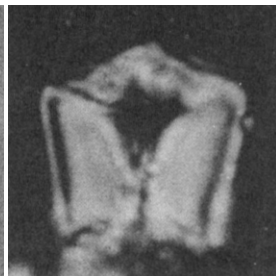
AMP/143



142



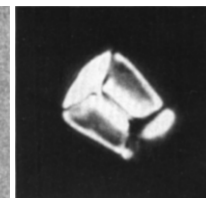
RPH73/144



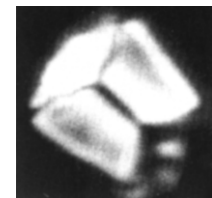
145



SE08/146

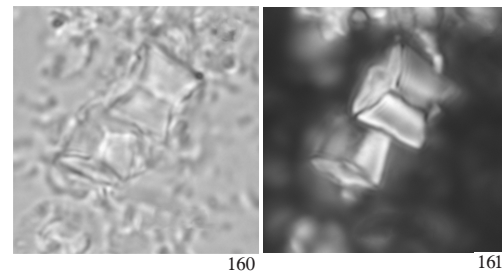
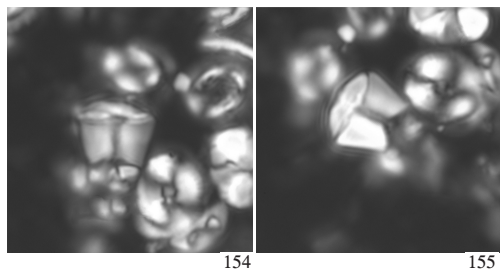
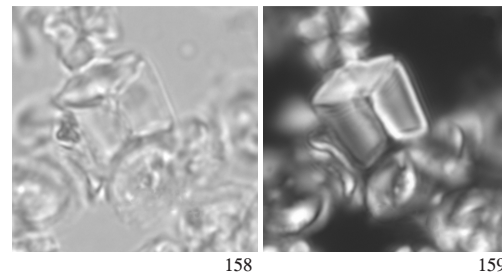
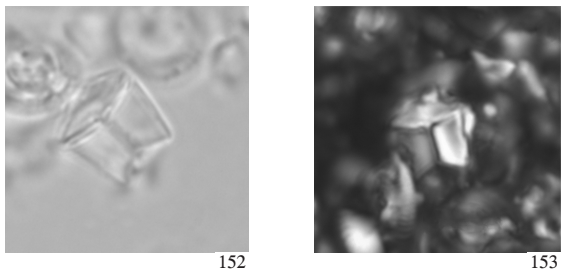
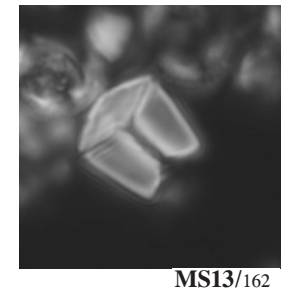
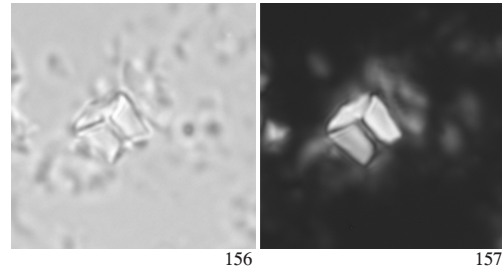
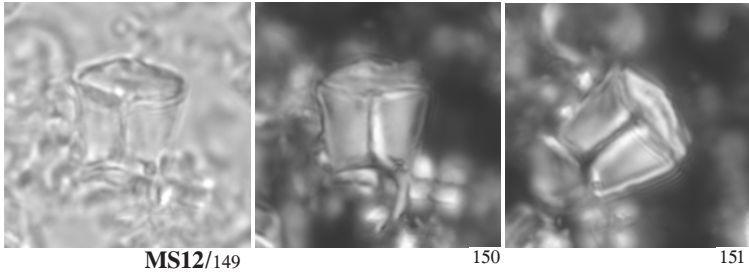


147



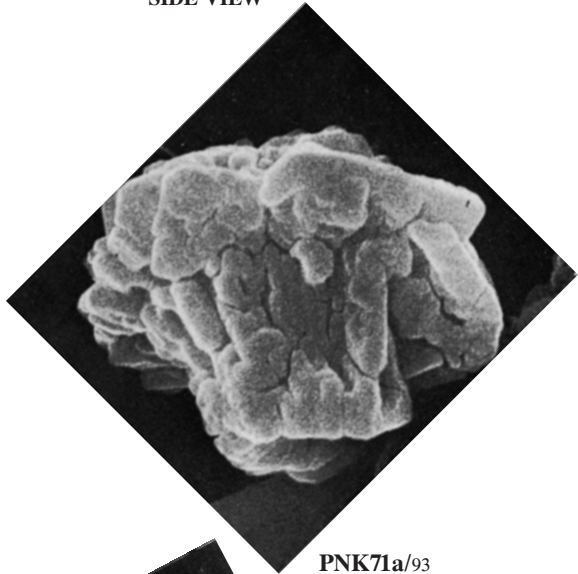
148

Lithoptychius pileatus (continued)



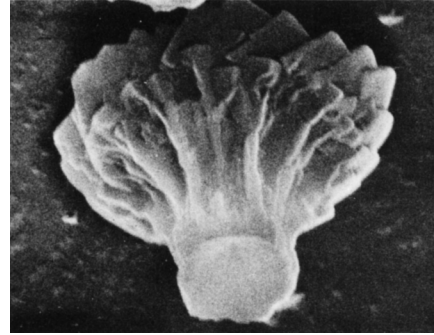
Lithoptychius janii (continued)

SIDE VIEW

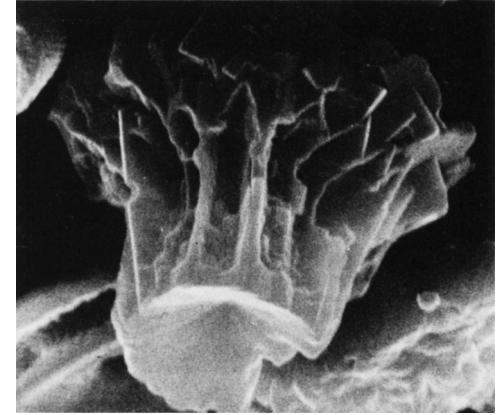


PNK71a/93

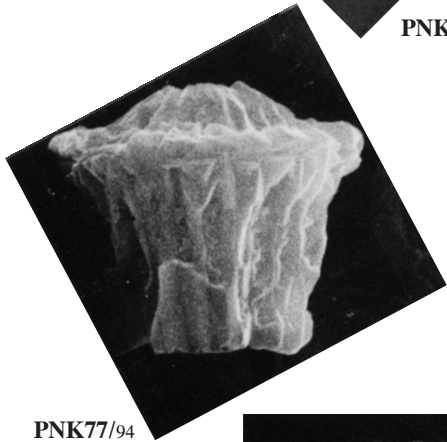
PROXIMAL FACE



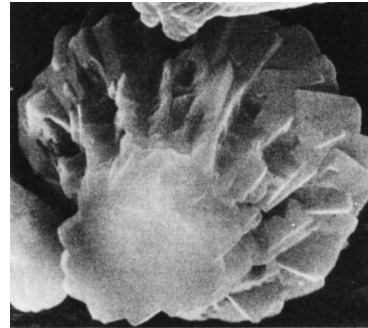
OH79/96



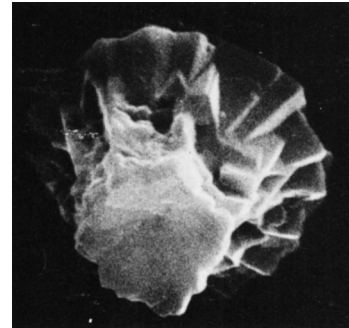
97



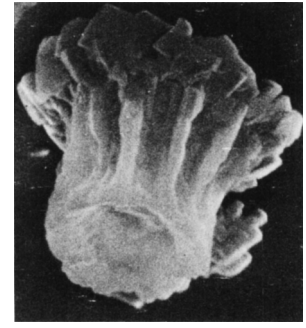
PNK77/94



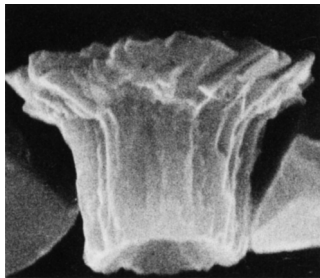
98



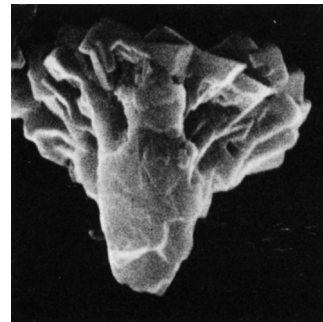
99



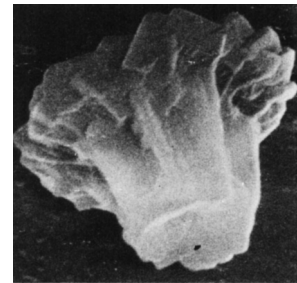
100



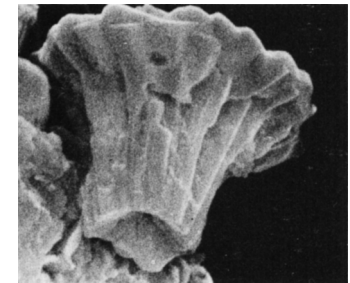
95



101



102

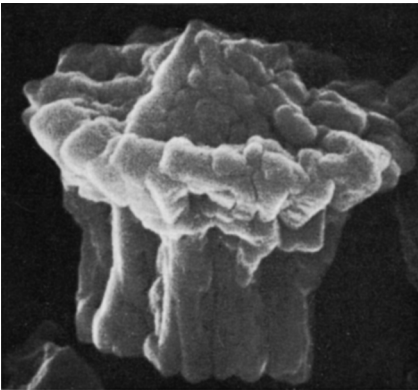


103

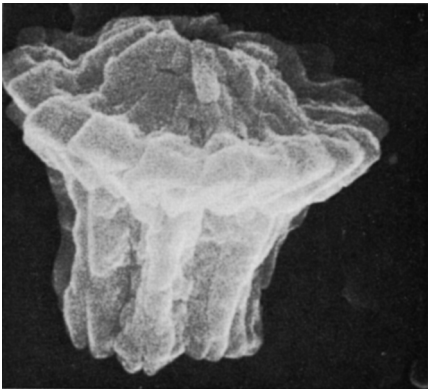
Lithoptychius janii (continued)

DISTAL FACE

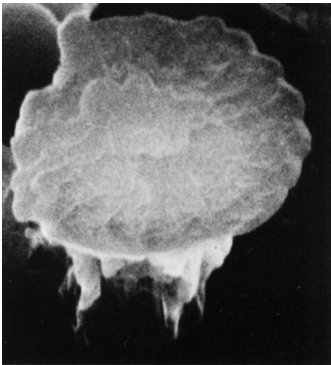
H



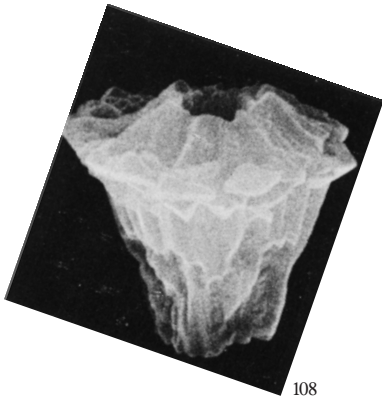
PNK71a/104



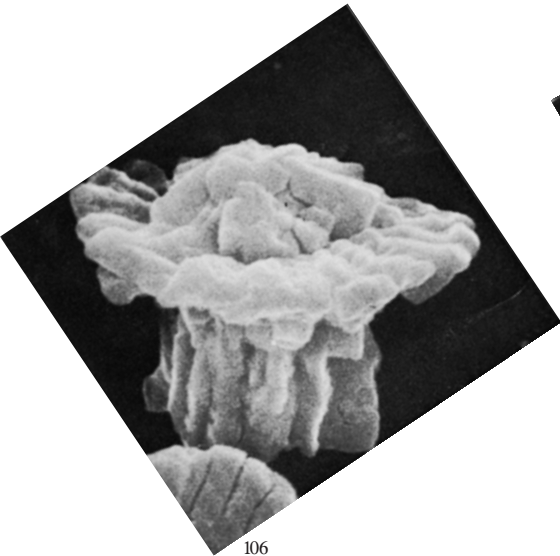
105



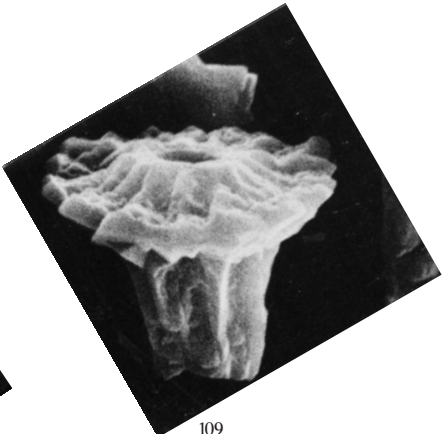
PNK77/107



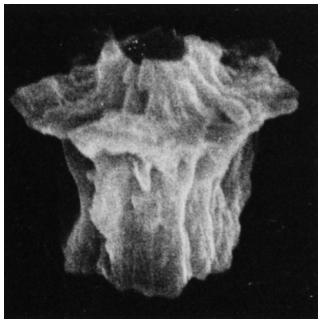
108



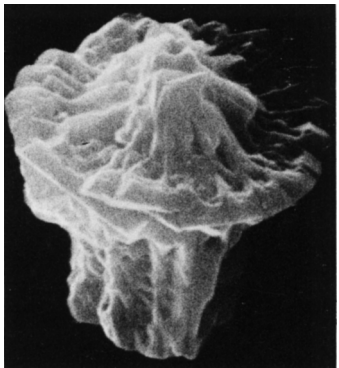
106



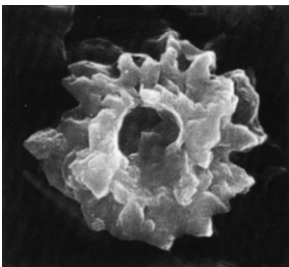
109



110



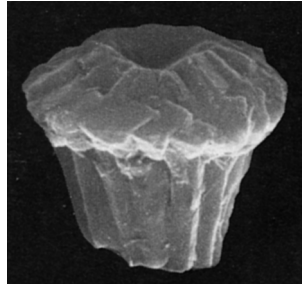
111



RPH73/112

Lithoptychius merloti (continued)

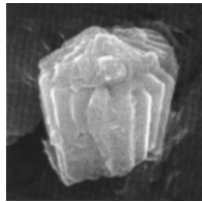
SIDE VIEW



RAJT79/131

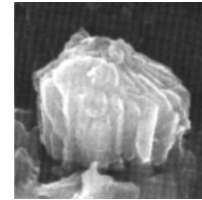
Lithoptychius pileatus (continued)

SIDE VIEW



SE08/163

DISTAL FACE



SE08/164

Lithoptychius stegastos Aubry & Bord in Aubry et al. 2011

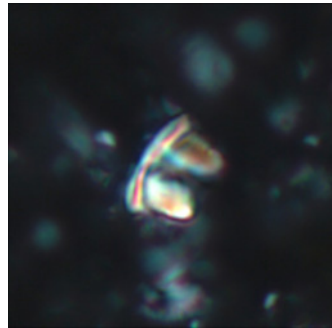
Lithoptychius sp. A [= *Fasciculithus* sp. 1 Okada & Thierstein 1972, p. 523, pl. 6, figs. 6a, b.]

Lithoptychius bitectus (Romein) Aubry in Aubry et al. 2011 [= *Fasciculithus bitectus* Romein 1979]

Lithoptychius barakati (El Dawoody) n. comb. [= *Fasciculithus barakati* El-Dawoody 1988, p. 555, 556, pl. 1, figs. 5-7]

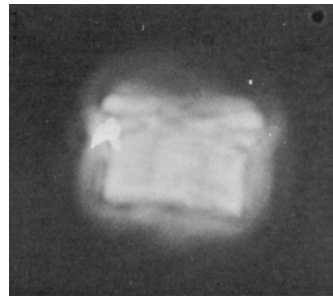


AMP11/165

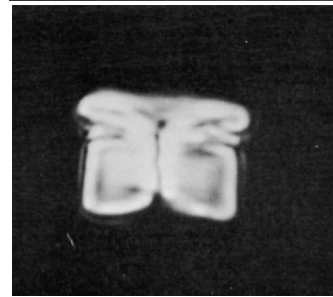


166

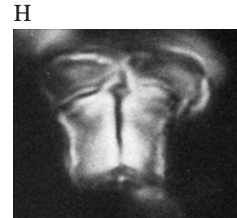
[Continued on page 56]



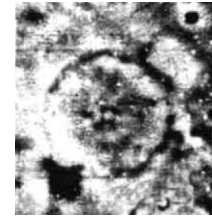
OH79/189



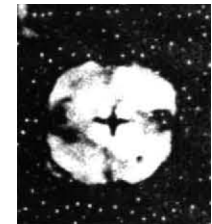
190



RAJT79/192



EDASA88/218



219

Lithoptychius stegastos

- H: 3.5–5 μm ; column W: 3.5–5 μm ; cone: 5–6.5 μm x 0.5–1.5 μm .

- E. Paleocene (I. NP4). Egypt.

- Fasciculith with a thin concavo-convex, sheet-like cone overlapping a wide column with a large axial canal. Column cylindrical, wider than tall, with strongly concave proximal face, gently convex distal one. Cone extending slightly beyond periphery of column, forming a broad angle with it. In CN cone shows thin calyptra surmounting the more prominent collaret. A sharp extinction line marks the contact between the collaret and column. The extinction line between the collaret and calyptra is parallel to the former but much weaker. Axial canal terminated distally by a tiny central body.

≠ from the somewhat similar *L. bitectus*, *L. janii* and *L. pileatus* by a combination of characters. In *L. bitectus* the distal side of the column is also convex but the cone is robust, with angular sides, and it is essentially comprised of the calyptra, not the collaret. In *L. janii*, the collaret is prominent, forming the flaring sides of the cone, the distal face of the column is concave, and the calyptra is entirely comprised within the diameter of the collaret. In *L. pileatus* the distal face of the column is also concave and the cone is entirely comprised within it. As in *L. stegastos*, the collaret and calyptra are difficult to distinguish in *L. pileatus*.

- AMP11 (p. 272).

Lithoptychius sp. A

- 6 μm x 5.8 μm

- M. Paleocene (NP5–NP6). N. Atlantic Ocean (DSDP Site 384).

- This form closely resembles *Fasciculithus pileatus* but differs from it by having a cylindrical body instead of a tapered one and by having a much thinner basal plate.

- OH79 (p. 523), AMP (p. 29).

Lithoptychius bitectus

- 6–8 μm x 7–8 μm

- Paleocene (NP4–NP5). Spain.

- Column consisting of 20 to 30 elements with smooth outer surfaces, tapering slightly in proximal direction, with a conical basal depression. The central body has a triangular cross section in side view; it is larger in earlier specimens than in later ones. Cone extending both in distal and lateral direction; it extends to, or almost to the margin of the column. It is covered by a convex, centrally depressed, distal cycle of elements. The sutures in this cycle are oblique counterclockwise in distal view. Its diameter is larger than that of the column and the cone.

≠ from *L. janii* by the presence of a distal cycle;

≠ from spp. of *Heliolithus* by the orientation of the extinction lines in distal or proximal view: in *L. bitectus* they are parallel to the polarization directions, while they make an angle with these in *Heliolithus*.

— Evolved from *L. ulii* and evolved into *Heliolithus elegans* (Romein, 1979, p. 77).

- RAJT79 (p. 149), AMP11 (p. 273).

Lithoptychius barakati

- 7 μm

- M. Paleocene (NP5–NP6). Dakhla Shales, Egypt.

- Specimens of relatively long cylindrical form with a plane view appearing as a rosette of about 20 rounded petals. One end is distinctly concave, slightly angular inwards, and the other end is nearly planar to slightly convex. Surface in side view is ornamented by characteristic longitudinal ridges, transversely cut by thinner and thinner striations.

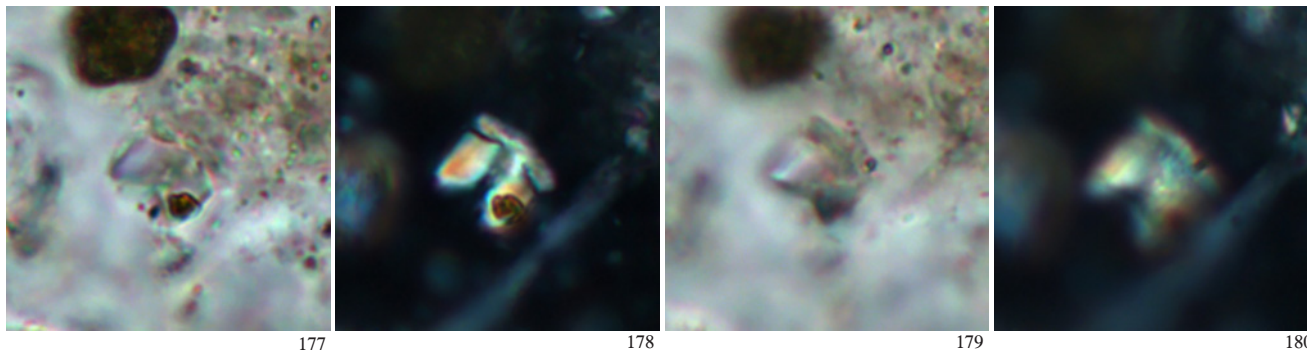
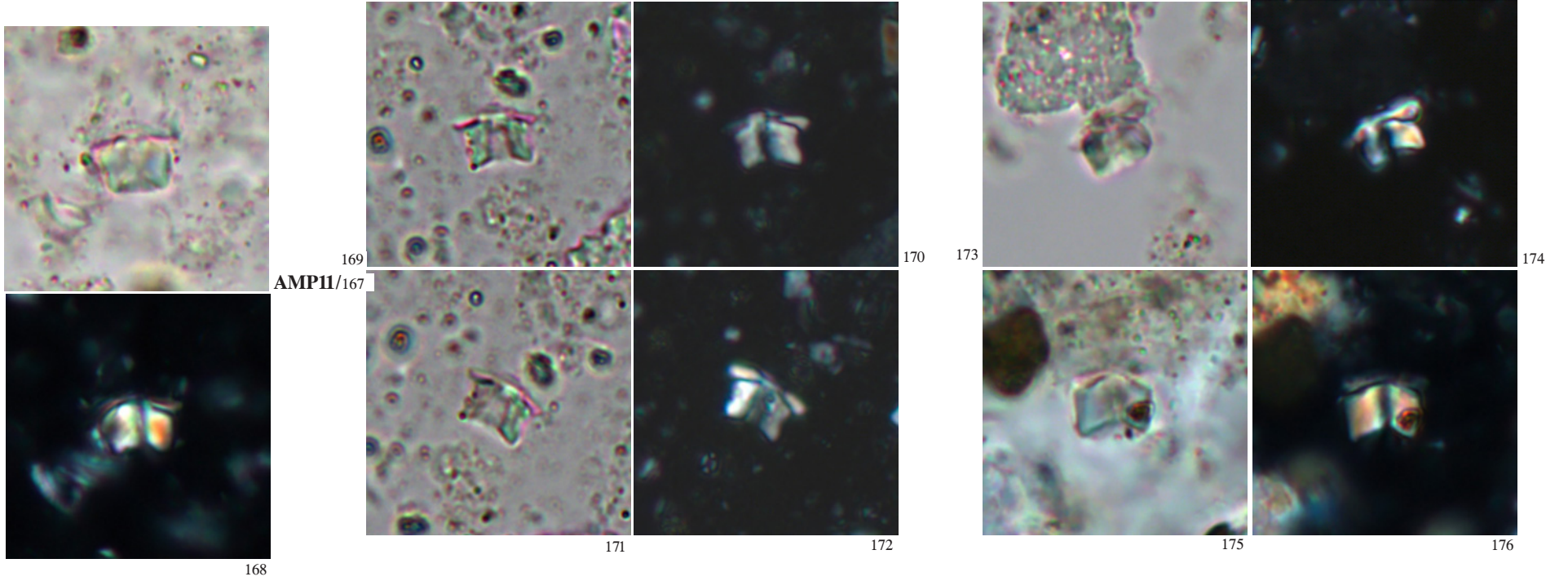
≠ from *F. involutus* by its relatively long cylindrical shape and the more rounded petal-like elements; also its surface is ornamented by longitudinal ridges crossed by finer striations.

- Remarks: abundant in Zone NP5 and rare in the lower part of Zone NP6 at Gebel Duwi.

— The holotype of *L. barakati* is shown in distal view, which is insufficiently diagnostic. The two paratypes, illustrated in side view, correspond to two different species; therefore although a valid name, *L. barakati* is a superficial taxon.

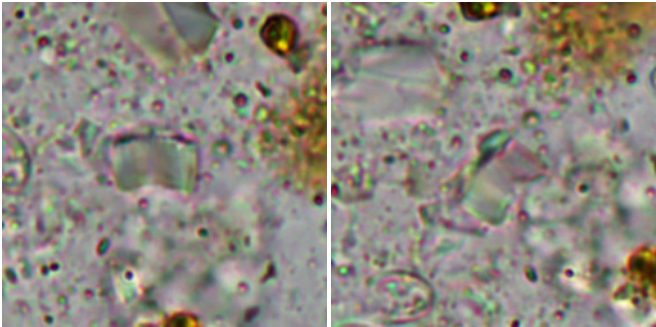
- EDASA88 (p. 555, 556), AMP (p. 29).

Lithoptychius stegastos (continued)

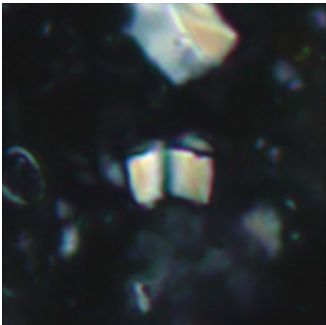


Lithoptychius stegastos (continued)

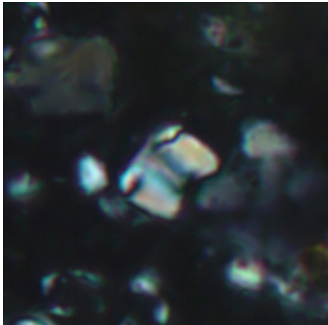
AMP11/181



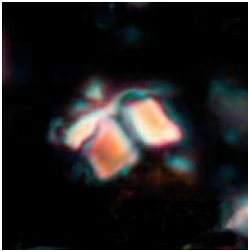
182



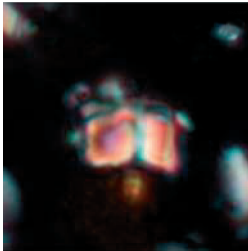
183



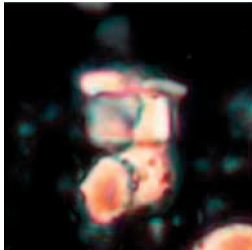
184



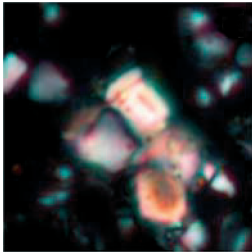
BG09/185



186



187

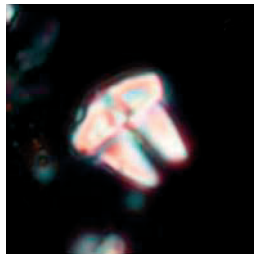


188

Lithoptychius bitectus (continued)



AMP/193



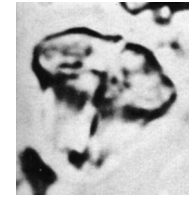
194



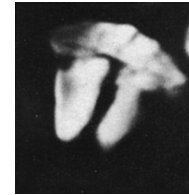
HBU80/195



196



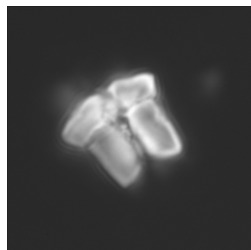
MS85/197



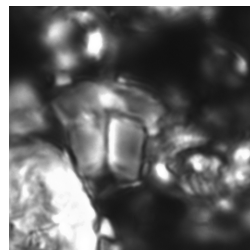
198



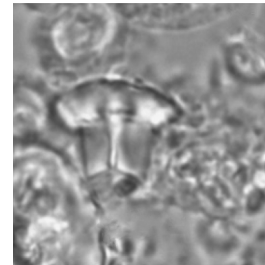
MS12/200



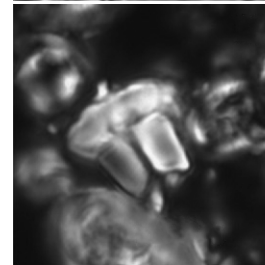
201



202



MS13/203

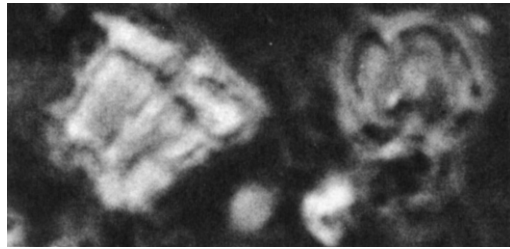


204

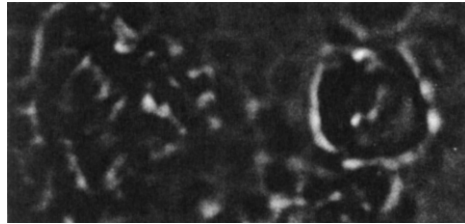


PNK77/205

Lithoptychius bitectus (continued)



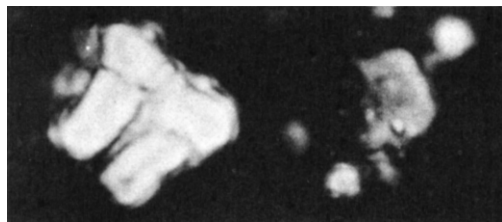
RPH73/206



207



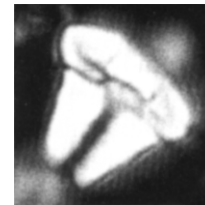
208



209



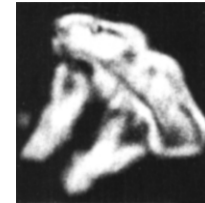
SE08/210



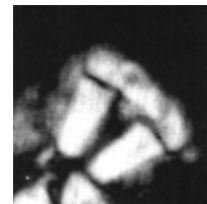
211



212



213

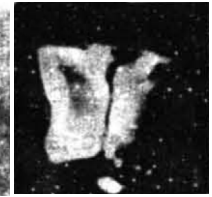


214

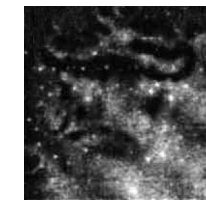
Fasciculithus barakati (continued)



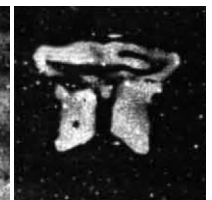
EDASA88/220



221



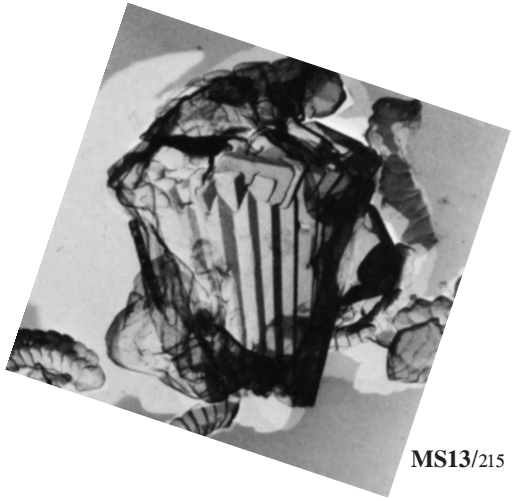
222



223

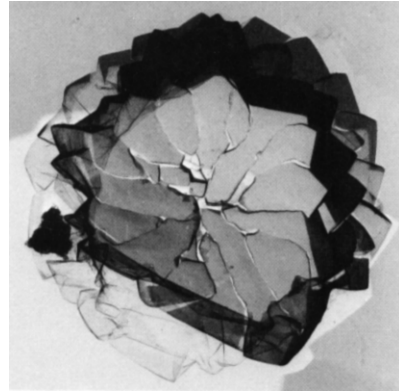
Lithoptychius bitectus (continued)

SIDE VIEW



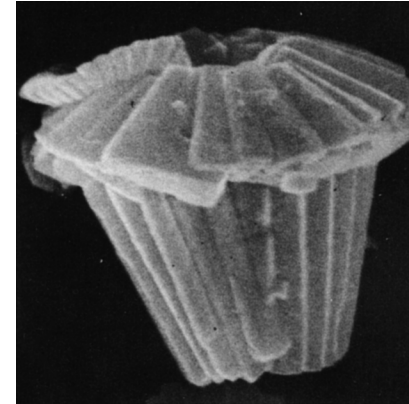
MS13/215

PROXIMAL FACE



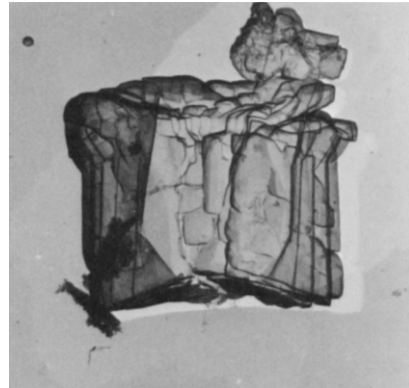
MS13/216

DISTAL FACE



HBU80/217

Lithoptychius sp. A (continued)



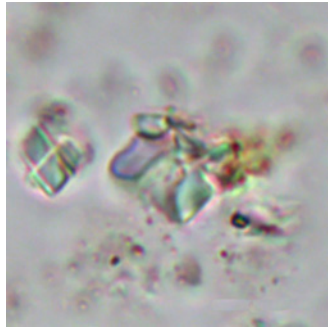
MS13/191

Lithoptychius sp. B [= *Lithoptychius* sp. 1
Aubry et al. 2011, p. 272, pl. 7, figs. 1a-d]

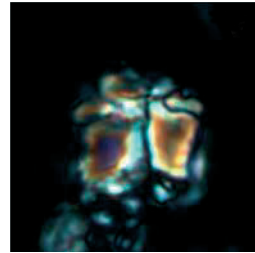
Lithoptychius sp. C [= *Fasciculithus* sp.
3 Bernaola et al. 2009, figs. 4v, 5a-d]

Lithoptychius schmitzii Monechi, Reale,
Bernaola & Balestra 2013 [= *Lithoptychius*
sp. 2 Aubry, Bord & Rodriguez 2011]

Lithoptychius sp. D [= *Fasciculithus* sp. 1
Prins 1971 pl. 6, figs. 5a-c]

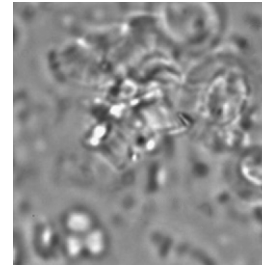


AMP11/224

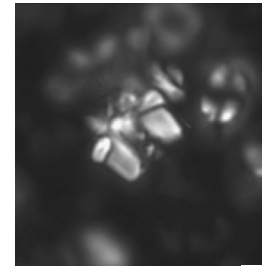


BG09/244

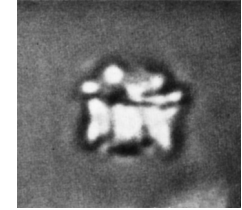
H



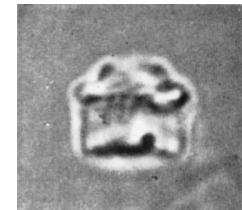
MS13/244



245



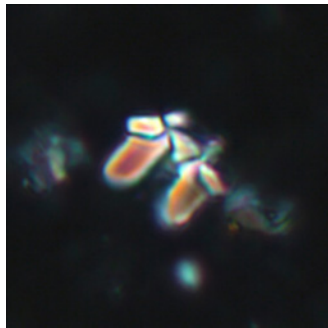
PB71/262



263



264



225

[Continued on page 66]

Lithoptychius sp. B

- 5–7 μm x 5–7 μm

- E. Paleocene (l. NP4). Egypt.

- Distinctive fasciculith, wider than high. The column is typically broader than high and possesses a broad central canal. Its proximal face is deeply concave proximally. Its distal surface is faceted, giving the impression that the different units of the fasciculiths are imbricated in one another. The innermost facet forms a triangular groove in which the central body is inserted. The outermost facet is occupied by the collaret, triangular in section and extending well beyond the periphery of the column with which it forms a sharp angle. The low, narrow, subvertical calyptra is inserted between the central body and the collaret to rests on the medial facet carved on the distal face of the column. The large central body is in the shape of an inverted cone (forming an isocetes triangle in axial view). Its base forms the bottom of the broad cavity delineated by the calyptra.

— In describing *Lithoptychius* sp. 2 Aubry et al. (2011, p. 272) commented (corrected text): *Lithoptychius* sp. 2 differs from *Lithoptychius* sp. 1 by 1) the shape of the column with distally convergent sides, 2) the shape and position of the collaret which is like a horizontal platform that is not restricted to the periphery of the column, and 3) by the shape of the low and broad calyptra which is curved inwards in lateral view. In *Lithoptychius* sp. 1 the section of the calyptra is triangular, pointing distally. The contact between the column and collaret is essentially horizontal in *Lithoptychius* sp. 2. It is strongly oblique in *Lithoptychius* sp. 1.

— The authors remarked (p. 272) that this taxon may correspond to *Fasciculithus* sp. 3 of Bernola, Martín-Rubio and Baceta, 2009, figs. 5A-D.

- AMP11 (p. 272), AMP (p. 29).

Lithoptychius sp. C

- ~6.5 μm x 6.5 μm

- E. Paleocene (l. Danian). Zumaya, Spain.

- Only illustrations were provided for this taxon.

- BG09 (p.84), AMP (p. 29).

Lithoptychius schmitzii

- 4.5–7.1 μm x 3.5–5.2 μm .

- l. E. Paleocene (l. Danian). South Atlantic (ODP 1262), Egypt, Spain.

- Rectangular column, broader than high and with a broad central canal which thickness may be as much as one third the width of the column. Collaret triangular in section, always extending beyond the periphery of the column. Calyptra subvertical, low, and narrow. It is inserted between the central body and the collaret on the distal face of the column.

≠ from *L. varolii* in the wider broad central canal and the smaller, concave and less prominent calyptra.

≠ from *L. chowii* in the wider central canal, the more evident collaret and the smaller and more delicate calyptra.

— Monechi et al. (2013, p. 38) indicated that the concept of *L. schmitzii* encompasses that of *Lithoptychius* sp. 1 Aubry, Bord & Rodriguez 2011, pl. 7, figs. 1a-d, 2a-d, 3a-d, 4a, b, 5a-c, 6a-c, and, questionably, of *Fasciculithus* sp. 3 Bernola, Martín-Rubio & Baceta 2009, figs. 5A-D. In the light of the description of *L. schmitzii*, the two latter taxa appear to comprise distinct morphotypes, some referable to *L. schmitzii*, others to as yet undescribed taxa. *L. schmitzii* is clearly synonym with *Lithoptychius* sp. 2 Aubry, Bord & Rodriguez 2011, pl. 8, figs. 1a-d. The following synonymy is proposed: *L. schmitzii* was previously cited as *Lithoptychius* sp. 2 Aubry, Bord & Rodriguez 2011, pl. 8, figs. 1a-d; *Lithoptychius* sp. 1 Aubry, Bord & Rodriguez 2011, pl. 7, figs. 2a-d, 6a-c; *Fasciculithus* sp. 3 Bernola, Martín-Rubio & Baceta 2009, fig. 5D.

- AMP11 (p. 272).

Lithoptychius sp. D

- ~6 μm x 4 μm

- L. Paleocene.

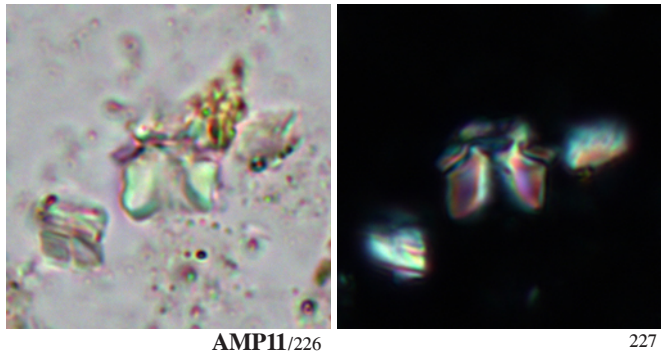
- “Plate covering the distal side of the tube [column], with a circular structure with central cavity, the apical spine, on top.”

- Prins (1971, p. 1027) described this taxon in relation to *F. tympaniformis* which he viewed as its ancestor: “the spiny part of *F. tympaniformis* develops into a plate...”. He also viewed this new taxon as ancestral to *Heliolithus*.

— Prins (1971) illustrated two specimens of the new taxon. Although they both belong, clearly, to *Lithoptychius*, they also represent distinct species. The specimen illustrated in plate 6, figs. 4a-c is assigned here to *L. janii*.

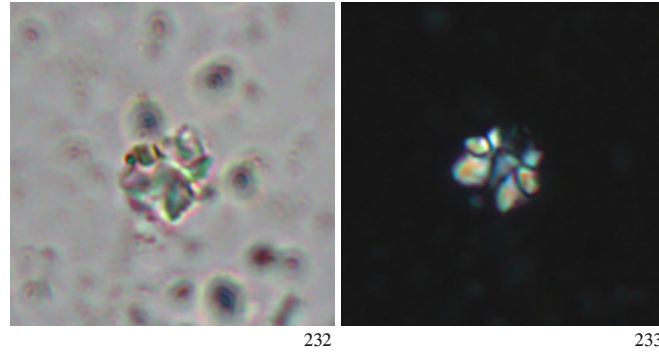
- PB71 (p. 1027), AMP (p. 29).

Lithoptychius sp. B (continued)



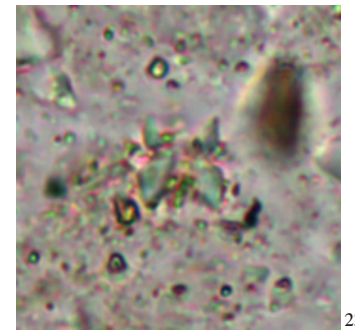
AMP11/226

227

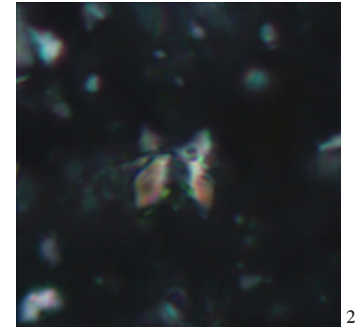


232

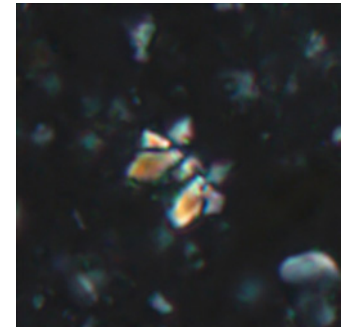
233



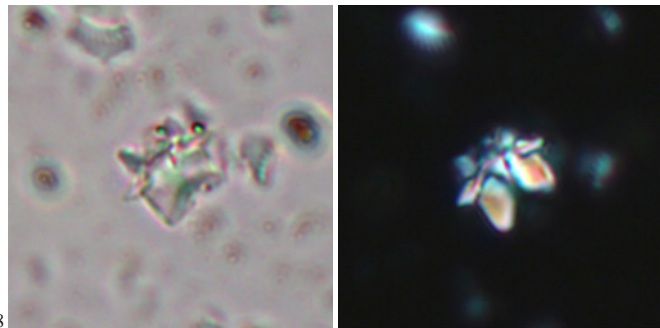
238



239

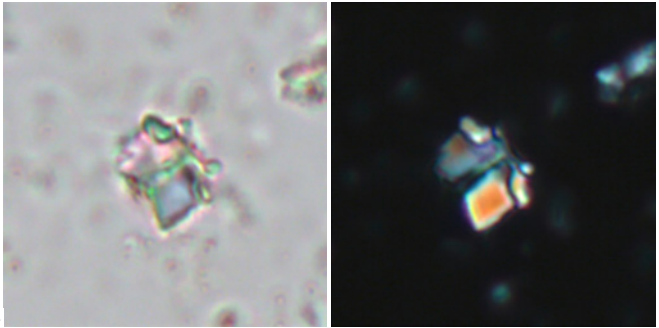


240



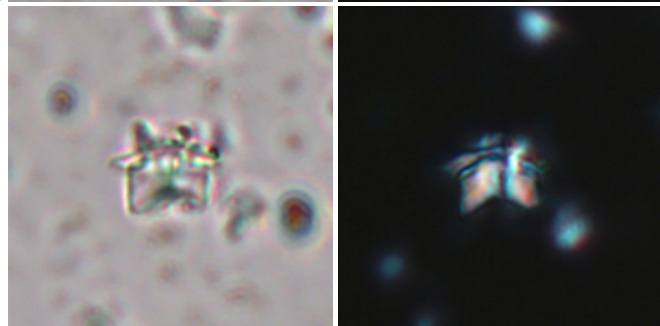
228

229



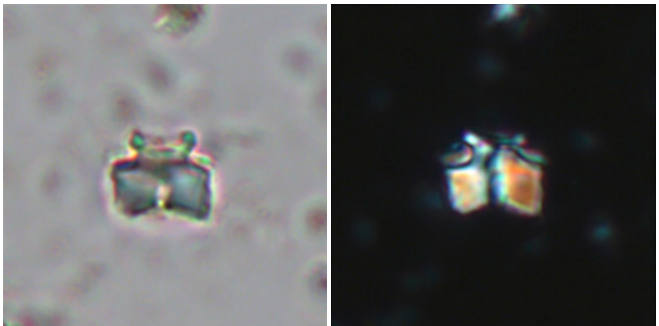
234

235



230

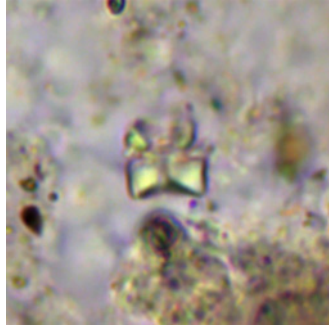
231



236

237

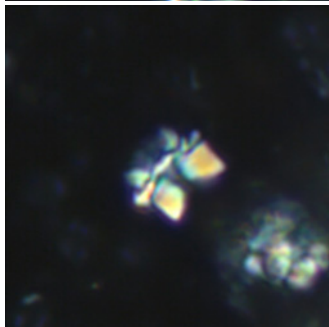
Lithoptychius sp. B (continued)



AMP11/241

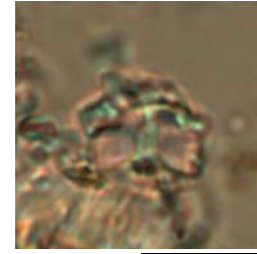


242

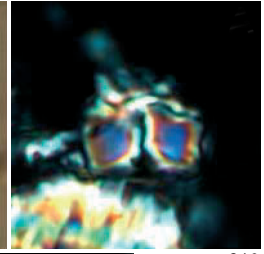


243

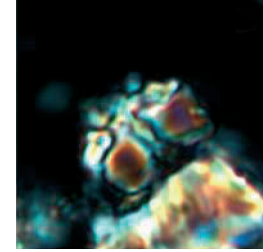
Lithoptychius sp. C (continued)



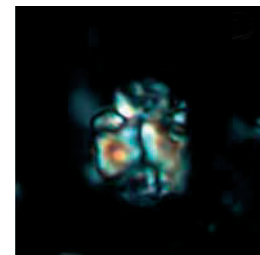
BG09/245



246

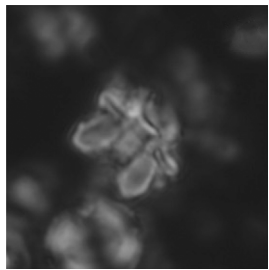


247

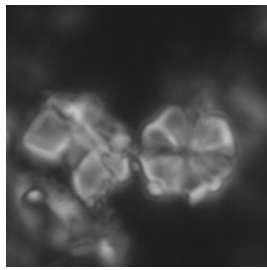


248

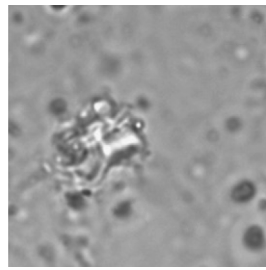
Lithoptychius schmitzii (continued)



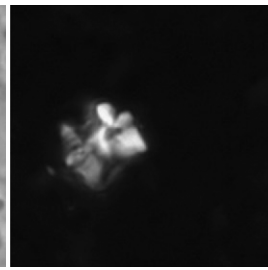
MS13/246



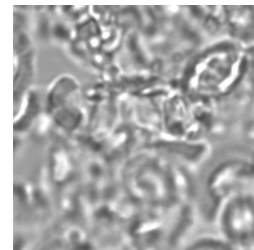
247



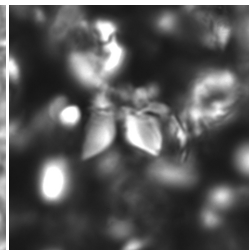
248



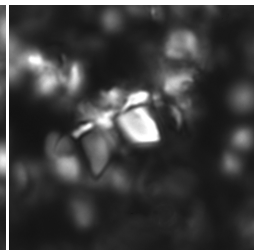
249



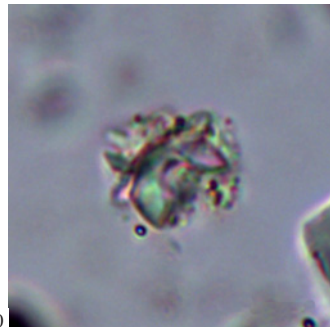
MS12/254



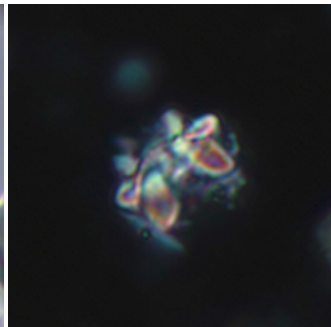
255



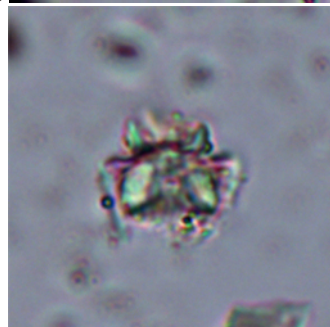
256



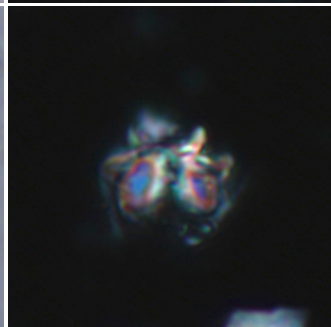
AMP11/250



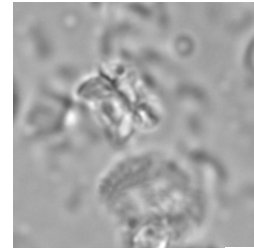
251



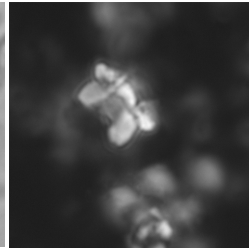
252



253

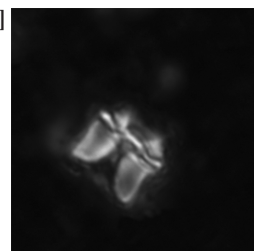


257

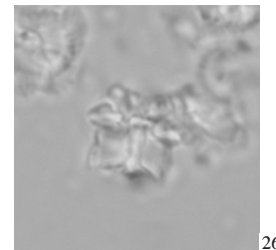


2548

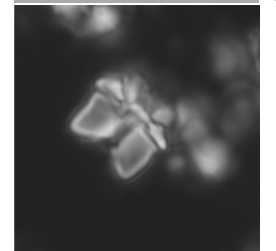
[cf.]



259



260



261

Lithoptychius vertebratoides (Steurbaut & Sztrákos) Aubry in Aubry et al. 2011 [= *Fasciculithus vertebratoides* Steurbaut & Sztrákos 2008; = *Fasciculithus janii* Perch-Nielsen 1971a, pl. 14, figs. 37-39]

H



SE08/265

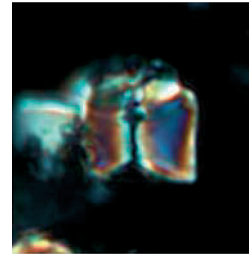
Lithoptychius ulii (Perch-Nielsen) Aubry et al. 2011 [= *Fasciculithus ulii* Perch-Nielsen 1971]



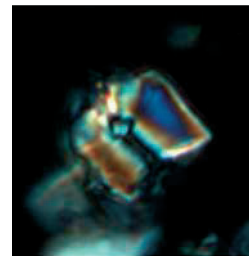
PNK71a/287

288

Lithoptychius sp. E [= *Fasciculithus* sp. 5 Bernaola, Martín-Rubio & Baceta 2009 figs. 5i, j]

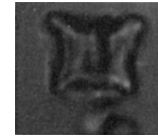


BG09/339

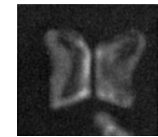


340

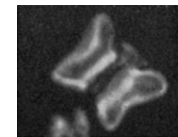
Lithoptychius billii (Perch-Nielsen) Aubry et al. 2011 [= *Fasciculithus billii* Perch-Nielsen 1971]



PNK71a/341



342



343

Lithoptychius vertebratoides

- 5.6–7.2 μm x 5.6–8 μm

- E. Paleocene (l. Danian) (l. NP4).

- Egg-timer-shaped fasciculith in side view, resembling fish vertebrae. Proximal column with series of conspicuous surface ridges and deep grooves, strongly birefringent with irregular color pattern. Low distal cone present, consisting of a cylindrical ring of elements with a width $\sim 1/3$ maximum width of the fasciculith. In single polarized light this ring forms two low knobby protrusions.

\neq from *L. janii* (Perch-Nielsen, 1971, pl. 5, fig. 1 = holotype) by the egg-timer shape, absence of distal cap and difference in birefringence (“irregular pattern with higher order colors e.g. deep blue”, Steurbaut and Sztrákos, 2008, p. 24).

- Remarks. Early forms ($\sim 5.6 \mu\text{m}$ x $5.6 \mu\text{m}$; width at center $\sim 4.5 \mu\text{m}$) much smaller than later ones ($7.2 \mu\text{m}$ x $8 \mu\text{m}$; width at center $\sim 5.6 \mu\text{m}$).

- SE08 (p. 25, 26), PNK71a (p. –), AMP11 (p. 272).
UNIT 5

Lithoptychius ulii

- 5–7 μm x 5–10 μm

- L. Paleocene (NP9). Bay of Biscay (DSDP, Site 119), Atlantic.

- [Almost parallel-sided column made of a variable number of protruding or inflated elements. Distal side topped with a truncated cone consisting of one or more flat cycles of elements. The height of the column, that of the cone, the number of wedges and the total size of the sp. vary greatly.]

\neq from *L. janii* by the absence of a flange;
 \neq from *L. bobii* by the cylindrical distal structure;
 \neq from *L. billii* by the presence of a distal structure.

— FAD in NP4. LAD given in NP5 by Romein (1979, p. 77), but in NP7 by Varol (1989, p. 276).

— Was thought to have evolved from *L. magnus* (Romein, 1979, p. 77).

— The collaret in *L. ulii* is inserted within the distal end of the column, barely extending above it (see holotype: Perch-Nielsen 1971a, pl. 2, fig. 3). As a result in cross-polarized light only weak extinction lines delineate the collaret from the column and calyptra (Aubry in Aubry et al., 2011, p. 273).

- PNK71a (p. 350), AMP11 (p. 273).

Lithoptychius sp. E

- $\sim 6 \mu\text{m}$ x $6.6 \mu\text{m}$

- E. Paleocene (l. Danian). Zumaya, Spain.

- Only illustrations were provided for this taxon.

- BG09 (p. –), AMP (p. 29).

Lithoptychius billii

- 5–8 μm x 5–8 μm

- M. Paleocene (NP5). Bay of Biscay (DSDP Site 119), Atlantic.

- [Column slightly widened at the distal and proximal ends, but without a distinct flange. Composed of wedges separated by deep furrows. Distal end flat, consisting of several concentric cycles of small elements.]

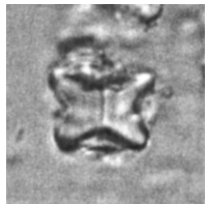
\neq from other spp. by the flat distal side, the length of the depressions between the wedges and the angles of the column.

— The flat distal side is similar to the distal side of *Discoaster multiradiatus*.

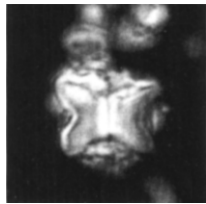
— Restricted to upper Zone NP5 (Romein, 1979, p. 77).

- PNK71a (p. 352), AMP11 (p. 272).

Lithoptychius vertebratoides (continued)



SE08/266



267



270



268



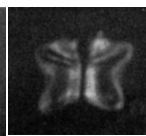
271



269



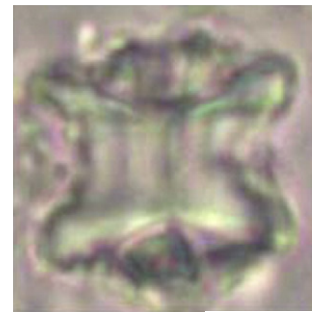
PNK71a/275



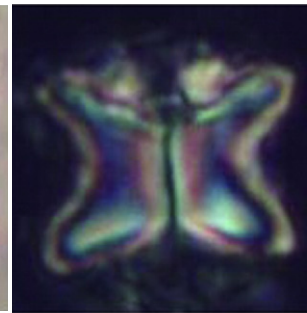
276



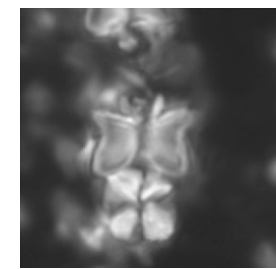
277



DTJ10/272



273



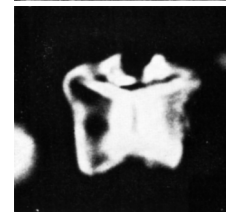
MS13/274



PB71/278



279



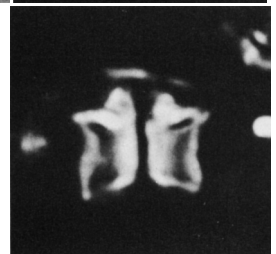
280



PDF78/281

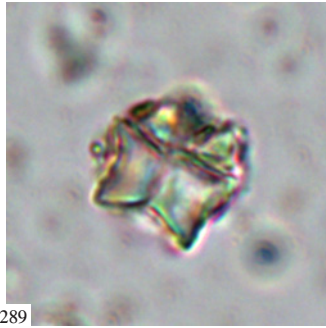
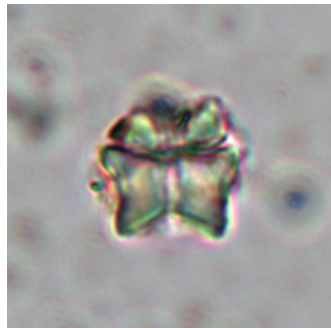


282



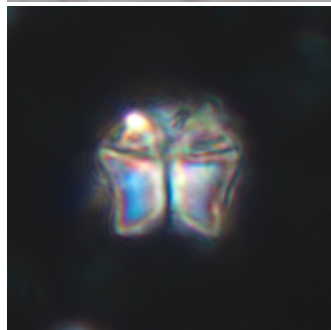
283

Lithoptychius ulii (continued)

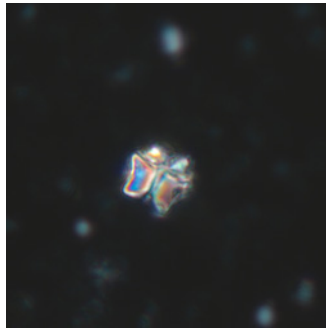


AMP11/289

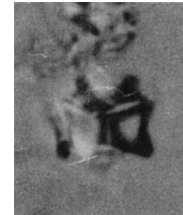
291



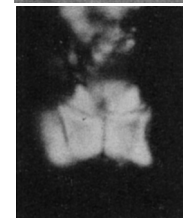
290



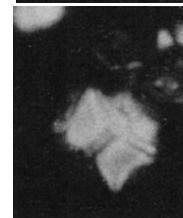
292



PNK77/293

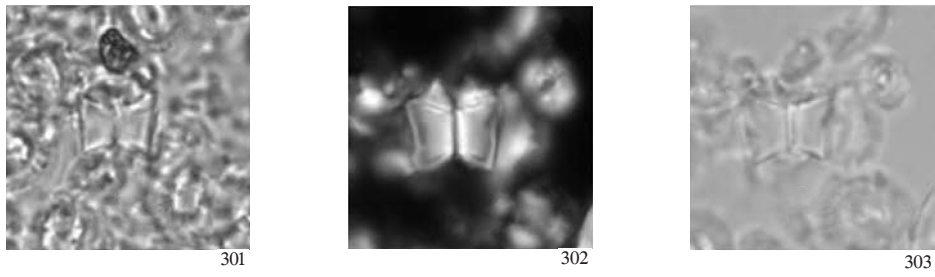
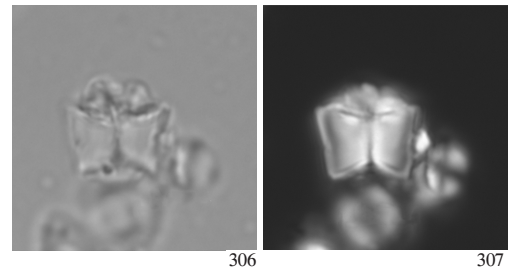
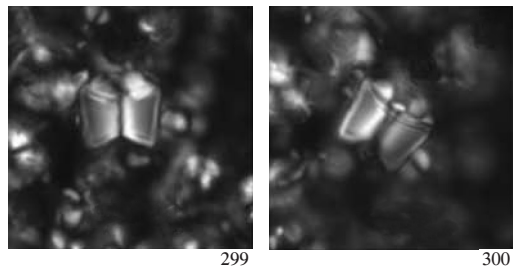
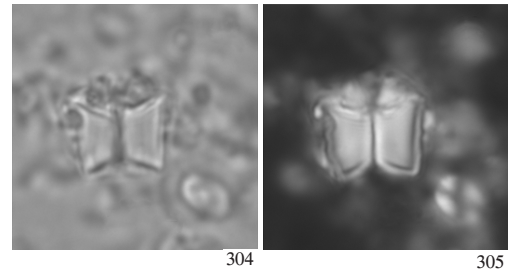
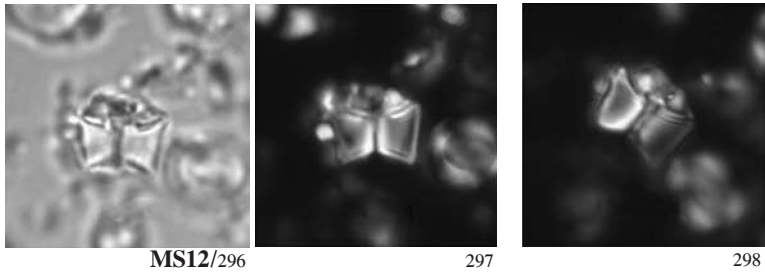


294

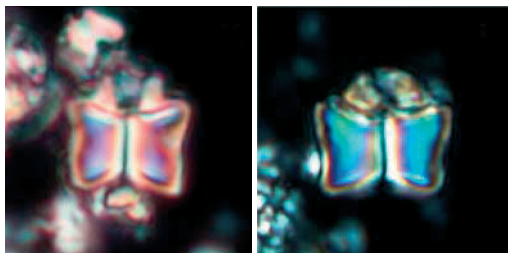


295

Lithoptychius ulii (continued)

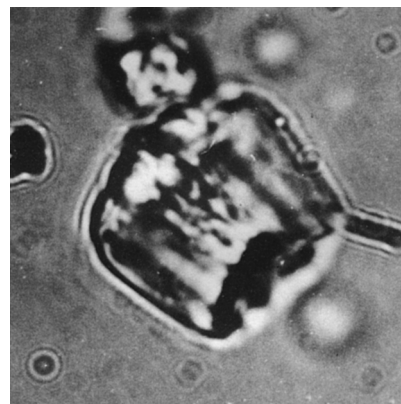


Lithoptychius ulii (continued)

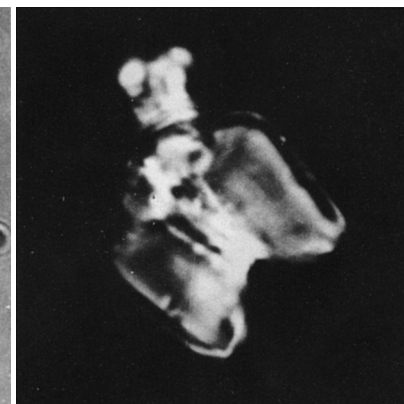


BG09/308

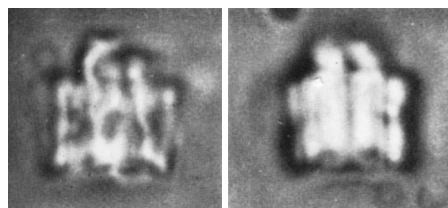
309



MS85/310

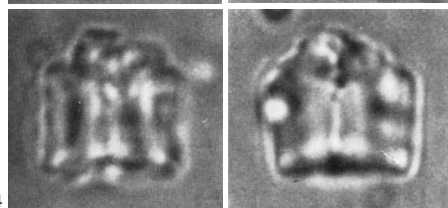


311



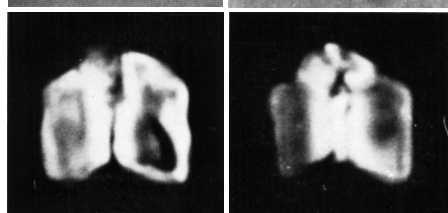
PB71/312

313



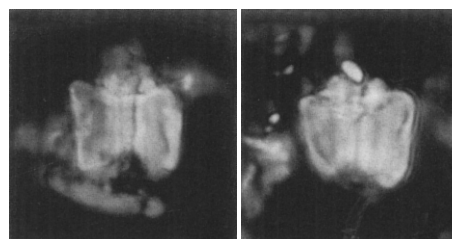
314

315



316

317

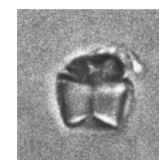


SE02/318

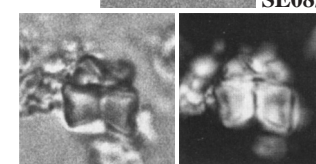
319



320

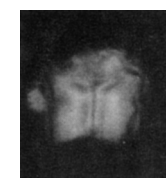


SE08/321



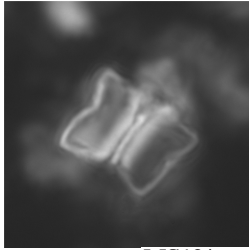
322

323

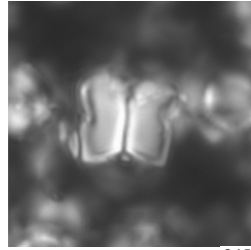


24/324

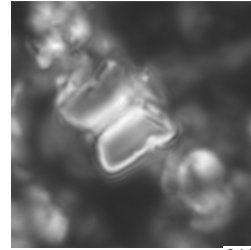
Lithoptychius billii (continued)



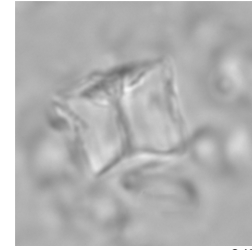
MS12/344



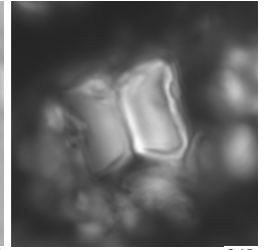
345



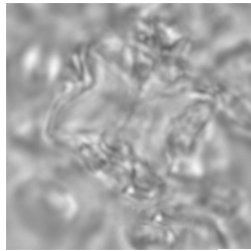
346



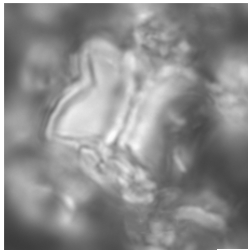
347



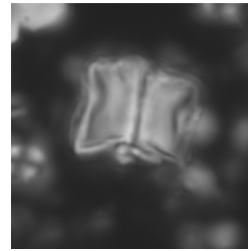
348



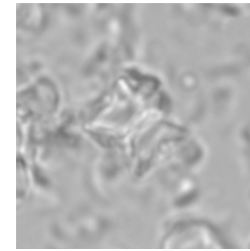
349



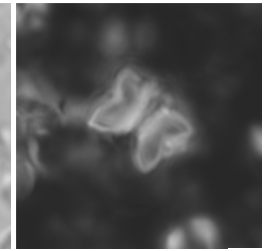
350



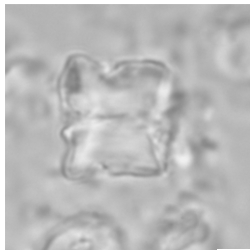
351



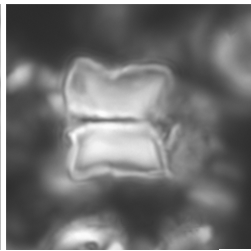
352



353

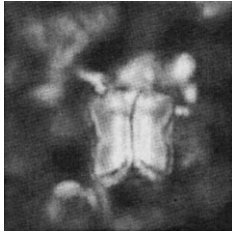


354

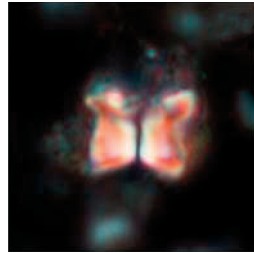


355

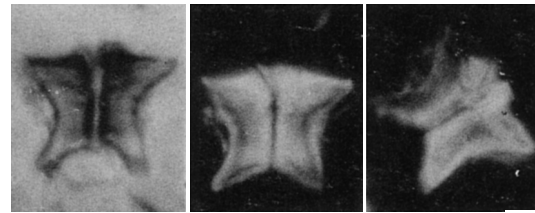
Lithoptychius billii (continued)



AC07/356



BG09/357



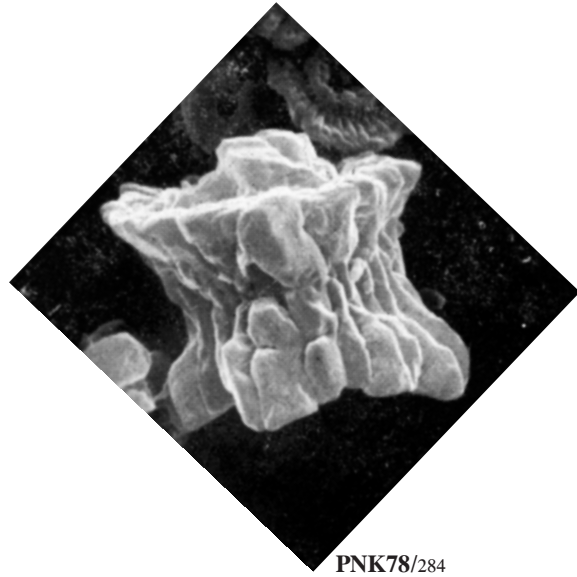
PNK77/358

359

360

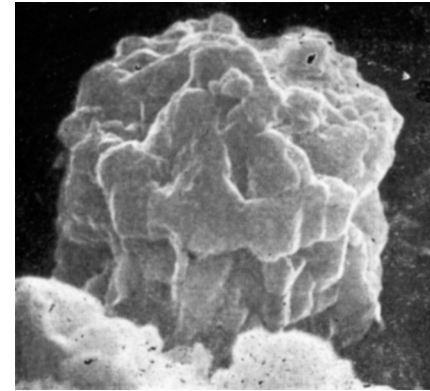
Lithoptychius vertebratoides (continued)

SIDE VIEW

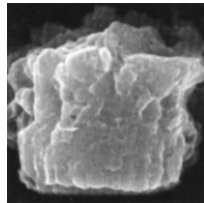


PNK78/284

DISTAL FACE



PNK78/286



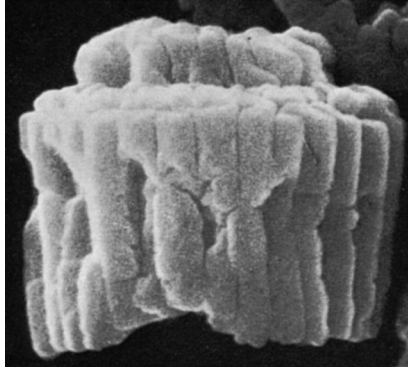
SE08/285

Lithoptychius ulii (continued)

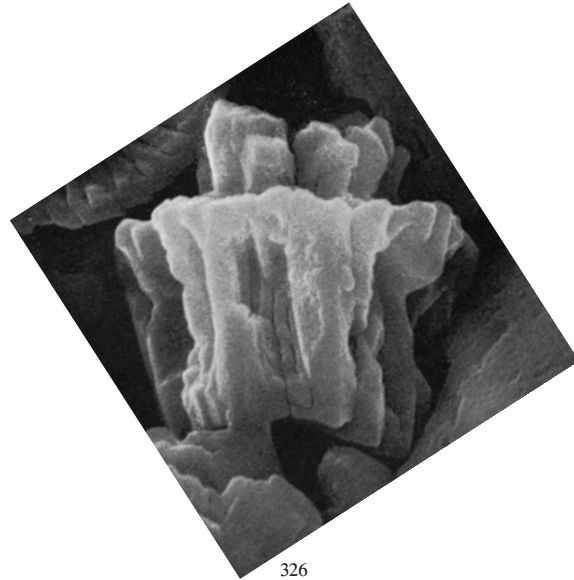
SIDE VIEW

PROXIMAL FACE

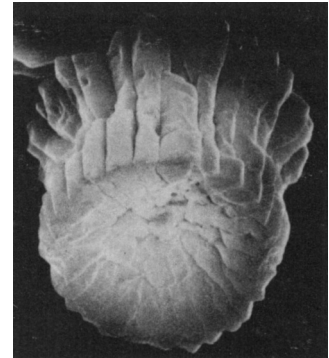
H



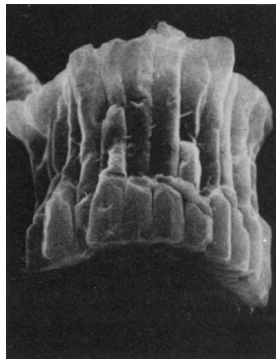
PNK71a/325



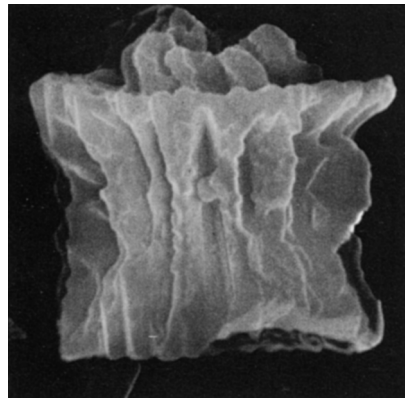
326



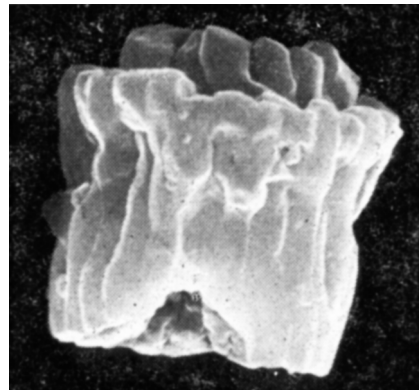
PNK77/330



PNK77/327



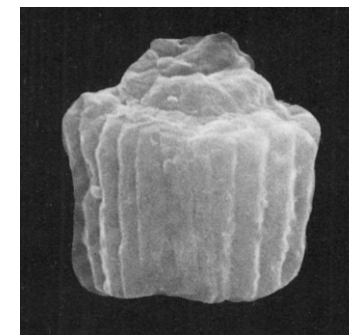
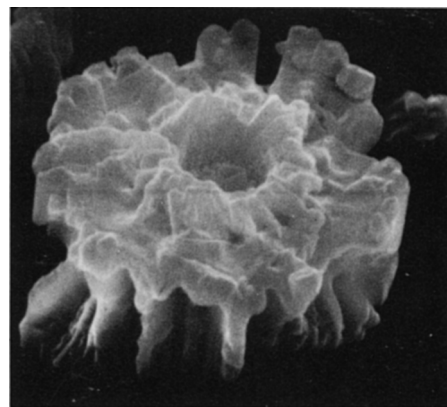
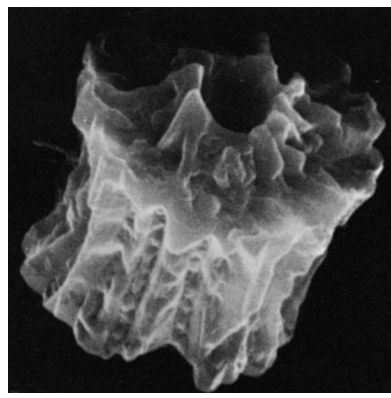
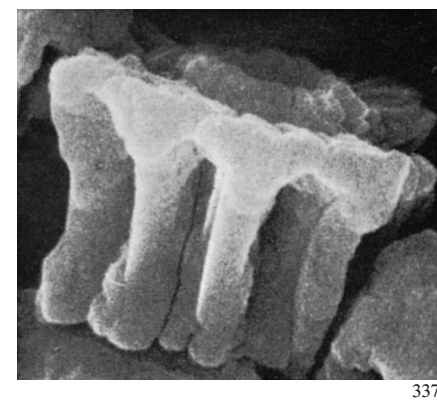
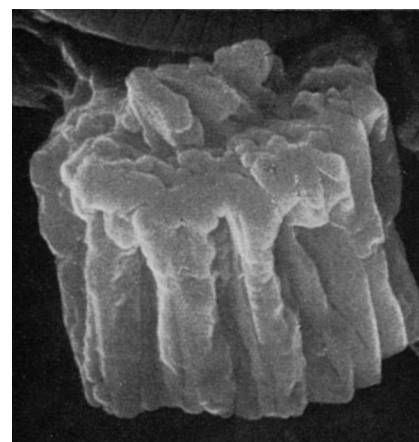
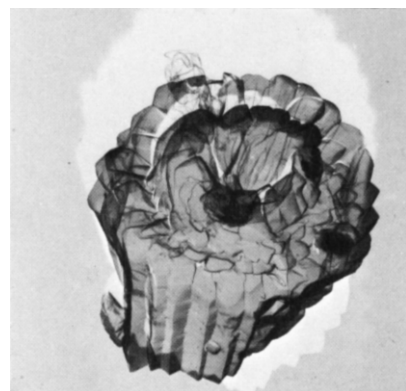
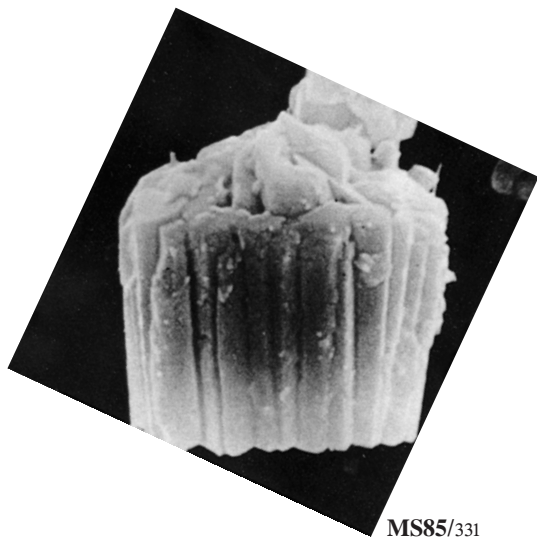
328



PNK78/329

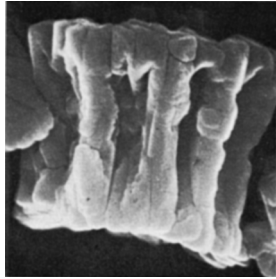
Lithoptychius ulii (continued)

DISTAL FACE

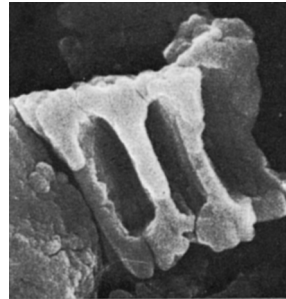


Lithoptychius billii (continued)

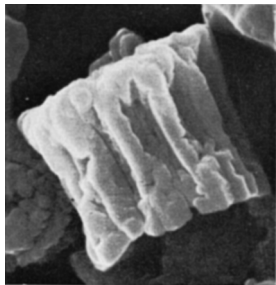
SIDE VIEW



PNK71a/361

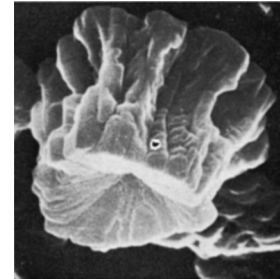


363

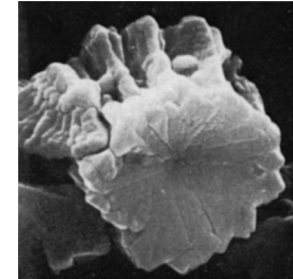


362

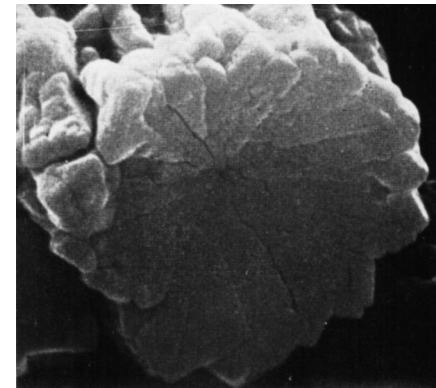
PROXIMAL FACE



PNK71a/364



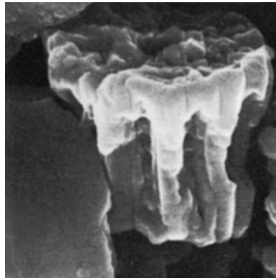
365



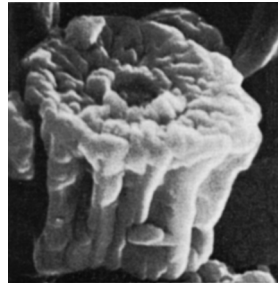
PNK71b/366

Lithoptychius billii (continued)

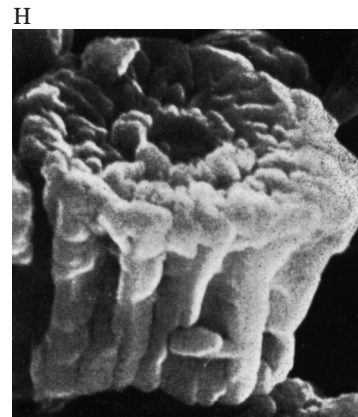
DISTAL FACE



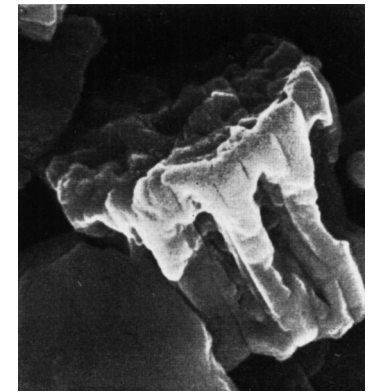
PNK71a/367



368



H
PJ77/369



370

Figure References

- AC07.** AGNINI, C., FORNACIARI, E., RAFFI, I., RIO, D., RÖHL, U. and WESTERHOLD, T., 2007. *Marine Micropaleontology*, 64: 215–248.
(356): 2/7 (as *Fasciculithus billii*)
- AMP11.** AUBRY, M.–P., BORD, D. and RODRIGUEZ, O., 2011. *Micropaleontology*, 57: 269–287.
(5-16): 9/1a-d, 2a-d, 3a-d (*L. varolii*)
(17-20): 9/4a-d (*L. varolii*)
(33-36): 4/1a-d (*L. collaris*)
(37-48): 4/1e-1p (*L. collaris*)
(49-52): 4/2a-d (*L. collaris*)
(57-60): 5/1a-d (*L. felis*)
(61-72): 5/2a-d, 3a-d, 4a-d (*L. felis*)
(73-76): 5/5a-d (*L. felis*)
(86-89): 8/2a-d (*L. jani*)
(116-119): 8/3a-d (*L. merloti*)
(165-168): 6/1a-d (*L. stegastos*)
(169-180): 6/2a-d, 3a, b, 4a-f (*L. stegastos*)
(181-184): 6/5a-d (*L. stegastos*)
(224-227): 7/1a-d (*Lithoptychius* sp. 1)
(228-231): 7/2a-d (as *Lithoptychius* sp. 1)
(241-243): 7/6a-c (as *Lithoptychius* sp. 1)
(232-240): 7/4a, b, 3a-d, 5a-c (*Lithoptychius* sp. 1)
(250-253): 8/1a-d (*Lithoptychius* sp. 2)
(289-292): 8/4a-d (*L. ulii*)
- AMP.** AUBRY, M.–P., this volume.
- BG09.** BERNAOLA, G., MARTIN–RUBIO, M. and BACETA, J. J., 2009. *Geologica Acta*, 7: 79–92.
(21-23): 4/S-U (as *Fasciculithus* sp. 2)
(143): 5/T (*F. pileatus*)
(185-188): 5/E-H (as *Fasciculithus* sp. 4)
(193-194): 5/N, O (as *Fasciculithus jani*)
(244): 4/V (as *Fasciculithus* sp. 3)
(245-248): 5/A-C, D (as *Fasciculithus* sp. 3)
(308, 309): 5/K, L (as *Fasciculithus ulii*)
(339, 340): 5/I, J (as *Fasciculithus* sp. 5)
(357): 5/M (as *Fasciculithus billi*)
- BD73a.** BUKRY, D., 1973a. In: Heezen, B. C., MacGregor, I. D., et al., *Initial Reports of the Deep Sea Drilling Project*, 20, 307–317. Washington, D. C.: U.S. Government Printing Office.
(135, 136): 1/7, 8 (as *F. pileatus*)
(137-140): 2/2-5 (as *F. pileatus*)
(141): 1/9 (as *F. pileatus*)
(142): 2/1 (as *F. pileatus*; =*F. bitectus*?)
- DTJ10.** DINARÈS-TURELL, J., STOYKOVA, K., BACETA, J. I., IVANOV, M. and PUJALTE, V., 2010. *Palaeogeography, Palaeoclimatology, Palaeoecology*, 12: 169–191.
(24-26): 5/19, 18, 17 (17, 18: as *Fasciculithus* sp. 2 or sp. 3 of Bernaola; 19: as *Fasciculithus* sp. 2 of Bernaola)
(272, 273): 3/12–11 (as *Fasciculithus vertebratoides*)
- EDASA88.** EL-DAWOODY, A.S.A., 1988. *Bulletin of the Faculty of Sciences*, Cairo University, 56: 549-564.
(218, 219): 1/5a, b (as *Fasciculithus barakati*)
(220-223): 1/6a, b, 7a, b (as *Fasciculithus barakati*)
- HBU80.** HAQ, B. U. and AUBRY, M.–P., 1980. In: Salem, M. J. and Busrewil, M. T. (Eds.), *The geology of Libya, Volume 1*, 271–304. London: Academic Press.
(132-134): 1/11-13 (as *F. stonehengi*) (? syn. *F. bitectus*)
(195, 196): 1/7, 8 (as *F. jani*)
- MS85.** MONECHI, S., 1985. In: Heath G. R., Burckle L. H., et al., *Initial Reports of the Deep Sea Drilling Project*, 86, 301–336. Washington, D. C.: U.S. Government Printing Office.
(197, 198): 7/7a, b (as *F. pileatus*)
(217): 7/4 (as *F. pileatus*; same specimen as 7/7a, b)
(310, 311): 7/6a, b (as *F. ulii*)
(331): 7/3 (as *F. ulii*; same specimen as 7/6a, b)
- MS12.** MONECHI, S., REALE, V., BERNAOLA, G. and BALESTRA, B., 2012. *Micropaleontology*, 58: 351–365.
(27-32): 4/9, 10, 14, 15, 17, 16 (*L. varolii*)
(53-56): 4/2, 1, 3, 4 (as *L. chowii*)
(77, 78): 3/15–14 (as *L. schmitzii*)
(120-122): 3/13, 11, 12 (as *L. cf. L. jani*)
(149-161): 5/3, 1, 2, 4, 5-7, 9, 8, 11, 10, 13, 12 (*L. pileatus*)
(200-202): 3/25, 24, 20 (as *L. jani*)
(254-261): 3/5, 3, 4, 7, 6, 9, 8, 10 (*L. schmitzii*)
(296-303): 4/20, 18, 19, 21-25 (*L. ulii*)
(304-307): 3/19, 18, 17, 16 (*L. ulii*)
(344-355): 5/14–16, 18, 17, 20, 19, 21, 23, 22, 25, 24 (*L. billii*)
- MS13.** MONECHI, S., REALE, V., BERNAOLA, G. and BALESTRA, B., 2013. *Marine*

- Micropaleontology*, 98: 28–40.
 (162): 1/19 (*L. pileatus*)
 (203, 204): 1/22–21 (as *L. jani*)
 (244–249): 1/9, 8, 13, 14, 12, 11 (*L. schmitzii*)
 (274): 1/24 (*L. vertebratooides*)
- OH79.** OKADA, H. and THIERSTEIN, H. R., 1979. In: Tucholke, B. E., Vogt, P. R., et al., *Initial Reports of the Deep Sea Drilling Project*, 43, 507–573. Washington, D. C.: U.S. Government Printing Office.
 (189, 190): 6/10b, a (as *Fasciculithus* sp. 1)
 (191): 17/8 (as *Fasciculithus* sp. 1)
 (215, 216): 17/2, 3 (as *F. pileatus*)
 (332): 17/7 (as *F. ulii*)
- PJ77.** PAVŠIČ, J., 1977. *Geologija Razprave in Porocila*, 20: 33–57.
 (113–115): 7/1–3 (as *F. merloti*) (Figs. 1, 3: *L. jani* or *L. bitectus*; Fig. 2: *L. pileatus*)
- PNK71a.** PERCH–NIELSEN, K., 1971a. *Meddelelser fra Dansk Geologisk Forening*, 20: 347–361.
 (93): 5/4. (as *F. jani*)
 (104–106): 5/1–3. (as *F. jani*; 2, 3: also Perch–Nielsen 71c, pl. 1, figs. 2, 3)
 (275–277): 14/37–39 (as *F. jani*)
 (287, 288): 14/17, 18 (as *F. ulii*)
 (325, 326): 2/3, 2 (as *F. ulii*)
 (336, 337): 2/1, 4 (as *F. ulii*)
 (341–343): 14/31–33 (as *F. billii*)
 (361, 362): 5/6, 9 (as *F. billii*)
 (363): 4/11 (as *F. billii*)
 (364, 365): 5/7, 10 (as *F. billii*; 5, 8, 10: also Perch–Nielsen, 1971c, pl. 1, figs. 6–8 reproduced herein)
 (367, 368): 5/5, 8 (as *F. billii*; 5, 8, 10: also Perch–Nielsen, 1971c, pl. 1, figs. 6–8 reproduced herein)
- PNK71b.** PERCH–NIELSEN, K., 1971b. In: Farinacci, A. (Ed.), *Proceedings of the II Planktonic Conference, Roma 1970, Volume 2*. 939–980. Rome: Ediz. Tecnoscienza.
 (366): 1/6 (as *F. billii*; also Perch 71a, pl. 5, 10)
 (369, 370): 1/8, 7 (as *F. billii*; also Perch 71a, pl. 5, 10, 8)
- PNK77.** PERCH–NIELSEN, K., 1977. In: Supko, P. R., Perch–Nielsen, K., et al., *Initial Reports of the Deep Sea Drilling Project*, 39, 699–823. Washington, D. C.: U.S. Government Printing Office.
 (93–103): 12/9, 13, 2–5, 8, 10–12 (as *F. jani*)
 (107–111): 12/14–18 (as *F. jani*)
 (205): 49/26 (as *F. jani*)
 (293–295): 49/23–25 (as *F. ulii*)
 (327): 10/20 (as *F. ulii*)
 (328): 11/1 (as *F. ulii*)
 (330): 10/18 (as *F. ulii*)
 (333): 10/19 (as *F. ulii*)
 (334): 11/2 (as *F. ulii*)
 (335): 11/3 (as *F. ulii*)
 (358–360): 49/27–29 (as *F. aff. billii*)
- PNK78.** PERCH–NIELSEN, K., SADEK, A., BARAKAT, M. G. and TELEB, F., 1978. *Annales des Mines et de la Géologie*, 28: 337–403.
 (284): 15/9 (as *Fasciculithus* sp.)
 (286): 15/10 (as *Fasciculithus* sp.)
 (329): 15/8 (as *Fasciculithus ulii*)
- PB71.** PRINS, B., 1971. In: Farinacci, A. (Ed.), *Proceedings of the II Planktonic Conference, Roma, 1970, Volume 1*: 1017–1037. Rome: Ediz. Tecnoscienza.
 (90–92): 6/4a–c (as *Fasciculithus* spec. 1)
 (123–125): 6/12a–c (as *Discoasteroides megastypus*)
 (262–264): 6/5a–c (as *Fasciculithus* spec. 1)
 (278–280): 6/3a–c (as *F. tympaniformis* / *Fasciculithus* spec. 1)
 (312, 314, 316): 6/1a–c (as *F. tympaniformis*)
 (313, 315, 317): 6/2a–c (as *F. tympaniformis*)
- PDF78.** PROTO DECIMA, F., MEDIZZA, F. and TODESCO, L., 1978. In: Bolli, H. M., Ryan, W. B. F., et al., *Initial Reports of the Deep Sea Drilling Project*, 40, 571–634. Washington, D. C.: U.S. Government Printing Office.
 (281–283): 12/1a–c (as *Fasciculithus jani*)
- RAJT79.** ROMEIN, A. J. T., 1979. *Utrecht Micropaleontological Bulletins*, 22: 1–231.
 (131): 5/1 (as *F. jani*)
 (192): 9/15 (as *F. bitectus*)
 (338): 4/7 (as *F. ulii*)
- RPH73.** ROTH, P. H., 1973. In: Winterer, E. L., Ewing, J. L., et al., *Initial Reports of the Deep Sea Drilling Project*, 17, 695–795. Washington, D. C.: U.S. Government Printing Office.
 (144, 145): 16/2a, b (as *Fasciculithus* sp. cf. *F. ulii*)
 (206–209): 16/1a–d (as *Fasciculithus* sp. cf. *F. ulii*)
- SE02.** STEURBAUT, E. and SZTRÁKOS, K., 2002. *Revue de Micropaléontologie*, 45: 195–219.
 (112): 3/11 (as *F. jani*)
 (126): 4/10 (as *F. pileatus*)
 (127, 128): 3/10a, b (as *F. jani*)
 (318–320): 4/11–13 (as *F. ulii*)

SE08. STEURBAUT, E. and SZTRÁKOS, K., 2008. *Marine Micropaleontology*, 67: 1-29.

(1-4): 2/18a, b, 17a, b (as *F. varolii*)

(146-148): 3/25b, a, 26 (as *F. pileatus*)

(163, 164): 3/23, 24 (as *F. pileatus*)

(210-214): 3/11-15 (as *F. jani*)

(266-271): 3/1a, b, 2a, b, 3, 4 (as *F. vertebratoides*)

(265): 3/5 (as *F. vertebratoides*)

(285): 3/21 (as *F. vertebratoides*)

(321-323): 2/19, 20a, b (as *F. ulii*)

VO89. VAROL, O., 1989. In: Crux, J. A. and van Heck, S. E. (Eds.), *Nannofossils and their applications*, 267-310. Chichester: Ellis Horwood Limited.

(79-81): 12.5/11-13 (as *F. chowi*)

(129, 130): 12.5/1, 2 (as *F. jani*)

(324): 12.5/10 (as *F. ulii*)

VO13. VAROL, O., 2013. Personal e-mail communication to author of 16 April 2013

(82-85): four unpublished photographs of *L. chowii*, from paratype locality

FASCICULITHUS

HIGHLIGHTS:

- Honeycomb fasciculiths consisting of two monocyclic structural units: the column and calyptra.
- Fasciculiths are convex distally with calyptra ranging from gently conical to needle-shaped.
- 14 formally described species, with at least one synonymy; two forms in open nomenclature.
- Size range: 4–17 μm x 6–17 μm .
- Coccosphere unknown.
- Stratigraphic range: Zone NP5 to NP9/NP10 zonal boundary.
- *Lithoptychius* was the most likely ancestor.

SELECTED READING

Perch-Nielsen, 1971a; Raffi and de Bernardi, 2008; Romein, 1979; Wise and Wind, 1977.

INTRODUCTION

Fasciculithus tympaniformis and *F. involutus* are the quintessential fasciculiths: pyramidal to conical with a broad base, gently tapering towards the distal end, and divided by a narrow central canal that confers bilateral symmetry. *Fasciculithus involutus* is representative of most species in the genus, in that the alveolar pattern on the column has the typical honeycomb texture. In light microscopy and in side view, whether using bright field or crossed nicols, the *Fasciculithus* fasciculiths appear to be formed of two symmetrical longitudinal units. The (proximal) column and the (distal) calyptra are each a monocyclic structural unit, although the suture is not accentuated by a dark line in cross-polarized light.

MORPHOLOGY AND STRUCTURE

Morphology – As seen in side view and longitudinal section, the fasciculiths are cylindrical to broadly conical (text-figs. 1, 2). The proximal end may be slightly to strongly concave. The distal end may be rounded, or extend into a needle-shape projection which, in some species, is as tall as the main body of the fasciculith. The central canal along the vertical axis opens distally (e.g., *F. sidereus*: Bybell and Self-Trail, 1995, pl. 16, fig. 4a, 5a; *F. thomasii*: op. cit., pl. 17, fig. 4a; *F. involutus*, op. cit., pl. 16, fig. 16a) and proximally (e.g., *F. sidereus*: op. cit., pl. 16, fig. 3a; *F. involutus*: op. cit., pl. 16, fig. 7b). The distal opening is narrow and may be obliterated because of overgrowth (e.g., Perch-Nielsen, 1971a, pl. 1, fig. 7). In most species, the surface of the column is pitted with depressions aligned in superposed rows, creating a honeycomb pattern (e.g., Bown and Pearson, 2009, fig. 4, lower two rows).

Because external morphology is essentially determined by internal structure, additional morphologic characters are discussed below in the description of structural characters.

Structure – The fasciculiths of *Fasciculithus* are comprised of a column and a calyptra that, while separate monocyclic units, are prolongation of one another, so that (in most species) they are only distinguishable by the different orientation of their elements as seen in the SEM.

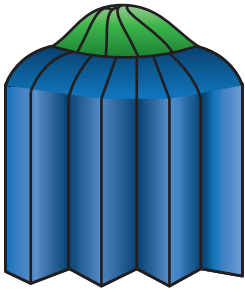
Column: This structural unit consists of a single cycle of ~15 to 25 tall elements that are wedge-shaped in cross section and

arranged radially around the central canal (e.g., Wise and Wind, 1977, pl. 15, figs. 1, 2; text-fig. 3). In *F. tympaniformis*, the elements are essentially regularly arranged so as to confer a rosette shape to the proximal face, although with an modified LS pattern (e.g., Wise and Wind, 1977, pl. 16, fig. 3; text-figs. 3a, 4). However, in most species, the elements are paired so that the proximal face of the column is stellate while its sides exhibit a pattern of broad grooves alternating with pronounced, vertical ridges (e.g., *F. schaubii*, Perch-Nielsen, 1971a, pl. 7, fig. 6; *F. richardii*, ibid., pl. 8, fig. 2; text-figs. 3b, 5). The ridges are narrow, regular and straight, with vertical sutures that mark the contact between adjacent elements (e.g., *F. schaubii*, Perch-Nielsen, 1971a, pl. 7, fig. 6; *F. liliana*, ibid., pl. 6, fig. 4; also visible in the LM: e.g., *F. hayi*, Haq, 1971, pl. 1, fig. 3). In the grooves, the elements are deeply pitted, producing the typical honeycomb alveolar pattern with fenestrae arranged in one to five superposed concentric rows (text-figs. 5b, 6b). In some species single rows occur in the upper half of the column. Overgrowth and recrystallization often alter the regularity of this distinctive pattern.

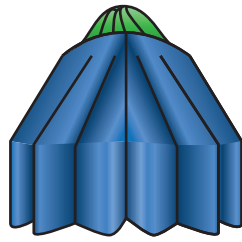
The column is always concave proximally, but several distal configurations are possible (text-figs. 1, 2). Where the distal end is flat (as in *F. aubertae*, Perch-Nielsen, 1971a, pl. 2, fig. 6), the calyptra separates easily from the column. In most taxa, however, the upper part of the column tends to develop a lateral shoulder, above which the column decreases gradually in diameter. In some species, the column ends in a V-shaped concavity, into which the calyptra fits (e.g., *F. clinatus*, Monechi, 1985, pl. 7, figs. 5B, C; *F. bobii*, Perch-Nielsen, 1971a, pl. 3, figs. 1-3). Most commonly, however, the column ends in a narrow platform upon which the calyptra rests (e.g., *F. schaubii*, Perch-Nielsen, 1971a, pl. 9, fig. 1; *F. alanii*, Perch-Nielsen, 1971a, pl. 9, fig. 4; *F. richardii*, pl. 9, fig. 2). In these cases, a discrete furrow generally marks the suture line between column and calyptra (e.g., *F. richardii*, Perch-Nielsen, 1971a, pl. 9, fig. 2).

Only few proximal views of *Fasciculithus* fasciculiths are available. It is possible that a tiny inner proximal cycle occurs (e.g., *F. sidereus*, Bybell and Self-Trail, 1995, pl. 16, fig. 3a). This cycle is reminiscent of the inner proximal cycle in *Biantholithus*.

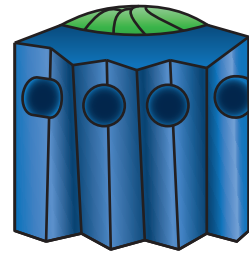
Calyptra: This consists of a single cycle of dextrally imbricated elements with oblique sutures oriented anticlockwise (e.g., *F. tym-*



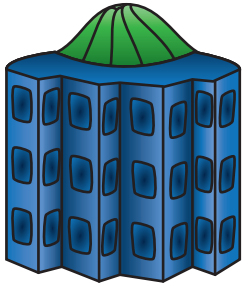
F. tympaniformis



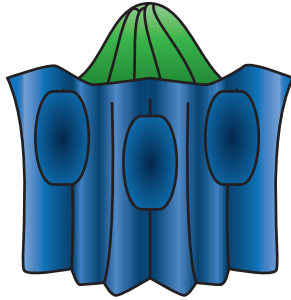
F. clinatus



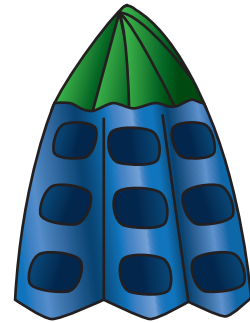
F. aubertae



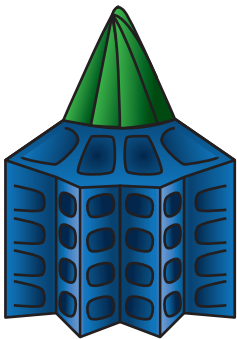
F. involutus



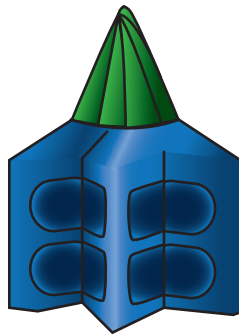
F. bobii



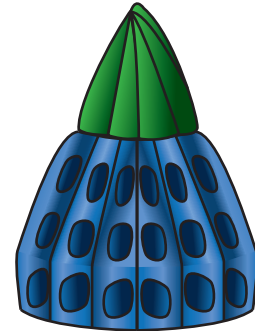
F. thomasi



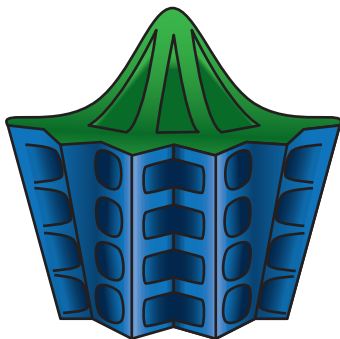
F. schaubii



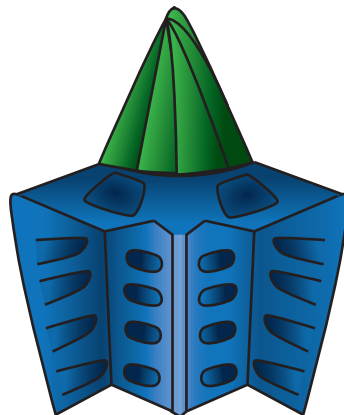
F. lilianae



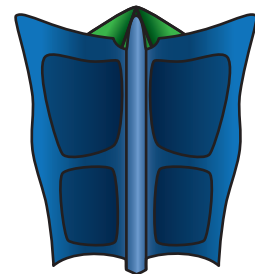
F. alanii



F. tonii



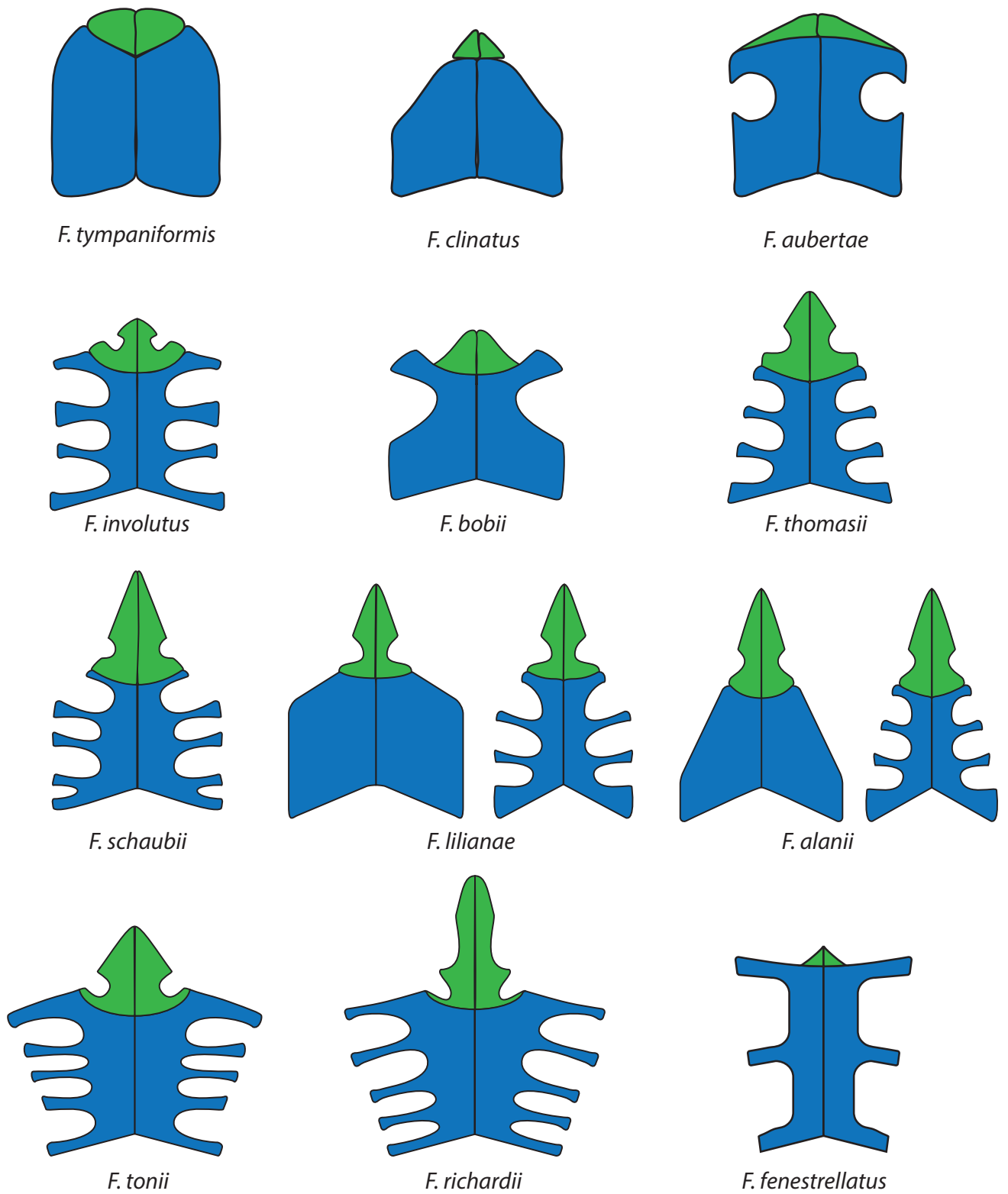
F. richardii



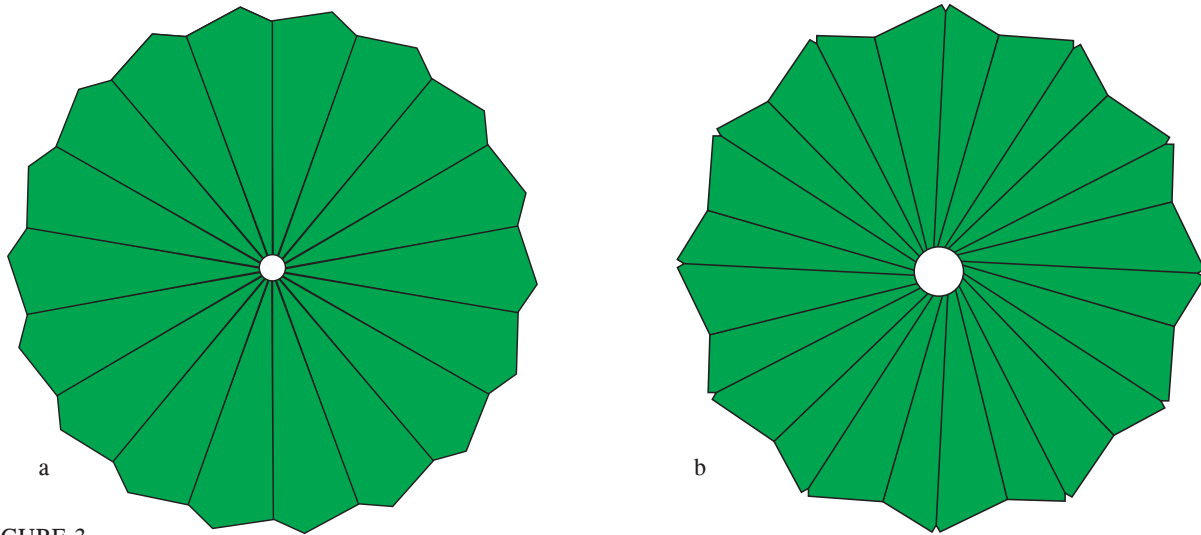
F. fenestrellatus

TEXT-FIGURE 1

Side view of *Fasciculithus* fasciculiths, showing the calyptra over the column, and the honeycomb pattern present in most species. Refer to species descriptions in "units" for size of fasciculiths of different species.



TEXT-FIGURE 2
 Longitudinal sections of the *Fasciculithus* fasciculiths illustrated in text-fig. 1.



TEXT-FIGURE 3

Structure of the column in *Fasciculithus fasciculithus* as seen from the proximal face.

- a: typical rosette-shaped pattern, with regularly spaced elements.
- b: slightly derived rosette-shaped pattern, in which the elements are weakly organized in pairs. Note that the LSp pattern is preserved.

paniformis, Perch-Nielsen, 1971a, pl. 1, fig. 7; *F. involutus*, Wise and Wind, 1976, pl. 15, figs. 3; text-fig. 4d). This configuration is readily seen when the elements of the calyptra are gently inclined towards the vertical axis of the fasciculith (as in *F. tympaniformis*, where the calyptra is a low cone). In other fasciculiths, the elements of the calyptra are arranged on edge, with their long axes essentially parallel to the vertical axis of the fasciculith, creating a needle-shaped calyptra in which the characteristic imbrication of the elements is perceptible in their slight twist (e.g., *F. alanii*, Perch-Nielsen, 1971a, pl. 9, fig. 4; *F. richardii*, Perch-Nielsen, 1971a, pl. 5, fig. 3; pl. 9, figs. 2, 4; text-figs. 1, 2).

Previous authors have overlooked the calyptra in distally needle-shaped fasciculiths, because the outer edge of its elements are aligned with the vertical ridges of the column, giving a false impression of structural continuity from one end of the fasciculith to the other (e.g., *F. alanii*, Perch-Nielsen, 1971a, pl. 9, fig. 4; *F. richardii*, op. cit., pl. 8, fig. 6). On the other hand, the calyptra is reduced to a thin cycle in *F. sidereus* (Bybell and Self-Trail, 1995, pl. 16, fig. 4b; text-figs. 6c, d).

Discussion

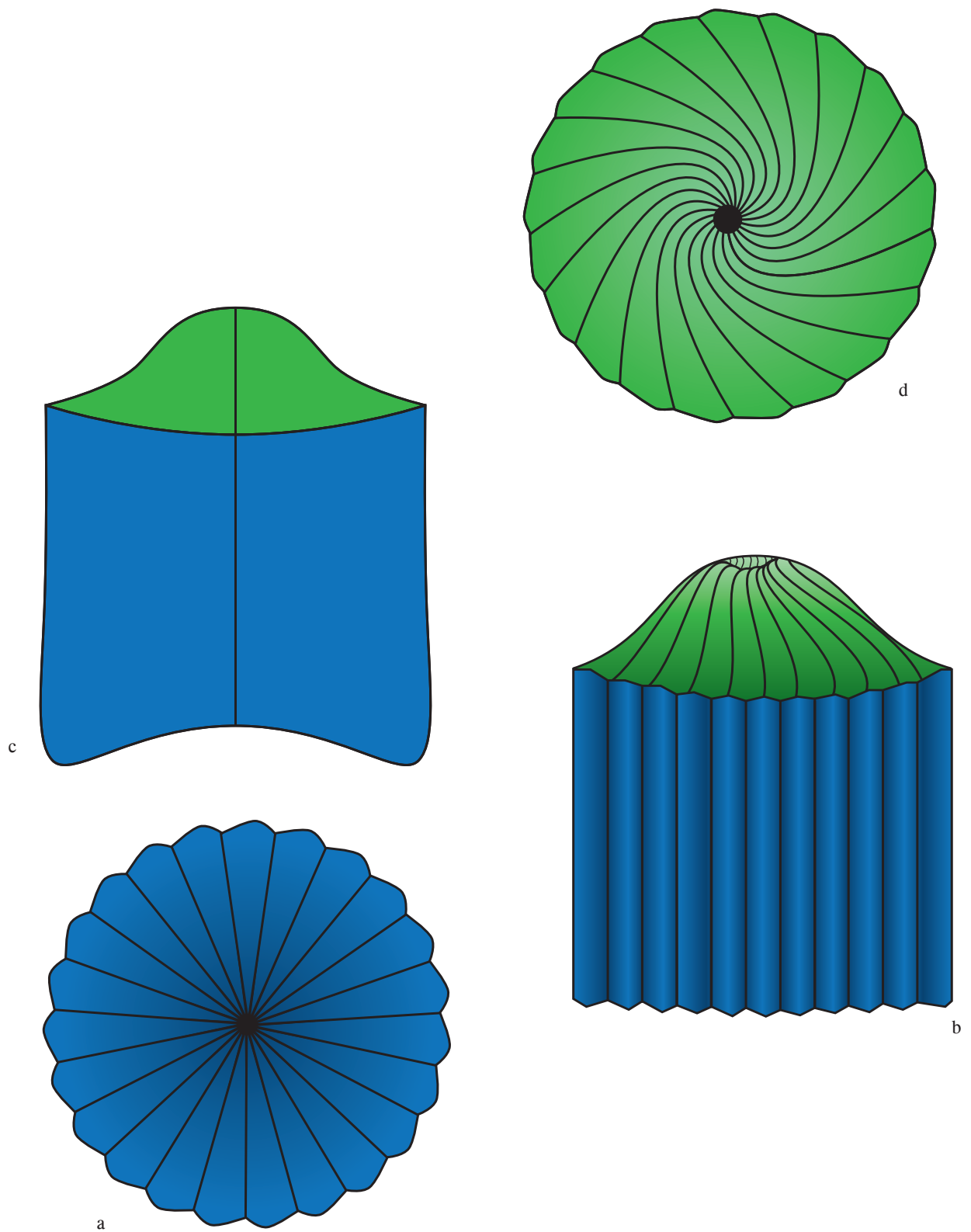
The primary or secondary nature of the honeycomb pattern of the *Fasciculithus* fasciculith is important because of the significance that may be attached to it. If secondary, it is indicative of sharply differentiated zones of solubility during diagenesis (Wise and Wind, 1977) which could come from comparably uneven calcification by the living cell (Raffi and De Bernardi, 2008). If this pattern is a primary feature, however, its presence in most species must have adaptive significance. The consistent manifestation of the pattern, regardless of sedimentary context (see below) suggests that it is in fact a primary feature.

In comparing the abundance and preservation of specimens assigned to *F. involutus* in biosiliceous sediments alternating with those of *F. tympaniformis* in the coccolith oozes of the Upper Paleocene on the Falkland Plateau, Wise and Wind (1977) observed that the fasciculiths in the silica-rich sediments, assumed to be deposited near the base of the CCD, were moderately to heavily etched, and that

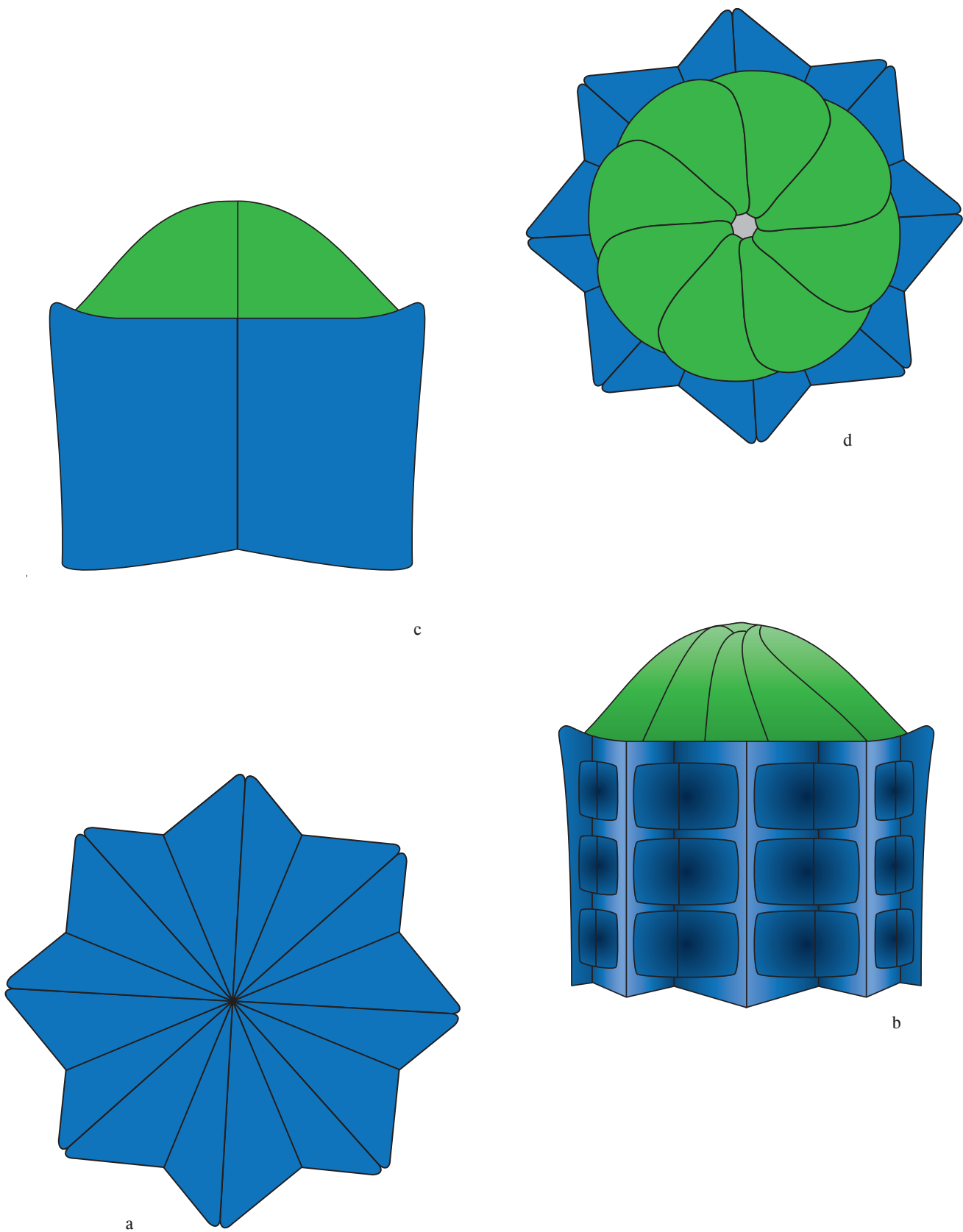
those in the carbonate rich sediments, apparently deposited well above the CCD, were somewhat overgrown (text-fig. 7). From this, the authors concluded that “*Fasciculithus involutus* is probably an etched form of *F. tympaniformis*” (op. cited, p. 295; emphasis mine). Romein (1979) disagreed with this conclusion, remarking (op. cit., p. 154) that, in plane view, *F. involutus* has a stellate outline whereas *F. tympaniformis*, even when strongly etched, has a circular outline.

In a comparative study of the abundance and preservation of coccolith assemblages in pre-, syn- and post-PETM sediments, Raffi and De Bernardi (2008) interpret PETM fasciculiths with delicate elements and fenestrae as weakly calcified, in opposition to the well-preserved pre- and post PETM fasciculiths that are massive and heavily calcified (text-fig. 8). In the same vein as Wise and Wind (1977), these authors described *Fasciculithus thomasii* as a “weakly calcified *F. tympaniformis* in which the column appears strongly etched and has an irregular pseudo-cylindrical structure with an alveolar surface (figs. 9C, F, 11B [text-fig. 8]) and without distinct wedge-shaped elements”. Describing *F. thomasii* as a weakly calcified *F. tympaniformis* is as problematic as identifying *F. involutus* as a poorly preserved *F. tympaniformis*, since morphological evidence again contradicts the synonymy. Even though *F. thomasii* and *F. tympaniformis* both have a circular outline in plane view, the column is parallel-sided in *F. tympaniformis* but tapering in *F. thomasii*, while the calyptra is needle-shaped in the latter species and rounded in the former.

Two main lines of evidence indicate that the honeycomb fenestrae are primary features. More often than not, the elements of the column in specimens from deep-sea oozes and chalks exhibit smooth crystal faces and angular sides indicative of the secondary overgrowths of calcite that form in such oversaturated deposits (Wise, 1977; see also Martini, 1976, pl. 11, figs. 4-6). While such smoothed-over specimens have been characterized by Raffi and De Bernardi (2008, fig. 11A) as “normal nannoliths”, they are much more likely to fall in the category of overgrown fasciculiths in which morphologic (and taxonomic) differences are mostly obscured.



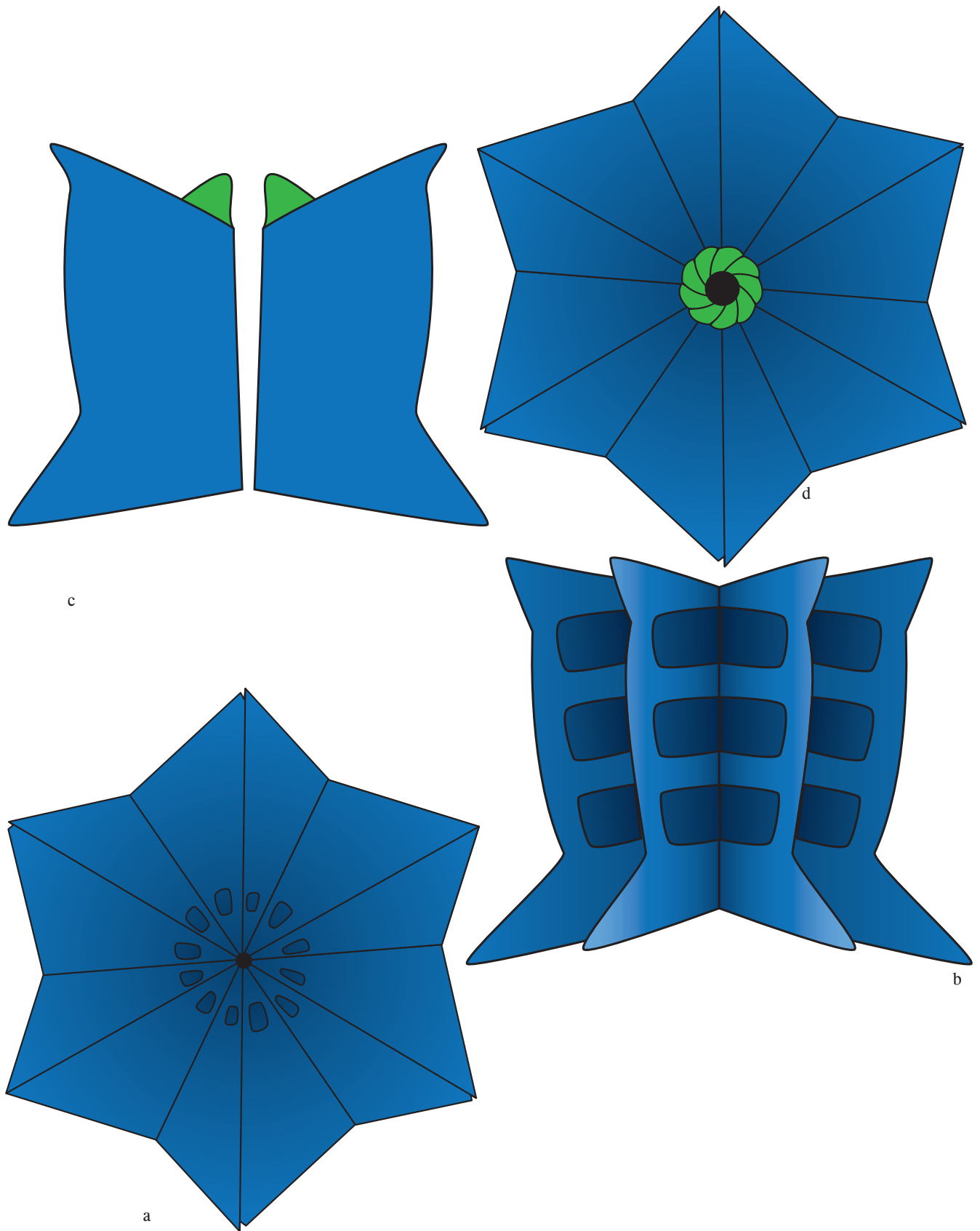
TEXT-FIGURE 4
General morphology and structure of a *Fasciculithus fasciculith*.
 a: proximal face.
 b: side view.
 c: longitudinal section.
 d: distal face.



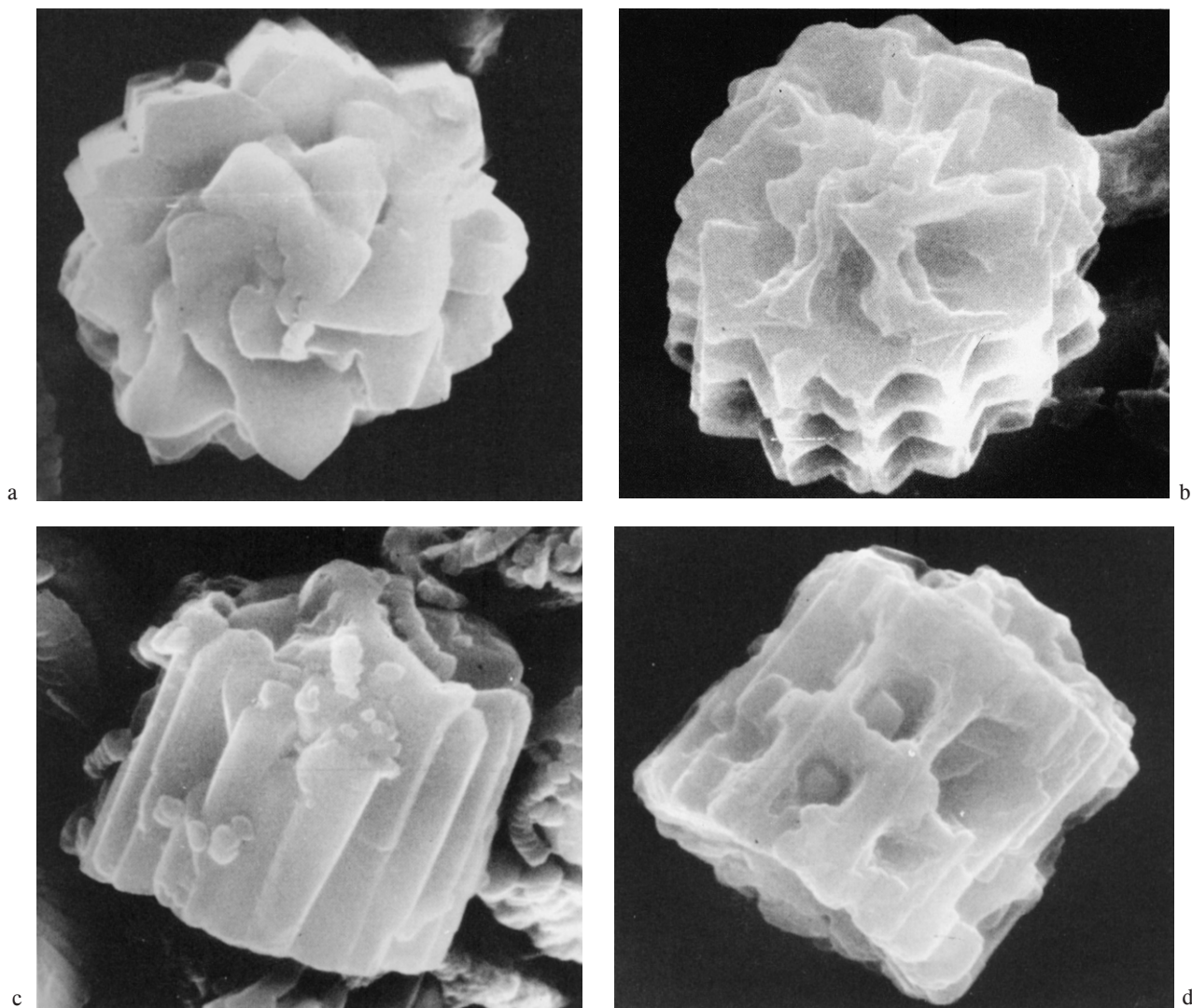
TEXT-FIGURE 5

Strongly derived structure of the column in some *Fasciculithus fasciculithus*.

- a: stellate pattern in which the elements are strongly organized in pairs. Note that the LSp pattern is preserved.
- b: side view of the column, with deep re-entrants.
- c: longitudinal section.
- d: distal face.



TEXT-FIGURE 6
Morphology and structure of the fasciculith of *F. sidereus*.
 a: proximal face.
 b: side view.
 c: longitudinal section.
 d: distal face.



TEXT-FIGURE 7

“Non-etched (or overgrown)” and “etched” fasciculiths of *F. involutus* recovered from the upper Paleocene of the Falkland Plateau (Wise and Wind, 1977). Note the angular sides and smooth crystal surface of the left specimens, indicative of recrystallization, and the regular pattern of alveolae in the so-called “etched” specimens (right). The fine structural details have been lost following recrystallization of the two left specimens whereas they are beautifully preserved on the distal face of the top right specimen, and partly preserved on the column of the bottom right one.

a, b: distal views (pl. 15, figs. 3, 6).

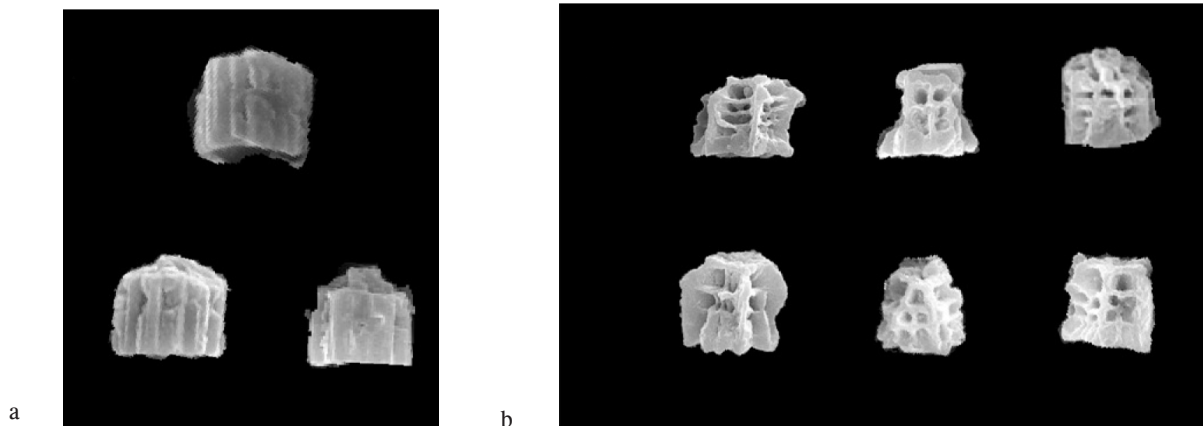
c, d: oblique proximal view (pl. 16, figs. 5, 6).

A second line of evidence comes from fasciculiths preserved in clay-rich, epicontinental sediments such as those of New Jersey and Maryland (Bybell and Self-Trail, 1995). These specimens exhibit rounded rather than sharp edges, just as in living coccoliths, without flat crystal faces. Such fasciculiths exhibit delicate morphology and structure, with remarkable evenness and symmetry (text-fig. 9) neither of which could be the product of dissolution. While local dissolution may have enlarged natural alveoles, and overgrowth may have fattened the ridges between them, dissolution alone could not have transformed the surface of a “normal coccolith” into a zone of evenly arranged and equally sized pits that would qualify to be called a honeycomb, whereas the opposite effect of calcite overgrowth to obscure a honeycomb is clearly possible. Likewise, the fasciculiths recovered from the Upper Paleocene of Tanzania (Bown and Pearson, 2009), with their exceptionally pristine preservation (Bown et al., 2008), also exhibit a remarkably regular and symmetrical alveolar pattern (text-fig. 10).

There can be little doubt, therefore, that the honeycomb alveolar pattern found in species of *Fasciculithus* is primary rather than the effect of post-depositional circumstances. For this reason, the “weakly calcified” fasciculiths of *F. thomasii* illustrated by Raffi and De Bernardi (2008, fig. 11b) from the PETM interval must in fact be well preserved honeycombed fasciculiths, which have avoided being secondarily overgrown into “normal” specimens because the seawater and sediments were undersaturated in calcium carbonate during the PETM (Zachos et al. 2005).

Extinction patterns

Romein (1979, p. 148) has described the extinction and color patterns of the fasciculiths. In the standard orientation for distal view (cone upwards, concave side of column downwards) the lines of extinction “are parallel to the cross-hairs, and bisect each other in the centre of the nannolith”, and “the second and the fourth quadrant are blue; the others are yellow”. In the standard orienta-



TEXT-FIGURE 8

“Normal” (a) and “weakly calcified” (b) fasciculiths recovered from the PETM interval at South Atlantic ODP Site 1262. (Raffi and De Bernardi, 2008, figs. 11a, b.) The “normal fasciculiths” show angular sides and crystalline faces, and compare well with the recrystallized specimen in text-fig. 7c. The “weakly calcified fasciculiths” compare well with the well-preserved honeycomb fasciculiths from the Clayton Core (see text-fig. 9).

a: specimens identified as *F. tympaniformis*.

b: specimens identified as *F. thomasii* and transitional species between *F. tympaniformis* and *F. thomasii*.

tion for side view (cone pointing in the positive direction of the Y-cross-hair, base of the column parallel to the X-cross-hair) “a straight median extinction line can be observed in the column and the cone. In some species the line is curved in the cone”; “the left half of the nannolith is blue, the other half is yellow” (text-fig. 11).

Romein (loc. cit.) also noted:

“In the L.M., and in plane view, *Fasciculithus* can easily be distinguished from the closely related *Heliolithus* with the aid of the extinction lines; the angle between the lines and the cross-hairs is 0° in *Fasciculithus*, while it is about 20° in *Heliolithus*”.

BIOLOGY, PHYSIOLOGY AND ECOLOGY

Biology

The coccosphere of *Fasciculithus* is unknown. It can be easily imagined as formed of juxtaposed fasciculiths radiating around the cell (text-figs. 12a, b). The honeycomb fasciculiths were particularly light and delicate (see above); however, considering their shape, the heterococcolith-stage was most likely non-motile.

Physiology

The central canal ensured gas, mineral and nutrient exchanges between the cell and the environment as in other fasciculiths, but without the mediation of a central body as in *Gomphiolithus* and *Lithoptychius*.

The honeycomb morphology of the fasciculiths allowed for a large surface area to be in contact with the environment, while the deep recesses of the alveolae served as traps for food particles or bacteria (text-figs. 12, 13). These coccoliths can be interpreted as high-

ly adapted for enhanced mixotrophic physiology in the oligotrophic Late Paleocene Ocean.

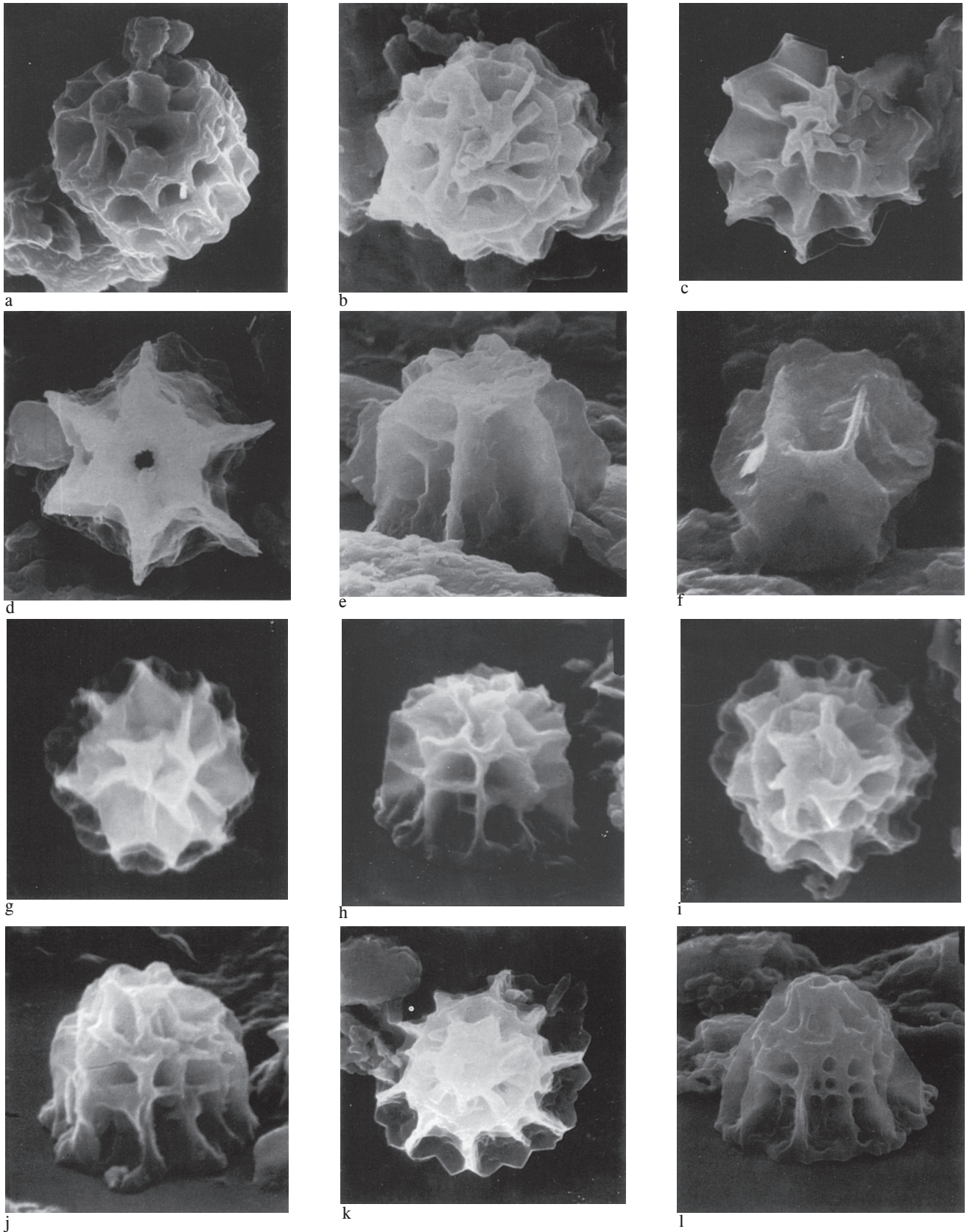
Ecology

The distribution of the genus is latitude-dependent. It is unknown at northern high latitudes in the North Sea area (Varol, 1989, 1998; Clemmensen and Thomsen, 2005). However, it occurred at higher southern latitudes, as for instance during the Late Paleocene at 50° latitude on the Falkland Plateau (Wise and Wind, 1977) where *Fasciculithus tympaniformis* was abundant during episodes of global warmth.

EVOLUTIONARY HISTORY

Origin

The oldest formally described species of *Fasciculithus* is *F. tympaniformis*, which Romein (1979, fig. 40) suggested was evolved from *Fasciculithus* [vel *Lithoptychius*] *ulii*. Agnini et al. (2008, fig. 5) considered that the abundance patterns of specimens in the lower Selandian sediments recovered from Walvis Site 1262 demonstrated a “*F. ulii*/*F. tympaniformis* intergrade”, described as consisting of “... transitional forms between *F. tympaniformis* and other *Fasciculithus* species, namely *Fasciculithus ulii*-*F. chowii* gr., *Fasciculithus pileatus*, and *Fasciculithus billii*-*Fasciculithus jani* gr.” (op. cit., p. 223; text-fig. 14). It is difficult to imagine how several distinct species could contain morphotypes transitional with the single species *F. tympaniformis*, and also how *Lithoptychius billii* and *L. jani* could be united in a single taxonomic group (see Genus *Lithoptychius*, this volume, for differences between these taxa). This interpretation of an evolutionary lineage is based on superficial morphologic convergence/similarity, without regard for the feasibility of the interpretation. The specimen older than *F. tympaniformis* and illustrated from Core 1262C-10H-4W under the



TEXT-FIGURE 9

Honeycomb fasciculoliths recovered from the Upper Paleocene Zone NP9 in the Clayton Core, New Jersey (photographs from Bybell and Self-Trail, 1995). Note the regular arrangement of the elements of the calyptra and of the vertical ridges and alveolae in the column.

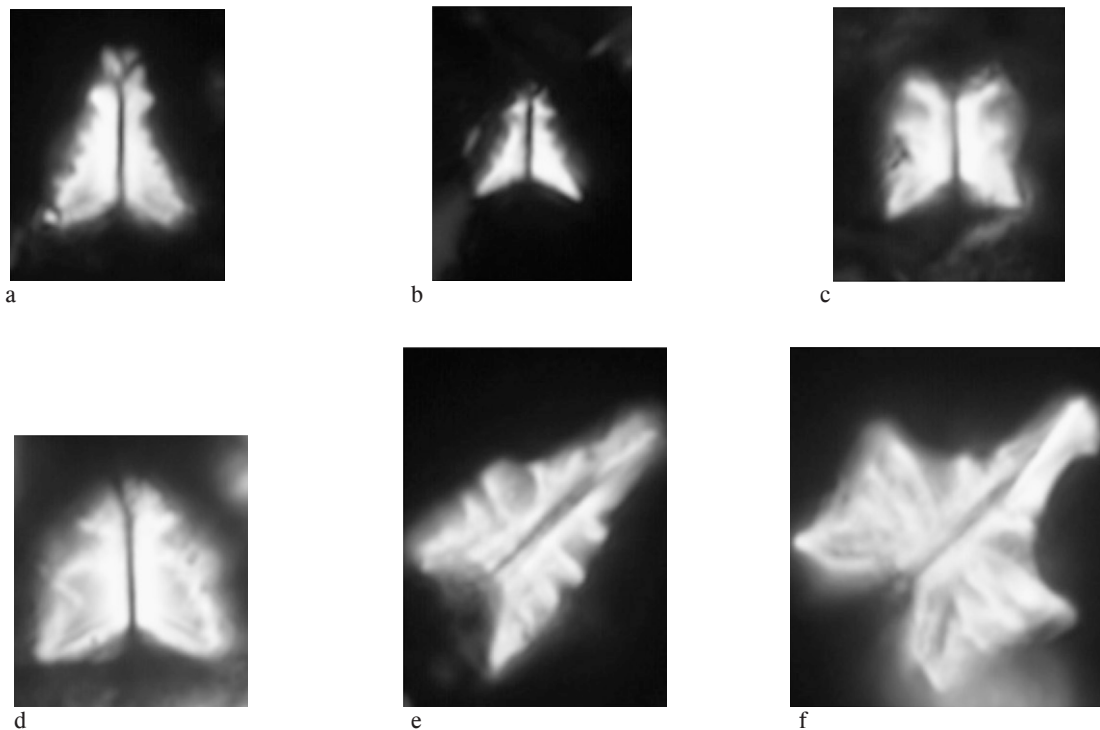
a, b, c: *F. involutus*, pl. 15, figs. 3a, 4a, 5a.

d-e (same specimen), f: *F. sidereus*, pl. 16, figs., 4a, b, 5a.

g-h (same specimen), i-l (same specimen), j- k (same specimen): *F. thomasii*, pl. 17, figs. 1a, b, 2a, b, 3a, b.

a-d, f, g, i, j: distal faces; e, h, k, l: side views.

(Taxonomic assignment as per Bybell and Self-Trail, 1995).



TEXT-FIGURE 10

Honeycomb fasciculiths recovered from the Upper Paleocene Zone NP9 at TDP Site 14 in Tanzania (photographs from Bown and Pearson, 2009, fig. 4, lower two rows, partim). Note the remarkable bilateral symmetry exhibited by these specimens, and the evenly arranged alveolae that penetrate deeply in the column.

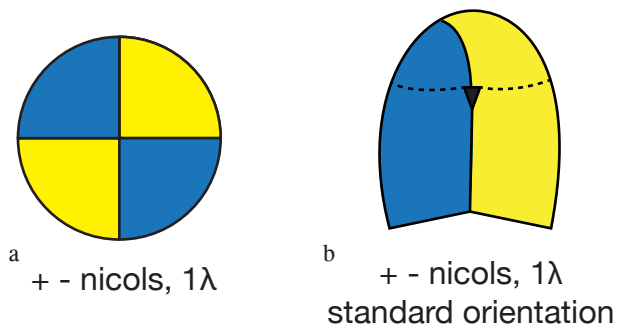
a: *Fasciculithus alanii*; b: *F. thomasii*; c: *Fasciculithus* sp. A; d: *F. lilianeae*; e: *F. schaubii*; f: *F. richardii* (taxonomic assignment as per Bown and Pearson, 2009).

name “*F. ulii* transitional to *Fasciculithus tympaniformis* (op. cit. pl. 2, fig. 4) may not be typical of *L. ulii*, but its wide canal and broad albeit low calyptra are not attributes of *F. tympaniformis*. Any transition between *L. ulii*–*F. tympaniformis* would require SEM studies to demonstrate the progressive reductions of the calyptra and collaret, with ultimately the loss of the latter, and disappearance of the central body.

Romein (1979) remarked that the earliest morphotypes of *F. tympaniformis* possessed a central body that was lost in the course of Biochron NP5. *Lithoptychius billii* shows that a *Lithoptychius*–*Fasciculithus* lineage is feasible (text-fig. 15). Both the calyptra and collaret are tiny in this species, being tucked at the center of the depressed distal end of the column. In fact, *L. billii* would be a convincing stem species if its FAD was firmly established in late Biochron NP4 (Varol, 1989, 1998), i.e., older than the FAD of *F. tympaniformis*. In contrast to Varol, Romein (1979) located this FAD in late Biochron NP5, and Agnini et al. (2007, table 1) estimated that the *F. tympaniformis* group evolved 508 kyr prior to *L. billii*.

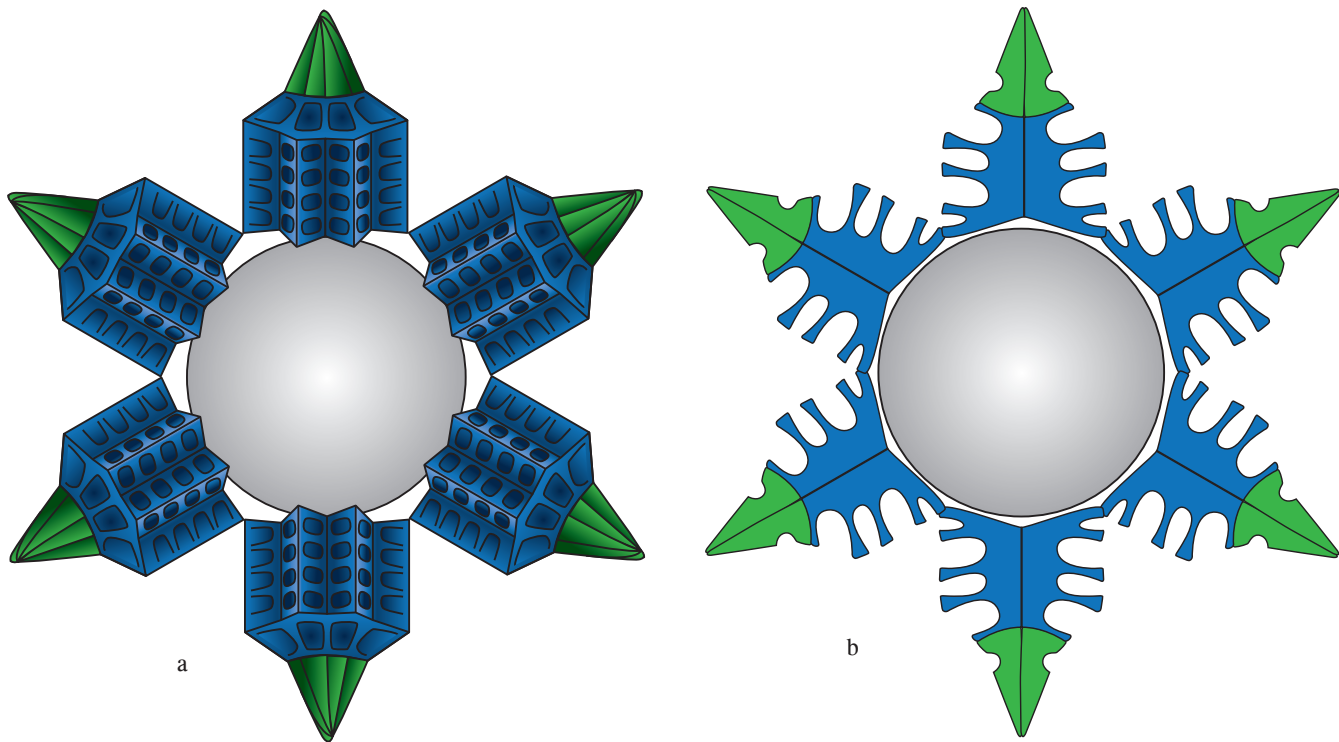
In summary, a *Lithoptychius* lineage is possible, but the species involved are unknown. The informally described taxon *Fasciculithus* sp. Steurbaut & Sztrákos (2008, p. 26, pl. 2, fig. 22), recovered from the same stratigraphic level as the oldest *F. tympaniformis* in the Loubieng Quarry at Pont Labau (Aquitaine Basin, France), is evidence that the lineage may include other early species as well as *F. tympaniformis*.

Finally, it cannot be excluded that *Fasciculithus* arose directly from *Biantholithus*. This would have only required a thickening



TEXT-FIGURE 11

Extinction patterns of *Fasciculithus fasciculiths* in standard orientation of distal [a] and side views [b]. (From Romein, 1979, p. 147.)



TEXT-FIGURE 12

Tentative reconstructions of the coccospheres of *F. schaubii*.

- a: cell in equatorial section and fasciculiths in side view.
- b: cell in equatorial section and fasciculiths in longitudinal section.

of the column of *Biantholithus* and a reduction of the calyptra, two structural changes that are less profound than those necessitated by a *Lithoptychius-Fasciculithus* lineage. Nevertheless, a *Lithoptychius-Fasciculithus* lineage is favored here. Monechi et al. (2013) illustrated a specimen thought to be transitional between *Biantholithus* and *Fasciculithus* (text-fig. 17), but this illustration is inconclusive.

Phylogeny

Romein (1979) was first to describe the diversification of *Fasciculithus* during Late Paleocene (Biochron NP7 to NP9) as consisting in the divergence from *F. tympaniformis* of three groups of species which differed in combinations of size, general shape, presence/absence of a calyptra, and the presence/absence as well as the number of rows of fenestrae (text-fig. 16). As it is now established that all *Fasciculithus* species possess a calyptra, this phylogenetic interpretation requires revision based on a careful stratophenotypic analysis.

Honeycombs fasciculiths are characteristic of most, but not all species of *Fasciculithus*. The earliest (*F. tympaniformis* and *Fasciculithus* sp. Steurbaut & Sztrákos) do not show clear evidence of such an alveolar pattern; the fenestrae, if present, were very shallow and in a single row near the distal end of the column, as suggested by light microscopy observations. The fasciculiths of *F. tympaniformis* are rather like overgrown fluted fasciculiths of *Lithoptychius* and perhaps for this reason they possessed elongate vertical depressions in the column (which would constitute strong evidence in favor of a *Lithoptychius-Fasciculithus* lineage). Of all subsequent *Fasciculithus*, only *F. clinatus*, which likely evolved directly from *F. tympaniformis* during Biochron NP7, was similarly without a noticeable honeycomb pattern. The other species in the genus had one (*F. aubertae*) or multiple rows of fenestrae. In many of these species, the elements of the calyptra were also

TEXT-FIGURE 13 (next page)

Tentative reconstructions of coccospheres.

- Cell in equatorial section and fasciculiths in longitudinal section.
- a: *F. tympaniformis*.
- b: *F. alanii*.
- c: *F. thomasii*.
- d: *F. tonii*.
- e: *F. lilianae*.

The cells are arbitrarily shown as approximately the same size. However, cell size was likely different in different species at different times.

arranged so as to delineate fenestrae (e.g., *F. involutus*, text-fig. 7b; *F. thomasii*, text-figs. 9g-l). A satisfactory identification of lineages among these species will require detailed stratophenotypic analysis.

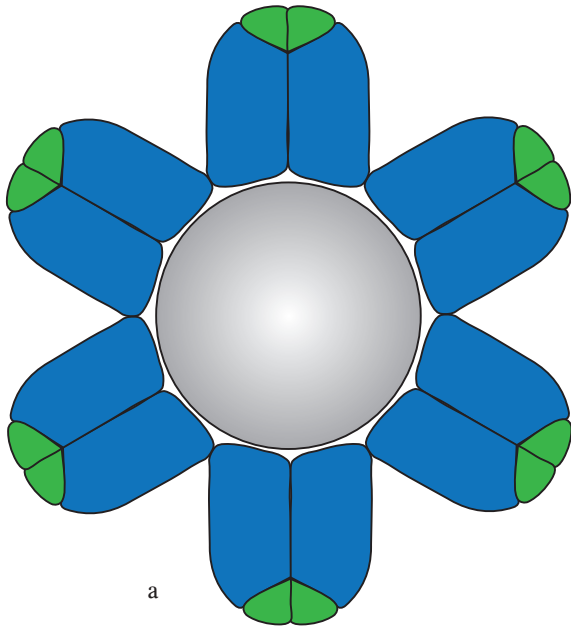
Diversity

Fasciculithus achieved maximum diversity during Biochron NP9, between ~55.9 and 55.5 Ma, although its species were still common after the Paleocene/Eocene Thermal Maximum (PETM) (see e.g., Bybell and Self-Trail, 1995, figs. 13, 16, 17). Their diversity declined thereafter until extinction in late Biochron NP9.

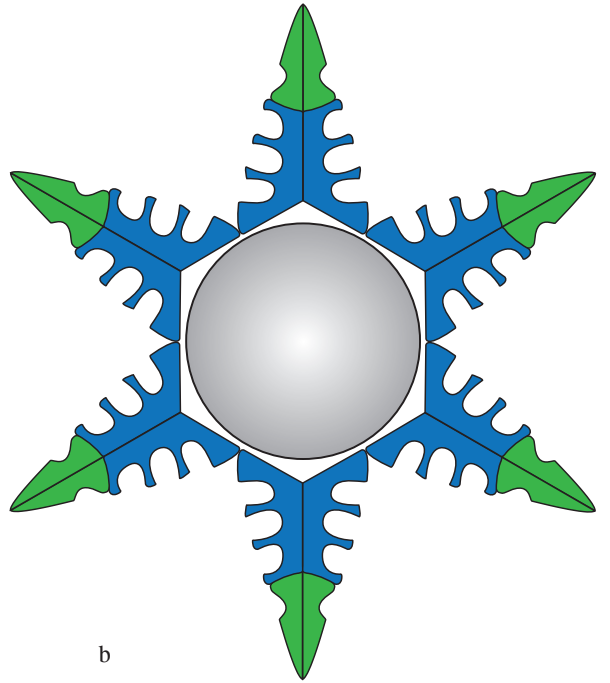
STRATIGRAPHY

Biostratigraphy

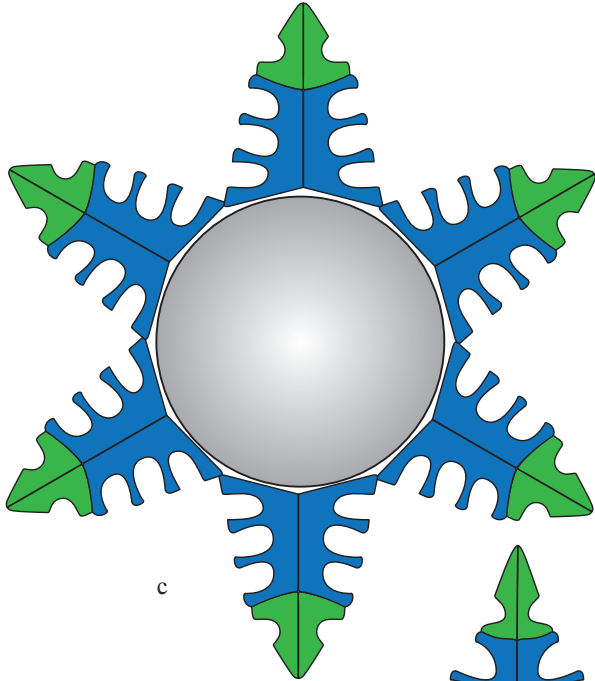
Fasciculithus tympaniformis is one of the most important marker species of the Paleocene. It serves to anchor stratigraphic sections when other, less reliable, markers (e.g., *Ellipsolithus macellus*, *Heliolithus* species) are not present, and its upper range limit



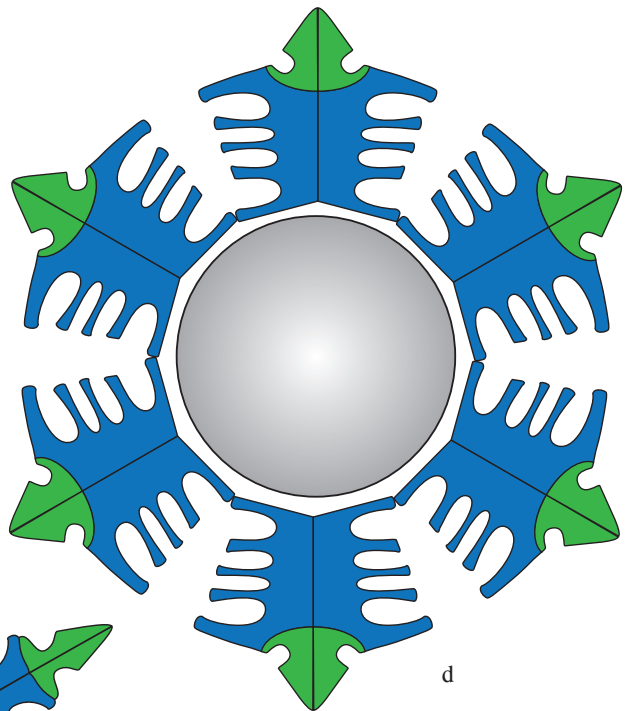
a



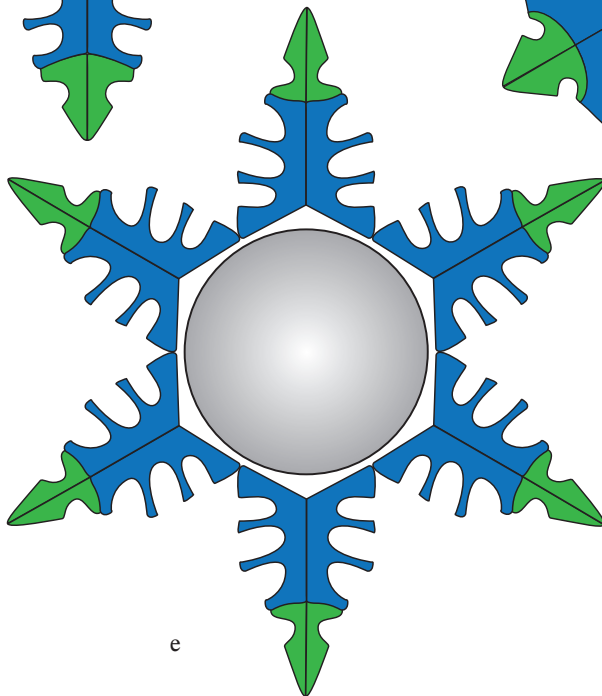
b



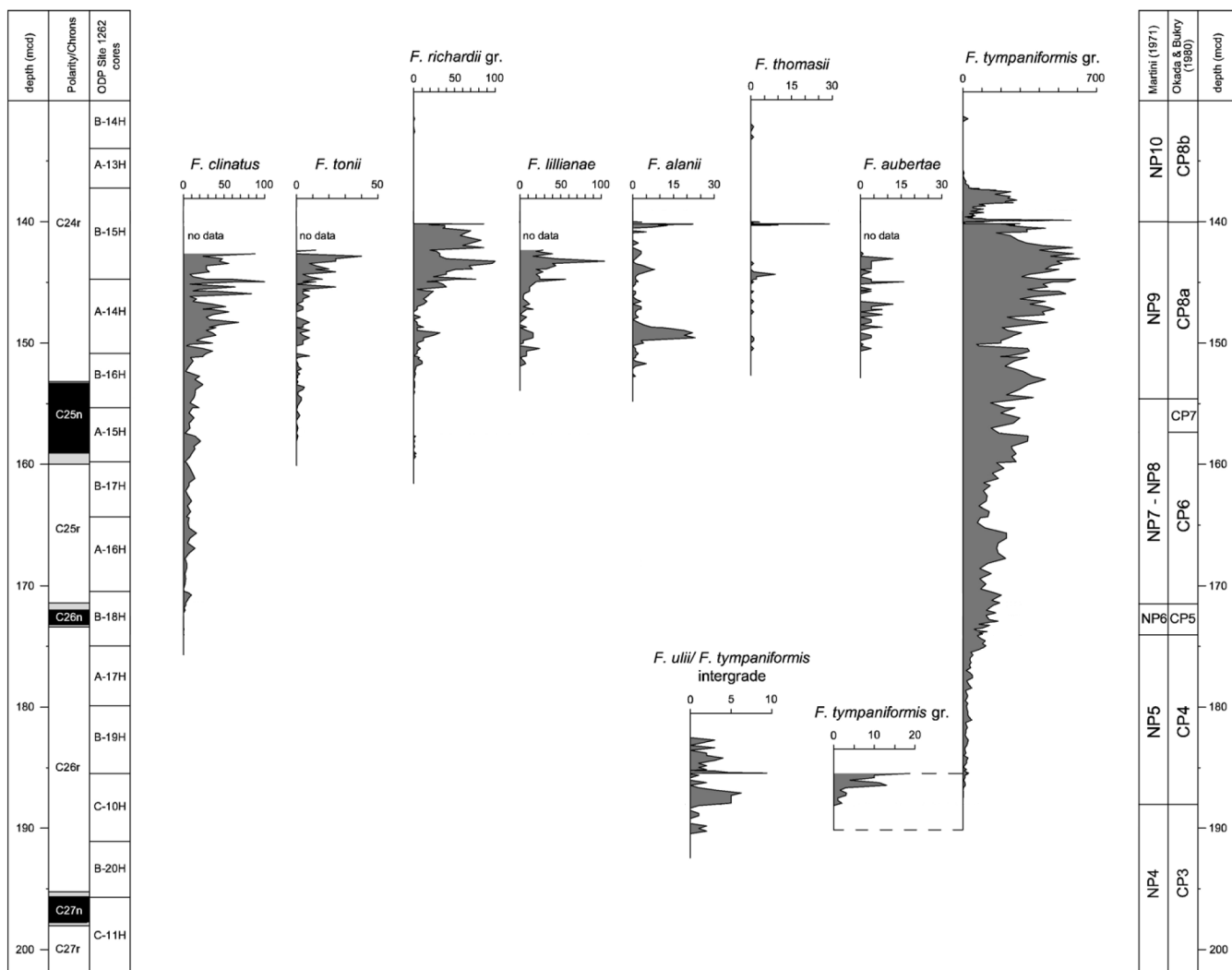
c



d



e



TEXT-FIGURE 14

Abundance patterns of honey-comb fasciculiths at Site 1262. (Modified from Agnini et al., 2007, fig. 5.)

approximates the NP9/NP10 zonal boundary in the absence of the markers *Tribrachiatus bramlettei* and *Heliodiscoaster diastypus*.

The LO of *F. tympaniformis* has been incorporated in the main zonal schemes (text-fig. 18). Hay and Mohler (in Hay et al., 1967) introduced the *Fasciculithus tympaniformis* Zone, the LO of the nominating taxon defining its base. It is known as Zone NP5 (Martini, 1970, 1971) and Zone CP4 (Okada and Bukry, 1980). Varol (1989) also used the LO of *F. tympaniformis* to define the *Cruciplacolithus subrotundus/Neochiastozygus saepes* [NTp8/NTp9] zonal boundary. He further named three (sub)zones after *Fasciculithus* species: *Fasciculithus lillianae* Zone (NTp18), *Fasciculithus hayi* Zone (NTp19), and *Fasciculithus involutus* Zone (NTp20), the latter being defined as the interval between the HOs of *F. hayi* and *F. tympaniformis*.

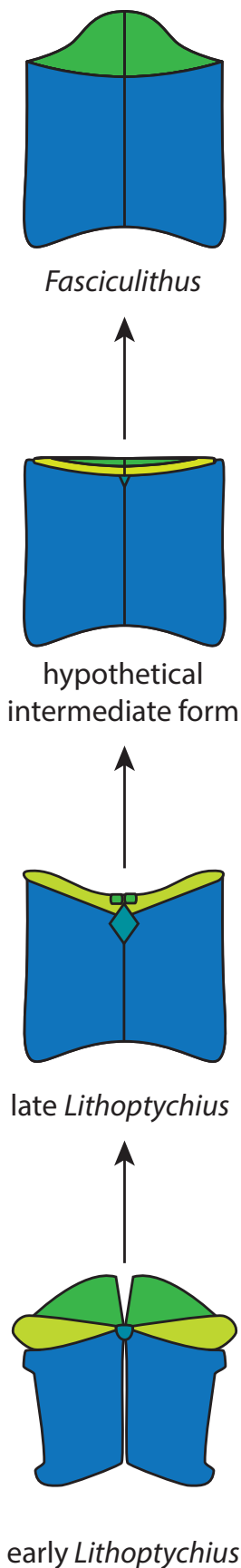
Fasciculithus involutus is a controversial taxon. It has been placed in synonymy with *F. tympaniformis* (Wise and Wind, 1977) apparently under the misapprehension as to diagenetic effects; (see "Structure: Discussion" above). It is often reported from Zone NP5, and even from upper Zone NP4 (e.g., Steurbaut and Sztrákos, 2008; Monechi et al., 2013). It is also the honeycomb fasciculith, formally described from Zone NP8 in the Lodo Formation, and also reported from Zone NP9 (Bramlette and Sullivan, 1961), with a restricted stratigraphic range (see also Romein, 1979).

Several biostratigraphic events among *Fasciculithus* species stand out. They are 1) the LOs of *F. alanii*, *F. hayi* and *F. lillianae* in lower Subzone NP9a (also NTp16B) and 2) the HO of *F. alanii* at the NP9a/b zonal boundary, thus marking the Paleocene/Eocene boundary. According to Varol (1989) the HOs of *F. hayi* (marking the top of Zone NTp19) and *F. tonii* are very close to this horizon.

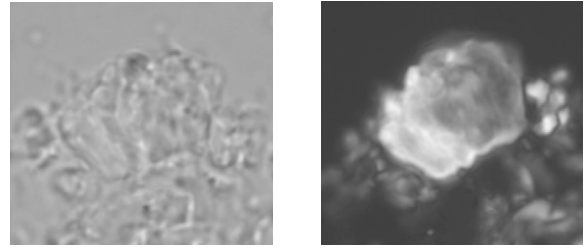
The *Discoaster multiradiatus* (NP9) Zone is subdivided into three subzones (NP9a, b, c; Aubry and Salem, 2012). Subzone NP9b is characterized by the so-called "RD assemblage" that is comprised of *Rhombaster* spp. and asymmetrical discoasters such as *Heliodiscoaster araneus* and *H. anartios*. The extent of subzone NP9b equates with the Carbon Isotope Excursion (CIE) (Kahn and Aubry, 2004) whose onset characterizes the Paleocene/Eocene boundary (Aubry et al., 2007). The HO of *F. alanii* marks the top of Subzone NP9a, thus characterizing a level just below the onset of the CIE (Monechi et al., 2000; Dupuis et al., 2003; Aubry et al., 2007; Agnini et al., 2007). The NP9c/NP10 zonal boundary is defined by the LO of *Tribrachiatus bramlettei* which may be approximated by the HO of *F. tympaniformis*.

CHRONOSTRATIGRAPHY

The LO of *F. tympaniformis* may help approximate the base of the Selandian Stage, although it is a younger stratigraphic horizon



TEXT-FIGURE 15
Tentative interpretation of the *Lithoptychius*–*Fasciculithus* transition.



TEXT-FIGURE 16
“Transitional form between *Biantholithus* and *Fasciculithus* in lateral view.” (From Monechi et al., 2013, pl. 1, figs. 4, 3.)

(text-fig. 19). Until a GSSP for the base of the Eocene Series was defined, the HO of *Fasciculithus tympaniformis* served to approximate the Paleocene/Eocene boundary. As this boundary is now globally correlated on the basis of the Carbon Isotope Excursion (CIE) (Aubry et al., 2007), the extinction of *Fasciculithus* is an Early Eocene event.

On the other hand, the HO (at the NP9a/b subzonal boundary) of the easily identifiable *Fasciculithus alanii* can now be used to approximate the chronostratigraphic boundary.

BIOCHRONOLOGY

The FAD of *Fasciculithus* is tied to Chron C26r (Agnini et al., 2007; Monechi et al., 2013), its LAD to mid-Chron C24r (text-fig. 20).

Calibration of biochronologic events among *Fasciculithus* species includes the following:

- LAD *F. tympaniformis*: mid Chron C24r.532; ~55.0 Ma
- LAD *F. alanii*: early Chron C24r.647; ~55.5 Ma
- FAD *F. alanii*: earliest Chron C24r.960; ~55.8 Ma
- FAD *F. richardii* (group): Chron C25n.033; ~56.1 Ma
- FAD *F. tonii*: Chron C25n.812; ~56.3 Ma
- FAD *F. clinatus*: Chron C26n.401; ~57 Ma
- FAD *F. tympaniformis*: Chron C26r.672; ~59.7 Ma

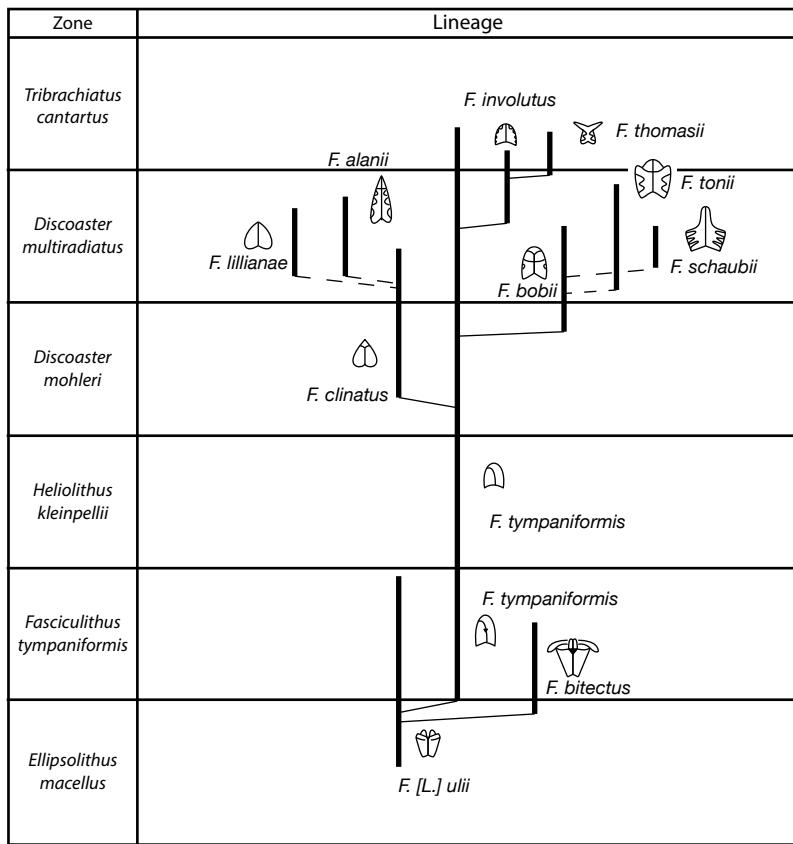
The calibrations above are based on magnetobiostratigraphic integration at ODP Site 1262 (Agnini et al., 2007), but the numerical chronology is based on the magnetostratigraphy in Cande and Kent (1992, 1995).

TAXONOMY

Generic taxonomy

Genus: *Fasciculithus* Bramlette & Sullivan, 1961

Type Species: *Fasciculithus involutus* Bramlette & Sullivan, 1961.



TEXT-FIGURE 17 (left)
Suggested lineages in *Fasciculithus*. (Modified from Romein, 1979, text-fig. 40.)

TEXT-FIGURE 18 (below)
Zonal schemes based on the stratigraphic ranges of *Fasciculithus* species.

	Hay & Mohler in Hay et. al 1967	Martini 1990, 1971	Bukry 1973 Okada & Bukry 1980	Varol 1989	Aubry herein	Wise and Wind 1977
⊥ <i>T. bramlettei</i>		NP10				
⊥ <i>F. tympaniformis</i>		NP9				
⊥ <i>F. hayi</i>				<i>Fasciculithus involutus</i> NTp20	<i>Fasciculithus</i> NP9c	
⊥ <i>F. lillianae</i>				<i>Fasciculithus hayi</i> Zone NTp19		
⊥ <i>D. araneus</i>					RD subzone NP9b	
⊥ <i>D. araneus</i>						
⊥ <i>Rhombaster</i> spp.						
⊥ <i>F. alanii</i>					<i>F. alanii</i> - <i>D. multiradiatus</i> NP9a concurrent subzone NP8	
⊥ <i>D. multiradiatus</i>		NP9 NP8	CP8 CP7	NP16A NP16B		
⊥ <i>C. Heliolithus universus</i>						
⊥ <i>H. kleinPELLii</i>		NP6	CP5	<i>Neochiastozygus saepes</i> Zone NTp9		<i>Fasciculithus involutus</i> Zone
⊥ <i>N. neocrassus</i>	<i>Fasciculithus tympaniformis</i> Zone	<i>Fasciculithus tympaniformis</i> Zone NP5	<i>Fasciculithus tympaniformis</i> Zone CP4			
⊥ <i>F. tympaniformis</i>		NP4	CP3	<i>Fasciculithus janii</i> subzone NTp8c		

“Forms of short cylindrical shape, appearing as a bundle of short rods with two or three encircling bands suggestive of a much shortened fascis. End view appearing as a rosette of about ten elements, with one concave and the other protruding in the central area.

“Although showing marked variations, especially in the compactness or solidity of the structure with varying degrees of calcification, which tends to obscure the surface features, this form-genus is distinctive, especially between crossed nicols. The side view shows extinction positions for each side at 25° to 30° from the central axis, and the end view shows an extinction cross indicating the radial arrangement of the heliolithid group” (Bramlette and Sullivan, 1961, p. 164).

Genus: *Fasciculithus* Bramlette & Sullivan, 1961 emend. Aubry in Aubry, Bord and Rodriguez 2011

Type Species: *Fasciculithus involutus* Bramlette & Sullivan, 1961, p. 164, plate 14, figures 1a-c, 2a, b, 3a, b, 4a, b, 5a, b.

“*Fasciculithus* comprised of a column with a narrow central canal, consisting of radially arranged wedge-shaped elements that meet along the vertical axis of the coccolith. The column is directly surmounted by the calyptra, consisting of a cycle of wedge-shaped elements with dextral imbrication separated by sutures with slight anti-clockwise curvature.

“*Fasciculithus* differs from *Lithoptychius* in being comprised of only two structural units. *Fasciculithus* has neither collaret nor central body. It differs from *Gomphiolithus* that is essentially formed by the column and possesses a central body.

“The genus *Fasciculithus* diversified as part of the second radiation of the fasciculiths” (Aubry in Aubry et al., 2011, p. 273).

The species of *Fasciculithus* differ by the general shape and size of the fasciculiths, the distal shape of the column, the presence/absence of fenestrae, eventually the number of rows of fenestrae, and the shape and size of the calyptra.

The taxonomy of these fasciculiths is mostly stabilized. However, fundamental conceptual differences exist for some taxa. For instance, the LO of *F. involutus* is located in upper Zone NP9 by some authors (e.g., Romein, 1979; Perch-Nielsen, 1985, fig. 37; Agnini et al., 2007), even though the holotype is from Zone NP8, whereas this LO is located in Zone NP4 by others (e.g., Steurbaut and Sztárkos, 2008, p. 8, table 1).

In agreement with Wise and Wind (1977) but for opposite reasons, the loss of the original character of the surface through diagenetic alteration is a potential for taxonomic confusion.

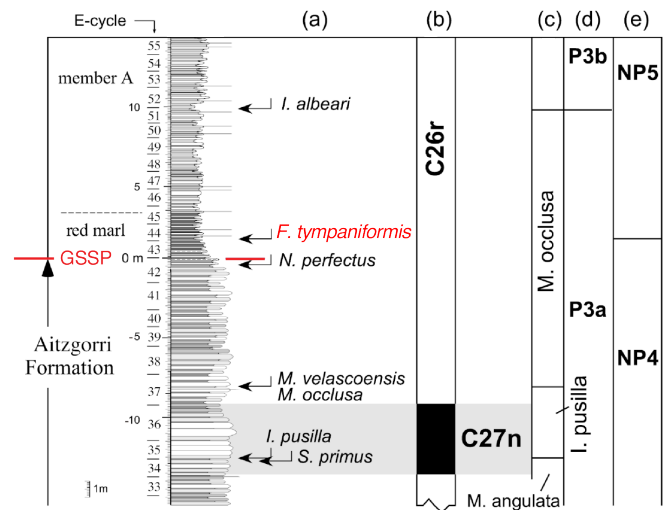
Revised species taxonomy

Fasciculithus sp. A

Basionym: *Fasciculithus* sp. Steurbaut & Sztárkos, 2008, p. 26, pl. 2, fig. 12.

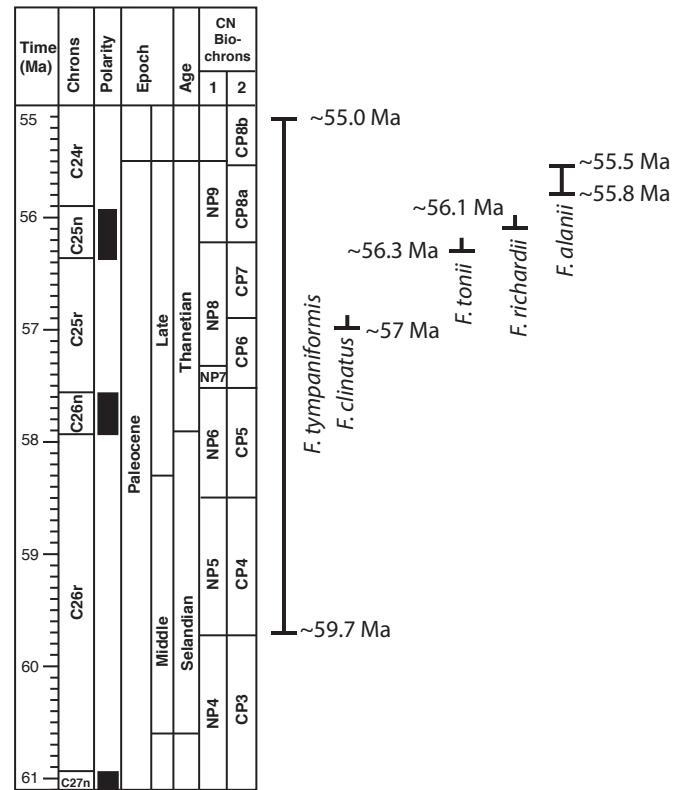
Fasciculithus sp. B

Basionym: *Fasciculithus* sp. 1 Bown 2005, p. 9, pl. 12, figs. 25-27.



TEXT-FIGURE 20

FAD of *F. tympaniformis* as recorded in the GSSP section at Zumaia, for the base of the Selandian Stage. (Modified from Schmitz et al., 2011, fig. 13.)



TEXT-FIGURE 20

Biochronology of *Fasciculithus* species.

Magnetobiochronologic framework from Berggren et al. (1995) updated (Wade et al., 2011, and herein).

Key of Determination

- I. Fasciculiths with a conical calyptra. Units 1–3
- *F. sidereus*
 - *F. clinatus*
 - *F. aubertae*
 - *F. lobus*
 - *Fasciculithus* sp. A
 - *F. tympaniformis*
 - *F. involutus*
 - *F. bobii*
 - *F. lingfengensis*
 - *F. thomasi*
 - *F. schaubii*
 - *F. lillianae*
 - *F. alanii*
- II. Fasciculiths with a needle-shaped calyptra. Units 4–6
- *F. tonii*
 - (*F. mitreus*)
 - *F. richardii*
 - *F. hayii*
 - *F. fenestrellatus*
 - *Fasciculithus* sp. B

Fasciculithus sidereus Bybell & Self-Trail 1995

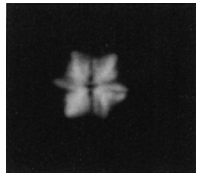
Fasciculithus clinatus Bukry 1971

Fasciculithus aubertae Haq & Aubry 1980

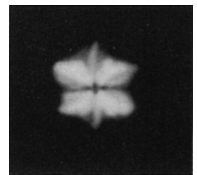
Fasciculithus lobus Bown 2010



BLM95/1



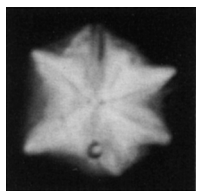
2



3

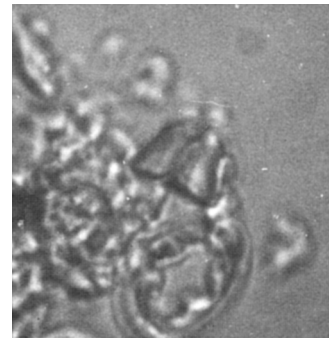


4



5

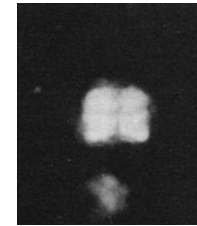
H



BD71/18



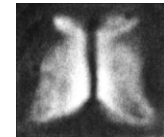
19



HBU80/25



BPR10/36



37



38

Fasciculithus sidereus

-Ø: 4.2–9.5 µm

- L. Paleocene-E. Eocene (NP9). New Jersey, USA.

- Distinctive fasciculith with five- or six-sided proximal column with numerous depressions and a central perforation on both concave ends. Column slightly broader at base than at top. Both ends pentagonal or hexagonal in well preserved specimens, star-shaped in partly dissolved specimens, rounded in very dissolved specimens. In lateral view, a vertical ridge is seen to connect distal and proximal apices. Ridges are delineated by longitudinal lateral depressions which are themselves divided by three to four superposed rows of small, alveolar pits.

- Remarks: “The top and basal disks of *F. sidereus* n. sp. are very different from any other species, and this species is easily identified both in the light microscope and in the SEM. Under the light microscope, the star shape is very diagnostic. *Fasciculithus sidereus* n. sp. does not closely resemble any other fasciculith, except in side view, where it might be possible to confuse badly dissolved specimens with *F. involutus*.

- BLM95 (p. 27, 28).

Fasciculithus clinatus

- 4–6 µm

- L. Paleocene. Northwestern Pacific Ocean.

- Small, simple; short conical column with a slightly rounded top that produces an almost triangular outline in side view. Base line essentially straight in side view, slightly longer than the upper sides, which are straight to slightly convex. In CN, a single median extinction band bisects the triangular outline.

≠ from other spp. by its small size and almost triangular outline;

≠ from the comparable small form *F. tympaniformis*, which is cylindrical with parallel instead of inclined sides;

≠ from *F. magnus*, which has inclined sides for only one half of its height and is much larger than *F. clinatus*;

≠ from spp. as *F. involutus* by the lack of the pit-and-ridge ornamentation.

— Ranges from NP7 to lower NP9 (Romein, 1979, p. 77).

— Evolved from *F. tympaniformis*. Transitional forms exist between the two species in NP7. (Romein, 1979, p. 152).

- BD71 (p. 318).

Fasciculithus aubertae

- 5–8 µm

- L. Paleocene (NP9). Jordan.

- Roughly rectangular outline with distal corners slightly rounded. Horizontal row of prominent pores between midway and one-third the width from the top. Crystal rays arranged in a bundle with slight outward ridges. Pores located between the crystal rays. In LM the row of pores appears like a horizontal groove.

- Seems to be restricted to NP9.

- HBU80 (p. 301).

Fasciculithus lobus

- 5.2–6.0 µm

- L. Paleocene (NP9b). Tanzania.

- Medium-sized fasciculith with concave top and bottom surfaces and a tapering column that has at least two deep indentations, resulting in a lobate outline. Overall, it has a rather angular, blocky outline.

≠ from most other fasciculiths by the concave top/distal surface, but also by its sloping and strongly lobate column.

- Remarks: Occurrence restricted to the PETM; may represent an excursion species.

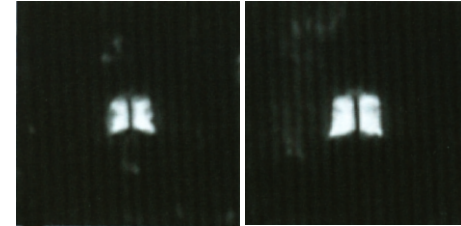
- BPR10 (p. 23).

Fasciculithus clinatus (continued)

Fasciculithus aubertae (continued)

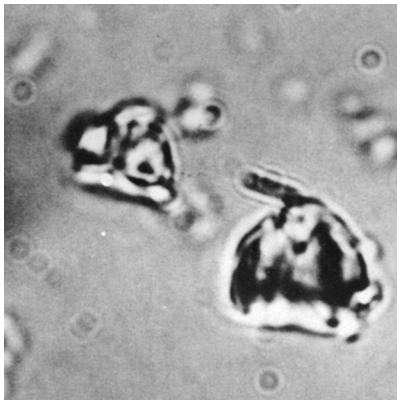


AC07/20

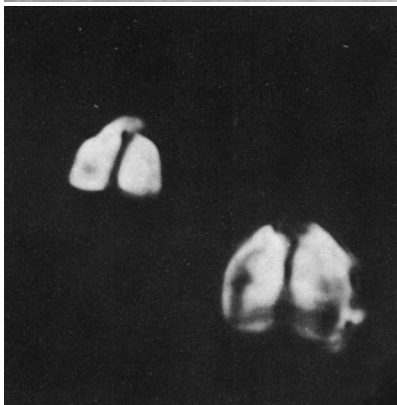


BPR05a/26

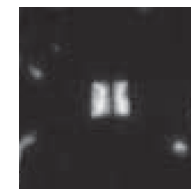
27



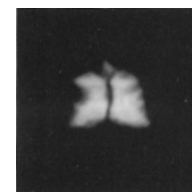
MS85/21



22



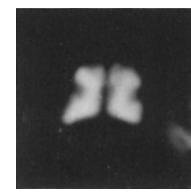
BPR05b/28



BLM95/29



30



31

Fasciculithus lobus (continued)



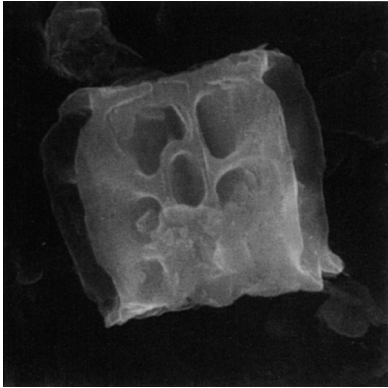
BPR10/39



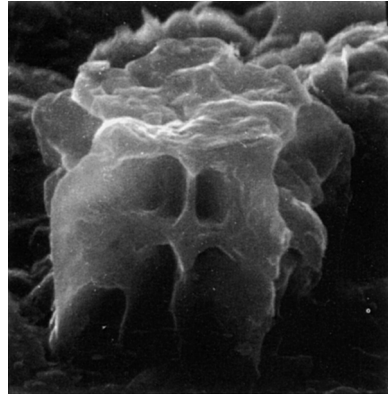
STJM11/40

Fasciculithus sidereus (continued)

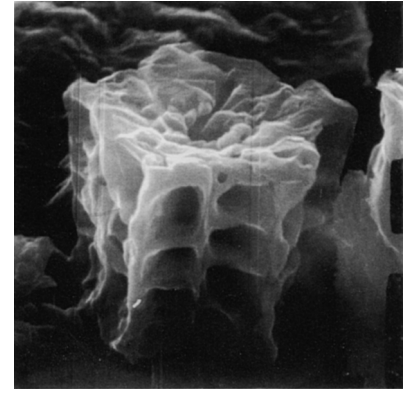
SIDE VIEW



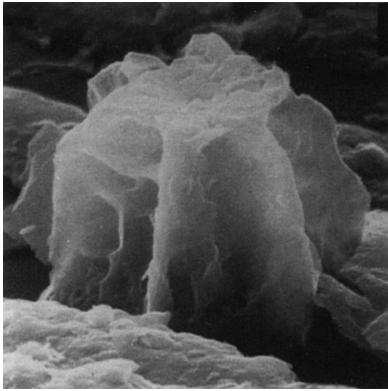
BLM95/6



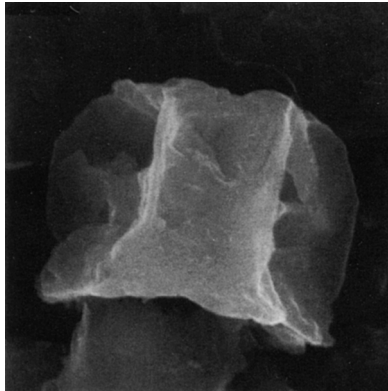
7



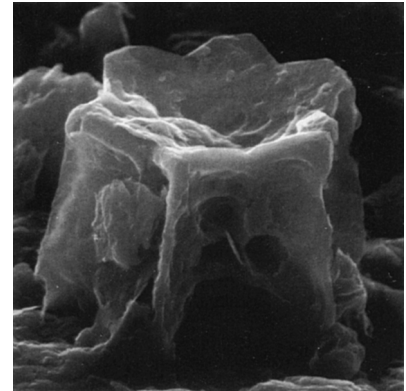
8



9



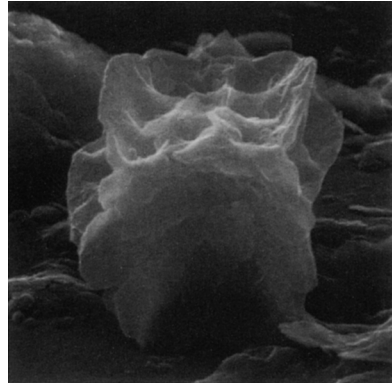
10



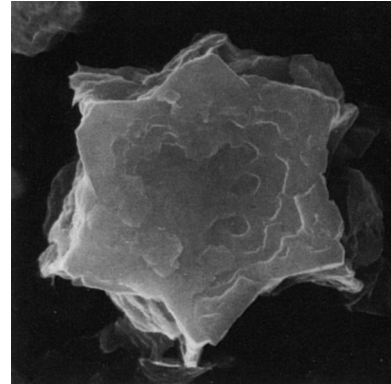
11

Fasciculithus sidereus (continued)

PROXIMAL FACE



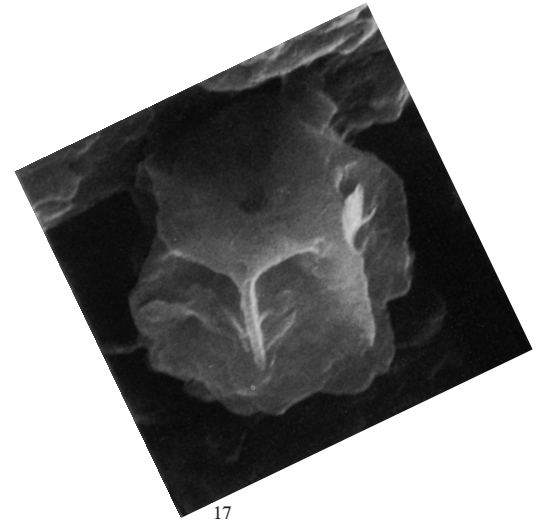
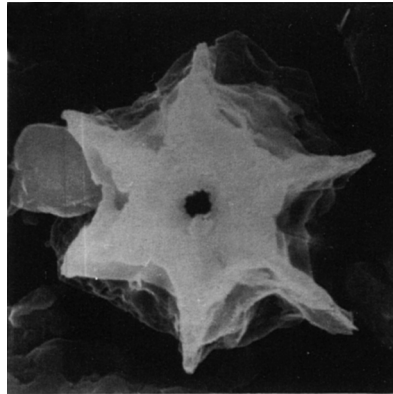
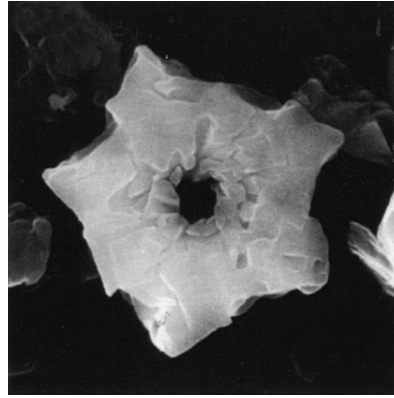
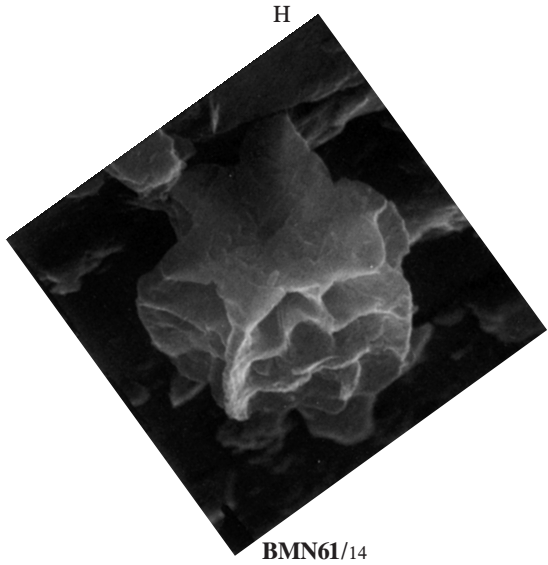
BLM95/12



13

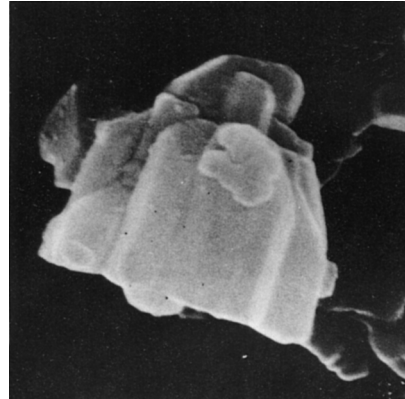
Fasciculithus sidereus (continued)

DISTAL FACE

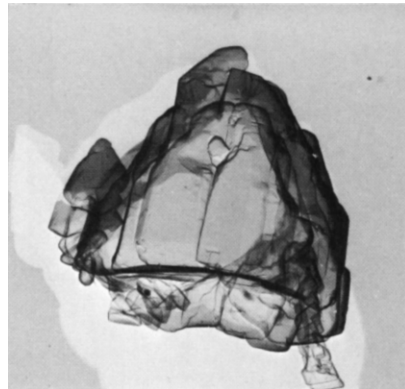


Fasciculithus clinatus (continued)

SIDE VIEW



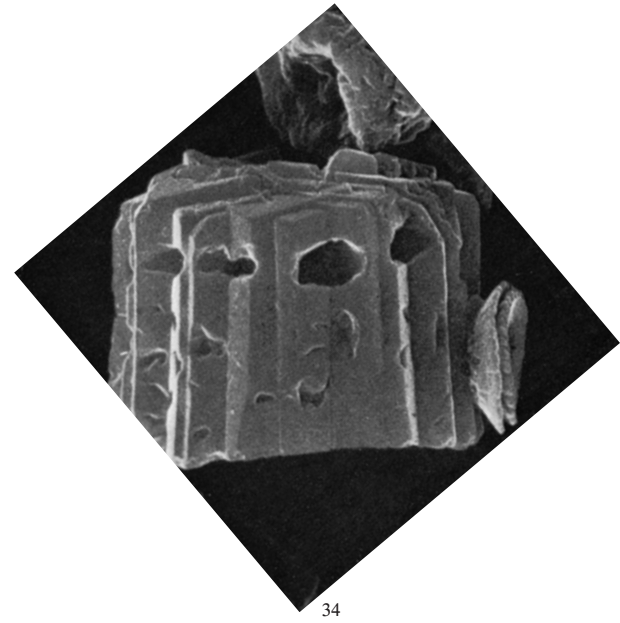
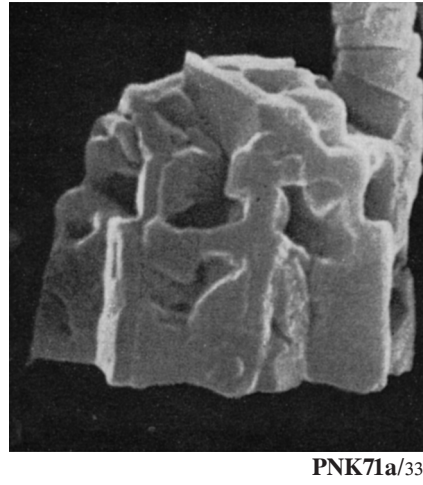
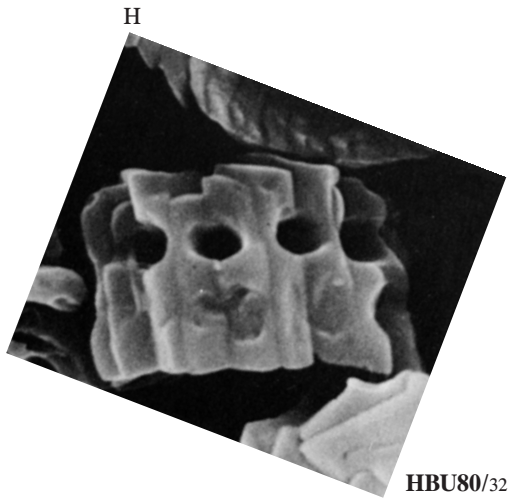
MS85/23



OH79/24

Fasciculithus aubertae (continued)

SIDE VIEW



Fasciculithus sp. A [= *Fasciculithus* sp. Steurbaut & Sztrákos 2008, p. 26, pl. 2, fig. 12]

Fasciculithus tympaniformis Hay & Mohler 1967

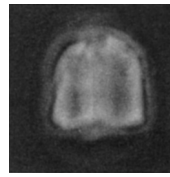
Fasciculithus involutus Bramlette & Sullivan 1961

Fasciculithus bobii Perch-Nielsen 1971

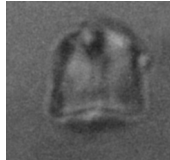
Fasciculithus lingfengensis Wang & Huang 1989



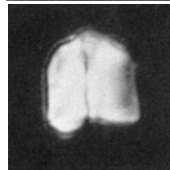
SE08/41



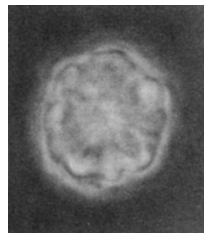
HWW67/42



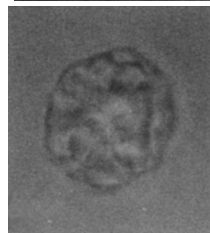
43



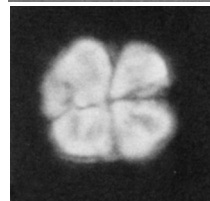
44



45

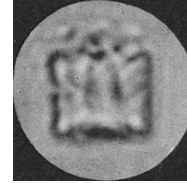


46



47

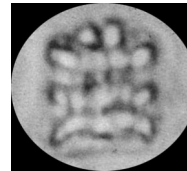
H



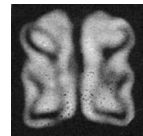
BMN61/89



90



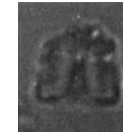
91



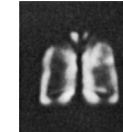
92



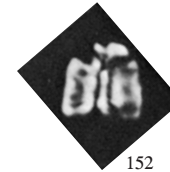
93



PNK71a/150



151



152



WC89/160



161



162

Fasciculithus sp. A

- 6.4 μm x 5.6 μm

- L. Paleocene (NP4). Aquitaine Basin, France.

- Small, with a proximally tapering column, consisting of a series of rather smooth elements with small depressions, especially in the most distal parts, and a dome-shaped very small cone. In side view, in CN, the longitudinal optical extinction line is bifurcated. On the basis of these characters these forms are grouped in a separate taxon, which shares features with *F. involutus* (optical colour pattern between CN; presence of depressions). However, differences, such as small size, tapering outline and configuration of the cone, exclude inclusion in *F. involutus*.

- SFR64 (p. 26), AMP (p. 103).

Fasciculithus tympaniformis

- 4–6 μm

- Paleocene. Aquitaine Basin, France.

- Short sub-cylindrical; one end slightly pointed, the other end concave. Column constructed of about 16 wedges, so arranged that their thin edges meet at the center and the thick ends form the outer surface of the column. Surface smooth, lacking ornamentation. In some specimens, a few tabular plates are present on the pointed end.

≠ from *F. involutus* by its smoothly finished outer surface.

— LO defines the base of NP5 (Martini, 1971, p. 752). LAD in the earliest Eocene within NP10 (Romein, 1979, p. 77).

— Evolved from *F. ulii*. Older specimens of the sp. have a central body that disappears in younger specimens (Romein, 1979, p. 77, p. 157).

- HWW67 (p. 447).

Fasciculithus involutus

- 5–13 μm

- Paleocene. Lodo Formation, California.

- Short cylindrical form, with end view appearing as a rosette of about ten rounded petals, both ends somewhat concave but with a small central knob in one end. Commonly compact, with surface ridges on cylindrical sides rather obscure.

- Remarks: Much of the variation in appearance of this sp. seems to be largely related to the solidity of construction by varying amounts of calcite deposition. However, subdivision of better characterized taxa within this genus elsewhere may permit their recognition among forms here included in the broadly defined sp.

— Wise and Wind (1977, p. 296) interpret this sp. as “an etched form of *F. tympaniformis*”. When well preserved, both spp. are distinct.

— FAD in earlier NP9 (Romein, 1979, p. 77).

— Present in Upper Paleocene cool assemblages (Bukry, 1973b, p. 887).

— Dissolution resistant sp. (Wise and Wind, 1977, p. 296).

- BMN61 (p. 164).

Fasciculithus bobii

- 8–10 μm x 8–10 μm

- L. Paleocene (NP9). Bay of Biscay (DSDP site 119), Atlantic.

- [Column made of wedge-shaped elements interrupted in the upper part by a row of depressions. Distal side topped by a very flat cone-shaped apical needle. The number of elements, of depressions, and the total size of the fasciculith vary greatly.]

≠ from other spp. by its flat cone-shaped needle, and its depressions-bearing column.

- Ranges in NP8 and part of NP9.

- PNK71a (p. 351).

Fasciculithus lingfengensis

- 5 μm x 6.6 μm

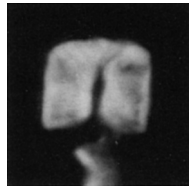
- Not given.

- [Fasciculith comprised of a distal and a proximal part. The distal part is deeply ensconced at the end of the proximal part. The latter is marked by transversal ridges. In CN at 45°, the fasciculith is divided into two bright areas, with extinction lines that highlight its contour. In CN at 0°, a median extinction line occurs as well as two curved extinction lines that delineate the distal part.]

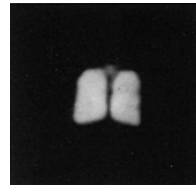
≠ from the similar *F. bobii* which possesses longitudinal ridges but lack transversal ones.

- WC89 (p. 224).

Fasciculithus tympaniformis (continued)



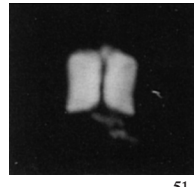
BLM95/48



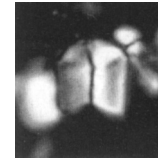
49



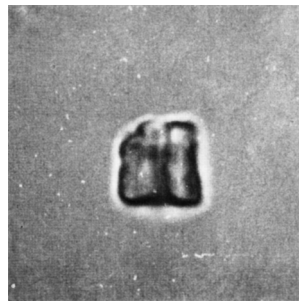
50



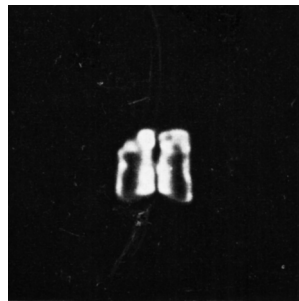
51



SE08/54



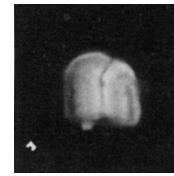
ME71/52



53



VO89/55

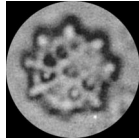


56

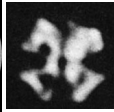
Fasciculithus involutus (continued)



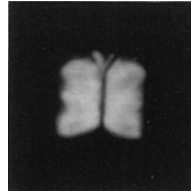
BPR10/94



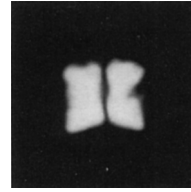
BMN61/95



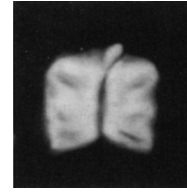
96



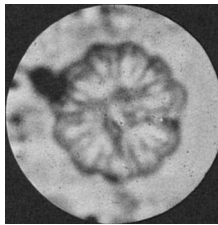
BLM95/101



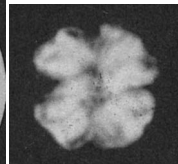
102



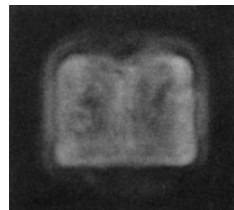
103



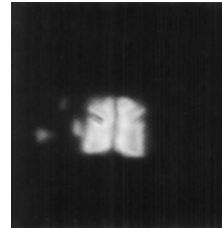
97



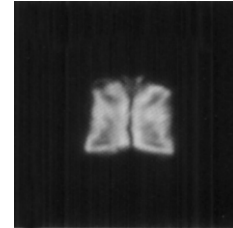
98



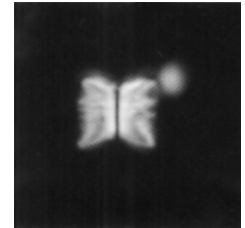
HWW67/104



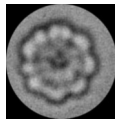
STJM11/110



111



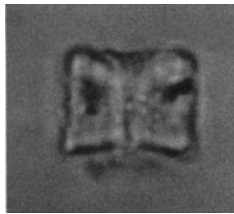
112



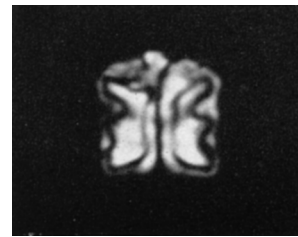
99



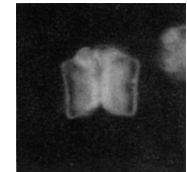
100



105



SFR64/113



VO89/115



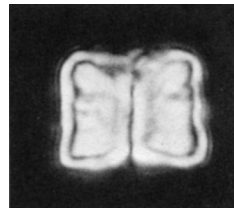
PNK71a/107



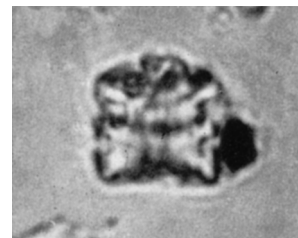
108



109



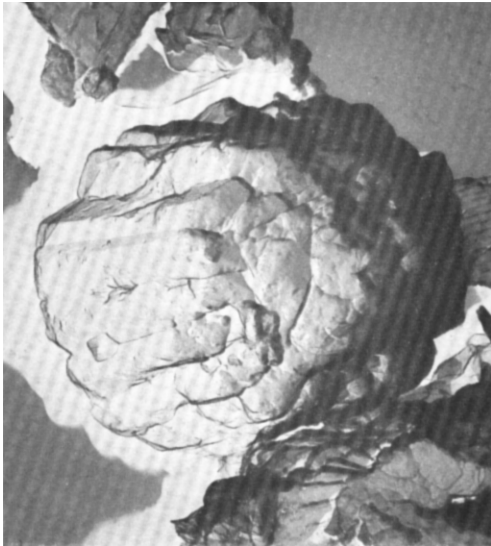
106



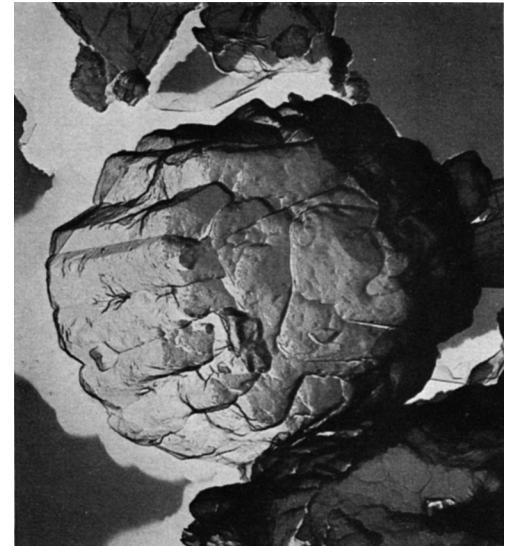
114

Fasciculithus tympaniformis (continued)

DISTAL FACE



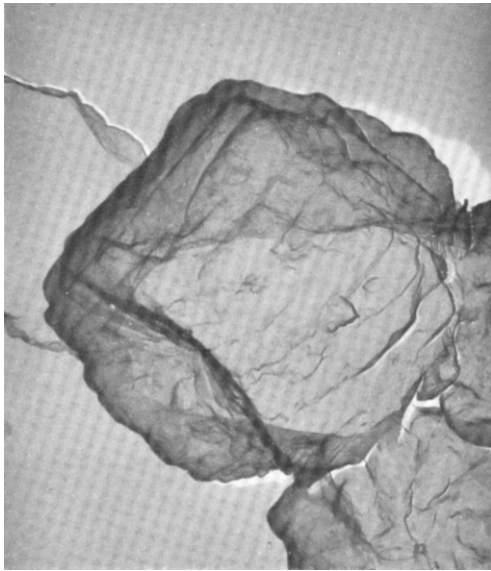
HWW67/57



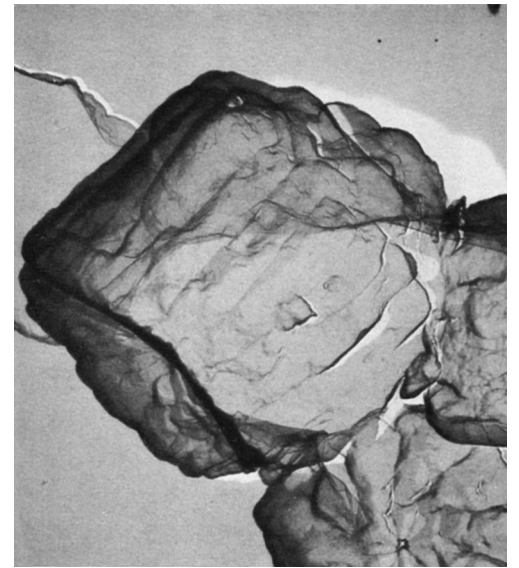
58

Fasciculithus tympaniformis (continued)

SIDE VIEW



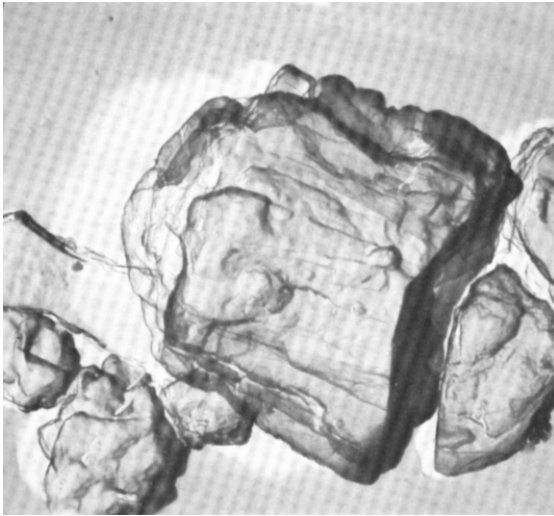
HWW67/59



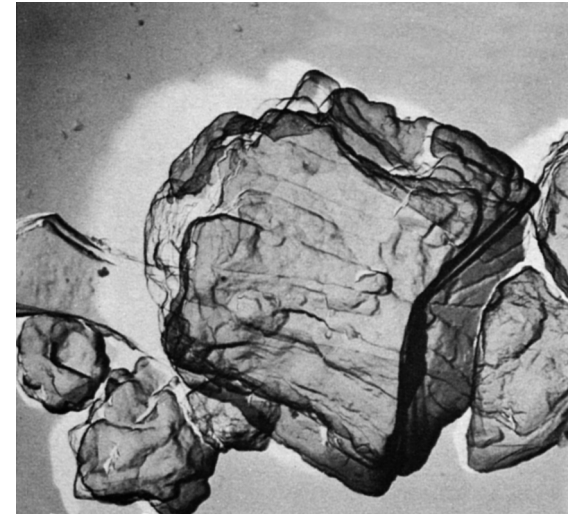
60

Fasciculithus tympaniformis (continued)

SIDE VIEW



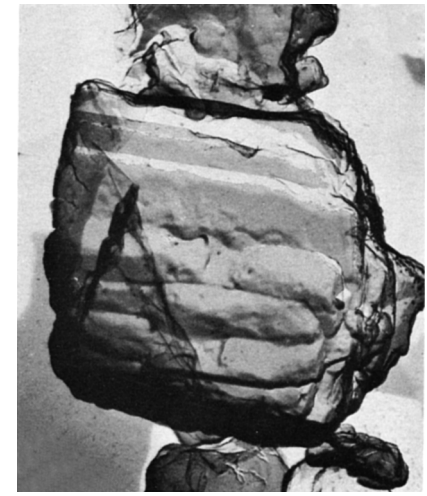
HWW67/61



62



63



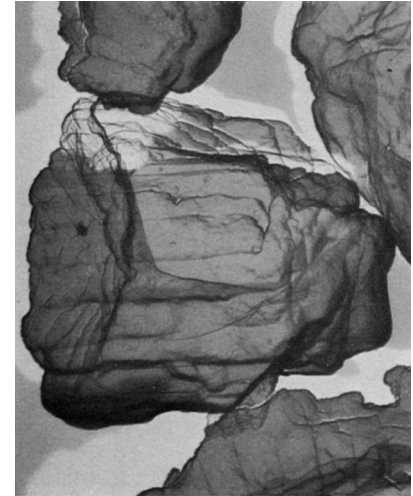
64

Fasciculithus tympaniformis (continued)

SIDE VIEW



HWW67/65

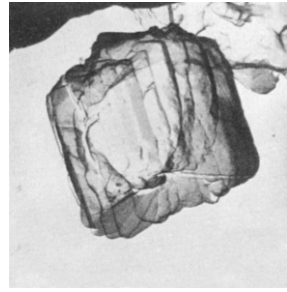


66

Fasciculithus tympaniformis (continued)

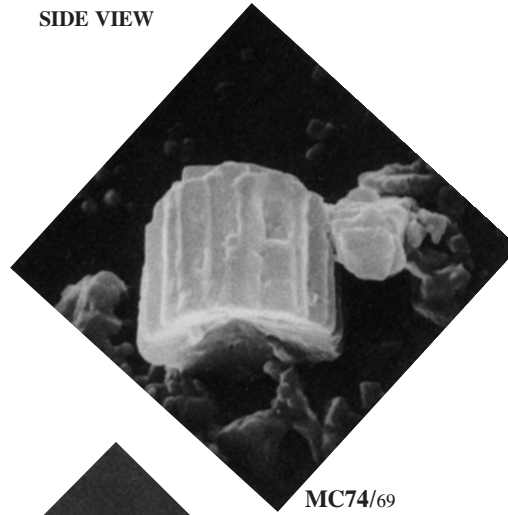


HWW67/67



68

SIDE VIEW



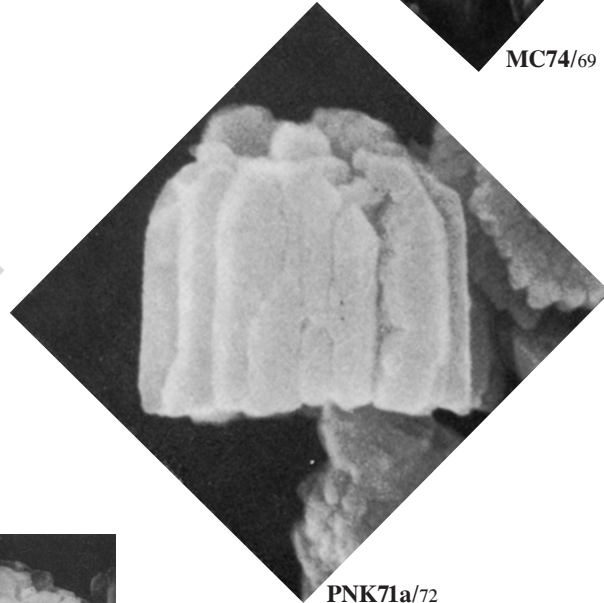
MC74/69



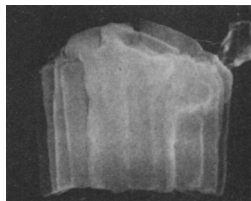
OH79/70



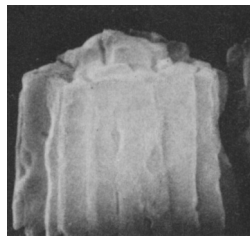
71



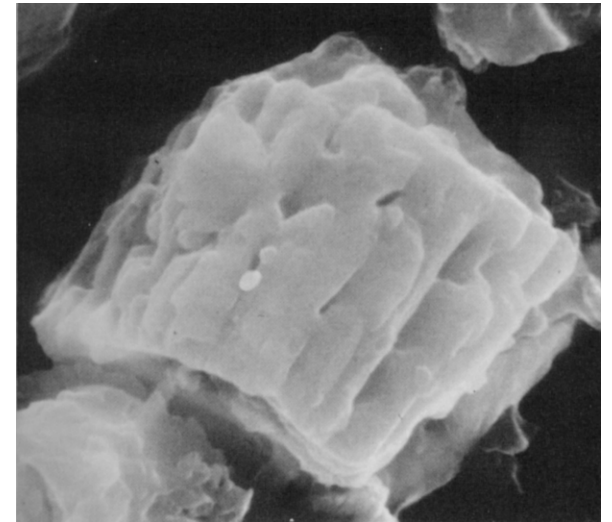
PNK71a/72



PNK77/73



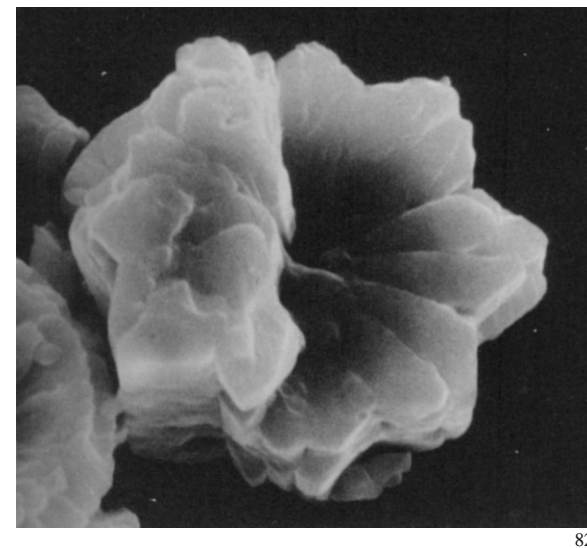
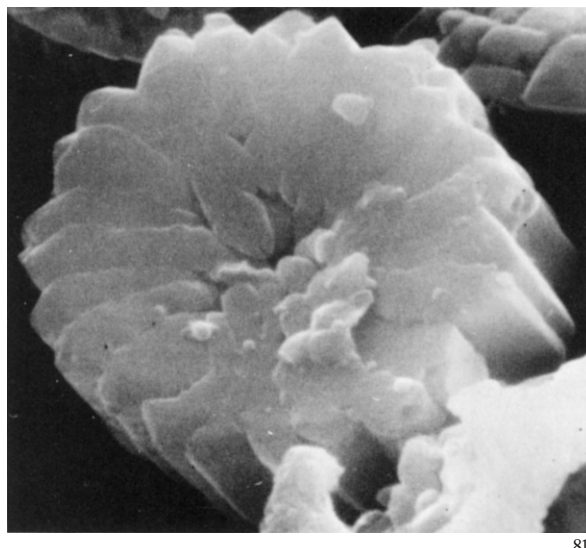
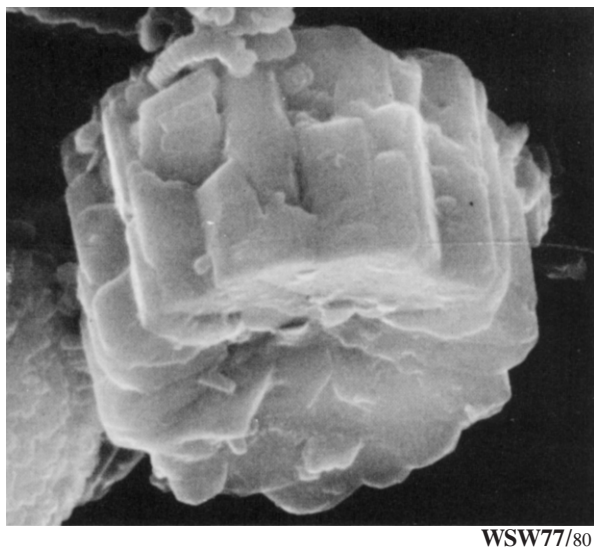
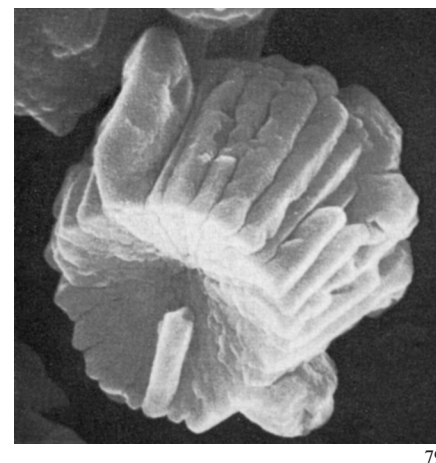
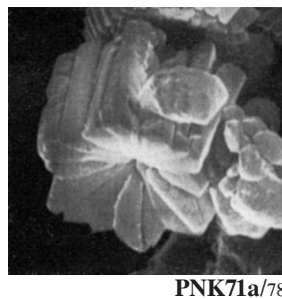
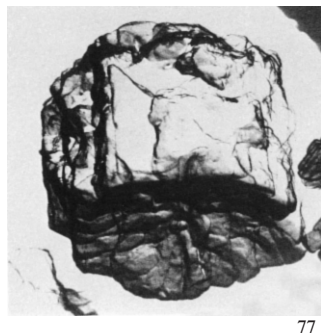
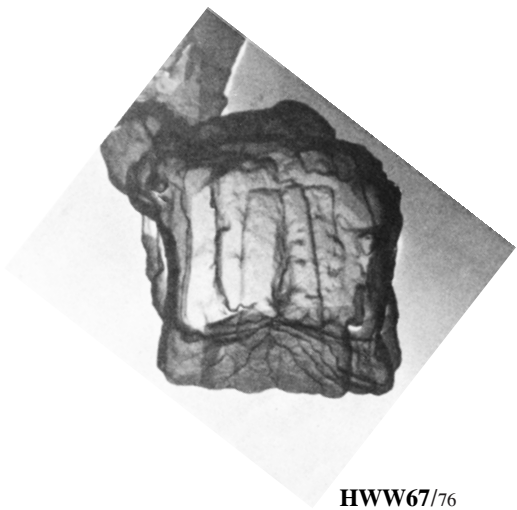
74



WSW77/75

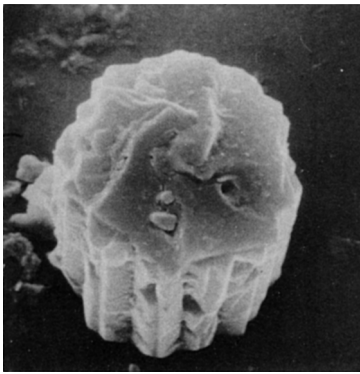
Fasciculithus tympaniformis (continued)

PROXIMAL FACE

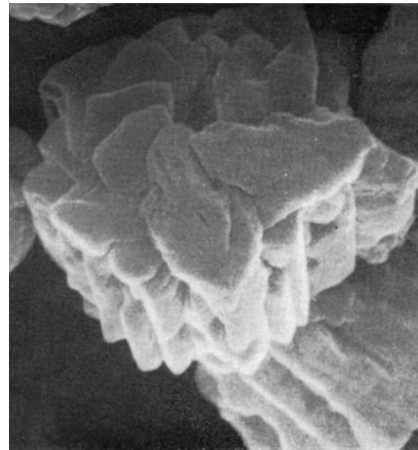


Fasciculithus tympaniformis (continued)

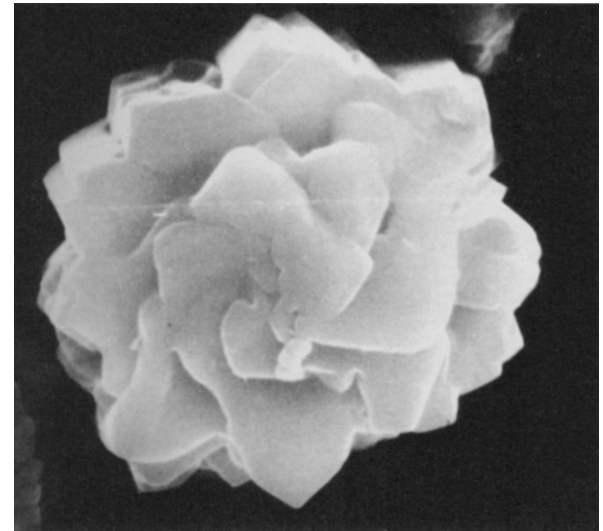
DISTAL FACE



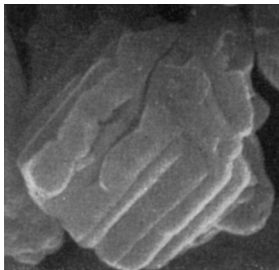
MC74/83



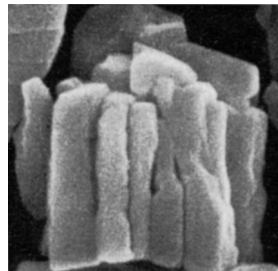
PNK71a/84



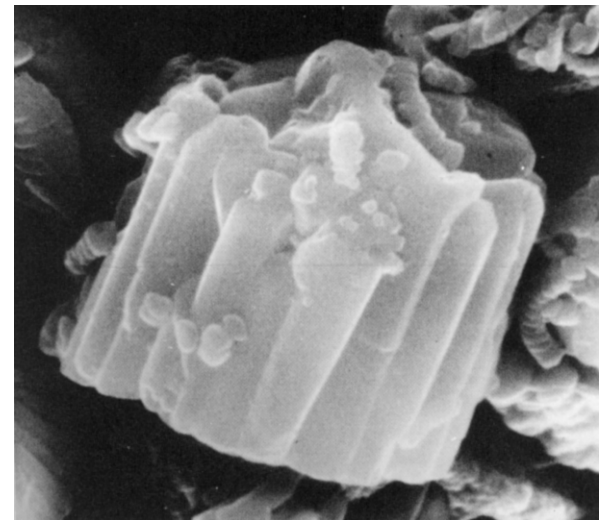
SFR64/87



85



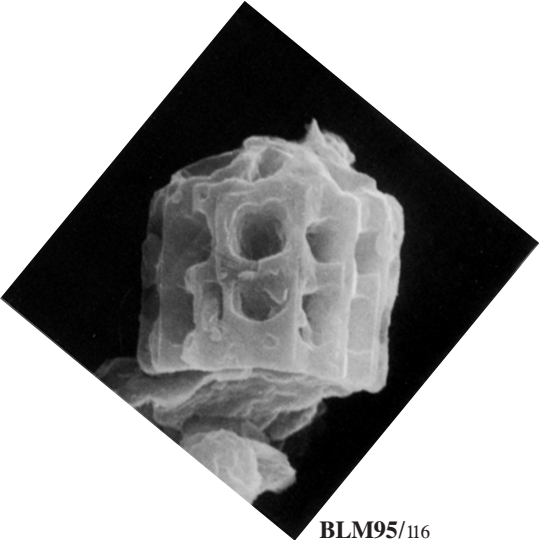
86



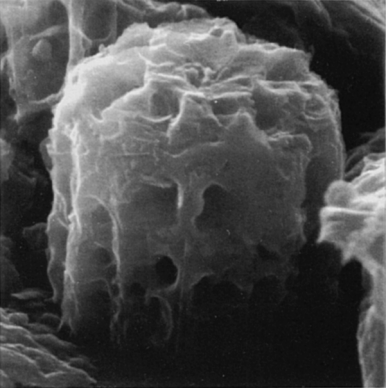
88

Fasciculithus involutus (continued)

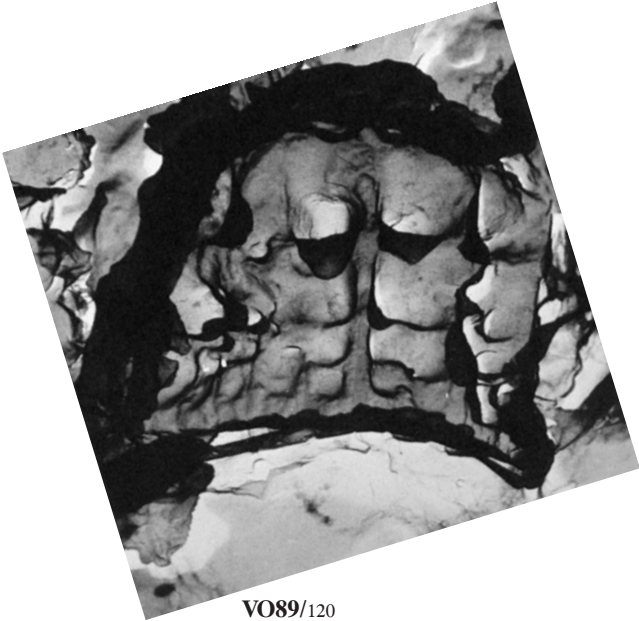
SIDE VIEW



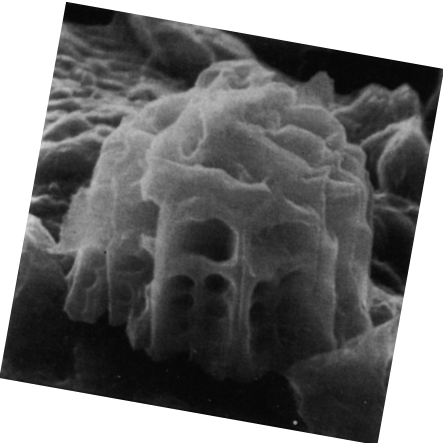
BLM95/116



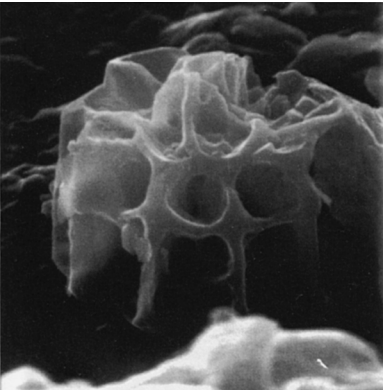
117



VO89/120



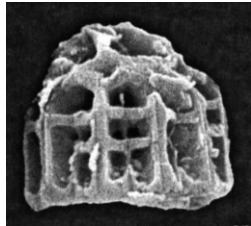
118



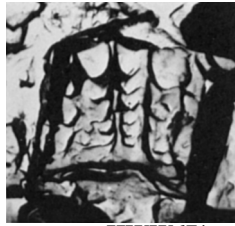
119

Fasciculithus involutus (continued)

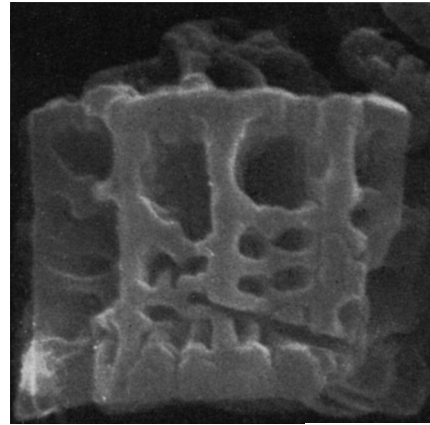
SIDE VIEW



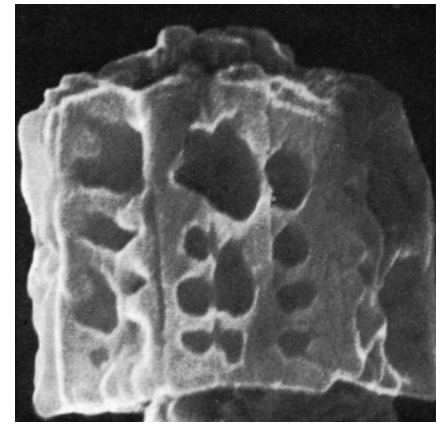
BPR10/121



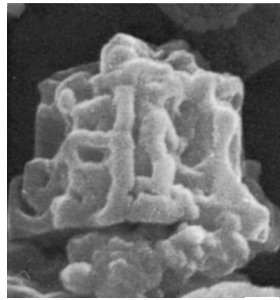
HWW67/122



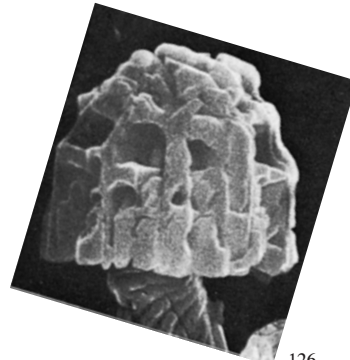
PNK71a/123



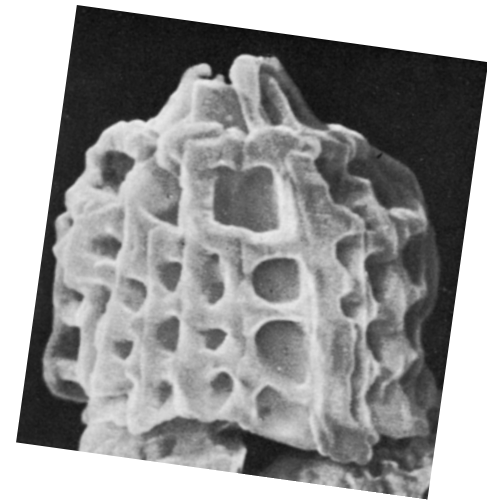
124



125



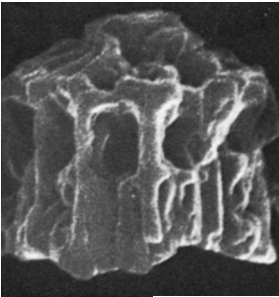
126



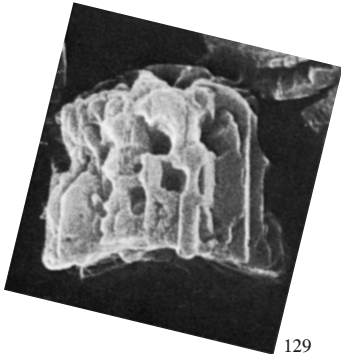
127

Fasciculithus involutus (continued)

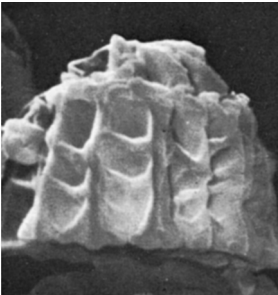
SIDE VIEW



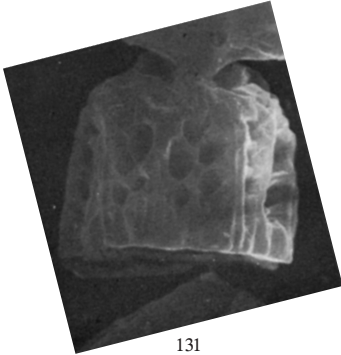
PNK71a/128



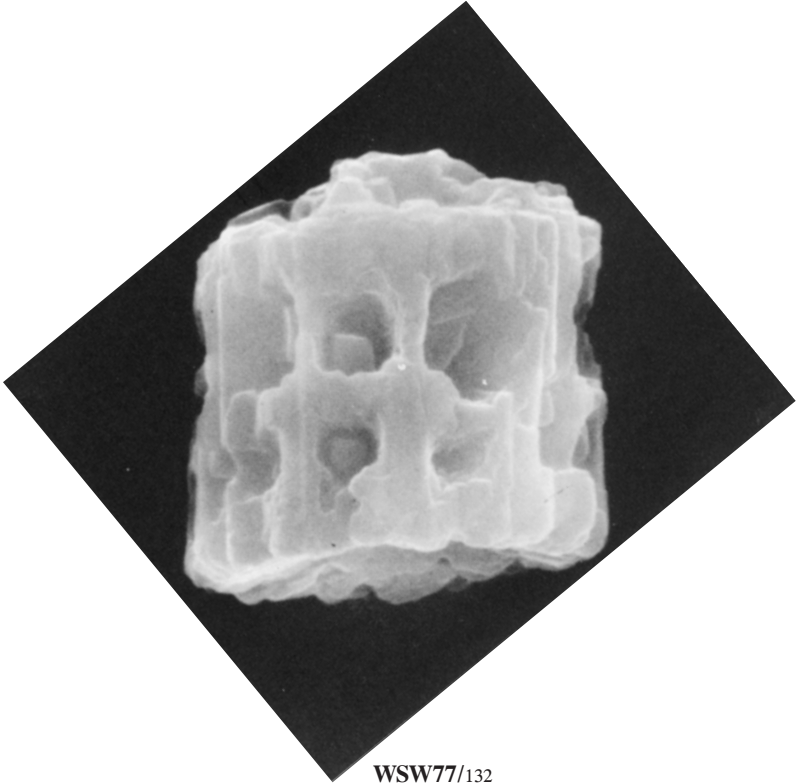
129



130



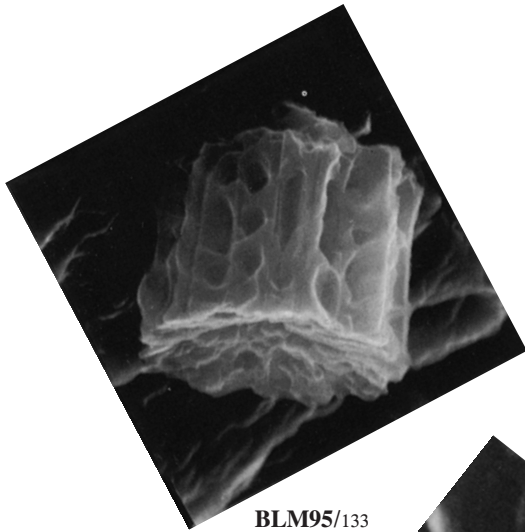
131



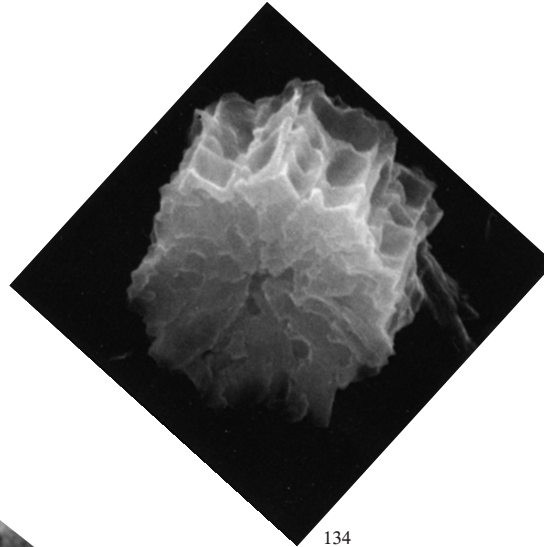
WSW77/132

Fasciculithus involutus (continued)

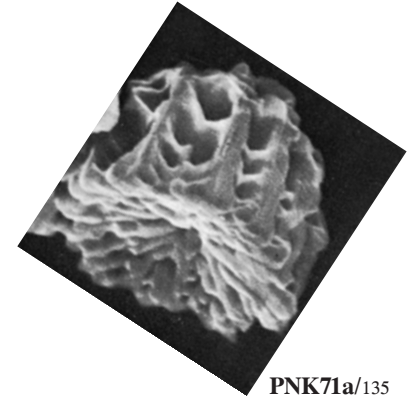
PROXIMAL FACE



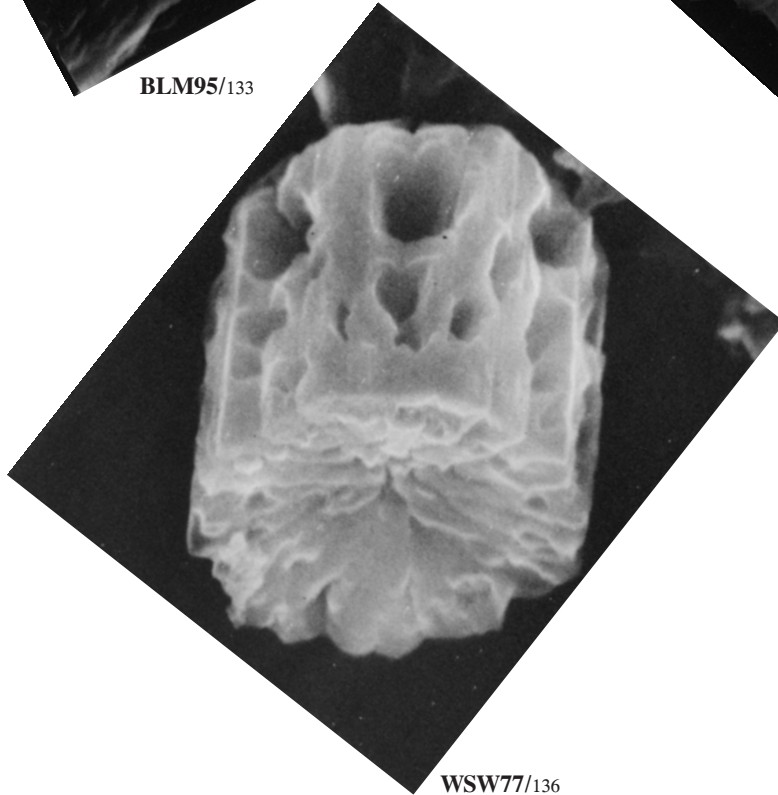
BLM95/133



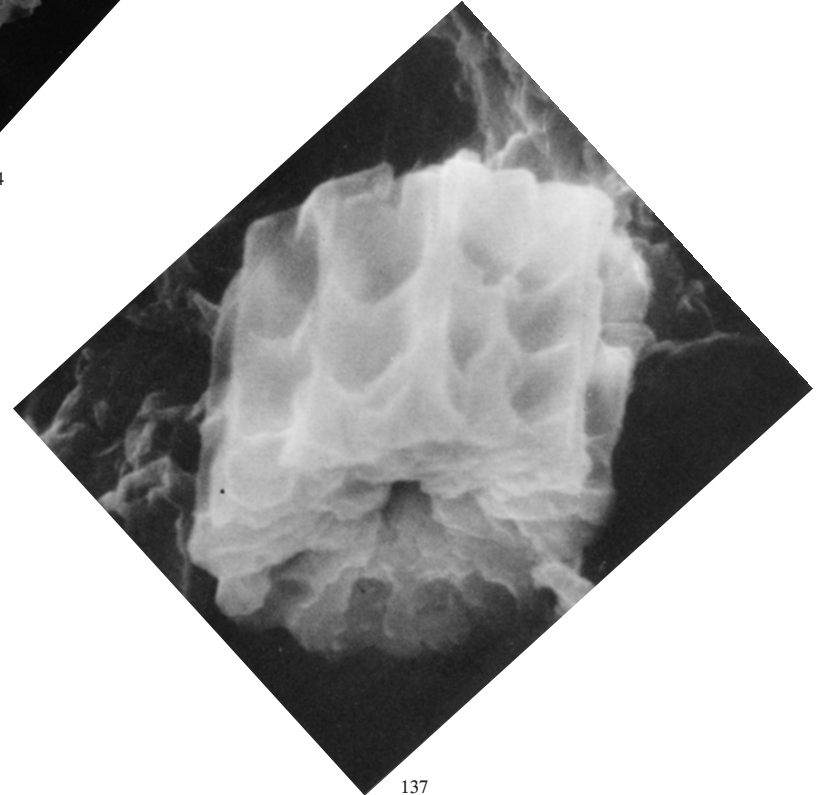
134



PNK71a/135



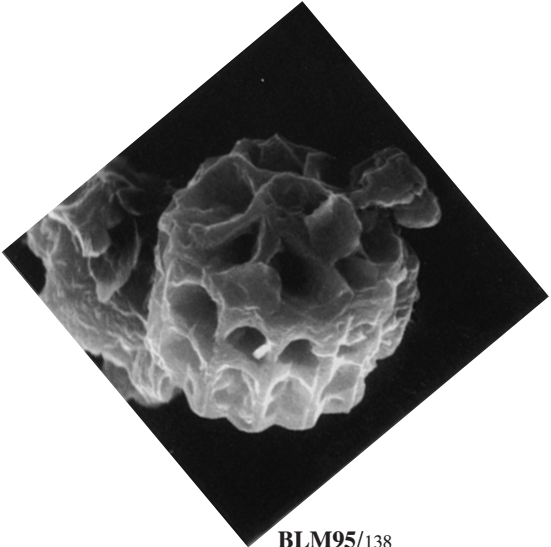
WSW77/136



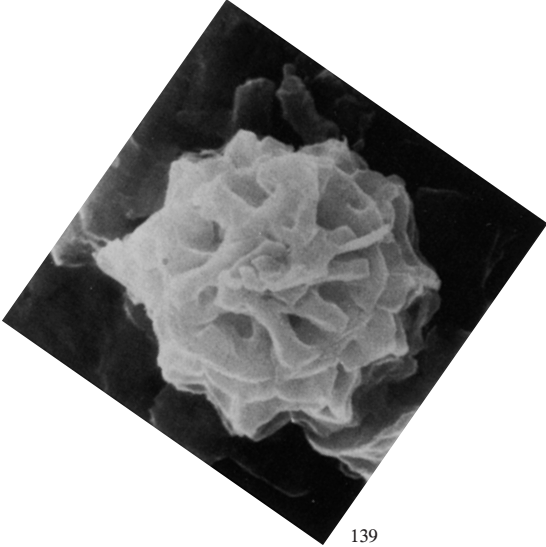
137

Fasciculithus involutus (continued)

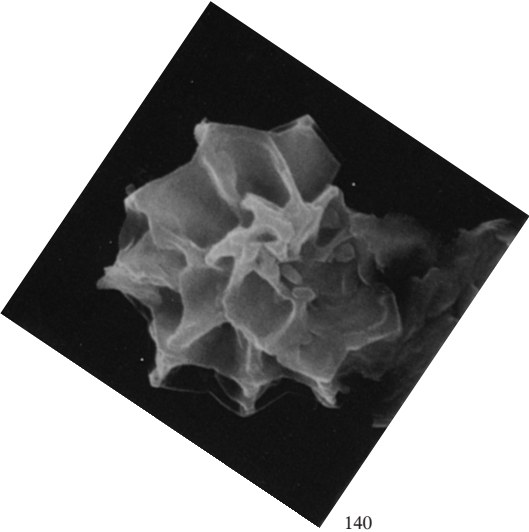
DISTAL FACE



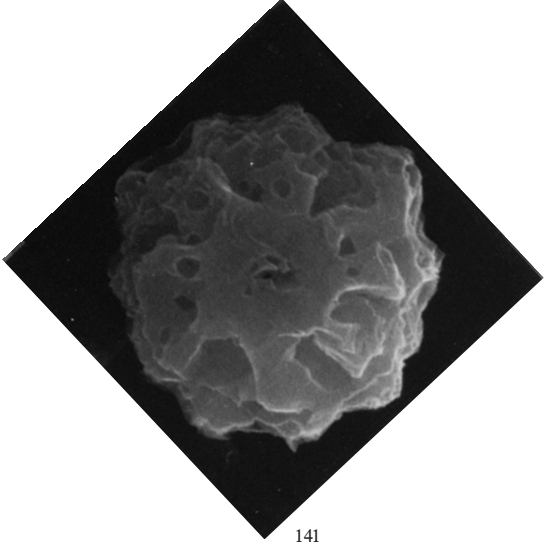
BLM95/138



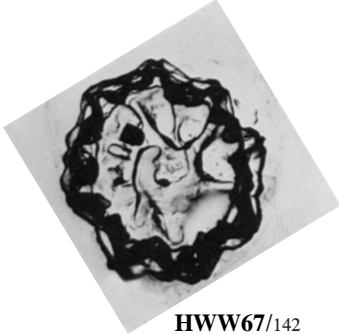
139



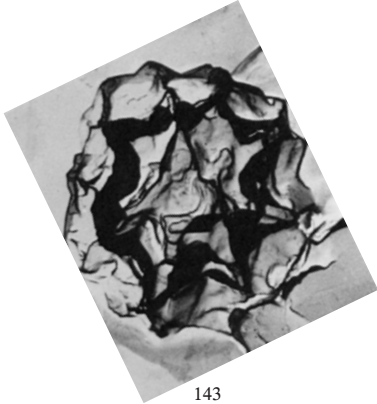
140



141



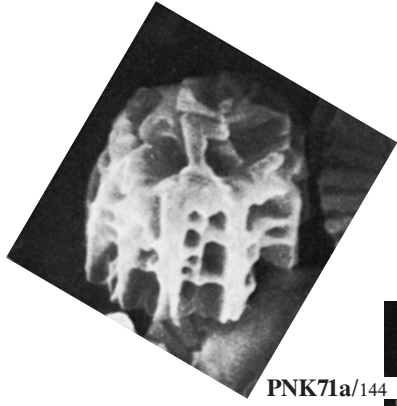
HWW67/142



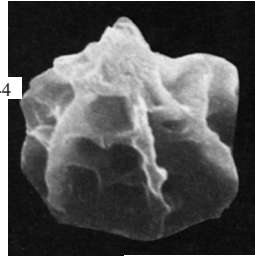
143

Fasciculithus involutus (continued)

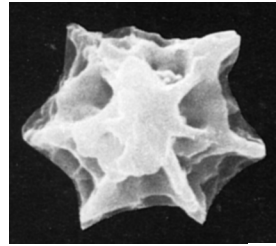
DISTAL FACE



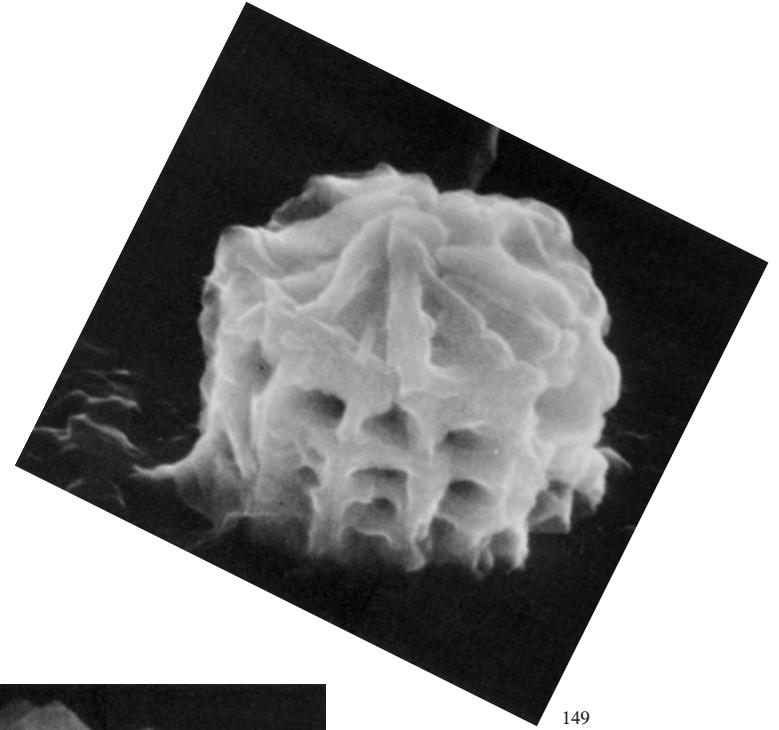
PNK71a/144



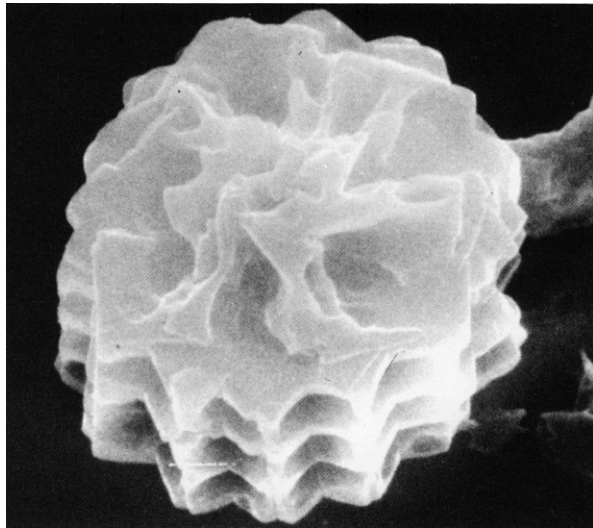
RAJT79/145



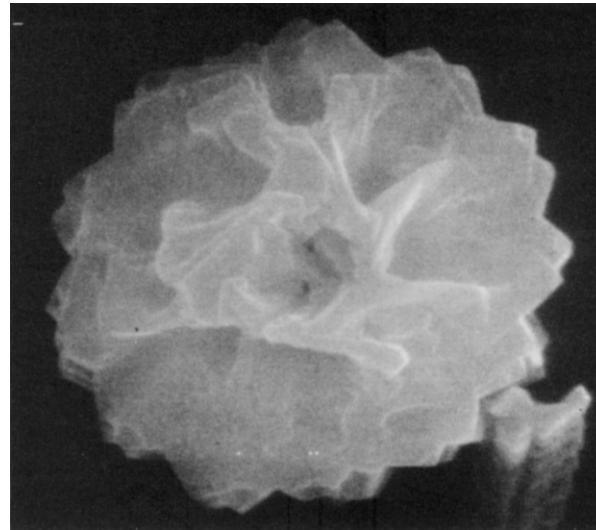
146



149



WSW77/147

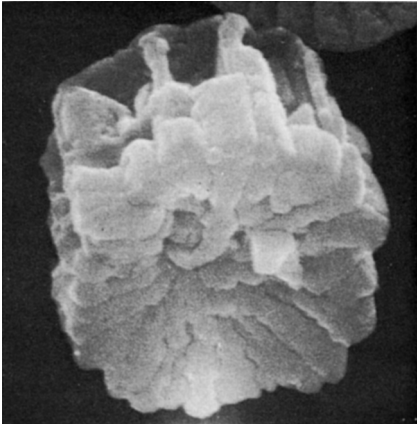


148

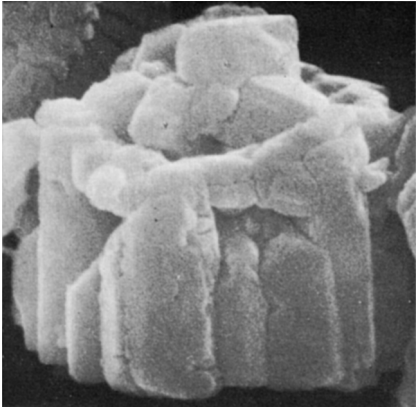
Fasciculithus bobii (continued)

PROXIMAL FACE

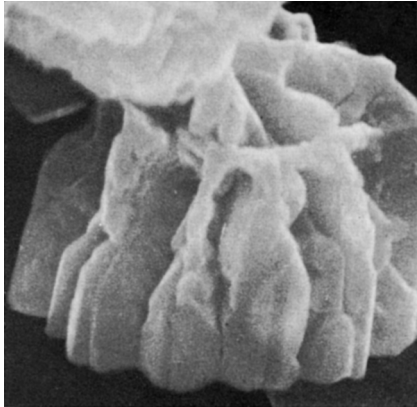
SIDE VIEW



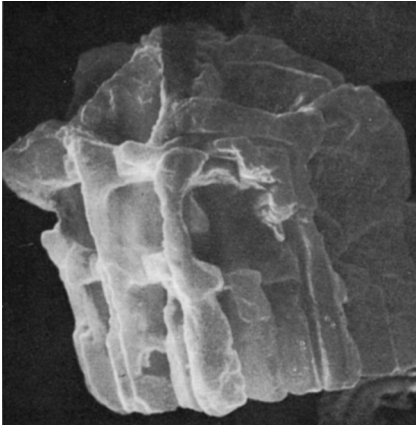
PNK71a/153



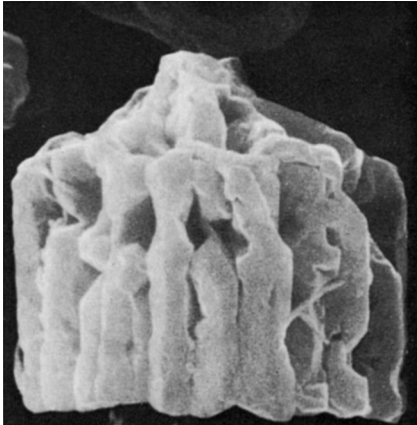
PNK71a/154



155



156

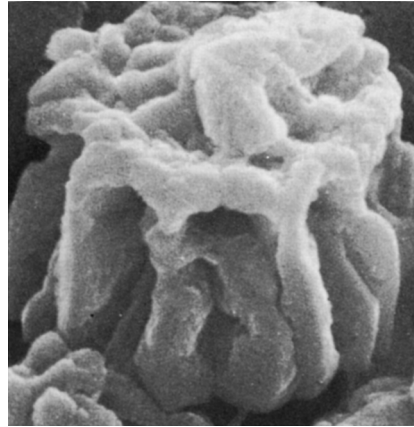


157

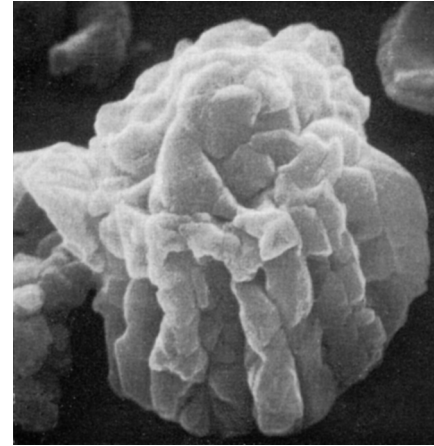
Fasciculithus bobii (continued)

DISTAL FACE

H



PNK71a/158



159

Fasciculithus thomasi Perch-Nielsen 1971

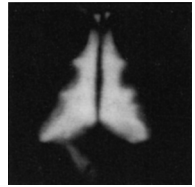
Fasciculithus schaubii Hay & Mohler 1967

Fasciculithus lilianae Perch-Nielsen 1971

Fasciculithus alanii Perch-Nielsen 1971

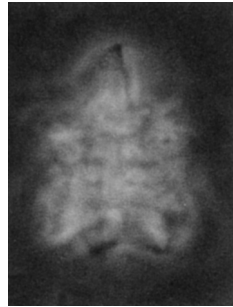


BMN61/163

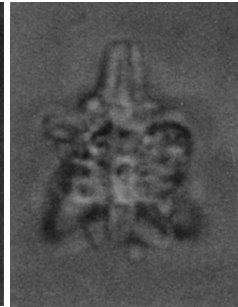


164

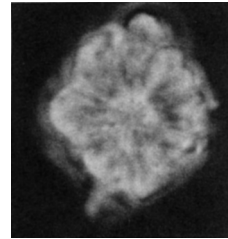
HWW67/180



181



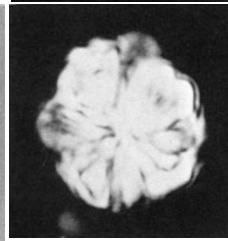
182



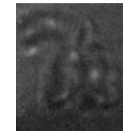
183



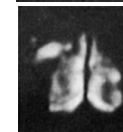
184



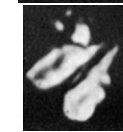
185



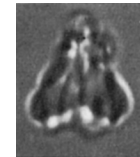
PNK71a/198



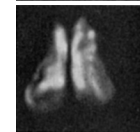
199



200



PNK71a/208



209

Fasciculithus thomasii

- 5–6 μm x 5–6 μm

- L. Paleocene (NP9). Bay of Biscay (DSDP Site 119), Atlantic.

- [Distally narrowing column topped by a sharp distal needle, both showing an alveolar pattern. The needle is hardly separated from the column.]

≠ from other spp. by its general shape and its alveolar pattern.

— Short ranging sp., mainly restricted to the lowest part of NP10 (Romein, 1979, p. 77).

Fasciculithus schaubii

- 7–10 μm x 5–8 μm

- L. Paleocene (NP9). Aquitaine Basin, France.

- Base roughly prismatic, having six concave sides bearing vertical rows of pits, each row having four pits. Between the pits are ridges, and between the rows of pits are ribs forming the edges of the prism. The pyramid surmounting the base is smooth but stubby and only about half the height of the base. The surface of the base opposite the pyramid is slightly concave.

≠ from *F. involutus* which lacks the pyramid.

— Restricted to NP9 (Romein, 1979, p. 77).

Fasciculithus lilianae

- 6–10 μm x 7–11 μm

- L. Paleocene (NP9). Bay of Biscay (DSDP Site 119), Atlantic.

- [Simple column consisting of distinct wedges topped by a sharp distinctive apical needle.]

≠ from other spp. by its simply-built column, made of a smaller number of wedges and its sharp needle.

— Restricted to NP9 (Romein, 1979, p. 77).

Fasciculithus alanii

- 6–8 μm x 7–9 μm

- L. Paleocene (NP9). Bay of Biscay (DSDP Site 119), Atlantic.

- [Column with a star-shaped cross section, consisting of wedge-shaped elements. Rare depressions. Slender and high apical needle consisting of a row of lateral elements of the column.]

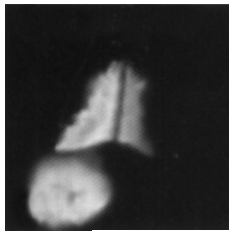
≠ from other spp. by its apical needle and the outline of its cross section.

— Restricted to NP9 (Romein, 1979, p. 77).

Fasciculithus thomasi (continued)

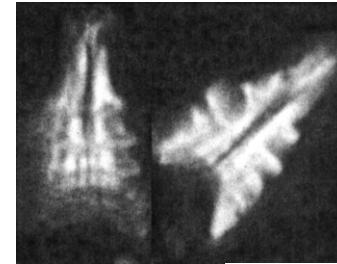


BPR10/165

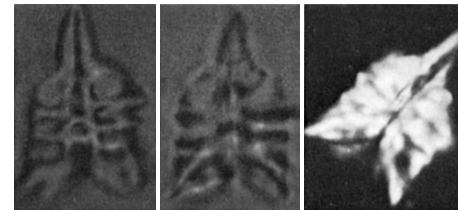


STJM11/166

Fasciculithus schaubii (continued)



BPR10/186



PNK71a/187

188

189

Fasciculithus lilianae (continued)



BPR10/201



202

Fasciculithus alanii (continued)

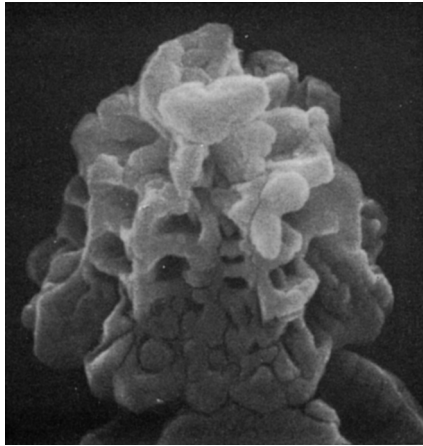


BPR10/210

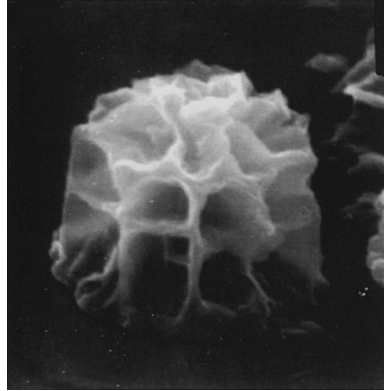
Fasciculithus thomasi (continued)

SIDE VIEW

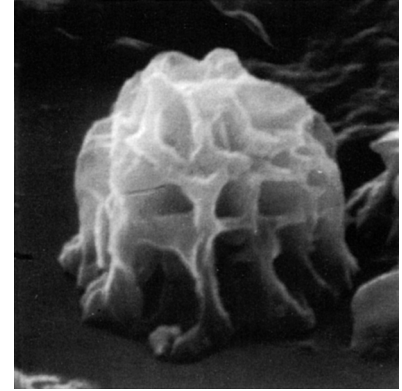
H



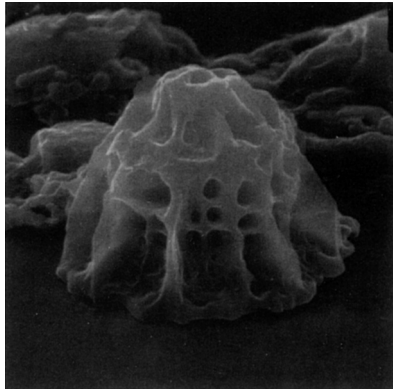
PNK71a/167



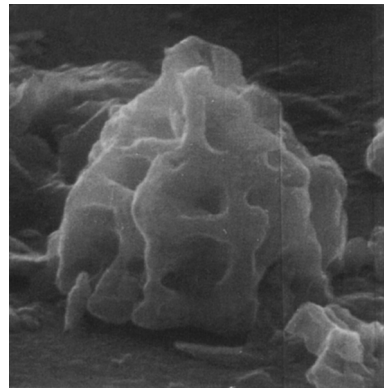
BLM95/168



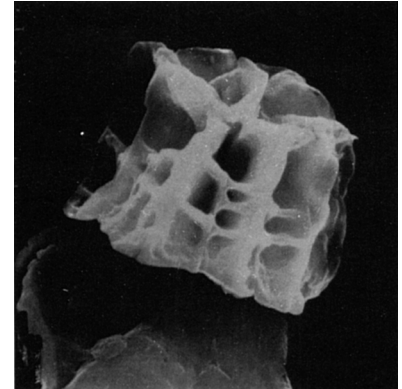
169



170



171

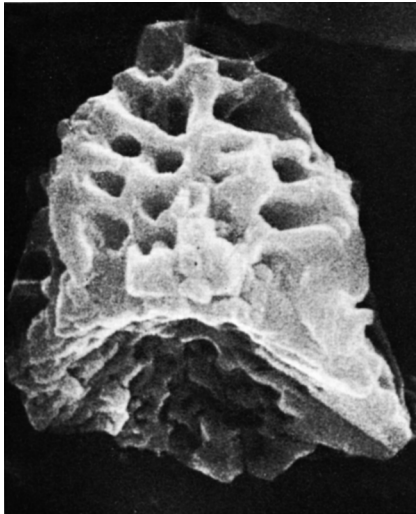


172

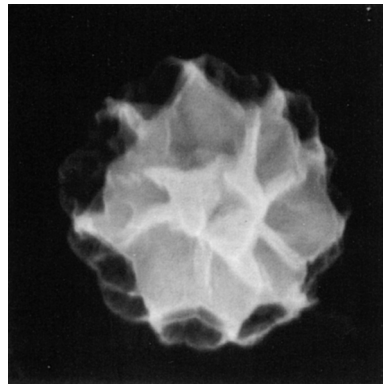
Fasciculithus thomasi (continued)

PROXIMAL FACE

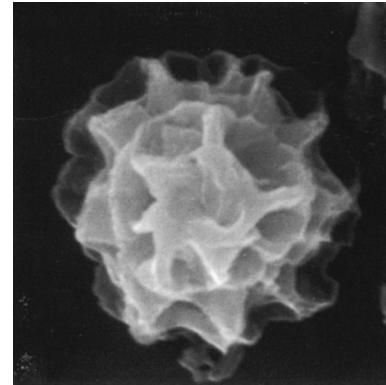
DISTAL FACE



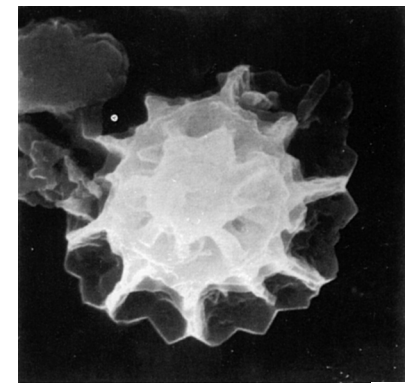
PNK71a/173



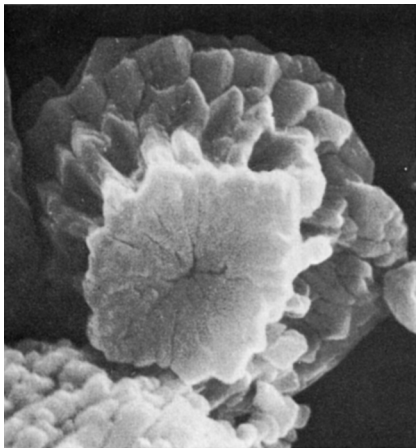
BLM95/175



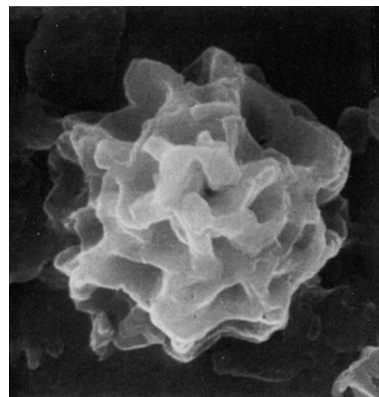
176



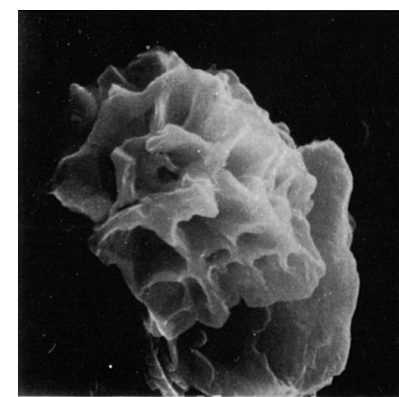
177



174



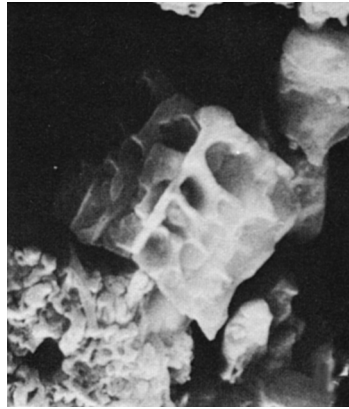
178



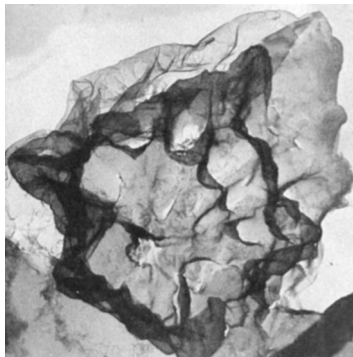
179

Fasciculithus schaubii (continued)

SIDE VIEW



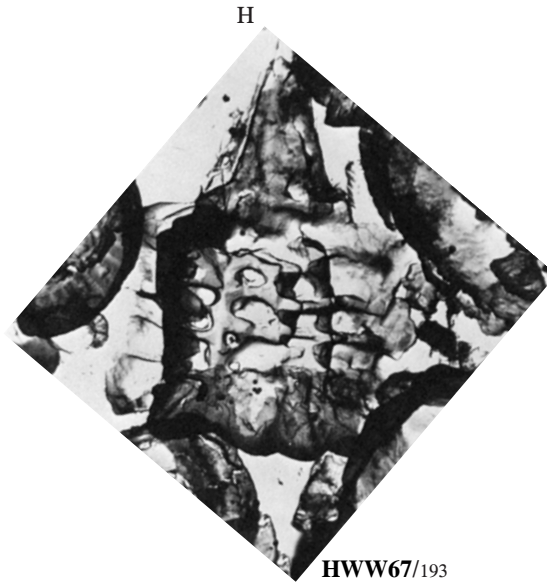
HBU80/192



HWW67/190



191

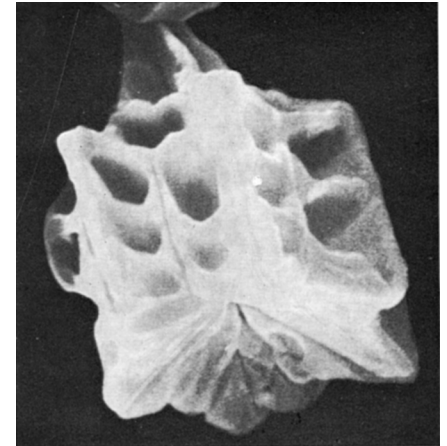


HWW67/193

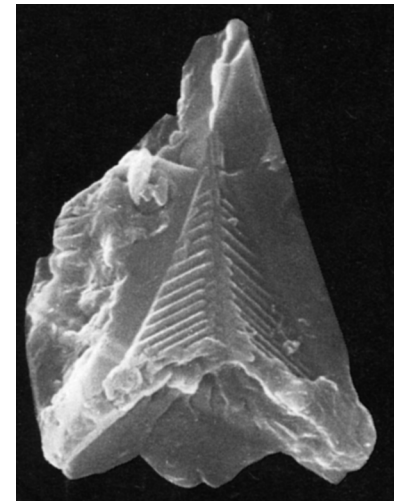


194

PROXIMAL FACE



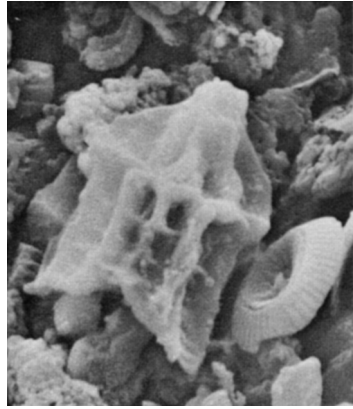
PNK71a/195



RAJT79/196

Fasciculithus schaubii (continued)

DISTAL FACE



HBU80/196



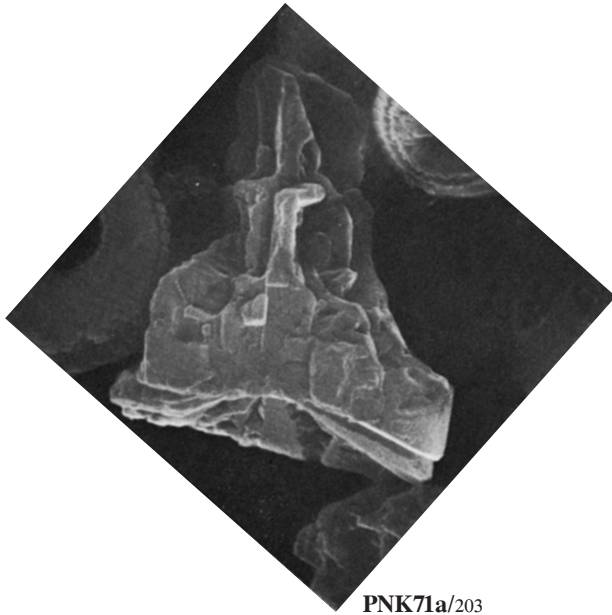
PNK71a/197

Fasciculithus lilianae (continued)

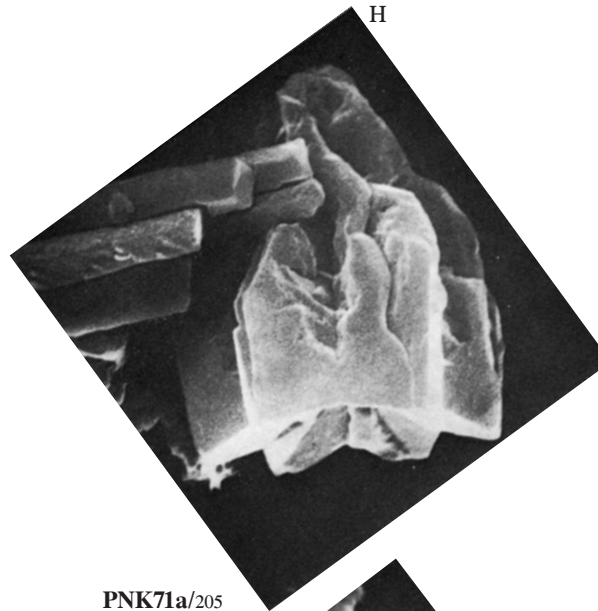
SIDE VIEW

PROXIMAL FACE

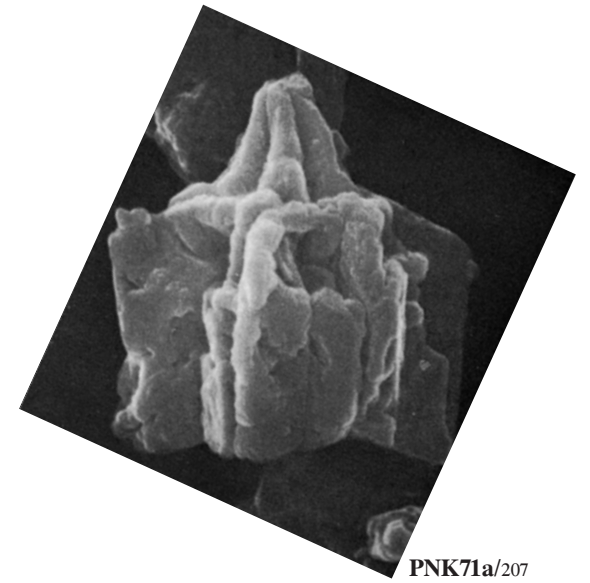
DISTAL FACE



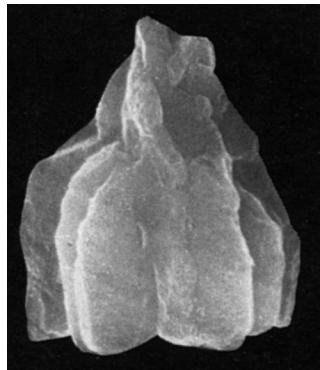
PNK71a/203



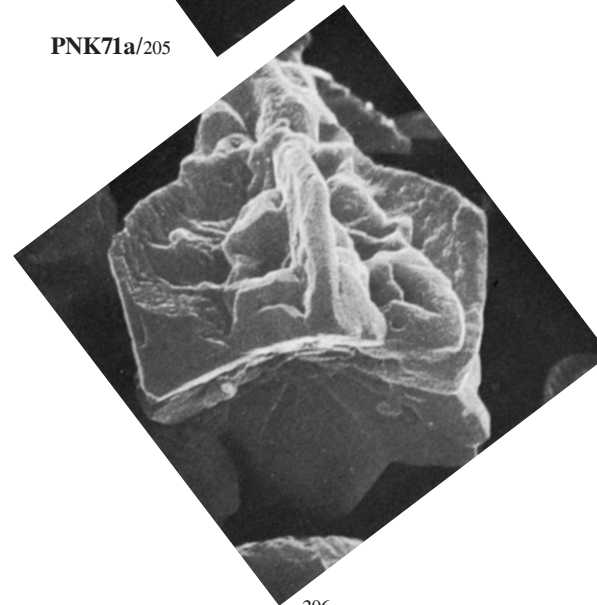
PNK71a/205



PNK71a/207



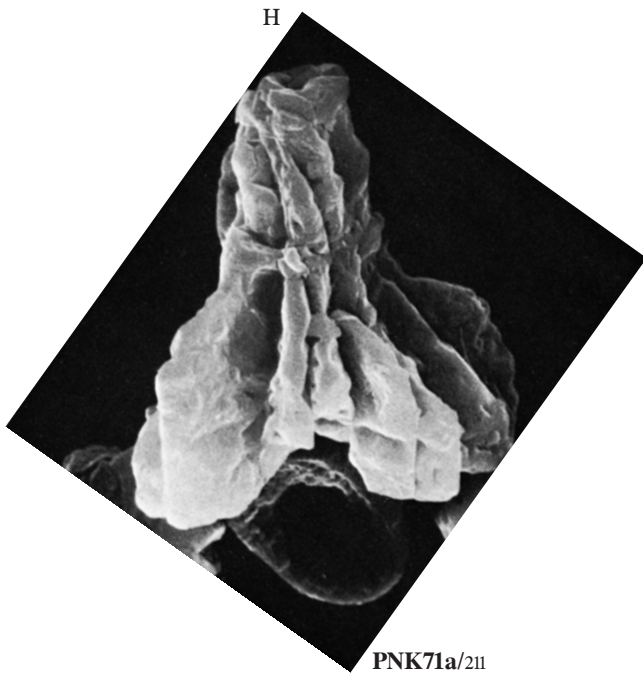
RAJT79/204



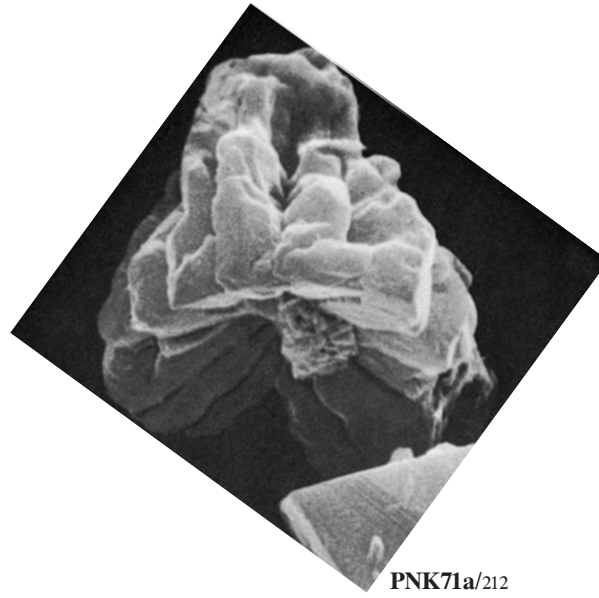
206

Fasciculithus alanii (continued)

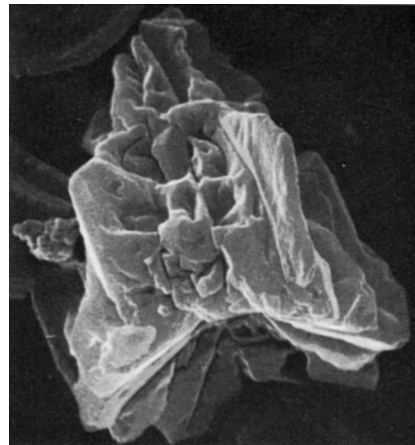
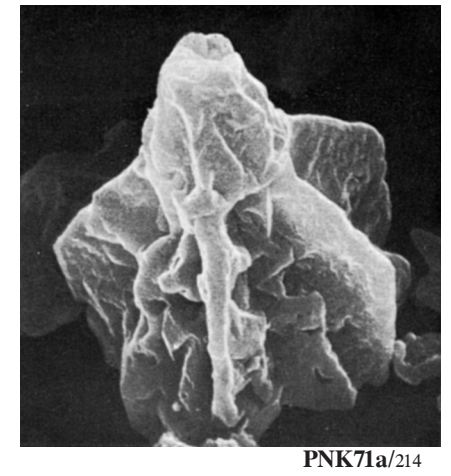
SIDE VIEW



PROXIMAL FACE



DISTAL FACE



Fasciculithus tonii Perch-Nielsen 1971

Fasciculithus mitreus Gartner 1971

Fasciculithus richardii Perch-Nielsen 1971

Fasciculithus hayii Haq 1971

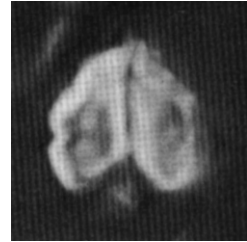


PNK71a/215

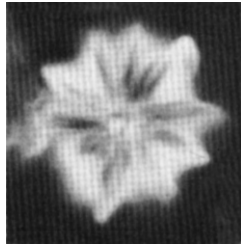


216

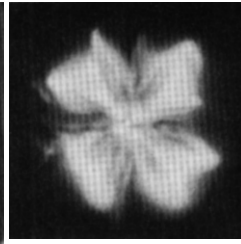
H



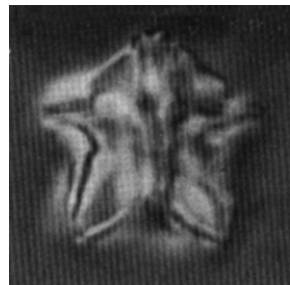
GS71/221



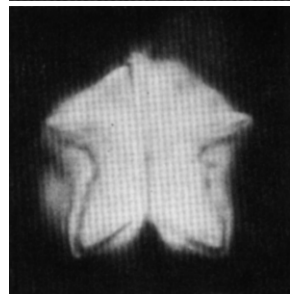
222



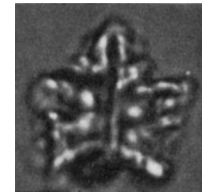
223



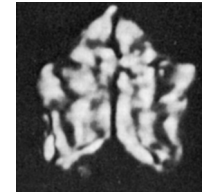
BD71/224



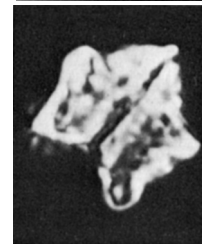
225



PNK71a/229



230

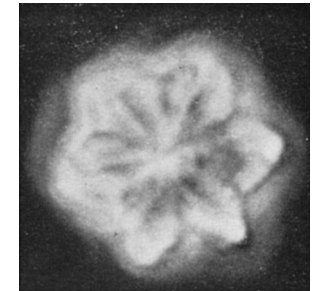


231

H



HBU71/249



250

Fasciculithus tonii

- 12–17 μm x 14–17 μm

- L. Paleocene (NP9). Bay of Biscay (DSDP Site 119), Atlantic.

- [Large size. Column strongly widening towards the distal side, decorated with several large depressions. Distal end topped with a needle consisting of spirally arranged elements.]

≠ from other spp. by its size, the spiral structure of its needle and the aspect of the column.

— Restricted to NP9 (Romein, 1979, p. 77).

- PNK71a (p. 354).

Fasciculithus mitreus

- 9–12 μm

- L. Paleocene (Lower part of NP9). Blake Plateau, Atlantic.

- Mitre-shaped with stellate or crudely polygonal cross section, concave base and distally expanding column surmounted and terminated by a broad cone. Column constructed of radially arranged tabular calcite crystallites separated by furrows at the periphery.

≠ from *F. tympaniformis* in that it is commonly larger, expands distally, and has a distinct conical “top”;

≠ from *F. schaubi*, which has a regularly pitted surface and a short stem.

— Gartner’s original illustrations figure two different forms, probably equivalent to *F. tonii* (Gartner, 1971, pl. 3, figs. 3a, b) and *F. hayi* (op. cit., pl. 3, fig. 4a, pl. 4, fig. 1).

- GS71 (p. 109).

Fasciculithus richardii

- 6–10 μm

- L. Paleocene (NP9). Bay of Biscay (DSDP Site 119), Atlantic.

- [Column having a rectangular, often square, outline decorated with depressions arranged in several horizontal and vertical rows. The outline can be polygonal: the column is then nearly as wide as high. Apical needle slightly separated from the column.]

≠ from other spp. by its outline.

— “... considered as a variant of *F. schaubi*, which has a low number of elements” (Romein, 1979, p. 153).

- PNK71a (p. 355).

Fasciculithus hayii

- ~ 8 μm

- L. Paleocene (NP9). West central Persia.

-**Simply constructed base of about six radiating elements surmounted by a short spine, resembling an asterolith in outline.

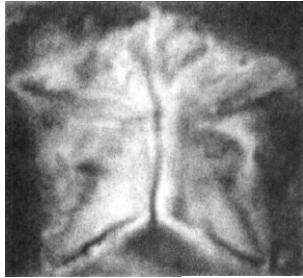
- In side view, the base shows a simple construction resembling *F. schaubi*, but including more acute angles at bottom and top.

— Possibly a variant of *F. schaubi*.

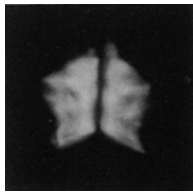
- HBU71 (p. 32).

Fasciculithus tonii (continued)

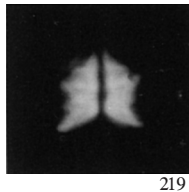
Fasciculithus richardii (continued)



BPR10/217



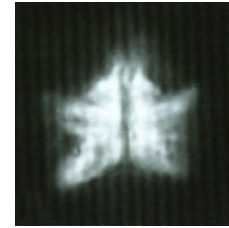
BLM95/218



219



BPR05a/232



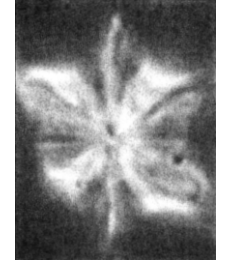
233



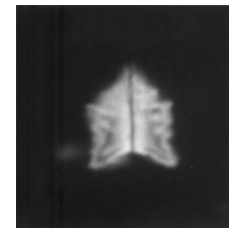
BPR10/234



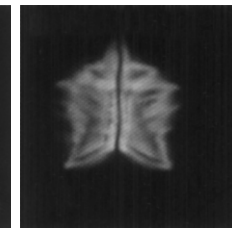
235



236



STJM11/237



238

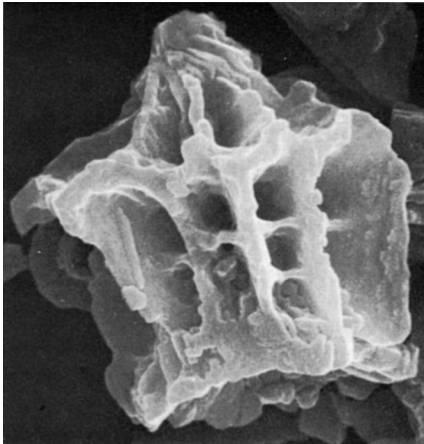
Fasciculithus tonii (continued)

Fasciculithus mitreus (continued)

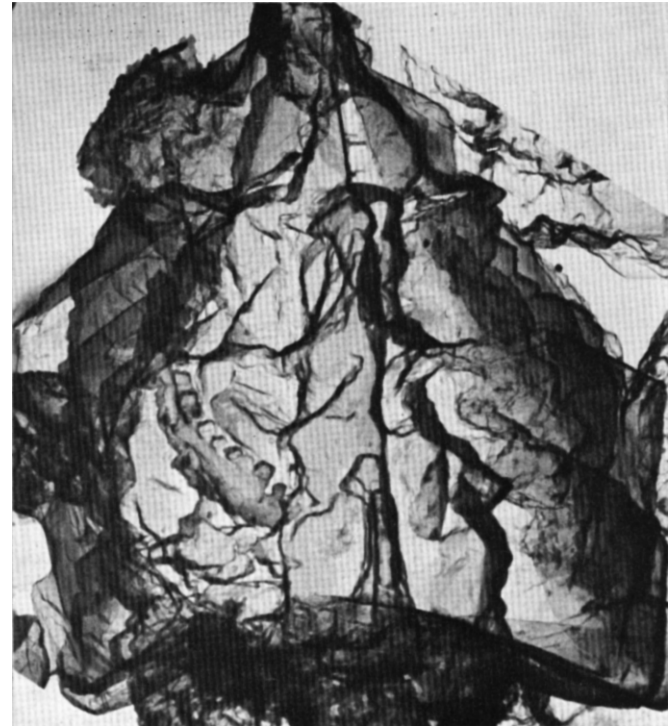
SIDE VIEW

SIDE VIEW

H



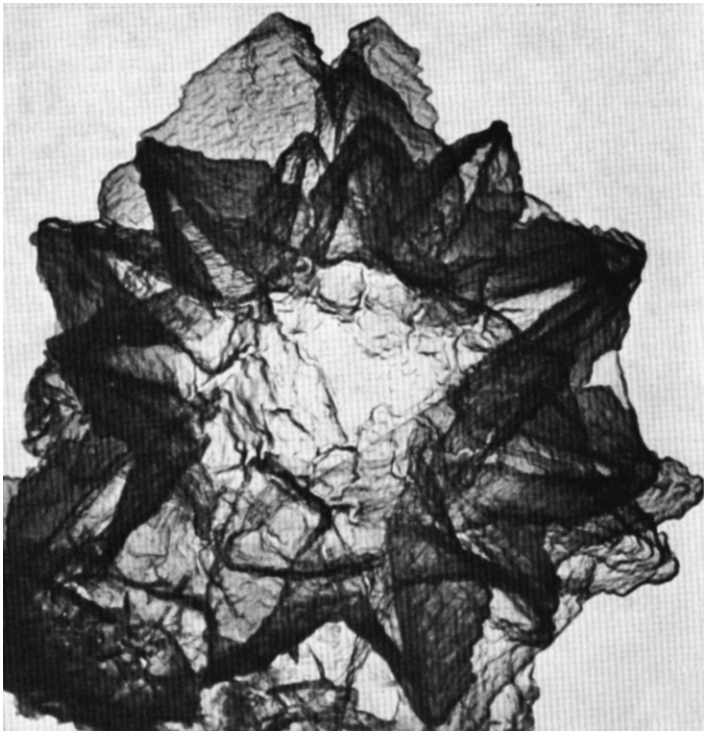
PNK71a/220



GS71/226

Fasciculithus mitreus (continued)

DISTAL FACE



GS71/227

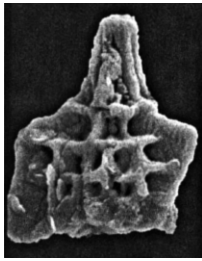


228

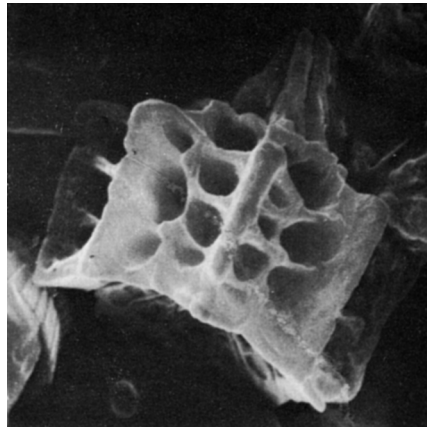
Fasciculithus richardii (continued)

SIDE VIEW

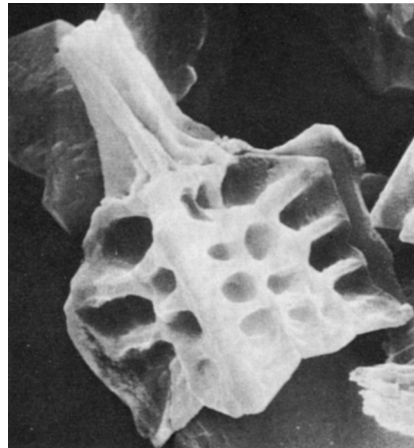
PROXIMAL FACE



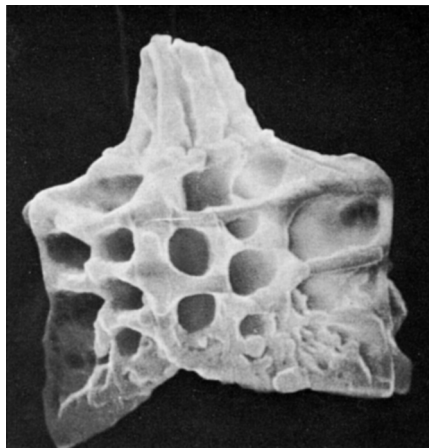
BPR10/239



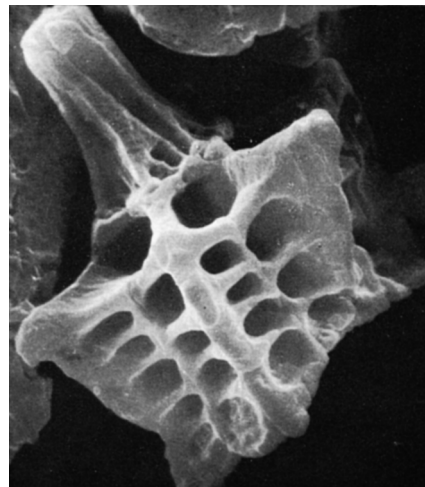
PNK71a/240



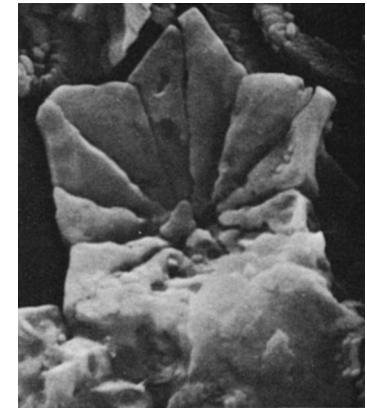
241



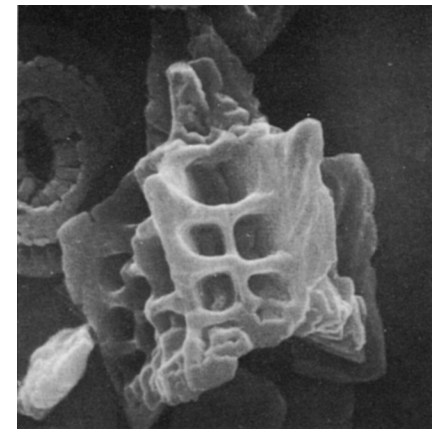
242



243



GS71/244

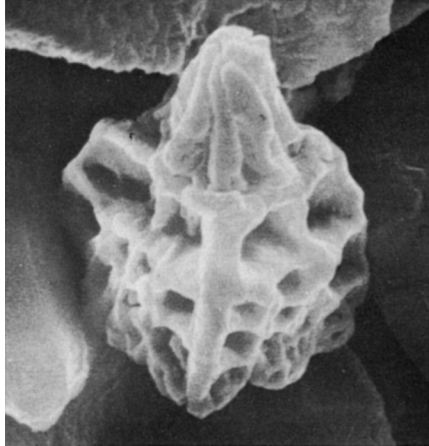


PNK71a/245

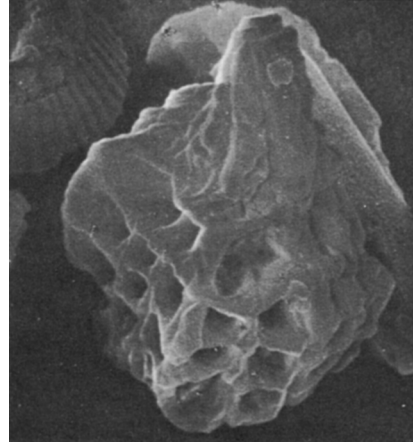
Fasciculithus richardii (continued)

DISTAL FACE

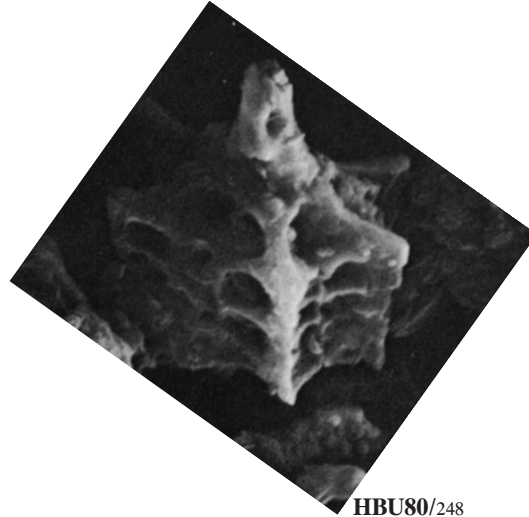
H



PNK71a/246



247



HBU80/248

Fasciculithus fenestrellatus Bown 2005

Fasciculithus sp. B [= *Fasciculithus* sp. 1 Bown 2005, p. 9, pl. 12, figs. 25-27]



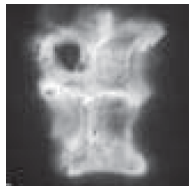
BPR05b/251



252



253



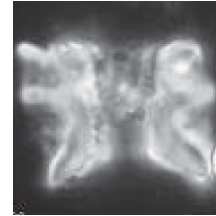
254



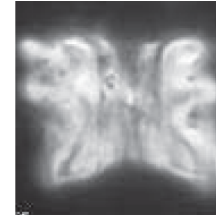
255



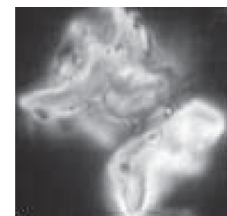
256



BPR05b/257



258



259

Fasciculithus fenestrellatus

- 12.3 μm x 9.8 μm
- L. Paleocene (NP9a). Shatsky Rise (Site 1208), northwest Pacific Ocean.
- Large, tall, tapering towards its base; ornamented with large rectangular fenestrae delineated by distinct longitudinal and transversal ridges. Fasciculith higher than wide.
- Remarks. The LM image is not the typical two blocks seen in smaller fasciculiths, the median extinction line being indistinct.

- BPR05b (p. 9).

Fasciculithus sp. B

- 11.0 μm x 14.4 μm
- L. Paleocene (Subzone NP9a). Shatsky Rise (Site 1208), northwest Pacific Ocean.
- Large fasciculith tapering slightly towards its base, ornamented by thick, rounded, protruding ridges. Broader than tall with a rather wide central opening. The LM image is not the typical two blocks seen in smaller fasciculiths.

- BPR05b (p. 9), AMP (p. 103).

Figure References

- AC07.** AGNINI, C., FORNACIARI, E., RAFFI, I., RIO, D., RÖHL, U. and WESTERHOLD, T., 2007. *Marine Micropaleontology*, 64: 215–248.
(20): 2/8 (as *F. clinatus*)
- AMP.** AUBRY, M.–P., this volume.
- BPR05a.** BOWN, P. R., 2005a. *Journal of Nannoplankton Research*, 27: 21–95.
(26, 27): 40/16, 17 (*F. aubertae*)
(232, 233): 40/31, 32 (*F. richardii*)
- BPR05b.** BOWN, P. R., 2005b. In: Bralower, T. J., Premoli Silva, I. and Malone, M. J., *Proceedings of the Ocean Drilling Program, Scientific Results, 198*, 1–44. College Station, Texas: Ocean Drilling Program.
(28): 12/3 (*F. aubertae*)
(251–256): 12/19–24 (*F. fenestrellatus*)
(257–259): 12/25–27 (*Fasciculithus* sp. 1)
- BPR10.** BOWN, P. R., 2010. *Journal of Nannoplankton Research*, 31: 11–38.
(36–38): 11/21–23 (*F. lobus*)
(39): 11/24 (*F. sidereus*)
(94): 11/20 (*F. involutus*)
(121): 11/ 18 (*F. involutus*)
(165): 11/15 (*F. thomasi*)
(186): 11/28 (two photographs; *F. schaubii*)
(201, 202): 11/16, 17 (*F. liliana*)
(210): 11/14 (*F. alanii*)
(217): 11/12 (as *F. tonii*)
(234–236): 11/26 (two photographs), 27 (*F. richardii*)
(239): 11/25 (*F. richardii*)
- BMN61.** BRAMLETTE, M. N. and SULLIVAN, F. R., 1961. *Micropaleontology*, 7: 129–188.
(89–93): 14/3a, b, 1a, b, c (*Fasciculithus involutus*)
(95–100): 14/2a, b, 4a, b, 5a, b (*Fasciculithus involutus*)
- BD71.** BUKRY, D., 1971. *Transactions of the San Diego Society of Natural History*, 16: 303–327.
(18, 19): 4/8, 9 (*F. clinatus*)
- BLM95.** BYBELL, L. M. and SELF–TRAIL, J. M., 1995. Washington D.C.: U.S. Geological Survey. Professional Paper 1554, 36 pp.
(1–5): 36/6–9, 11 (*F. sidereus*)
(6–11): 16/1b, 2, 3b, 4b, 5b, 6b (*F. sidereus*)
(12, 13): 16/1c, 6a (*F. sidereus*)
(14–17): 16/1a, 3a, 4a, 5a (*F. sidereus*)
(29–31): 35/12–14 (*F. aubertae*)
(48–51): 36/14, 15, 19, 20 (*F. tympaniformis*)
(101–103): 36/1–3 (*F. involutus*)
(116–119): 15/3b, 6b, 4b, 5b (*F. involutus*)
(138–141): 15/3a, 4a, 5a, 6a (*F. involutus*)
(133, 134): 15/7a, b (*F. involutus*)
(163, 164): 36/12, 13 (*F. thomasi*)
(168–172): 17/1b, 2b, 3b, 4b, 5a (*F. thomasi*)
(175–179): 17/1a, 2a, 3a, 4a, 5b (*F. thomasi*)
(218, 219): 36/5, 10 (*F. schaubii*)
- GS71.** GARTNER, S., 1971. *Tulane Studies in Geology and Paleontology*, 8 (1970–1971): 101–121.
(221–225): 3/4a–c, 3a, b (as *F. mitreus*)
(226): 3/1 (as *F. mitreus*)
(227): 3/2 (as *F. mitreus*)
(228): 4/1 (as *F. mitreus*)
- HB71.** HAQ, B. U., 1971. *Stockholm Contributions in Geology*, 25: 1–56.
(249, 250): 1/3, 2 (as *F. hayi*)
- HB80.** HAQ, B. U. and AUBRY, M.–P., 1980. In: Salem, M. J. and Busrewil, M. T. (Eds.), *The geology of Libya, Volume 1*, 271–304. London: Academic Press.
(25): 1/14 (as *F. aubertae*)
(32): 5/1 (as *F. aubertae*)
(192): 5/3 (as *F. schaubii*)
(196): 5/4 (as *F. schaubii*)
(244): 5/5 (as *F. hayi*)
(248): 5/6 (as *F. hayi*)
- HWW67.** HAY, W. W. and MOHLER, H. P., 1967. *Journal of Paleontology*, 41: 1505–1541.
(42–44): 204/13–15 (as *F. tympaniformis*)
(45–47): 204/10–12 (as *F. tympaniformis*)
(62, 63): 205/4, 8 (as *F. tympaniformis*)
(76, 77): 205/7, 5 (as *F. tympaniformis*)
(104–106): 204/4, 8, 9 (as *F. involutus*)
(120): 203/9 (as *F. involutus*)
(122): 203/6 (as *F. involutus*)
(142, 143): 203/1, 3 (as *F. involutus*)
(180–185): 204/1–3, 5–7 (as *F. schaubii*)
(190–94): 203/7, 2, 10, 4 (as *F. schaubii*)

- HWW67.** HAY, W. W., MOHLER, H. P., ROTH, P. H., SCHMIDT, R. R. and BOUDREAUX, J. E., 1967. *Transactions of the Gulf Coast Association of Geological Societies*, 17: 428–480.
 (57, 59, 61, 63, 65): 8/1, 2, 4, 3, 5 (as *F. tympaniformis*; the five figures form two sets one on each plate for stereoscopic viewing)
 (58, 60, 62, 64, 66): 9/1, 2, 4, 3, 5 (as *F. tympaniformis*; the five figures form two sets one on each plate for stereoscopic viewing)
- ME71.** MARTINI, E., 1971. In: Farinacci, A. (Ed.), *Proceedings of the II Planktonic Conference, Roma, 1970, Volume 2*, 739–785. Rome: Ediz. Tecnoscienza.
 (52, 53): 1/11, 12 (*F. tympaniformis*)
- MS85.** MONECHI, S., 1985. In: Heath G. R., Burckle L. H., et al., *Initial Reports of the Deep Sea Drilling Project*, 86, 301–336. Washington, D. C.: U.S. Government Printing Office.
 (21, 22): 7/5A, B (*F. clinatus*)
 (23): 7/2 (*F. clinatus*)
- MC74.** MÜLLER, C., 1974. In: Simpson, E. S. W., Schlich, R., et al., *Initial Reports of the Deep Sea Drilling Project*, 25, 579–633. Washington, D. C.: U.S. Government Printing Office.
 (69): 5/6 (*F. tympaniformis*)
 (83): 5/7 (*F. tympaniformis*)
- OH79.** OKADA, H. and THIERSTEIN, H. R., 1979. In: Tucholke, B. E., Vogt, P. R., et al., *Initial Reports of the Deep Sea Drilling Project*, 43, 507–573. Washington, D. C.: U.S. Government Printing Office.
 (24): 17/1 (as *F. crinatus*, *err. pro cit.*)
 (70, 71): 17/6, 5 (as *F. tympaniformis*)
- PNK71a.** PERCH-NIELSEN, K., 1971a. *Meddelelser fra Dansk Geologisk Forening*, 20: 347–361.
 (33, 34): 2/6, 5 (as *Fasciculithus* sp. 1)
 (72): 1/5 (*F. tympaniformis*)
 (78, 79): 1/1, 4 (*F. tympaniformis*)
 (84-86): 1/7, 3, 2 (*F. tympaniformis*)
 (107-109): 14/28-30 (*F. involutus*)
 (123-126): 4/1, 2, 6, 9 (*F. involutus*)
 (127): 7/5 (*F. involutus*)
 (128-131): 4/8, 10, 4, 7 (*F. involutus*)
 (135): 4/3 (*F. involutus*)
 (144): 4/5 (*F. involutus*)
 (150-152): 14/34-36 (*F. bobii*)
 (153-157): 3/4, 1, 2, 5, 6 (*F. bobii*)
 (158): 3/3 (*F. bobii*)
- (159): 1/6 (*F. bobii*)
 (167): 6/5 (as *F. thomasii*)
 (173): 9/3 (*F. thomasii*)
 (174): 6/6 (as *F. thomasii*)
 (187-189): 14/25-27 (*F. schaubi*)
 (195): 7/6 (*F. schaubi*)
 (197): 9/1 (*F. schaubi*)
 (198-200): 14/40-42 (as *F. liliana*)
 (203): 6/3 (*F. liliana*)
 (205): 6/1 (*F. liliana*)
 (206): 7/3 (as *F. alanii*)
 (207): 6/4 (as *F. alanii*)
 (208, 209): 14/13, 14 (as *F. alanii*)
 (211): 9/4. (as *F. alanii*)
 (212): 6/2 (as *F. alanii*)
 (213, 214): 7/1, 2 (as *F. alanii*)
 (215, 216): 14/15, 16 (*F. tonii*)
 (220): 7/4 (*F. tonii*)
 (229-231): 14/5-7 (*F. richardii*)
 (240-242): 8/2, 3, 4 (as *F. richardii*)
 (243): 9/2 (as *F. richardii*)
 (245): 8/1 (as *F. richardii*)
 (246, 247): 8/5, 6 (as *F. richardii*)
- PNK77.** PERCH-NIELSEN, K., 1977. In: Supko, P. R., Perch-Nielsen, K., et al., *Initial Reports of the Deep Sea Drilling Project*, 39, 699–823. Washington, D. C.: U.S. Government Printing Office.
 (73, 74): 10/22, 23 (as *F. tympaniformis*)
- PJJ90.** POSPICHAL, J. J. and WISE, S. W., 1990. In: Barker, P. F., Kennett, J. P., et al., *Proceedings of the Ocean Drilling Program, Scientific Results*, 113, 613–638. College Station, Texas: Ocean Drilling Program.
 (35): 3/7 (as *F. involutus*)
- RAJT79.** ROMEIN, A. J. T., 1979. *Utrecht Micropaleontological Bulletins*, 22: 1–231.
 (145, 146): 5/4, 5 (as *F. involutus*)
 (196): 5/2 (as *F. schaubii*)
 (204): 5/3 (as *F. liliana*)
- STJM11.** SELF-TRAIL, J. M., 2011. *Journal of Nannoplankton Research*, 32: 1–28.
 (40): 8/14 (as *F. thomasii*)
 (110-112): 8/5–7 (as *F. inversus*)
 (166): 8/13 (*F. thomasii*)
 (237, 238): 8/9, 10 (*F. richardii*)
- SE08.** STEURBAUT, E. and SZTRÁKOS, K., 2008. *Marine Micropaleontology*, 67: 1–29.

(41): 2/22 (as *Fasciculithus* sp.)

(54): 2/25 (*F. tympaniformis*)

SFR64. SULLIVAN, F. R., 1964. *University of California Publications in Geological Sciences*, 44: 163–228.

(113, 114): 12/9b, 9a (*F. involutus*)

VO89. VAROL, O., 1989. In: Crux, J. A. and van Heck, S. E. (Eds.), *Nannofossils and their applications*, 267–310. Chichester: Ellis Horwood Limited.

(55, 56): 12.5/8, 9 (as *F. tympaniformis*)

(115): 12.5/5 (as *F. involutus*)

WC89. WANG, C. and HUANG, W., 1989. *Cenozoic paleobiota of the continental shelf of the East China Sea (Donghai). Micropaleontological volume*, 202–252. Beijing: Geological Publishing House. (Research Party Marine Geology, Ministry of Geological Sciences).

(160-162): 72/1-3 (as *F. lingfengensis*)

WSW77. WISE, S. W. and WIND, F. H., 1977. In: Barker, P. F., Dalziel, I. W. D., et al., *Initial Reports of the Deep Sea Drilling Project*, 36: 269–491. Washington, D. C.: U.S. Government Printing Office.

(75): 15/1 (as *F. involutus*)

(80, 81): 16/1, 3 (as *F. involutus*)

(82): 15/5 (as *F. involutus*)

(87): 15/3 (as *F. involutus*)

(88): 16/5 (as *F. involutus*)

(132): 16/6 (*F. involutus*)

(136, 137): 16/2, 4 (*F. involutus*)

(147-149): 15/6, 4, 2 (*F. involutus*)

BOMOLITHUS

HIGHLIGHTS:

- Two species.
- Coccoliths consisting of three structural units, intermediate between fasciculiths and more complex helioliths.
- Collaret and calyptra united in the “cone”.
- Size range: 7–11 μm .
- Coccosphere unknown.
- Stratigraphic Range: upper Zone NP4?–lowermost Zone NP8.
- Evolved from *Lithoptychius*.
- Evolved into *Heliotrochus*.

SELECTED READING

Romein, 1979; Roth, 1973; Steurbaut, 1998; Varol, 1989.

INTRODUCTION

The coccoliths for which the genus *Bomolithus* was erected share characters with both the *Lithoptychius*–fasciculiths and the *Heliotrochus*–helioliths, and they may be classified in either group. They are placed here among helioliths because of closer similarity in basic structure.

Romein (1979) and Aubry (1989) did not consider it necessary to distinguish *Bomolithus* from *Heliolithus* (including *Heliotrochus*) and placed the two genera in synonymy. However, *Bomolithus* exhibits characters that are transitional between *Lithoptychius* and *Heliolithus* (*s. l.*), occupying a pivotal place in the history of the Suborder Eudiscoasterineae. Its presence in the initial diversification of the small Family Heliolithaceae at the origin of the highly diversified families Helio-discoasteraceae and Eu-discoasteraceae, provides evidence of phylogenetic unity within the suborder.

MORPHOLOGY AND STRUCTURE

Coccoliths

Bomolithus elegans is the type of the genus and the discussion below is essentially based on it. *Heliolithus rotundus* has been tentatively, albeit informally, transferred to *Bomolithus* by Steurbaut (1998) based on a re-interpretation of this coccolith such that the collaret and calyptra form a characteristic cone (op. cit, fig. 8, bottom left). This re-interpretation is accepted here, although this taxon is poorly known.

Morphology – The helioliths of *Bomolithus* are thick, robust, and of medium size (7 to 11 μm). They are circular in transverse section (text-fig. 1). As seen in side view their lower part is either cylindrical or in the shape of an inverted truncated cone, and with a concave proximal face. This supports two superposed, closely appressed units, each cup-shaped and flaring distally. The distal face is concave.

Structure – SEM illustrations of *Bomolithus* helioliths are few, and almost all of secondarily overgrown specimens. Consequently, it is difficult to give a detailed description of the original, undoubt-

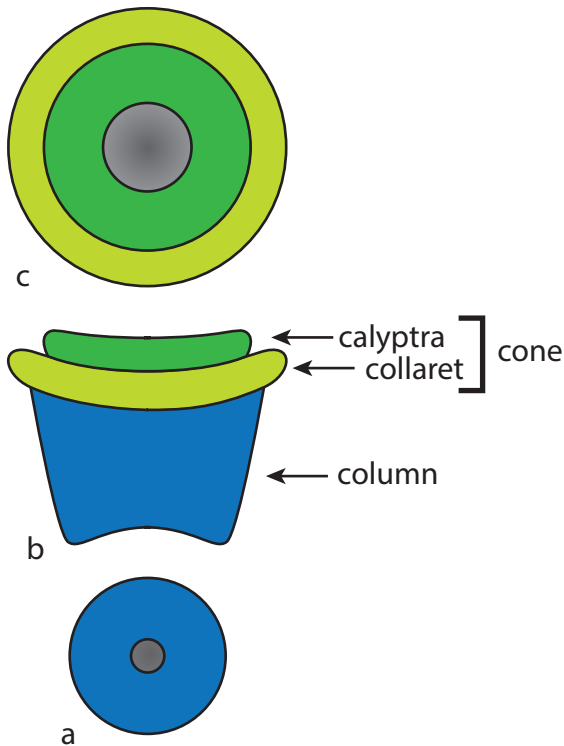
edly delicate coccoliths by reference to these now massive specimens. General structural characters, however, can be easily determined (see also Romein, 1979, p. 78, 156).

The coccoliths are comprised of three structural units: column, collaret and calyptra (text-fig. 2).

The (proximal) column is monocyclic and consists of 25 to 40 tall elements arranged tangentially, with sutures curved clockwise as seen in proximal view (e.g., Okada and Thierstein, 1979, pl. 14, fig. 2; text-fig. 2a). The center of the proximal face is occupied by a large opening at the end of an axial canal (op. cit.).

The median and distal structural units consist of as many elements as the column, and are alike as seen in lateral view except for the latter being smaller (text-fig. 2b). The distal unit is easily identified as the calyptra with the dextral imbrication of its elements and their sutures oriented anticlockwise (e.g., Okada and Thierstein, 1979, pl. 14, fig. 1; text-fig. 2c). One of the specimens of *B. elegans* illustrated by Perch-Nielsen et al. (1978, pl. 16, fig. 7) shows that the calyptra is comprised of two concentric cycles, with the outer cycle being wider (text-fig. 2d). The inner cycle occupies a low depression formed by the outer cycle at the center of the distal face (see Okada and Thierstein, 1979, pl. 14, fig. 1). It is difficult to determine whether the imbrication of the elements and the orientation of the sutures are identical in the two cycles, although this is highly probable considering that the cycles are no longer distinct in markedly overgrown specimens (e.g., Perch-Nielsen et al., 1978, pl. 16, fig. 8). The diameter of the inner cycle appears to be only slightly larger than the proximal opening. The calyptra is also bicyclic in *B. rotundus*, the inner cycle being slightly raised above the outer cycle in contrast to *B. elegans*.

Located between column and calyptra, the monocyclic median structural unit would, in principle, be directly comparable to the collaret. However, its tabular elements are imbricate sinistrally (text-figs. 2c, d) as seen in proximal view of some specimens (e.g., Roth, 1973, pl. 15, fig. 1), with sutures oriented anticlockwise (e.g., Okada and Thierstein, 1979, pl. 14, fig. 2), which is opposite to the characters of the collaret in *Lithoptychius* (as for instance illustrated in *L. jani*, see Perch-Nielsen, 1977, pl. 12,



TEXT-FIGURE 1

Morphology of the *Bomolithus heliolith*. a: proximal view; b: side view; c: distal view. (The etymology of the genus name is Gr. *bomos*, altar and Gr. *lithos*, stone).

fig. 9, or *L. merloti*, see Romein, 1979, pl. 5, fig. 1). It is unclear whether these are genuine characters of the median cycle. The specimen illustrated by Okada and Thiertein (1979, pl. 14, fig. 1) would seem to indicate that the elements are non-imbricate and with sutures curved anticlockwise.

Extinction patterns

The standard orientations are those established by Romein (1979, p. 155). In the standard orientation for distal view, the broadest face of the heliolith faces upwards. In the standard orientation for side view, the edge of the distal cycle is parallel to the X-cross-hair and the axis of the column is parallel to the Y-cross-hair. In side view, the extinction pattern in cross-polarized light is similar to that of *Lithoptychius* fasciculiths, with an extinction line along the axis of symmetry dividing the coccolith into two identical halves. In addition, the sutures between column and collaret and between collaret and calyptra are highlighted as black lines. Importantly there is no central body. In distal view, only the column is birefringent, producing a “dark cross with practically straight arms” (Roth, 1973, p. 734). As a result, the diameter of the coccolith in such view appears lesser in cross-polarized light than in bright field.

BIOLOGY, PHYSIOLOGY AND ECOLOGY

Biology

The coccosphere of *B. elegans* is unknown, but can be imagined with the coccoliths juxtaposed around the cell, forming as many circular cups broadly opened outwards (text-fig. 3).

Physiology

The complex structure of the calyptra implies specialization. The cup-shape of the cone (calyptra + collaret) suggests adaptive morphology towards collection of food particles for mixotrophic physiology.

Ecology

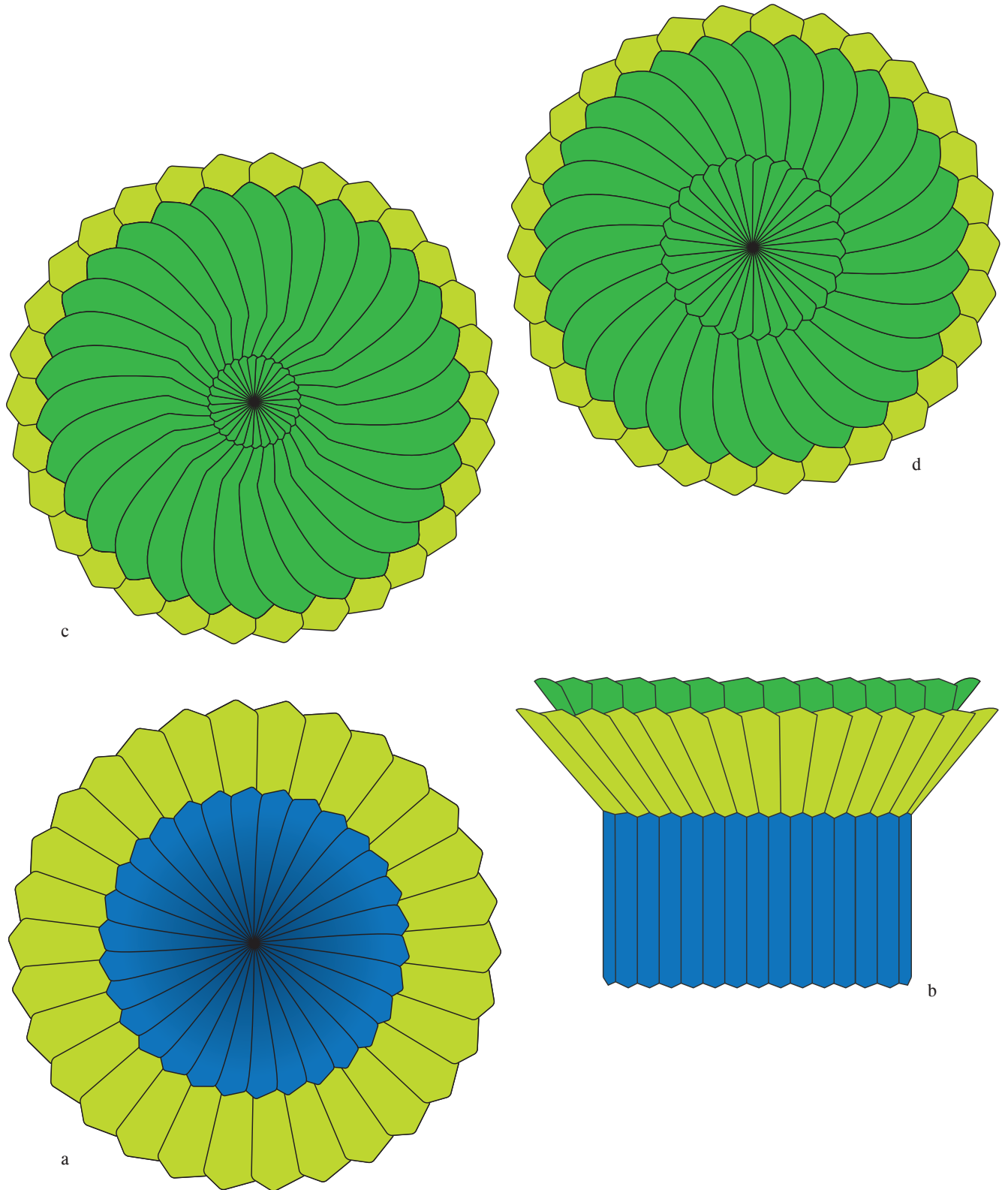
Bomolithus is known only from the low-latitudes. It has been reported from the Central Pacific Ocean, South and North Atlantic Oceans, and Tethys area (Roth, 1973; Haq and Lohmann 1976; Perch-Nielsen, 1977; Perch-Nielsen et al., 1978; Okada and Thierstein 1979; Romein, 1979; Agnini et al., 2007; Steurbaut and Sztráchos, 2008; Dinares et al., 2010; text-fig. 4).

EVOLUTIONARY HISTORY

Origin

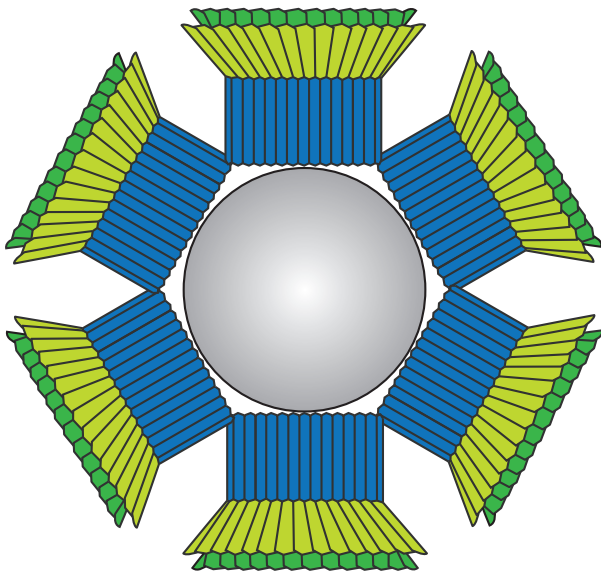
The helioliths of *Bomolithus* are reminiscent of the fasciculiths of *Lithoptychius* (see above), and it would seem likely that one is derived from the other. However, the illustrations of well-preserved specimens are too few to confidently document such a transition at this time.

The helioliths of *Bomolithus* are in the general shape of a fasciculith of *Lithoptychius*. The morphologic difference between the two concerns the shape of the calyptra, which is convex distally in *Lithoptychius* but concave distally in *Bomolithus* (text-fig. 5). This is a minor difference that required no structural change. The two coccoliths are also alike in having a tripartite construction. The proximal and distal units of the heliolith are clearly homologous with the column and calyptra of the fasciculith. The column exhibits a minor difference, in consisting of radial elements in *Lithoptychius*, but tangentially arranged elements in *Bomolithus*. Another minor difference concerns the calyptra, which is monocyclic in *Lithoptychius* and bicyclic in *Bomolithus*. A more significant difference is the imbrication of the elements of the median unit in *Bomolithus*, which is opposite to that of the elements of the collaret in *Lithoptychius* (see above) and raises the question whether the two units are in fact homologous. This would require that the *Lithoptychius*-*Bomolithus* transition involved a re-orientation of the elements of the collaret, in conflict with the principle of permanency of the characters of morphostructural units. Romein (1979, p. 78, 79) has shown, however, that insertion of a gypsum plate during observation in cross polarized light results in a color distribution that is the same in *Lithoptychius bitectus* and *Bomolithus elegans*, which led him to infer that the latter arose from the former (text-fig. 6). It is possible that, occasionally, some significant character (here imbrication) of a specific structural unit may be permanently changed within a lineage (as seen also in the *Biantholithus*-*Sphenolithus* transition; see Aubry 2014a, Chapter *Sphenolithus*). It is also possible that the imbrication of the elements of the collaret in *Lithoptychius* was not as strict as it appears from the few well-preserved specimens that are so far available. Yet another possibility is that the collaret has sinistrally imbricate elements in *Lithoptychius*, but non-imbricate elements in *Bomolithus* (see above). The alternative to homology is that the median unit is analogous to the collaret, in which case this could have resulted from the doubling of the calyptra after disappearance of the collaret. The doubling of cycles during evolution is known to occur in closely related coccoliths (Perch-Nielsen, 1981b), and there is a definitive trend towards reduction of the collaret in *Lithoptychius* (as seen in *L. billii*; see this volume, Chapter *Fasciculithus*). The



TEXT-FIGURE 2

Structure of the *Bomolithus heliolith*. a: proximal face; b: side view; c, d: distal faces. Note the weak sinistral imbrication of the elements of the column as seen in proximal view and the slight clockwise orientation of the sutures (a); the structural similarity between the calyptra and the inverted collaret (with dextral imbrication and anticlockwise sutures) and the smaller cycle at the center of the calyptra. 2a-d: The structure of the calyptra in *Bomolithus* is not completely resolved: it may be comprised of more than two cycles; and the details of the central cycle is tentative in these drawings (c, d). Note the characteristic arrangement of the calyptra and inverted collaret to form the cone; note also that the elements are similarly imbricate in the three structural units (b).



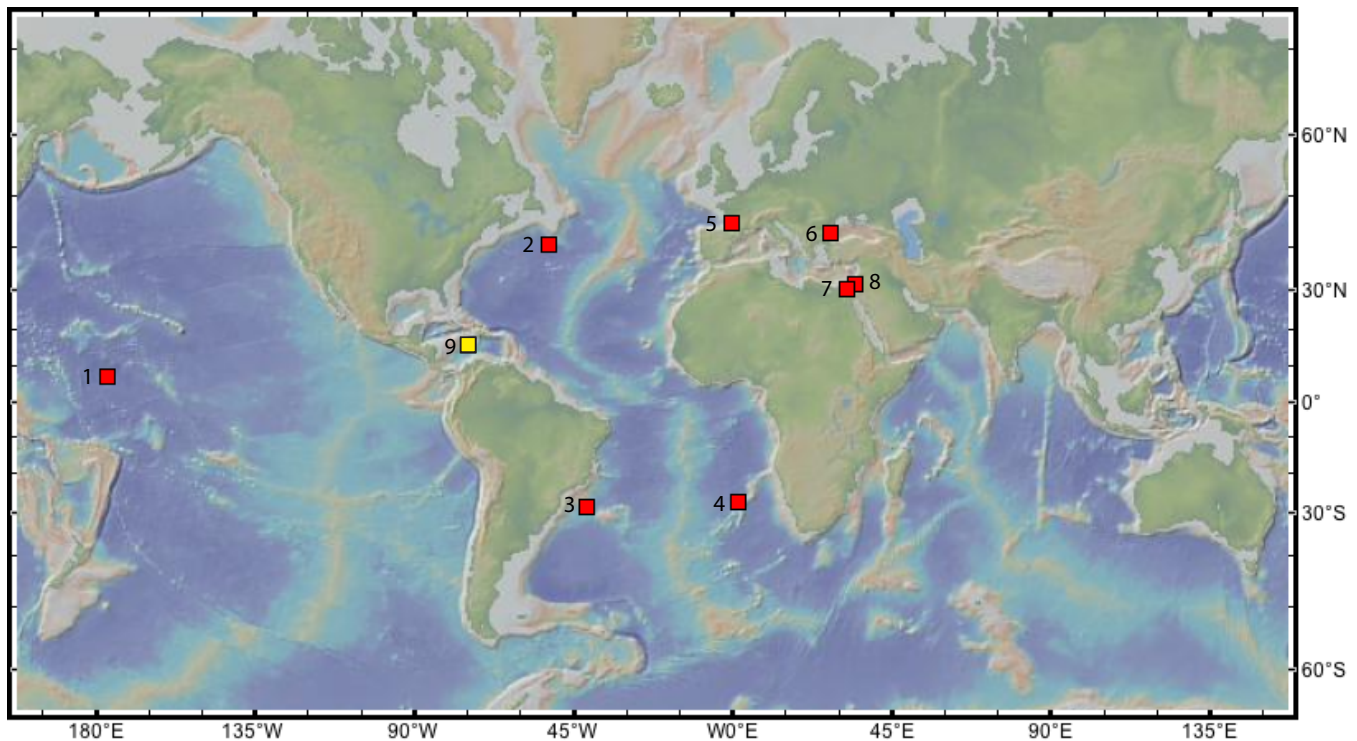
TEXT-FIGURE 3
Tentative reconstruction of the coccosphere of *B. elegans*.

recovery of well-preserved specimens of both genera will help clarify the matter. Until then, the median cycle in *Bomolithus* is provisionally regarded as the collaret, particularly because the loss of a structural unit to be immediately replaced with a similar one from a different source raises suspicion.

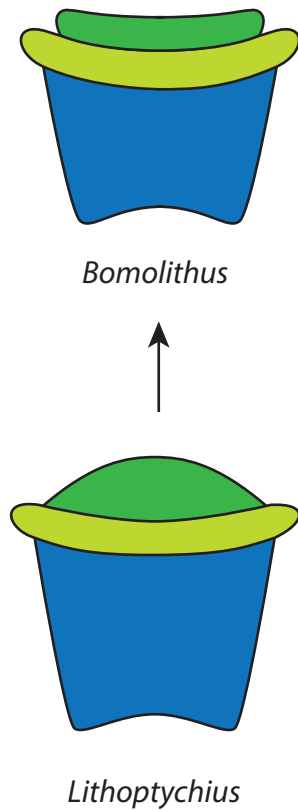
In summary, *Bomolithus* can only have arisen from a species of *Lithoptychius*. The transition involved 1) a change in the orientation of the elements of the column from radial to tangential with sutures oriented anticlockwise in distal view (Romein, 1979); 2) a distal expansion of the collaret (Romein, 1979) and a re-orientation of the imbrication of its elements; and 3) the differentiation of an inner cycle in the calyptra which is bicyclic in *Bomolithus*.

Phylogeny

Bomolithus is currently a bispecific genus that is sometimes incorporated in the generic concept of *Heliolithus*. However, its coccoliths are distinctive and characterized by the unique arrangement of the calyptra and collaret which, nested together, slope in opposite direction of the column. The generic description refers to this opposition (“The uppermost cycle slope[s] towards a central depression. The two lower cycles ... slope towards the periphery”). *Bomolithus elegans* is, however, closely related to *Heliotrochus cantabriae*, either by being part of the same lineage, or by the two taxa representing independent divergences from *Lithoptychius* (see Genus *Heliotrochus*, this volume).



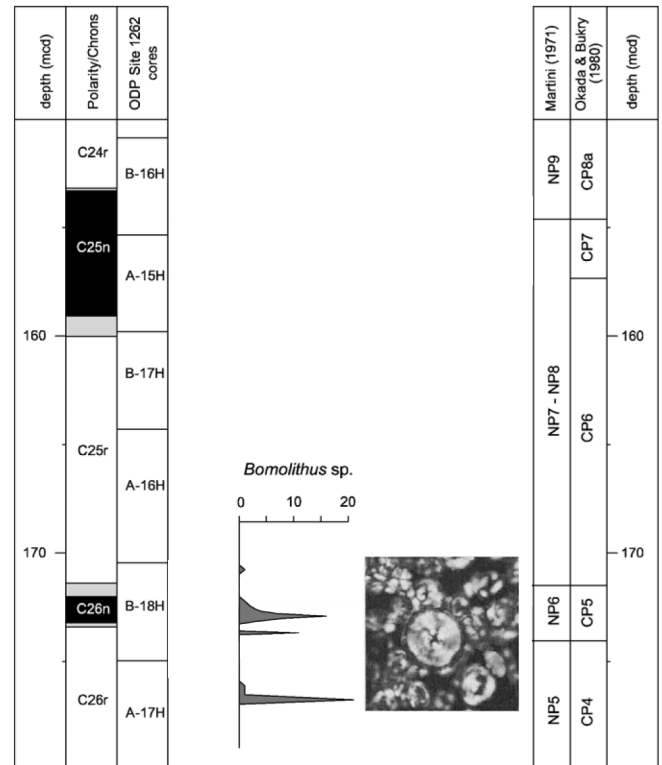
TEXT-FIGURE 4
Known geographic distribution of *Bomolithus* species.
Red: *B. elegans*: (1): DSDP Site 167-38, Magellan Rise Central Pacific (Roth, 1973); (2): DSDP site 384 (Okada and Thierstein, 1979); (3): DSDP 356 (Perch-Nielsen, 1977); (4) 1262A ODP leg 208 (Agnini et al., 2007); (5): S.W. Aquitaine, France (Steurbaut and Szttrachos, 2008); (6): Bjala, Bulgaria (Dinares et al., 2010); (7): Egypt (Perch-Nielsen, 1978); (8) Israel (Romein, 1979).
Yellow: *Faciculithus rotundas*: *B. rotundas*: DSDP site 152 (9) (Haq and Lohmann, 1976).
(Map from GMRT, Ryan 2009; <http://www.geomapapp.org>.)



TEXT-FIGURE 5
Morphologic comparison between a fasciculith of *Lithoptychius* and the heliolith of *Bomolithus*. Both in side view.

Zone	Lineage
<i>Discoaster multiradiatus</i>	
<i>Discoaster mohleri</i>	
<i>Heliolithus kleinpelli</i>	
<i>Fasciculithus tympaniformis</i>	 <i>H. elegans</i>
<i>Ellipsolithus macellus</i>	<i>Fasciculithus bitectus</i>

TEXT-FIGURE 6
Structural comparison between a “capped” fasciculith of *Lithoptychius* (*L. bitectus*) and the heliolith of *Bomolithus*, as deduced from crystallographic behavior (cross-polarized light and gypsum slide). (Modified from Romein, 1979, fig 41, who proposed that *L. bitectus* was the direct ancestor of *B. elegans*.)



TEXT-FIGURE 7
Abundance pattern of *Bomolithus* sp. at ODP Site 1262. (After Agnini et al., 2007, fig. 6 and pl. 2, fig. 21).

Diversity

Only one species, *Bomolithus elegans*, has been formally described but the taxon *Heliolithus? conicus* Perch-Nielsen is sometimes transferred to *Bomolithus*, which is not followed here on morphological and structural grounds. The identity of the specimen illustrated from the Upper Paleocene (Zone NP7) recovered at ODP Hole 1262A and referred to as *Bomolithus* sp. A (Agnini et al., 2007, pl. 2, fig. 21; text-fig. 7) cannot be confirmed from the single photograph available.

The two taxa described as *Bomolithus aquilus* Bown 2010 and *B. superbus* Bown 2010 from the lowermost Eocene (Zone NP9c) of Tanzania do not exhibit the structural characteristic of *Bomolithus*. In fact, their taxonomic assignment is ambiguous (see *Nomina dubia*, this volume).

STRATIGRAPHY

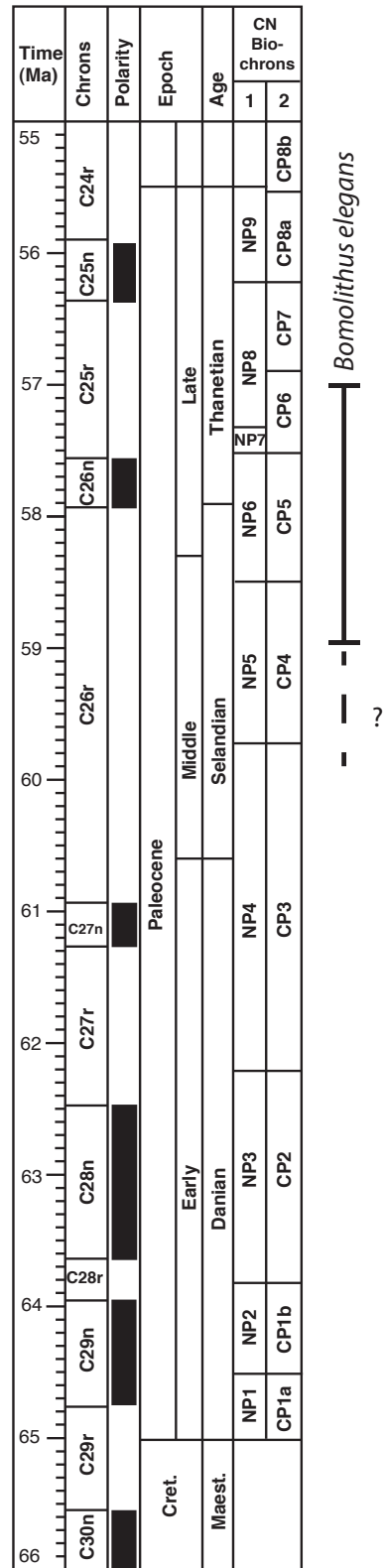
Biostratigraphy

According to Perch-Nielsen (1985, p. 480) the stratigraphic range of *B. elegans* extends from mid Zone NP5 to lower Zone NP8. This is in close agreement with Varol (1989, p. 277) who shows the species occurring from the base of Zone NP6 (and questionably in upper Zone NP5) to lower Zone NP8. This corresponds to the interval of Subzone NTp10B to Zone NTp13 in Varol's low to mid latitude zonal scheme, in which the HO of *Bomolithus elegans* is used as an alternative to the HO of *Zygodiscus clausus* to define the top of Zone NTp13 (op. cit., p. 280; text-fig. 8).

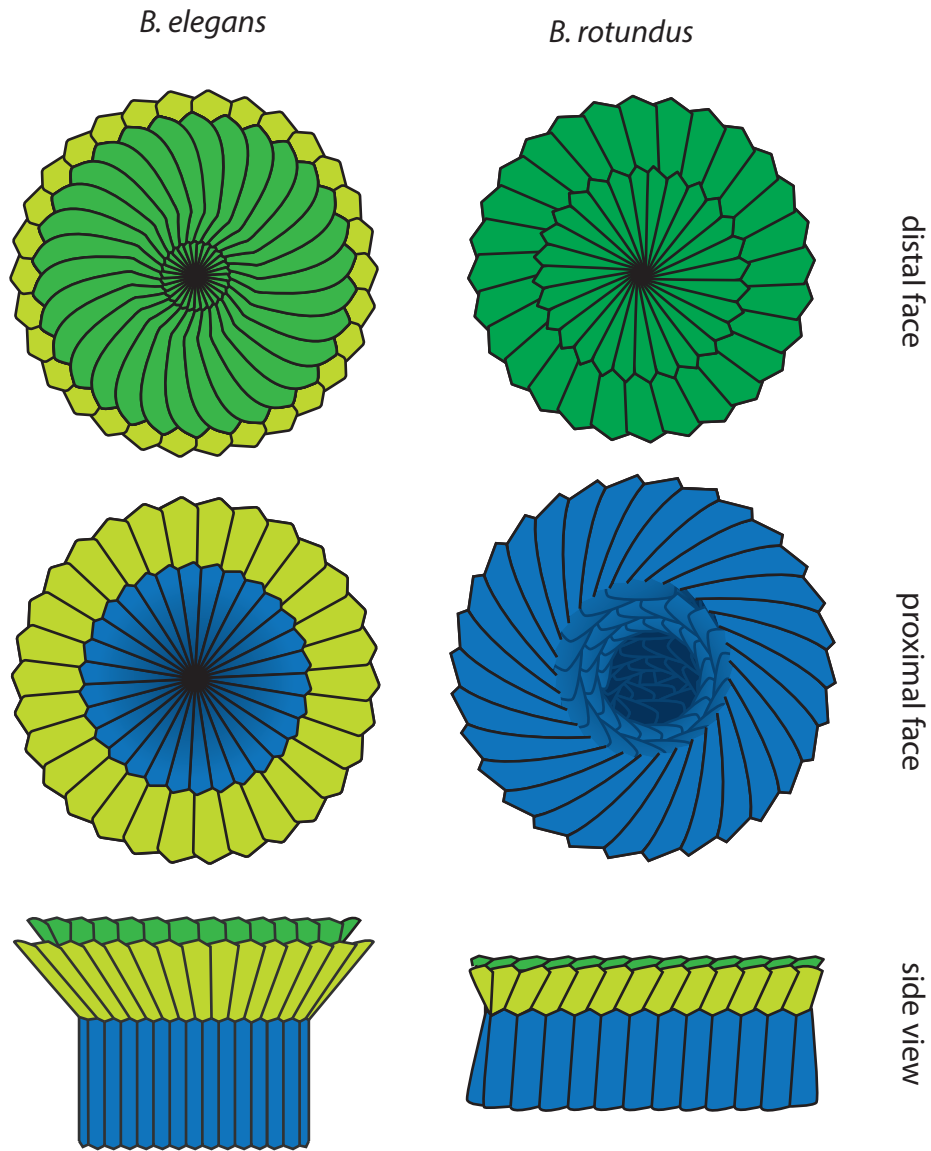
	Varol 1989	Martini 1971
† <i>B. elegans</i> † <i>Z. clausus</i>	NTP14	Zone NP8
	NTP13	
† <i>H. riedelii</i>	NTp12	Zone NP7

TEXT-FIGURE 8
Biozonal significance of *B. elegans*.

The range of *B. elegans* is, however, inconsistent between sections. The species was reported (and described) from a single level in Zone NP7 at DSDP Site 167-38-CC (Roth, 1973). It has since been reported from a) Zone NP5 at DSDP Site 356 (Perch-Nielsen, 1977, p. 748/722); b) Zone NP9 and a stratigraphic interval tentatively assigned to Zone NP6 in the Gebel Owaina section of Egypt (Perch-Nielsen et al. (1978); c) uppermost Zone NP5 and Zone NP6 in the Nahal Havdat section of Israel (Romein, 1979, p. 34); d) Zone NP6 at DSDP Site 384 (as *Heliolithus* aff. *cantabriae* Perch-Nielsen, Okada and Thierstein, 1979, p. 562/514); e) upper Zone NP6 to lower Zone NP8 in the Kokatsu section of Turkey (Varol, 1989b, fig. 12.3); and f) upper Zone NP4 in the Danian-Selandian Loubieng Section near Pont Labau, France (Steurbaut and Sztrákos, 2008, p. 8). This latter report is in agreement with Dinarès et al. (2010, fig. 10) who showed the Lowest Common Occurrence of the species slightly above the Chron C27n/C26r magnetozonal boundary in the Blaja section (Bulgaria). These are the oldest levels from which *B. elegans* has been reported. However, these two reports are questionable. The single illustration of a specimen from the Loubieng section (op. cit, pl. 3, fig. 17) is insufficient to determine whether the taxonomic identification is accurate. The two specimens illustrated from the Blaja section (op. cit., pl. 2, fig. 5 and pl. 5, fig. 6) are entirely birefringent whereas only the column is birefringent in *B. elegans*.



TEXT-FIGURE 9
Biochronology of *Bomolithus* (tentative). Magnetostratigraphy of Cande and Kent (1992, 1995).



TEXT-FIGURE 10

Comparison between species of *Bomolithus*.

Note that the tangential arrangement of the elements of the column is more pronounced in *B. rotundus* than in *B. elegans*.

Chronostratigraphy

Steurbaut and Sztrákó (2008, p. 23) have asserted that the LO of *B. elegans* may be used to approximate the Danian/Selandian boundary.

Biochronology

The FAD of *B. elegans* is placed at ~59 Ma. However, if the biostratigraphic succession in the Loubieng section can serve as a reference for biochronology (see above), the FAD of *B. elegans* is only slightly younger than the FAD of *Lithoptychius ulii* (60 Ma; text-fig. 9).

Agnini et al. (2007) have shown that the occurrence of *Bomolithus* sp. was discontinuous between (mid) Chron C26r and earliest Chron C25r and between (mid) Biochron NP5 and early Biochron NP7-NP8 undifferentiated. Assignment of this taxon to *Bomolithus* requires verification.

TAXONOMY

Generic taxonomy

Genus: *Bomolithus* Roth, 1973 emend.

Type Species: *Bomolithus elegans* Roth, 1973.

Diagnosis:

“Circular coccolith consisting of three cycles of elements. The uppermost cycle is higher than the others and the elements slope towards a central depression. The two lower cycles are sinistrally imbricate and slope towards the periphery.

“*Heliolithus* differs from *Bomolithus* in having only two cycles of elements in the shape of two partial cones joined at truncate apices. *Fasciculithus* lacks the lower

cycles which slope towards the periphery. *Toweius* has a much lower inner cycle of elements and is usually elliptical” (Roth, 1973, p. 734).

Emended diagnosis: Helioliths in which the calyptra and median structural unit (or collaret) are associated in a cone that flares distally in opposition to the column that flares in proximal direction. The calyptra is comprised of two or more cycles.

Bomolithus helioliths differ from *Heliotrochus* helioliths that also consist of three well developed structural units in having a collaret oriented as the calyptra. In *Heliotrochus*, the collaret in association with the column form the pillar which is markedly distinct from the calyptra.

Remarks: In his description of the genus, Roth did not refer to the extinction pattern of the coccoliths. However, in describing *B. elegans*, he (also p. 734) commented “In the light microscope under cross-polarized light only the central part (i.e., the upper cycle) is bright with a dark cross with practically straight arms. The two lower cycles are extinct”, adding “*Bomolithus elegans* n. sp. has a cylindrical upper cycle with two lower cycles attached to it and only the center is bright in cross-polarized light”. Roth oriented the coccolith upside down, referring to the column as “upper cycle”. Thus, in plane view and cross-polarized light, only the column is birefringent in *Bomolithus*, implying that complementary images in bright field and crossed nicols are necessary to comprehensively illustrate its species.

Specific taxonomy

Only two species are currently assigned to *Bomolithus* (text-fig. 10). Published illustrations show marked morphologic differences among specimens of *B. elegans*, in particular with regard to the height of the column, which may indicate either large intraspecific variability, or greater species diversity.

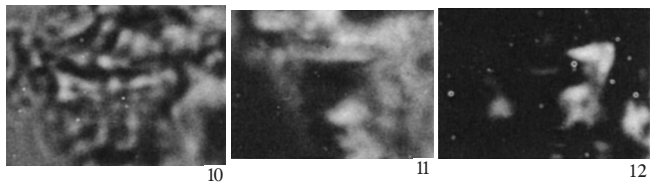
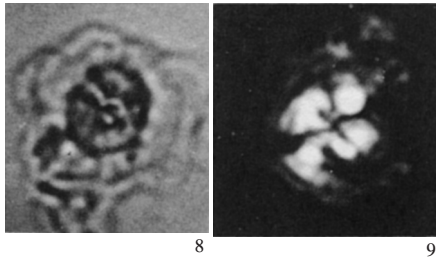
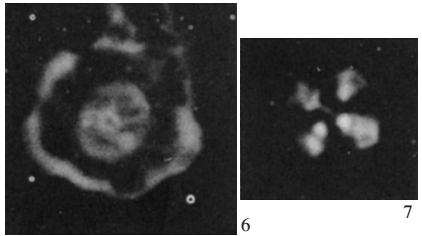
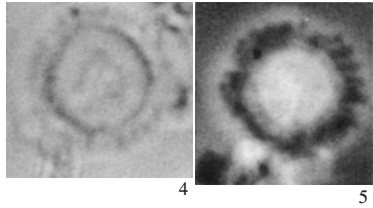
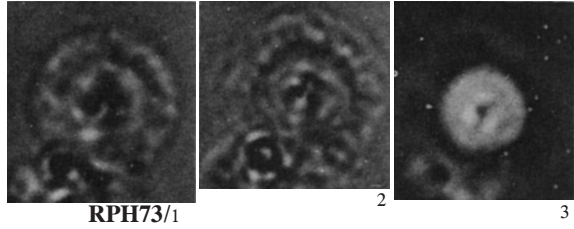
Revised species taxonomy

Bomolithus rotundus (Haq & Lohmann) n. comb.

Basionym: *Fasciculithus rotundus* Haq & Lohmann, 1976, p. 183, pl. 4, figs. 8, 9.

Bomolithus elegans Roth 1973

Bomolithus rotundus (Haq & Lohmann) n. comb. [= *Fasciculithus rotundus* Haq & Lohmann 1976, p. 183, pl. 4, figs. 8, 9]



Bomolithus elegans

- 7–11 μm x 7–9 μm

- Paleocene (NP7). Magellan Rise (DSDP Site 167), Central Pacific.

-The upper cycle [in fact the proximal cycle, or column] is the highest one and is composed of about 24 irregular wedge-shaped elements which slope towards a crater-like central depression. Not all the elements reach the center. There is an irregular hole in the center of the depression. The next lower [upper] cycle consists of about 24 tabular sinistrally imbricate elements which slope towards the periphery of the coccolith. The next lower [upper or overlying] cycle seems to be of the same basic construction. So far it has only been observed in side view. In the light microscope under cross-polarized light only the central part (i.e., the upper [proximal] cycle [column]) is bright with a dark cross with practically straight arms. The two lower [distal] cycles are extinct.

≠ from *H. riedelii* which has two conical cycles which are bright under CN.

— Romein (1979, p. 156) indicated that the cycles are comprised of 25 to 40 elements. The column is high, proximally flaring or parallel-sided. The median cycle is well differentiated with elements imbricated anticlockwise in proximal view.

— The stratigraphic distribution of this taxon is poorly established. Reports in Zone NP4 are questionable.

- RPH73 (p. 734).

Bomolithus rotundus

- ~7 μm x 8 μm

- L. Paleocene (NP7). Lower flank of Nicaragua Rise, Caribbean.

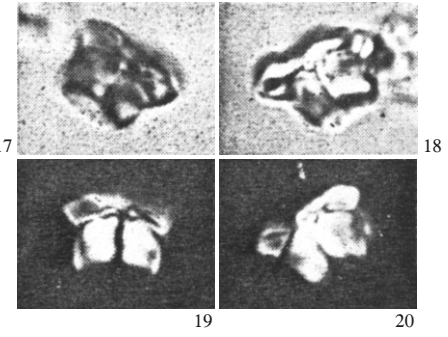
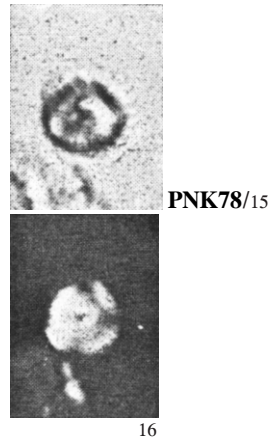
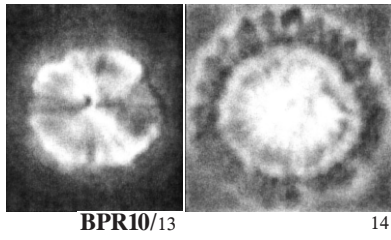
- Bundles of short cylindrical crystal-rods, topped by semi-spherical “crown” which is slightly larger in diameter than the bundle. Crystal-rods vary in number from about 30 to 40.

- *Bomolithus rotundus* might be the intermediate form in a *H. cantabriae* - *H. megastypus* lineage.

— Tentative but informal re-assignment of *Heliolithus rotundus* to *Bomolithus* was proposed earlier by Steurbaut (1998).

- HBU76 (p. 182), AMP (p. 169).

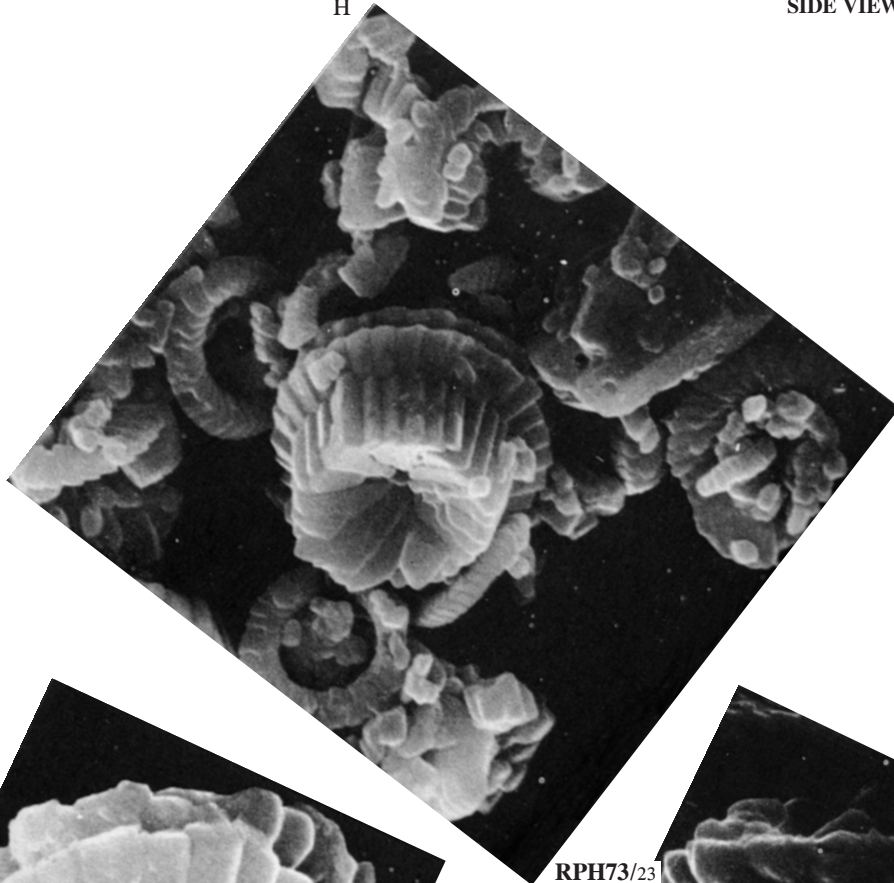
Bomolithus elegans (continued)



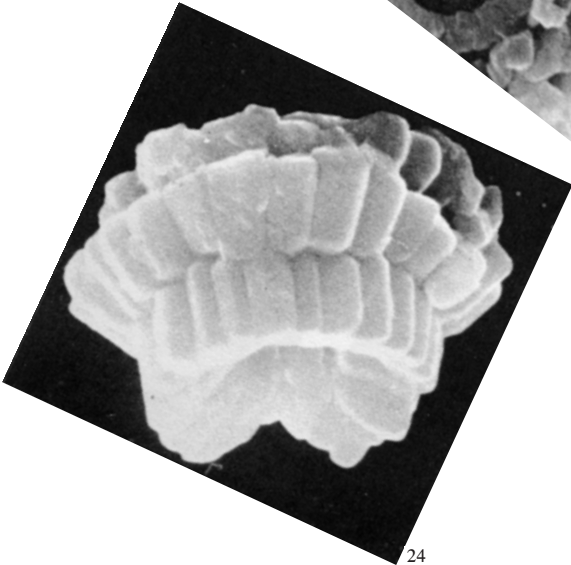
Bomolithus elegans (continued)

H

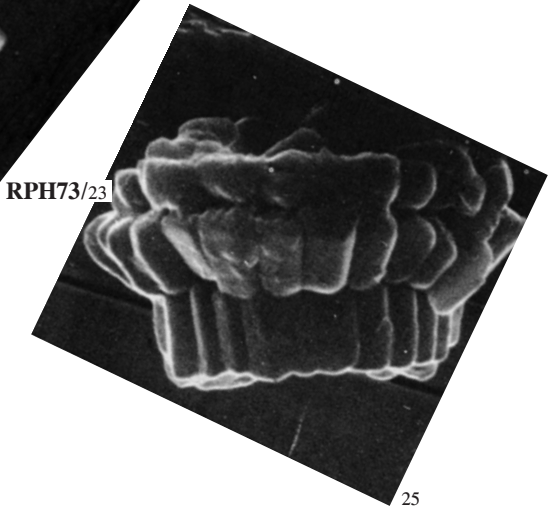
SIDE VIEW



PNK78/26

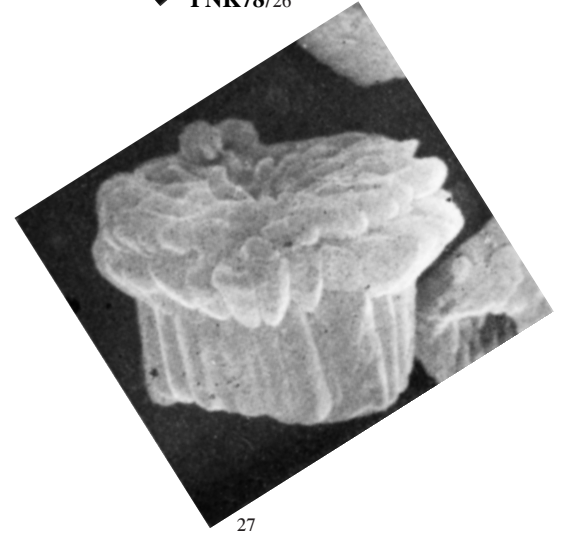


24



RPH73/23

25



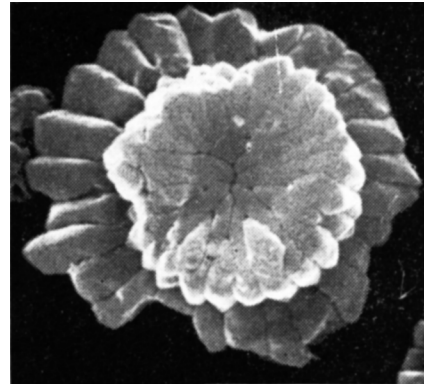
27

Bomolithus elegans (continued)

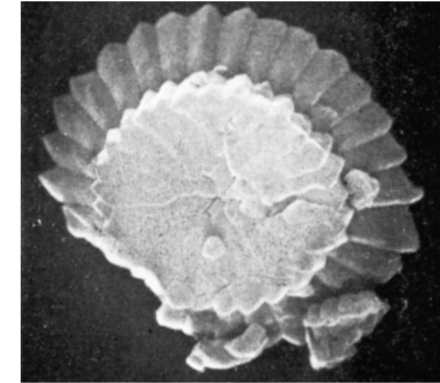
PROXIMAL FACE



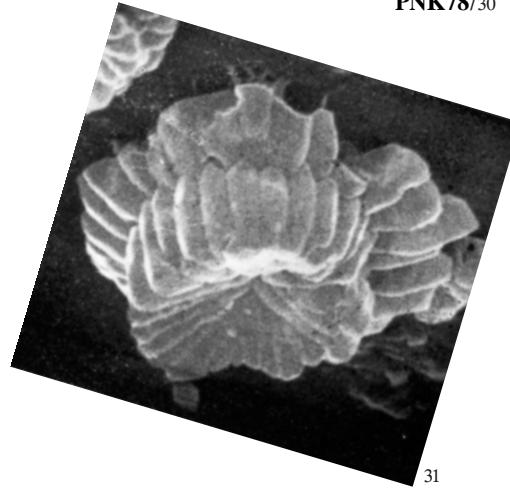
OH79/28



PNK78/30



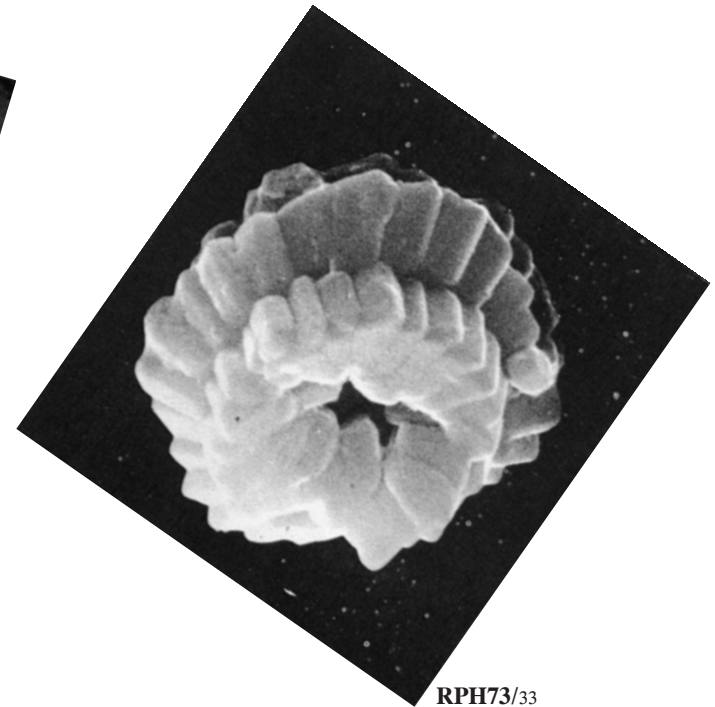
32



31



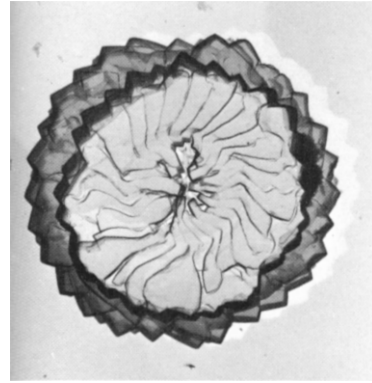
PNK77/29



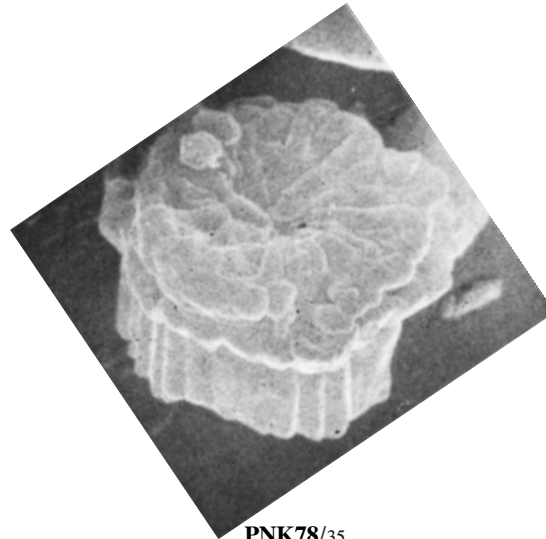
RPH73/33

Bomolithus elegans (continued)

DISTAL FACE



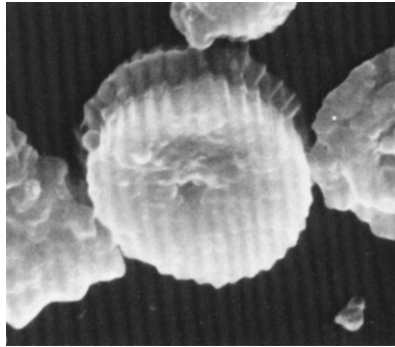
OH79/34



PNK78/35

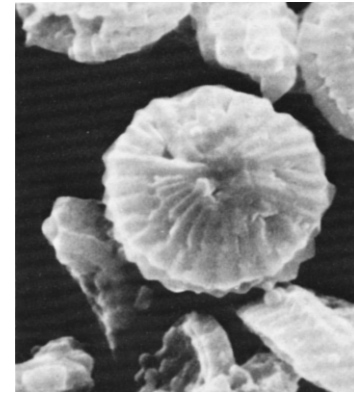
Bomolithus rotundus (continued)

PROXIMAL FACE



HBU76/36

DISTAL FACE



HBU76/37

Figure References

- AMP.** AUBRY, M.-P., this volume.
- BPR10.** BOWN, P. R.. 2010. *Journal of Nannoplankton Research*, 31: 11–38.
(13, 14): 10/5 (two images; *B. elegans*)
- HBU76.** HAQ, B. U. and LOHMANN, G. P., 1976. *Marine Micropaleontology*, 1: 119–194.
(36, 37): 4/9, 8 (as *Fasciculithus rotundus*)
- OH79.** OKADA, H. and THIERSTEIN, H. R., 1979. In: Tucholke, B. E., Vogt, P. R., et al., *Initial Reports of the Deep Sea Drilling Project*, 43, 507–573. Washington, D. C.: U.S. Government Printing Office.
(28): 14/2 (as *Heliolithus* aff. *cantabriae*)
(34): 14/1 (as *Heliolithus* aff. *cantabriae*)
- PNK77.** PERCH-NIELSEN, K., 1977. In: Supko, P. R., Perch-Nielsen, K., et al., *Initial Reports of the Deep Sea Drilling Project*, 39, 699–823. Washington, D. C.: U.S. Government Printing Office.
(29): 12/1 (*B. elegans*)
- PNK78.** PERCH-NIELSEN, K., SADEK, A., BARAKAT, M. G. and TELEB, F., 1978. *Annales des Mines et de la Géologie*, 28: 337–403.
(15-20): 9/5, 6, 25-28 (*B. elegans*)
(26, 27): 16/7, 11 (*B. elegans*)
(30-32): 17/8, 11, 9 (*B. elegans*)
(35): 16/8 (*B. elegans*)
- RAJT79.** ROMEIN, A. J. T., 1979. *Utrecht Micropaleontological Bulletins*, 22: 1–231.
(21): 10/1 (as *Heliolithus elegans*)
- RPH73.** ROTH, P. H., 1973. In: Winterer, E. L., Ewing, J. L., et al., *Initial Reports of the Deep Sea Drilling Project*, 17, 695–795. Washington, D. C.: U.S. Government Printing Office.
(1-12): 15/3a-c, 4a, b, 6a-d, 5a-c (*B. elegans*)
(23-25): 15/1, 2a, b (*B. elegans*)
(33): 15/2c (*B. elegans*)
- SE08.** STEURBAUT, E. and SZTRÁKOS, K., 2008. *Marine Micropaleontology*, 67: 1–29.
(22): 4/27 (as *B. elegans*)

HELIOTROCHUS

HIGHLIGHTS

- Five species.
- Coccoliths thick, circular in distal and proximal views, consisting of three structural units.
- Collaret and column united in the “pillar”.
- Size range: 6–17 μm .
- Cocosphere unknown.
- Stratigraphic Range: Zone NP6 – Zone NP9.
- Life span: ~1.2 Ma (late Chron C26r to earliest Chron C24r).
- Very closely related to *Bomolithus* and *Lithoptychius*.
- Ancestor of *Heliodiscoaster*.

Selected references

Agnini, 2007; Hay et al., 1967; Perch-Nielsen, 1971c; Perch-Nielsen, 1977; Prins, 1971; Romein, 1977; Steurbaut, 1998; Varol, 1989.

INTRODUCTION

The genus *Heliolithus* has traditionally included coccoliths that display a mosaic of characters (shape, number of cycles, birefringence pattern) that unite its species in a tenuous manner. Most of these species form a natural grouping around *H. kleinpelli*, but the remaining group of species, including the generotype *H. riedelii*, is sufficiently different to raise doubts as to whether *Heliolithus* is a monophyletic genus. In view of the morphostructural differences found here between these two groups, there is little alternative but to accommodate the *H. kleinpelli* group in a new genus, for which the name of *Heliotrochus* is introduced, for the species level taxa *kleinpelli*, *cantabriae*, *megastypus*, *conicus* and *knoxii*.

MORPHOLOGY AND STRUCTURE

Morphology – In plane view the helioliths of *Heliotrochus* appear to essentially consist of two imbricated discs of different diameters and thicknesses. In lateral view they are essentially mushroom-shaped, either thin and broad or thick and columnar (text-fig. 1). The widest side of the heliolith is the distal side, as determined from the peripheral serration pattern and from comparison with the ancestral fasciculiths. This is in agreement with Romein (1979).

The (circular) proximal face is concave. The concavity may be shallow (e.g., *H. conicus*) or deep (e.g., *H. cantabriae*). The (circular) distal face is flat or centrally depressed. A central canal occurs, linking the distal and proximal sides of the coccolith. The distal end of the canal is obliterated in most helioliths, but in some specimens a wide circular opening occupies the center of the distal face (probably because of the loss of a cycle).

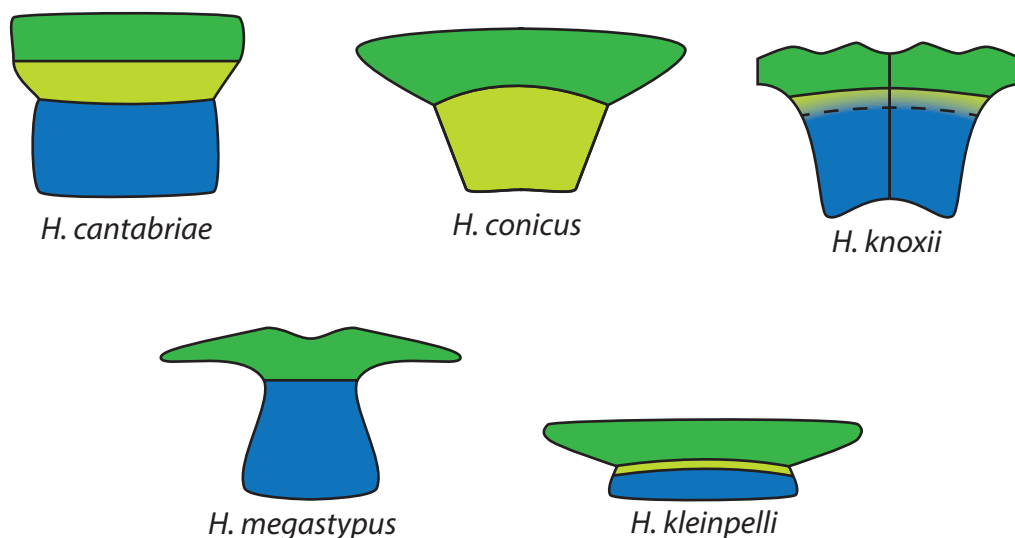
Structure – The structural description below is guided by the description of *H. kleinpelli* as seen in distal, proximal and side views. As always the LS pattern helps determine the proximal face of these coccoliths. *Heliotrochus* helioliths are comprised of three structural units: column, collaret and calyptra (text-figs. 2-5). As shown by a partly dissolved, partly overgrown heliolith (Perch-Nielsen 1971c; text-fig. 6), these are complex constructions whose

complete documentation would require description of the manner in which their structural units interlock. Whereas this is beyond the scope of this work, it implies that the longitudinal sections proposed below are highly simplified. This remark is valid for longitudinal sections of almost all coccoliths.

Column: This is a monocyclic unit, consisting of tangentially arranged elements. The sutures are oriented clockwise as seen in proximal view. The elements do not meet centrally but delineate a deep inner cavity (text-figs. 2a, 3a). The column in *H. cantabriae* compares well with that in *H. kleinpelli*, with tangentially arranged elements separated by sutures strongly bent clockwise forming a broad ring around a deep central cavity. In *H. megastypus* and *H. conicus* the column is compact (although short in the latter species) and without central depression, and the elements are also tangentially arranged although with sutures being less strongly curved (text-figs. 4a, 5a). The proximal face of the column is not illustrated in *H. knoxii*.

Collaret: The collaret is a monocyclic unit with non-imbricate elements and sutures oriented clockwise as seen in proximal view. The elements of the collaret and column interlock tightly as seen in side views of the helioliths (e.g., *H. kleinpelli*: Perch-Nielsen, 1971c, pl. 2, fig. 4). This median cycle is unambiguously identified as a low cycle in *H. cantabriae* in which it is readily comparable to that in *H. kleinpelli* (text-figs. 2a, 3b). The collaret is well developed in *H. conicus* in which it forms the bulk of the “pillar” (collaret + column), the column forming a low cycle much narrower than the collaret (in agreement with Perch-Nielsen’s interpretation, 1981a, fig. 3; text-figs. 4b, c). There is no visible collaret in *H. megastypus* (text-figs. 5b, c).

Calyptra: The calyptra is a polycyclic structural unit, consisting of (at least) three concentric cycles. Only the outer cycle is seen in both distal and proximal views of the helioliths. The calyptra can be best described from specimens of *H. kleinpelli* in which all cycles are comprised of the same number of elements with sutures curved anticlockwise. However the cycles differ with regard to the arrangements of the elements. Those of the inner and median cycles



TEXT-FIGURE 1
General shapes of *Heliotrochus* helioliths as seen in side view.

are imbricate dextrally (e.g., Okada and Thierstein, 1979, pl. 14, fig. 7; Perch-Nielsen et al., 1978, pl. 16, fig. 1; text-fig. 2d). Those of the outer cycle are non-imbricate (Perch-Nielsen, 1971c, pl. 2, fig. 2). Each element possesses on its proximal side a radial ridge that alternates with the sutures. This confers a corrugated aspect to the proximal surface of the cycle. None of the illustrated helioliths available here are sufficiently well preserved to allow a detailed description of the distal surface of the outer cycle of the calyptra. However, from the asymmetric overgrowth of the same elements on their distal side, it may be deduced that a corrugated ornamentation occurred there, similar to that seen on the proximal side. The innermost cycle is plug-like and seems to consist of radially arranged, lath-like elements. A very narrow but prominent ring with “tidy appearance” encircles this central cycle that is often lacking, leaving a gaping central hole at the mouth of the axial canal (text-fig. 7).

Illustrations that allow a detailed description of the calyptra are not available for all species. It is readily seen, however, from available illustrations of *H. cantabriae*, *H. conicus*, *H. knoxii* and *H. megastypus*, that the essentially flat or slightly depressed centrally distal face of their calyptra is directly comparable to that of *H. kleinPELLI* (e.g., *H. kleinPELLI*: Perch-Nielsen, 1971c, pl. 2, fig. 2; *H. cantabriae*: Perch-Nielsen et al., 1978, pl. 16, fig. 9; *H. conicus*: Haq and Aubry, 1980, pl. 6, fig. 7; *H. knoxii*: Steurbaut, 1998, pl. 2, fig. 15).

EXTINCTION PATTERNS

Romein (1979, p. 155, 156) has described the extinction lines in the species of *Heliolithus* that are now assigned to *Heliotrochus* as follows:

“In the standard orientation for distal view, the lines are laevogyre. The lines are straight over most of their length, and curve marginally. The straight parts make an angle of about 20° with the polarization directions in clockwise direction, in distal view. In the standard orientation for side view a straight, median extinction line can be observed”.

In the standard orientation for distal view, the side with the largest diameter is turned upwards; in the standard orientation for side view, the edge of the distal cycle is parallel to the X-cross-hair and the axis of the column is parallel to the Y-cross-hair.

Romein has also described the color patterns obtained in cross-polarized light with the gypsum slide added:

“In the standard orientation for distal view, the larger parts of the second and fourth quadrants are blue; the other sectors are yellow. In the standard orientation for side view, the left half of the column, the left half of the distal cycle and the right half of the median cycle are blue; the other halves are yellow” (text-fig. 8).

Helioliths of *Heliotrochus kleinPELLI*, *H. cantabriae* and *H. knoxii* are entirely birefringent in standard orientation for distal view. The calyptra is non birefringent in *H. conicus* and *H. megastypus*.

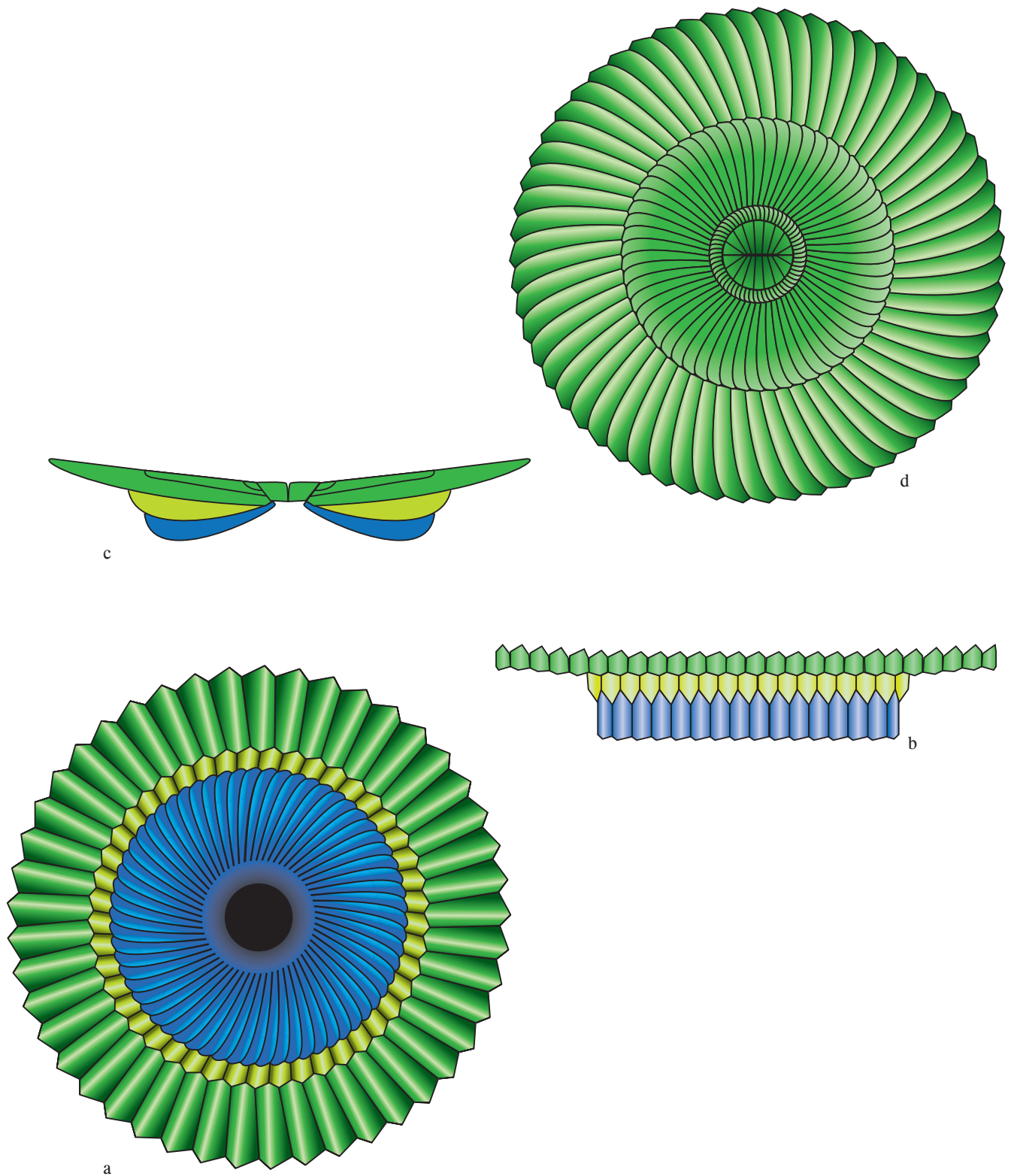
BIOLOGY AND ECOLOGY

Biology

The coccosphere of *Heliotrochus* is unknown. The variable shapes of helioliths indicate that the outline of the coccosphere would have been highly variable as well (text-fig. 9).

Physiology

Disc-shaped, and the broadest of the three structural units in most species, the calyptra confers a remarkable unity to the *Heliotrochus* helioliths, even though its structure is not fully resolved. This polycyclic calyptra is complex (text-fig. 2d, 3d, 4d, 5d, 7), suggesting that it was highly functional. The plug-like innermost cycle surrounded by a well-defined narrow ring occupies a location similar to the central body of *Lithoptychius*. The two may be homologous and they may have played a similar role, perhaps in controlling exchanges between the cell and seawater.

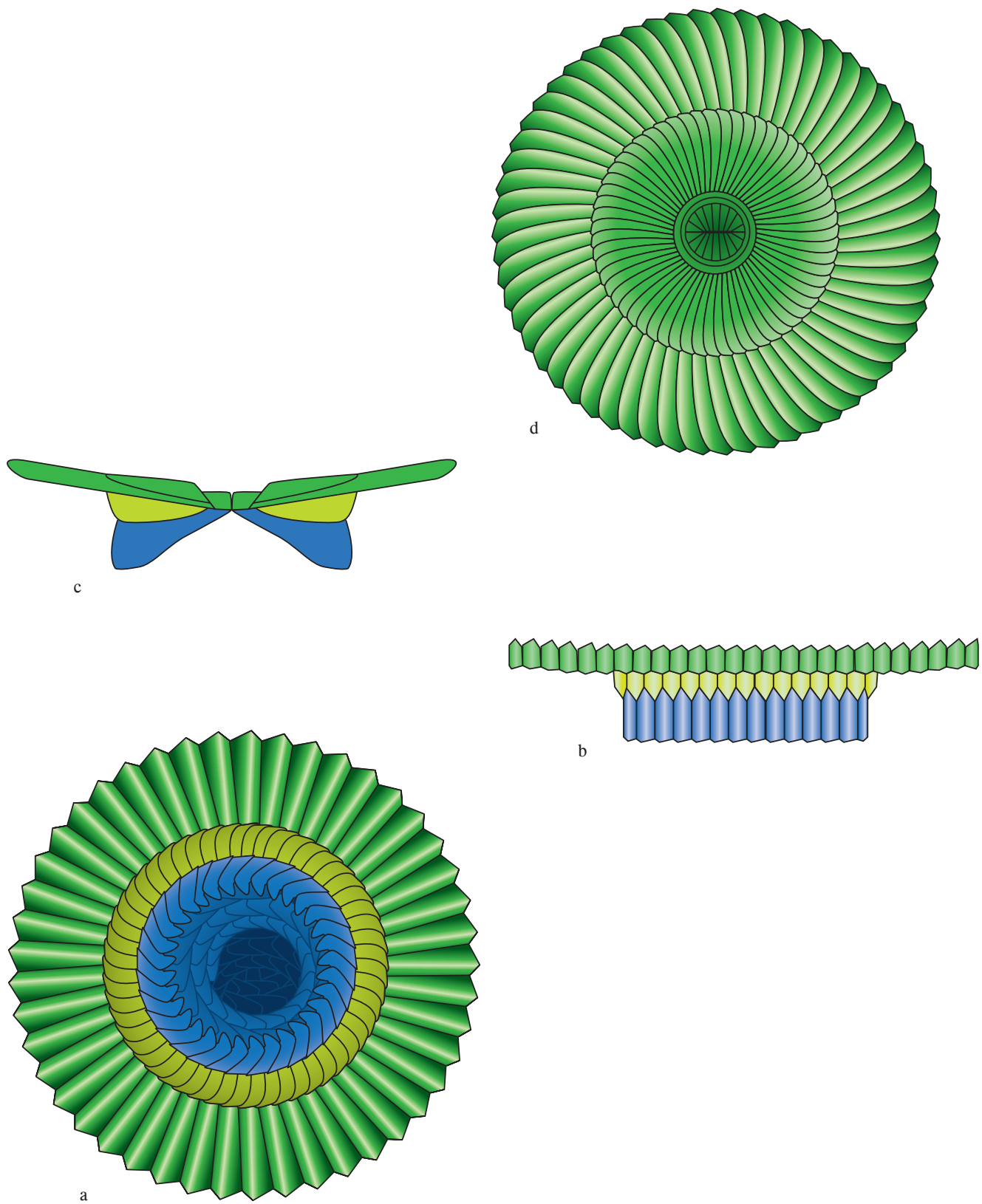


TEXT-FIGURE 2

Structure of *Heliotrochus kleinPELLI*.

- a: proximal face.
- b: side view.
- c: longitudinal cross section.
- d: distal face.

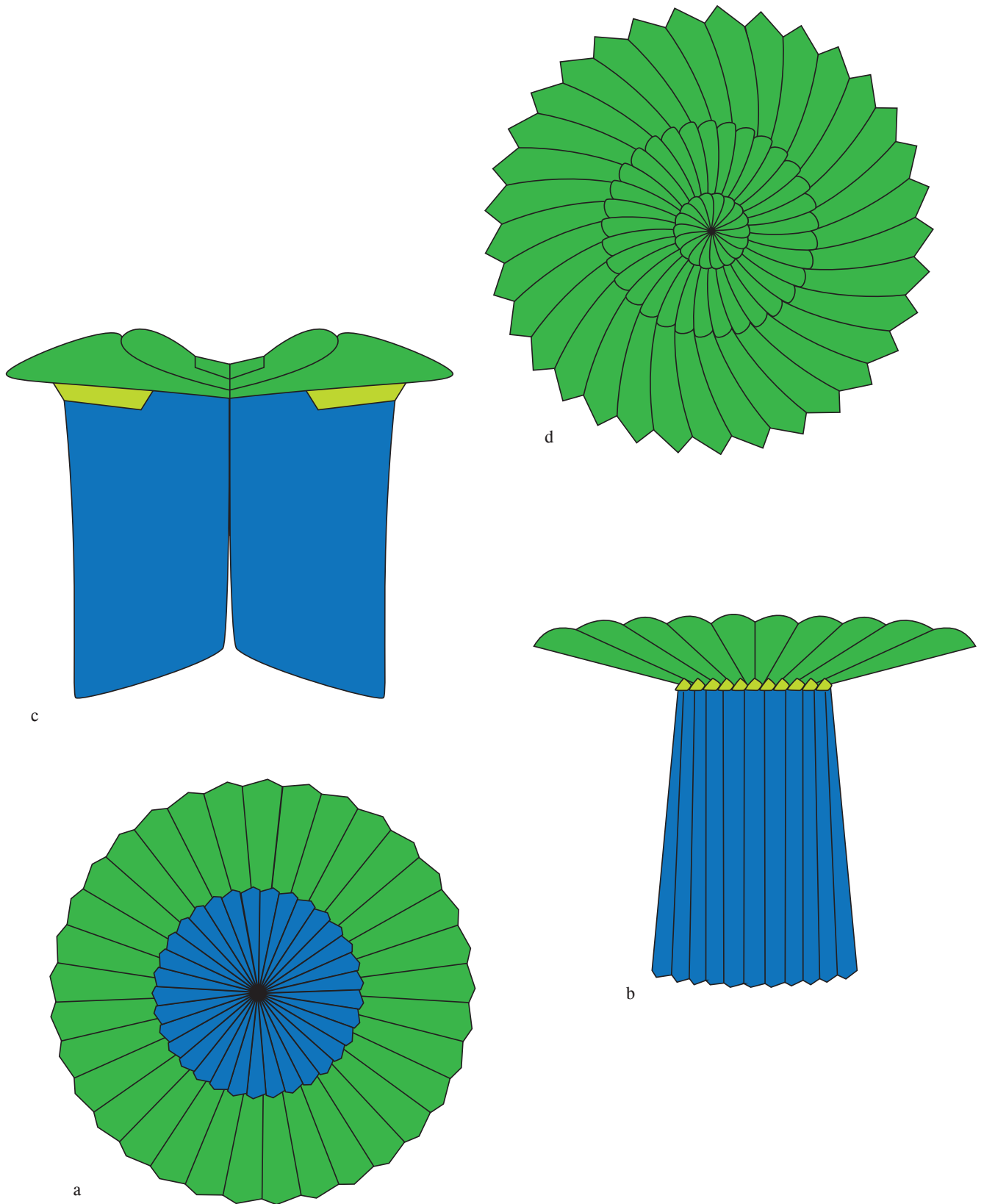
Note the polycyclic character of the calyptra, and the fact that, although in apparent concentric arrangement its cycles are in superposition, not in lateral juxtaposition. The column and collaret form the pillar. For the sake of simplicity the number of elements in the column has been kept to a minimum in the side view.



TEXT-FIGURE 3

Structure of *Heliotrochus cantabriae*.

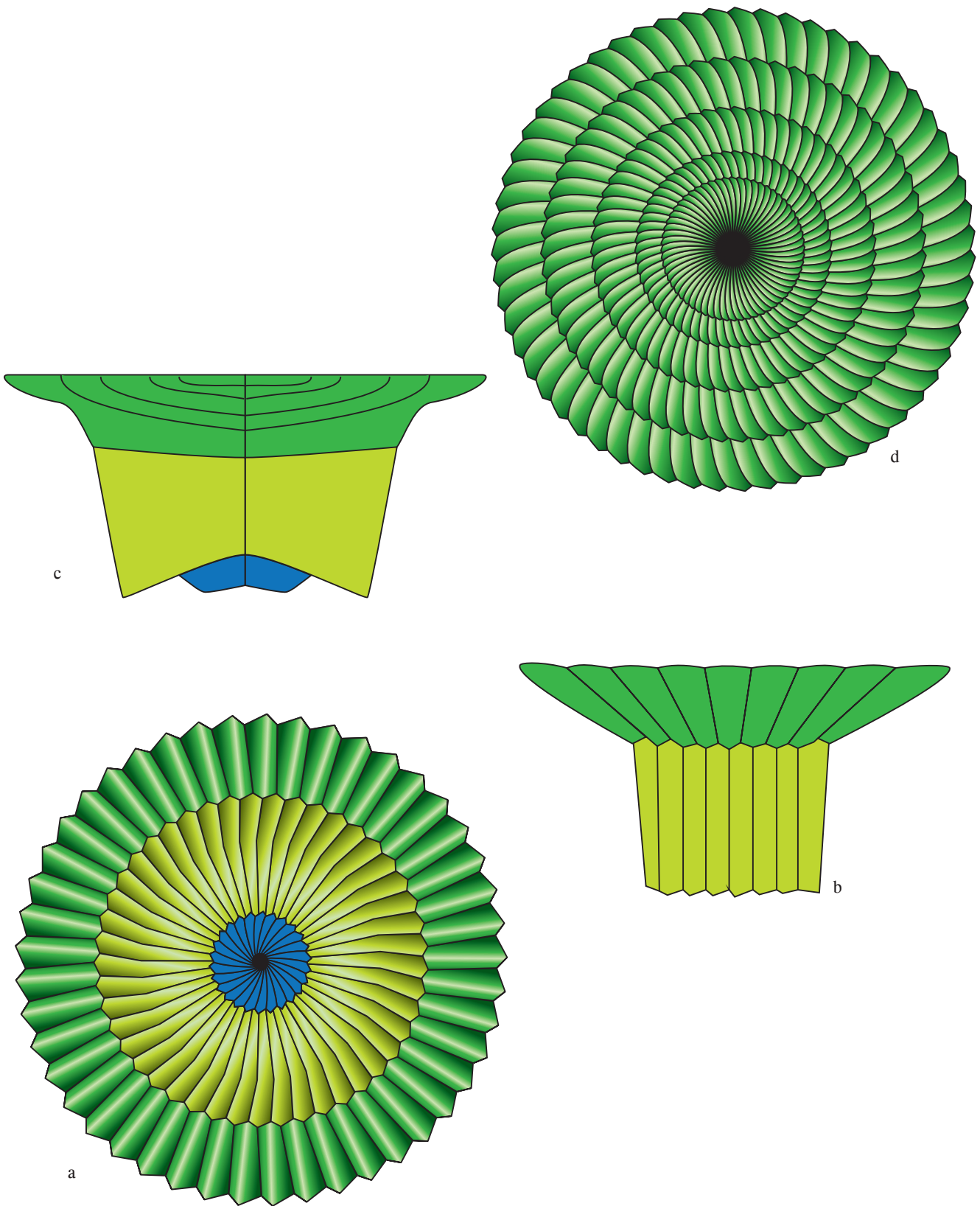
- a: proximal face.
- b: side view.
- c: longitudinal cross section.
- d: distal face. For further explanation, see text-fig. 2.



TEXT-FIGURE 4

Structure of *Heliotrochus megastypus*.

- a: proximal face.
- b: side view.
- c: longitudinal cross section. Side view and longitudinal cross section correspond to different specimen.
- d: distal face. For further explanation, see text-fig. 2.



TEXT-FIGURE 5

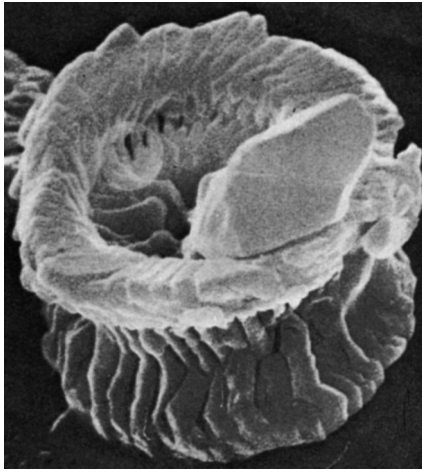
Structure of *Heliotrochus conicus*.

a: proximal face.

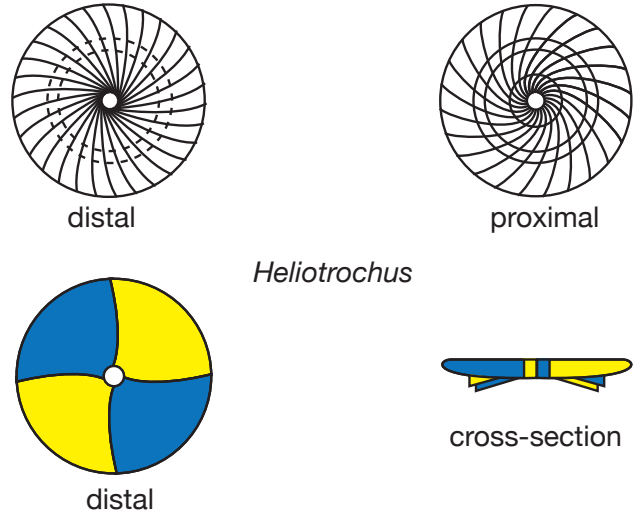
b: side view.

c: longitudinal cross section. Side view and longitudinal cross section correspond to different specimen.

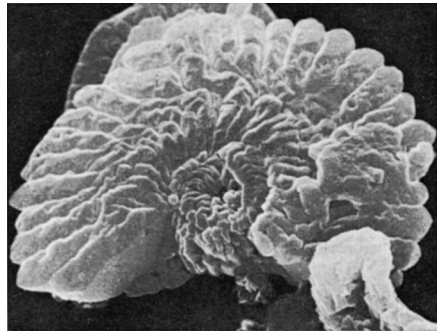
d: distal face. For further explanation, see text-fig. 2.



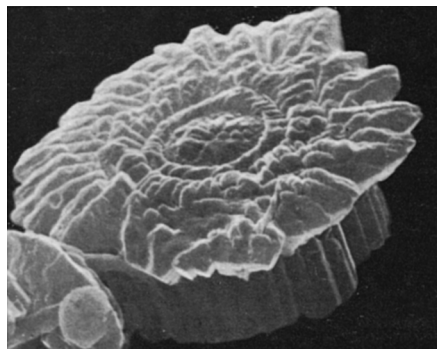
TEXT-FIGURE 6
Fine structure of a *heliotrochus heliolith* (*Heliolithus* ? sp. in Perch-Nielsen, 1971c, pl. 1, fig. 5).



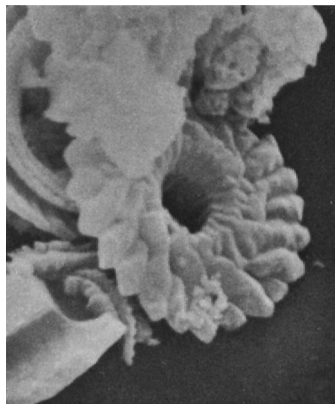
TEXT-FIGURE 8
Interpretation of the structure of helioliths of *Heliotrochus* and optical behavior. Extinction patterns in *Heliotrochus* in the standard orientations (after Romein, 1979, p. 155).



a



b



c

Overgrowth in most illustrated specimens has obliterated an original ornamentation of ridges, not only on the calyptra but the column as well (e.g., *H. kleinPELLI*: Perch-Nielsen, 1971c, pl. 2, fig. 2; text-fig. 2) that would have contributed to collect and refrain food particles. The ridge on the calyptra would also have funneled them toward the central plug.

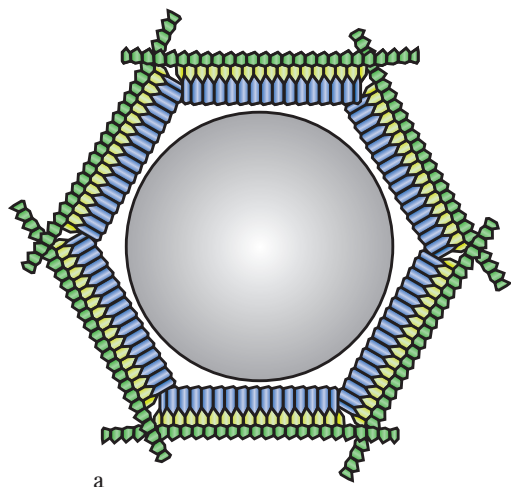
Ecology

Heliotrochus species may have shown preferences for mid latitudes (Backman, 1986), but they occurred at low latitudes, as well as in southern high latitudes (e.g. Weddell Sea: Pospichal and Wise, 1990). They were common on the edges of North Sea area (e.g., Steurbaut, 1998) as well as in other epicontinental settings (e.g., New Jersey margin; pers. obs.).

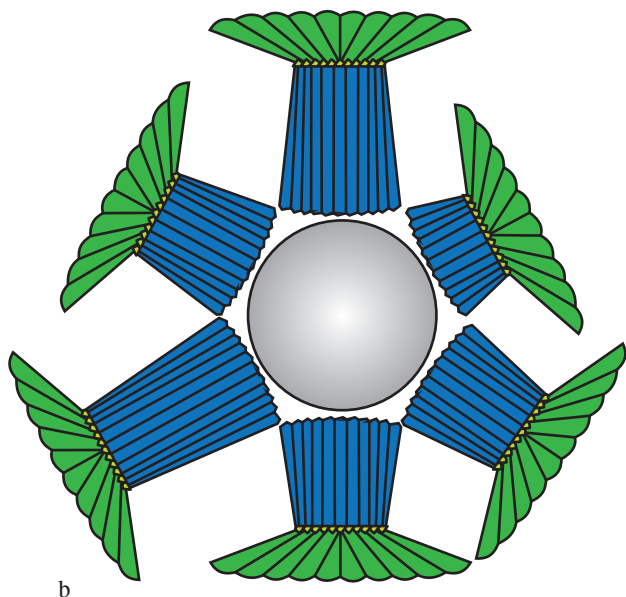
EVOLUTIONARY HISTORY

It may be useful to re-state here the differences between the helioliths of *Bomolithus* and of *Heliotrochus*. The coccoliths of the two genera exhibit the same tripartite structure, with similar imbrication of the elements and orientation of the sutures, and, importantly, their calyptra is composite. However, in *Bomolithus*

TEXT-FIGURE 7 (left)
Details of the distal face of the polycyclic calyptra in *Heliotrochus*. a: "*Heliolithus* ? sp." in Perch-Nielsen, 1971c, pl. 2, fig. 8; b: "*Discoasteroides* sp." in Perch-Nielsen, 1971c, pl. 1, fig. 7; c: "Top view of a ? *Heliolithus* sp." in Haq and Aubry, 1980, pl. 6, fig. 8. Note the four cycles forming the calyptra in (a), the tidiness of the third cycle, and the slight decrease in elevation from outer cycle to inner cycle. Note also, to the right in the dual arrangement of the elements of the outer cycle to form short spurs separated by deep grooves, reminiscent of the configuration of the elements of the column in *Fasciculithus*. Note the orientation of the elements of the outer cycle in (b), and the conical shape of the innermost, distinct cycle. Note the two cycles and the opening of the central canal (c). It is probable that the innermost cycle have been lost.



a



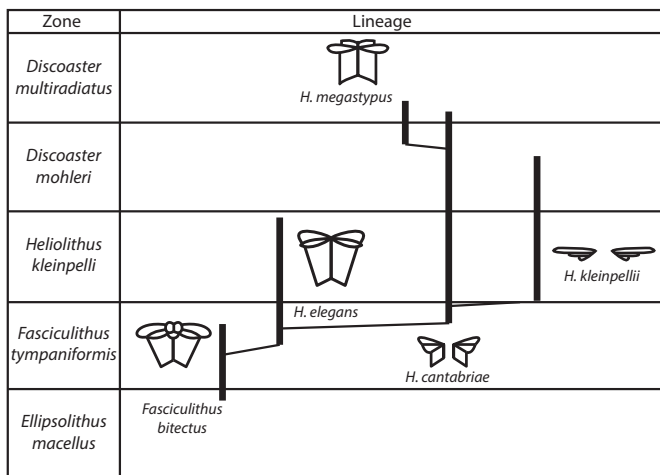
b

TEXT-FIGURE 9

Tentative reconstructions of the coccospheres of *Heliotrochus* species.

a: *H. kleinpellii*.

b: *H. megastypus*. The column varies considerably in size between specimens. This may represent intraspecific variability, pseudocryptic speciation or possibly coccosphere polymorphism as shown here.



TEXT-FIGURE 10

Structure of *Heliotrochus helioliths* and lineages. (After Romein, 1979, p. 79, fig. 41.) Note that Romein assigned these taxa to *Heliolithus*.

Bomolitus represents an intermediate stage, is difficult to determine. *Bomolitus* and *Heliotrochus* could have arisen independently from *Lithoptychius*, or in phylogenetic succession.

Romein (1979, p. 78, fig. 41; text-fig. 10) saw a one to one relationship between the structural units of *Lithoptychius* (his "*Fasciculithus bitectus*") and the species now grouped in *Heliotrochus*, and considered that the re-arrangement of the elements of the column from radial (*Lithoptychius*) to tangential (*Heliotrochus*) was the main transformation associated with an inferred *L. bitectus* – *B. [H.] elegans* – *H. cantabriae* lineage (text fig. 4). It should be noted that Romein regarded *Bomolitus* as a synonym of *Heliolithus* (including *Heliotrochus*), which does not conflict with the phylogeny discussed here. Perch-Nielsen (1981a) essentially agreed with Romein's interpretation of the lineage.

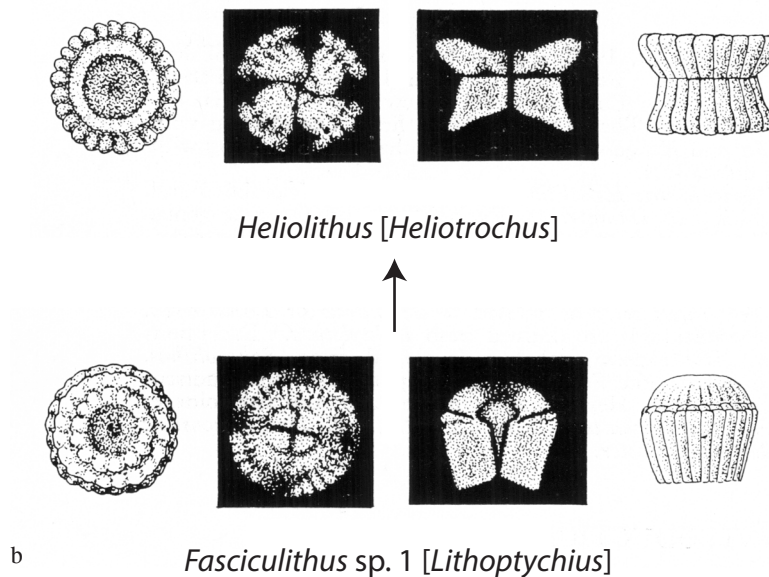
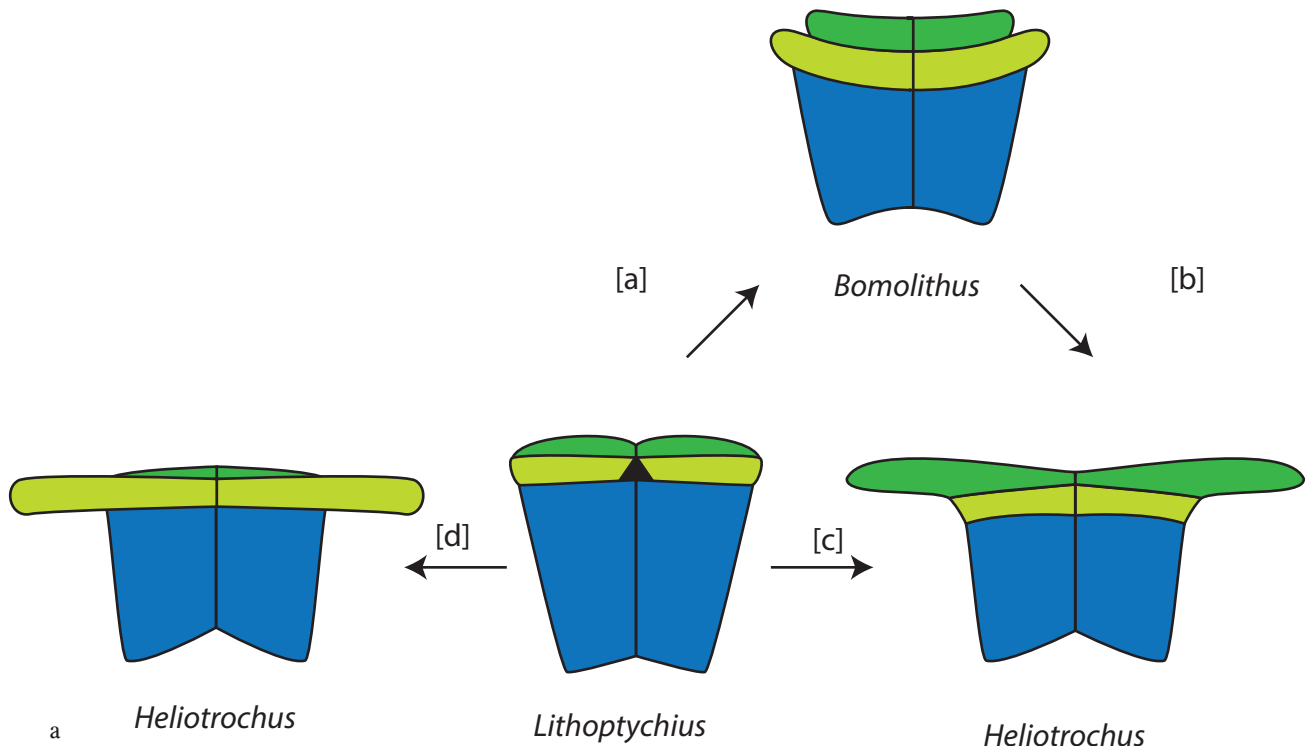
It is possible that *Bomolitus elegans* gave rise to *Heliotrochus cantabriae* through shrinkage of the collaret coincident with flattening and lateral expansion of the calyptra (text-fig. 11, evolutionary path [b]). But it is equally possible that *H. cantabriae* evolved directly from a species of *Lithoptychius* with a narrow collaret solely through lateral expansion of the calyptra (text-fig. 11a, evolutionary path [c]). This is one of the two evolutionary paths envisioned by Prins (1971, p. 1027). In the other path (text-fig. 11a, path [d]), the collaret of *Lithoptychius* expanded laterally while the calyptra regressed.

the calyptra and the collaret are oriented similarly with regard to the axis of rotation of the coccolith, and opposite to the column, which is not the case in *Heliotrochus*. Simply stated, in addition to their tripartite structure, these helioliths can be described as consisting of two superstructures. In *Bomolitus*, the superstructure is formed by the collaret and the calyptra. This is also the superstructure found in *Lithoptychius*, where it is referred to as the cone (following Romein, 1979). In *Heliotrochus*, the superstructure is formed by the column and collaret, referred above as the pillar.

Origin

Heliotrochus is plainly close to *Lithoptychius* and to *Bomolitus*. Whether it evolved directly from *Lithoptychius*, or whether

The median cycle in *Heliotrochus* and in *Bomolitus* are clearly homologous. Whether it is also homologous with the collaret of *Lithoptychius* requires further consideration (see genus *Bomolitus*, this volume). If it is homologous, as seems likely, then the collaret underwent a significant structural change during the evolutionary transition that involved a change in the imbrication of its elements from sinistral to dextral as seen in distal view. This resulted in the calyptra and collaret becoming essentially undifferentiated in the descendant taxa. That such a major structural change would occur only once is far more probable than to suppose that it occurred twice as *Bomolitus* and *Heliotrochus* evolved separately from *Lithoptychius*. However, this does not imply that *Bomolitus* is the direct ancestor of *Heliotrochus*, and it would be presumptuous to think that the lineages of these coccoliths that never occurred



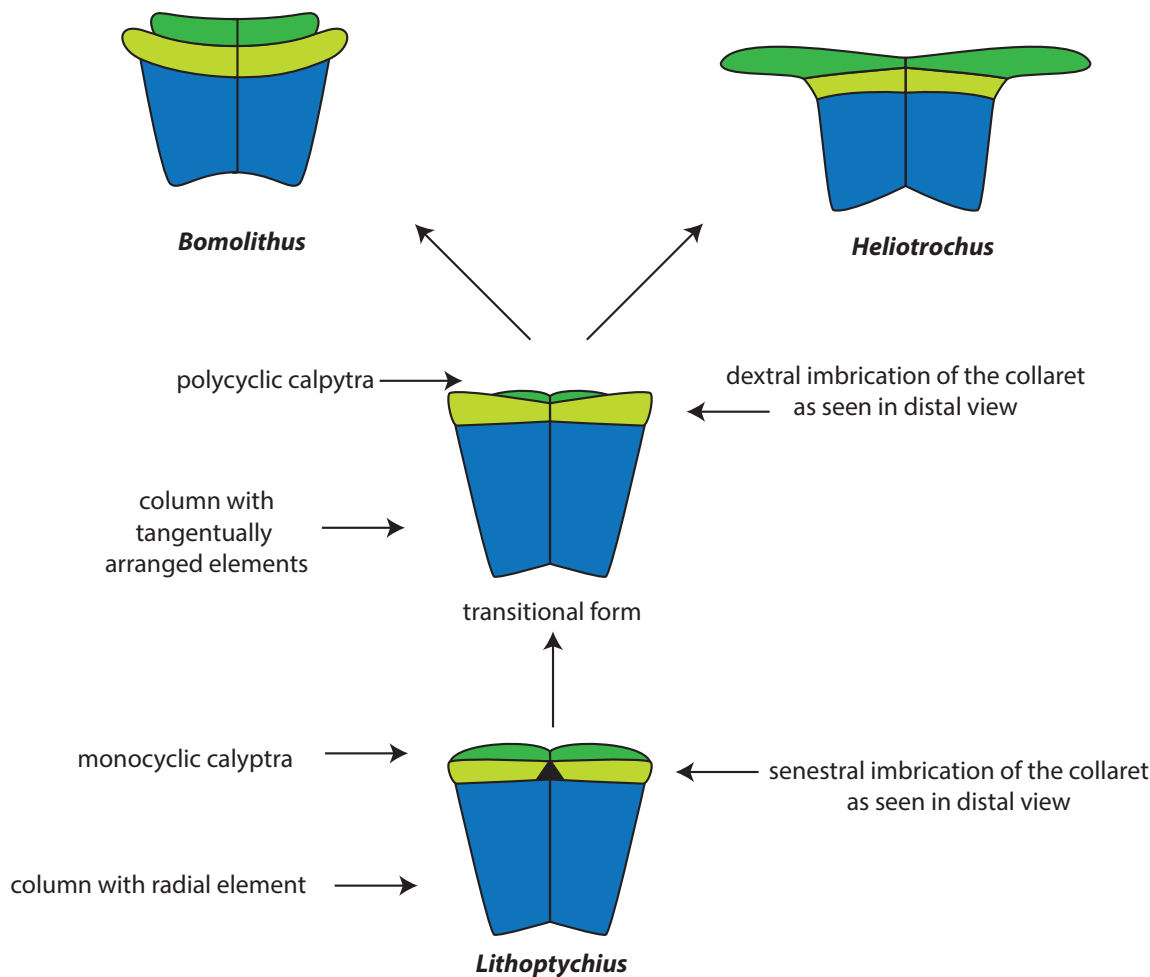
TEXT-FIGURE 11

Potential evolutionary paths between *Lithoptychius*, *Bomolithus* and *Heliotrochus*.

a: Path [a], in which the three taxa form a lineage, was proposed by Romein (1979). Path [c] proposed by Prins (1971) consists in the lateral expansion and flattening of the calyptra whereas path [d], also considered by Prins, consists in the expansion of the collaret and a reduction of the collaret.

b: Evolution of *Heliotrochus* from *Lithoptychius* (from Prins, 1971, pl. 1, figs. 6 and 7). Prins's illustrations leave no doubt that *Fasciculithus* sp. 1 is a species of *Lithoptychius*.

Prins commented "This undescribed form of *Fasciculithus* evolves into *Heliolithus* (pl. 1 fig. 7). In which way this transformation exactly took place, is not fully understood by me. It is well possible, that the flaring top part in *Heliolithus* represents the enlarged disc on top of the proximal column in *Fasciculithus* spec. 1. In this case the erect ring-like apical spine in *F. spec. 1* is strongly reduced in *Heliolithus*. It might also be, that the disc is reduced and that the erect apical spine in *F. spec. 1* bends more and more outwards in *Heliolithus*" adding, in a visionary fashion, "until it becomes nearly horizontal in the descendants of *Heliolithus*, the genera *Discoasteroides* and *Heliodiscoaster* (pl. 1 figs. 8, 10)" (op. cit., p. 1027). Prins' drawing of "*Heliolithus*" is more suggestive of a *Heliolithus* heliolith than of a *Heliotrochus* heliolith. However, his discussion implies that the drawing symbolizes both genera.



TEXT-FIGURE 12

Divergence of *Bomolithus* and *Heliotrochus* from *Lithoptychius*.

Hypothetical transitional form between *Lithoptychius* and *Bomolithus* and between *Lithoptychius* and *Heliotrochus*, with indication of the associated structural changes.

in great abundance could be restored so easily. It is at least as likely that *Bomolithus* and *Heliotrochus* evolved separately from a transient common ancestor that arose from *Lithoptychius*. The structural adjustments to the column (from radially to tangentially arranged elements with clockwise sutures in proximal view) and to the collaret would have occurred during the transition from *Lithoptychius* to the unknown intermediate form, from which *Bomolithus* and *Heliotrochus* each in turn diverged (text-fig. 12).

Phylogeny

Romein (1979; text-fig. 10) considered *Heliotrochus cantabriae* to be the stem species from which *H. kleinpelli*, and *H. megastypus* diverged. However, no lineage has been quantitatively described for the genus. Transitional forms between *H. cantabriae* and *H. kleinpelli* have been reported (Backman, 1986; Wei and Wise, 1989; Agnini et al., 2007; text-fig. 13), and evolution of one species into the other is highly feasible, involving nothing more than an expansion of the calyptra, thinning of the column and inwards migration of the collaret to become restricted to the diameter of the column. However, direct transition between the two species has not been demonstrated. The common and consistent occurrences of intermediate forms (the “*Heliolithus cantabriae*/*Heliolithus kleinpelli* intergrade”, text-fig. 13) through most of the ranges of both the ancestral taxon and its descendant at ODP

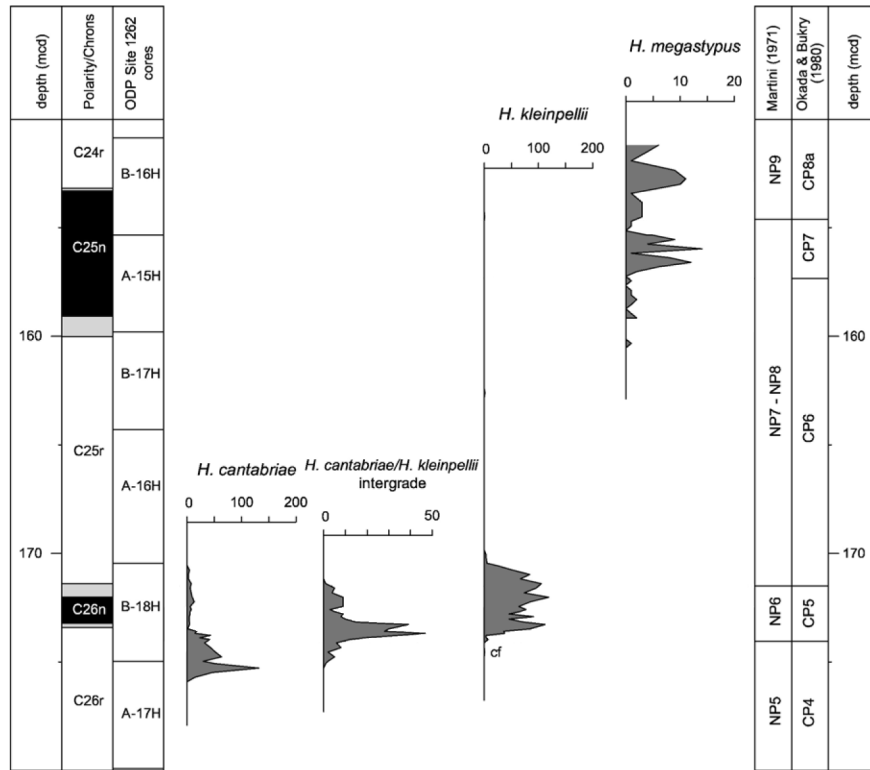
Site 1262 are in fact suspicious and raise the question of whether the putative intermediate specimens do not rather correspond to pseudocryptic species of either species.

Diversity

Only five species are assigned to the genus *Heliotrochus*, but published illustrations and personal light microscope observations suggest that diversity is much higher. For instance, specimens assigned to *H. megastypus* exhibit large differences in the morphology of the calyptra and the height of the pillar. In *H. kleinpelli* the calyptra may flare distally or be planar (compare Perch-Nielsen, 1971c, pl. 2, fig. 2 and Haq and Aubry, 1980, pl. 6, fig. 3). The collaret may be partly or completely integrated with the column (compare Perch-Nielsen, 1971c, pl. 2, fig. 4, in which the collaret is of the same diameter as the column, and Perch-Nielsen et al., 1978, pl. 17, fig. 4, in which the collaret is wider than the column). It is not known whether these differences represent intraspecific variability, indicate pseudocryptic speciation, or have some other undiscovered significance.

STRATIGRAPHY

The role of *Heliotrochus* species in Upper Paleocene biostratigraphy has been closely intertwined with that of *Heliolithus* species because they span a similar stratigraphic interval (text-fig. 14).



TEXT-FIGURE 13

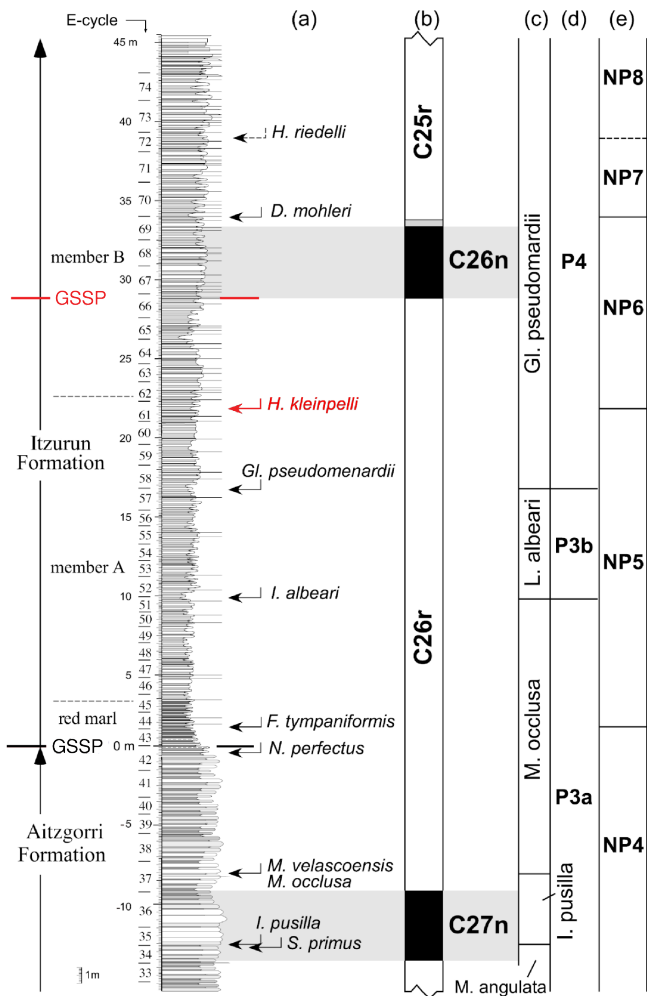
Abundance patterns of *Heliotrochus* species at ODP Site 2007. (Modified from Agnini et al., 2007, fig. 6.) The “*H. cantabrie/H. kleinpelli* intergrade” corresponds to putative transitional specimens between the two species.

	Bramlette and Sullivan 1961	Mohler and Hay in Hay et al. 1967	Martini 1970, 1971	Perch-Nielsen 1972	Bukry 1973	Okada and Bukry 1980	Romein 1979	Perch-Nielsen 1981	NTp17 ^a				
T <i>H. atkasii</i> - - - -	<i>Discoaster multiradiatus</i> Zone	<i>D. multiradiatus</i> Zone		<i>D. multiradiatus</i> Zone	<i>D. multiradiatus</i> Zone	CP8	<i>D. multiradiatus</i> Zone	NP9	NTp16				
T <i>Ht. cantabrie</i> - - - -										NTp16B ³			
⊥ <i>Hd. multiradiatus</i> - - - -									NTp16A ²				
T <i>Ht. kleinpelli</i> - - - -	<i>Heliolithus riedeli</i> Zone	<i>H. riedeli</i> Zone	<i>H. riedeli</i> Zone	<i>Discoaster nobilis</i> Zone	<i>D. nobilis</i> Zone	CP7	<i>D. mohleri</i> Zone	NP7/8	NTp15 ¹				
T <i>H. riedeli</i> - - - -									NTp14				
⊥ <i>Hd. nobilis</i> - - - -													
⊥ <i>H. riedeli</i> - - - -													
⊥ <i>Hd. driereri</i> - - - -									NTp12				
⊥ <i>Hd. mohleri</i> [<i>D. gemmeus</i>] - - - -	<i>Heliolithus kleinpelli</i> Zone	<i>D. gemmeus</i> Zone	<i>D. gemmeus</i> Zone	<i>D. gemmeus</i> Zone	<i>Discoaster mohleri</i> Zone	CP6	<i>H. kleinpelli</i> Zone	NP6	<i>Cruciplacolithus latipons</i> Subzone NTp10B				
⊥ <i>Ht. kleinpelli</i> - - - -													
				<i>Fasciculithus tympaniformis</i> Zone								CP4	<i>F. tympaniformis</i> Zone

⁵*Placozygus sigmoides* Zone
⁴*Discoaster lenticularis* Subzone
³*Heliolithus atkasii* Subzone
²*Heliolithus cantabrie* Zone
¹*Hornibrookina australis* Zone

TEXT-FIGURE 14

Zonal schemes based on the stratigraphic ranges of *Heliotrochus* species.

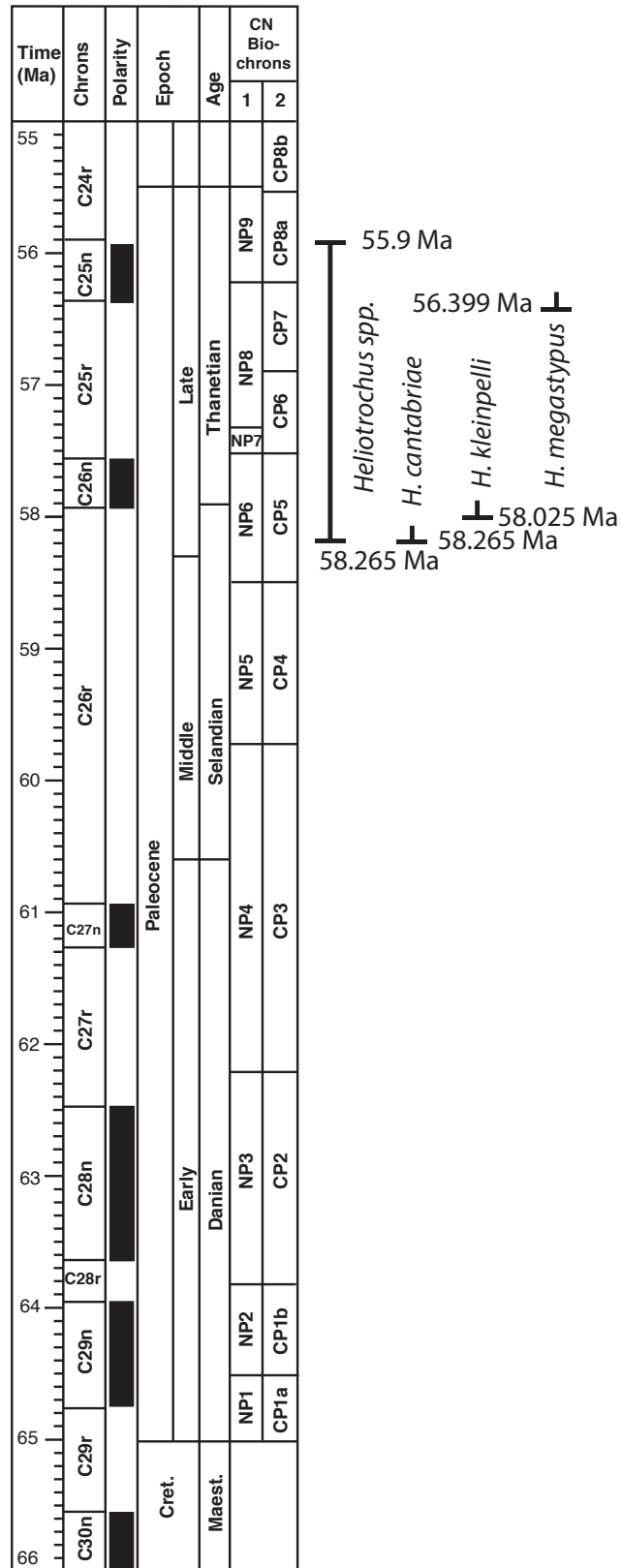


TEXT-FIGURE 15
GSSP for the base of the Thanetian Stage and Upper Paleocene Subseries at Zumaya and LO of *Heliotrochus kleinpelli* (marker of the base of Zone NP6). (Modified from Schmitz et al., 2011, fig. 13.)

At the same time as they formalized the *Heliolithus riedeli* Zone of Bramlette and Sullivan 1961, Mohler and Hay (op. cit., p. 455) introduced the “*Heliolithus kleinpelli* Zone”, which became Zone NP6 ((Martini, 1970, p. 560; 1971, p. 753) and Zone CP 5 (Okada and Bukry, 1980, p. 322). This is the interval between the LOs of *Heliolithus* [now *Heliotrochus*] *kleinpelli* and “*Discoaster gemmeus*” (now *Heliodiscoaster mohleri*).

Heliotrochus kleinpelli has a broad geographic range and is found in oceanic as well as epicontinental sediments. Its LO is thus a dependable, broadly correlatable horizon.

The low to mid latitude zonal scheme of Varol (1989) makes the most out of the ranges of *Heliotrochus* species, relying on the LO of *Heliotrochus kleinpelli* and also on its HO and that of *Heliotrochus cantabriae* (text-fig. 14). The complete stratigraphic ranges of *Heliotrochus* species are difficult to determine, however, because of their generally low abundances and sporadic occurrences. For indeterminate reasons, species of *Heliotrochus* seem to occur inconsistently throughout their ranges (e.g., *H. kleinpelli*: Wei and Wise, 1989, fig. 3; *H. kleinpelli*, *H. riedeli*: Monechi and Thierstein, 1985, fig. 4). Varol’s placement of the HO/LAD of *H.*



TEXT-FIGURE 16
Biochronology of *Heliotrochus* species. Magnetobiochronologic framework from Berggren et al. (1995) updated (Wade et al., 2011, and herein).

cantabriae in Zone NP9 is well supported (Romein, 1979; Perch-Nielsen, 1985). However, this species, with a range of Zone NP5-NP9, was reported only from Zone NP6 at Site 1262 (Agnini et al., 2007; text-fig. 13). The date of 57.656 Ma determined for the HO of the species at this latter site (op. cit., table 1) thus does not correspond to the LAD of the species but to a local disappearance of indeterminate significance.

Wei and Wise (1989) presented magnetobiostratigraphic evidence for marked diachrony of *H. kleinpelli*. However, interpretation of diachrony requires objective analysis of stratigraphic sections to decipher the presence of unconformities, leading Berggren et al. (1995) to question the report of diachrony by these authors. In any case it will be difficult to test *Heliolithus* and *Heliotrochus* species for diachrony considering their inconsistent stratigraphic occurrences.

CHRONOSTRATIGRAPHY

The GSSP for the base of the Thanetian Stage is placed at a lithologic horizon in the cliffs along the Itzurun Beach at Zumaia (Spain) which corresponds to the Chron C26n/C26r magnetic reversal and located slightly above (6.5 m) the LO of *H. kleinpelli* (Schmitz et al., 2011). Thus, in the absence of magnetostratigraphy, the LO of *H. kleinpelli* may help to approximate the base of the Thanetian Stage (text-fig. 15).

CHRONOLOGY

The life span of *Heliotrochus* extends from late Chron C26r to a level close to the Chron C25n/C24r magnetic reversal (text-fig. 16).

The FAD of the oldest species, *H. cantabriae* and *H. kleinpelli*, have been tied to late Chron C26r (e.g., Berggren et al., 2000; Agnini et al., 2007; Schmitz et al., 2011).

Based on quantitative analysis of coccolithophores in the Paleocene at ODP Site 1262 and in reference to the magnetostratigraphy of Cande and Kent (1992, 1995), datums are located as follows (Agnini et al., 2007, table 1):

– FAD *H. megastypus*: 56.399 Ma

– FAD *H. kleinpelli*: 58.025 Ma

– FAD *H. cantabriae*: 58.265 Ma

TAXONOMY

As explained above the genus *Heliotrochus* is introduced for helioliths that differ from *Heliolithus riedelii* by their structure.

Generic taxonomy

Genus: *Heliotrochus* new genus

Type Species: *Heliotrochus kleinpelli* (Sullivan) n. comb. (= *Heliolithus kleinpelli* Sullivan, 1964, p. 193, pl. 12, figs. 5a, b).

Heliotrochus helioliths are mushroom-shaped, and consist of three structural units such that the column and collaret are closely associated to form a *pillar* whereas the thin and broad calyptra expands well beyond the distal edge of the pillar. The calyptra is polycyclic, with an outer cycle of non-imbricate elements and inner cycles of dextrally imbricate elements. It is birefringent in some species, non-birefringent in others. The elements are trihedral and

arranged in such a manner that both the column and calyptra are strongly fluted.

The shape of species varies with the relative width and thickness of the pillar and calyptra. The original trihedral shape of the elements is rarely preserved, with post-mortem overgrowth having transformed these delicate coccoliths into massive fossils.

The helioliths of *Heliotrochus* differs from those of *Bomolithus* in having a column associated with the collaret to form the pillar. In *Bomolithus* the collaret is associated with the calyptra to form a cone.

The helioliths of *Heliolithus* are diabolo-shaped, and consists essentially of the column and calyptra, the collaret being vestigial.

Species taxonomy

Species of the genus *Heliotrochus* differ by their general lateral outline and the relative development of the three structural units (text-fig. 17).

Unlike the other species that are entirely birefringent, *Heliolithus megastypus* and *H. conicus* are partly birefringent, in that only the pillar but not the calyptra produces an extinction cross. This has been seen by some authors (e.g., Steurbaut, 1998; Bown and Dunkley Jones, 2006; Bown, 2010) as a sufficient reason to re-assign them to *Bomolithus* despite the fact that they do not possess a *Bomolithus*-like cone.

Heliolithus rotundus was tentatively (but informally) transferred to *Bomolithus* by Steurbaut (1998), based on a re-interpretation of the coccolith in which the collaret and calyptra form a cone (op. cit, fig. 8, bottom left). This has been followed here.

The difficulty in determining the presence/absence of the median structural unit leads to ambiguous interpretations of some species, most acutely for *H. megastypus*. Romein (1979, p. 157) interpreted it as consisting of a “high column, a wide median cycle and a very reduced distal cycle” (see also Steurbaut, 1998, fig. 8). In contrast, *H. megastypus* is interpreted here as consisting of a high column, a very reduced collaret and a wide calyptra. Romein’s “very reduced distal cycle” is in fact the inner cycle of the calyptra in this species. The small elements seen at the contact between column and calyptra in some specimens of this species (e.g., Perch-Nielsen, 1971c, pl. 1, fig. 6) can be regarded as remnants of the collaret.

Revised species taxonomy

Heliotrochus cantabriae (Perch-Nielsen) n. comb.

Basionym: *Heliolithus cantabriae* Perch-Nielsen, 1971, p. 55, pl. 2, figs. 3, 5, pl. 7, figs. 33-36.

Heliotrochus conicus (Perch-Nielsen) n. comb.

Basionym: *Heliolithus*(?) *conicus* Perch-Nielsen, 1971, p. 56, pl. 1, figs. 1-3, pl. 7, figs. 37, 38.

Heliotrochus kleinpelli (Sullivan) n. comb.

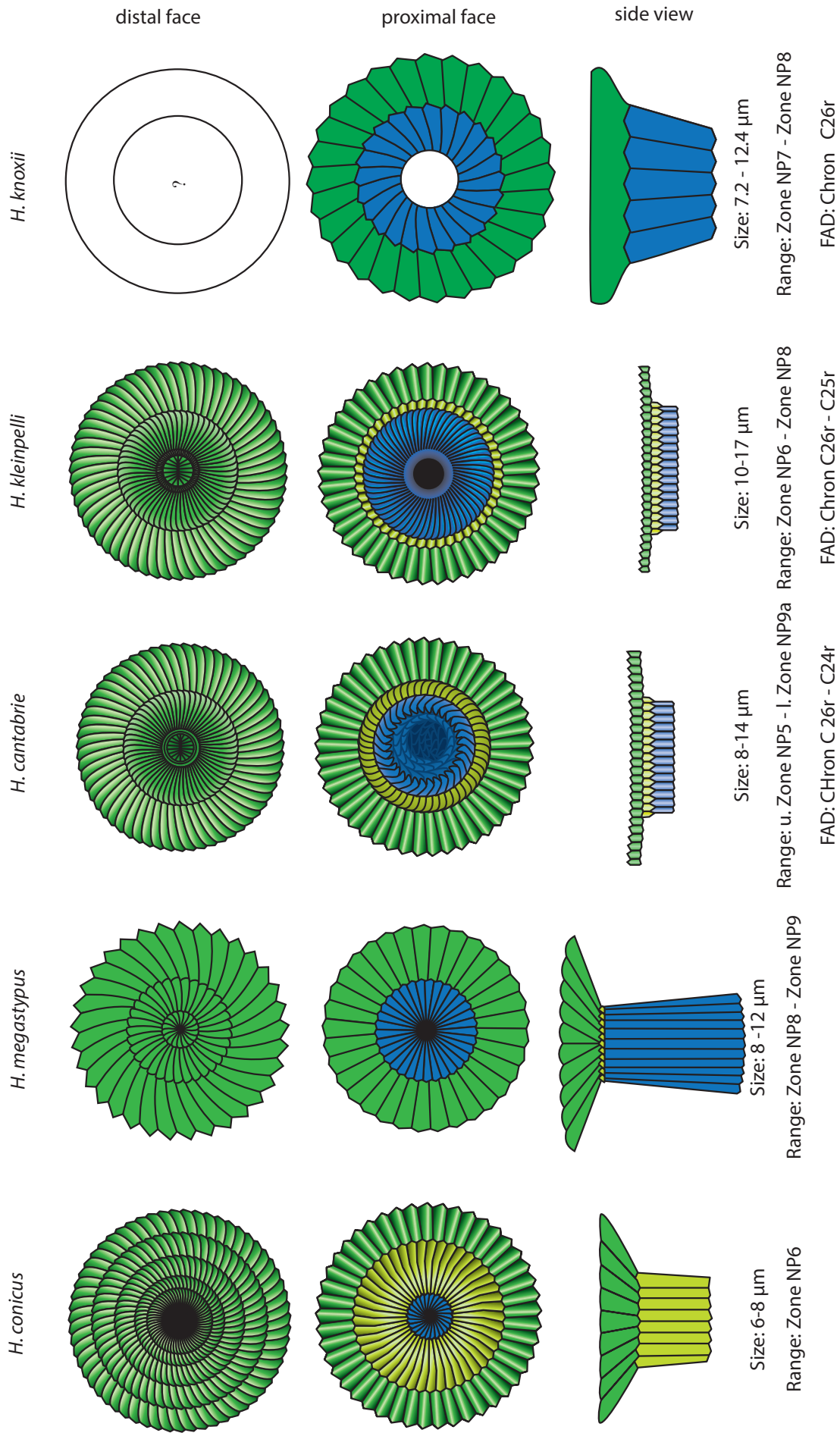
Basionym: *Heliolithus kleinpelli* Sullivan, 1964, p. 193, pl. 12, figs. 5a, b; not *Heliolithus* aff. *H. riedelii* Bramlette & Sullivan 1961, pl. 14, fig. 12.

Heliotrochus knoxii (Steurbaut) n. comb.

Basionym: *Heliolithus knoxii* Steurbaut 1998, p. 132-134, pl. 4, figs. 23a, b.

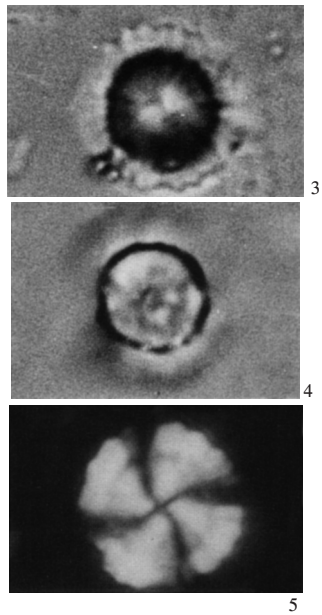
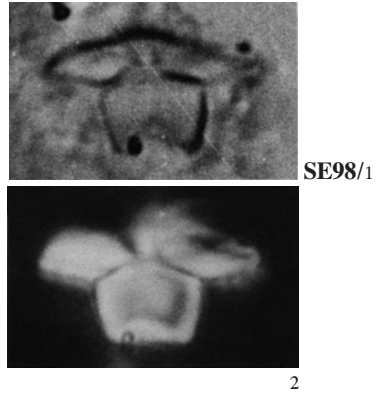
Heliotrochus megastypus (Bramlette & Sullivan) n. comb

Basionym: *Discoasteroides megastypus* Bramlette & Sullivan, 1961, p. 163, pl. 13, figs. 14a-d, 15a-c.

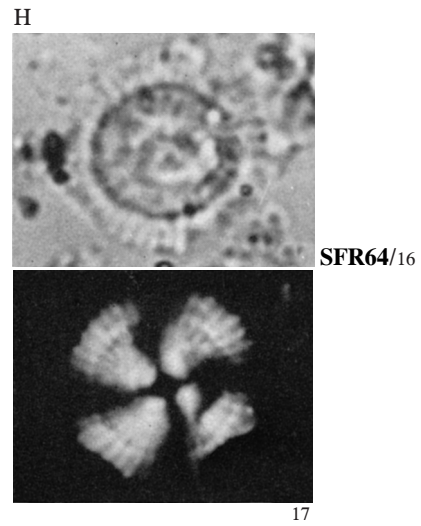


TEXT-FIGURE 16
Comparison between *Heliotrochus* species.

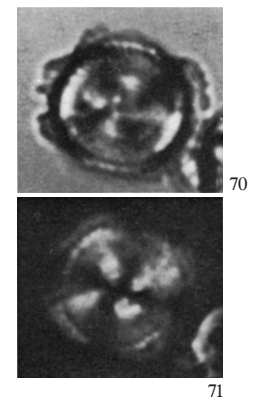
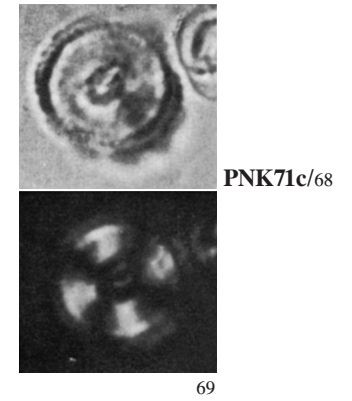
Heliotrochus knoxii (Steurbaut) n. comb. [= *Heliolithus knoxii* Steurbaut 1998, p. 132-134, pl. 4, figs. 23a, b]



Heliotrochus kleinpelli (Sullivan) n. comb. [= *Heliolithus kleinpelli* Sullivan 1964, p. 193, pl. 12, figs. 5a, b; not *Heliolithus* aff. *H. riedeli* Bramlette & Sullivan 1961, pl. 14, fig. 12]



Heliotrochus cantabriae (Perch-Nielsen) n. comb. [= *Heliolithus cantabriae* Perch-Nielsen 1971, p. 55, pl. 2, figs. 3, 5, pl. 7, figs. 33-36]



Heliotrochus knoxii

- max Ø: 7.2–12.4 µm (mean = 9.3 µm); Ø column: 3.6–6.4 µm (mean = 5 µm); H: ~4 µm

- L. Paleocene (NP7-NP8). NW Europe.

- Small, almost circular, hat-shaped nannolith, consisting of 2 cycles of elements which differ considerably in diameter and height. Large distal cycle with 28 to 35 elements (commonly ~32), with an almost flat distal surface and a small distal central opening. Smaller cycle (column) thick, trapezoidal, about half the Ø of the other cycle, with a strongly concave proximal surface. Both cycles are birefringent in CN, with slightly curved extinction lines.

≠ from *H. aktasii* by the construction of the distal cycle which is very thin and flat in *H. knoxii*;

≠ from *H. kleinpellii* which is larger, has 3 cycles, and a proximal cycle ~70% the Ø of the distal cycle;

≠ from *H. bukryi* that it resembles in side view, in the latter having a much lower and considerably smaller column (~one third the Ø of the larger cycle).

- SE98 (p. 132-134), AMP (p. 193).

Heliotrochus kleinPELLII

- 10–17 µm

- L. Paleocene. Lodo Fm., California.

-** Specimens consisting of three closely appressed cycles. Column and median cycles about two thirds the diameter of the distal cycle, both showing about 45 radiating petal-like elements. Small central depression.

≠ from *H. riedelii* in being larger, more appressed, and in having a greater number of radiating elements.

— LO defines base of NP6 (Martini, 1971, p. 753). It ranges through NP8.

- SFR64 (p. 193), AMP (p. 193).

Heliotrochus cantabriae

- 8–14 µm x 7–11 µm

- L. Paleocene (NP6). Bay of Biscay, DSDP Site 119, Atlantic.

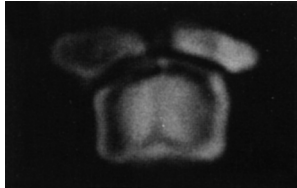
- [High column consisting of tangential to concentrically arranged plates, slightly depressed proximally, with a narrow central opening. Median cycle of about the same diameter but lower than the column. Slightly larger distal cycle which is flat or distally concave.]

≠ from *H. kleinPELLII* in its higher column, narrower central canal and the relatively smaller diameter of the distal cycle.

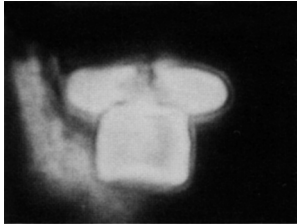
— Ranges from upper NP5 through lower NP9 (Romein, 1979, p. 79).

- PNK71b (p. 55), AMP (p. 193).

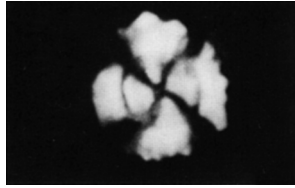
Heliotrochus knoxii (continued)



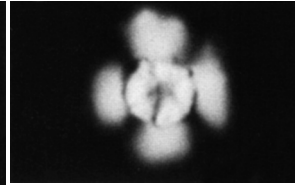
SE98/6



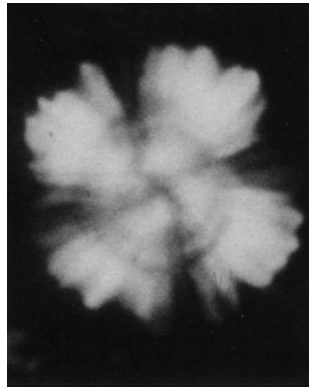
7



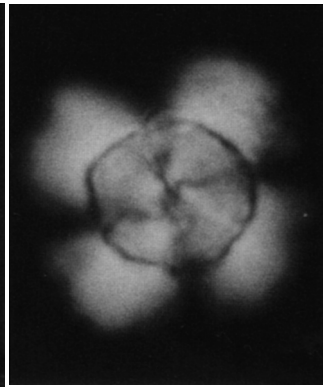
8



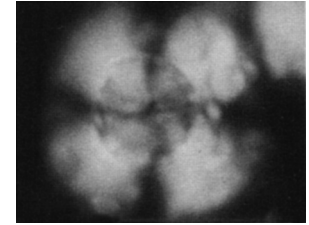
9



10



11



12

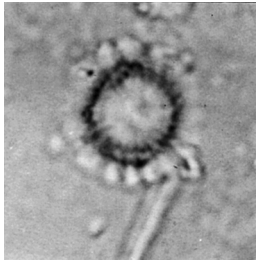


SE02/13

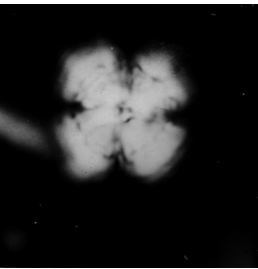


14

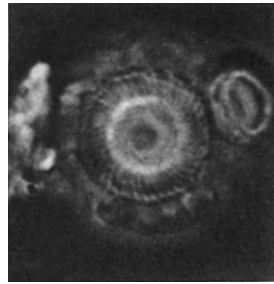
Heliotrochus kleinpelli (continued)



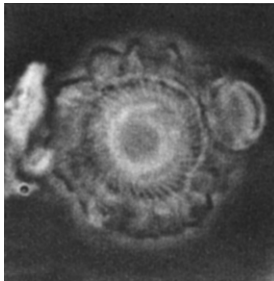
AMP86/18



19



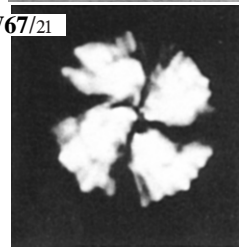
HWW67/21



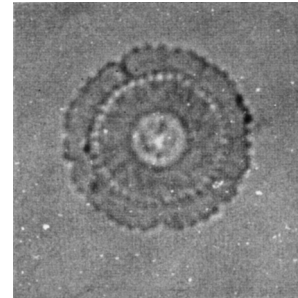
22



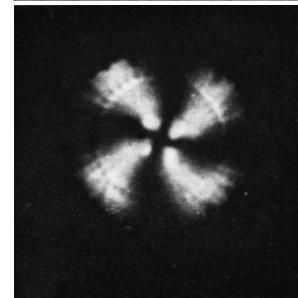
23



24



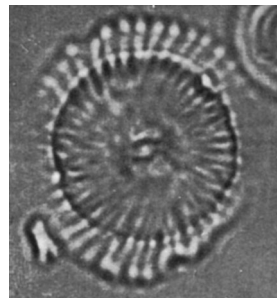
ME71/25



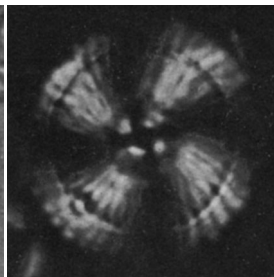
26



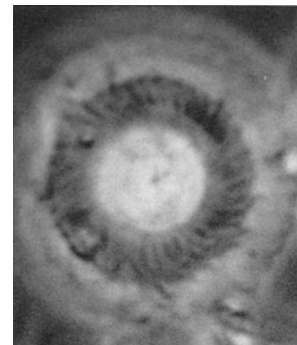
BMN61/20



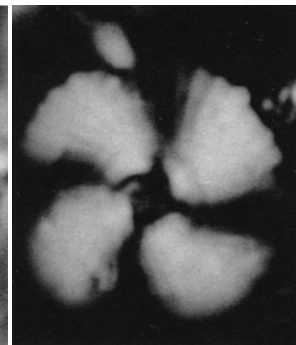
PNK71c/27



28

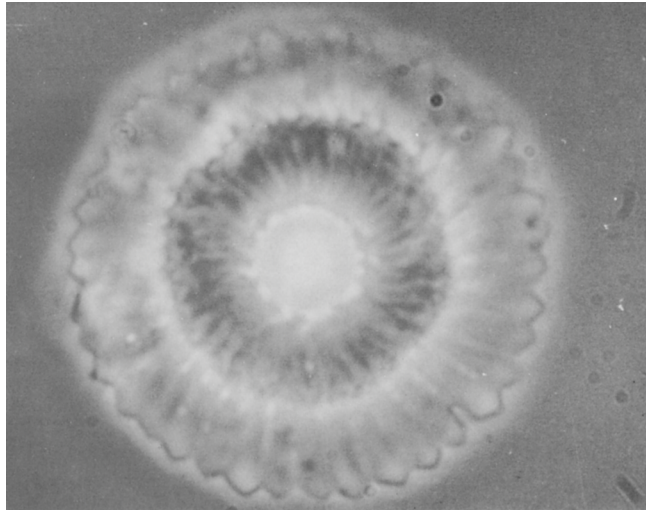


PJJ90/29

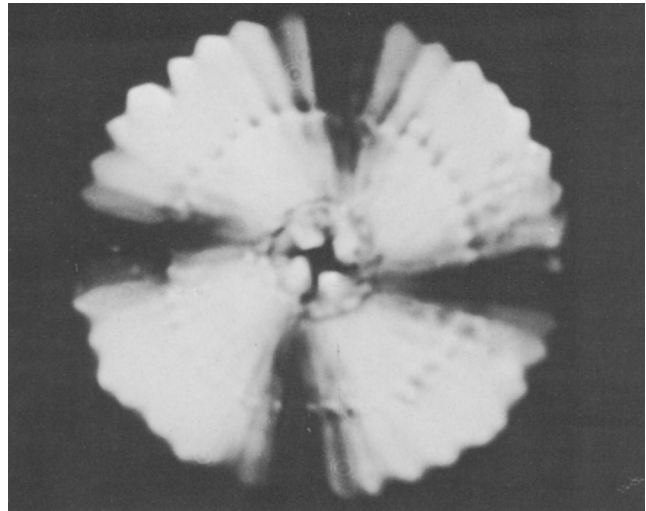


30

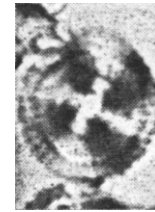
Heliotrochus kleinpelli (continued)



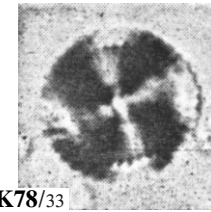
OT79/31



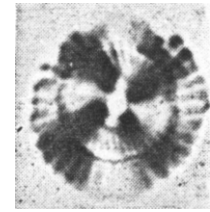
32



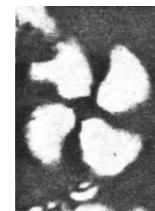
PNK78/33



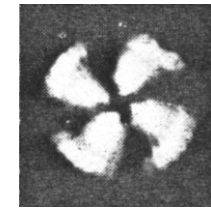
35



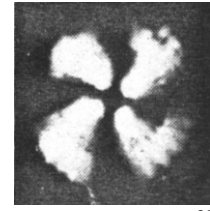
37



34



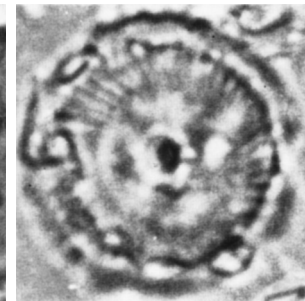
36



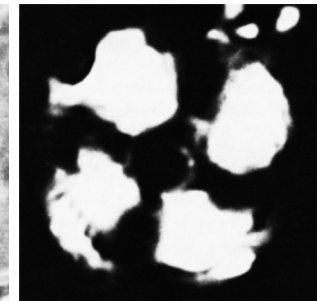
38



PB71/39

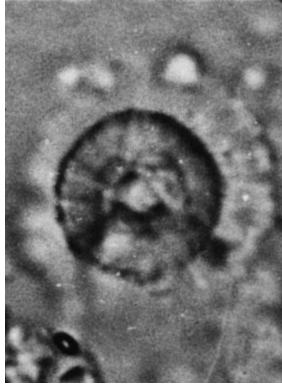


40

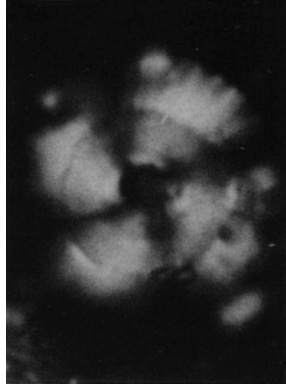


41

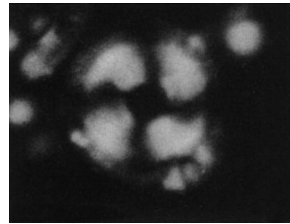
Heliotrochus kleinpelli (continued)



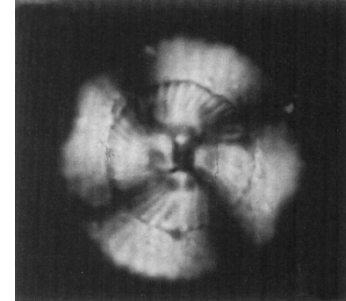
SE98/42



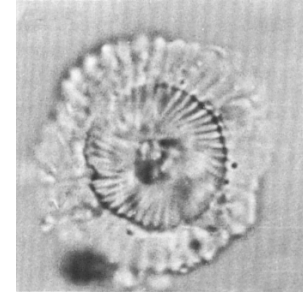
43



44



SE02/45

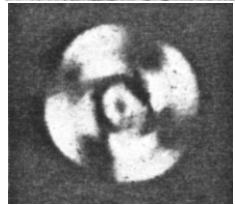


46

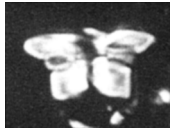
Heliotrochus cantabriae (continued)



PNK78/72



73

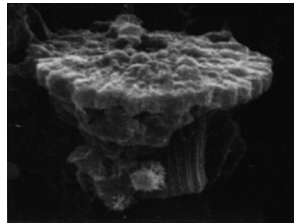


RAJT79/74

Heliotrochus knoxii (continued)

SIDE VIEW

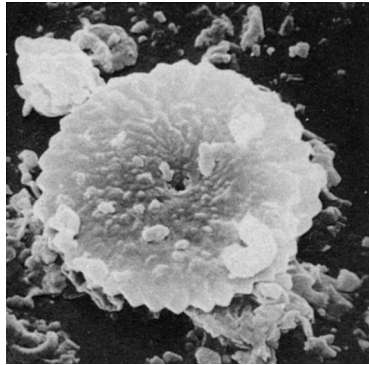
H



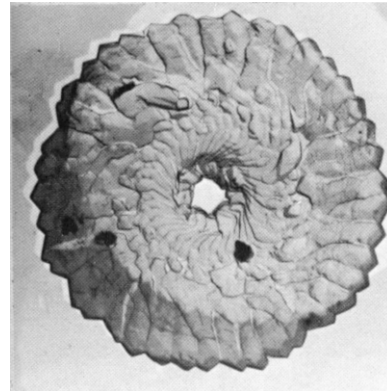
SE98/15

Heliotrochus kleinpelli (continued)

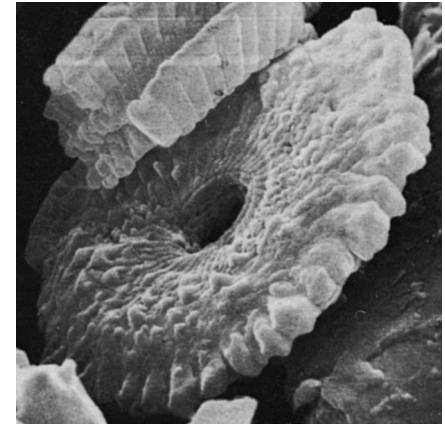
DISTAL FACE



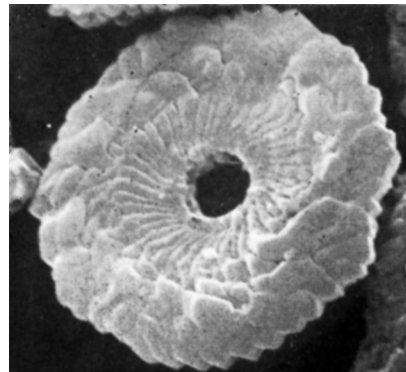
MC74/47



OT79/48



PNK71c/49



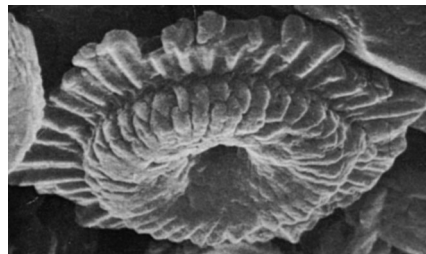
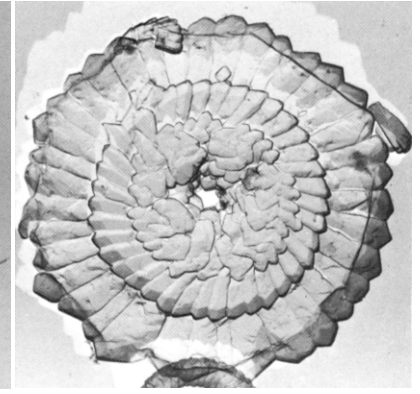
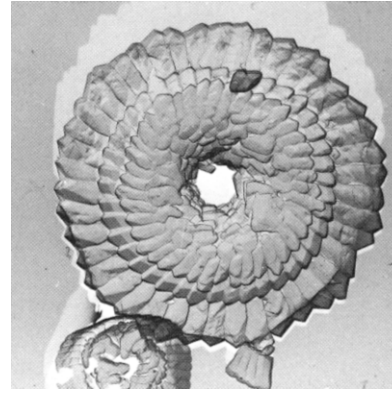
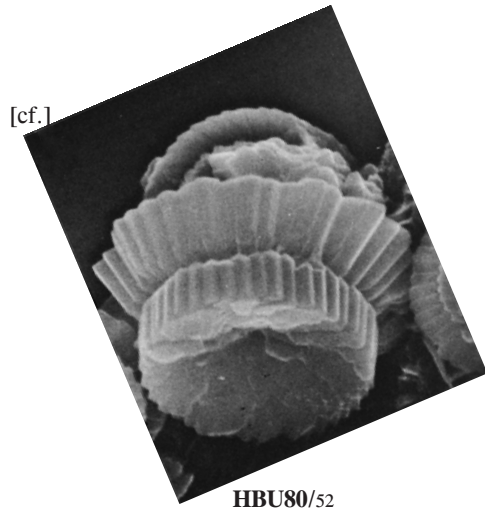
PNK78/50



51

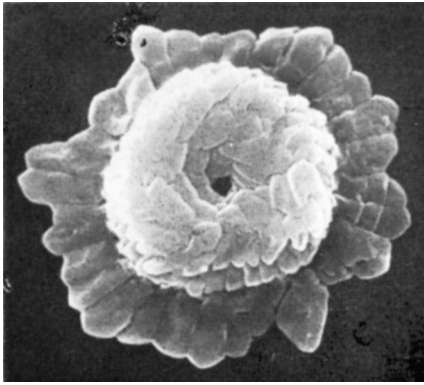
Heliotrochus kleinpelli (continued)

PROXIMAL FACE

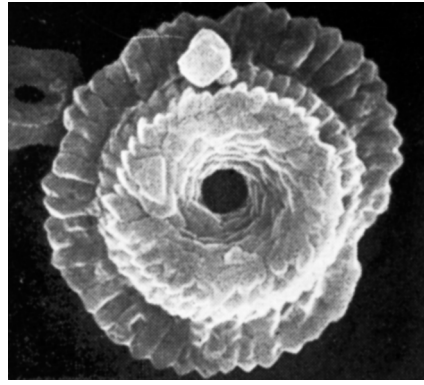


Heliotrochus kleinpelli (continued)

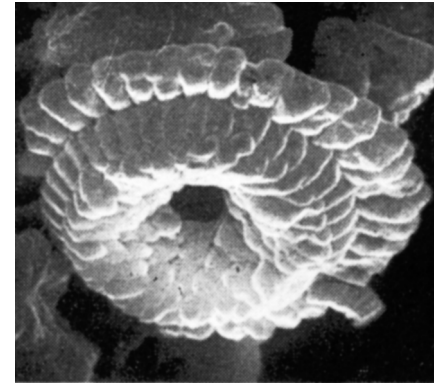
PROXIMAL FACE



PNK78/59



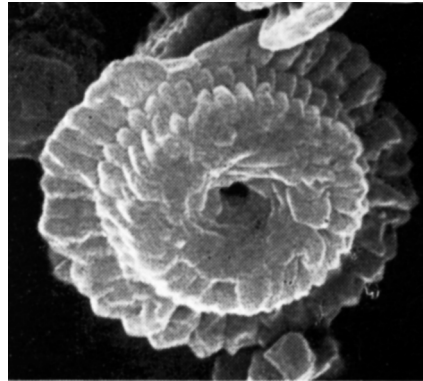
60



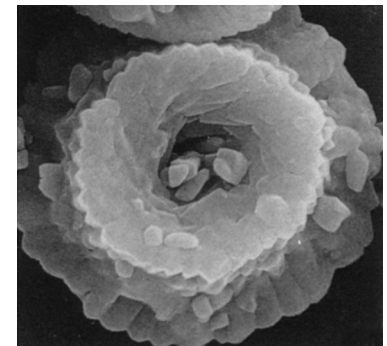
61



62



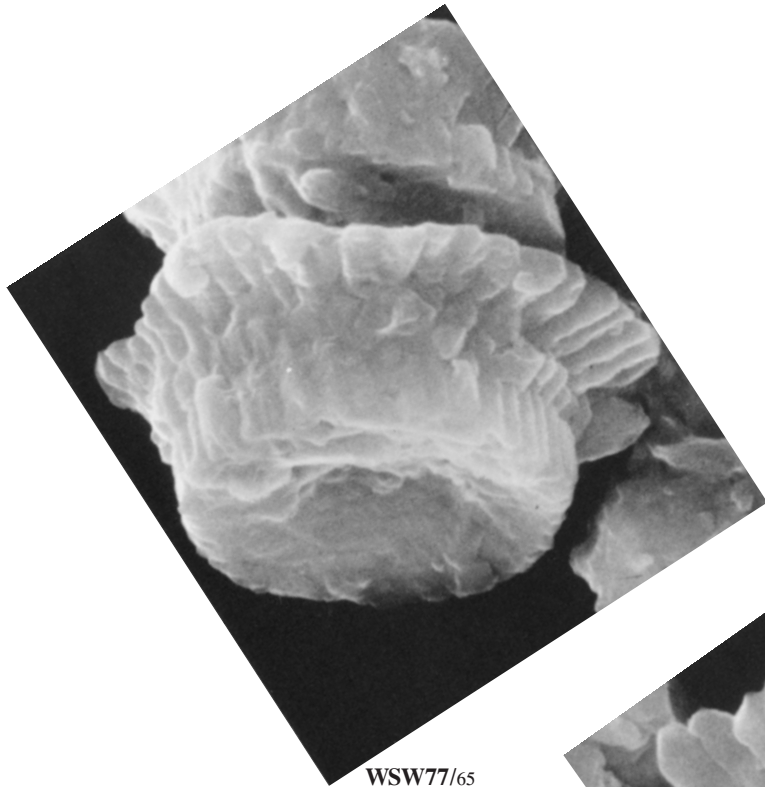
63



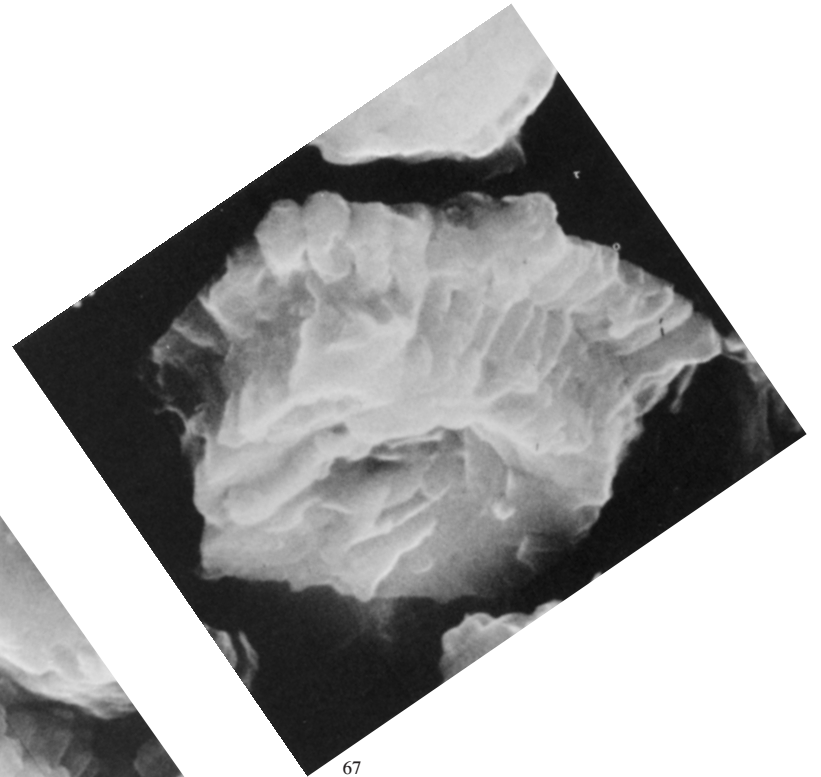
PJJ90/64

Heliotrochus kleinpelli (continued)

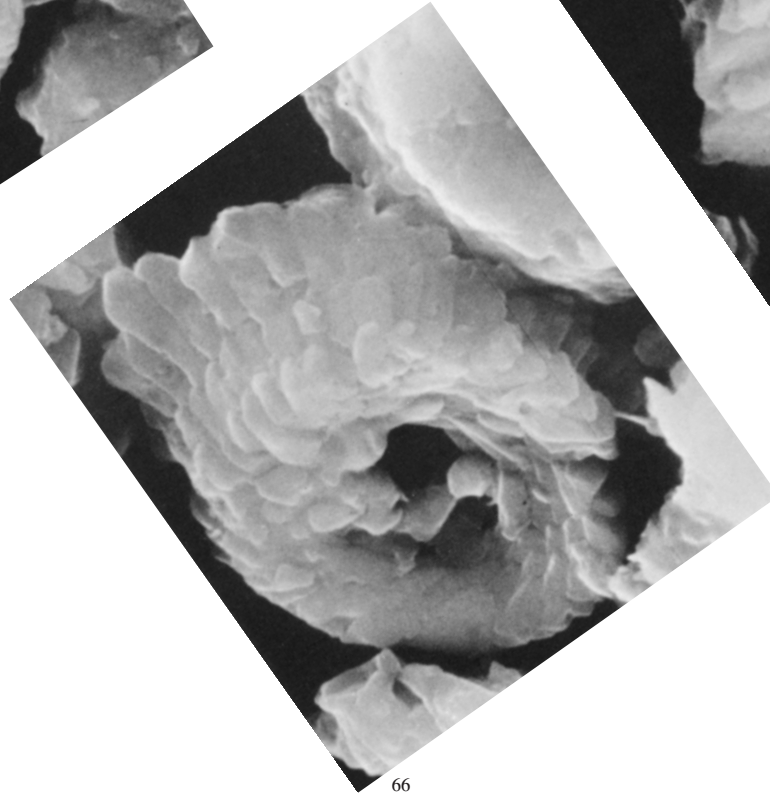
PROXIMAL FACE



WSW77/65



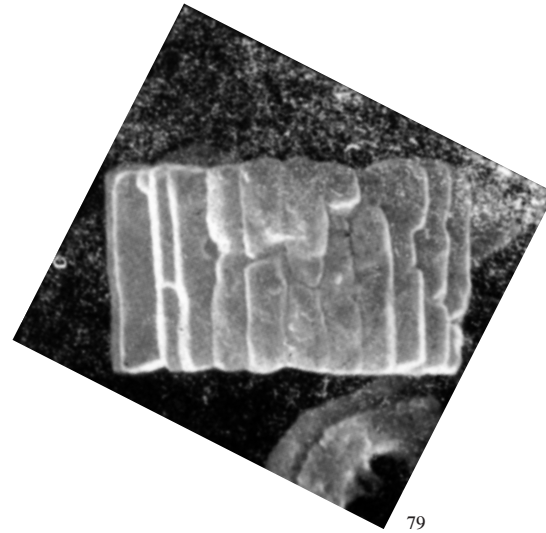
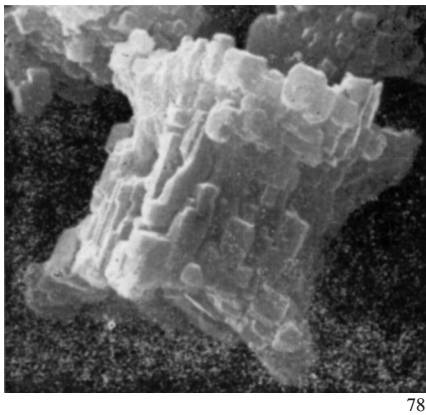
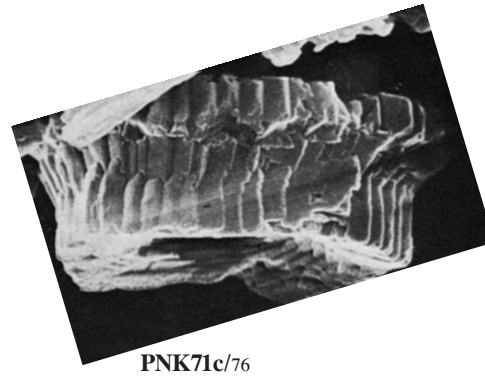
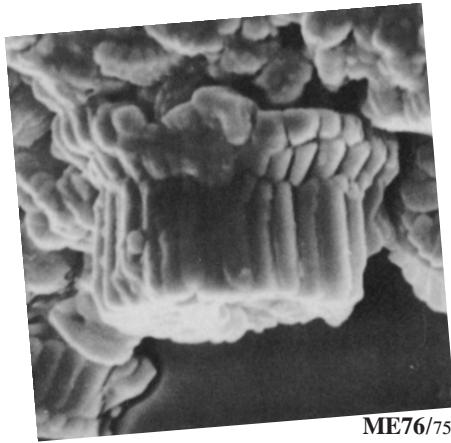
67



66

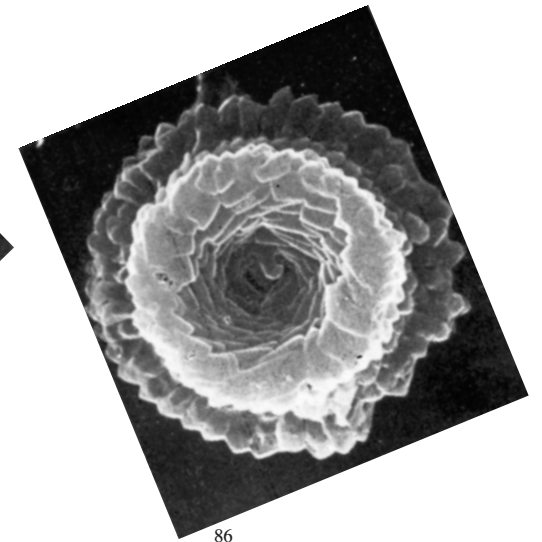
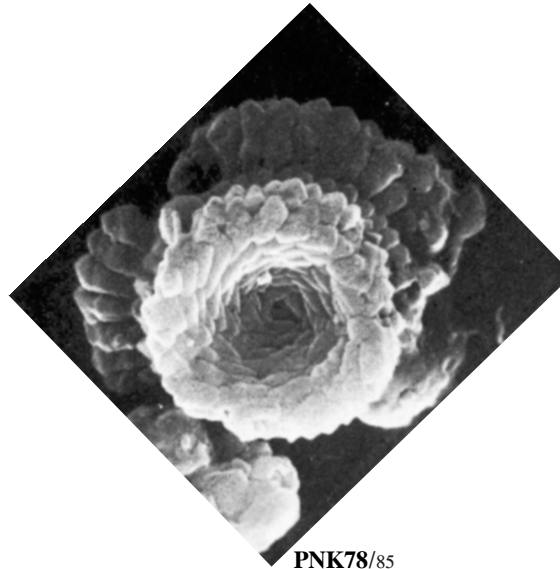
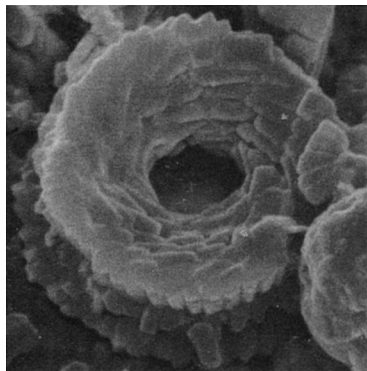
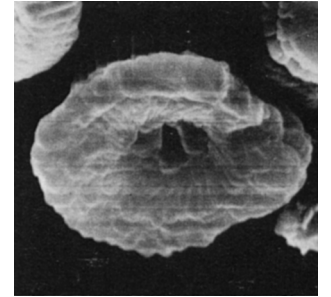
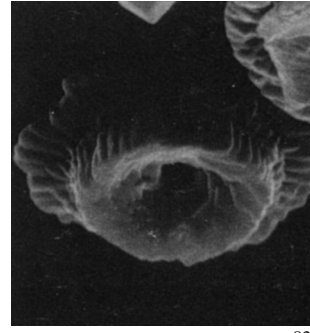
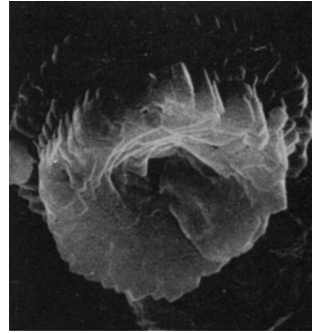
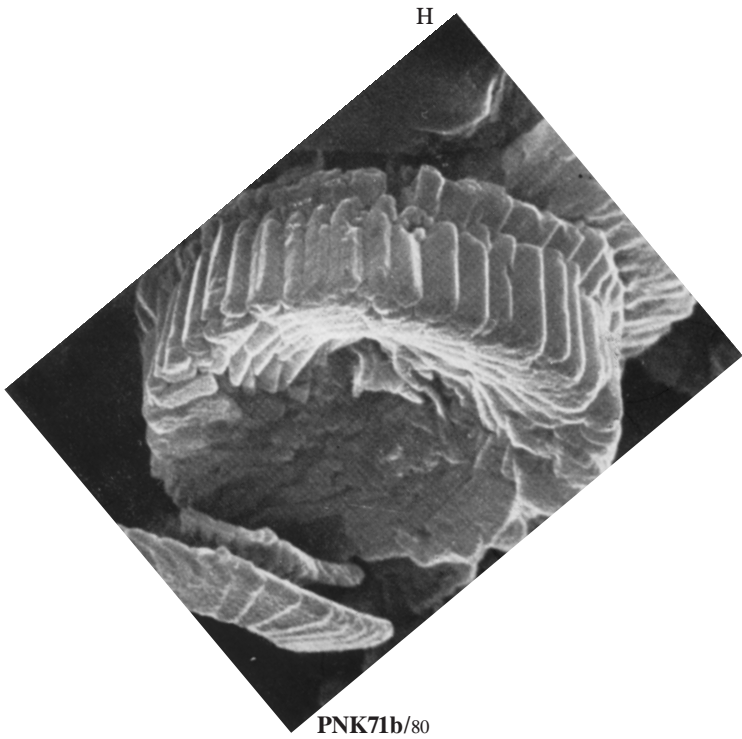
Heliotrochus cantabriae (continued)

SIDE VIEW



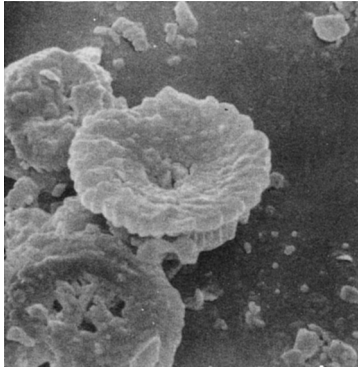
Heliotrochus cantabriae (continued)

PROXIMAL FACE

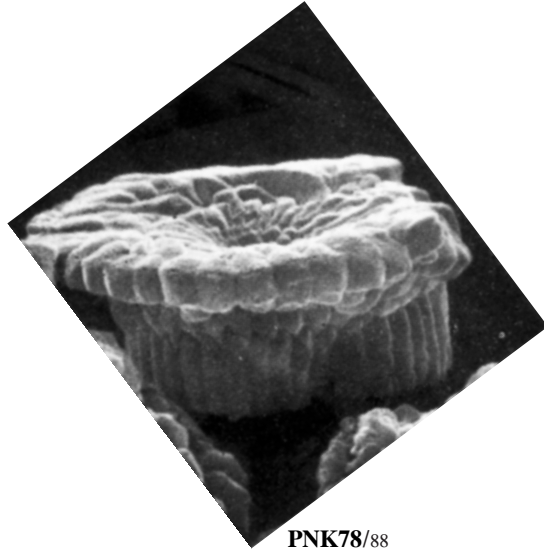


Heliotrochus cantabriae (continued)

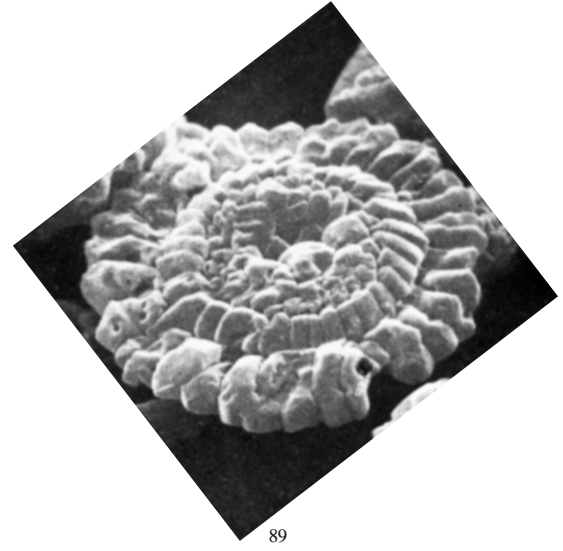
DISTAL FACE



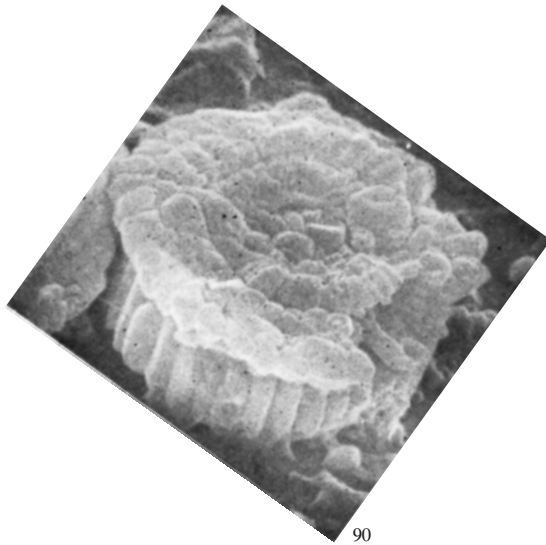
MC74/87



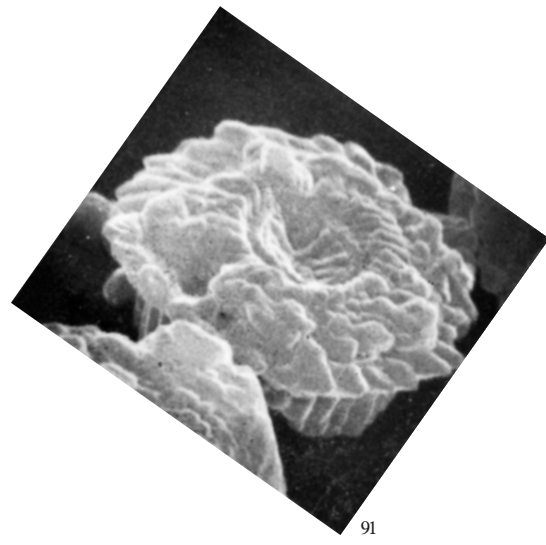
PNK78/88



89



90



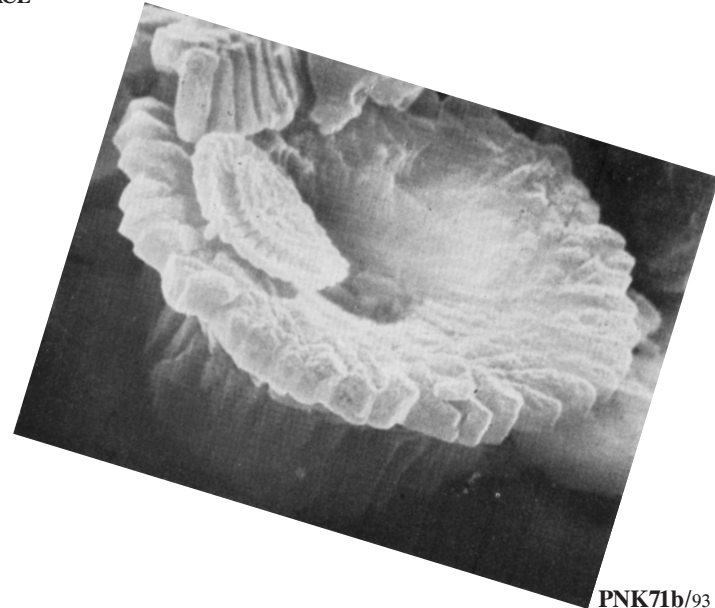
91

Heliotrochus cantabriae (continued)

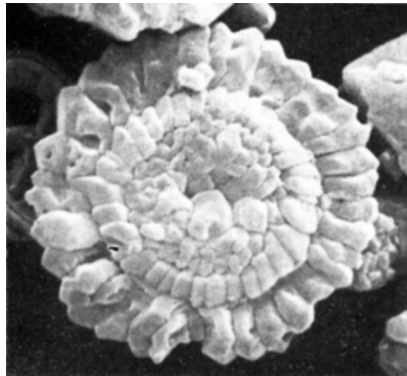
DISTAL FACE



PNK71c/92



PNK71b/93



PNK78/94



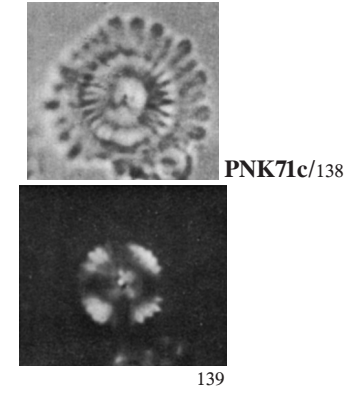
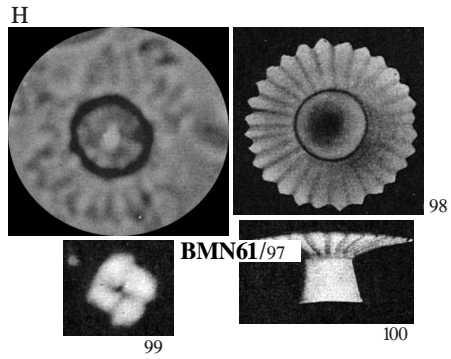
95



96

Heliotrochus megastypus (Bramlette & Sullivan) n. comb [= *Discoasteroides megastypus* Bramlette & Sullivan 1961, p. 163, pl. 13, figs. 14a-d, 15a-c]

Heliotrochus conicus (Perch-Nielsen) n. comb. [= *Heliolithus*(?) *conicus* Perch-Nielsen 1971, p. 56, pl. 1, figs. 1-3, pl. 7, figs. 37, 38]



Heliotrochus megastypus

- 8–12 μm

- Paleocene. Lodo Fm., California.

-** Mushroom-shaped. Proximal cycle having about 30 delicate rays, joined throughout their length, with rounded to bluntly pointed tips. Large flaring median cycle with a terminal \emptyset about one half that of the proximal cycle, with end depressed or concave and depression continuing as a small hole down most of the stem. Very reduced distal cycle.

- Remarks: In contrast to the heavy stem, the delicate rays of this form are very difficult to see in plan view in Canada balsam. Between CN, the plan and side views of the large stem show the radiate structure of heliolithids, whereas the petals, which are like the ortholithid discoasters, show no distinct birefringence in plan view. The plan view of *Heliolithus riedelii* appears much like this sp., similarly oriented, in TL, but between CN the radiate petals of *Heliolithus riedelii* are quite different in their distinct birefringence and extinction cross.

— As remarked by Romein (1979, p. 157), “all previous authors have assigned this species to the genus *Discoasteroides* because of the presence of a ‘heliolithic’ stem. In the type species of this genus (*Discoasteroides kuepperi*), however, this stem is formed by a proximal elongation of the rays and is not a separate structure as in *Heliotrochus megastypus*.”

— Transitional forms between *Heliotrochus megastypus* and *D. multiradiatus* occur frequently in the lower part of NP9 and in NP8 (Romein, 1979).

— Ranges in NP8 and lower NP9 (Romein, 1979).

- BMN61 (p. 163), RAJT79 (p. 157), AMP (p. 193).

Heliotrochus conicus

- ~6–8 μm

- L. Paleocene (NP6). Bay of Biscay (DSDP Site 119), Atlantic.

- [Serrate, low cone-shaped distal cycle. High conical median cycle. Very low funnel-shaped column.]

≠ from *Heliolithus riedelii* by its conical structure;

≠ from *Heliolithus megastypus* by the proportion of the different units.

- *Heliotrochus conicus* is characterized by its very reduced column, flaring distal cycle and unusually well-developed median cycle.

- PNK71b (p. 56), AMP (p. 193).

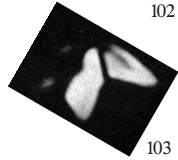
Heliotrochus megastypus (continued)



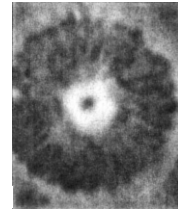
BMN61/101



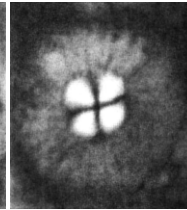
102



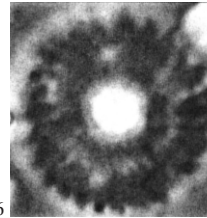
103



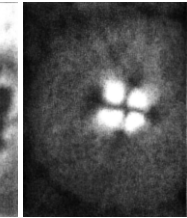
BPR10/104



105



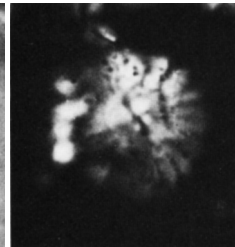
106



107



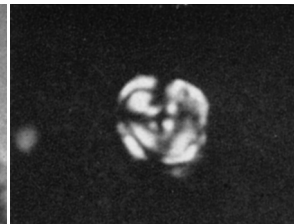
PDF75/108



109

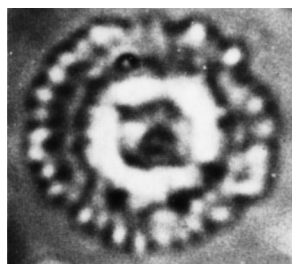


SFR64/110

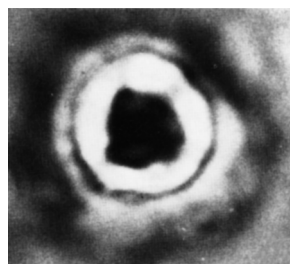


111

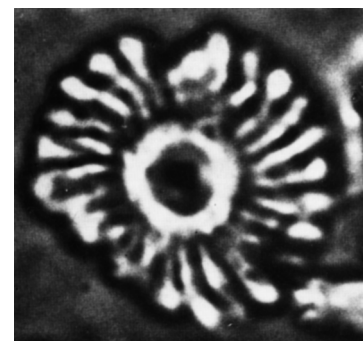
Heliotrochus megastypus (continued)



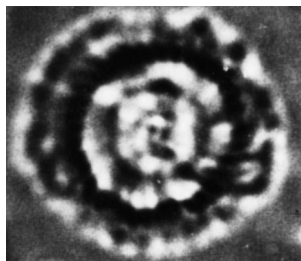
PB71/112



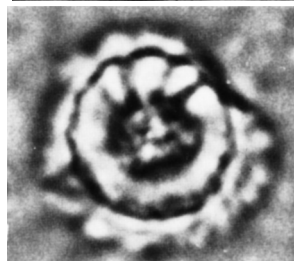
115



119



113



116



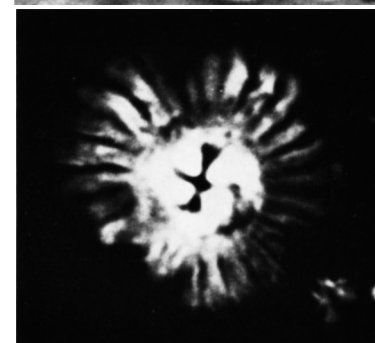
120



114



117



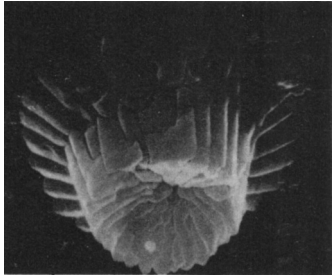
121



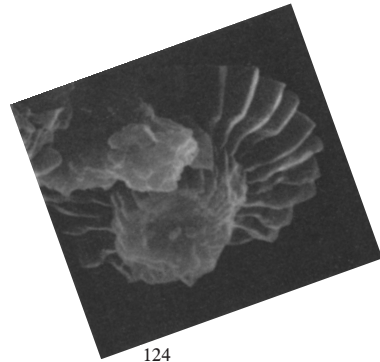
118

Heliotrochus megastypus (continued)

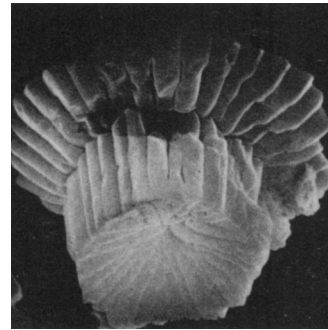
PROXIMAL FACE



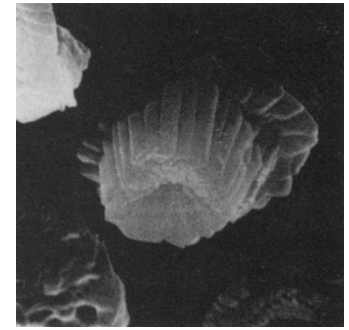
PNK77/122



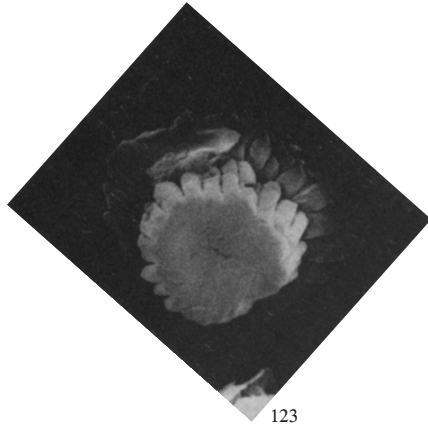
124



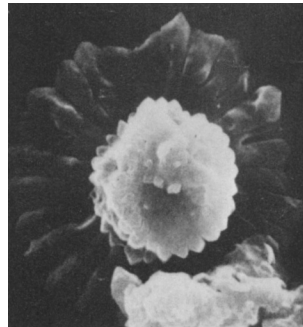
125



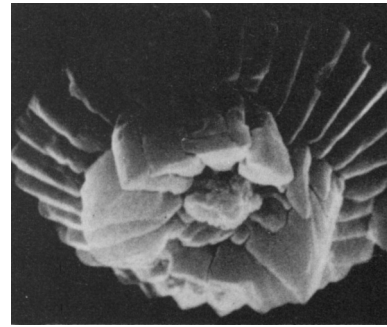
126



123



127



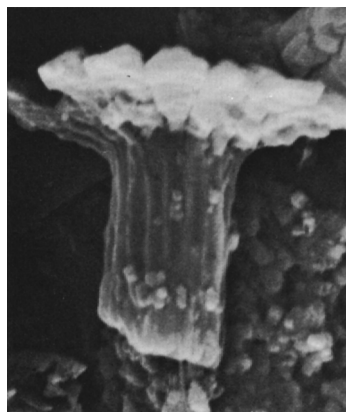
128



129

Heliotrochus megastypus (continued)

SIDE VIEW

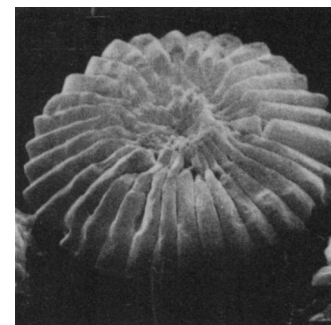


HBU80/130

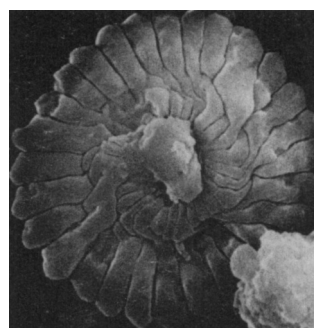
DISTAL FACE



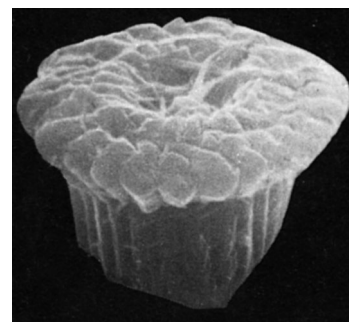
PNK77/133



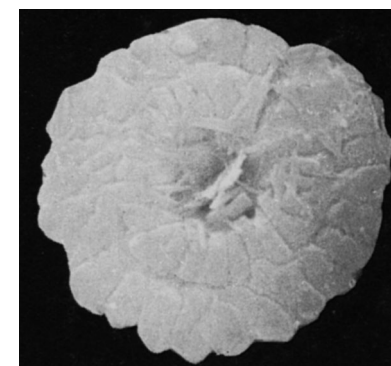
134



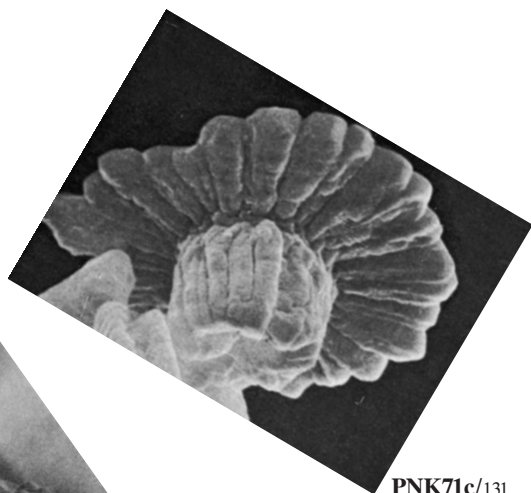
135



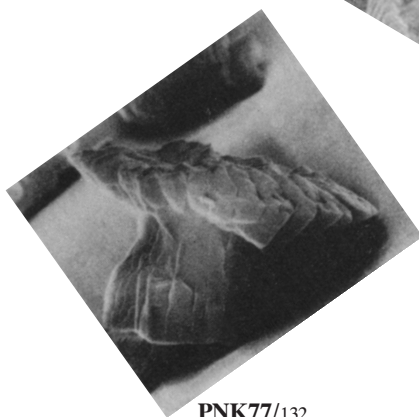
RAJT79/136



137



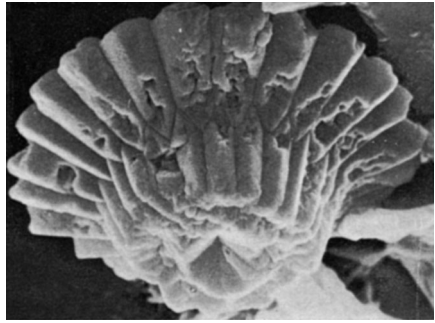
PNK71c/131



PNK77/132

Heliotrochus conicus (continued)

SIDE VIEW

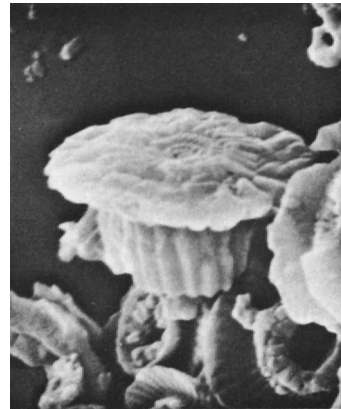


PNK71c/140



HBU80/141

DISTAL FACE



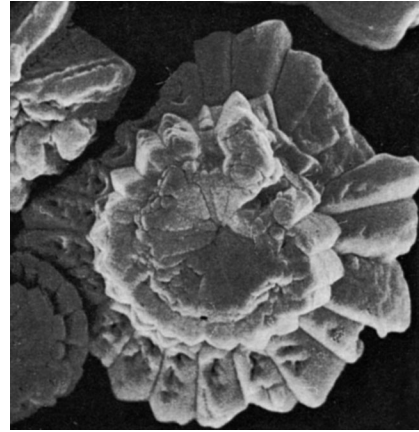
HBU80/142

Heliotrochus conicus (continued)

PROXIMAL FACE



BPR10/143



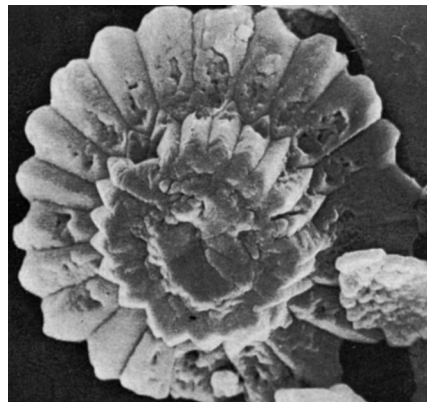
PNK71c/146



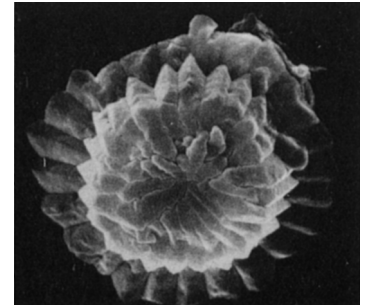
144



145



147



PNK77/148

Figure Reference

- AMP86.** AUBRY, M.-P., 1986. *Palaeogeography, Palaeoclimatology, Palaeoecology*, 55: 267–334.
(18, 19): 1/21, 22 (*Heliolithus kleinPELLI*; also Aubry 1983, pl. 1, figs. 21, 22)
- AMP.** AUBRY, M.-P., this volume.
- BPR10.** BOWN, P. R., 2010. *Journal of Nannoplankton Research*, 31: 11–38.
(104-107): 10/6, 7 (two images, each; as *B. megastypus*)
- BMN61.** BRAMLETTE, M. N. and SULLIVAN, F. R., 1961. *Micropaleontology*, 7: 129–188.
(20): 14/12 (as *Heliolithus* aff. *riedelii*)
(97-100): 13/14a, d, c, b (as *Discoasteroides megastypus*)
(101-103): 13/15a-c (as *Discoasteroides megastypus*)
- HBU80.** HAQ, B. U. and AUBRY, M.-P., 1980. In: Salem, M. J. and Busrewil, M. T. (Eds.), *The geology of Libya, Volume 1*, 271–304. London: Academic Press.
(52): 6/3 (*Heliolithus kleinPELLI*; [cf.])
(130): 7/3 (as *Discoasteroides ? megastypus*)
(141, 142): 6/2, 7 (*Heliolithus conicus*)
(143-145): 6/5, 1, 4 (*Heliolithus conicus*)
- HWW67.** HAY, W. W. and MOHLER, Heliolithus P., 1967. *Journal of Paleontology*, 41: 1505–1541.
(21-24): 199/4-7 (*Heliolithus kleinPELLI*)
- ME71.** MARTINI, E., 1971. In: Farinacci, A. (Ed.), *Proceedings of the II Planktonic Conference, Roma, 1970, Volume 2*, 739–785. Rome: Ediz. Tecnoscienza.
(25, 26): 1/13, 14 (*Heliolithus kleinPELLI*)
- ME76.** MARTINI, E., 1976. In: Schlander, S. C., Jackson, E. D., et al., *Initial Reports of the Deep Sea Drilling Project*, 33, 383–423. Washington, D. C.: U.S. Government Printing Office.
(75): 2/6 (as *Heliolithus* cf. *cantabriae*)
- MC74.** MÜLLER, C., 1974. In: Simpson, E. S. W., Schlich, R., et al., *Initial Reports of the Deep Sea Drilling Project*, 25, 579–633. Washington, D. C.: U.S. Government Printing Office.
(47): 1/3 (*Heliolithus kleinPELLI*)
(53): 1/2 (*Heliolithus kleinPELLI*)
(81): 1/9 (*Heliolithus cantabriae*)
(87): 1/8 (*Heliolithus cantabriae*)
- OT79.** OKADA, Heliolithus and THIERSTEIN, Heliolithus R., 1979. In: Tucholke, B. E., Vogt, P. R., et al., *Initial Reports of the Deep Sea Drilling Project*, 43, 507–573.
Washington, D. C.: U.S. Government Printing Office.
(31, 32): 4/8a, b (*Heliolithus kleinPELLI*)
(48): 14/7 (*Heliolithus kleinPELLI*)
(54, 55): 14/5, 6 (*Heliolithus kleinPELLI*)
- PNK71c.** PERCH-NIELSEN, K., 1971c. *Meddelelser fra Dansk Geologisk Forening*, 21:51–66.
(27, 28): 7/26, 27 (*Heliolithus kleinPELLI*)
(56, 57): 2/2, 4 (*Heliolithus kleinPELLI*)
(49): 2/6 (*Heliolithus kleinPELLI*)
(68-71): 7/33-36 (*Heliolithus cantabriae*)
(76): 2/3 (*Heliolithus? cantabriae*)
(92): 2/5 (*Heliolithus cantabriae*)
(131): 1/6 (as *Discoasteroides megastypus*)
(138, 139): 7/37, 38 (as *Heliolithus? conicus*)
(140): 1/2 (as *Heliolithus? conicus*)
(146, 147): 1/1, 3 (as *Heliolithus? conicus*)
- PNK71b.** PERCH-NIELSEN, K., 1971b. In: Farinacci, A. (Ed.), *Proceedings of the II Planktonic Conference, Roma 1970, Volume 2*. 939–980. Rome: Ediz. Tecnoscienza.
(80): 2/11 (*Heliolithus cantabriae*; also Perch-Nielsen, 1971, pl. 2, figs. 1, 7: as *Heliolithus? cantabriae*)
(93): 2/10 (*Heliolithus cantabriae*; also Perch-Nielsen, 1971, pl. 2, figs. 1, 7: as *Heliolithus? cantabriae*)
- PNK77.** PERCH-NIELSEN, K., 1977. In: Supko, P. R., Perch-Nielsen, K., et al., *Initial Reports of the Deep Sea Drilling Project*, 39, 699–823. Washington, D. C.: U.S. Government Printing Office.
(82-84): 13/9, 13, 17 (*Heliolithus? cantabriae*)
(122-128): 10/7-9, 11-13, 16 (as *Discoasteroides megastypus*)
(129): 13/14 (as *Discoasteroides megastypus* (?))
(132-135): 10/6, 10, 15, 14 (as *Discoasteroides megastypus*)
(148): 13/5 (as *Heliolithus? conicus*)
- PNK78.** PERCH-NIELSEN, K., SADEK, A., BARAKAT, M. G. and TELEB, F., 1978. *Annales des Mines et de la Géologie*, 28: 337–403.
(33-38): 9/7, 8, 11, 12, 13, 14 (*Heliolithus kleinPELLI*)
(50, 51): 16/1, 5 (*Heliolithus kleinPELLI*)
(58): 15/4 (*Heliolithus kleinPELLI*)
(59-63): 17/1, 4-7 (*Heliolithus kleinPELLI*)

(72, 73): 9/9, 10 (*Heliolithus cantabriae*)
(77-79): 15/1, 12, 3 (*Heliolithus cantabriae*)
(85, 86): 17/2, 3 (*Heliolithus cantabriae*)
(88-91): 16/2, 6, 4, 12 (*Heliolithus cantabriae*)
(94, 95): 16/3, 9 (*Heliolithus cantabriae*)
(96): 15/6 (*Heliolithus cantabriae*)

(65-67): 11/4, 5, 3 (*Heliolithus kleinPELLI*)

PJJ90. POSPICHAL, J. J. and WISE, S. W., 1990. In: Barker, P. F., Kennett, J. P., et al., *Proceedings of the Ocean Drilling Program, Scientific Results, II3*, 613–638. College Station, Texas: Ocean Drilling Program.

(29, 30): 3/10c, b (*Heliolithus kleinPELLI*; a same as b, c)

(64): 3/10a (*Heliolithus kleinPELLI*)

PB71. PRINS, B., 1971. In: Farinacci, A. (Ed.), *Proceedings of the II Planktonic Conference, Roma, 1970, Volume 1*: 1017–1037. Rome: Ediz. Tecnoscienza.

(39-41): 8/2a-c (*Heliolithus kleinPELLI*)

(112-121): 8/3a-c, 5a-d; 6a-c (as *Discoasteroides megastypus*)

PDF75. PROTO DECIMA, F., ROTH, P. *Heliolithus* and TODESCO, L., 1975. In: Bolli, H. M. (Ed.) *Monografia micropaleontologica sul Paleocene e l'Eocene di Possagno, Schweizerische Paläontologische Abhandlungen*, 97: 35–55, 149–161.

(108, 109): 4/19a, b (as *Discoasteroides megastypus*)

RAJT79. ROMEIN, A. J. T., 1979. *Utrecht Micropaleontological Bulletins*, 22: 1–231.

(74): 10/2 (*Heliolithus cantabriae*)

(136, 137): 5/7, 8 (*Heliolithus megastypus*)

SE98. STEURBAUT, E., 1998. *Palaeontographica, Abt. A*, 247: 91–156.

(1-5): 2/10b, a, 12b, c, a (*Heliolithus knoxii*)

(6-12): 2/11, 13, 9a, b, 17a, b, 14 (*Heliolithus knoxii*)

(15): 2/15 (*Heliolithus knoxii*)

(42-44): 2/18a, b, 16 (*Heliolithus kleinPELLI*)

SE02. STEURBAUT, E. and SZTRÁKOS, K., 2002. *Revue de Micropaléontologie*, 45: 195–219.

(13, 14): 4/23a, b (*Heliolithus knoxii*)

(45, 46): 3/1a, b (*Heliolithus kleinPELLI*)

SFR64. SULLIVAN, F. R., 1964. *University of California Publications in Geological Sciences*, 44: 163–228.

(16, 17): 12/5a, b (*Heliolithus kleinPELLI*)

(110, 111): 12/3a, b (as *Discoasteroides megastypus*)

WSW77. WISE, S. W. and WIND, F. *Heliolithus*, 1977. In: Barker, P. F., Dalziel, I. W. D., et al., *Initial Reports of the Deep Sea Drilling Project*, 36: 269–491. Washington, D. C.: U.S. Government Printing Office.

GENUS HELIOLITHUS

HIGHLIGHTS:

- Two species.
- Coccoliths diablo-shaped, circular in distal and proximal views.
- Size range: 7–11 μm .
- Cocosphere unknown.
- Stratigraphic Range: Zone NP6–lower Zone NP9.
- Life span: ~700 kyr (late Chron C26r to earliest Chron C24r).

SELECTED READING

Hay et al., 1967; Perch-Nielsen, 1971; Perch-Nielsen, 1977; Siesser et al., 1987; Steurbaut, 1998; Varol, 1989.

INTRODUCTION

The name *Heliolithus* has traditionally applied to a small number of Late Paleocene helioliths that are circular with radial symmetry. Despite their wide morphologic diversity as seen in side view, these have previously been grouped in a single taxonomic entity because they share the characteristic of strong birefringence with two prominent orthogonal extinction lines when examined in cross-polarized light. Analysis of their structure herein shows, however, that these helioliths fall into two independent groupings, such that the genus *Heliolithus* Bramlette & Sullivan 1961 is biphyletic. The genus *Heliolithus* is retained for the helioliths that conform to the structure of the type-species, *Heliolithus riedelii*, while the other group has been placed in the new genus *Heliotrochus* (this volume).

MORPHOLOGY AND STRUCTURE

Coccoliths

Morphology – The helioliths of *Heliolithus* (emend.) are circular in plane view, as in all helioliths, but they are typically diablo-shaped in side view, as if consisting of two superposed truncated cones of different width and height (text-fig. 1). As indicated by the peripheral serration pattern (see below), the broader and lower cone is proximal (in agreement with Bramlette and Sullivan, 1961, pl. 14, fig. 9b). This orientation is opposite to that of the helioliths of *Heliotrochus* that are broadest distally.

Structure – SEM illustrations of the helioliths of *Heliolithus* are few, and most document their side view. However, their proximal face is known from two well-preserved specimens, and their distal face from another one (respectively, Siesser et al., 1989, pl. 8, fig. 8, Steurbaut, 1998, pl. 16, fig. 18; Okada and Thierstein, 1979, pl. 14, fig. 8). These helioliths are comprised of two main structural units with, in some, the remnant of a third one located at their contact. These are readily identified as the column, calyptra and collaret (text-figs. 2a–d).

Column: The cone-shaped column consists of thin, wedge-shaped, non-imbriate elements that fan-out proximally in an orderly fashion (text-fig. 2a). The sutures between elements curve in clock-

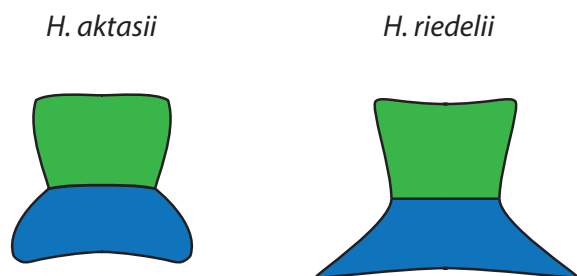
wise direction. The proximal end of each element is beveled in such a manner as to produce the distinctive L-S serration pattern (e.g., Siesser et al., 1987, pl. 3, fig. 8). A tall distal ridge runs in the middle of each element, conferring to the outer side of the column a regular corrugated pattern of alternating radial ridges and valleys (e.g., Siesser et al., 1987, pl. 3, figs. 9, 10; Steurbaut, 1998, pl. 1, fig. 18; text-figs. 2b, c). Similar ridges run also on the inner side of the column, but weaker, and it is possible that regularly spaced knobs created with them a concentric pattern of shallow depressions (e.g., Steurbaut, 1998, pl. 1, fig. 18).

The elements would appear to abut a narrow cycle of small elements at the inner distal end of the column (e.g., Siesser et al., 1987, pl. 3, fig. 8). However, this is insufficiently well preserved to be describable.

Calyptra: The cone-shaped calyptra consists of thin, wedge-shaped elements that fan out in distal direction (text-figs. 2b–d). These elements imbricate dextrally and their sutures curve anticlockwise (Okada and Thierstein, 1979, pl. 14, fig. 8). On the outside each element possesses a radial ridge so that the calyptra exhibits the same pattern of valleys and ridges as the outer surface of the column (text-fig. 2b). Interestingly, ridges and valleys are almost in continuity between the two structural units (e.g., Steurbaut, 1998, pl. 1, fig. 19).

Collaret: Only two structural units are readily visible in most helioliths of *Heliolithus*. However, some specimens exhibit a partially developed third cycle (e.g., Siesser et al., 1987, pl. 3, fig. 10; text-figs. 2b, c), which is interpreted here as the collaret.

Extinction patterns – The standard orientations for optical behavior are those described by Romein (1979, p. 153). In the standard orientation for distal view the broadest side faces upwards. In this orientation the extinction lines are curved counterclockwise (laevogyre), being straight over most of their length and curving peripherally, and the orthogonal extinction cross forms an angle of ~20° with the directions of polarization in clockwise direction. In the standard orientation for side view the edge of the distal cycle is parallel to the X-cross-hair and the axis of the column is parallel to the Y-cross-hair. In side view the extinction line is aligned with the axis of symmetry of the coccolith, and the contact between column and calyptra is marked by a black line.



TEXT-FIGURE 1
General shapes of *Heliolithus*-helioliths as seen in side view.

BIOLOGY, ECOLOGY AND DIVERSITY

Biology

The coccosphere of *Heliolithus* is unknown. The delicate helioliths would have probably surrounded the cell in a uniform fashion (text-fig. 3). Presumably the heliolith-bearing cell would have been non-motile.

Physiology

Heliolithus riedelii and *H. aktasii* stand out by their funnel-shaped column and calyptra that differentiate them readily from the helioliths of *Heliotrochus*. Their shape and the elaborated corrugated pattern on their inner as well as outer surface indicate that these are also highly specialized helioliths. If these structures reflect adaptations to mixotrophic physiology as thought here, these helioliths represent a morphologic strategy different from that of *Heliotrochus*. In the *Heliolithus* helioliths, the corrugated surface would have increased the surface of the coccolith in contact with seawater at the same time as the valleys would have channeled food particles and symbiotic cells alike towards the center of the coccolith and towards the cell surface. The outer ridges may also have strengthened these delicate structures serving as buttresses to preserve the conical shape.

Ecology

Heliolithus species are rarely abundant. They are usually more common in epicontinental settings but they also occur in oceanic sediments.

EVOLUTIONARY HISTORY

Origin

Unlike the heliolith of *Heliotrochus*, the origin of the *Heliolithus* heliolith is not readily apparent, due to its unique morphology. There are, however, some indications that it could have derived from the *Bomolitus* heliolith. First, these two coccoliths have roughly the same morphology, and both the cone-shaped calyptra and cone-shaped column of *Heliolithus* could have naturally developed from, respectively, the distal and proximal extension of the flaring calyptra and column of *Bomolitus*. Secondly, their structure is directly comparable, even though the heliolith of *Bomolitus*

possesses a well-developed collaret and that of *Heliolithus* does not. However, as indicated above, remnants of a collaret are present in *Heliolithus*, in which dextrally imbricated elements can be seen in side view, just as in *Bomolitus* (compare Siesser et al., 1987, pl. 3, fig. 10 with Roth, 1973, pl. 15, fig. 1). *Heliolithus* can thus have evolved from *Bomolitus* with simple modification of the calyptra and column and regression of the collaret (text-fig. 4).

Phylogeny

Heliolithus aktasii evolved (from a *Bomolitus* species) during Biochron NP6 and would be directly or indirectly ancestral to *H. riedelii*.

Diversity

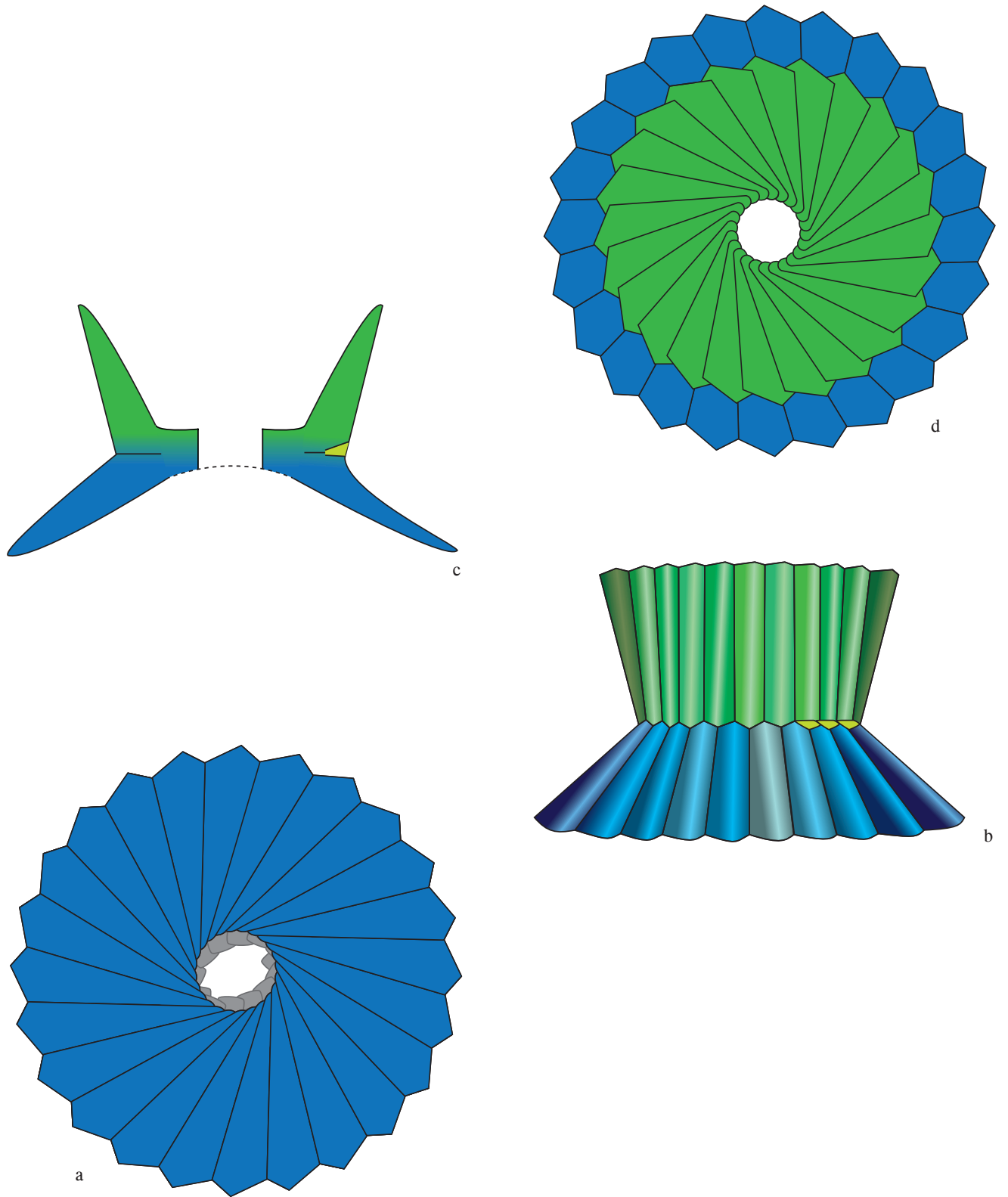
The significance of the large differences in heliolith size within *Heliolithus riedelii* is unknown. It may reflect intraspecific variability, or pseudocryptic speciation. It may also reflect coccolith dimorphism on single coccospheres. The introduction of *H. aktasii*, based on the shape of the free ends of the column and calyptra suggests that *Heliolithus* is more diverse than would appear.

STRATIGRAPHY

The potential of helioliths in biozonal subdivision of the stratigraphic record was recognized as early as 1961, during the initial development of coccolith biostratigraphy (Bramlette and Sullivan, 1961; Stradner, 1961). Bramlette and Sullivan (op. cit.) introduced the first Paleocene biostratigraphic unit based on coccolith occurrences (those of *Heliolithus riedeli* and *Heliodiscoaster helianthus*), provisionally named the "*Heliolithus riedeli* Zone". This was subsequently adopted by Mohler and Hay (in Hay et al., 1967, p. 455) for the interval between the LOs of *H. riedeli* and *Heliodiscoaster multiradiatus*, and codified by Martini (1970, p. 560; 1971, p. 754) as Zone NP8 (text-fig. 5)

The geographic distribution of *Heliolithus riedelii* is somewhat unpredictable. Regarded by most authors as restricted to epicontinental deposits, it may also occur in oceanic oozes where it is rare (e.g., ODP Site 865, Allison Guyot, Central Pacific Ocean, Bralower and Mutterlose, 1995) or common (e.g., DSDP Sites 384, 386, Okada and Thierstein, 1979; Berggren et al., 2000; DSDP Site 550, Goban Spur, Müller, 1985; ODP Sites 689 and 690, Pospichal and Wise, 1990). However, it was not found, for instance, in the Paleocene of the Bay of Biscay (Perch-Nielsen, 1972) nor in the western South Atlantic (Perch-Nielsen, 1977). To remedy the problem of the sporadic geographic occurrences of *H. riedeli*, Romein (1979, p. 54) emended the definition of the "*Discoaster mohleri* Zone" so as to encompass the *Heliolithus riedeli* Zone. Other authors (e.g., Perch-Nielsen, 1972; Bukry, 1973) have introduced alternative markers (such as *Helio-discoaster nobilis*) with a LO that approximates that of *H. riedelii* to subdivide the interval between the LOs of *H. mohleri* and *H. multiradiatus*. A pragmatic solution is to combine Zones NP7 and NP8 in a single, undifferentiated NP7/8 zonal interval (e.g., Perch-Nielsen, 1981).

The low to mid latitude zonal scheme of Varol (1989) makes the most out of the ranges of *Heliolithus* species, relying on the LO of *Heliolithus riedeli* but also on its HO and that of *Heliolithus aktasii* (text-fig. 5). The complete stratigraphic ranges of *Heliolithus* species are as difficult to determine as those of *Heliotrochus* species, however, because of their generally low abundances and sporadic occurrences. For instance, placement of the HO of *H. riedeli* in Zone NP8 is challenged by the report of this species in Zone NP9 in Northwest Europe (Bignot et al., 1994; Steurbaut, 1998) unless



TEXT-FIGURE 2

Structure of *Heliolithus riedelii*.

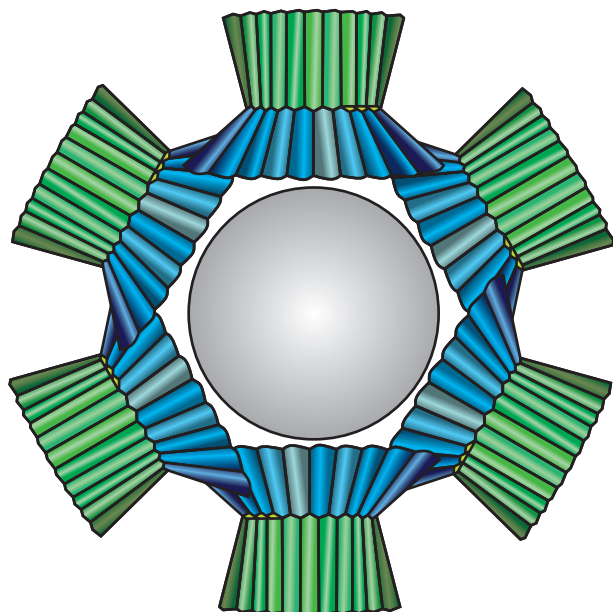
a: proximal face. The innermost structure of the heliolith is unknown at this time.

b: side view. Note the pattern of ridges on the column and calyptra as well as the remnant of a collaret (right side).

c: longitudinal cross section. The structure of the central part of the heliolith is unknown, whether on the proximal or distal face.

A remnant of a collaret is tentatively shown (right side).

d: distal face.



TEXT-FIGURE 3
Tentative reconstruction of the coccosphere of *Heliolithus*
 (*Heliolithus riedelii* in this model). Cell seen in cross section.
 Helioliths in side view.

the specimens there should belong to *Heliolithus aktasii*. The latter species occurs from Zone NP7 to lower Zone NP9, and its HO marks the NTp16B/NTp17 zonal boundary (Varol., 1989).

For indeterminate reasons, species of *Heliolithus* seem to occur inconsistently throughout their ranges (e.g., *H. riedelii*: Monechi and Thierstein, 1985, fig. 4).

Chronostratigraphy

Although without special significance in modern chronostratigraphy, *Heliolithus riedelii* was a key species for correlating the Thanetian stratotypic of Engand (Thanet Beds) to the deep sea stratigraphy (Aubry et al., 1986).

CHRONOLOGY

The FAD of *Heliolithus riedelii* is tied to early Chron C25r (See Aubry et al., 1986; Schmitz et al., 2011; text-figs. 6, 7).

The LAD of *H. aktasii* is predictably located in earliest Chron C24r.

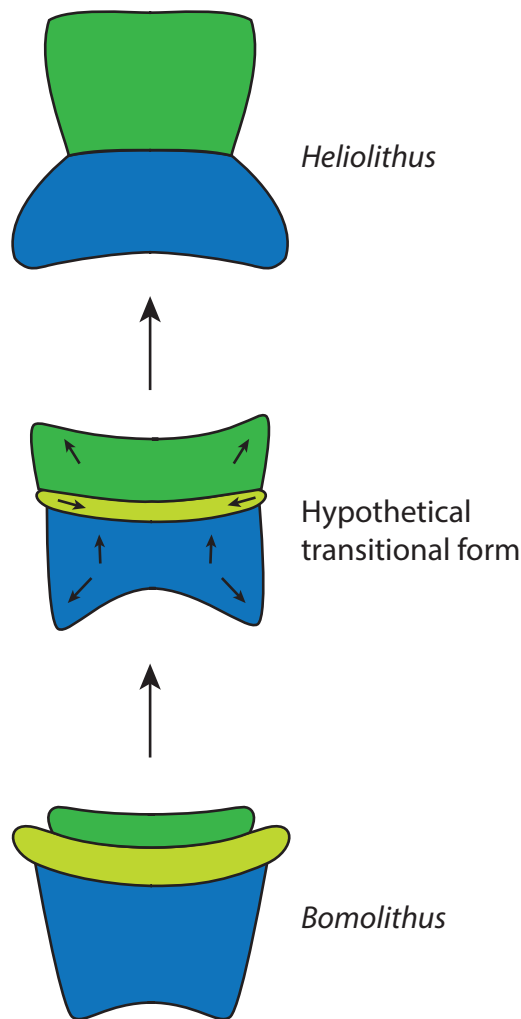
TAXONOMY

Generic taxonomy

Genus: *Heliolithus* Bramlette & Sullivan, 1961 emend.

Type Species: *Heliolithus riedelii* Bramlette & Sullivan, 1961

“Forms consisting of two partial cones joined at truncate apices and having concave basal ends. The larger of the conical parts is more appressed or flaring and shows more distinctly the many thin radiate elements of construction.



TEXT-FIGURE 4
Tentative interpretation of the evolution of *Heliolithus* from *Bomololithus*.

“Specimens in Canada balsam are more apparent between crossed nicols than in normal transmitted light, and the heliolithid radial arrangement of component calcite elements is especially conspicuous in end view, which shows the sharply defined cross of the extinction lines” (Bramlette and Sullivan, 1961, p. 164).

Emended Diagnosis: Diabolo-shaped helioliths, consisting of column and calyptra flaring in opposite direction, both consisting of trihedral elements arranged so as to produce a pattern of ridges and valleys on their outer surface. The column is lower but broader than the calyptra. The remnant of a collaret may be present in some specimens.

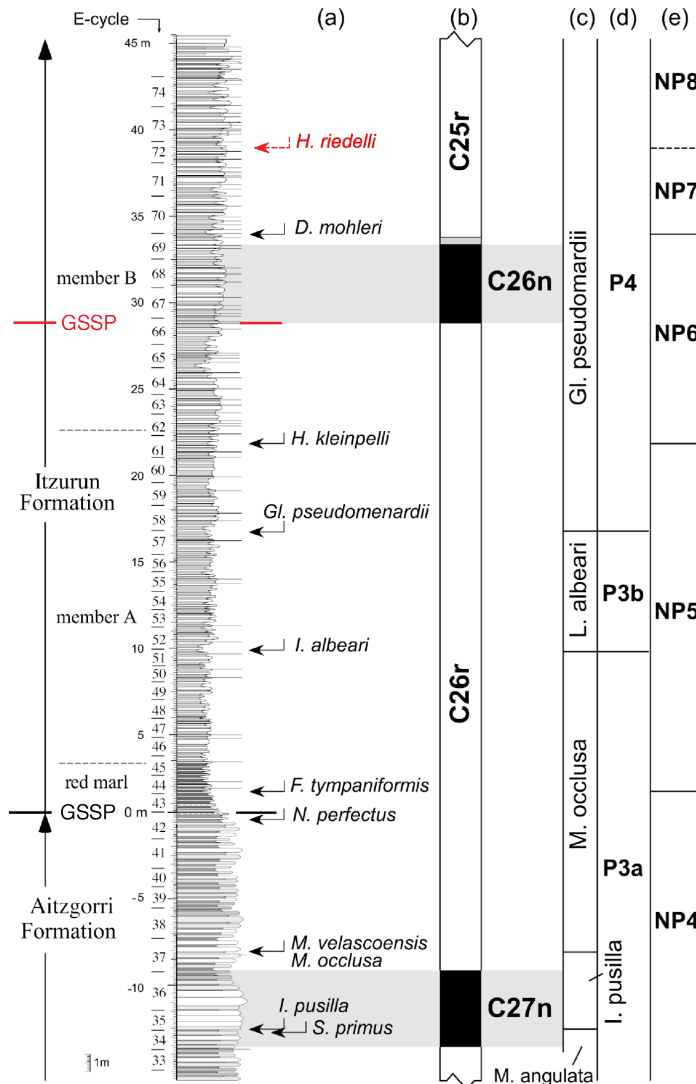
The inner structure of the *Heliolithus* heliolith is indeterminate at this time, and it is unknown whether the calyptra is polycyclic or not. As with other coccoliths of the Order Discoasterales, *Heliolithus* helioliths were delicate structure, prone to massive recrystallization. Both the column and the calyptra were externally fluted.

	Bramiette and Sullivan 1961	Mohler and Hay in Hay et al. 1967	Martini 1970, 1971	Perch-Nielsen 1972	Bukry 1973	Okada and Bukry 1980	Romein 1979	Perch-Nielsen 1981	NTp17 ⁵
T <i>H. atkasii</i>	Discoaster multiradiatus Zone	<i>D. multiradiatus</i> Zone		<i>D. multiradiatus</i> Zone	<i>D. multiradiatus</i> Zone	CP8	<i>D. multiradiatus</i> Zone	NP9	NTp16
T <i>Ht. cantabriae</i>									
└ <i>Hd. multiradiatus</i>									NTp16A ²
T <i>Ht. kleinpelli</i>	Heliolithus riedeli Zone	<i>H. riedeli</i> Zone	<i>H. riedeli</i> Zone	<i>Discoaster nobilis</i> Zone	<i>D. nobilis</i> Zone	CP7	<i>D. mohleri</i> Zone	NP7/8	NTp15 ¹
T <i>H. riedeli</i>									NTp14
└ <i>Hd. nobilis</i>									
└ <i>H. riedeli</i>									
T <i>Hd. drieveri</i>									NTp12
└ <i>Hd. mohleri</i> [<i>D. gemmeus</i>]	Discoaster gemmeus Zone	<i>D. gemmeus</i> Zone	<i>D. gemmeus</i> Zone	<i>D. gemmeus</i> Zone	<i>Discoaster mohleri</i> Zone	CP6		NP6	Cruciplacolithus latipons Subzone NTp10B
└ <i>Ht. kleinpelli</i>									
└ <i>Ht. kleinpelli</i>	Heliolithus kleinpelli Zone	<i>H. kleinpelli</i> Zone	<i>H. kleinpelli</i> Zone	<i>H. kleinpelli</i> Zone	<i>H. kleinpelli</i> Zone	CP5	<i>H. kleinpelli</i> Zone		
	Fasciculithus tympaniformis Zone					CP4	<i>F. tympaniformis</i> Zone	NP5	Multiparis ponticus Subzone NTp10A

TEXT-FIGURE 5

Zonal schemes based on the stratigraphic ranges of *Heliolithus* species.

⁵Placozygus sigmoides Zone
⁴Discoaster lenticularis Subzone
³Heliolithus atkasii Subzone
²Heliolithus cantabriae Zone
¹Hornibrookina australis Zone



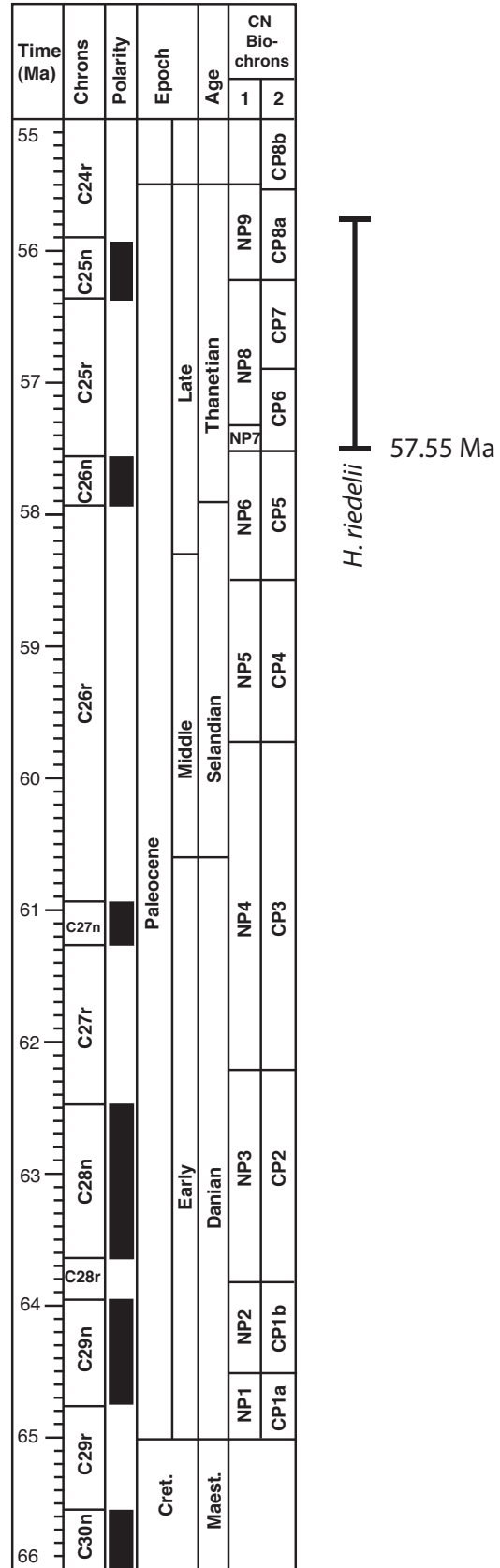
TEXT-FIGURE 6

FAD of *H. riedeli* as recorded in the GSSP section at Zumaia, for the base of the Upper Paleocene (Thanetian Stage). (Modified from Schmitz et al., 2011, fig. 13.)

Heliolithus helioliths differs from *Heliotrochus* helioliths by their shape, in which the proximal end of the column is broader than the distal end of the calyptra in the former group, and by the vestigial character of the collaret in them.

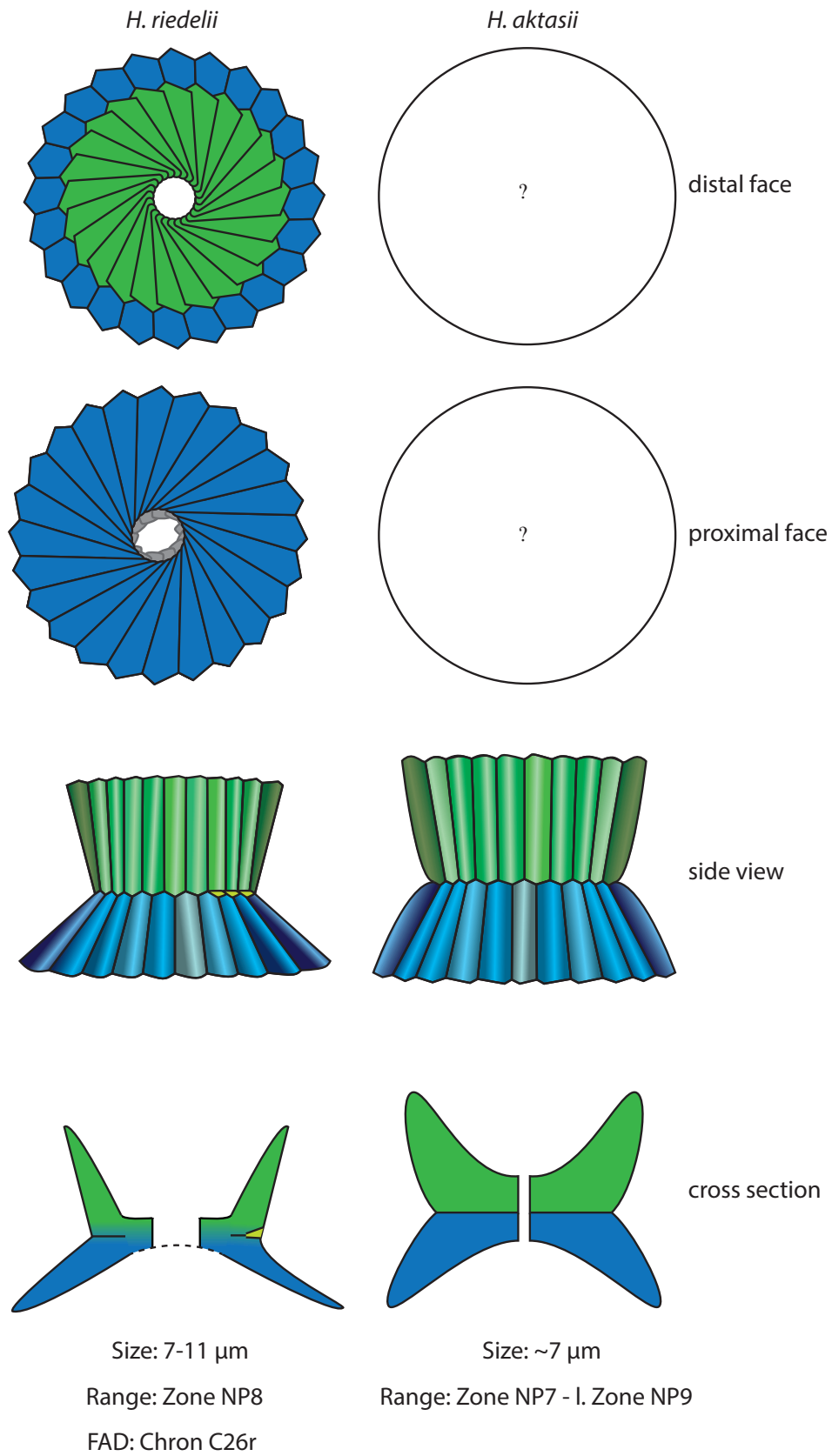
Specific taxonomy

Only two species have been described. They differ by the shape of the proximal end of the column and the distal end of the calyptra. Both are gently curved inwards in *H. atkasii* whereas they are flaring in *H. riedelii* (text-fig. 8). It is unclear whether overgrowth has a negative effect on the distinction between the two taxa.



TEXT-FIGURE 7

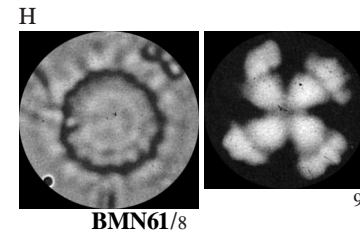
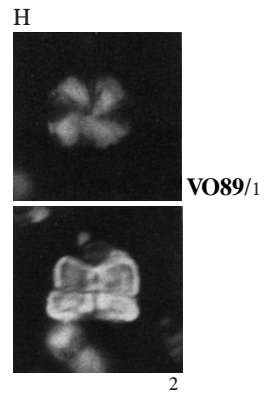
Biochronology of *Heliolithus* species. Magnetobiochronologic framework from Berggren et al. (1995) updated (Wade et al., 2011, and herein).



TEXT-FIGURE 8
Comparison between *Heliolithus* species.

Heliolithus aktasii Varol 1989

Heliolithus riedelii Bramlette & Sullivan 1961



Heliolithus aktasii

- ~7.1 μm x H: 7.0 μm

- L. Paleocene (NTp12). Mid and low latitude worldwide, including Turkey, Iran Java, India, S. Atlantic Ocean.

- A small form having a distal cycle and a column which are almost equal in diameter. Strongly birefringent in CN.

≠ from *H. cantabriae* and *B. elegans* in having no median cycle;

≠ from *H. riedelii* by having an inflated distal cycle instead of flaring outwards and distally as in the latter species. Both species have a serrated outer rim in plan view.

Heliolithus riedelii

- 7–11 μm

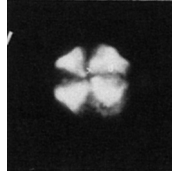
- L. Paleocene. Lodo Fm., California.

-** Two conical-shaped parts joined at truncate apices. Conical ends vary from being similar to having one distinctly more appressed and greater diameter of base. Thin peripheral part of conical bases showing about 20 petal-like elements; small hole present in the thick central part.

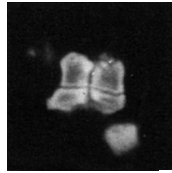
— LO defines base NP8 (Martini, 1971, p. 754). However, it is not always a reliable marker because it occurs mainly in epicontinental areas.

— Shallow water marker.

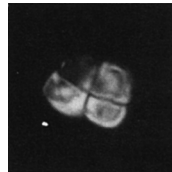
Heliolithus aktasii (continued)



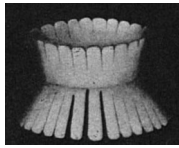
VO89/3



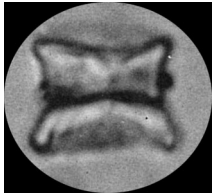
4



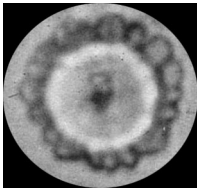
5



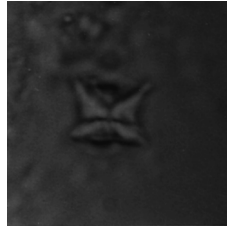
BMN61/10



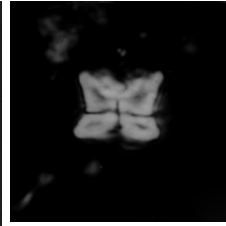
II



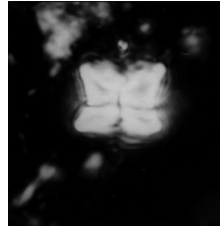
12



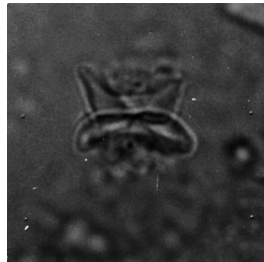
AMP86/13



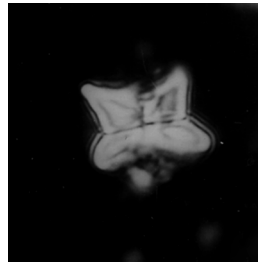
14



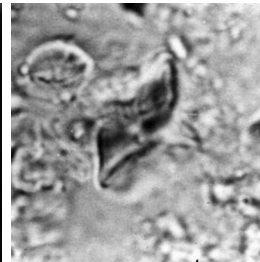
15



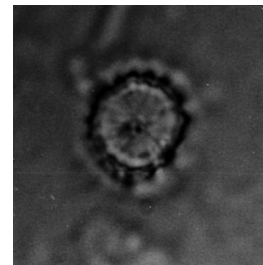
16



17

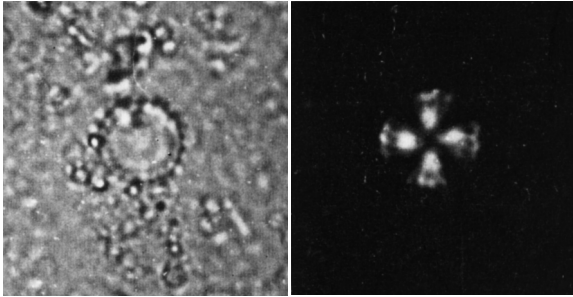


18



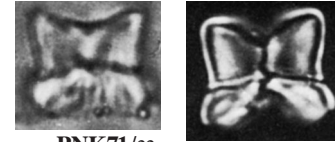
19

Heliolithus riedelii (continued)



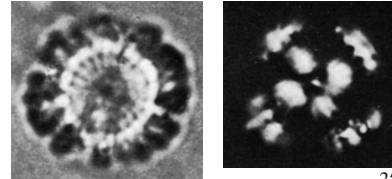
ME71/20

21



PNK71/22

23

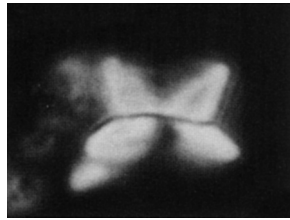


24

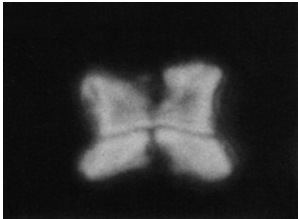
25



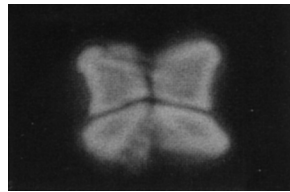
SE98/26



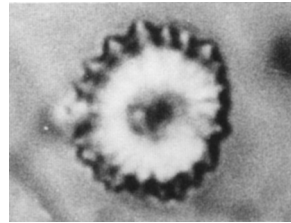
27



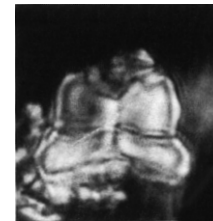
28



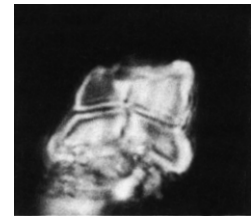
29



30

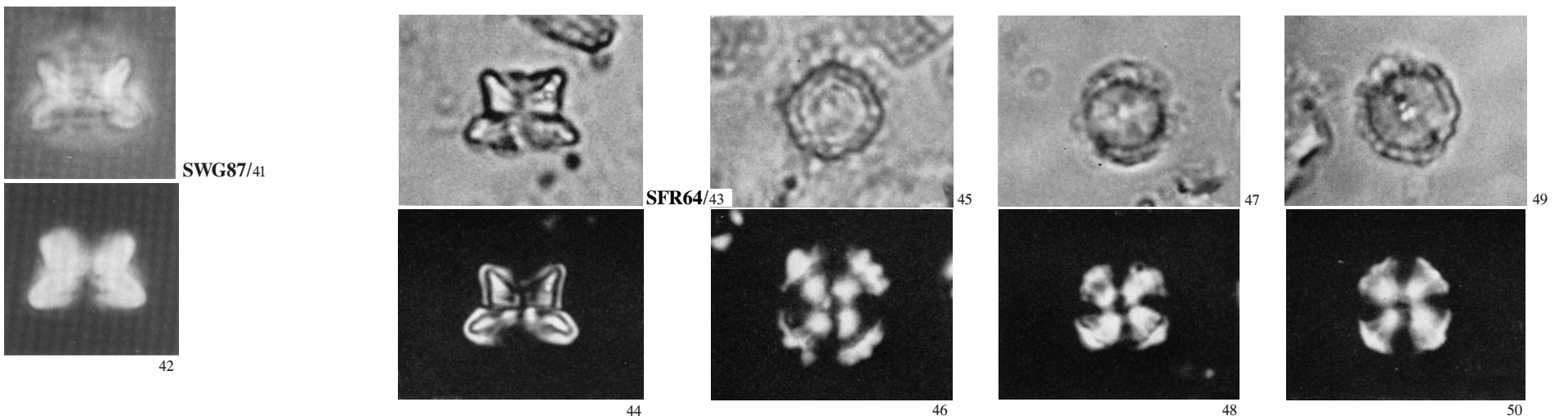
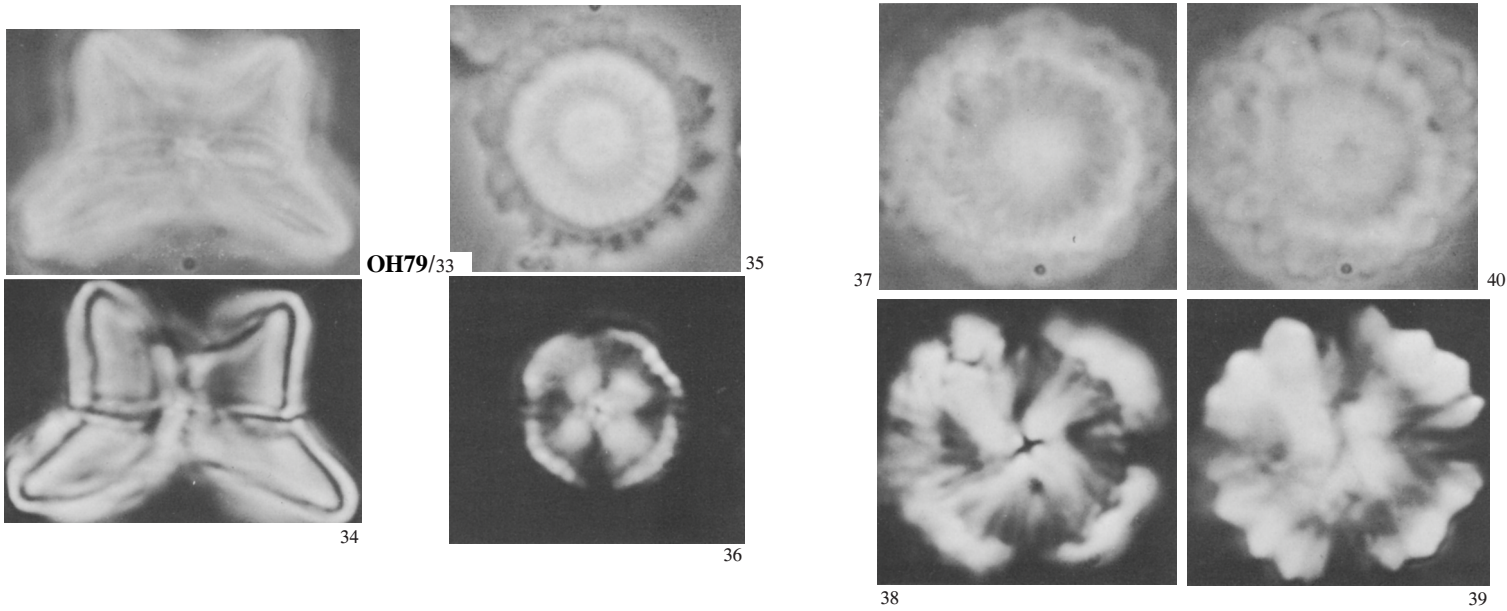


SE02/31



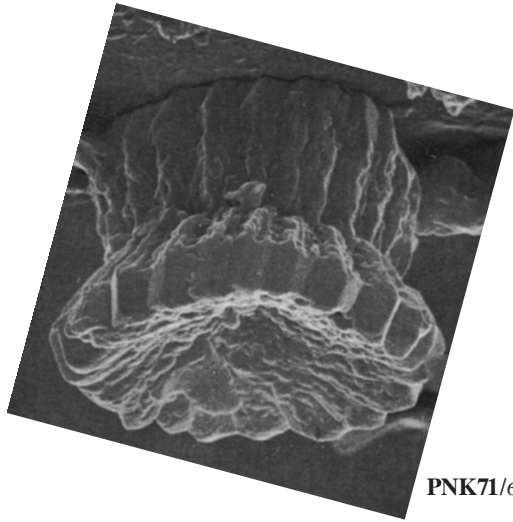
32

Heliolithus riedelii (continued)

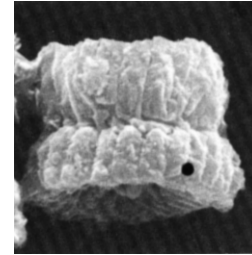


Heliolithus aktasii (continued)

PROXIMAL FACE



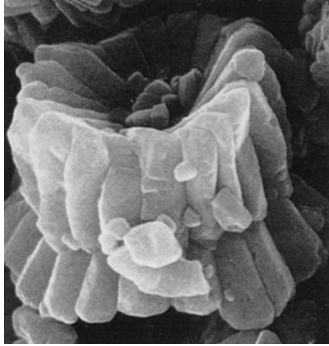
SIDE VIEW



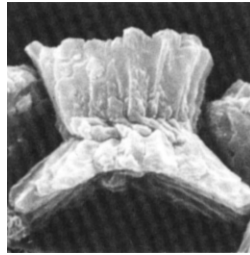
SWG87/7

Heliolithus riedelii (continued)

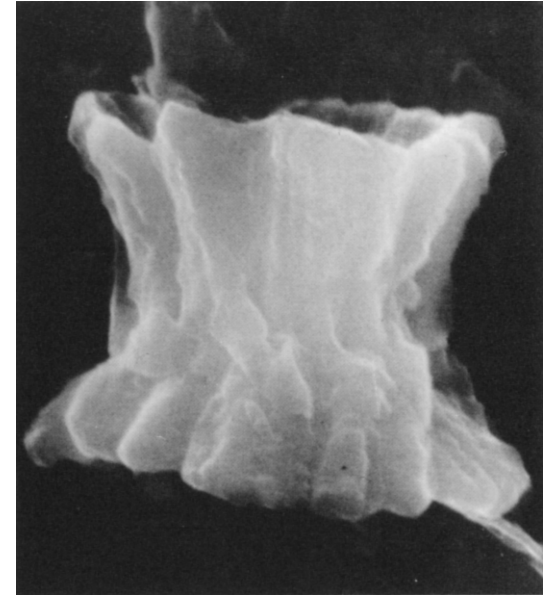
SIDE VIEW



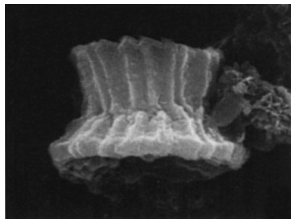
PJJ90/51



SWG87/52



WSW77/54



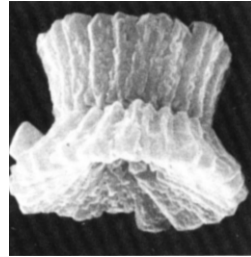
SE98/53

Heliolithus riedelii (continued)

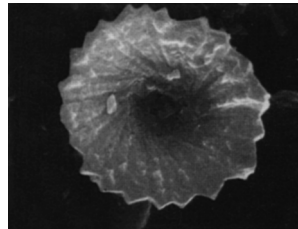
PROXIMAL FACE



SWG87/55



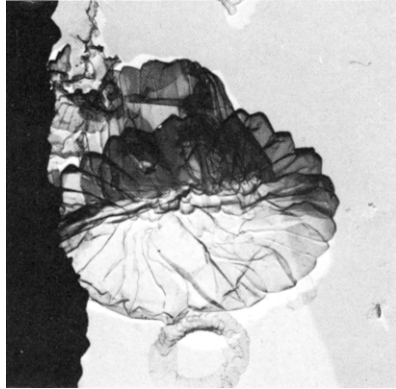
56



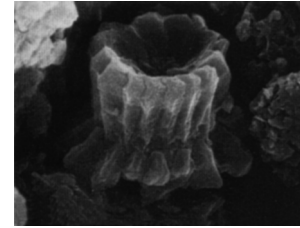
SE98/57

Heliolithus riedelii (continued)

DISTAL FACE

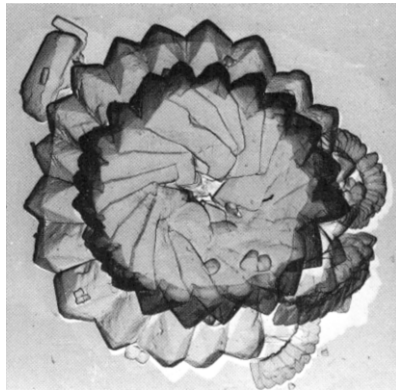


OH79/58

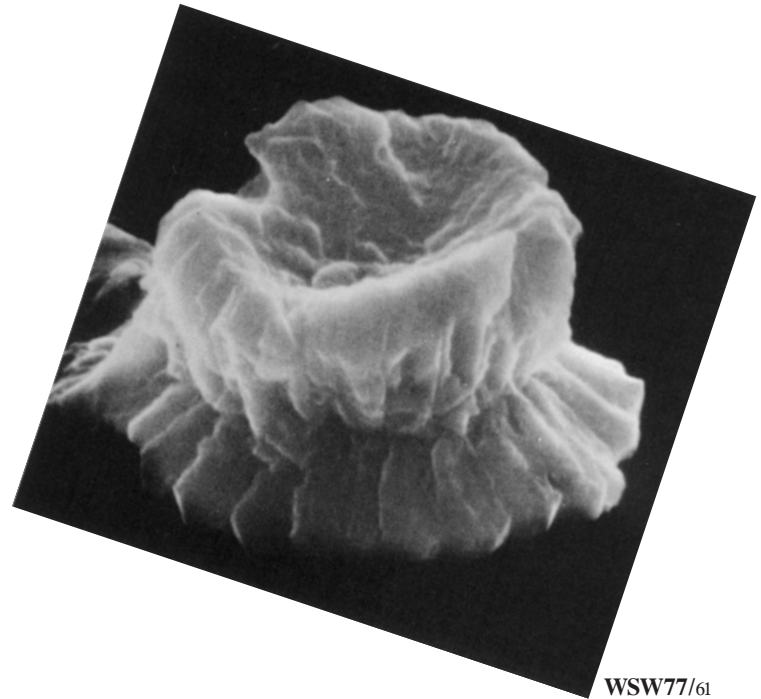


SE98/60

[cf.]



59



WSW77/61

Figure References

- AMP86.** AUBRY, M.-P., 1986. *Palaeogeography, Palaeoclimatology, Palaeoecology*, 55: 267–334.
(13-19): 1/14-18, 20, 19 (*H. riedelii*; 14-16 as *H. cantabriae*; also Aubry 1983, pl.1, figs. 14-20)
- AMP.** AUBRY, M.-P., this volume.
- BMN61.** BRAMLETTE, M. N. and SULLIVAN, F. R., 1961. *Micropaleontology*, 7: 129–188.
(8, 9): 14/9a, c (*Heliolithus riedelii*)
(10-12): 14/9b, 10, 11 (*Heliolithus riedelii*)
- ME71.** MARTINI, E., 1971. In: Farinacci, A. (Ed.), *Proceedings of the II Planktonic Conference, Roma, 1970, Volume 2*, 739–785. Rome: Ediz. Tecnoscienza.
(20, 21): 1/15, 16 (*H. riedelii*)
- OH79.** OKADA, H. and THIERSTEIN, H. R., 1979. In: Tucholke, B. E., Vogt, P. R., et al., *Initial Reports of the Deep Sea Drilling Project, 43*, 507–573. Washington, D. C.: U.S. Government Printing Office.
(33-40): 4/6b, a, 4b, a, 5c, a, d, b (*H. riedelii*)
(58, 59): 14/9, 8 (*H. riedelii*)
- PNK71.** PERCH-NIELSEN, K., 1971c. *Meddelelser fra Dansk Geologisk Forening*, 21: 51–66.
(6): 1/4 (*H. riedelii*)
(22-25): 7/28, 29, 39, 40 (*H. riedelii*)
- PJJ90.** POSPICHAL, J. J. and WISE, S. W., 1990. In: Barker, P. F., Kennett, J. P., et al., *Proceedings of the Ocean Drilling Program, Scientific Results*, 113, 613–638. College Station, Texas: Ocean Drilling Program.
(51): 3/11 (*Heliolithus* sp. cf. *Heliolithus riedelii*)
- SWG87.** SIESSER, W. G., WARD, D. and LORD, A. R., 1987. *Journal of Micropalaeontology*, 6: 85–102.
(7): 3/11 (*H. riedelii*)
(41, 42): 2/10, 11 (*H. riedelii*)
(52): 3/10 (*H. riedelii*)
(55, 56): 3/8, 9 (*H. riedelii*)
- SE98.** STEURBAUT, E., 1998. *Palaeontographica, Abt. A*, 247: 91–156.
(26-30): 1/21, 20, 22, 24, 23 (*H. riedelii*)
(53, 54): 1/16, 17 (*H. riedelii*)
(57): 1/18 (*H. riedelii*)
- (60): 1/19 (*H. riedelii*)
- SE02.** STEURBAUT, E. and SZTRÁKOS, K., 2002. *Revue de Micropaléontologie*, 45: 195–219.
(31, 32): 3/14, 15 (*H. riedelii*)
- SFR64.** SULLIVAN, F. R., 1964. *University of California Publications in Geological Sciences*, 44: 163–228.
(43-50): 12/8a, b, 4a, b, 6a, b, 7a, b (*H. riedelii*)
- VO89.** VAROL, O., 1989. In: Crux, J. A. and van Heck, S. E. (Eds.), *Nannofossils and their applications*, 267–310. Chichester: Ellis Horwood Limited.
(1,2): 12.5/24, 25 (*H. aktasii*)
(3-5): 12.5/21-23 (*H. aktasii*)
- WSW77.** WISE, S. W. and WIND, F. H., 1977. In: Barker, P. F., Dalziel, I. W. D., et al., *Initial Reports of the Deep Sea Drilling Project, 36*: 269–491. Washington, D. C.: U.S. Government Printing Office.
(54): 11/2 (as *H. riedelii*)
(61): 11/1 (as *H. riedelii*)

HIGHLIGHTS:

- 3.5–11 μm .
- Four formally described species; three synonyms; two informal taxa.
- Poorly known coccolith consisting of superposed polycyclic structural units.
- Assignment to Discoasterales based on LS_{prox} peripheral pattern of serration.
- Evolutionary origin unknown.
- Most common in epicontinental and hemipelagic sediments.
- Ranges from Lower Eocene (Zone NP11) to Lower Pliocene.
- Only one taxon, *H. situliformis*, with well known stratigraphic range.

SELECTED READING

Gartner, 1969a; Perch-Nielsen, 1977; Theodoridis, 1984.

INTRODUCTION

Hayella Gartner 1969a (non *Hayella* Roth 1969) is among the genera whose taxonomic position has been most unstable. For example, in its initial description Gartner (1969a) assigned it to the Family Heliolithaceae, albeit tentatively, while Hay (1977), Perch-Nielsen (1977), Young and Bown (1997), and Bown (2005a) regarded it as a genus *incertae sedis*. Perch-Nielsen (1985) earlier transferred it to the Family Coccolithaceae, while Bown and Jones (2006) subsequently placed it in the Family Calcidiscaceae. Finally, Dunkley Jones and Bown (2009, p. 380) returned it to the category of “placolith coccoliths *incertae sedis*”.

These taxonomic assignments were, of course, determined by various interpretations of relationships seen in the *Hayella* coccoliths. While some authors have refrained from placing them in a morphologic group, others have recognized in them the basic morphology of a placolith, leading to their assignments to families of the Order Coccolithales Schwarz, 1932 emend. Edvardsen & Eikrem in Edvardsen et al., 2000. Gartner (1969, p. 32), however, refuted this interpretation when he wrote:

“The two rims suggest relationship to placoliths, but in *Hayella situliformis* the collar comprises most of the body, and the shields are reduced to mere rims. The most nearly similar genus is *Heliolithus*, species of which are constructed on the plan of two truncated cones joined at their narrow ends”.

Hayella is placed here in the Order Discoasterales because of details of its construction, discussed below. Fundamentally, however, the absence of a divide that would delineate a central area and a margin, and the serration pattern at the outer edge of the cycles, strongly suggest assignment to this order in the newly erected Family Hayellaceae.

MORPHOLOGY AND STRUCTURE

Hayella situliformis is the most extensively illustrated species of the genus, principally in Perch-Nielsen (1977). However, this coc-

colith is complex and a comprehensive description of its structure would necessitate numerous additional illustrations of the distal and proximal sides (text-fig. 1) of well preserved specimens.

Morphology – The coccoliths of *Hayella* are tall, vase-like, and circular in transverse section. They are characterized in side view by the presence of two rims, one being narrow and proximal and the other being broad and distal. The sides diverge in distal direction above the proximal rim, then flare almost horizontally to form a broader distal rim, and, in some species, is further constricted into a low distal cycle.

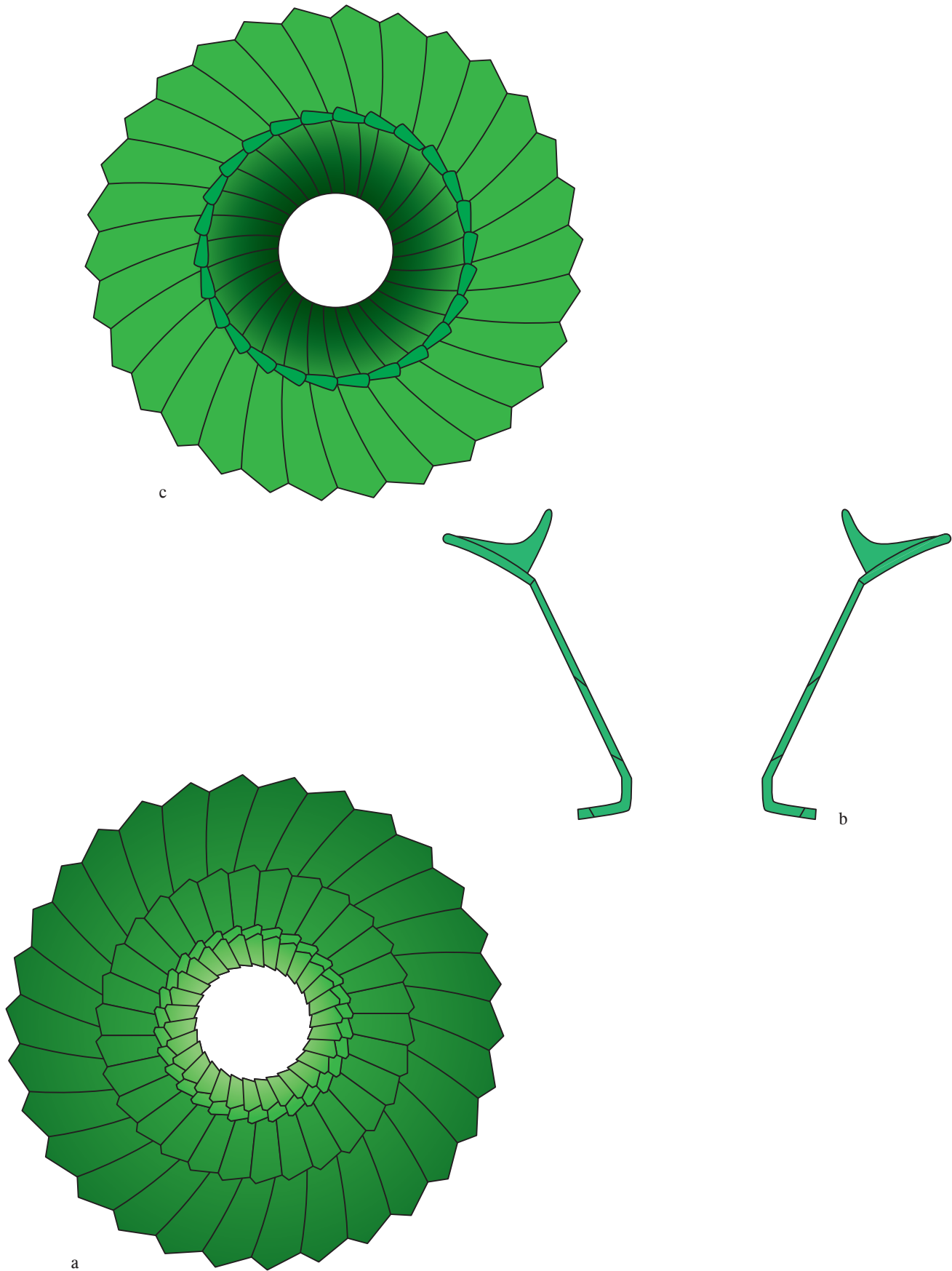
The coccolith was initially oriented with the broadest rim considered as proximal (Gartner, 1969, pl. 1, figs. 4, 6). This resulted in a convex proximal end and a concave distal end, delineated by vertical elements. This orientation is properly reversed here, such that the coccolith has a gently concave proximal face of the proximal rim (e.g., Perch-Nielsen, 1977, pl. 44, fig. 1).

Structure – It is convenient to describe the coccolith as comprised of a low proximal structural unit (essentially the proximal, or lower, rim) surmounted by an inverted, truncated cone-shaped distal structural unit.

In proximal view, the proximal structure appears to be comprised of two interlocked cycles, one of them being the lower rim. The imbrication of the elements and orientation of the sutures cannot be firmly described at this time, except for the sutures of the outer cycle curving clockwise (see Perch-Nielsen, 1977, pl. 44, fig. 1).

The tall proximal part of the distal structure is formed of at least three superposed interlocked tiers (which excludes any structural relation to a placolith). Each tier is formed by a cycle of tangentially arranged lath-shaped elements. The two lower cycles consist of sub-vertically arranged rod-like elements inclined anticlockwise.

The most distal tier flares laterally to form the broad distal (or upper) rim typical of the genus. This rim is concave proximally, convex distally. Its outer edge clearly exhibits the LS serration pattern when seen in proximal view (Perch-Nielsen, 1977, pl. 44, fig.



TEXT-FIGURE 1

Morphology and structure of *Hayella*.

- a: proximal face.
- b: longitudinal section.
- c: distal face.

2, 3, 6; Müller, 1974, pl. 15, fig. 5; Roth, 1973, pl. 1, fig. 6), which is a diagnostic character of the Order Discoasterales. The elements would appear to be non-imbricate with sutures oriented anticlockwise on the distal surface of this rim.

The upper rim is overlain at the inner periphery by a narrow cycle of elongate elements with strong sinistral imbrication (Perch-Nielsen, 1977, pl. 44, fig. 7; Roth, 1973, pl. 1, fig. 6). This cycle smoothly delineates the large, circular distal opening.

The coccolith structure is fragile, and it is not rare to find isolated cycles in sediments. Some have been described as separate taxa (*Cyclolithella aprica* Roth, 1973; *Cyclolithella? neoaprica* Bukry 1985).

Extinction patterns

The *Hayella* coccoliths are entirely and brightly birefringent in standard orientations for distal and side views. In the standard orientation for distal view, the broadest rim of the coccolith faces upwards. In this orientation the orthogonal extinction lines are straight over most of their length, fanning out peripherally. In the standard orientation for side view, the axis of the coccolith is parallel to the Y-cross-hair and the gently concave proximal edge is parallel to the X-cross-hair. In this position a median extinction line runs along the axis of the coccolith.

BIOLOGY, ECOLOGY, AND DIVERSITY

Biology

The coccosphere of *Hayella* is unknown. A coccosphere of *H. situliformis* is tentatively reconstructed here (text-fig. 2).

Physiology

The shape of the coccolith, characterized by its large inner cavity and the external area extended into a rim, is suggestive of adaptation to mixotrophic physiology.

Ecology

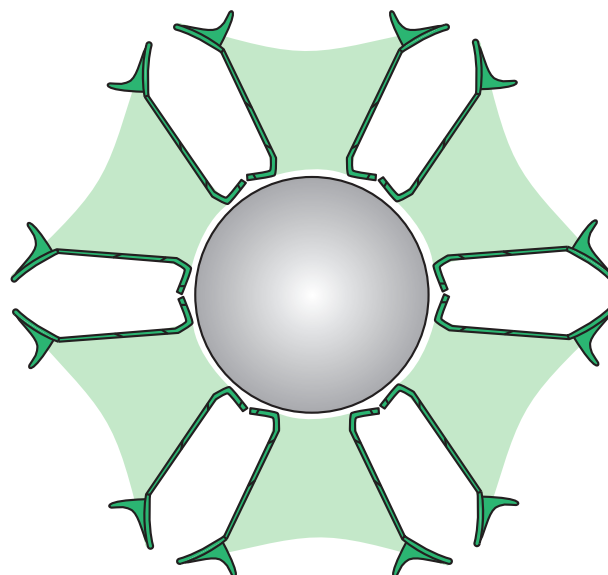
Hayella occurred at low latitudes, and was most common in oceanic areas not far from continental masses (Gartner, 1971).

EVOLUTIONARY HISTORY

Origin

The origin of *Hayella* is obscured by the fact that it is difficult, at this time, to identify in its coccolith the two main structural units characteristic of the Order Discoasterales, i.e., column and calyptra. This is because the proximal face and rim of the individual coccoliths are poorly illustrated. The recognition of these features would, however, be the ultimate test of whether *Hayella* is properly assigned to the order. *Hayella* is an isolated, very derived coccolith, and whether it will be possible to retrace its origin is questionable.

Prins (1971, p. 1027) endorsed Gartner's suggestion that *Hayella* may have evolved from *Heliolithus*.



TEXT-FIGURE 12

Tentative reconstructions of the coccosphere *H. situliformis*. Cell in equatorial section and coccolith in longitudinal section. Light green highlights inner part of coccolith.

Phylogeny

Except for *H. situliformis*, other species are poorly illustrated, and their stratigraphic ranges are poorly known.

Diversity

The genus is comprised of four formally recognized species with a collective temporal span of Early Eocene through Early Pliocene. The specimens illustrated by Bown (2005a) and Bown and Jones (2006) as *Hayella simplex* do not exhibit the characters of the genus.

BIOSTRATIGRAPHY

The range of *Hayella* is discontinuous. *Hayella gauliformis* is known from the Lower Eocene (Zone NP12; Troëlsen and Quadros 1971), *H. situliformis* from the Upper Eocene–Lower Oligocene (Perch-Nielsen, 1985), *H. aperta* from the Lower and Middle Miocene (Zone NN1/NN2 to NN6; Theodoridis, 1984, [?]Perch-Nielsen, 1977, p. 750) and *H. challengerii* from the Upper Miocene (Zone NN11-lower Zone NN12; Müller, 1974; *Coccolithus pelagicus* Zone to *Calcidiscus leptoporus* Zone of Theodoridis, 1974) and Lower Pliocene (Müller, 1974).

An informal *Hayella* sp. has been illustrated from the Lower Eocene Ieper Formation (Zone NP12) in Belgium (Steurbaut, 1991). It had been previously described and illustrated as *Cyclococcolithus* sp. from the Den Hoorn and Brussel Formations (both of Zone NP14) of Belgium (Steurbaut, 1990, p. 49, table 1, p. 53). Finally, *Cyclolithella* sp. was described, without illustration, as a “Small circular coccolith (6 μ m) with raised inner margin around the central opening, somewhat similar to *Cyclolithella aprica* Roth 1973 (see Roth, 1973:730, pl. 11, fig. 4-6; pl. 12, fig. 1-4)” (Steurbaut, 1990, p. 53), occurring in Zone NP11 of the Ieper Formation of Belgium (op. cit., p. 48, table 1).

The most commonly reported species is *Hayella situliformis*, found mostly in hemipelagic sediments (Gartner, 1971, p. 104). The LO of this species defines the base of the *Hayella situliformis* Zone, which is the interval between the LO of the nominate species and the LO of *Isthmolithus recurvus* (Gartner, 1971, p. 106; text-fig. B). This zone is approximately equivalent to Zone NP18 of Martini (1971), as indicated by the LO of *Chiasmolithus oamaruensis* and *Helicosphaeroides reticulatus* near the base of the zone, and the HO of *Chiasmolithus grandis* below the top of the underlying *Helicopontosphaera compacta-Chiasmolithus grandis* Zone (Gartner, 1971). Its HO is close to the HOs of *Ericsonia formosa* and *Reticulofenestra umbilicus* (Gartner, 1971).

CHRONOSTRATIGRAPHY

Hayella species have not been employed in formal chronostratigraphy. Based on the current GSSP-defined E/O boundary (Premoli Silva and Jenkins, 1993), this species has a known range from Priabonian into Rupelian. However, if the GSSP for the base of the Oligocene should be redefined so that it can be correlated by Isotopic Event O11 (Miller et al., 1991), then *Hayella situliformis* would be useful as an approximate marker for the Eocene/Oligocene boundary in hemipelagic stratigraphy.

BIOCHRONOLOGY

The temporal range of *Hayella* species have not been securely tied to magnetochronology. The FAD of *H. situliformis* is close to the LAD of *Chiasmolithus grandis* and to the FAD of *C. oamaruensis*. Its LAD is close to those of *Ericsonia formosa* (~33 Ma) and *Reticulofenestra umbilicus* (~32 Ma) (text-fig. 3).

TAXONOMY

Generic taxonomy

Genus: *Hayella* Gartner, 1969

Type Species: *Hayella situliformis* Gartner, 1969.

“Heliolithid calcareous body in the shape of a truncated cone with the smaller end closed, bearing a peripheral rim-like flange at both ends and a constricted lip at the wider open end” (Gartner, 1969a, p. 32).

Aubry (1989, p. 215) commented:

“Roth (1969) proposed the generic name *Hayella* for a calcareous nannofossil from the Lower Oligocene Red Bluff Clay of Alabama. He assigned one species to the genus, which he named *Hayella elegans*. *Hayella elegans* Roth, however, is a junior synonym of *Ilseolithina* n.g. Stradner (in Stradner and Adamiker, 1966), and therefore is invalid. Gartner (1969a) also proposed the generic name *Hayella* for a calcareous nannofossil, this form being from the Shubuta Clay Member of the Upper Eocene Yazoo Formation of Mississippi. He assigned one species to the genus, *Hayella situliformis*.

“As *Hayella* Gartner has the earlier publication date, it has priority over *Hayella* Roth, and the latter is both a junior synonym of *Ilseolithina* Stradner, and a junior homonym of *Hayella* Gartner” (Gartner, 1969b, p. 490).

In agreement with Theodoridis (1984, p. 83) *Nannocorbis* Müller, 1974 is a synonym of *Hayella* Gartner 1969.

Genus: *Nannocorbis* Müller, 1974

Type Species: *Nannocorbis challengerii* Müller, 1974.

“Forms tube-shaped with distinct externally turned rims at both ends” (Müller, 1974, p. 593).

Species taxonomy

Species differ by their size (height and width) and shape. *Hayella aperta*, *H. challengerii*, and *H. gauliformis* differ from *H. situliformis* by the absence of a marked distal cycle above the upper rim.

Revised species taxonomy

Hayella sp. A

Basionym: *Hayella* sp. Steurbaut, 1991, pl. 2, figs. 24, 25; = *Cyclococcolithus* sp. Steurbaut, 1990, p. 53, pl. 1, figs. 8a, b, 9a, b, 10, 11.

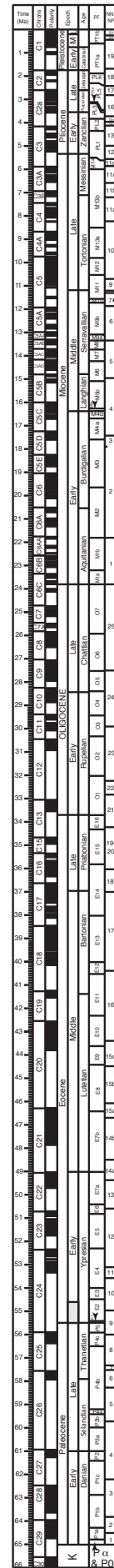
Hayella sp. B (Perch-Nielsen) n. comb.

Basionym: *Hayella* sp. Perch-Nielsen, 1977, pl. 45, figs. 3, 6, 10.

Hayella sp. Perch-Nielsen, 1977, pl. 45, figs. 3, 6, 10.

TEXT-FIGURE 3

Biochronology of *Hayella* species. Magnetobiochronologic framework from Cande and Kent (1992, 1995) with updated biochronology.



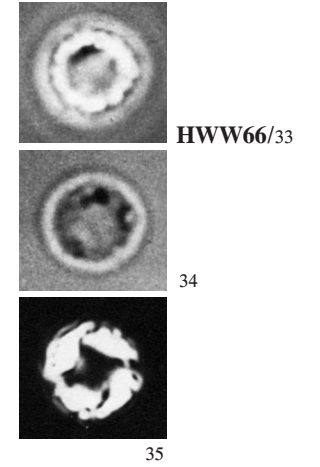
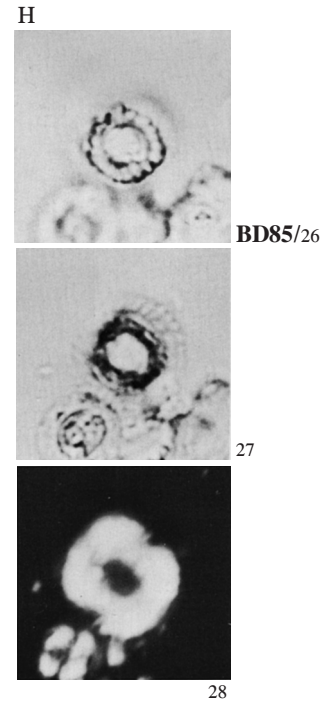
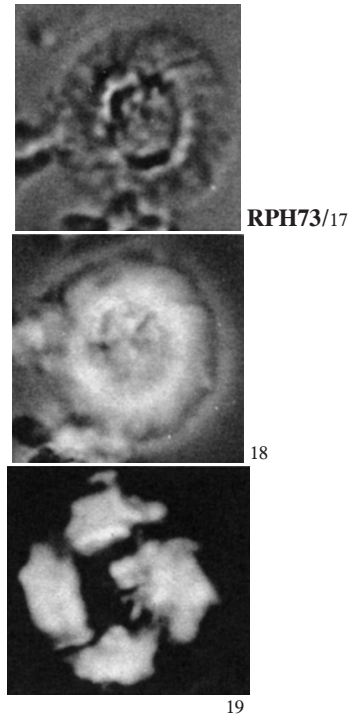
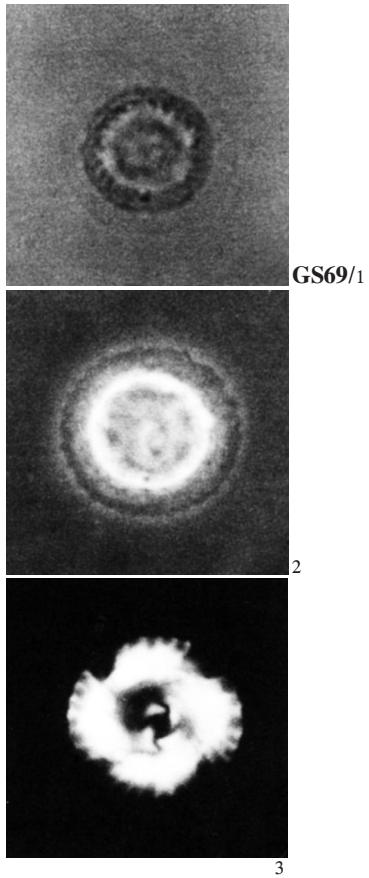
Hayella
 H. situliformis 37 Ma

Hayella situliformis Gartner 1969

Cyclolithella aprica Roth 1973

Hayella neoaprica (Bukry) n. comb. [= *Cyclolithella? neoaprica* Bukry 1985, p. 600, pl. 1, figs. 8-10]

Coronocyclus serratus Hay, Mohler, & Wade 1966, pl 11, figs. 1, 2, 3



Hayella situliformis

- ~10–12 μm

- L. Eocene. Shubuta Clay, Mississippi.

- Bucket-like calcareous body, circular or slightly elliptical in cross section with one rim at the narrower closed end and another rim at the larger open end. Constructed of 25 to 32 elements, inclined slightly to form a dextral spiral. The elements continue into both rims, terminate radially at the closed end but are moderately oblique in the rim at the open end. A short constricted extension of the wall, terminating in a circular to slightly elliptical opening extends beyond the rim at the open end.

- Remarks: This sp. has some superficial similarities to several calcareous nannofossil genera but probably is not closely related to any of these forms. The two rims suggest relationship to placoliths, but in *H. situliformis* the collar comprises most of the body, and the shields are reduced to mere rims. The most nearly similar genus is *Heliolithus* spp. which are constructed on the plan of two truncated cones joined at their narrow ends. *Hayella* is here assigned tentatively to the family Heliolithaceae.

- Its first occurrence closely corresponds to the first occurrences of *Chiasmolithus oamaruensis* and *Helicosphaera reticulata* and to the last occurrence of *C. grandis*, near the top of the middle Eocene (Gartner, 1971, p. 105).

— Occurs at low latitudes (Perch-Nielsen, 1972, p. 1006).

- GS69 (p. 32).

Cyclolithella aprica

- ~9 μm

- M. Eocene. Central Pacific.

- This species has a circular shield composed of about 32 to 34 sinistrally imbricate elements. The outer margin is serrate. The central area is almost one half the size of the whole coccolith. The inner margin of the shield is raised and consists of a cycle of laths with strongly clockwise inclined sutures. Due to secondary calcite overgrowths some of the elements of this inner rim cycle are completely fused to the elements of the shield. In the L.M., the individual elements in the shield can be distinguished. In C.N. the extinction figure consists of four slightly flaring bars.

≠ from *Cyclolithella robusta* by its serrate margin and by the raised rim along the central area.

— *C. aprica* is the isolated basal part of *Hayella situliformis* Perch-Nielsen (1977, p. 750).

- RPH73 (p. 730).

Hayella neoaprica

- 7–11 μm

- E. Oligocene (NP21). Atlantic Ocean.

- Form with a medium-sized, circular basal shield and an elevated tube cycle. Both the basal and tube cycle have sinistrally inclined crystallites in apical view. The periphery of each cycle is serrate. The tube opening occupies about a third the diameter of the basal shield and the outer tube wall occupies about half that diameter. The basal shield is composed of 25 to 35 crystallites and the tube cycle of 18 to 22 crystallites, both structures are bright in CN. Crystallites in the low relief basal shield are more distinct in CN.

≠ from *C. aprica* by a thicker and taller tube cycle and a much smaller central tube opening;

≠ from other circular coccoliths, e.g., *C. formosus*, by the much higher optic relief of the tube cycle than the basal shield as seen with a single polarizer.

- BD85 (p. 600), AMP (p. 248).

Coronocyclus serratus

- ~5 μm

- L. Eocene (NP19). Caucasus.

— As suggested by Gartner (1969a, p. 34) Paratype UI-H-2097 of *Coronocyclus serratus* illustrated by Hay et al. (1966) from the Upper Eocene *Isthmolithus recurvus* Zone at Nal Chik (Caucasus) does not match the holotype of this species (op. cit., pl. 11, fig. 4), but is a representative of *Hayella situliformis*.

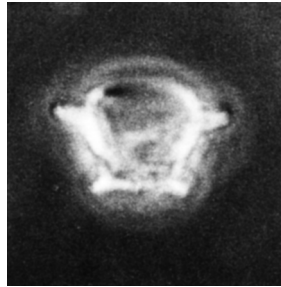
- HWW66 (p. 394).

Hayella situliformis (continued)

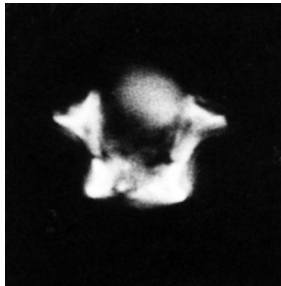
Hayella aprica (continued)



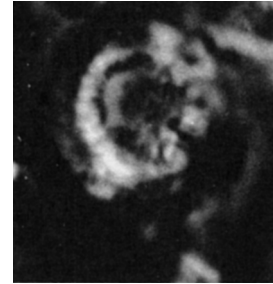
GS69/4



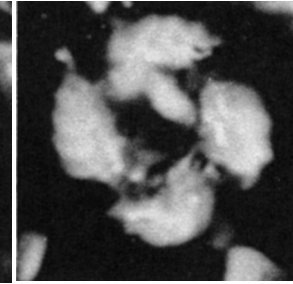
5



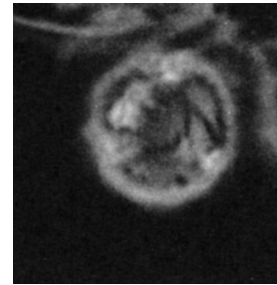
6



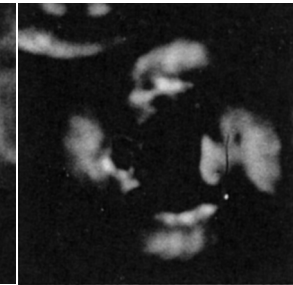
RPH73/20



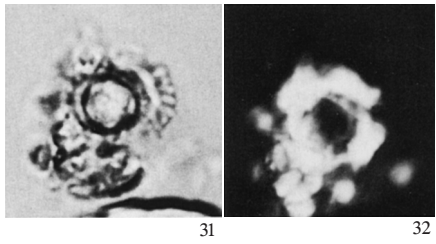
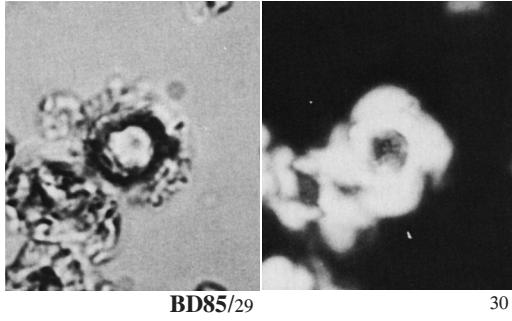
21



22

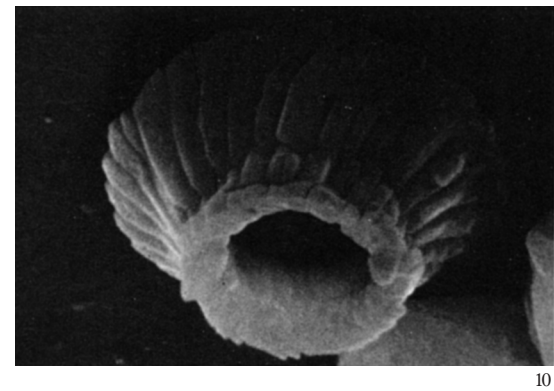
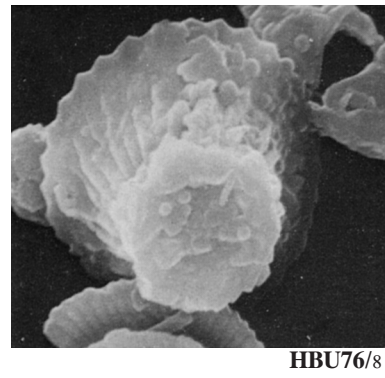
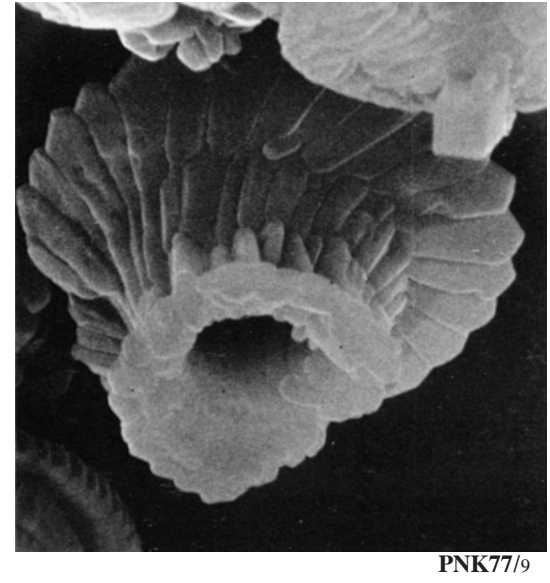
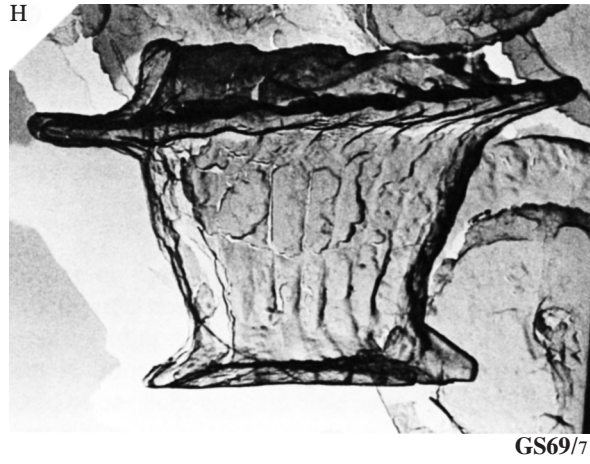


23



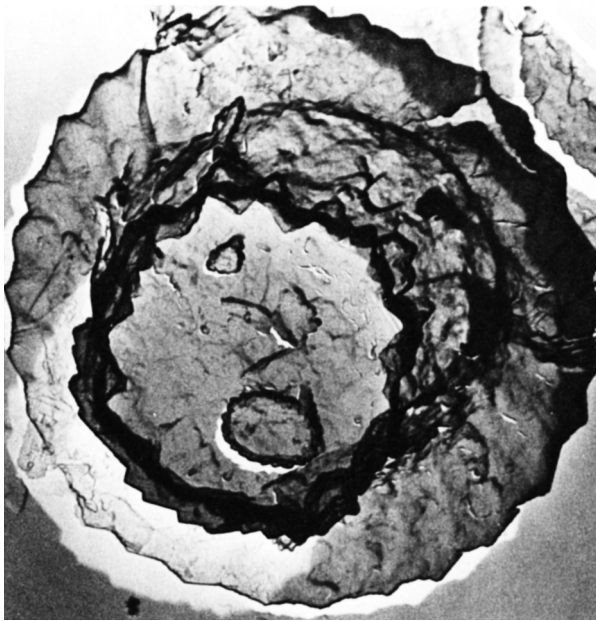
Hayella situliformis (continued)

SIDE VIEW

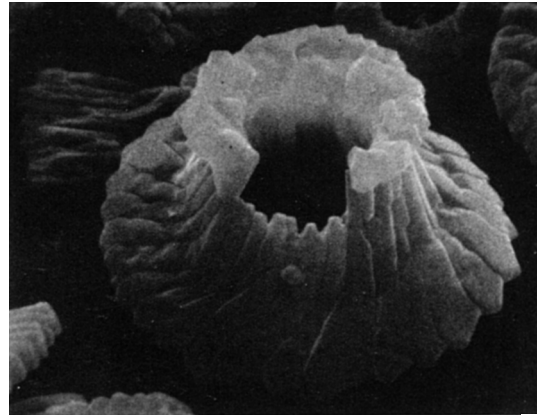


Hayella situliformis (continued)

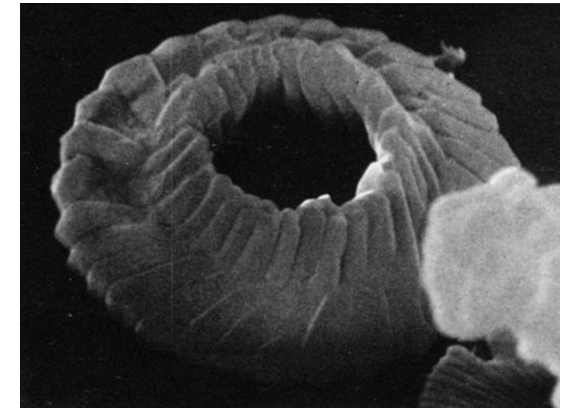
PROXIMAL FACE



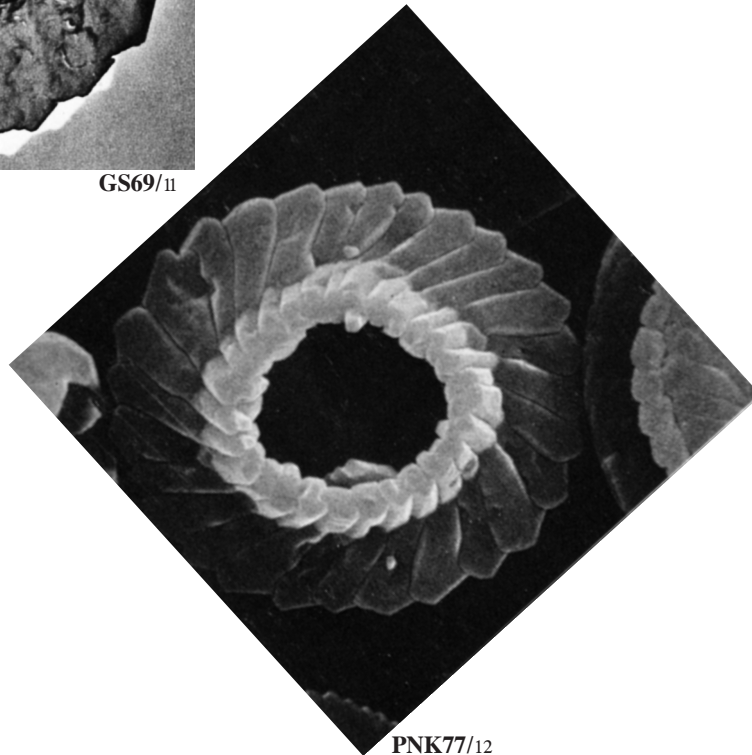
GS69/11



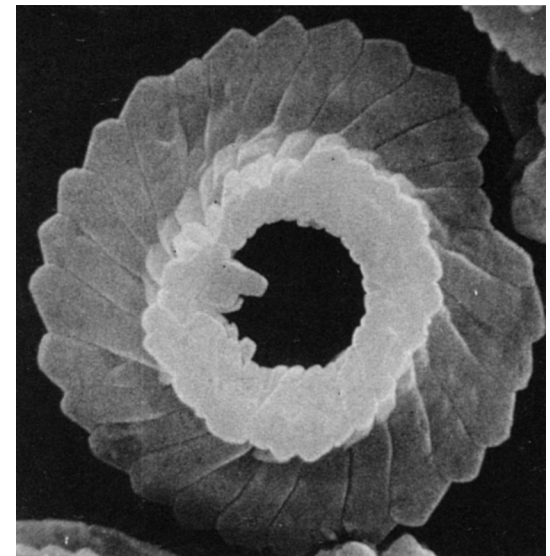
13



14



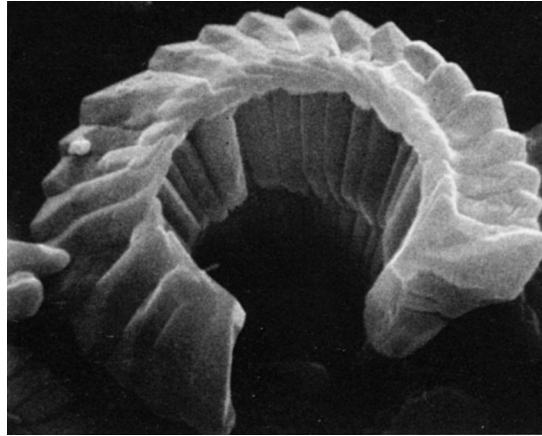
PNK77/12



15

Hayella situliformis (continued)

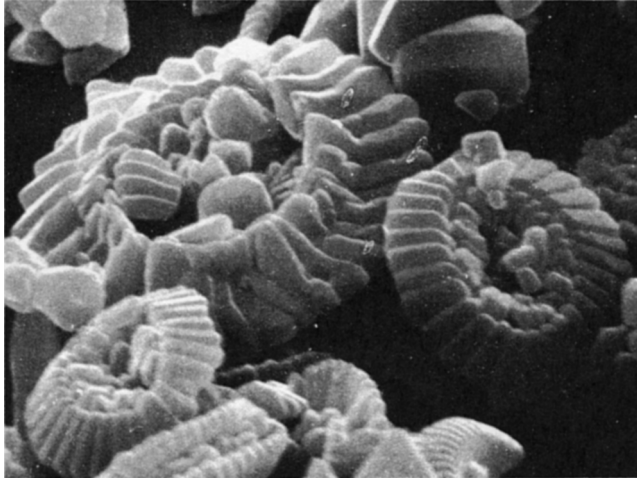
DISTAL FACE



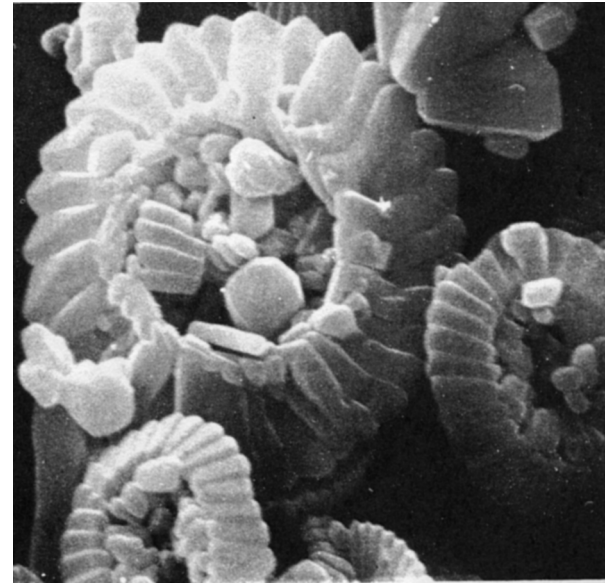
PNK77/16

DISTAL FACE

H



RPH73/24



25

Hayella? gauliformis Troëlsen & Quadros 1971

Hayella sp. A [= *Hayella* sp. Steurbaut 1991, pl. 2, figs. 24, 25; = *Cyclococcolithus* sp. Steurbaut 1990, p. 53, pl. 1, figs. 8a, b, 9a, b, 10, 11]

Hayella aperta Theodoridis 1984

Hayella challengeri (Müller) Theodoridis 1984 [= *Nannocorbis challengeri* Müller 1974]

Hayella sp. B (Perch-Nielsen) n. comb. [= *Hayella* sp. Perch-Nielsen 1977, pl. 45, figs. 3, 6, 10]



TJC71/36



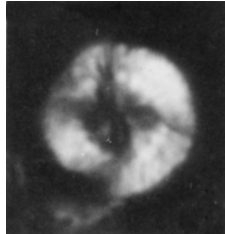
37



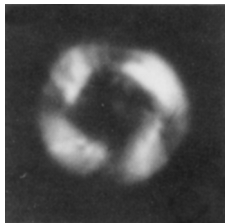
38



39

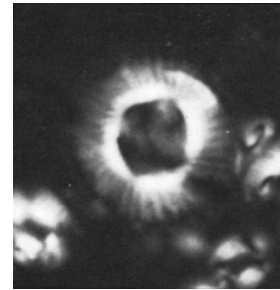


SE91/41

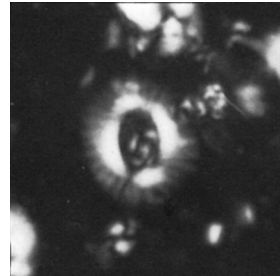


42

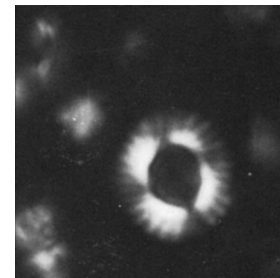
H



TS84/49



50



51

Hayella? gauliformis

- ~6.8 μm

- E. Eocene (NP12). Brazil.

- [Bucket-shaped body, circular to slightly elliptical in cross section, with a rim at each end. Both ends seem to be open. Wall with delicate transverse striae.]

≠ from *H. situliformis* by the absence of an extension of the wall at the widest end. Also, the narrowest end seems to be open in *H. ? gauliformis*, whereas it is closed in *H. situliformis*.

- Remarks: The striae visible on the wall of this sp. may be an optical artifact, and may not reflect the real structure of the wall.

- TJC71 (p. 602).

Hayella sp. A

- 7–9 μm

- M. Eocene (Zone NP14). Knokke Well Den Hoorn and Brussel Formations, Belgium.

- Circular; outer cycle of 30 to 35 elements with anti-clockwise oblique sutures; central area closed by radial elements. In CP light, outer cycle is very bright and central area is only faintly illuminated with a central fairly broad extinction cross.

- Remarks: “This form is related to *Cyclococcolithus hirsutus* Müller 1970 and *Cyclococcolithus hoerstgensis* Müller 1970 known respectively from the Middle Oligocene of Belgium and the Upper Oligocene of Germany (see Müller, 1970:93, pl. 9, figs. 1-4 and 94; pl. 9, figs 5-8). However, since no SEM photos are available of any of these three forms it is difficult to decide whether the Knokke material represents a new species or not”. (Sturbaut, 1990, p. 53).

— Two specimens illustrated (without description except for mention “distal view” in figure caption) from the Ieper Formation (Roubaix Clay Member) under the name *Hayella* sp. by Sturbaut (1991). They were recovered from Zone NP12, in Nannozone IIIb2 of Sturbaut (1991).

— If synonymy above is correct (based on Sturbaut’s designation of “*Hayella* sp.” 1991, p. 265) this taxon ranges from NP12 (partim) and NP14.

- SE90 (p. 53), SE91 (p. 265), AMP (p. 248).

Hayella aperta

- Miocene ([?NN1] NN2–NN6). Atlantic Ocean (Sierra Leone Rise, DSDSP Site 369A).

- Calcareous body resembling a short conical tube, with 30 to 35 elements that imbricate dextrally (when observed from the smaller base of the cone); at both ends of the tube they terminate radially and form two narrow shields.

≠ from *H. situliformis* by the shorter cone and the large opening at the narrow end of the tube; ≠ from *H. gauliformis* which has comparable openings but a longer cone; ≠ from *H. challengerii* which is much smaller.

Remarks: “*H. aperta* superficially resembles *G. rotula*, in plane view, but it is easily distinguished by its brighter birefringence and its conical shape which becomes apparent when the level of focus of the light microscope is changed.”

- MC74 (p. 82).

Hayella challengerii

- 3.4–5 μm

- L. Miocene – E. Pliocene. Western Indian Ocean.

- Twenty to twenty-five robust elements which form the short tube, turned externally at each end. At the base, only a narrow rim is developed while at the distal side the rim is widened by an additional ring of elements. Elements of the rim arranged radially, and turned back to a vertical direction in the wall of the tube.

— Perch-Nielsen (1977) questionably assigned to *Hayella* sp. (p. 750) a coccolith recovered from the Upper Miocene (Zone NN12) at South Atlantic DSDP Site 354 (but illustrated it as *H. situliformis* (p. 807, 810, pl. 41, fig. 10.) This coccolith was assigned to *H. challengerii* by Theodoridis (1984). However, the specimen illustrated by Perch-Nielsen would seem more elongate than *H. challengerii*, which is short and broad.

— Ranges from lower Zone NN11 to lower Zone NN12 in the Mediterranean area (Theodoridis, 1984).

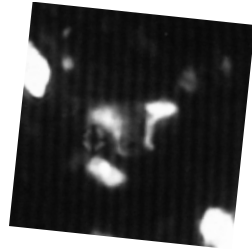
- PNK77 (p. 593), TS84 (p. 83).

Hayella sp. B

— Perch-Nielsen (1977) illustrated three incomplete coccoliths recovered from the Lower Miocene (Zone NN2) at South Atlantic DSDP Site 356, questionably referring them to *Hayella?* sp. It is possible that these specimens correspond to *Hayella aperta* Theodoridis 1984.

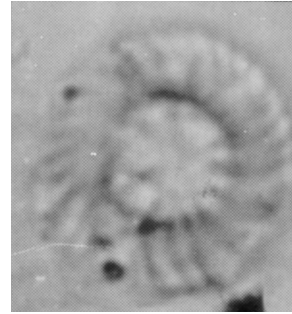
- PNK77 (p. –).

Hayella? gauliformis (continued)

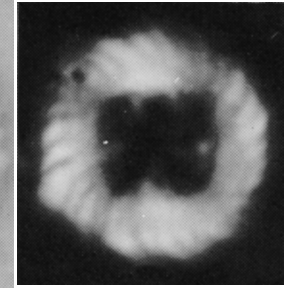


BPR05a/40

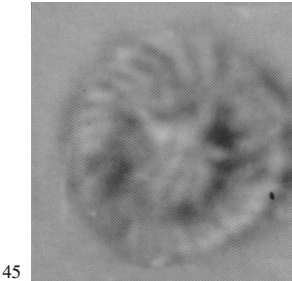
Hayella sp. A (continued)



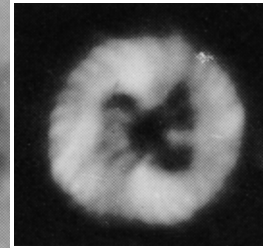
SE90/43



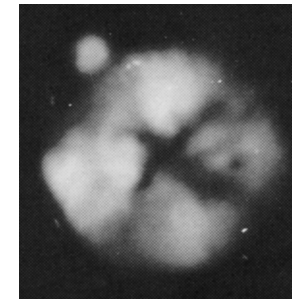
44



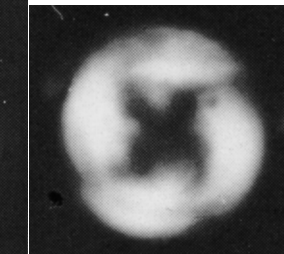
45



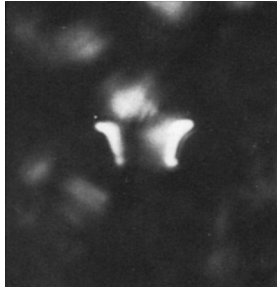
46



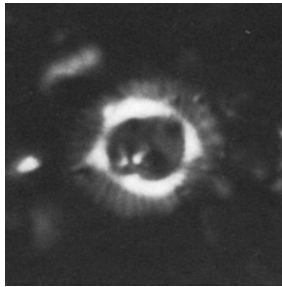
47



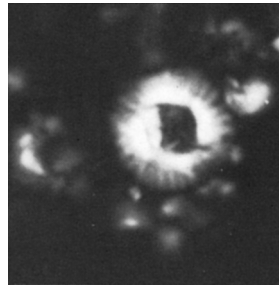
48



TS84/52



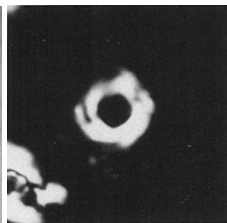
53



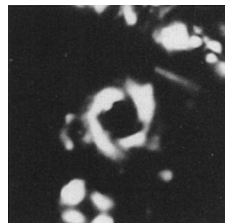
54



RD90/55



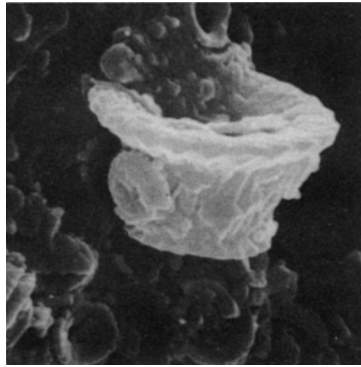
56



57

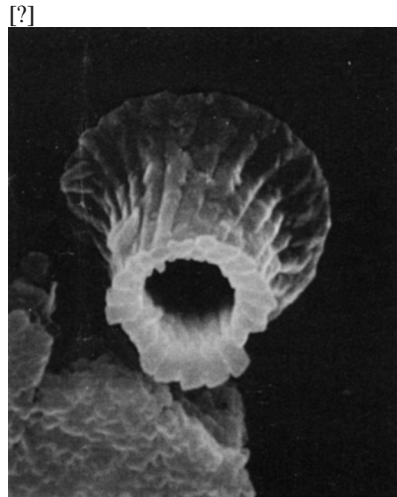
Hayella challengeri (continued)

SIDE VIEW



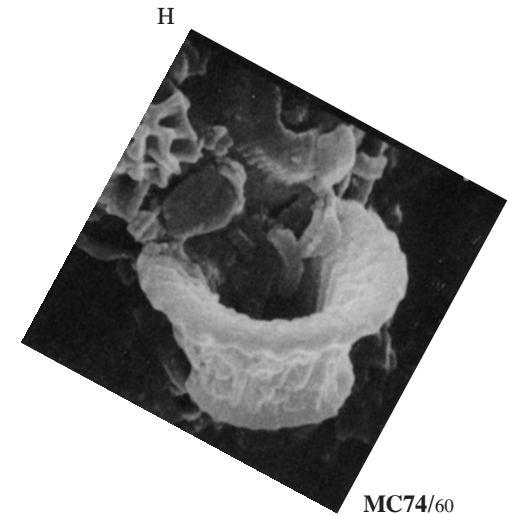
MC74/58

PROXIMAL FACE



PNK77/59

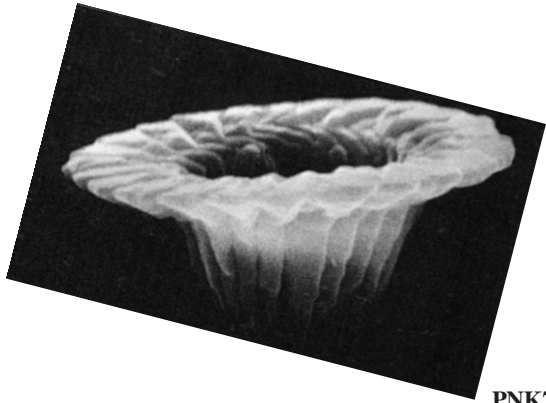
DISTAL FACE



MC74/60

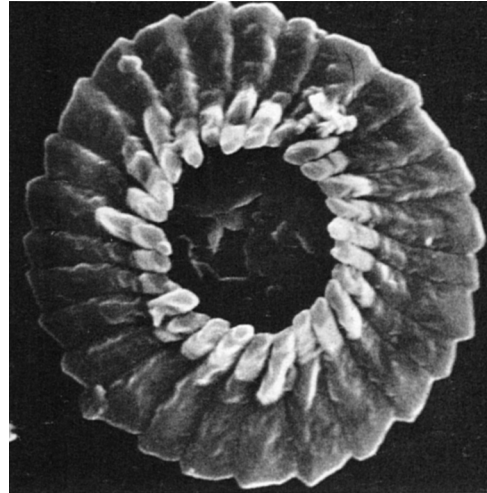
Hayella sp. B (continued)

SIDE VIEW



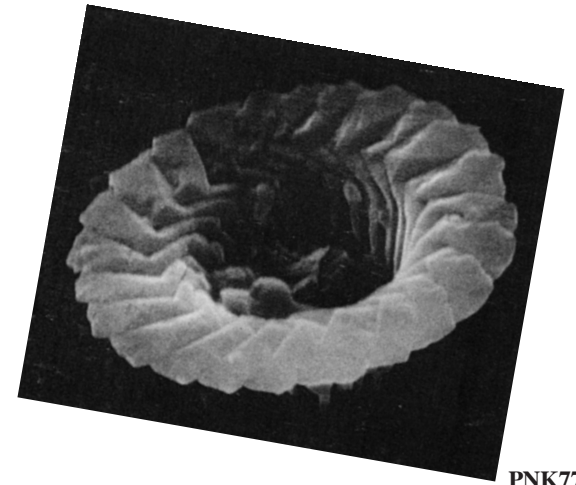
PNK77/61

PROXIMAL FACE



PNK77/62

DISTAL FACE



PNK77/63

Figure References

- AMP.** AUBRY, M.-P., this volume.
- BPR05a.** BOWN, P. R., 2005a. *Journal of Nannoplankton Research*, 27: 21–95.
(40): 10/35 (*H. gauliformis*)
- BD85.** BUKRY, D., 1985. In: Bougault H., Cande S. C., et al., *Initial Reports of the Deep Sea Drilling Project*, 82, 591–603, Washington, D. C.: U.S. Government Printing Office.
(26-28): 1/8-10 (as *Cyclolithella neoaprica*)
(29-32): 1/6, 7, 11, 12 (as *Cyclolithella neoaprica*)
- GS69.** GARTNER, S., 1969a. *Micropaleontology*, 15: 31–34.
(1-3): 1/5b, a, c (*H. situliformis*)
(4-6): 1/4b, a, c (*H. situliformis*)
(7): 1/6 (*H. situliformis*)
(11): 1/7 (*H. situliformis*)
- HBU76.** HAQ, B. U. and LOHMANN, G. P., 1976. *Marine Micropaleontology*, 1: 119–194.
(8): 6/12 (as *Discoasteroides megastypus*)
- HWW66.** HAY, W. W., MOHLER, H. P. and WADE, M., 1966. *Calcareous nannofossils from Nal'chik* (Northwest Caucasus). *Eclogae Geologicae Helveticae*, 59: 379–399.
(33-35): 11/1-3 (as *Coronocycus serratus*)
- MC74.** MÜLLER, C., 1974. In: Simpson, E. S. W., Schlich, R., et al., *Initial Reports of the Deep Sea Drilling Project*, 25, 579–633. Washington, D. C.: U.S. Government Printing Office.
(58, 60): 15/4, 5 (as *Nannocorbis challengerii*)
- PNK77.** PERCH-NIELSEN, K., 1977. In: Supko, P. R., Perch-Nielsen, K., et al., *Initial Reports of the Deep Sea Drilling Project*, 39, 699–823. Washington, D. C.: U.S. Government Printing Office.
(59): 41/10 (as *H. situliformis*)
(9, 10): 44/1, 4 (*H. situliformis*)
(12-15): 44/6, 2, 5, 3 (*H. situliformis*)
(16): 44/7 (*H. situliformis*)
(61-63): 45/3, 10, 6 (as *Hayella?* sp.)
- RD90.** RIO, D., FORNACIARI, I. and RAFFI, I., 1990. In: Duncan, R. A., Backman, J., Peterson, L. C., et al., *Proceedings of the Ocean Drilling Program, Scientific Results*, 115, 175–235. College Station, Texas: Ocean Drilling Program.
(55-57): 14/1a, b, 2 (*H. aperta*)
- RPH73.** ROTH, P. H., 1973. In: Winterer, E. L., Ewing, J. L., et al., *Initial Reports of the Deep Sea Drilling Project*, 17, 695–795. Washington, D. C.: U.S. Government Printing Office.
(17-19): 12/4c, b, a (as *Cyclolithella aprica*)
(20-23): 12/1a, b, 2a, b (as *Cyclolithella aprica*)
(24, 25): 11/4, 6 (as *Cyclolithella aprica*)
- SE91.** STEURBAUT, E., 1991. *Bulletin de la Société belge de géologie*, 97: 251–285.
(41, 42): 2/24, 25 (as *Hayella* sp.)
- SE90.** STEURBAUT, E., 1990. In: Laga, P. and Vanderberghe, N., Eds., *The Knokke Well (11E/138) with a description of the Den Haan (22W/276) and Oostduinkerke (35E/142) wells*, 47–62. Bruxelles: Service géologique de la Belgique. Mémoire pour servir à l'Explication des Cartes géologiques et minières de la Belgique, 29.
(43-48): 1/8b, a, 9a, b, 10, 11 (as *Cyclococcolithus* sp.)
- TS84.** THEODORIDIS, S., 1984. *Utrecht Micropaleontological Bulletins*, 32: 1–271.
(49-51): 3/3, 5, 6 (*H. aperta*)
(52-54): 3/4, 7, 8 (*H. aperta*)
- TJC71.** TROËLSEN, J. C. and QUADROS, L. P., 1971. *Academia Brasileira de Ciências, Anales*, 43, suplemento: 577–609. (Simpósio Brasileiro do Paleontologia).
(36-39): 7/115-118 (*Hayella?* *gauliformis*)

HIGHLIGHTS:

- ~5–9 μm .
- Enigmatic coccoliths from the Paleocene.
- Illustrated from Jordan and the North Atlantic Ocean (Bay of Biscay).
- Known from Zone NP7 (?NP8).

SELECTED READING

Bralower and Mutterlose, 1995; Haq and Aubry, 1980; Perch–Nielsen, 1972.

DISCUSSION

Three specimens of an enigmatic coccolith named *Heliolithus floris* were described from the Upper Paleocene of Jordan by Haq and Aubry (1980). These incomplete specimens are comprised of at least two structural units with a shape and structure that are not known in other coccoliths. One structural unit consists of a tall, thin and flaring cycle of joint elements with radial sutures, which is reminiscent of the column of some sphenoliths. As seen in distal view, the serration at the periphery of this cycle exhibits the SL pattern (op. cit., pl. 6, figs. 9, 10). This, and the radial elements, indicate a taxonomic position in the Order Discoasterales. The other structural unit is a thin and narrow rim at the distal end of the column (op. cit., pl. 6, fig. 11). The specimens are generally poorly preserved and exhibit evidence of dissolution and overgrowth (op. cit., pl. 6, fig. 10 and pl. 6, figs. 9, 11, respectively).

An unnamed specimen clearly related to *H. floris* was illustrated from the Upper Paleocene Zone NP7 at DSDP Site 119 (Bay of Biscay) by Perch–Nielsen (1972, pl. 21, fig. 3). This specimen differs from *H. floris* in having a less flaring column, and a pattern of furrows along the elements whereas the best-preserved specimen from Jordan (op. cit., pl. 6, fig. 10) shows a longitudinal ridge running in the middle of each element. These differences may be diagenetic effects.

Two specimens assigned to *H. floris*, illustrated in light microscopy (Bralower and Mutterlose, 1995, pl. 6, figs. 12–13, 19–20), have been recovered at ODP Site 865 on Allison Guyot, Mid-Pacific Mountains, from an interval assigned to Zone CP6 of Okada and Bukry (1980) and undifferentiated Zones NP7–8 (Martini, 1971). These specimens would indicate that the column is non-birefringent, unlike the distal cycle. It remains to be confirmed, however, if these specimens really belong to *H. floris*.

A specimen with a similar extinction pattern albeit with fewer elements than Bralower and Mutterlose’s specimens was also illustrated from Zone NP9 in Tanzania by Bown (2010, fig. 5, third specimen from the right).

TAXONOMY

Assignment of the species *floris* to *Heliolithus* is clearly unjustified. With a morphology and structure unknown in other coccoliths of the Order Discoasterales, the taxon is currently a systematic orphan. The erection of a new genus for this material would benefit, however, from comprehensive description of better-preserved and fully documented specimens.

Heliolithus floris is more suitably placed in open nomenclature.

Genus *A. floris* (Haq & Aubry) Aubry 2014 [= *Heliolithus floris* Haq & Aubry 1980]

Genus *A. floris*

- ~9 μ m
- L. Paleocene. Jordan.
- ** A short proximal column that flares slightly at the proximal end. Thin distal cycle, also slightly flaring.
- The assignment of this sp. to *Heliolithus* is questionable.

Genus *A. floris* (continued)

PROXIMAL FACE

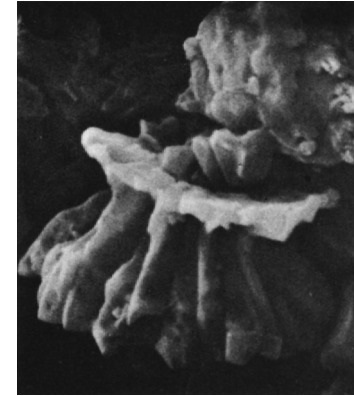
SIDE VIEW



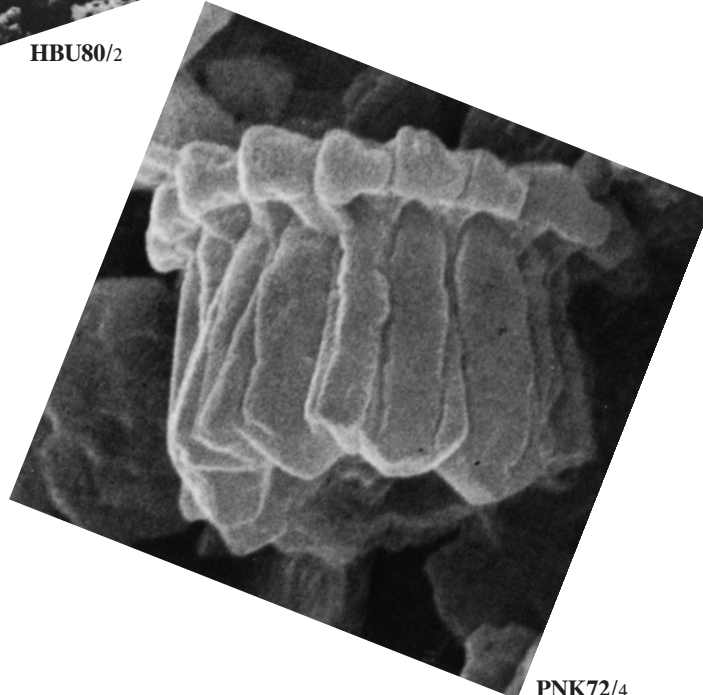
HBU80/1



HBU80/2



3



PNK72/4

Figure References

1. **AMP.** AUBRY, M.-P., this volume.
2. **HBUS80.** HAQ, B. U. and AUBRY, M.-P., 1980. In: Salem, M. J. and Busrewil, M. T. (Eds.), *The geology of Libya, Volume 1*, 271–304. London: Academic Press.
(1): 6/9 (as *Heliolithus floris*)
(2, 3): 6/10, 11 (as as Gen. et Sp. indet.; cone shaped specimens bottom and side view)
3. **PNK72.** PERCH-NIELSEN, K., 1972. In: Supko, P. R., Perch-Nielsen, K., et al., *Initial Reports of the Deep Sea Drilling Project, 12*, 1003–1069. Washington, D. C.: U.S. Government Printing Office.
(4): 14/3 (as Gen. et sp. indet.)

INTRODUCTION

Four taxa have been assigned to genera of the Order Discoasterales although they do not display their characters. These taxa are regrouped here until new information help clarifying their taxonomic position.

Heliolithus crassus Müller 1976

Heliolithus crassus is an enigmatic taxon (text-fig. 1) recovered from Upper Pleistocene sediments. Known from five coccoliths, two of them illustrated in bright field and cross-polarized light, the other three in the SEM, it exhibits the morphology and extinction patterns of the helioliths of *Heliotrochus* and, like them, possesses a wide, disc-shaped structural unit associated with a tall, narrow, cone-shaped structural unit. There is no indication of a third cycle unless the specimen illustrated in plate 3, fig. 3 represents the face opposite to that of the other two specimens. The specimens are rather poorly preserved, with the larger structural unit strongly etched at the periphery, with non-imbricate elements and sutures curved clockwise, in an arrangement similar of that of the elements of the column of *Heliotrochus* as seen in proximal view. The elements of the narrower but thicker unit are imbricate dextrally, with the sutures inclined anticlockwise as in a calyptra. These characters are opposite to those seen in *Heliotrochus* helioliths, in the sense that the calyptra is always thinner and broader than the column in the latter genus.

Heliolithus crassus is more suitably placed in open nomenclature, and it is provisionally included in the Family *Heliolithaceae*.

Hayella simplex Bown & Jones 2006

This Middle Eocene taxon is known only from distal and proximal views illustrated in bright field and cross-polarized light. It is assigned to *Hayella* Gartner 1969 based on its vacant central area but it does not display the elevation characteristic of this genus. The taxonomic position of this taxon is thus questionable.

Bomolithus supremus Bown 2010 and *Bomolithus aquilus* Bown 2010

Bown (2010, p. 23) commented that due to the lack of adequate illustrations, the taxonomy of the “nannoliths closely allied to the discoasters” was “rather poor at both generic and species levels” and summarized the situation as follows:

“Typically, the genus *Heliolithus* Bramlette & Sullivan, 1961 [i.e., *Heliotrochus* n. gen. herein] is used for taxa that have birefringent images, *Bomolithus* for forms with a single, birefringent cycle that is narrower than the diameter of the nannolith (although simply the possession of three cycles, not the crystallography, has been used as a diagnostic criterion by some. e.g. Romein, 1979), and both *Discoaster* [*Heliodiscoaster* (Tan) herein] and *Bomolithus* have been used for taxa where the birefringent cycle is narrow.”

Linking the degree of birefringence exhibited by these coccoliths to the development of the R- and V- units, he proposed an evolutionary trend “first towards reduction in the width of the birefringent (R-unit) cycle (in *Bomolithus*) and, second, towards loss of cycles,

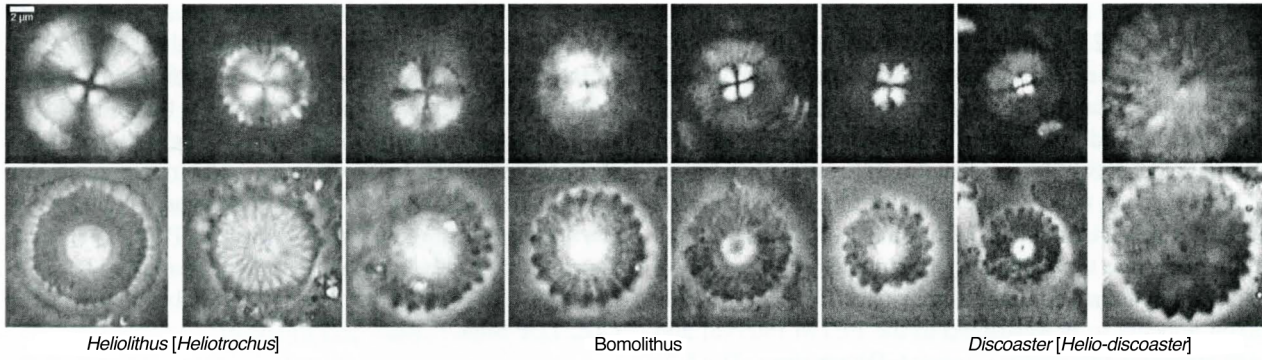
until only one, the V-unit, remains (in *Discoaster*)” (text-fig. 1). In practice, *Bomolithus* was “used for taxa where the birefringent cycle is narrower than the diameter of the nannolith”, but also included “a new species, *Bomolithus aquilus*, where several cycles are present, but they are non-birefringent”; a definition that is at odds with that of the genus, as defined.

Bown’s criteria (2010) for *Bomolithus* are unrelated to those used by Roth (1973), who made no reference to the extinction pattern of the coccoliths. Instead, Roth introduced this genus to distinguish a group with a specific arrangement of three cycles (see *Bomolithus*, this volume). While extinction patterns are a practical means to classify coccoliths, several authors have worked with little success, to develop a comprehensive definition of heliolith genera based on the association of morphostructure and number of birefringent cycles. The absence of a demonstrable relationship between morphostructure and extinction patterns among helioliths and early asteroliths has led to inconsistent classifications (see CC-B, Order Discoasterales).

In the absence of clear relation between morphostructure and extinction patterns in helioliths, priority must be given to morphostructure as the original criterion for recognition of *Bomolithus*. As a case in point, neither of the specimens assigned to *Bomolithus supremus* and *Bomolithus aquilus* on the basis of extinction patterns display the shape and structure characteristic of the coccoliths of *Bomolithus* Roth 1973.

Bomolithus aquilus Bown 2010 described from the Upper Paleocene (Zone NP9) in Tanzania, is based on poorly preserved material, including the holotype (op. cit., pl. 10, fig. 2), and its taxonomic position is dubious.

Bomolithus supremus Bown and Jones 2006 was also described from the Upper Paleocene (Zone NP9) in Tanzania. The specimen illustrated in scanning electron microscopy (Bown, 2010, pl. 10, fig. 8) is an asterolith seen in distal view. If it is representative of the taxon, the latter is assignable to *Heliodiscoaster*, and it is possibly synonymous with *Heliodiscoaster protomultiradiatus* Wei 1998 (see CC-D, *Heliodiscoaster*).



TEXT-FIGURE 1

Evolutionary trend from *Heliolithus* (*Heliotrochus* herein) to *Discoaster* [*Heliodiscoaster* herein] via *Bomolithus* as reflected by changes in the extinction pattern of the coccoliths. (From Bown, 2010, fig. 5: “LM images (upper row XPL, lower row PC) representing the range of morphologies seen in the genera *Heliolithus* (two furthest left images), *Bomolithus*, and *Discoaster* (two furthest right images). Images from TDP Site 19 (NP6), except for last four on the right, which are from TDP Site 14 (NP9).”)

Genus *B crassus* (Müller) n. comb. [= *Heliolithus crassus* Müller 1976]



BPR05/1



2



3



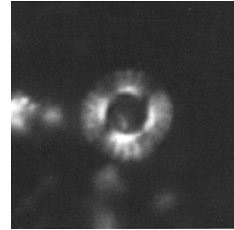
4

Hayella simplex Bown & Jones 2006 [= *Hayella* sp. Bown 2005]

H

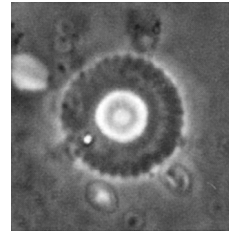


BPR06/5

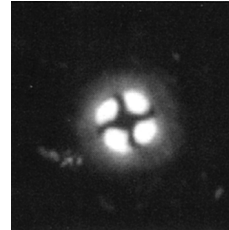


6

Bomolithus supremus Bown and Jones 2006



BPR06/14

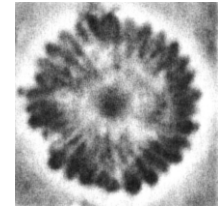


15

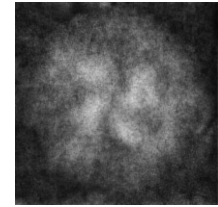


16

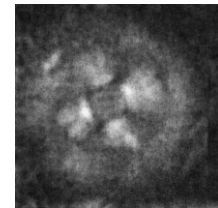
Bomolithus aquilus Bown 2010



BPR10/30



31



32

Genus *B crassus*

- 10–13 μm

- L. Pleistocene (NN21). Red Sea.

- [Flat median cycle made of about 30 radial elements. Narrow distal cycle consisting of about 18 small elements. Proximal column more or less thickened, made of 30 elements in low spiral arrangement, strongly birefringent.]

≠ from *H. kleinpellii* by its much smaller size and by the more thickened column.

— Probably a reworked specimen of *H. kleinpellii*.

Hayella simplex

- 5–7 μm

- M. Eocene (NP14b-NP16). Tanzania.

- Medium sized, circular coccolith with an open, vacant central area. Shield elements distinct and show obliquity. The shield image is brighter towards the inner edge.

≠ from *H. situliformis* in lacking the elevated cycle characteristic of this sp.

— This taxon does not exhibit the characters of the genus. Its taxonomic position is uncertain at this time.

Bomolithus aquilus

- 8.2–9.0 μm

- L. Paleocene (NP9b above CIE). Tanzania.

- Medium-sized, circular heliolith with at least two discernable cycles in the LM, both of which are dark in XPL. The cycles comprise around 40 visible radial elements, and the central area is typically closed.

≠ from other *Bomolithus* spp. and *Heliolithus* spp. by the absence of a birefringent cycle.

Bomolithus supremus

- 5.3–8.3 μm

- L. Paleocene (NP9b above CIE). Tanzania.

- A circular nannolith that typically appears to comprise three distinct cycles, with only the innermost exhibiting birefringence in XPL; the central area is a narrow hole or closed. The outermost cycle is dark in PC and the distinct elements show obliquity. The innermost cycle shows white interference colours and is crossed by thick extinction lines that are rotated approximately 5° from axial.

≠ from other species of *Bomolithus* Roth, 1973, in being less elevated and of younger age except for *Bomolithus/Discoaster megastypus* Bramlette & Sullivan, 1961 (e.g. Perch-Nielsen, 1985; Steurbaut, 1998); ≠ from the similar *Bomolithus conicus* (Perch-Nielsen, 1971c), in having a more distinctly birefringent inner cycle and a younger stratigraphic range (Zone NP9 vs. Zone NP6).

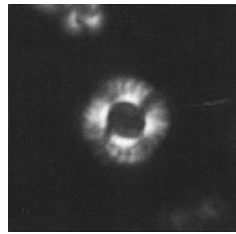
- MC76 (p. 51), AMP (p.277).

- BPR06 (p. 18), BPR05 (p. –).

- BPR10 (p. 23)

- BPR06 (p. 23)

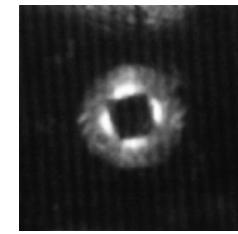
Hayella simplex (continued)



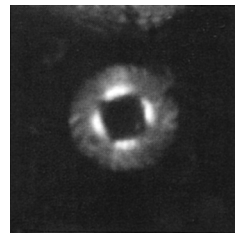
BPR06/7



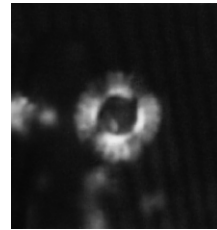
BPR05/9



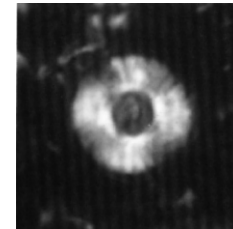
11



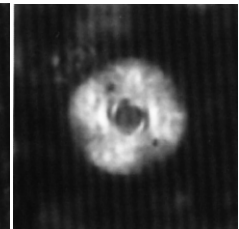
8



10



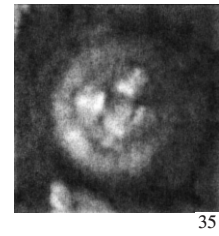
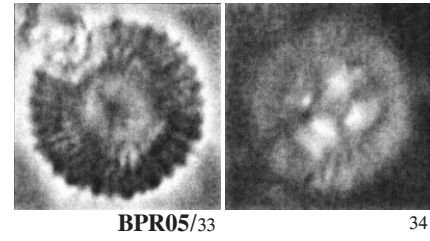
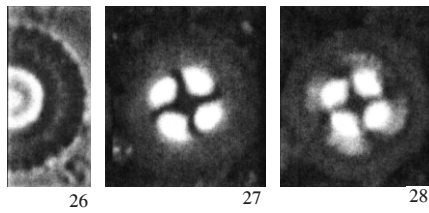
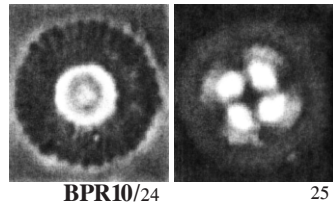
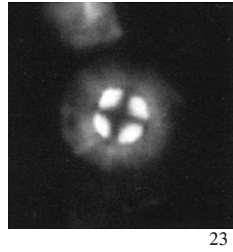
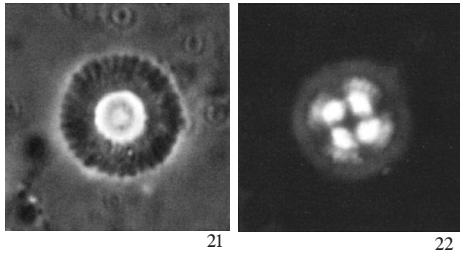
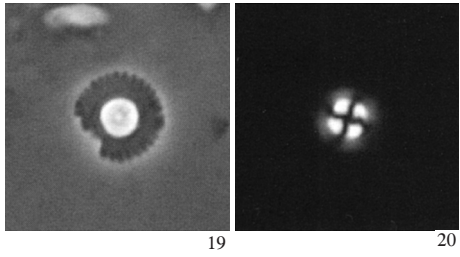
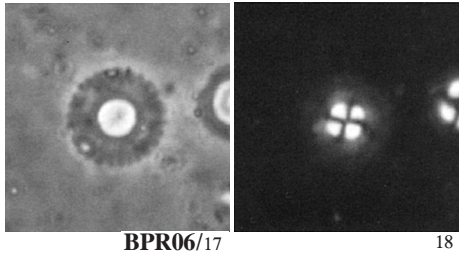
12



13

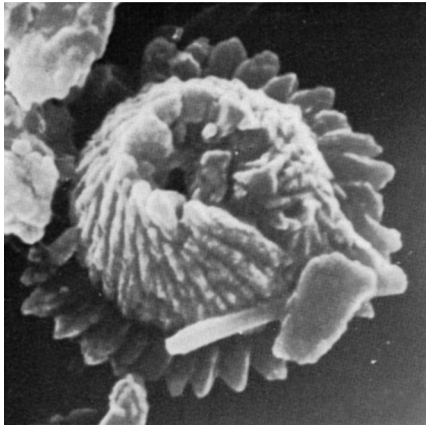
Bomolithus supremus (continued)

Bomolithus aquilus (continued)

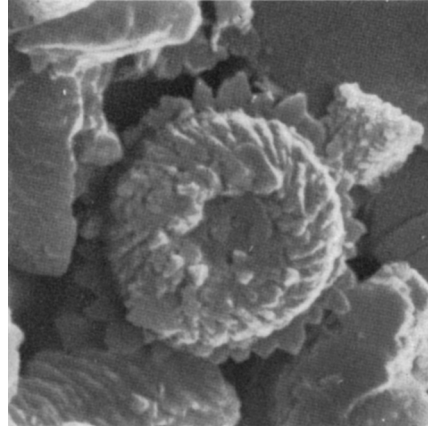


Genus B (continued)

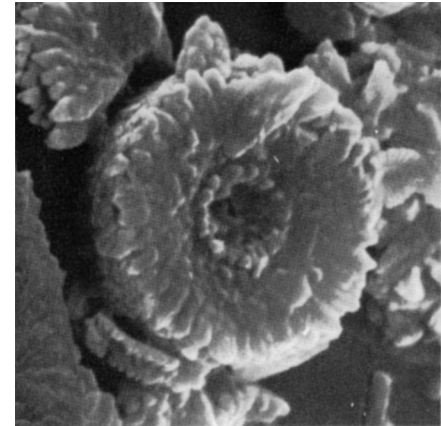
H



5/5



6



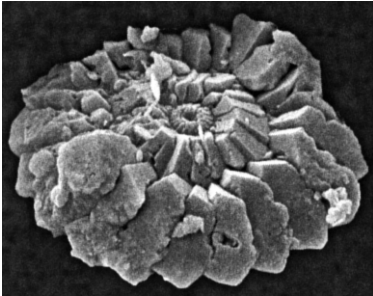
7

Bomolithus supremus (continued)

Bomolithus aquilus (continued)

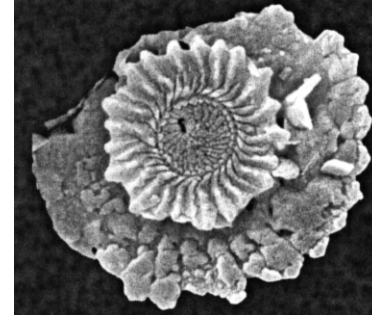
DISTAL FACE

[?]



BPR10/29

[?]



BPR10/36

Figure References

1. **AMP.** AUBRY, M.-P., this volume.
2. **BPR05.** BOWN, P. R., 2005a. *Journal of Nannoplankton Research*, 27: 21–95.
(9-13): 10/2, 1, 3-5 (as *Hayella?* sp.)
3. **BPR10.** BOWN, P. R., 2010. *Journal of Nannoplankton Research*, 31: 11–38.
(24-28): 10/9 (two pictures), 10 (three pictures) (*B. supremus*)
(29): 10/8 (*B. supremus*)
(30-32): 10/2 (three pictures) (*B. aquilus*)
(33-35): 10/3 (two pictures), 4 (*B. aquilus*)
(36): 10/1 (*B. aquilus*)
4. **BPR06.** BOWN, P. R. and DUNKLEY JONES, T. D., 2006. *Journal of Nannoplankton Research*, 28(1): 17-34.
(5, 6): 1/14, 13 (*H. simplex*)
(7, 8): 1/12, 15 (*H. simplex*)
(14-16): 7/32, 31, 30 (*B. supremus*)
(17-23): 7/26, 25, 28, 27, 34, 33, 29 (*B. supremus*)
6. **MC76.** MÜLLER, C., 1976. *Geologisches Jahrbuch, D*, 17: 33–77.
(1-4): 4/7-10 (*H. crassus*)
(5-7): 3/1-3 (*H. crassus*)

REFERENCES

- AGNINI, C., FORNACIARI, E., RAFFI, I., RIO, D., RÖHL, U. and WESTERHOLD, T., 2007. High resolution nannofossil biochronology of middle Paleocene to Early Eocene at ODP Site 1262: Implications for calcareous nannoplankton evolution. *Marine Micropaleontology*, 64: 215–248.
- AGNINI, C., FORNACIARI, E. and RAFFI, I., 2008. Three new species of calcareous nannofossil from Late Palaeocene and Early Eocene assemblages (Ocean Drilling Program Site 1262, Walvis Ridge, SE Atlantic Ocean). *Journal of Nannoplankton Research*, 30: 51–56.
- AUBRY, M.–P., 1986. Paleogene calcareous nannoplankton stratigraphy of northwestern Europe. *Palaeogeography, Palaeoclimatology, Palaeoecology*, 55: 267–334.
- AUBRY, M.–P., 1989. *Handbook of Cenozoic Calcareous nannofossils, volume 3*. New York: Micropaleontology Press, 279 pp.
- AUBRY, M.–P., 1998. Early Paleogene calcareous nannoplankton evolution: A tale of climatic amelioration. In: Aubry, M.–P., Lucas, S. and Berggren, W. A., *Late Paleocene–Early Eocene climatic and biotic events in the marine and terrestrial records*, 158–203. New York: Columbia University Press.
- AUBRY, M.–P., *Cenozoic Coccolithophores: Discoasterales. CC-B*. New York: Micropaleontology Press. Atlas of Micropaleontology series, 3 volumes, (in press).
- AUBRY, M.–P., BORD, D. and RODRIGUEZ, O., 2011. New taxa of the Order Discoasterales Hay 1977. *Micropaleontology*, 57: 269–287.
- AUBRY, M.–P., HAILWOOD, E. and TOWNSEND, H., 1986. Magneto- and calcareous nannofossil stratigraphy of the lower Paleogene of the Hampshire - London Basin. *Journal geological Society London*, v. 143, p. 729-735.
- AUBRY, M.–P., OUDA, KH., DUPUIS, C., BERGGREN, W. A., VAN COUVERING, J. A. and the Members of the Working Group on the Paleocene/Eocene Boundary, 2007. Global Standard Stratotype-section and Point (GSSP) for the base of the Eocene Series in the Dababiya Section (Egypt). *Episodes*, 30(4): 271-286.
- AUBRY, M.–P., RODRIGUEZ, O., BORD, D., GODFREY, L., SCHMITZ, B. and KNOX, R. W.O' B., 2012. The first radiation of the fasciculiths: Morphologic adaptations of the coccolithophores to oligotrophy. *Austrian Journal of Earth Sciences*, v. 105 (1): 29-38.
- AUBRY, M.–P. and SALEM, R., 2012. The Dababiya Core: A Window into Paleocene to Early Eocene depositional history in Egypt based on coccolith stratigraphy. In Berggren, W. A. and Ouda, Kh., *Early Paleogene history of Upper Egypt: The Dababiya Corehole*. Stratigraphy, v. 9, nos. 3-4: 287-346.
- BACKMAN, J., 1986. Late Paleocene to Middle Eocene calcareous nannofossil biochronology from the Shatsky Rise, Walvis Ridge and Italy. *Palaeogeography, Palaeoclimatology, Palaeoecology*, 57: 43–59.
- BERGGREN, W. A., AUBRY, M.–P., VAN FOSSEN, M., KENT, D. V., NORRIS, R. D. and QUILLÉVÉRÉ, F., 2000. Integrated Paleocene Calcareous Plankton Magnetobiochronology and Stable Isotope Stratigraphy: DSDP Site 384 (NW Atlantic Ocean). *Palaeogeography, Palaeoclimatology, Palaeoecology*, 159: p. 1-51.
- BERGGREN, W. A., KENT, D. V., SWISHER, C. C. and AUBRY, M.–P., 1995. A revised Cenozoic geochronology and chronostratigraphy. In: Berggren, W. A., Kent, D. V., Aubry, M.–P. and Hardenbol, J. (Eds.), *Geochronology, time scales and stratigraphic correlation; framework for an historical geology*, 129–212. Tulsa: Society of Economic Paleontologists and Mineralogists. Special publication, 54.
- BERNAOLA, G., MARTIN–RUBIO, M. and BACETA, J. J., 2009. New high resolution calcareous nannofossil analysis across the Danian/Selandian transition at the Zumaya section: Comparison with South Tethys and Danish sections. *Geologica Acta*, 7: 79–92.
- BIGNOT, G., JANIN, M.–C. and GUERNET, C., 1994. Mise en évidence de la Zone de nannofossiles calcaires NP 9 dans le Thanétien de Rollet (Bassin de Paris). *Bulletin d'Information des Géologues du Bassin de Paris*, 31: 25-28.
- BOWLES, J., 2006. Data report: revised magnetostratigraphy and magnetic mineralogy of sediments from Walvis Ridge, Leg 208. In: XXX., *Proceedings of the Ocean Drilling Program, Scientific Results, 208*, 1–24. College Station, Texas: Ocean Drilling Program. (http://www-odp.tamu.edu/publications/208_SR/VOLUME/CHAPTERS/206.PDF).
- BOWN, P. R., 2005a. Palaeogene calcareous nannofossils from the Kilwa and Lindi areas of coastal Tanzania (Tanzania Drilling Project 2003–4). *Journal of Nannoplankton Research*, 27: 21–95.
- BOWN, P. R., 2005b. Cenozoic calcareous nannofossil biostratigraphy, ODP leg 198 Site 1208 (Shatsky Rise, Northwest Pacific Ocean). In: Bralower, T. J., Premoli Silva, I. and Malone, M. J., *Proceedings of the Ocean Drilling Program, Scientific Results, 198*, 1–44. College Station, Texas: Ocean Drilling Program.
- BOWN, P. R., 2010. Calcareous nannofossils from the Paleocene/Eocene Thermal Maximum interval in southern Tanzania (TDP Site 14). *Journal of Nannoplankton Research*, 31: 11–38.
- BOWN, P. R. and DUNKLEY JONES, T. D., 2006. New Palaeogene calcareous nannofossil taxa from coastal Tanzania: Tanzania Drilling Project Sites 11 to 14. *Journal of Nannoplankton Research*, 28(1); 17-34.
- BOWN, P. R., DUNKLEY JONES, T., LEES, J. A., RANDELL, R., MIZZI, J., PEARSON, P. N., COXALL, H. R., YOUNG, J. R., NICHOLAS, C. J., KAREGA, A., SINGANO, J. and WADE, B. S., 2009. The paleogene kilwa group of coastal Tanzania: A calcareous microfossil Konservat-Lagerstätte. *Bulletin of the Geological Society of America*, 120: 3–12.

- BOWN, P. R. and PEARSON, P. N., 2009. Calcareous plankton evolution and the Paleocene/Eocene thermal maximum event: New evidence from Tanzania. *Marine Micropaleontology*, 71: 60–70.
- BRALOWER T. J. and MUTTERLOSE, J., 1995. Calcareous nannofossil biostratigraphy of Site 865, Allison Guyot, Central Pacific Ocean: a tropical Paleogene reference section. In: Winterer E. L., Sager W. W. and Sinton J. M. (Eds.), *Proceedings of the Ocean Drilling Program, Scientific Results, 143*, 31–74. College Station, Texas: Ocean Drilling Program.
- BRAMLETTE, M. N. and SULLIVAN, F. R., 1961. Coccolithophorids and related nannoplankton of the Early Tertiary in California. *Micropaleontology*, 7: 129–188.
- BUKRY, D., 1971. Cenozoic calcareous nannofossils from the Pacific Ocean. *Transactions of the San Diego Society of Natural History*, 16: 303–327.
- BUKRY, D., 1973a. Phytoplankton stratigraphy, Leg 20, Deep Sea Drilling Project Leg 20, western Pacific Ocean. In: Heezen, B. C., MacGregor, I. D., et al., *Initial Reports of the Deep Sea Drilling Project, 20*, 307–317. Washington, D. C.: U.S. Government Printing Office.
- BUKRY, D., 1973b. Coccolith and silicoflagellate stratigraphy, Tasman Sea and southwestern Pacific Ocean, Deep Sea Drilling Project Leg 21. In: Burns R. E., Andrews J. E., et al., *Initial Reports of the Deep Sea Drilling Project, 21*, 885–893. Washington, D. C.: U.S. Government Printing Office.
- BUKRY, D., 1973c. Low-latitude coccolith biostratigraphic zonation. In: Edgar, N. T., Saunders, J. B., et al., *Initial Reports of the Deep Sea Drilling Project, 15*, 685–703. Washington, D. C.: U.S. Government Printing Office.
- BUKRY, D., 1978. Cenozoic Coccolith and silicoflagellate stratigraphy, offshore Northwest Africa, Deep Sea Drilling Project, Leg 41. In: Lancelot Y., Seibold E., et al., *Initial Reports of the Deep Sea Drilling Project, 41*, 689–707. Washington, D. C.: U.S. Government Printing Office.
- BUKRY, D., 1985. Mid-Atlantic Ridge coccolith and silicoflagellate biostratigraphy, DSDP Sites 558 and 563. In: Bougault H., Cande S. C., et al., *Initial Reports of the Deep Sea Drilling Project, 82*, 591–603, Washington, D. C.: U.S. Government Printing Office.
- BUKRY, D. and PERCIVAL., S. F., 1971. New Tertiary calcareous nannofossils. *Tulane Studies in Geology and Paleontology*, 8: 123–146.
- BYBELL, L. M. and SELF-TRAIL, J. M., 1995. *Evolutionary, biostratigraphic, and taxonomic study of calcareous nannofossils from a continuous Paleocene–Eocene boundary section in New Jersey*. Washington D.C: U.S. Geological Survey. Professional Paper 1554, 36 pp.
- CANDE, S. C. and KENT, D. V., 1992. A New Geomagnetic Polarity Time Scale for the Late Cretaceous and Cenozoic. *Journal of Geophysical Research*, 97(B10): 13,917–13,951.
- CANDE, S. C. and KENT, D. V., 1995. Revised calibration of the geomagnetic polarity timescale for the Late Cretaceous and Cenozoic. *Journal of Geophysical Research*, 100(B4), 6093–6095.
- CLEMMENSEN, A. and THOMSEN, E., 2005. Palaeoenvironmental changes across the Danian–Selandian boundary in the North Sea Basin. *Palaeogeography, Palaeoclimatology, Palaeoecology*, 215: 351–384
- DINARÈS-TURELL, J., STOYKOVA, K., BACETA, J. I., IVANOV, M. and PUJALTE, V., 2010. High-resolution intra- and interbasinal correlation of the Danian–Selandian transition (Early Paleocene): The Bjala section (Bulgaria) and the Selandian GSSP at Zumaia (Spain). *Palaeogeography, Palaeoclimatology, Palaeoecology*, 12: 169–191.
- DUNKLEY JONES T., BOWN, P. R. and PEARSON, P. N., 2009. Exceptionally well preserved upper Eocene to lower Oligocene calcareous nannofossils (Prymnesiophyceae) from the Pande Formation (Kilwa Group), Tanzania. *Journal of Systematic Palaeontology*, 7: 359–411.
- DUPUIS, C., AUBRY, M.-P., STEURBAUT, E., BERGGREN, W.A., OUDA, KH., MAGIONCALDA, R., CRAMER, B.S., KENT, D.V., SPEIJER, R.P. and HEILMANN-CLAUSEN, C., 2003. The Dababiya Quarry Section: Lithostratigraphy, clay mineralogy, geochemistry and Paleontology, *Micropaleontology*, vol. 49, Supplement, 41–59.
- EDVARDBSEN, B., EIKREM, W., GREEN, J. C., ANDERSEN, R. A., STAYY, S. Y. M. and MEDLIN, L. K., 2000. Phylogenetic reconstructions of the Haptophyta inferred from 18S ribosomal DNA sequences and available morphological data. *Phycologia*, 39: 19–35
- EL-DAWOODY, A.S.A., 1988. New calcareous nannoplankton species from the Paleocene rocks in southern Egypt. *Bulletin of the Faculty of Sciences*, Cairo University, 56: 549–564.
- FAROUK, S. and FARIS, M., 2013. Calcareous nannofossil and foraminiferal bio-events of the Danian–Selandian transition of the Quseir area, northwestern Red Sea margin, Egypt. *Micropaleontology*, 59: 201–222.
- FUQUA, L. M., BRALOWER, T. J., ARTHUR, M. A., PATZKOWSKY, M. E., 2008. Evolution of calcareous nannoplankton and recovery of marine food webs after the Cretaceous–Paleocene mass extinction. *Palaios*, 23: 185–194.
- GARTNER, S., 1969a. Two new calcareous nannofossils from the Gulf Coast Eocene. *Micropaleontology*, 15: 31–34.
- GARTNER, S., 1969b. *Hayella* Roth and *Hayella* Gartner. *Micropaleontology*, 15: 490.
- GARTNER, S., 1971. Calcareous nannofossils from the JOIDES Blake Plateau cores, and revision of Paleogene nannofossil zonation. *Tulane Studies in Geology and Paleontology*, 8 (1970–1971): 101–121.

- HAQ, B. U., 1971. Paleogene calcareous nannoflora. Part I. The Paleocene of west-central Persia and the Upper Paleocene-Eocene of West Pakistan. *Stockholm Contributions in Geology*, 25: 1–56.
- HAQ, B. U. and AUBRY, M.–P., 1980. Early Cenozoic calcareous nannoplankton biostratigraphy and palaeobiogeography of North Africa and the Middle East and trans-Tethyan correlations. In: Salem, M. J. and Busrewil, M. T. (Eds.), *The geology of Libya, Volume 1*, 271–304. London: Academic Press.
- HAQ, B. U. and LOHMANN, G. P., 1976. Early Cenozoic calcareous nannoplankton biogeography of the Atlantic Ocean. *Marine Micropaleontology*, 1: 119–194.
- HAY, W. W., 1977. Calcareous nannofossils. In: Ramsay, A. T. S., *Oceanic micropaleontology, Volume 2*, 1055–1200. London: Academic Press.
- HAY, W. W. and MOHLER, H.–P., 1967. Calcareous nannoplankton from early Tertiary rocks at Pont Labau, France, and Paleocene–Early Eocene correlations. *Journal of Paleontology*, 41: 1505–1541.
- HAY, W. W., MOHLER, H. P. and WADE, M., 1966. Calcareous nannofossils from Nal'chik (Northwest Caucasus). *Eclogae Geologicae Helveticae*, 59: 379–399.
- HAY, W. W., MOHLER, H. P., ROTH, P. H., SCHMIDT, R. R. and BOUDREAUX, J. E., 1967. Calcareous nannoplankton zonation of the Cenozoic of the Gulf Coast and Caribbean–Antillean area, and transoceanic correlation. *Transactions of the Gulf Coast Association of Geological Societies*, 17: 428–480.
- KAHN, A. and AUBRY, M.–P., 2004. Provincialism in the calcareous nannoplankton during the Paleocene-Eocene thermal maximum: constrain on timing and duration. *Marine Micropaleontology*, 52: 117–131.
- MARTINI, E., 1970. Standard Paleogene calcareous nannoplankton zonation. *Nature*, 226: 560–561.
- MARTINI, E., 1971. Standard Tertiary and Quaternary calcareous nannoplankton zonation. In: Farinacci, A. (Ed.), *Proceedings of the II Planktonic Conference, Roma, 1970, Volume 2*, 739–785. Rome: Ediz. Tecnoscienza.
- MARTINI, E., 1976. Cretaceous to Recent calcareous nannoplankton from the Central Pacific Ocean (DSDP Leg 33). In: Schlander, S. C., Jackson, E. D., et al., *Initial Reports of the Deep Sea Drilling Project, 33*, 383–423. Washington, D. C.: U.S. Government Printing Office.
- MILLER, K.G., WRIGHT, J.D. and FAIRBANKS, R.G., 1991. Unlocking the Ice House: Oligocene–Miocene oxygen isotopes, eustasy, and margin erosion. *Journal of Geophysical Research*, 96: 6829–6848.
- MONECHI, S., 1985. Campanian to Pleistocene calcareous nannofossil stratigraphy from the Northwest Pacific Ocean, Deep Sea Drilling Project Leg 86. In: Heath, G. R., Burckle, L. H. et al., *Initial Reports of the Deep Sea Drilling Project, 86*, 301–336. Washington, D. C.: U.S. Government Printing Office.
- MONECHI, S., ANGORI, E. and VON SALIS, K., 2000. Calcareous nannofossil turnover around the Paleocene/Eocene transition at Alamedilla (southern Spain). *Bulletin de la Société géologique de France*, 171: 477–489.
- MONECHI, S., REALE, V., BERNAOLA, G. and BALESTRA, B., 2012. Taxonomic review of early Paleocene fasciculiths. *Micropaleontology*, 58: 351–365.
- MONECHI, S., REALE, V., BERNAOLA, G. and BALESTRA, B., 2013. The Danian/Selandian boundary at Site 1262 (South Atlantic) and in the Tethyan region: Biomagnetostratigraphy, evolutionary trends in fasciculiths and environmental effects of the latest Danian event. *Marine Micropaleontology*, 98: 28–40.
- MÜLLER, C., 1970. Nannoplankton aus dem Mittel-Oligozän von Norddeutschland und Belgien. *Neues Jahrbuch für Geologie und Paläontologie, Abhandlungen*, 135: 82–101.
- MÜLLER, C., 1974. Calcareous nannoplankton, Leg 25 (western Indian Ocean). In: Simpson, E. S. W., Schlich, R., et al., *Initial Reports of the Deep Sea Drilling Project, 25*, 579–633. Washington, D. C.: U.S. Government Printing Office.
- MÜLLER, C., 1976. Nannoplankton–Gemeinschaften aus dem Jung–Quartär des Golfes von Aden und des Roten Meeres. *Geologisches Jahrbuch, D*, 17: 33–77.
- MÜLLER, C., 1985. Biostratigraphic and paleoenvironmental interpretation of the Goban Spur region based on a study of calcareous nannoplankton. In: Gracianski, P. D., de, Poag, C. W., et al., *Initial Reports of the Deep Sea Drilling Project, 80(1)*, 573–599. Washington, D. C.: U.S. Government Printing Office.
- OKADA, H. and BUKRY, D., 1980. Supplementary modification and introduction of code numbers to the low-latitude coccolith biostratigraphic zonation (Bukry, 1973; 1975). *Marine Micropaleontology*, 5: 321–325.
- OKADA, H. and THIERSTEIN, H. R., 1979. Calcareous nannoplankton—Leg 43, Deep Sea Drilling Project. In: Tucholke, B. E., Vogt, P. R., et al., *Initial Reports of the Deep Sea Drilling Project, 43*, 507–573. Washington, D. C.: U.S. Government Printing Office.
- PAVŠIČ, J., 1977. Nannoplankton v zgornjekrednih in paleocenskih plasteh na Goriškem (Nannoplankton from the Upper Cretaceous and Paleocene beds in the Goriča region.) [Slovenian with English summary.] *Geologija Razprave in Poročila*, 20: 33–57.
- PERCH–NIELSEN, K., 1971a. Einige neue Coccolithen aus dem Paleozän der Bucht von Biskaya. *Meddelelser fra Dansk Geologisk Forening*, 20: 347–361.
- PERCH–NIELSEN, K., 1971b. Durchsicht tertiärer Coccolithen. In: Farinacci, A. (Ed.), *Proceedings of the II Planktonic Conference, Roma 1970, Volume 2*. 939–980. Rome: Ediz. Tecnoscienza.

- PERCH-NIELSEN, K., 1971c. Neue Coccolithen aus dem Paleozän von Dänemark, der Bucht von Biskaya und dem Eozän der Labrador See. *Meddelelser fra Dansk Geologisk Forening*, 21: 51–66.
- PERCH-NIELSEN, K., 1972. Remarks on Late Cretaceous to Pleistocene coccoliths from the North Atlantic. In: Laughton, A. S., Berggren, W. A., et al., *Initial Reports of the Deep Sea Drilling Project, 12*, 1003–1069. Washington, D. C.: U.S. Government Printing Office.
- PERCH-NIELSEN, K., 1977. Albian to Pleistocene calcareous nannofossils from the western South Atlantic, DSDP Leg 39. In: Supko, P. R., Perch-Nielsen, K., et al., *Initial Reports of the Deep Sea Drilling Project, 39*, 699–823. Washington, D. C.: U.S. Government Printing Office.
- PERCH-NIELSEN, K., 1981a. Les coccolithes du Paléocène près de El Kef, Tunisie, et leurs ancêtres. *Cahiers de Micropaléontologie*, 3: 7–23.
- PERCH-NIELSEN, K., 1981b. New Maastrichtian and Paleocene calcareous nannofossils from Africa, Denmark, the USA and the Atlantic, and some Paleocene lineages. *Eclogae Geologicae Helvetiae*, 74: 831–863.
- PERCH-NIELSEN, K., 1985. Cenozoic calcareous nannofossils. In: Bolli, H. M., Saunders, J. B. and Perch-Nielsen, K. (Eds.), *Plankton Stratigraphy*, 427–554. Cambridge: Cambridge University Press.
- PERCH-NIELSEN, K., SADEK, A., BARAKAT, M. G. and TELEB, F., 1978. Late Cretaceous and Early Tertiary calcareous nannofossil and planktonic foraminifera zones from Egypt. Actes du VI^e Colloque Africain de Micropaléontologie, Tunis, 1974. *Annales des Mines et de la Géologie*, 28: 337–403.
- POSPICHAL, J. J. and WISE, S. W., 1990. Paleocene to middle Eocene calcareous nannofossils of ODP Sites 689 and 690, Maud Rise, Weddell Sea. In: Barker, P. F., Kennett, J. P., et al., *Proceedings of the Ocean Drilling Program, Scientific Results, 113*, 613–638. College Station, Texas: Ocean Drilling Program.
- PREMOLI SILVA, I. and JENKINS, D. G., 1993. Decision on the Eocene-Oligocene boundary Stratotype. *Episodes*, 16: 379–382.
- PRINS, B., 1971. Speculations on relations, evolution, and stratigraphic distribution of discoasters. In: Farinacci, A. (Ed.), *Proceedings of the II Planktonic Conference, Roma, 1970, Volume I*: 1017–1037. Rome: Ediz. Tecnoscienza.
- PROTO DECIMA, F., ROTH, P. H. and TODESCO, L., 1975. Nannoplankton calcareo del Paleocene e dell' Eocene della sezione di Possagno. In: Bolli H. M. (Ed.) *Monografia micropaleontologica sul Paleocene e l'Eocene di Possagno, Schweizerische Paläontologische Abhandlungen*, 97: 35–55, 149–161.
- PROTO DECIMA, F., MEDIZZA, F. and TODESCO, L., 1978. Southeastern Atlantic Leg 40 calcareous nannofossils. In: Bolli, H. M., Ryan, W. B. F., et al., *Initial Reports of the Deep Sea Drilling Project, 40*, 571–634. Washington, D. C.: U.S. Government Printing Office.
- RAFFI, I. and DE BERNARDI, B., 2008. Response of calcareous nannofossils to the Paleocene-Eocene thermal maximum: Observations on composition, preservation and calcification in sediments from ODP Site 1263 (Walvis Ridge — SW Atlantic). *Marine Micropaleontology*, 69: 119–138.
- RIO, D., FORNACIARI, I. and RAFFI, I., 1990. Late Oligocene through early Pleistocene calcareous nannofossils from western equatorial Indian Ocean (leg 115). In: Duncan, R. A., Backman, J., Peterson, L. C., et al., *Proceedings of the Ocean Drilling Program, Scientific Results, 115*, 175–235. College Station, Texas: Ocean Drilling Program.
- ROMEIN, A. J. T., 1979. Lineages in Early Paleogene calcareous nannoplankton. *Utrecht Micropaleontological Bulletins*, 22: 1–231.
- ROTH, P. H., 1969. Calcareous nannoplankton zonation of Oligocene sections in Alabama (USA), on the islands of Trinidad and Barbados (W. I.), and the Blake Plateau (E. Coast of Florida, U. S. A.). *Eclogae Geologicae Helvetiae*, 61 (1968): 459–465.
- ROTH, P. H., 1973. Calcareous nannofossils — Leg 17, Deep Sea Drilling Project. In: Winterer, E. L., Ewing, J. L., et al., *Initial Reports of the Deep Sea Drilling Project, 17*, 695–795. Washington, D. C.: U.S. Government Printing Office.
- RYAN, W.B.F., S.M. CARBOTTE, S. M., COPLAN, J. O., O'HARA, S., MELKONIAN, A., ARKO, R. WEISSEL, R. A., FERRINI, V., GOODWILLIE, A., NITSCHKE, F., BONCZKOWSKI, J. and ZEMSKY, R., 2009. Global Multi-Resolution Topography synthesis, *Geochemistry, Geophysics, Geosystems*, 10, Q03014, doi:10.1029/2008GC002332.
- SCHWARZ, E., 1932. Beiträge zur Entwicklungsgeschichte der Protophyten. IX. Der Formwechsel von *Ochrosphaera neapolitana*. *Archiv für Protistenkunde*, 77: 434–462.
- SCHMITZ, B., PUJALTE, V., MOLINA, E., MONECHI, S., ORUE-ETXEBARRIA, X., SPEIJER, R. P., ALEGRET, L., APELLANIZ, E., ARENILLAS, I., AUBRY, M.-P., BACETA, J.-I., BERGGREN, W. A., BERNAOLA, G., CABALLERO, F., CLEMMENSEN, A., DINARÈS-TURELL, J., DUPUIS, C., HEILMANN-CLAUSEN, C., ORÚS, A. H., KNOX, R., MARTÍN-RUBIO, M., ORTIZ, S., PAYROS, A., PETRIZZO, M. R., VON SALIS, K., SPRONG, J., STEURBAUT, E. and THOMSEN, E., 2011. The global Stratotype Sections and Points for the bases of the Selandian (Middle Paleocene) and Thanetian (Upper Paleocene Paleocene) stages at Zumaia, Spain. *Episodes*, 34 (4), 220–243.
- SELF-TRAIL, J. M., 2011. Paleogene calcareous nannofossils of the South Dover Bridge core, Southern Maryland (USA). *Journal of Nannoplankton Research*, 32: 1–28.
- SIESSER, W. G., WARD, D. and LORD, A. R., 1987. Calcareous nannoplankton biozonation of the Thanetian stage (Palaeocene) in the type area. *Journal of Micropalaeontology*, 6: 85–102.

- SPRONG, J., SPEIJER, R. P. and STEURBAUT, E. 2009. Biostratigraphy of the Danian/Selandian transition in the southern Tethys. Special reference to the Lowest Occurrence of planktic foraminifera *Igorina albeari*. *Geologica Acta*, 7: 63-77. DOI: 10.1344/105.000000271
- STEURBAUT, E., 1990. Calcareous nannoplankton assemblages from the Tertiary in the Knokke Borehole. In: Laga, P. and Vanderberghe, N., Eds., *The Knokke Well (IIE/138) with a description of the Den Haan (22W/276) and Oostduinkerke (35E/142) wells*, 47–62. Bruxelles: Service géologique de la Belgique. Mémoire pour servir à l'Explication des Cartes géologiques et minières de la Belgique, 29.
- STEURBAUT, E., 1991. Ypresian calcareous nannoplankton biostratigraphy and palaeogeography of the Belgian Basin. *Bulletin de la Société belge de géologie*, 97: 251–285.
- STEURBAUT, E., 1998. High-resolution holostratigraphy of Middle Paleocene to Early Eocene strata in Belgium and adjacent areas. *Palaeontographica, Abt. A*, 247: 91–156.
- STEURBAUT, E and SZTRÁKOS, K., 2002. The Paleogene of the Gan-Rébénacq road section (Aquitaine, France): Integrated stratigraphy, foraminifera and calcareous nannofossils. *Revue de Micropaléontologie*, 45: 195–219.
- STEURBAUT, E and SZTRÁKOS, K., 2008. Danian/Selandian boundary criteria and North Sea basin—Tethys correlations based on calcareous nannofossil and foraminiferal trends in SW France. *Marine Micropaleontology*, 67: 1–29.
- STRADNER, H., 1961. Vorkommen von Nannofossilien im Mesozoikum und Alttertiär. *Erdöl-Zeitschrift*, 77: 77–88.
- SULLIVAN, F. R., 1964. Lower Tertiary nannoplankton from the California Coast Ranges, 1. Paleocene. *University of California Publications in Geological Sciences*, 44: 163–228.
- THEODORIDIS, S., 1984. Calcareous nannofossil biozonation of the Miocene and revision of the helicoliths and discoasters. *Utrecht Micropaleontological Bulletins*, 32: 1–271.
- TROËLSEN, J. C. and QUADROS, L. P., 1971. Distribuição bioestratigráfica dos nanofósseis em sedimentos marinhos (Aptiano–Mioceno) do Brasil. *Academia Brasileira de Ciências, Anales*, 43, suplemento: 577–609. (Simpósio Brasileiro do Paleontologia).
- VAN ITTERBEECK, J., SPRONG, J., DUPUIS, C., SPEIJER, R.P. and STEURBAUT, E., 2007. Danian/Selandian boundary stratigraphy and ostracod records from Sidi Nasseur, Tunisia. *Marine Micropaleontology*, 62: 211–234.
- VAROL, O., 1989. Palaeocene calcareous nannofossil biostratigraphy. In: Crux, J. A. and van Heck, S. E. (Eds.), *Nannofossils and their applications*, 267–310. Chichester: Ellis Horwood Limited.
- VAROL, O., 1998. Paleogene. In: Bown, P. R. (ed.), *Calcareous Nannofossil Biostratigraphy*, 200–224. London: Kluwer Academic Publishers.
- WANG, C. and HUANG, W., 1989. Calcareous nannofossils. In: Research Party of Marine Geology, Ministry of Geology and Mineral Resources and Institute of Geology, Chinese Academy of Geological Sciences, (Eds.). *Cenozoic Paleobiota of the Continental Shelf of the East China Sea (Donghai)*. Micropaleobotanica Volume. Beijing: Geological Publishing House, 202–252.
- WEI, W. and WISE, S. W., 1989. Paleogene calcareous nannofossil magnetobiochronology: Results from South Atlantic DSDP Site 516. *Marine Micropaleontology*, 14: 119–152.
- WISE, S. W., jr., 1977. Chalk formation: Early diagenesis. In: Andersen, N. R. and Malahoff, A. (eds.), *The Fate of Fossil Fuel CO₂ in the Oceans*, 717–739. New York: Plenum Publishing Corporation.
- WISE, S. W., jr. and WIND, F. H., 1977. Mesozoic and Cenozoic calcareous nannofossils recovered by DSDP Leg 36 drilling on the Falkland Plateau, southwest Atlantic sector of the southern Ocean. In: Barker, P. F., Dalziel, I. W. D., et al., *Initial Reports of the Deep Sea Drilling Project*, 36: 269–491. Washington, D. C.: U.S. Government Printing Office.
- YOUNG, J. R. and BOWN, P. R., 1997. Cenozoic calcareous nanoplankton classification. *Journal of Nannoplankton Research*, 19: 36–47.
- ZACHOS, J. C., KROON, D., BLUM, P., et al., 2004. Early Cenozoic Extreme Climates: The Walvis Ridge Transect. *Proceedings of the Ocean Drilling Program, Preliminary Results*, 208. College Station, Texas: Ocean Drilling Program. (http://www-odp.tamu.edu/publications/208_SR/VOLUME/CHAPTERS/206.PDF).
- ZACHOS, J.C., RÖHL, U., SCHELLENBERG, S.A., SLUIJS, A., HODELL, D.A., KELLY, D.C., THOMAS, E., NICOLO, M., RAFFI, I., LOURENS, L.J., MCCARREN, H., KROON, D., 2005. Rapid acidification of the ocean during the Paleocene–Eocene Thermal Maximum. *Science*, 308: 1611–1615.

APPENDIX 1: ALPHABETIC LIST OF TAXA

Bold face: valid formal names

Regular face, underlined: synonyms

Regular face: informal names

Bomolithus Roth, 1973

Bomolithus Roth, 1973 emend

Bomolithus aquilus Bown, 2010

Bomolithus elegans Roth, 1973

Bomolithus supremus Bown & Jones, 2006

Bomolithus rotundus (Haq & Lohmann) n. comb. [= *Fasciculithus rotundus* Haq & Lohmann, 1976]

Coronocyclus serratus Hay, Mohler, & Wade, 1966, pl 11, figs. 1, 2, 3

Cyclolithella aprica Roth, 1973

Fasciculithus Bramlette & Sullivan, 1961

Fasciculithus Bramlette & Sullivan, 1961 emend Aubry in Aubry et al., 2011

Fasciculithus alanii Perch-Nielsen, 1971

Fasciculithus aubertae Haq & Aubry, 1981

Fasciculithus bobii Perch-Nielsen, 1971

Fasciculithus clinatus Bukry, 1971

Fasciculithus fenestrellatus Bown, 2005

Fasciculithus hayii Haq, 1971

Fasciculithus involutus Bramlette & Sullivan, 1961

Fasciculithus lilianae Perch-Nielsen, 1971

Fasciculithus lingfengensis Wang & Huang, 1989

Fasciculithus lobus Bown 2010

Fasciculithus mitreus Gartner, 1971

Fasciculithus richardii Perch-Nielsen, 1971

Fasciculithus schaubi Hay & Mohler, 1967

Fasciculithus sidereus Bybell & Self-Trail 1995

Fasciculithus thomasii Perch-Nielsen, 1971

Fasciculithus tonii Perch-Nielsen, 1971

Fasciculithus tympaniformis Hay & Mohler, 1967

Fasciculithus sp. A [= *Fasciculithus* sp. Steurbaut & Sztrákos,

2008, p. 26, pl. 2, fig. 12]

Fasciculithus sp. B [= *Fasciculithus* sp. 1 Bown 2005, p. 9, pl. 12, figs. 25-27]

Genus *A floris* Haq & Aubry, 1980

Genus *B crassus* (Müller) n. comb. [= *Heliolithus crassus* Müller, 1976]

Gomphiolithus Aubry in Aubry, Bord & Rodriguez 2011

Gomphiolithus magnicordis (Romein) Aubry & Rodriguez in Aubry et al., 2011 [= *Fasciculithus magnicordis* Romein, 1979]

Gomphiolithus magnus (Bukry & Percival) Aubry & Rodriguez in Aubry et al., 2011 [= *Fasciculithus magnus* Bukry & Percival, 1971]

Hayella Gartner, 1969

Hayella aperta Theodoridis, 1984

Hayella challengeri (Müller) Theodoridis, 1984 [= *Nannocorbis challengeri* Müller, 1974]

Hayella? gauliformis Troëlsen & Quadros, 1971

Hayella neoaprica (Bukry) n. comb. [= *Cyclolithella? neoaprica* Bukry, 1985, p. 600, pl. 1, figs. 8-10]

Hayella simplex Bown & Jones, 2006 [= *Hayella* sp. Bown, 2005]

Hayella situliformis Gartner, 1969

Hayella sp. A [= *Hayella* sp. Steurbaut, 1991, pl. 2, figs. 24, 25; = *Cyclococcolithus* sp. Steurbaut, 1990, p. 53, pl. 1, figs. 8a, b, 9a, b, 10, 11]

Hayella sp. B (Perch-Nielsen) n. comb. [= *Hayella* sp. Perch-Nielsen, 1977, pl. 45, figs. 3, 6, 10]

Heliolithus Bramlette & Sullivan, 1961

Heliolithus Bramlette & Sullivan, 1961 emend.

Heliolithus aktasii Varol, 1989

Heliolithus crassus Müller, 1976

Heliolithus floris Haq & Aubry, 1981

Heliolithus riedelii Bramlette & Sullivan, 1961

Heliotrochus new genus

Heliotrochus cantabriae (Perch-Nielsen) n. comb. [= *Heliolithus cantabriae* Perch-Nielsen, 1971, p. 55, pl. 2, figs. 3, 5, pl. 7, figs. 33-36]

Heliotrochus conicus (Perch-Nielsen) n. comb. [= *Heliolithus(?) conicus* Perch-Nielsen, 1971, p. 56, pl. 1, figs. 1-3, pl. 7, figs. 37, 38]

Heliotrochus kleinpelli (Sullivan) n. comb. [= *Heliolithus klein-*

PELLI Sullivan; not *Heliolithus* aff. *H. riedeli* Bramlette & Sullivan 1961]

Heliotrochus knoxii (Steurbaut) n. comb. [= *Heliolithus knoxii* Steurbaut 1998]

Heliotrochus megastypus (Bramlette & Sullivan) n. comb [= *Discoasteroides megastypus* Bramlette & Sullivan, 1961, p. 163, pl. 13, figs. 14a-d, 15a-c]

Lithoptychius Aubry in Aubry, Bord and Rodriguez 2011

Lithoptychius barakati (El Dawoody) n. comb. [= *Fasciculithus barakati* El-Dawoody 1988, p. 555, 556, pl. 1, figs. 5-7]

Lithoptychius bitectus (Romein) Aubry in Aubry et al., 2011 [= *Fasciculithus bitectus* Romein, 1979]

Lithoptychius billii (Perch-Nielsen) Aubry in Aubry et al., 2011 [= *Fasciculithus billii* Perch-Nielsen, 1971]

Lithoptychius chowii (Varol) Aubry in Aubry et al., 2011 [= *Fasciculithus chowii* Varol, 1989]

Lithoptychius collaris Aubry & Rodriguez in Aubry et al., 2011

Lithoptychius felis Aubry & Bord in Aubry et al., 2011

Lithoptychius janii (Perch-Nielsen) Aubry in Aubry et al., 2011 [= *Fasciculithus janii* Perch-Nielsen, 1971]

Lithoptychius merloti (Pavsic) Aubry in Aubry et al., 2011 [= *Fasciculithus merloti* Pavsic, 1977]

Lithoptychius pileatus (Bukry) Aubry in Aubry et al., 2011 [= *Fasciculithus pileatus* Bukry, 1973; = *Fasciculithus* sp. cf. *F. ulii*, Roth, 1973]

Lithoptychius schmitzii Monechi, Reale, Bernaola & Balestra, 2013 [= *Lithoptychius* sp. 2 Aubry, Bord & Rodriguez, 2011]

Lithoptychius stegastos Aubry & Bord in Aubry et al., 2011

Lithoptychius stonehengii (Haq & Aubry) Aubry in Aubry et al., 2011 [= *Fasciculithus stonehengei* Haq & Aubry, 1980]

Lithoptychius ulii (Perch-Nielsen) Aubry in Aubry et al., 2011 [= *Fasciculithus ulii* Perch-Nielsen, 1971]

Lithoptychius varolii (Steurbaut & Sztrákos) Aubry & Rodriguez in Aubry et al., 2011 [= *Fasciculithus varoli* Steurbaut & Sztrákos, 2008]

Lithoptychius vertebratoides (Steurbaut & Sztrákos) Aubry in Aubry et al., 2011 (= *Fasciculithus vertebratoides* Steurbaut & Sztrákos, 2008) [= *Fasciculithus janii* Perch-Nielsen, 1971]

Lithoptychius sp. A [= *Fasciculithus* sp. 1 Okada & Thierstein, 1972, p. 523, pl. 6, figs. 6a, b.]

Lithoptychius sp. B [= *Lithoptychius* sp. 1 Aubry et al., 2011, p. 272, pl. 7, figs. 1a-d]

Lithoptychius sp. C [= *Fasciculithus* sp. 3 Bernaola et al., 2009, figs. 4v, 5a-d]

Lithoptychius sp. D [= *Fasciculithus* sp. 1 Prins 1971, pl. 6, figs. 5a-c]

Lithoptychius sp. E [= *Fasciculithus* sp. 5 Bernaola, Martín-Rubio & Baceta 2009, figs. 5i, j]

Nannocorbis Müller, 1974

**APPENDIX 2: SUPPLEMENTARY INFORMATION ON ILLUSTRATIONS LISTED IN
"FIGURE REFERENCES"**

Gomphiolithus

Reference	Species	Plate/ Figure	Height (μm)	Magnification	Age	Formation	Location
Agnini et al. 2007	as <i>F. magnus</i>	2/1		1200	M. Pal-E. Eoc		Angola Basin, SE Atlantic Ocean
Bukry and Percival 1971	as <i>F. magnus</i>	4/9		2000	E. Paleocene		Shatsky Ridge, Pacific Ocean
		4/10		<i>id</i>	<i>id</i>		<i>id</i>
		4/11		<i>id</i>	<i>id</i>		<i>id</i>
		4/12		<i>id</i>	<i>id</i>		<i>id</i>
Monechi et al. 2012	<i>G. magnus</i>	1/2	10		<i>id</i>		Walvis Ridge, SE Atlantic
		1/1	10		<i>id</i>		<i>id</i>
		1/4	8.9		<i>id</i>		<i>id</i>
		1/3	8.9		<i>id</i>		<i>id</i>
		1/6	7.1		<i>id</i>		<i>id</i>
		1/5	7.1		<i>id</i>		<i>id</i>
		1/8	7.9		<i>id</i>		<i>id</i>
		1/7	7.9		<i>id</i>		<i>id</i>
		1/10	8.9		<i>id</i>		<i>id</i>
		1/9	8.9		<i>id</i>		<i>id</i>
		1/12	10		<i>id</i>		<i>id</i>
		1/11	10		<i>id</i>		<i>id</i>
	<i>G. magnicordis</i>	1/15	6.8		<i>id</i>		<i>id</i>
		1/14	6.8		<i>id</i>		<i>id</i>
		1/13	6.8		<i>id</i>		<i>id</i>
		1/21	5		<i>id</i>		<i>id</i>
		1/20	5		<i>id</i>		<i>id</i>
		1/17	7.9		<i>id</i>		<i>id</i>
		1/16	7.9		<i>id</i>		<i>id</i>
		1/19	7.1		<i>id</i>		<i>id</i>
		1/18	7.1		<i>id</i>		<i>id</i>
		1/23	6.8		<i>id</i>		<i>id</i>
1/22	6.8		<i>id</i>		<i>id</i>		
1/25	7.9		<i>id</i>		<i>id</i>		
1/24	7.9		<i>id</i>		<i>id</i>		
Monechi et al. 2013	<i>G. magnus</i>	1/7	6.4		Danian-Se-landian		Wombat Plateau, Indian Ocean
		1/6	6.4		<i>id</i>		<i>id</i>
	<i>G. magnicordis</i>	1/10	9.5		<i>id</i>		North Atlantic
		1/5	10		<i>id</i>		<i>id</i>

Gomphiolithus (continued)

Reference	Species	Plate/ Figure	Height (μm)	Magnification	Age	Formation	Location
Perch- Nielsen 1977	as <i>F. magnus</i>	49/10		2000	E. Paleocene		São Paulo Plateau,
		49/16		<i>id</i>	<i>id</i>		Western South Atlantic
		49/22		<i>id</i>	<i>id</i>		<i>id</i>
		11/9		4700	Danian-Se- landian		<i>id</i>
		11/8		<i>id</i>	<i>id</i>		<i>id</i>
		11/11		<i>id</i>	<i>id</i>		<i>id</i>
		11/12		<i>id</i>	<i>id</i>		<i>id</i>
		11/10		<i>id</i>	<i>id</i>		<i>id</i>
		11/5		<i>id</i>	<i>id</i>		<i>id</i>
		11/6		<i>id</i>	<i>id</i>		<i>id</i>
		11/4		<i>id</i>	<i>id</i>		<i>id</i>
		11/7		<i>id</i>	<i>id</i>	<i>id</i>	
Romein 1979	as <i>F. magnus</i>	9/14		2500	Paleocene	Jorquera, Car- avaca Section	Spain
	as <i>F. magni- cordis</i>	9/12		1500	<i>id</i>	<i>id</i>	<i>id</i>
		9/13		2500	<i>id</i>	<i>id</i>	<i>id</i>
Steurbaut and Sztrákos 2008	as <i>F. magnus</i>	2/7		1420	Danian	Lasseube Fm	SW France
		2/8		1700	<i>id</i>	<i>id</i>	<i>id</i>
		2/9		1750	<i>id</i>	<i>id</i>	<i>id</i>
		2/10a		1500	<i>id</i>	<i>id</i>	<i>id</i>
		2/10b		<i>id</i>	<i>id</i>	<i>id</i>	<i>id</i>
		2/11		<i>id</i>	<i>id</i>	<i>id</i>	<i>id</i>
		2/12		1600	<i>id</i>	<i>id</i>	<i>id</i>
	as <i>F. magni- cordis</i>	2/13		3000	<i>id</i>	<i>id</i>	<i>id</i>

Reference	Species	Plate/ Figure	Height (μm)	Diameter (μm)	Magnifica- tion	Age	Formation	Location
Agnini et al. 2007	as <i>Fasciculithus billii</i>	2/7			1200	M. Pal-E. Eoc		Angola Basin, SE Atlantic
Aubry et al. 2011	<i>L. varolii</i>	9/1a	5.8			Danian - Se- landian	Dakhla Shale, Qreiya Section	Gebel Abu Had, Upper Egypt
		9/1b	4.6			<i>id</i>	<i>id</i>	<i>id</i>
		9/1c	4.6			<i>id</i>	<i>id</i>	<i>id</i>
		9/1d	4.6			<i>id</i>	<i>id</i>	<i>id</i>
		9/2a	5			<i>id</i>	<i>id</i>	<i>id</i>
		9/2b	5			<i>id</i>	<i>id</i>	<i>id</i>
		9/2c	5			<i>id</i>	<i>id</i>	<i>id</i>
		9/2d	5			<i>id</i>	<i>id</i>	<i>id</i>
		9/3a	5.8			<i>id</i>	<i>id</i>	<i>id</i>
		9/3b	5.8			<i>id</i>	<i>id</i>	<i>id</i>
		9/3c	5.8			<i>id</i>	<i>id</i>	<i>id</i>
		9/3d	5.8			<i>id</i>	<i>id</i>	<i>id</i>
		9/4a	3.8			<i>id</i>	<i>id</i>	<i>id</i>
		9/4b	3.8			<i>id</i>	<i>id</i>	<i>id</i>
		9/4c	3.8			<i>id</i>	<i>id</i>	<i>id</i>
		9/4d	3.8			<i>id</i>	<i>id</i>	<i>id</i>
	<i>L. collaris</i>	4/1a	7.1			<i>id</i>	<i>id</i>	<i>id</i>
		4/1b	7.1			<i>id</i>	<i>id</i>	<i>id</i>
		4/1c	7.1			<i>id</i>	<i>id</i>	<i>id</i>
		4/1d	7.1			<i>id</i>	<i>id</i>	<i>id</i>
		4/1e	7.1			<i>id</i>	<i>id</i>	<i>id</i>
		4/1f	7.1			<i>id</i>	<i>id</i>	<i>id</i>
		4/1g	7.1			<i>id</i>	<i>id</i>	<i>id</i>
		4/1h	7.1			<i>id</i>	<i>id</i>	<i>id</i>
		4/1i	7.1			<i>id</i>	<i>id</i>	<i>id</i>
		4/1j	7.1			<i>id</i>	<i>id</i>	<i>id</i>
		4/1k	7.1			<i>id</i>	<i>id</i>	<i>id</i>
		4/1l	7.1			<i>id</i>	<i>id</i>	<i>id</i>
		4/1m	7.1			<i>id</i>	<i>id</i>	<i>id</i>
		4/1n	7.1			<i>id</i>	<i>id</i>	<i>id</i>
		4/1o	7.1			<i>id</i>	<i>id</i>	<i>id</i>
		4/1p	7.1			<i>id</i>	<i>id</i>	<i>id</i>
		4/2a	5.4			<i>id</i>	<i>id</i>	<i>id</i>
		4/2b	5.4			<i>id</i>	<i>id</i>	<i>id</i>
4/2c	5.4			<i>id</i>	<i>id</i>	<i>id</i>		
4/2d	5.4			<i>id</i>	<i>id</i>	<i>id</i>		
<i>L. felis</i>	5/1a	4.6			<i>id</i>	<i>id</i>	<i>id</i>	
	5/1b	4.6			<i>id</i>	<i>id</i>	<i>id</i>	

Lithoptychius (continued)

Reference	Species	Plate/ Figure	Height (μm)	Diameter (μm)	Magnifica- tion	Age	Formation	Location	
Aubry et al. 2011	<i>L. felis</i>	5/1c	4.6			Danian - Se- landian	Dakhla Shale, Qreiya Section	Gebel Abu Had, Upper Egypt	
		5/1d	4.6			<i>id</i>	<i>id</i>	<i>id</i>	
		5/2a	4.6			<i>id</i>	<i>id</i>	<i>id</i>	
		5/2b	4.6			<i>id</i>	<i>id</i>	<i>id</i>	
		5/2c	4.6			<i>id</i>	<i>id</i>	<i>id</i>	
		5/2d	4.6			<i>id</i>	<i>id</i>	<i>id</i>	
		5/3a	5			<i>id</i>	<i>id</i>	<i>id</i>	
		5/3b	5			<i>id</i>	<i>id</i>	<i>id</i>	
		5/3c	5			<i>id</i>	<i>id</i>	<i>id</i>	
		5/3d	5			<i>id</i>	<i>id</i>	<i>id</i>	
		5/4a	4.6			<i>id</i>	<i>id</i>	<i>id</i>	
		5/4b	4.6			<i>id</i>	<i>id</i>	<i>id</i>	
		5/4c	4.6			<i>id</i>	<i>id</i>	<i>id</i>	
		5/4d	4.6			<i>id</i>	<i>id</i>	<i>id</i>	
		5/5a	5.4			<i>id</i>	<i>id</i>	<i>id</i>	
		5/5b	5.4			<i>id</i>	<i>id</i>	<i>id</i>	
	5/5c	5.4			<i>id</i>	<i>id</i>	<i>id</i>		
	5/5d	5.4			<i>id</i>	<i>id</i>	<i>id</i>		
		<i>L. janii</i>	8/2a	7.1			<i>id</i>	Dababiya Quarry	Near Luxor, Egypt
			8/2b	7.1			<i>id</i>	<i>id</i>	<i>id</i>
8/2c			7.1			<i>id</i>	<i>id</i>	<i>id</i>	
8/2d			7.1			<i>id</i>	<i>id</i>	<i>id</i>	
	<i>L. merloti</i>	8/3a	5.8			<i>id</i>	<i>id</i>	<i>id</i>	
		8/3b	5.8			<i>id</i>	<i>id</i>	<i>id</i>	
		8/3c	5.8			<i>id</i>	<i>id</i>	<i>id</i>	
		8/3d	5.8			<i>id</i>	<i>id</i>	<i>id</i>	
	<i>L. stegastos</i>	6/1a	3.8			<i>id</i>	Dakhla Shale, Qreiya Section	Gebel Abu Had, Upper Egypt	
		6/1b	3.8			<i>id</i>	<i>id</i>	<i>id</i>	
		6/1c	3.8			<i>id</i>	<i>id</i>	<i>id</i>	
		6/1d	3.8			<i>id</i>	<i>id</i>	<i>id</i>	
		6/2a	3.8			<i>id</i>	<i>id</i>	<i>id</i>	
		6/2b	3.8			<i>id</i>	<i>id</i>	<i>id</i>	
		6/2c	3.8			<i>id</i>	<i>id</i>	<i>id</i>	
		6/2d	3.8			<i>id</i>	<i>id</i>	<i>id</i>	
		6/3a	3.3			<i>id</i>	<i>id</i>	<i>id</i>	
		6/3b	3.3			<i>id</i>	<i>id</i>	<i>id</i>	
		6/4a	5.4			<i>id</i>	<i>id</i>	<i>id</i>	
		6/4b	5.4			<i>id</i>	<i>id</i>	<i>id</i>	
6/4c	5.4			<i>id</i>	<i>id</i>	<i>id</i>			

Lithoptychius (continued)

Reference	Species	Plate/ Figure	Height (μm)	Diameter (μm)	Magnifica- tion	Age	Formation	Location
Aubry et al. 2011	<i>L. stegastos</i>	6/4e	5.4			Danian - Se- landian	Dakhla Shale, Qreiya Section	Gebel Abu Had, Upper Egypt
		6/4f	5.4			<i>id</i>	<i>id</i>	<i>id</i>
		6/5a	3.5			<i>id</i>	<i>id</i>	<i>id</i>
		6/5b	3.5			<i>id</i>	<i>id</i>	<i>id</i>
		6/5c	3.5			<i>id</i>	<i>id</i>	<i>id</i>
		6/5d	3.5			<i>id</i>	<i>id</i>	<i>id</i>
	<i>L. sp. 1</i>	7/1a	5.4			<i>id</i>	<i>id</i>	<i>id</i>
		7/1b	5.4			<i>id</i>	<i>id</i>	<i>id</i>
		7/1c	5.4			<i>id</i>	<i>id</i>	<i>id</i>
		7/1d	5.4			<i>id</i>	<i>id</i>	<i>id</i>
		7/2a	4.6			<i>id</i>	<i>id</i>	<i>id</i>
		7/2b	4.6			<i>id</i>	<i>id</i>	<i>id</i>
		7/2c	4.6			<i>id</i>	<i>id</i>	<i>id</i>
		7/2d	4.6			<i>id</i>	<i>id</i>	<i>id</i>
		7/6a	4.2			<i>id</i>	<i>id</i>	<i>id</i>
		7/6b	4.2			<i>id</i>	<i>id</i>	<i>id</i>
		7/6c	4.2			<i>id</i>	<i>id</i>	<i>id</i>
		7/4a	3.8			<i>id</i>	<i>id</i>	<i>id</i>
		7/4b	3.8			<i>id</i>	<i>id</i>	<i>id</i>
		7/3a	4.6			<i>id</i>	<i>id</i>	<i>id</i>
		7/3b	4.6			<i>id</i>	<i>id</i>	<i>id</i>
		7/3c	4.6			<i>id</i>	<i>id</i>	<i>id</i>
		7/3d	4.6			<i>id</i>	<i>id</i>	<i>id</i>
		7/5a	4.4			<i>id</i>	<i>id</i>	<i>id</i>
	7/5b	4.4			<i>id</i>	<i>id</i>	<i>id</i>	
	7/5c	4.4			<i>id</i>	<i>id</i>	<i>id</i>	
	<i>L. sp. 2</i>	8/1a	4.6			<i>id</i>	<i>id</i>	<i>id</i>
		8/1b	4.6			<i>id</i>	<i>id</i>	<i>id</i>
		8/1c	4.6			<i>id</i>	<i>id</i>	<i>id</i>
		8/1d	4.6			<i>id</i>	<i>id</i>	<i>id</i>
	<i>L. ulii</i>	8/4a	6.9			<i>id</i>	<i>id</i>	<i>id</i>
		8/4b	6.9			<i>id</i>	<i>id</i>	<i>id</i>
8/4c		6.9			<i>id</i>	<i>id</i>	<i>id</i>	
8/4d		6.9			<i>id</i>	<i>id</i>	<i>id</i>	

Lithoptychius (continued)

Reference	Species	Plate/ Figure	Height (μm)	Diameter (μm)	Magnifica- tion	Age	Formation	Location
Bernaola et al. 2009	as <i>F.</i> sp. 2	4/S	4.1			Danian - Se- landian	Zumaia Section	Western Pyrenees, Spain
		4/T	5.8			<i>id</i>	<i>id</i>	<i>id</i>
		4/U	5.9			<i>id</i>	<i>id</i>	<i>id</i>
	as <i>F. pileatus</i>	5/T	4.8			<i>id</i>	<i>id</i>	<i>id</i>
	as <i>F.</i> sp. 4	5/E	4.2			<i>id</i>	<i>id</i>	<i>id</i>
		5/F	3.1			<i>id</i>	<i>id</i>	<i>id</i>
		5/G	3.1			<i>id</i>	<i>id</i>	<i>id</i>
		5/H	3.1			<i>id</i>	<i>id</i>	<i>id</i>
	as <i>F. janii</i>	5/N	4.8			<i>id</i>	<i>id</i>	<i>id</i>
		5/O	5			<i>id</i>	<i>id</i>	<i>id</i>
	as <i>F.</i> sp. 3	4/V	5.2			<i>id</i>	<i>id</i>	<i>id</i>
		5/A	4.2			<i>id</i>	<i>id</i>	<i>id</i>
		5/B	4.2			<i>id</i>	<i>id</i>	<i>id</i>
		5/C	4.2			<i>id</i>	<i>id</i>	<i>id</i>
5/D		4.2			<i>id</i>	<i>id</i>	<i>id</i>	
as <i>F. ulii</i>	5/K	5.4			<i>id</i>	<i>id</i>	<i>id</i>	
	5/L	5.8			<i>id</i>	<i>id</i>	<i>id</i>	
as <i>F.</i> sp. 5	5/I	4.6			<i>id</i>	<i>id</i>	<i>id</i>	
	5/J	4.6			<i>id</i>	<i>id</i>	<i>id</i>	
as <i>F. billi</i>	5/M	3.8			<i>id</i>	<i>id</i>	<i>id</i>	
Bukry 1973a	as <i>F. pileatus</i>	1/7			2000	L. Paleocene		Western Pacific Ocean
		1/8			<i>id</i>	<i>id</i>	<i>id</i>	
		2/2			<i>id</i>	<i>id</i>	<i>id</i>	
		2/3			<i>id</i>	<i>id</i>	<i>id</i>	
		2/4			<i>id</i>	<i>id</i>	<i>id</i>	
		2/5			<i>id</i>	<i>id</i>	<i>id</i>	
		1/9			<i>id</i>	<i>id</i>	<i>id</i>	
		2/1			<i>id</i>	<i>id</i>	<i>id</i>	
Dinarés-Turell et al. 2010	as <i>F.</i> sp. 2	5/19			3000	Danian-Selandi- an	Bjala E Sec- tion	Bjala, Bulgaria
	as <i>F.</i> sp. 2 or 3	5/18			<i>id</i>	<i>id</i>	<i>id</i>	<i>id</i>
		5/17			<i>id</i>	<i>id</i>	<i>id</i>	<i>id</i>
	as <i>F. vertebra- toides</i>	3/12			<i>id</i>	<i>id</i>	Bjala 1 Section	<i>id</i>
		3/11			<i>id</i>	<i>id</i>	<i>id</i>	<i>id</i>

Reference	Species	Plate/ Figure	Height (μm)	Diameter (μm)	Magnifica- tion	Age	Formation	Location
El-Dawoody 1988	as <i>F. barakati</i>	1/5a		7		Paleocene	Dakhla Shale	Gebel Duwi, Red Sea Coast, Egypt
		1/5b		7		<i>id</i>	<i>id</i>	<i>id</i>
		1/6a		7		<i>id</i>	<i>id</i>	<i>id</i>
		1/6b		7		<i>id</i>	<i>id</i>	<i>id</i>
		1/7a		7		<i>id</i>	<i>id</i>	<i>id</i>
		1/7b		7		<i>id</i>	<i>id</i>	<i>id</i>
Haq and Aubry 1980	as <i>F. stonehengi</i>	1/11			2000	e. Cenozoic		Middle East
		1/12			<i>id</i>	<i>id</i>	<i>id</i>	
		1/13			<i>id</i>	<i>id</i>	<i>id</i>	
	as <i>F. janii</i>	1/7			<i>id</i>	<i>id</i>		<i>id</i>
1/8				<i>id</i>	<i>id</i>		<i>id</i>	
Monechi 1985	as <i>F. pileatus</i>	7/7a			2800	L. Paleocene		Shatsky Ridge, NW Pacific Ocean
		7/7b			<i>id</i>	<i>id</i>	<i>id</i>	
		7/4			7000	<i>id</i>	<i>id</i>	<i>id</i>
	as <i>F. ulii</i>	7/6a			2800	<i>id</i>		<i>id</i>
		7/6b			<i>id</i>	<i>id</i>	<i>id</i>	
		7/3			4200	<i>id</i>	<i>id</i>	<i>id</i>
Monechi et al. 2012	<i>L. varolii</i>	4/9	5.8			E. Paleocene		Walvis Ridge, Southeast Atlantic
		4/10	5.8			<i>id</i>	<i>id</i>	<i>id</i>
		4/14	5.8			<i>id</i>	<i>id</i>	<i>id</i>
		4/15	4.2			<i>id</i>		Gebel Abu Had, Egypt
		4/17	4.6			<i>id</i>	<i>id</i>	<i>id</i>
		4/16	4.6			<i>id</i>	<i>id</i>	<i>id</i>
	as <i>L. chowii</i>	4/2	5.8			<i>id</i>		Walvis Ridge, Southeast Atlantic
		4/1	5.8			<i>id</i>	<i>id</i>	<i>id</i>
		4/3	6.3			<i>id</i>	<i>id</i>	<i>id</i>
		4/4	6.3			<i>id</i>	<i>id</i>	<i>id</i>
	as <i>L. schmitzii</i>	3/15	3.8			<i>id</i>		Gebel Abu Had, Egypt
		3/14	5			<i>id</i>	<i>id</i>	<i>id</i>
	as <i>L. cf. L. janii</i>	3/13	5			<i>id</i>		Walvis Ridge, Southeast Atlantic
		3/11	5.4			<i>id</i>	<i>id</i>	<i>id</i>
		3/12	5.4			<i>id</i>	<i>id</i>	<i>id</i>
	<i>L. pileatus</i>	5/3	7.1			<i>id</i>		<i>id</i>
		5/1	7.5			<i>id</i>	<i>id</i>	<i>id</i>
		5/2	7.5			<i>id</i>	<i>id</i>	<i>id</i>
		5/4	6.3			<i>id</i>	<i>id</i>	<i>id</i>
		5/5	5.4			<i>id</i>	<i>id</i>	<i>id</i>

Lithoptychius (continued)

Reference	Species	Plate/ Figure	Height (μm)	Diameter (μm)	Magnifica- tion	Age	Formation	Location
Monechi et al. 2012	<i>L. pileatus</i>	5/6	4.2			E. Paleocene		Walvis Ridge, Southeast Atlantic
		5/7	4.2			<i>id</i>		<i>id</i>
		5/9	4.2			<i>id</i>		<i>id</i>
		5/8	3.8			<i>id</i>		<i>id</i>
		5/11	6.3			<i>id</i>		<i>id</i>
		5/10	6.7			<i>id</i>		<i>id</i>
		5/13	5			<i>id</i>		<i>id</i>
		5/12	5			<i>id</i>		<i>id</i>
	as <i>L. janii</i>	3/25	5.8			<i>id</i>		<i>id</i>
		3/24	6.3			<i>id</i>		<i>id</i>
		3/20	6.3			<i>id</i>		<i>id</i>
	<i>L. schmitzii</i>	3/5	3.8			<i>id</i>		<i>id</i>
		3/3	4.2			<i>id</i>		<i>id</i>
		3/4	4.6			<i>id</i>		<i>id</i>
		3/7	3.3			<i>id</i>		<i>id</i>
		3/6	3.3			<i>id</i>		<i>id</i>
		3/9	5.8			<i>id</i>		<i>id</i>
		3/8	5			<i>id</i>		<i>id</i>
		3/10	5			<i>id</i>		Gebel Abu Had, Egypt
	<i>L. ulii</i>	4/20	5.4			<i>id</i>		Walvis Ridge, Southeast Atlantic
		4/18	5.8			<i>id</i>		<i>id</i>
		4/19	5.8			<i>id</i>		<i>id</i>
		4/21	5.4			<i>id</i>		<i>id</i>
		4/22	5.4			<i>id</i>		<i>id</i>
		4/23	5.4			<i>id</i>		<i>id</i>
		4/24	6.3			<i>id</i>		<i>id</i>
		4/25	5			<i>id</i>		<i>id</i>
		3/19	6.3			<i>id</i>		<i>id</i>
		3/18	6.7			<i>id</i>		<i>id</i>
		3/17	6.3			<i>id</i>		<i>id</i>
		3/16	6.3			<i>id</i>		<i>id</i>
		<i>L. billii</i>	5/14	6.7			<i>id</i>	
	5/15		5.8			<i>id</i>		<i>id</i>
5/16	5.4				<i>id</i>		<i>id</i>	
5/18	6.7				<i>id</i>		<i>id</i>	
5/17	6.7				<i>id</i>		<i>id</i>	
5/20	7.1				<i>id</i>		<i>id</i>	
5/19	7.1				<i>id</i>		<i>id</i>	
5/21	6.3			<i>id</i>		<i>id</i>		

Reference	Species	Plate/ Figure	Height (μm)	Diameter (μm)	Magnifica- tion	Age	Formation	Location
Monechi et al. 2012	<i>L. billii</i>	5/23	5.8			E. Paleocene		Walvis Ridge, Southeast Atlantic
		5/22	4.6			<i>id</i>		<i>id</i>
		5/25	7.1			<i>id</i>		<i>id</i>
		5/24	7.1			<i>id</i>		<i>id</i>
Monechi et al. 2013	<i>L. pileatus</i>	1/19	6.3			Danian-Selandi- an		<i>id</i>
		as <i>L. janii</i>	1/22	6.3			<i>id</i>	<i>id</i>
		1/21	6.3			<i>id</i>	<i>id</i>	
	<i>L. schmitzii</i>	1/9	4.3			<i>id</i>		Gebel Abu Had, Egypt
		1/8	4.3			<i>id</i>		<i>id</i>
		1/13	5.3			<i>id</i>		Walvis Ridge, SE Atlantic
		1/14	5.3			<i>id</i>		<i>id</i>
		1/12	3.7			<i>id</i>		Gebel Abu Had, Egypt
	1/11	4.3			<i>id</i>		<i>id</i>	
<i>L. vertebra- toides</i>	1/24	5.3			<i>id</i>		Walvis Ridge, SE Atlantic	
Okada and Thierstein 1979	as <i>F. pileatus</i>	17/2	5.8			M. Paleocene		<i>J</i> -Anomaly Ridge, W. North Atlantic Ocean
		17/3		5		<i>id</i>		<i>id</i>
	as <i>F. ulii</i>	17/7		6.9		<i>id</i>		<i>id</i>
	as <i>F. sp. 1</i>	6/10a	5			<i>id</i>		NW Atlantic Ocean
		6/10b	5			<i>id</i>		<i>id</i>
		17/8	5.5			<i>id</i>		<i>id</i>
as <i>F. pileatus</i>	17/2	6.2			<i>id</i>		<i>id</i>	
	17/3		5.2		<i>id</i>		<i>id</i>	
as <i>F. ulii</i>	17/7		6.2		<i>id</i>		<i>id</i>	
Pavšič 1977	as <i>F. merloti</i>	7/1			1500	Paleocene		Podsabotin Village, Slovenia
		7/2			<i>id</i>	<i>id</i>	<i>id</i>	
		7/3			<i>id</i>	<i>id</i>	<i>id</i>	
Perch-Nielsen 1971a	as <i>F. janii</i>	5/4			10000	<i>id</i>		Bay of Biscay
		5/1			10900	<i>id</i>	<i>id</i>	
		5/2			10000	<i>id</i>	<i>id</i>	
		5/3			8800	<i>id</i>	<i>id</i>	
		14/37			2000	<i>id</i>	<i>id</i>	
		14/38			<i>id</i>	<i>id</i>	<i>id</i>	
	14/39			<i>id</i>	<i>id</i>	<i>id</i>		
	as <i>F. ulii</i>	14/17				<i>id</i>	<i>id</i>	<i>id</i>
		14/18				<i>id</i>	<i>id</i>	<i>id</i>
2/3					12400	<i>id</i>	<i>id</i>	

Lithoptychius (continued)

Reference	Species	Plate/ Figure	Height (μm)	Diameter (μm)	Magnifica- tion	Age	Formation	Location
Perch-Nielsen 1971a	as <i>F. ulii</i>	2/2			9400	Paleocene		Bay of Biscay
		2/1			7300	<i>id</i>		<i>id</i>
		2/4			13800	<i>id</i>		<i>id</i>
	as <i>F. billii</i>	14/31			2000	<i>id</i>		<i>id</i>
		14/32			<i>id</i>	<i>id</i>		<i>id</i>
		14/33			<i>id</i>	<i>id</i>		<i>id</i>
		5/6			6000	<i>id</i>		<i>id</i>
		5/9			5700	<i>id</i>		<i>id</i>
		4/11			7650	<i>id</i>		<i>id</i>
		5/7			5100	<i>id</i>		<i>id</i>
		5/10			5000	<i>id</i>		<i>id</i>
		5/5			6500	<i>id</i>		<i>id</i>
5/8			7300	<i>id</i>		<i>id</i>		
Perch-Nielsen 1971b	as <i>F. billii</i>	1/6			8600	Eocene		Cantabria Sea- mount, Bay of Biscay
		1/8			10000	<i>id</i>		<i>id</i>
		1/7			7700	<i>id</i>		<i>id</i>
Perch-Nielsen 1977	as <i>F. janii</i>	12/9			7000	Paleocene		São Paulo Plateau, Atlantic Ocean
		12/13			<i>id</i>	<i>id</i>		<i>id</i>
		12/2			<i>id</i>	<i>id</i>		<i>id</i>
		12/3			<i>id</i>	<i>id</i>		<i>id</i>
		12/4			<i>id</i>	<i>id</i>		<i>id</i>
		12/5			<i>id</i>	<i>id</i>		<i>id</i>
		12/8			<i>id</i>	<i>id</i>		<i>id</i>
		12/10			<i>id</i>	<i>id</i>		<i>id</i>
		12/11			<i>id</i>	<i>id</i>		<i>id</i>
		12/12			<i>id</i>	<i>id</i>		<i>id</i>
		12/14			<i>id</i>	<i>id</i>		<i>id</i>
		12/15			<i>id</i>	<i>id</i>		<i>id</i>
		12/16			<i>id</i>	<i>id</i>		<i>id</i>
		12/17			<i>id</i>	<i>id</i>		<i>id</i>
	12/18			<i>id</i>	<i>id</i>		<i>id</i>	
	49/26			2000	<i>id</i>		<i>id</i>	
	as <i>F. ulii</i>	49/23			<i>id</i>	<i>id</i>		<i>id</i>
		49/24			<i>id</i>	<i>id</i>		<i>id</i>
		49/25			<i>id</i>	<i>id</i>		<i>id</i>
		10/20			6000	<i>id</i>		Ceara Rise, Atlan- tic Ocean
11/1				5400	<i>id</i>		São Paulo Plateau, Atlantic Ocean	

Lithoptychius (continued)

Reference	Species	Plate/ Figure	Height (μm)	Diameter (μm)	Magnifica- tion	Age	Formation	Location	
Perch-Nielsen 1977		10/18			7500	Maastrichtian		Ceara Rise, Atlan- tic Ocean	
		10/19			7000	<i>id</i>		<i>id</i>	
		11/2			6800	<i>id</i>		São Paulo Plateau, Atlantic Ocean	
		11/3			<i>id</i>	<i>id</i>		<i>id</i>	
	as <i>F. aff. billii</i>	49/27			2000	<i>id</i>		<i>id</i>	
		49/28			<i>id</i>	<i>id</i>		<i>id</i>	
49/29				<i>id</i>	<i>id</i>		<i>id</i>		
Perch-Nielsen et al. 1978	as <i>F. sp.</i>	15/9			4500	L. Paleocene	Kilabiya Chalk, Owaina Shale	Gebel Oweina, Nile Valley, Egypt	
		15/10			7000	M. Paleocene	Lower Owaina Shale	<i>id</i>	
	as <i>F. ulii</i>	15/8			9100	L. Paleocene	Kilabiya Chalk, Owaina Shale	<i>id</i>	
Prins 1971	as <i>F. sp. 1</i>	6/4a			2500	x		x	
		6/4b			<i>id</i>	x		x	
		6/4c			<i>id</i>	x		x	
	as <i>Discoaster-oides megastypus</i>	6/12a			<i>id</i>	x		x	
		6/12b			<i>id</i>	x		x	
		6/12c			<i>id</i>	x		x	
	as <i>F. sp. 1</i>	6/5a			<i>id</i>	x		x	
		6/5b			<i>id</i>	x		x	
		6/5c			<i>id</i>	x		x	
	as <i>F. tympani-formis/ F. sp. 1</i>	6/3a			<i>id</i>	x		x	
		6/3b			<i>id</i>	x		x	
		6/3c			<i>id</i>	x		x	
	as <i>F. tympani-formis</i>	6/1a			<i>id</i>	x		x	
		6/1b			<i>id</i>	x		x	
		6/1c			<i>id</i>	x		x	
		6/2a			<i>id</i>	x		x	
		6/2b			<i>id</i>	x		x	
		6/2c			<i>id</i>	x		x	
	Proto Decima et al. 1978	as <i>F. janii</i>	12/1a			2800	Paleocene		SE Atlantic Ocean
			12/1b			<i>id</i>	<i>id</i>		<i>id</i>
			12/1c			<i>id</i>	<i>id</i>		<i>id</i>
Romein 1979	as <i>F. janii</i>	5/1			6000	L. Paleocene	Jorquera, Car- avaca Section	Spain	
	as <i>F. bitectus</i>	9/15			25000	M. Paleocene	Nahal Avdat	Israel	
	as <i>F. ulii</i>	4/7			6000	Paleocene	Jorquera, Car- avaca Section	Spain	

Lithoptychius (continued)

Reference	Species	Plate/ Figure	Height (μm)	Diameter (μm)	Magnifica- tion	Age	Formation	Location	
Roth 1973	as <i>F. sp.</i>	16/2a			3000	E. Paleocene		Magellan Rise,	
	cf. <i>F. ulii</i>	16/2b			<i>id</i>	<i>id</i>		Central Pacific Basin	
		16/1a			<i>id</i>	<i>id</i>		<i>id</i>	
		16/1b			<i>id</i>	<i>id</i>		<i>id</i>	
		16/1c			<i>id</i>	<i>id</i>		<i>id</i>	
		16/1d			<i>id</i>	<i>id</i>		<i>id</i>	
Steurbaut and Sztrákos 2002	as <i>F. janii</i>	3/11		6		Selandian	Gan-Rébénacq Road Section	Aquitaine, France	
	as <i>F. pileatus</i>	4/10	8.3			<i>id</i>	<i>id</i>	<i>id</i>	
	as <i>F. janii</i>	3/10a		6		<i>id</i>	<i>id</i>	<i>id</i>	
		3/10b		6		<i>id</i>	<i>id</i>	<i>id</i>	
as <i>F. ulii</i>	4/11	8.3			<i>id</i>	<i>id</i>	<i>id</i>		
	4/12	7.8			<i>id</i>	<i>id</i>	<i>id</i>		
	4/13	7.8			<i>id</i>	<i>id</i>	<i>id</i>		
Steurbaut and Sztrákos 2008	as <i>F. varolii</i>	2/18a			1520	Danian	Lasseube Fm	Southwest France	
		2/18b			<i>id</i>	<i>id</i>	<i>id</i>	<i>id</i>	
		2/17a			1330	<i>id</i>	<i>id</i>	<i>id</i>	
		2/17b			<i>id</i>	<i>id</i>	<i>id</i>	<i>id</i>	
	as <i>F. pileatus</i>	3/25b				1530	Selandian	Pont-Labau Fm	<i>id</i>
		3/25a				<i>id</i>	<i>id</i>	<i>id</i>	<i>id</i>
		3/26				3000	<i>id</i>	<i>id</i>	<i>id</i>
		3/23				3430	<i>id</i>	<i>id</i>	<i>id</i>
		3/24				4000	<i>id</i>	<i>id</i>	<i>id</i>
	as <i>F. janii</i>	3/11				1930	<i>id</i>	<i>id</i>	<i>id</i>
		3/12				2780	<i>id</i>	<i>id</i>	<i>id</i>
		3/13				3125	<i>id</i>	<i>id</i>	<i>id</i>
		3/14				2860	<i>id</i>	<i>id</i>	<i>id</i>
		3/15				3000	Danian	Lasseube Fm	<i>id</i>
	as <i>F. vertebra- toides</i>	3/1a				1670	Selandian	Pont-Labau Fm	<i>id</i>
		3/1b				<i>id</i>	<i>id</i>	<i>id</i>	<i>id</i>
		3/2a				2800	Danian	Lasseube Fm	<i>id</i>
		3/2b				<i>id</i>	<i>id</i>	<i>id</i>	<i>id</i>
		3/3				2810	<i>id</i>	<i>id</i>	<i>id</i>
3/4					1670	<i>id</i>	<i>id</i>	<i>id</i>	
3/5					1360	Selandian	Pont-Labau Fm	<i>id</i>	
3/21				2890	<i>id</i>	<i>id</i>	<i>id</i>		
as <i>F. ulii</i>	2/19				1700	Danian	Lasseube Fm	<i>id</i>	
	2/20a				1400	<i>id</i>	<i>id</i>	<i>id</i>	
	2/20b				<i>id</i>	<i>id</i>	<i>id</i>	<i>id</i>	

Lithoptychius (continued)

Reference	Species	Plate/ Figure	Height (μm)	Diameter (μm)	Magnifica- tion	Age	Formation	Location
Varol 1989	as <i>F. chowi</i>	12.5/11	5			E. Paleocene	Kokaksu Sec- tion	Zonguldak, North- ern Turkey
		12.5/12	3.3			<i>id</i>	<i>id</i>	<i>id</i>
		12.5/13	4.4			<i>id</i>		North Sea Area (Block 21)
	as <i>F. janii</i>	12.5/1	3.9			Paleocene	Kokaksu Sec- tion	Zonguldak, North- ern Turkey
		12.5/2	5			<i>id</i>	<i>id</i>	<i>id</i>
	as <i>F. ulii</i>	12.5/10	6.7			L. Paleocene	<i>id</i>	<i>id</i>

Fasciculithus

Reference	Species	Plate/ Figure	Height (μm)	Diameter (μm)	Magnifica- tion	Age	Formation	Location
Agnini et al. 2007	as <i>F. clinatus</i>	2/8			1200	M. Pal-E. Eoc		SE Atlantic Ocean
Bown 2005a	<i>F. aubertae</i>	40/16	2			L. Paleocene		Coastal Tanzania
		40/17	2.4			L. Pal-E. Eoc		<i>id</i>
	<i>F. richardii</i>	40/31	7.2			L. Paleocene		<i>id</i>
		40/32	7.2			<i>id</i>		<i>id</i>
Bown 2005b	<i>F. clinatus</i>	12/3	2.5			<i>id</i>		Shatsky Rise, NW Pacific Ocean
	<i>F. fenestrel- latus</i>	12/19	8.5			<i>id</i>		<i>id</i>
		12/20	8			<i>id</i>		<i>id</i>
		12/21	10			<i>id</i>		<i>id</i>
		12/22	10			<i>id</i>		<i>id</i>
		12/23	11			<i>id</i>		<i>id</i>
		12/24	10.5			<i>id</i>		<i>id</i>
	<i>Fasciculithus</i> sp. 1	12/25	8.5			<i>id</i>		<i>id</i>
		12/26	9			<i>id</i>		<i>id</i>
12/27		9			<i>id</i>		<i>id</i>	

Fasciculithus (continued)

Reference	Species	Plate/ Figure	Height (μm)	Diameter (μm)	Magnifica- tion	Age	Formation	Location
Bown 2010	<i>F. lobus</i>	11/21	5.5			PETM		Shatsky Rise, NW Pacific Ocean
		11/22	5.8			<i>id</i>		<i>id</i>
		11/23	4.5			<i>id</i>		<i>id</i>
	<i>F. sidereus</i>	11/24	5.8			L. Paleocene		<i>id</i>
	<i>F. involutus</i>	11/20	4.3			PETM		<i>id</i>
		11/18	4.3			<i>id</i>		<i>id</i>
	<i>F. thomasi</i>	11/15	3.3			L. Paleocene		<i>id</i>
	<i>F. schaubii</i>	11/28	10			<i>id</i>		<i>id</i>
	<i>F. lilianae</i>	11/16	6			<i>id</i>		<i>id</i>
		11/17	5			<i>id</i>		<i>id</i>
	<i>F. alanii</i>	11/14	6			<i>id</i>		<i>id</i>
	as <i>F. tonii</i>	11/12	14			<i>id</i>		<i>id</i>
	<i>F. richardii</i>	11/26	12.5			<i>id</i>		<i>id</i>
11/27		11.8			<i>id</i>		<i>id</i>	
11/25		7.5			<i>id</i>		<i>id</i>	
Bramlette and Sullivan 1961	<i>F. involutus</i>	14/3a	5			Paleocene	Lodo Fm	Fresno County, Central California, USA
		14/3b	5			<i>id</i>	<i>id</i>	<i>id</i>
		14/1a	7.7			<i>id</i>	<i>id</i>	<i>id</i>
		14/1b	6.8			<i>id</i>	<i>id</i>	<i>id</i>
		14/1c	7.7			<i>id</i>	<i>id</i>	<i>id</i>
		14/2a		5.8		<i>id</i>	<i>id</i>	<i>id</i>
		14/2b		5.8		<i>id</i>	<i>id</i>	<i>id</i>
		14/4a		8.2		<i>id</i>	<i>id</i>	<i>id</i>
		14/4b		7.7		<i>id</i>	<i>id</i>	<i>id</i>
		14/5a		5.3		<i>id</i>	<i>id</i>	<i>id</i>
		14/5b		4.8		<i>id</i>	<i>id</i>	<i>id</i>
Bukry 1971	<i>F. clinatus</i>	4/8			2000	L. Paleocene		Shatsky Rise, NW Pacific Ocean
		4/9			<i>id</i>	<i>id</i>		<i>id</i>
Bybell and Self-Trail 1995	<i>F. sidereus</i>	36/6		4.2		<i>id</i>		Gloucester County, New Jersey, USA
		36/7		4.7		<i>id</i>		<i>id</i>
		36/8		5.6		E. Eocene		<i>id</i>
		36/9		4.5		L. Paleocene		<i>id</i>
		36/11		9.5		E. Eocene		<i>id</i>
		16/1b	4.1			L. Paleocene		<i>id</i>
		16/2	4.7			<i>id</i>		<i>id</i>
		16/3b	3.2			<i>id</i>		Camden County, New Jersey, USA
		16/4b	4.2			<i>id</i>		Gloucester County, New Jersey, USA
		16/5b	3.3			<i>id</i>		<i>id</i>

Reference	Species	Plate/ Figure	Height (μm)	Diameter (μm)	Magnifica- tion	Age	Formation	Location
Bybell and Self-Trail 1995	<i>F. sidereus</i>	16/6b	4.9			L. Paleocene		Gloucester County, New Jersey, USA
		16/1c	4.1			<i>id</i>		<i>id</i>
		16/6a	4.9			<i>id</i>		<i>id</i>
		16/1a	4.1			<i>id</i>		<i>id</i>
		16/3a	3.2			<i>id</i>		Camden County, New Jersey, USA
		16/4a	4.2			<i>id</i>		Gloucester County, New Jersey, USA
		16/5a	3.3			<i>id</i>		<i>id</i>
	<i>F. aubertae</i>	35/12	3.8			<i>id</i>		<i>id</i>
		35/13	3.5			<i>id</i>		Camden County, New Jersey, USA
		35/14	2.3			<i>id</i>		Gloucester County, New Jersey, USA
	<i>F. tympaniformis</i>	36/14	5.4			<i>id</i>		Camden County, New Jersey, USA
		36/15	4.2			<i>id</i>		<i>id</i>
		36/19	4.7			<i>id</i>		Gloucester County, New Jersey, USA
		36/20	4.7			<i>id</i>		<i>id</i>
	<i>F. involutus</i>	36/1	4.7			E. Eocene		<i>id</i>
		36/2	3.5			L. Paleocene		<i>id</i>
		36/3	6.3			<i>id</i>		<i>id</i>
		15/3b	7.4			<i>id</i>		Camden County, New Jersey, USA
		15/6b	4.8			<i>id</i>		<i>id</i>
		15/4b	3.6			<i>id</i>		Gloucester County, New Jersey, USA
		15/5b	3.9			<i>id</i>		Camden County, New Jersey, USA
		15/3a	7.4			<i>id</i>		<i>id</i>
		15/4a	3.6			<i>id</i>		Gloucester County, New Jersey, USA
		15/5a	3.9			<i>id</i>		Camden County, New Jersey, USA
		15/6a	4.8			<i>id</i>		<i>id</i>
		15/7a	3.1			<i>id</i>		Gloucester County, New Jersey, USA
		15/7b	3.1			<i>id</i>		<i>id</i>
	<i>F. thomasii</i>	36/12	7.8			<i>id</i>		<i>id</i>
		36/13	8.3			<i>id</i>		<i>id</i>
		17/1b	4.3			<i>id</i>		Stafford County, Virginia, USA
		17/2b	4.1			<i>id</i>		Camden County, New Jersey, USA
		17/3b	4.3			<i>id</i>		Gloucester County, New Jersey, USA

Fasciculithus (continued)

Reference	Species	Plate/ Figure	Height (μm)	Diameter (μm)	Magnifica- tion	Age	Formation	Location
Bybell and Self-Trail 1995	<i>F. thomasii</i>	17/4b	3.7			L. Paleocene		Gloucester County, New Jersey, USA
		17/5a	4.1			<i>id</i>		<i>id</i>
		17/1a	4.3			<i>id</i>		Stafford County, Virginia, USA
		17/2a	4.1			<i>id</i>		Camden County, New Jersey, USA
		17/3a	4.3			<i>id</i>		Gloucester County, New Jersey, USA
		17/4a	3.7			<i>id</i>		<i>id</i>
		17/5b	4.1			<i>id</i>		<i>id</i>
	<i>F. schaubii</i>	36/5	8.4			<i>id</i>		<i>id</i>
36/10		5.7			<i>id</i>		<i>id</i>	
Gartner 1971	as <i>F. mitreus</i>	3/4a			2500	<i>id</i>		Blake Plateau, Atlantic Ocean
		3/4b			<i>id</i>	<i>id</i>		<i>id</i>
		3/4c			<i>id</i>	<i>id</i>		<i>id</i>
		3/3a			<i>id</i>	<i>id</i>		<i>id</i>
		3/3b			<i>id</i>	<i>id</i>		<i>id</i>
		3/1			10000	<i>id</i>		<i>id</i>
		3/2			<i>id</i>	<i>id</i>		<i>id</i>
4/1			<i>id</i>	<i>id</i>		<i>id</i>		
Haq 1971	as <i>F. hayi</i>	1/3			4000	Paleocene	Tang-E-Bijar Section	Bijar Valley, West- Central Persia
		1/2			<i>id</i>	<i>id</i>	<i>id</i>	<i>id</i>
Haq and Aubry 1980	as <i>F. aubertae</i>	1/14			2000			North Africa/ Middle East
		5/1		8.2			Jabal-um-Re- jam Section	Jordan
	as <i>F. schaubii</i>	5/3	6.3				<i>id</i>	<i>id</i>
		5/4	19	12.5			<i>id</i>	<i>id</i>
	as <i>F. hayi</i>	5/5		11.4			<i>id</i>	<i>id</i>
5/6			11			<i>id</i>	<i>id</i>	
Hay and Mohler 1967	as <i>F. tympani- formis</i>	204/13			2250	Pal-E. Eoc		Pont Labau, France
		204/14			<i>id</i>	<i>id</i>		<i>id</i>
		204/15			<i>id</i>	<i>id</i>		<i>id</i>
		204/10			<i>id</i>	<i>id</i>		<i>id</i>
		204/11			<i>id</i>	<i>id</i>		<i>id</i>
		204/12			<i>id</i>	<i>id</i>		<i>id</i>
		205/4			4500	<i>id</i>		<i>id</i>
		205/8			<i>id</i>	<i>id</i>		<i>id</i>
		205/7			<i>id</i>	<i>id</i>		<i>id</i>
		205/5			<i>id</i>	<i>id</i>		<i>id</i>
	as <i>F. involutus</i>	204/4			2250	<i>id</i>		<i>id</i>

Fasciculithus (continued)

Reference	Species	Plate/ Figure	Height (μm)	Diameter (μm)	Magnifica- tion	Age	Formation	Location		
Hay and Mohler 1967	as <i>F. involutus</i>	204/8			2250	Pal-E. Eoc		Pont Labau, France		
		204/9			<i>id</i>	<i>id</i>		<i>id</i>		
		203/9			9000	<i>id</i>		<i>id</i>		
		203/6			4500	<i>id</i>		<i>id</i>		
		203/1			<i>id</i>	<i>id</i>		<i>id</i>		
		203/3			<i>id</i>	<i>id</i>		<i>id</i>		
	as <i>F. schaubi</i>	204/1			2250	<i>id</i>			<i>id</i>	
		204/2			<i>id</i>	<i>id</i>			<i>id</i>	
		204/3			<i>id</i>	<i>id</i>			<i>id</i>	
		204/5			<i>id</i>	<i>id</i>			<i>id</i>	
		204/6			<i>id</i>	<i>id</i>			<i>id</i>	
		204/7			<i>id</i>	<i>id</i>			<i>id</i>	
		203/7			4500	<i>id</i>			<i>id</i>	
		203/2			<i>id</i>	<i>id</i>			<i>id</i>	
		203/10			<i>id</i>	<i>id</i>			<i>id</i>	
		203/4			<i>id</i>	<i>id</i>			<i>id</i>	
		Hay et al. 1967	as <i>F. tympani- formis</i>	8/1			9000	Paleocene		<i>id</i>
				8/2			<i>id</i>	<i>id</i>		<i>id</i>
8/4					7000	<i>id</i>		<i>id</i>		
8/3					<i>id</i>	<i>id</i>		<i>id</i>		
8/5					<i>id</i>	<i>id</i>		<i>id</i>		
9/1					9000	<i>id</i>		<i>id</i>		
9/2					<i>id</i>	<i>id</i>		<i>id</i>		
9/4					7000	<i>id</i>		<i>id</i>		
9/3					<i>id</i>	<i>id</i>		<i>id</i>		
9/5					<i>id</i>	<i>id</i>		<i>id</i>		
Martini 1971	<i>F. tympani- formis</i>	1/11	5.4		~ 2000	<i>id</i>		<i>id</i>		
		1/12	4.8		<i>id</i>	<i>id</i>		<i>id</i>		
Monechi 1985	<i>F. clinatus</i>	7/5A			2800	M. Paleocene		NW Pacific Ocean		
		7/5B			<i>id</i>	<i>id</i>		<i>id</i>		
		7/2			9800	<i>id</i>		<i>id</i>		
Müller 1974	<i>F. tympani- formis</i>	5/6			5000	Paleocene		Western Indian Ocean		
		5/7			<i>id</i>	<i>id</i>		<i>id</i>		
Okada and Thierstein 1979	as <i>F. crinatus</i> , err. pro cit.	17/1	5			M. Paleocene		Western North Atlantic Ocean		
	as <i>F. tympani- formis</i>	17/6	4			<i>id</i>		<i>id</i>		
		17/5	5.1			<i>id</i>		<i>id</i>		

Fasciculithus (continued)

Reference	Species	Plate/ Figure	Height (μm)	Diameter (μm)	Magnifica- tion	Age	Formation	Location
Perch-Nielsen 1971a	as <i>Fasciculithus</i> sp. 1	2/6			8200	Paleocene		Bay of Biscay
		2/5			14600	<i>id</i>		<i>id</i>
	<i>F. tympaniformis</i>	1/5			14200	<i>id</i>		<i>id</i>
		1/1			4800	<i>id</i>		<i>id</i>
		1/4			7700	<i>id</i>		<i>id</i>
		1/7			7000	<i>id</i>		<i>id</i>
		1/3			7500	<i>id</i>		<i>id</i>
		1/2			8600	<i>id</i>		<i>id</i>
		<i>F. involutus</i>	14/28			2000	<i>id</i>	
	14/29				<i>id</i>	<i>id</i>		<i>id</i>
	14/30				<i>id</i>	<i>id</i>		<i>id</i>
	4/1				10200	<i>id</i>		<i>id</i>
	4/2				11100	<i>id</i>		<i>id</i>
	4/6				9200	<i>id</i>		<i>id</i>
	4/9				7500	<i>id</i>		<i>id</i>
	7/5				10000	<i>id</i>		<i>id</i>
	4/8				9900	<i>id</i>		<i>id</i>
	4/10				8100	<i>id</i>		<i>id</i>
	4/4				9100	<i>id</i>		<i>id</i>
	4/7				6100	<i>id</i>		<i>id</i>
	4/3				9800	<i>id</i>		<i>id</i>
	4/5				7800	<i>id</i>		<i>id</i>
	<i>F. bobii</i>	14/34			2000	<i>id</i>		<i>id</i>
		14/35			<i>id</i>	<i>id</i>		<i>id</i>
		14/36			<i>id</i>	<i>id</i>		<i>id</i>
		3/4			9900	<i>id</i>		<i>id</i>
		3/1			11400	<i>id</i>		<i>id</i>
		3/2			10400	<i>id</i>		<i>id</i>
		3/5			5600	<i>id</i>		<i>id</i>
		3/6			11200	<i>id</i>		<i>id</i>
		3/3			12000	<i>id</i>		<i>id</i>
		1/6			6400	<i>id</i>		<i>id</i>
	<i>F. thomasi</i>	6/5			10200	<i>id</i>		<i>id</i>
9/3				6600	<i>id</i>		<i>id</i>	
6/6				8900	<i>id</i>		<i>id</i>	
<i>F. schaubi</i>	14/25			2000	<i>id</i>		<i>id</i>	
	14/26			<i>id</i>	<i>id</i>		<i>id</i>	
	14/27			<i>id</i>	<i>id</i>		<i>id</i>	
	7/6			10200	<i>id</i>		<i>id</i>	

Fasciculithus (continued)

Reference	Species	Plate/ Figure	Height (μm)	Diameter (μm)	Magnifica- tion	Age	Formation	Location
Perch-Nielsen 1971a	<i>F. schaubi</i>	9/1			5600	Paleocene		Bay of Biscay
	as <i>F. liliana</i> e	14/40			2000	<i>id</i>		<i>id</i>
		14/41			<i>id</i>	<i>id</i>		<i>id</i>
		14/42			<i>id</i>	<i>id</i>		<i>id</i>
	<i>F. liliana</i> e	6/3			6600	<i>id</i>		<i>id</i>
		6/1			9700	<i>id</i>		<i>id</i>
	as <i>F. alanii</i>	7/3			9100	<i>id</i>		<i>id</i>
		6/4			7200	<i>id</i>		<i>id</i>
		14/13			2000	<i>id</i>		<i>id</i>
		14/14			<i>id</i>	<i>id</i>		<i>id</i>
		9/4			6600	<i>id</i>		<i>id</i>
		6/2			11500	<i>id</i>		<i>id</i>
		7/1			6100	<i>id</i>		<i>id</i>
		7/2			7300	<i>id</i>		<i>id</i>
	<i>F. tonii</i>	14/15			2000	<i>id</i>		<i>id</i>
		14/16			<i>id</i>	<i>id</i>		<i>id</i>
		7/4			4300	<i>id</i>		<i>id</i>
	<i>F. richardii</i>	14/5			2000	<i>id</i>		<i>id</i>
		14/6			<i>id</i>	<i>id</i>		<i>id</i>
		14/7			<i>id</i>	<i>id</i>		<i>id</i>
		8/2			6400	<i>id</i>		<i>id</i>
		8/3			6500	<i>id</i>		<i>id</i>
		8/4			8000	<i>id</i>		<i>id</i>
9/2				6400	<i>id</i>		<i>id</i>	
8/1				5800	<i>id</i>		<i>id</i>	
8/5				7000	<i>id</i>		<i>id</i>	
8/6			8400	<i>id</i>		<i>id</i>		
Perch-Nielsen 1977	as <i>F. tympani-</i> <i>formis</i>	10/22			10000	L. Paleocene		Ceará Rise, West- ern South Atlantic
		10/23			<i>id</i>	<i>id</i>		<i>id</i>
Pospichal and Wise 1990	as <i>F. involutus</i>	3/7			3500	<i>id</i>		Maud Rise, South- ern Ocean
Romein 1979	as <i>F. involutus</i>	5/4			6000	<i>id</i>	Jorquera,	Spain
		5/5			<i>id</i>	<i>id</i>	Caravaca Sec- tion	<i>id</i>
	as <i>F. schaubii</i>	5/2			<i>id</i>	<i>id</i>	<i>id</i>	<i>id</i>
	as <i>F. liliana</i> e	5/3			<i>id</i>	<i>id</i>	<i>id</i>	<i>id</i>

Fasciculithus (continued)

Reference	Species	Plate/ Figure	Height (μm)	Diameter (μm)	Magnifica- tion	Age	Formation	Location
Self-Trail 2011	as <i>F. thomasii</i>	8/14	3			E. Eocene		Southern Mary- land, USA
	as <i>F. inversus</i>	8/5	4.1			L. Paleocene		<i>id</i>
		8/6	5.3			E. Eocene		<i>id</i>
		8/7	4.5			L. Paleocene		<i>id</i>
	<i>F. thomasii</i>	8/13	6			<i>id</i>		<i>id</i>
	<i>F. richardii</i>	8/9	6.8			<i>id</i>		<i>id</i>
8/10		8.6			<i>id</i>		<i>id</i>	
Steurbaut and	as <i>Fasciculi- thus</i> sp.	2/22			1520	Selandian	Pont-Labau Fm	Southwest France
Sztrákósz 2008	<i>F. tympani- formis</i>	2/25			<i>id</i>	<i>id</i>	<i>id</i>	<i>id</i>
Sullivan 1964	<i>F. involutus</i>	12/9b	7.6			Paleocene		California, USA
		12/9a	7.6			<i>id</i>		<i>id</i>
Varol 1989	as <i>F. tympani- formis</i>	12.5/8	2.8			L. Paleocene		Walvis Ridge, South Atlantic Ocean
		12.5/9	5			<i>id</i>		<i>id</i>
	as <i>F. involutus</i>	12.5/5	4.4			<i>id</i>		India
Wang and Huang 1989	as <i>F. lingfen- gensis</i>	72/1			3000	Cenozoic		East China Sea (Donghai)
		72/2			<i>id</i>	<i>id</i>		<i>id</i>
		73/3			<i>id</i>	<i>id</i>		<i>id</i>
Wise and Wind 1977	as <i>F. involutus</i>	15/1			7000	Paleocene		Pont Labau, France
		16/1			<i>id</i>	<i>id</i>		x
		16/3			11000	<i>id</i>		x
		15/5			10000	<i>id</i>		Falkland Plateau, Southern Ocean
		15/3			<i>id</i>	<i>id</i>		<i>id</i>
		16/5			9000	<i>id</i>		x
	<i>F. involutus</i>	16/6			7000	<i>id</i>		Falkland Plateau, Southern Ocean
		16/2			8000	<i>id</i>		<i>id</i>
		16/4			9000	<i>id</i>		<i>id</i>
		15/6			7000	<i>id</i>		<i>id</i>
		15/4			x	<i>id</i>		x
		15/2			10000	<i>id</i>		Lodo Fm Fresno County, Central California, USA

Reference	Species	Plate/ Figure	Diameter (μm)	Magnifica- tion	Age	Formation	Location
Bown 2010	<i>B. elegans</i>	10/5	7.7		L. Pal-E. Eoc		Near Pande, Southern Tanzania
Haq and Lohmann 1976	as <i>Fasciculi- thus rotundus</i>	4/9	6.5		L. Paleocene		Nicaragua Rise, Caribbean Sea
		4/8	6.8		<i>id</i>		<i>id</i>
Okada & Thierstein 1979	as <i>Heliolithus</i>	14/2	5.5		M. Paleocene		Western North Atlantic Ocean
	aff. <i>cantabriae</i>	14/1	6		<i>id</i>		<i>id</i>
Perch-Nielsen 1977	<i>B. elegans</i>	12/1		14000	Paleocene		São Paulo Plateau, Western South Atlantic
Perch-Nielsen et al. 1978	<i>B. elegans</i>	9/5		~ 2000	e. Tert		Nile Valley, Egypt
		9/6		<i>id</i>	<i>id</i>		<i>id</i>
		9/25		<i>id</i>	<i>id</i>		<i>id</i>
		9/26		<i>id</i>	<i>id</i>		<i>id</i>
		9/27		<i>id</i>	<i>id</i>		<i>id</i>
		9/28		<i>id</i>	<i>id</i>		<i>id</i>
		16/7		7200	L. Paleocene	Kilabiya Chalk,	Gebel Oweina, Nile Valley, Egypt
		16/11		8600	<i>id</i>	Owaina Shale	<i>id</i>
		17/8		7600	<i>id</i>	<i>id</i>	<i>id</i>
		17/11		7500	<i>id</i>	<i>id</i>	<i>id</i>
		17/9		3500	<i>id</i>	<i>id</i>	<i>id</i>
		16/8		8600	<i>id</i>	<i>id</i>	<i>id</i>
Romein 1979	as <i>Heliolithus elegans</i>	10/1		1500	E. Eocene	Nahal Avdat	Israel
Roth 1973	<i>B. elegans</i>	15/3a		3000	L. Paleocene		Central Pacific Basin
		15/3b		<i>id</i>	<i>id</i>		<i>id</i>
		15/3c		<i>id</i>	<i>id</i>		<i>id</i>
		15/4a		<i>id</i>	<i>id</i>		<i>id</i>
		15/4b		<i>id</i>	<i>id</i>		<i>id</i>
		15/6a		<i>id</i>	<i>id</i>		<i>id</i>
		15/6b		<i>id</i>	<i>id</i>		<i>id</i>
		15/6c		<i>id</i>	<i>id</i>		<i>id</i>
		15/6d		<i>id</i>	<i>id</i>		<i>id</i>
		15/5a		<i>id</i>	<i>id</i>		<i>id</i>
		15/5b		<i>id</i>	<i>id</i>		<i>id</i>
		15/5c		<i>id</i>	<i>id</i>		<i>id</i>
		15/1		5000	<i>id</i>	<i>id</i>	<i>id</i>
		15/2a		11000	<i>id</i>	<i>id</i>	<i>id</i>
		15/2b		<i>id</i>	<i>id</i>	<i>id</i>	<i>id</i>
		15/2c		<i>id</i>	<i>id</i>	<i>id</i>	<i>id</i>
Sturbaut and Sztrákos 2008	<i>B. elegans</i>	4/27	4.5		Selandian	Gan-Rébénacq Road Section	Aquitaine, France

Reference	Species	Plate/ Figure	Height (μm)	Diameter (μm)	Magnifica- tion	Age	Formation	Location
Aubry 1986	<i>H. kleinPELLI</i>	1/21			1750	Thanetian	Thanet Beds	Herne Bay, Kent, England
		1/22			<i>id</i>	<i>id</i>	<i>id</i>	<i>id</i>
Bown 2010	as <i>B. megastypus</i>	10/6			2180	L. Paleocene		Near Pande, S. Tanzania
		10/7			<i>id</i>	<i>id</i>		<i>id</i>
Bramlette and	as <i>Heliolithus</i> aff. <i>riedelii</i>	14/2		13.3		e. Tertiary		California, USA
Sullivan 1961	as <i>Discoasteriodes megastypus</i>	13/14a		3.9		Paleocene	Lodo Fm	Fresno County, Central California, USA
		13/14d		10.2		<i>id</i>	<i>id</i>	<i>id</i>
		13/14c		3.9		<i>id</i>	<i>id</i>	<i>id</i>
		13/14b	4.4	9.7		<i>id</i>	<i>id</i>	<i>id</i>
		13/15a	5.3	9.7		<i>id</i>	<i>id</i>	<i>id</i>
		13/15b	5.3	9.7		<i>id</i>	<i>id</i>	<i>id</i>
		13/15c	5.3			<i>id</i>	<i>id</i>	<i>id</i>
Haq and Aubry 1980	<i>H. kleinPELLI</i>	6/3		12.8		Pal-Eoc	Jabal-um-Re- jam Section	Jordan
	as <i>Discoasteroides?</i> <i>megastypus</i>	7/3		8.8		<i>id</i>	<i>id</i>	<i>id</i>
	<i>H. conicus</i>	6/2		11		<i>id</i>	<i>id</i>	<i>id</i>
		6/7		9		<i>id</i>	<i>id</i>	<i>id</i>
		6/5		8.3		<i>id</i>	<i>id</i>	<i>id</i>
		6/1		8		<i>id</i>	<i>id</i>	<i>id</i>
		6/4		9		<i>id</i>	<i>id</i>	<i>id</i>
Hay and Mohler 1967	<i>H. kleinPELLI</i>	199/4			2250	Pal-E. Eocene		Pont Labau, France
		199/5			<i>id</i>	<i>id</i>	<i>id</i>	
		199/6			<i>id</i>	<i>id</i>	<i>id</i>	
		199/7			<i>id</i>	<i>id</i>	<i>id</i>	
Martini 1971	<i>H. kleinPELLI</i>	1/13		12.3	2000	M. Paleocene	Boongerooda Greensand	Thoothawarra Village, West Australia
		1/14		11.8	<i>id</i>	<i>id</i>	<i>id</i>	<i>id</i>
Martini 1976	as <i>Heliolithus</i> cf. <i>cantabriae</i>	2/6			6500	E. Paleocene		Central Pacific Ocean
Müller 1974	<i>H. kleinPELLI</i>	1/3			2500	Paleocene		Southern Mada- gascar Basin, Western Indian Ocean
		1/2			<i>id</i>	<i>id</i>		<i>id</i>
	<i>H. cantabriae</i>	1/9			5000	<i>id</i>		<i>id</i>
		1/8			2500	<i>id</i>		<i>id</i>

Heliotrochus (continued)

Reference	Species	Plate/ Figure	Height (μm)	Diameter (μm)	Magnifica- tion	Age	Formation	Location
Okada and Thierstein 1979	<i>H. kleinpelli</i>	4/8a		8.1		M. Paleocene		<i>J</i> -Anomaly Ridge,
		4/8b		7.8		<i>id</i>		Western North Atlantic
		14/7		12.8		<i>id</i>		<i>id</i>
		14/5		11.7		<i>id</i>		<i>id</i>
		14/6		10.8		<i>id</i>		<i>id</i>
Perch-Nielsen 1971c	<i>H. kleinpelli</i>	7/26			2000	Paleocene		Bay of Biscay
		7/27			<i>id</i>	<i>id</i>		<i>id</i>
		2/2			5400	<i>id</i>		<i>id</i>
		2/4			6000	<i>id</i>		<i>id</i>
		2/6			7600	<i>id</i>		<i>id</i>
	<i>H. cantabriae</i>	7/33			2000	<i>id</i>		<i>id</i>
		7/34			<i>id</i>	<i>id</i>		<i>id</i>
		7/35			<i>id</i>	<i>id</i>		<i>id</i>
		7/36			<i>id</i>	<i>id</i>		<i>id</i>
	<i>H.?</i> <i>cantabriae</i>	2/3			5500	<i>id</i>		<i>id</i>
	<i>H. cantabriae</i>	2/5			<i>id</i>	<i>id</i>		<i>id</i>
	as <i>Discoaster- oides mega- stypus</i>	1/6			6500	<i>id</i>		<i>id</i>
	as <i>H.?</i> <i>conicus</i>	7/37			2000	<i>id</i>		<i>id</i>
		7/38			<i>id</i>	<i>id</i>		<i>id</i>
		1/2			7000	<i>id</i>		<i>id</i>
1/1				9800	<i>id</i>		<i>id</i>	
1/3				6400	<i>id</i>		<i>id</i>	
Perch-Nielsen 1971b	<i>H. cantabriae</i>	2/11			10000	<i>id</i>		Cantabria Sea- mount,
		2/10			9000	<i>id</i>		Bay of Biscay
Perch-Nielsen 1977	<i>H.?</i> <i>cantabriae</i>	13/9			5000	<i>id</i>		Ceará Rise, Atlan- tic Ocean
		13/13			4200	<i>id</i>		<i>id</i>
		13/17			4000	<i>id</i>		<i>id</i>
	as <i>Discoaster- oides megastypus</i>	10/7			10000	<i>id</i>		<i>id</i>
		10/8			<i>id</i>	<i>id</i>		<i>id</i>
		10/9			<i>id</i>	<i>id</i>		<i>id</i>
		10/11			8000	<i>id</i>		<i>id</i>
		10/12			10000	<i>id</i>		<i>id</i>
		10/13			<i>id</i>	<i>id</i>		<i>id</i>
		10/16			<i>id</i>	<i>id</i>		<i>id</i>
	as <i>Discoaster- oides megasty- pus?</i>	13/14			9000	<i>id</i>		<i>id</i>

Heliotrochus (continued)

Reference	Species	Plate/ Figure	Height (μm)	Diameter (μm)	Magnifica- tion	Age	Formation	Location	
Perch-Nielsen 1977	<i>as Discoaster- oides megastypus</i>	10/6			7500	<i>id</i>		<i>id</i>	
		10/10			<i>id</i>	<i>id</i>	<i>id</i>		
		10/15			<i>id</i>	<i>id</i>	<i>id</i>		
		10/14			9000	<i>id</i>	<i>id</i>		
	<i>as H.? conicus</i>	13/5			5000	<i>id</i>		<i>id</i>	
Perch-Nielsen et al. 1978	<i>H. kleinPELLI</i>	9/7			~ 2000	e. Tert		Nile Valley, Egypt	
		9/8			<i>id</i>	<i>id</i>	<i>id</i>		
		9/11			<i>id</i>	<i>id</i>	<i>id</i>		
		9/12			<i>id</i>	<i>id</i>	<i>id</i>		
		9/13			<i>id</i>	<i>id</i>	<i>id</i>		
		9/14			<i>id</i>	<i>id</i>	<i>id</i>		
		16/1			6500	L. Paleocene	Kilabiya Chalk	<i>id</i>	
		16/5			6000	<i>id</i>	<i>id</i>	Gebel Oweina,	
		15/4			5800	<i>id</i>	<i>id</i>	Nile Valley, Egypt	
		17/1	x			<i>id</i>	<i>id</i>	<i>id</i>	
		17/4	x			<i>id</i>	<i>id</i>	<i>id</i>	
		17/5	x			<i>id</i>	<i>id</i>	<i>id</i>	
		17/6	x			<i>id</i>	<i>id</i>	<i>id</i>	
	17/7	x			<i>id</i>	<i>id</i>	<i>id</i>		
	<i>H. cantabriae</i>	9/9				~ 2000	L. Creta-E. Tert		Nile Valley, Egypt
		9/10				<i>id</i>	<i>id</i>	<i>id</i>	
		15/1				10600	L. Paleocene	Kilabiya Chalk	Gebel Oweina,
		15/12				4900	M. Paleocene	Lower Owaina Shale	Nile Valley, Egypt
		15/3				7200	L. Paleocene	Kilabiya Chalk	<i>id</i>
17/2					6200	<i>id</i>	<i>id</i>	<i>id</i>	
17/3					5500	<i>id</i>	<i>id</i>	<i>id</i>	
16/2					8800	<i>id</i>	<i>id</i>	<i>id</i>	
16/6					4800	<i>id</i>	<i>id</i>	<i>id</i>	
16/4					8400	<i>id</i>	<i>id</i>	<i>id</i>	
16/12					7100	<i>id</i>	<i>id</i>	<i>id</i>	
16/3					4600	<i>id</i>	<i>id</i>	<i>id</i>	
16/9					7200	<i>id</i>	<i>id</i>	<i>id</i>	
15/6					7000	<i>id</i>	<i>id</i>	<i>id</i>	
Pospichal and Wise 1990		<i>H. kleinPELLII</i>	3/10c			3250	<i>id</i>		Maud Rise, Wed- dell Sea
			3/10b			<i>id</i>	<i>id</i>	<i>id</i>	
	3/10a				5500	<i>id</i>	<i>id</i>	<i>id</i>	

Heliotrochus (continued)

Reference	Species	Plate/ Figure	Height (μm)	Diameter (μm)	Magnifica- tion	Age	Formation	Location	
Prins 1971	<i>H. kleinpellii</i>	8/2a			2500	x		x	
		8/2b			<i>id</i>	x		x	
		8/2c			<i>id</i>	x		x	
	as <i>Discoaster- oides megastypus</i>	8/3a			<i>id</i>	x		x	
		8/3b			<i>id</i>	x		x	
		8/3c			<i>id</i>	x		x	
		8/5a			<i>id</i>	x		x	
		8/5b			<i>id</i>	x		x	
		8/5c			<i>id</i>	x		x	
		8/5d			<i>id</i>	x		x	
		8/6a			<i>id</i>	x		x	
		8/6b			<i>id</i>	x		x	
		8/6c			<i>id</i>	x		x	
Proto Decima et al. 1975	as <i>Discoaster- oides megastypus</i>	4/19a			1850	E. Eocene		Possagno, Italy	
		4/19b			<i>id</i>	<i>id</i>		<i>id</i>	
Romein 1979	<i>H. cantabriae</i>	10/2			1500	L. Paleocene	Nahal Avdat	Israel	
	<i>H. megastypus</i>	5/7			6000	<i>id</i>	<i>id</i>	<i>id</i>	
		5/8			<i>id</i>	<i>id</i>	<i>id</i>	<i>id</i>	
Steurbaut 1998	<i>H. knoxii</i>	2/10b	4.3			<i>id</i>	Argile de Louvil	Belgium	
		2/10a	4.3			<i>id</i>	<i>id</i>	<i>id</i>	
		2/12b		6.9		<i>id</i>	<i>id</i>	<i>id</i>	
		2/12c		6.9		<i>id</i>	<i>id</i>	<i>id</i>	
		2/12a		6.9		<i>id</i>	<i>id</i>	<i>id</i>	
		2/11	5.1			<i>id</i>	<i>id</i>	<i>id</i>	
		2/13	4.1			<i>id</i>	<i>id</i>	<i>id</i>	
		2/9a		9		<i>id</i>	<i>id</i>	<i>id</i>	
		2/9b		9		<i>id</i>	<i>id</i>	<i>id</i>	
		2/17a		13.6		<i>id</i>	<i>id</i>	<i>id</i>	
		2/17b		13.6		<i>id</i>	<i>id</i>	<i>id</i>	
		2/14		12		<i>id</i>	Tuffeau du Moulin Compensé	<i>id</i>	
		2/15	x			<i>id</i>	Argile de Louvil	<i>id</i>	
	<i>H. kleinpellii</i>	2/18a			11		E. Thanetian	Maaseik Clay Member	<i>id</i>
		2/18b			11		<i>id</i>	<i>id</i>	<i>id</i>
2/16				8		<i>id</i>	<i>id</i>	<i>id</i>	

Heliotrochus (continued)

Reference	Species	Plate/ Figure	Height (μm)	Diameter (μm)	Magnifica- tion	Age	Formation	Location
Sturbaut and Sztrákos 2008	<i>H. knoxii</i>	4/23a		8.8		Thanetian	Gan-Rébénacq Road Section	Aquitaine, France
		4/23b		8.8		<i>id</i>		<i>id</i>
	<i>H. kleinpellii</i>	3/1a		25		<i>id</i>	<i>id</i>	<i>id</i>
		3/1b		25		<i>id</i>	<i>id</i>	<i>id</i>
Sullivan 1964	<i>H. kleinpellii</i>	12/5a		12.7		Paleocene		California, USA
		12/5b		12.7		<i>id</i>		<i>id</i>
	as <i>Discoaster- oides megastypus</i>	12/3a		11.7		<i>id</i>		<i>id</i>
		12/3b		11.7		<i>id</i>		<i>id</i>
Wise and Wind 1977	<i>H. kleinpellii</i>	11/4			6000	<i>id</i>		Pont Labau, France
		11/5			7000	<i>id</i>		<i>id</i>
		11/3			6500	<i>id</i>		<i>id</i>

Heliolithus

Reference	Species	Plate/ Figure	Height (μm)	Diameter (μm)	Magnifica- tion	Age	Formation	Location		
Aubry 1986	<i>H. cantabriae</i>	1/14			1750	Thanetian	Thanet Beds	Herne Bay, Kent, England		
		1/15			<i>id</i>	<i>id</i>		<i>id</i>		
		1/16			<i>id</i>	<i>id</i>		<i>id</i>		
	<i>H. riedelii</i>	1/17				<i>id</i>	<i>id</i>	<i>id</i>		
		1/18				<i>id</i>	<i>id</i>	<i>id</i>		
		1/20				<i>id</i>	<i>id</i>	<i>id</i>		
Bramlette and Sullivan 1961	<i>H. riedelii</i>	14/9a		9.2		Paleocene	Lodo Forma- tion	Fresno County, Central California		
		14/9c		8.7		<i>id</i>			<i>id</i>	
		14/9b	6.8	9.2		<i>id</i>			<i>id</i>	<i>id</i>
		14/10	7.3	8.2		<i>id</i>			<i>id</i>	<i>id</i>
		14/11		9.7		<i>id</i>			<i>id</i>	<i>id</i>
Martini 1971	<i>H. riedelii</i>	1/15		5.4	2000	Thanetian	Reculver Silts	Reculver Towers, England		
		1/16		6.4	<i>id</i>	<i>id</i>		<i>id</i>	<i>id</i>	

Heliolithus (continued)

Reference	Species	Plate/ Figure	Height (μm)	Diameter (μm)	Magnifica- tion	Age	Formation	Location
Okada and Thierstein 1979	<i>H. riedelii</i>	4/6b	8.8			M. Paleocene		J-Anomaly Ridge, Western North Atlantic Ocean
		4/6a	8.8			<i>id</i>		<i>id</i>
		4/4b		9.1		L. Paleocene		<i>id</i>
		4/4a		6.2		<i>id</i>		<i>id</i>
		4/5c		10.9		M. Paleocene		<i>id</i>
		4/5a		10.6		<i>id</i>		<i>id</i>
		4/5d		11.8		<i>id</i>		<i>id</i>
		4/5b		10.9		<i>id</i>		<i>id</i>
		14/9		9.8		L. Paleocene		<i>id</i>
		14/8		8.8		<i>id</i>		<i>id</i>
Perch-Nielsen 1971c	<i>H. riedelii</i>	1/4			7500	Paleocene		Bay of Biscay
		7/28			2000	<i>id</i>		<i>id</i>
		7/29			<i>id</i>	<i>id</i>		<i>id</i>
		7/39			<i>id</i>	<i>id</i>		<i>id</i>
		7/40			<i>id</i>	<i>id</i>		<i>id</i>
Pospichal and Wise 1990	<i>H. riedelii</i>	3/11			5600	<i>id</i>		Maud Rise, Wed- dell Sea
Siesser et al. 1987	<i>H. riedelii</i>	3/11	5.1	5.9		<i>id</i>	Thanet Fm	SE England
		2/10			2850	<i>id</i>	<i>id</i>	<i>id</i>
		2/11			<i>id</i>	<i>id</i>	<i>id</i>	<i>id</i>
		3/10	9.3	10.7		<i>id</i>	<i>id</i>	<i>id</i>
		3/8		6		<i>id</i>	<i>id</i>	<i>id</i>
		3/9	8.3	10		<i>id</i>	<i>id</i>	<i>id</i>
Sturbaut 1998	<i>H. riedelii</i>	1/21	7.5			E. Thanetian	Chercq Mem- ber	Belgium
		1/20	4			<i>id</i>	<i>id</i>	<i>id</i>
		1/22	5			<i>id</i>	Sables de Bracheux	<i>id</i>
		1/24	4.8			<i>id</i>	Chercq Mem- ber	<i>id</i>
		1/23		7.3		<i>id</i>	<i>id</i>	<i>id</i>
		1/16	3.6			<i>id</i>	<i>id</i>	<i>id</i>
		1/17	x			<i>id</i>	<i>id</i>	<i>id</i>
		1/18		7.4		<i>id</i>	<i>id</i>	<i>id</i>
		1/19	5.2			<i>id</i>	<i>id</i>	<i>id</i>
Sturbaut and Sztrákos 2008	<i>H. riedelii</i>	3/14	8.3			Thanetian	Gan-Rébénacq	Aquitaine, France
		3/15	8.3			<i>id</i>	Road Section	<i>id</i>

Heliolithus (continued)

Reference	Species	Plate/ Figure	Height (μm)	Diameter (μm)	Magnifica- tion	Age	Formation	Location
Sullivan 1964	<i>H. riedelii</i>	12/8a	6.1			Paleocene		California, USA
		12/8b	6.1			<i>id</i>		<i>id</i>
		12/4a		10.2		<i>id</i>		<i>id</i>
		12/4b		10.2		<i>id</i>		<i>id</i>
		12/6a		8.1		<i>id</i>		<i>id</i>
		12/6b		8.1		<i>id</i>		<i>id</i>
		12/7a		8.1		<i>id</i>		<i>id</i>
		12/7b		8.1		<i>id</i>		<i>id</i>
Varol 1989	<i>H. aktasii</i>	12.5/24		5.6		L. Paleocene	Kokaksu Sec- tion	Zonguldak, North- ern Turkey
		12.5/25	5			<i>id</i>	<i>id</i>	<i>id</i>
		12.5/21		5.6		<i>id</i>	<i>id</i>	<i>id</i>
		12.5/22	3.9			<i>id</i>	<i>id</i>	<i>id</i>
		12.5/23	4.4			<i>id</i>	<i>id</i>	<i>id</i>
Wise and Wind 1977	as <i>H. riedelii</i>	11/2			10500	Paleocene	Lodo Fm	Fresno County, Central California, USA
		11/1			8000	<i>id</i>	<i>id</i>	

Hayella

Reference	Species	Plate/ Figure	Height (μm)	Diameter (μm)	Magnifica- tion	Age	Formation	Location
Bukry 1985	as <i>Cyclo- lithella neoaprica</i>	1/8			1900	Oligocene		Mid-Atlantic Ridge
		1/9			<i>id</i>	<i>id</i>	<i>id</i>	
		1/10			<i>id</i>	<i>id</i>	<i>id</i>	
		1/6			<i>id</i>	<i>id</i>	<i>id</i>	
		1/7			<i>id</i>	<i>id</i>	<i>id</i>	
		1/11			<i>id</i>	<i>id</i>	<i>id</i>	
		1/12			<i>id</i>	<i>id</i>	<i>id</i>	
Gartner 1969a	<i>H. situliformis</i>	1/5b			2500	L. Eocene	Shubuta Clay,	Clarke County, Mississippi, USA
		1/5a			<i>id</i>	<i>id</i>	Yazoo Fm	<i>id</i>
		1/5c			<i>id</i>	<i>id</i>	<i>id</i>	<i>id</i>
		1/4b			<i>id</i>	<i>id</i>	<i>id</i>	<i>id</i>
		1/4a			<i>id</i>	<i>id</i>	<i>id</i>	<i>id</i>
		1/4c			<i>id</i>	<i>id</i>	<i>id</i>	<i>id</i>
		1/6			10000	<i>id</i>	<i>id</i>	<i>id</i>
		1/7			<i>id</i>	<i>id</i>	<i>id</i>	<i>id</i>

Hayella (continued)

Reference	Species	Plate/ Figure	Height (μm)	Diameter (μm)	Magnifica- tion	Age	Formation	Location
Haq and Lohmann 1976b	<i>Discoasteroides megastypus</i>	6/12		8.8		Eocene		Blake Plateau, North Atlantic
Hay et al. 1966	as <i>Coronocylus serratus</i>	11/1			2500	L. Eocene		Nal'chik (Northwest Caucasus)
		11/2			<i>id</i>	<i>id</i>		<i>id</i>
		11/3			<i>id</i>	<i>id</i>		<i>id</i>
Müller 1974	as <i>Nannocorbis</i>	15/4			5000	Miocene		Mozambique Ridge, Western Indian Ocean
	<i>challengeri</i>	15/5			<i>id</i>	<i>id</i>		<i>id</i>
Perch-Nielsen	as <i>H. situliformis</i>	41/10			7000	<i>id</i>		Ceará Rise, Western South Atlantic
1977	<i>H. situliformis</i>	44/1			7500	L. Eocene		Rio Grande Rise, Western South Atlantic
		44/4			<i>id</i>	<i>id</i>		<i>id</i>
		44/6			<i>id</i>	<i>id</i>		<i>id</i>
		44/2			6000	<i>id</i>		<i>id</i>
		44/5			6800	<i>id</i>		<i>id</i>
		44/3			7500	<i>id</i>		<i>id</i>
		44/7			<i>id</i>	<i>id</i>		<i>id</i>
	as <i>Hayella?</i> sp.	45/10			<i>id</i>	E. Miocene		São Paulo Plateau, South Atlantic
		45/3			<i>id</i>	<i>id</i>		<i>id</i>
		45/6			<i>id</i>	<i>id</i>		<i>id</i>
Rio et al. 1990	<i>H. aperta</i>	14/1a			2400			Western Equatorial Indian Ocean
		14/1b			<i>id</i>			<i>id</i>
		14/2			<i>id</i>			<i>id</i>

Hayella (continued)

Reference	Species	Plate/ Figure	Height (μm)	Diameter (μm)	Magnifica- tion	Age	Formation	Location
Roth 1973	as <i>Cyclo- lithella aprica</i>	12/4c			3000	M. Eocene		Central Pa- cific Basin
		12/4b			<i>id</i>	<i>id</i>	<i>id</i>	
		12/4a			<i>id</i>	<i>id</i>	<i>id</i>	
		12/1a			<i>id</i>	<i>id</i>	<i>id</i>	
		12/1b			<i>id</i>	<i>id</i>	<i>id</i>	
		12/2a			<i>id</i>	<i>id</i>	<i>id</i>	
		12/2b			<i>id</i>	<i>id</i>	<i>id</i>	
		11/4			4800	<i>id</i>	<i>id</i>	
11/6			<i>id</i>	<i>id</i>	<i>id</i>			
Steurbaut 1991	as <i>Hayella</i> sp.	2/24		9.2		Ypresian	Roubaix Clay Mem- ber	West Flanders, Belgium
		2/25		9.2		<i>id</i>	<i>id</i>	<i>id</i>
Steurbaut 1990	as <i>Cyclococ- colithus</i> sp.	1/8b		10		Lutetian	Den Hoorn Fm	Knokke Borehole, Belgium
		1/8a		8.3		<i>id</i>	<i>id</i>	<i>id</i>
		1/9a		7.5		<i>id</i>	Brussel Fm	<i>id</i>
		1/9b		6.5		<i>id</i>	<i>id</i>	<i>id</i>
		1/10		8.2		<i>id</i>	Den Hoorn Fm	<i>id</i>
		1/11		8.4		<i>id</i>	<i>id</i>	<i>id</i>
Theodoridis 1984	<i>H. aperta</i>	3/3			2447.5	Miocene		Eastern At- lantic, coast off Cape Bojador
		3/5			<i>id</i>	<i>id</i>	<i>id</i>	
		3/6			<i>id</i>	<i>id</i>	<i>id</i>	
		3/4			<i>id</i>	<i>id</i>	<i>id</i>	
		3/7			<i>id</i>	<i>id</i>	<i>id</i>	
		3/8			<i>id</i>	<i>id</i>	<i>id</i>	
Troëlsen and Quadros 1971	<i>Hayella?</i> <i>gauliformis</i>	7/115	3.7			E. Eocene		Brazil
		7/116	3.7			<i>id</i>		<i>id</i>
		7/117	4.3			<i>id</i>		<i>id</i>
		7/118	4.3			<i>id</i>		<i>id</i>

Genus indeterminate A

Reference	Species	Plate/ Figure	Height (μm)	Diameter (μm)	Magnifica- tion	Age	Formation	Location
Haq and Aubry 1980	as <i>Heliolithus floris</i>	6/9	5	8.6		Paleocene	Jabal-um-Rejam Section	Jordan
	as Gen. et sp. indet	6/10		11		Pal-E. Eoc	<i>id</i>	<i>id</i>
		6/11		8.3		<i>id</i>	<i>id</i>	<i>id</i>
Perch-Nielsen 1972	as Gen. et sp. indet	14/3			16400	Paleocene		North At- lantic

Nomina dubia

Reference	Species	Plate/ Figure	Height (μm)	Diameter (μm)	Magnifica- tion	Age	Formation	Location
Bown 2005a	<i>H. gauliformis</i>	10/35		1.7		M. Eocene		Coastal Tanzania
	as <i>Hayella?</i> sp.	10/2		5.3		<i>id</i>		<i>id</i>
		10/1		5.3		<i>id</i>		<i>id</i>
		10/3		6		<i>id</i>		<i>id</i>
		10/4		7		<i>id</i>		<i>id</i>
		10/5		7		<i>id</i>		<i>id</i>
Bown and Jones 2006	<i>H. simplex</i>	1/14		5.7		<i>id</i>		<i>id</i>
		1/13		5.4		<i>id</i>		<i>id</i>
		1/12		5.4		<i>id</i>		<i>id</i>
		1/15		6.6		<i>id</i>		<i>id</i>
Müller 1976	<i>H. crassus</i>	4/7		x	2000	Quaternary		Red Sea
		4/8		x	<i>id</i>	<i>id</i>		<i>id</i>
		4/9		x	<i>id</i>	<i>id</i>		<i>id</i>
		4/10		x	<i>id</i>	<i>id</i>		<i>id</i>
		3/1		x	7125	<i>id</i>		<i>id</i>
		3/2		x	6525	<i>id</i>		<i>id</i>
		3/3		x	<i>id</i>	<i>id</i>		<i>id</i>

INDEX — DISCOASTERALES

Regular: Text mention

Bold: Pictures

Italic: Index list

Bold and italic: Taxonomic description

-
- aktasii* *Heliolithus* p. 197, 226, 228, 234, 235, 236, 240.
- alanii* *Fasciculithus* p. 87, 88, 89, 90, 97, 99, 100, 101, 102, 104, 136, 137, 139, 145.
- aperta* *Hayella* p. 247, 248, 260, 261, 263, 267.
- aprica* *Cyclolithella* p. 247, 252, 253, 254, 259.
- aubertae* *Fasciculithus* p. 87, 88, 89, 97, 104, 106, 107, 108, 114.
- aquilus* *Bomolithus* p. 167, 277, 280, 281, 283, 286.
- barakati* *Lithoptychius* p. 30, 54, 55, 59.
- billii* *Lithoptychius* p. 17, 19, 22, 23, 24-28, 30, 33, 70, 71, 76, 77, 82, 83, 97, 164.
- bitectus* *Lithoptychius* p. 17, 19, 22, 29, 30, 43, 54, 55, 58, 59, 60, 164, 167, 188.
- bobii* *Fasciculithus* p. 87, 88, 89, 101, 104, 116, 117, 133, 134.
- Bomolithus aquilus* p. 167, 277, 280, 281, 283, 286.
- Bomolithus elegans* p. 163, 164, 166, 167-169, 170, 172, 173, 174, 176, 177, 178, 188, 235.
- Bomolithus rotundus* p. 163, 169, 170, 172, 173, 179, 193.
- Bomolithus supremus* p. 277, 280, 281, 283, 286.
- cantabriae* *Heliothrochus* p. 166, 168, 173, 181, 182, 184, 187, 188, 190-193, 196, 197, 202, 209-212, 229, 235.
- challengeri* *Hayella* p. 247, 248, 262, 263, 266.
- chowii* *Lithoptychius* p. 19, 24, 25, 26, 30, 32, 33, 40.
- clinatus* *Fasciculithus* p. 87, 88, 89, 97, 101, 102, 104, 106, 107, 108, 113.
- collaris* *Lithoptychius* p. 5, 17, 18, 19, 22-24, 25-28, 30, 32, 33, 36, 37.
- conicus* *Heliothrochus* p. 167, 181, 182, 186, 193, 194, 214, 215, 220, 221.
- Coronocyclus serratus* p. 252, 253.
- crassus* Genus B p. 277, 280, 281.
- crassus* *Heliolithus* p. 277, 280.
- Cyclolithella aprica* p. 247, 252, 253, 254, 259.
- elegans* *Bomolithus* p. 163, 164, 166, 167-169, 170, 172, 173, 174, 176, 177, 178, 188, 235.
- Fasciculithus alanii* p. 87, 88, 89, 90, 97, 99, 100, 101, 102, 104, 136, 137, 139, 145.
- Fasciculithus aubertae* p. 87, 88, 89, 97, 104, 106, 107, 108, 114.
- Fasciculithus bobii* p. 87, 88, 89, 101, 104, 116, 117, 133, 134.
- Fasciculithus clinatus* p. 87, 88, 89, 97, 101, 102, 104, 106, 107, 108, 113.
- Fasciculithus fenestrellatus* p. 88, 89, 104, 158, 159.
- Fasciculithus hayii* p. 104, 148, 149.
- Fasciculithus involutus* p. 9, 55, 87, 88, 89, 90, 94, 96, 97, 100, 101, 102, 103, 104, 107, 116, 117, 119, 127-132, 137.
- Fasciculithus lillianae* p. 100, 101, 104.
- Fasciculithus lingfengensis* p. 104, 116, 117.
- Fasciculithus lobus* p. 104, 106, 107, 109.
- Fasciculithus mitreus* p. 104, 148, 149, 152, 153.
- Fasciculithus richardii* p. 87, 88, 89, 90, 97, 102, 104, 148, 149, 150, 154, 155.
- Fasciculithus schaubii* p. 87, 88, 89, 97, 98, 101, 104, 136, 137, 138, 142, 143.
- Fasciculithus sidereus* p. 87, 90, 93, 96, 104, 106, 107, 110, 111, 112.
- Fasciculithus thomasii* p. 87, 88, 89, 90, 94, 95-97, 99, 101, 104, 136, 137, 138, 140, 141.
- Fasciculithus tonii* p. 88, 89, 99, 100, 101, 102, 104, 148, 149, 150, 152.
- Fasciculithus tympaniformis* p. 9, 24, 43, 65, 87, 88, 89, 90, 95, 97, 99, 100, 101, 102, 104, 107, 116, 117, 118, 120-126, 149, 167, 187, 191, 229.
- Fasciculithus* sp. A p. 97, 104, 116, 117.
- Fasciculithus* sp. B p. 104, 158, 159.
- felis* *Lithoptychius* p. 17, 18, 19, 22, 23, 25, 27, 28, 30, 32, 33, 38, 39.
- fenestrellatus* *Fasciculithus* p. 88, 89, 104, 158, 159.
- floris* Genus A p. 269, 272, 273, 274.
- floris* *Heliolithus* p. 269, 272.
- gauliformis* *Hayella*? p. 247, 248, 262, 263, 264.
- Genus A *floris* p. 269, 272, 273, 274.
- Genus B *crassus* p. 277, 280, 281.
- Gomphiolithus magnicordis* p. 2, 5, 8, 9, 12.
- Gomphiolithus magnus* p. 1, 2, 3, 5, 8, 9, 10, 11, 14, 15, 19.
- Hayella aperta* p. 247, 248, 260, 261, 263, 267.
- Hayella challengerii* p. 247, 248, 262, 263, 266.
- Hayella? gauliformis* p. 247, 248, 262, 263, 264.
- Hayella neoaprica* p. 247, 252, 253, 255.
- Hayella simplex* p. 277, 280, 281, 282.
- Hayella situliformis* p. 245, 247, 248, 249, 252, 253, 254, 256-258, 263, 281.
- Hayella* sp. A p. 248, 262, 263, 264.
- Hayella* sp. B p. 248, 262, 263, 267.
- hayii* *Fasciculithus* p. 104, 148, 149.
- Heliolithus aktasii* p. 197, 226, 228, 234, 235, 236, 240.
- Heliolithus floris* p. 269, 272.
- Heliolithus riedelii* p. 24, 168, 181, 191, 192, 193, 197, 215, 225, 226, 227, 228, 229, 230, 231, 234, 235, 237-239, 241-243.

- Heliotrochus cantabriae* p. 166, 168, 173, 181, **182, 184, 187**, 188, 190-193, **196, 197, 202, 209-212**, 229, 235.
- Heliotrochus conicus* p. 167, 181, **182, 186**, 193, **194, 214, 215, 220, 221**.
- Heliolithus crassus* p. 277, **280**.
- Heliotrochus kleinpelli* p. 24, 101, 102, 167, 181, **182, 183, 187, 188**, 190-193, **194, 196, 197, 199-201, 205-208**, 229, 281.
- Heliotrochus knoxii* p. 181, **182, 194, 196, 197, 198, 204**.
- Heliotrochus megastypus* p. 173, 181, **182, 185, 187, 188**, 190, 193, **194, 214, 215, 216-219**.
- involutus Fasciculithus* p. 9, 55, 87, **88, 89**, 90, **94, 96**, 97, 100, **101**, 102, 103, *104*, 107, **116, 117, 119, 127-132**, 137.
- jani Lithoptychius* p. 17, **18, 19, 22, 23**, 24, 25, 26, 29, 30, 33, **42, 43, 44, 48, 49, 55, 65, 71, 95, 163**.
- kleinpelli Heliotrochus* p. 24, 101, 102, 167, 181, **182, 183, 187, 188**, 190-193, **194, 196, 197, 199-201, 205-208**, 229, 281.
- knoxii Heliotrochus* p. 181, **182, 194, 196, 197, 198, 204**.
- lillianae Fasciculithus* p. 100, **101, 104**.
- lingfengensis Fasciculithus* p. *104, 116, 117*.
- Lithoptychius barakati* p. **30, 54, 55, 59**.
- Lithoptychius billii* p. 17, **19, 22, 23**, 24-28, 30, 33, **70, 71, 76, 77, 82, 83, 97, 164**.
- Lithoptychius bitectus* p. 17, **19, 22**, 29, 30, 43, **54, 55, 58, 59, 60**, 164, 167, 188.
- Lithoptychius chowii* p. **19, 24, 25, 26, 30, 32, 33, 40**.
- Lithoptychius collaris* p. 5, 17, **18, 19, 22-24, 25-28, 30, 32, 33, 36, 37**.
- Lithoptychius felis* p. 17, **18, 19, 22, 23, 25, 27, 28, 30, 32, 33, 38, 39**.
- Lithoptychius jani* p. 17, **18, 19, 22, 23**, 24, 25, 26, 29, 30, 33, **42, 43, 44, 48, 49, 55, 65, 71, 95, 163**.
- Lithoptychius merloti* p. **18, 19, 29, 30, 42, 43, 44, 45, 50, 164**.
- Lithoptychius pileatus* p. 17, **19, 24, 25-27, 29, 30, 33, 42, 43, 46, 47, 51, 55**.
- Lithoptychius schmitzii* p. 25, 30, **64, 65, 68**.
- Lithoptychius stegastos* p. 19, 25, 27, 28, 30, **54, 55, 56, 57**.
- Lithoptychius stonehengii* p. **22, 26, 29, 30, 42, 43, 45**.
- Lithoptychius ulii* p. 17, **19, 22, 24-29, 30, 33, 43, 55, 70, 71, 73-75, 80, 81, 95, 101, 169**.
- Lithoptychius vertebratoides* p. 17, **19, 22, 25, 26, 29, 30, 70, 71, 72, 78**.
- Lithoptychius varolii* p. 17, **18, 19, 22, 23, 25-28, 30, 32, 33, 34, 35**.
- Lithoptychius* sp. A p. 18, 25, 27, 30, **54, 55, 61**.
- Lithoptychius* sp. B p. 30, **64, 65, 66, 67**.
- Lithoptychius* sp. C p. 30, **64, 65, 67**.
- Lithoptychius* sp. D p. 30, **64, 65**.
- Lithoptychius* sp. E p. 30, **70, 71**.
- lobus Fasciculithus* p. *104, 106, 107, 109*.
- magnicordis Gomphiolithus* p. 2, 5, 8, 9, **12**.
- magnus Gomphiolithus* p. 1, 2, 3, 5, 8, 9, **10, 11, 14, 15, 19**.
- megastypus Heliotrochus* p. 173, 181, **182, 185, 187, 188**, 190, 193, **194, 214, 215, 216-219**.
- merloti Lithoptychius* p. **18, 19, 29, 30, 42, 43, 44, 45, 50, 164**.
- mitreus Fasciculithus* p. *104, 148, 149, 152, 153*.
- Nannocorbis* p. 248, 262.
- neoaprica Hayella* p. 247, **252, 253, 255**.
- pileatus Lithoptychius* p. 17, **19, 24, 25-27, 29, 30, 33, 42, 43, 46, 47, 51, 55**.
- riedelii Heliolithus* p. 24, 168, 181, 191, 192, 193, 197, 215, 225, **226, 227, 228, 229, 230, 231, 234, 235, 237-239, 241-243**.
- richardii Fasciculithus* p. 87, **88, 89, 90, 97, 102, 104, 148, 149, 150, 154, 155**.
- rotundus Bomolithus* p. 163, **169, 170, 172, 173, 179, 193**.
- schaubii Fasciculithus* p. 87, **88, 89, 97, 98, 101, 104, 136, 137, 138, 142, 143**.
- schmitzii Lithoptychius* p. 25, 30, **64, 65, 68**.
- serratus Coronocycclus* p. **252, 253**.
- sidereus Fasciculithus* p. 87, 90, **93, 96, 104, 106, 107, 110, 111, 112**.
- simplex Hayella* p. 277, **280, 281, 282**.
- situliformis Hayella* p. 245, **247, 248, 249, 252, 253, 254, 256-258, 263, 281**.
- sp. A *Fasciculithus* p. **97, 104, 116, 117**.
- sp. A *Hayella* p. 248, **262, 263, 264**.
- sp. B *Fasciculithus* p. *104, 158, 159*.
- sp. B *Hayella* p. 248, 262, **263, 267**.
- sp. A *Lithoptychius* p. **18, 25, 27, 30, 54, 55, 61**.
- sp. B *Lithoptychius* p. 30, **64, 65, 66, 67**.
- sp. C *Lithoptychius* p. 30, **64, 65, 67**.
- sp. D *Lithoptychius* p. 30, **64, 65**.
- sp. E *Lithoptychius* p. 30, **70, 71**.
- stegastos Lithoptychius* p. **19, 25, 27, 28, 30, 54, 55, 56, 57**.
- stonehengii Lithoptychius* p. **22, 26, 29, 30, 42, 43, 45**.
- supremus Bomolithus* p. 277, **280, 281, 283, 286**.
- thomasi Fasciculithus* p. 87, **88, 89, 90, 94, 95-97, 99, 101, 104, 136, 137, 138, 140, 141**.
- tonii Fasciculithus* p. **88, 89, 99, 100, 101, 102, 104, 148, 149, 150, 152**.
- tyimpaniformis Fasciculithus* p. 9, 24, 43, 65, 87, **88, 89, 90, 95, 97, 99, 100, 101, 102, 104, 107, 116, 117, 118, 120-126, 149, 167, 187, 191, 229**.
- ulii Lithoptychius* p. 17, **19, 22, 24-29, 30, 33, 43, 55, 70, 71, 73-75, 80, 81, 95, 101, 169**.
- vertebratoides Lithoptychius* p. 17, **19, 22, 25, 26, 29, 30, 70, 71, 72, 78**.
- Lithoptychius varolii* p. 17, **18, 19, 22, 23, 25-28, 30, 32, 33, 34, 35**.